

Synthetic Studies Towards Nocapyrone and Violapyrone Natural Products

By

Patryk Syta

*Thesis
Submitted to Flinders University
for the degree of*

Doctor of Philosophy (PhD)

College of Science and Engineering
November 2020

Declaration

I, the undersigned, certify that this thesis does not incorporate without acknowledgement any material previously submitted for a degree or diploma in any university; and that to the best of my knowledge and belief it does not contain any material previously published or written by another person except where due reference is made in the text.

Patryk Syta

December 2019

“Every failure is the price of tuition I have paid to learn a new lesson.”

- Paul Stamets, Mycelium Running

Acknowledgements

The pursuit of doctoral studies is an enormous challenge; it is the challenge of becoming an expert. The road to becoming an expert is paved with failure and uncertainty which can only overcome with determined curiosity, a drive to understand and utilise. Research of the unexplored can be overwhelming, uncertain and filled with trepidation; it is an exercise in delayed gratification of the highest calibre. One must surround oneself with a support network to navigate the turbulent endeavour that is the achievement of the title Doctor.

I have had the great fortune to be able to rely on the support of friends, family and mentors. Without their support and guidance, I would not be able to progress and achieve the things which I set out to do.

I would like to give special thanks to my doctoral advisor Dr Michael Perkins. He specifically headhunted me to conduct my honours year research within his laboratory and research group. My honours year cemented my passion for synthetic chemistry and drove me to pursue further research and doctoral studies. His hands-off mentorship style and honest criticism provided me the platform to grow independently as a researcher. It provided me the space to pursue my own, if sometimes misguided, ideas and provided me the opportunity to fail. His criticism and scepticism kept my pursuits honest but also provided the required challenge chase. I have grown within in laboratory and I must offer him my thanks.

My friends and family have been patiently and eagerly awaiting the submission of this doctoral thesis and my subsequent entrenchment into gainful employment. I am glad to oblige them. I wish to extend my thanks to my Mother, Grandmother and Sister for their continued support of my research and my poverty.

Special thanks must go out to Simone and Oliver, without whom I would be buried in a tumult of disorder.

Conference Presentations

The following list of conference presentations have been a result of work presented in this thesis.

1. 22nd International Conference on Organic Synthesis,
Palazzo dei Congressi, Florence, Italy
Poster presentation “Synthetic Studies Towards Pyrone Natural Products”*
2. 18th Tetrahedron Symposium Asia Edition, at The RACI Centenary Congress 2017,
Melbourne Convention Centre
Poster presentation “Synthetic Studies Towards Pyrone Natural Products”*
3. The 21st International Conference on Organic Synthesis,
IIT Bombay, Mumbai, India
Poster presentation “Synthetic Studies Towards Pyrone Natural Products”*
4. The RACI National Congress 2014, Adelaide Convention Centre,
15 minute oral presentation “Synthetic Studies Towards Nocapyrone C and D”

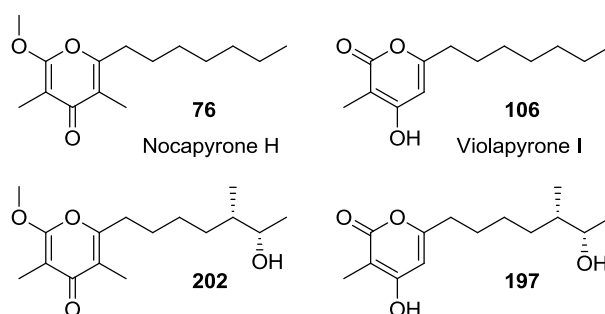
Scholarships

The following list of financial support was provided during the undertaking of this candidature.

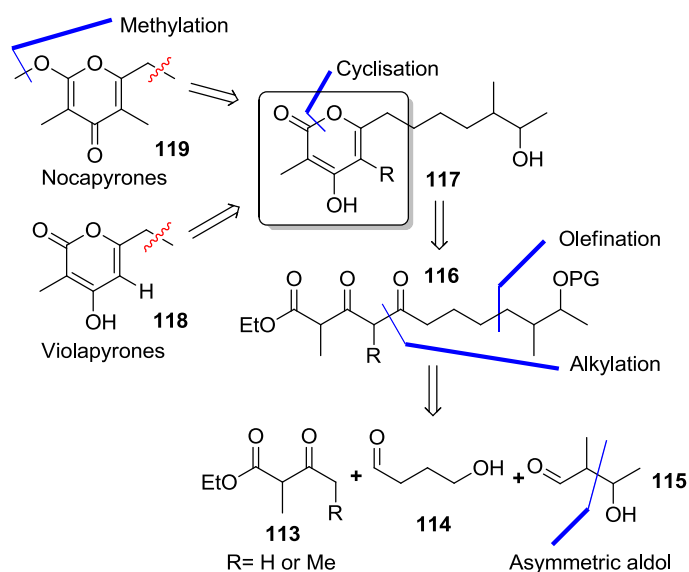
1. Australian Postgraduate Award, Provided by the Australian Government.
2. Research Student Conference Travel Grant, Provided by Flinders University

Thesis summary

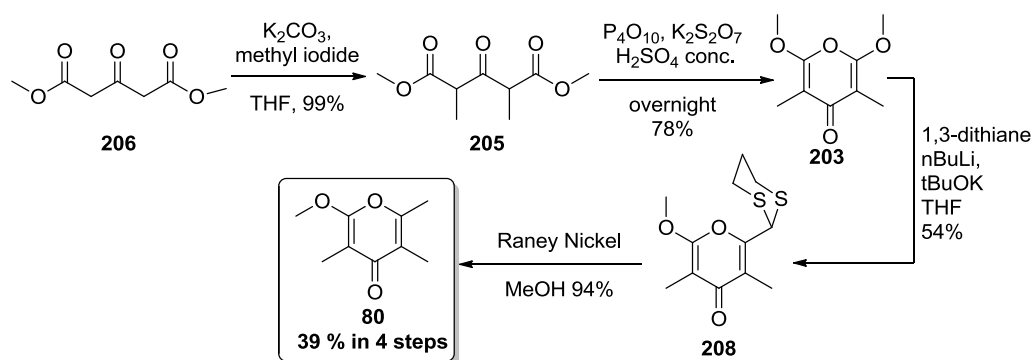
This doctoral thesis documents the investigation of stereocontrolled total synthesis of Nocapyrone and Violapyrone pyrone containing natural products. These independently isolated polyketide natural product families shared structural features, including pyrone cyclisation modes with C-6 substitution. From the natural product families 2 natural products, Violapyrone I **106** and Nocapyrone H **76**, and 2 natural product stereoisomers, Violapyrone E isomer **197** and (-)-Nocapyrone C **202**, were synthesised.



Building upon previous research from 2013, two synthetic strategies were investigated in the pursuit of Violapyrone E and Nocapyrone C natural products. The first generation synthetic strategy investigated the application of a convergent approach through early-stage pyrone preparation and side-chain coupling. The strategy was ultimately unsuccessful in realising the crucial coupling step between pyrone and side-chain fragments. The second-generation synthetic strategy investigated a linear approach, building the side chain up from asymmetric Crimmins aldol fragment and utilising late-stage pyrone preparation. This second-generation strategy was able to provide the natural products, Violapyrone I **106** and Nocapyrone H **76**, and stereoisomers, Violapyrone E isomer **197** and (-)-Nocapyrone C **202**. Analytical spectroscopic data was able to provide the evidence for the assigned characterisation.



This thesis also investigated the potential of preparing the α -methoxy- γ -pyrone synthon (**80**) through the desymmetrisation of α,α' -dimethoxy- γ -pyrone **203**. The preparation of α,α' -dimethoxy- γ -pyrone **203** and desymmetrisation to α -methoxy- γ -pyrone **80** previously demonstrated by De Paolis and co-workers was refined through intensive reaction screening and developed into a more robust protocol.



Glossary of abbreviations and non-standard terms

(-)-(Ipc)BOTf	diisopinocampheylboron triflate
(CH ₂) ₂ CHCHO	Isobutyraldehyde
(COCl) ₂	Oxaloyl chloride
[α]	Specific rotation
¹³ C	Carbon-13
1D	One-dimensional
¹ H	Proton
2D	Two-dimensional
Ac ₂ O	Acetic anhydride
AcCl	Acetyl chloride
AcOH	Acetic acid
ACP	Acyl carrier protein
APCI	Atmospheric pressure chemical ionisation
Aqu	Aqueous
AT	Acetyl transferase
aur	Aureothin
BF ₃ ·O(Et) ₂	Boron trifluoride diethyl etherate
BnBr	Benzyl bromide
Bu ₂ BOTf	Dibutylboron trifluoromethanesulfonate
BuOK	Potassium butoxide
Bz ₂ O	Benzoic anhydride
CaCO ₃	Calcium carbonate
CaH ₂	Calcium hydride
CBr ₄	Carbon tetrabromide
CDCl ₃	Chloroform deuterated
CDI	Carbonyldiimidazole
CF ₃ SO ₃ H	Trifluoromethanesulfonic acid
CH ₂ Cl ₂	Dichloromethane
CH ₃ CH ₂ COCl	Propionyl chloride
CH ₃ CN	Acetonitrile
CoA	Coenzyme A
CS ₂	Carbon disulfide
CsF	Caesium fluoride
CuBr·SMe ₂	Copper (I) bromide dimethyl sulfide
CuI	Copper iodide
DBU	1,3-Diazabicycloundec-7-ene
DCM	Dichloromethane
DH	Dehydratase
DIAD	Diisopropyl azodicarboxylate
DIBAL	Diisobutylaluminium hydride
DIPA	Diisopropylamine
DIPEA	Diisopropylethylamine
DMAP	4-Dimethylaminopyridine
DMF	Dimethylformamide
DMP	Dess-Martin periodinane

DMPU	1,3-Dimethyl-3,4,5,6-tetrahydro-2-pyrimidinone
DMSO	Dimethylsulfoxide
DNA	Deoxyribosenucleic acid
dr	Ratio of diastereomers
DH	Dehydratase
DS	Diastereomeric selectivity
ER	Enoyl reductase
Et ₂ O	Diethyl ether
Et ₃ N	Triethylamine
EtMgBr	Ethylmagnesium bromide
EtOAc	Ethyl acetate
EtOH	Ethanol
FSO ₂ OMe	Methyl fluorosulfonate
h	Hours
H ₂ SO ₃	Sulfurous acid
H ₂ SO ₄	Sulfuric acid
H ₃ PO ₄	Phosphoric acid
HCl	Hydrochloric acid
HDA	Diisopropylamine
^c Hex ₂ BCl	dicyclohexylboron chloride
HF	Hydrofluoric acid
HIV	Human immunodeficiency virus
HMPA	Hexamethylphosphoramide
HPLC	High performance liquid chromatography
HRESIMS	High-resolution mass spectrometry
ⁱ Pr ₂ NEt	N,N-Diisopropylamine
<i>i</i> -PrMgCl	Isopropylmagnesium chloride
IR	Infrared
<i>J</i>	Coupling constant
K ₂ CO ₃	Potassium carbonate
K ₂ S ₂ O ₇	Potassium pyrosulfate
kb	Kilobase
kbar	Kilobar
KMnO ₄	Potassium permanganate
KOH	Potassium hydroxide
KR	β-keto acyl synthase
KS	β-keto reductase
LDA	Lithium diisopropylamide
Li ₂ CO ₃	Lithium carbonate
LiAlH ₄	Lithium aluminium hydride
LiBH ₄	Lithium borohydride
LiHMDS	Lithium bis(trimethylsilyl)amide
lit.	Literature
M	Molecular ion (used in the context of mass spectrometry)
m/z	Mass-to-charge ratio
MAT	Malonyl-acetyl transferase
mCPBA	meta-Chloroperoxybenzoic acid
Me ₂ SO ₄	Dimethyl sulfate
MeI	Methyl iodide
MeNO ₂	Nitromethane
MeOH	Methanol
MeONa	Sodium methoxide
MeONH(Me)·HCl	N,O-Dimethylhydroxylamine hydrochloride salt
MeOTf	Methyl trifluoromethanesulfonate
MgCl ₂	Magnesium chloride

MHz	Megahertz
MIC	Minimum inhibitory concentration
MS	Mass spectrometry
MS	molecular sieves
MTPA	Methoxy(trifluoromethyl)phenylacetate
Na ₂ S ₂ O ₇	Sodium pyrosulfate
Na ₂ SO ₄	Sodium sulfate
NaCl	Sodium chloride
NaH	Sodium hydride
NaHCO ₃	Sodium bicarbonate
NaIO ₄	Sodium periodate
NaOH	Sodium hydroxide
nBuLi	n-Butyl lithium
ncp	nostocyclopeptide
NCS	N-Chlorosuccinimide
NH ₄ Cl	Ammonium chloride
NMP	N-Methyl-2-pyrrolidine
NMR	Nuclear magnetic resonance
PG	protecting group
P(OEt) ₃	Triethylphosphite
P ₂ O ₅	Phosphorous pentoxide
P ₄ O ₁₀	Phosphorous pentoxide
PCC	Pyrisinium chlorochromate
Pd(PPh ₃) ₄	Tetrakis(triphenylphosphine)palladium(0)
PhI(OCOCF ₃) ₂	[Bis(trifluoroacetoxy)iodo]benzene
PhLi	Phenyllithium
PKS	Polyketide synthase
PPA	Phenylpropanolamine
PPh ₃	Triphenylphosphine
ppm	Parts per million
PTSA	p-Toluenesulfonic acid
R	Any group with the prescribed limitations
Rf	Retention factor
RNA	Ribosenucleic acid
RT	Room temperature
SAM	S-Adenosyl methionine
SM	Starting material
SO ₃ -pyr	Pyridine sulfur trioxide complex
sp ²	trigonal planar molecular geometry
sp ³	tetrahedral molecular geometry
TBDPS	tert-Butyldiphenylsilyl
TBS	tert-Butyldimethylsilyl
TE	Thioesterase
TEMPO	(2,2,6,6-Tetramethylpiperidin-1-yl)oxyl
TFAA	Trifluoroacetic anhydride
THF	Tetrahydrofuran
TiCl ₄	Titanium tetrachloride
TLC	Thin layer chromatography
TMEDA	Tetramethylethylenediamine
TMSCl	Trimethylsilyl chloride
TosCl	4-Toluenesulfonyl chloride
UV	Ultraviolet
X4	Hexane
δC	Chemical shift of carbon nuclei (ppm)
δH	Chemical shift of hydrogen nuclei (ppm)

Contents

1	INTRODUCTION: NATURAL PRODUCTS, POLYKETIDES, PYRONES, AND THE ALDOL REACTION	1
1.1	Natural products and Drug Discovery	1
1.2	Polyketide biosynthesis relevant to pyrones.....	2
1.3	From polyketide backbone to primary core structures	7
1.4	Pyrones as structural motifs in polyketides natural products.	7
1.5	Synthetic approaches to pyrones motifs	9
1.6	Asymmetric Aldol and Chiral Auxiliaries.....	19
1.6.1	The aldol reaction in polyketide chain construction and asymmetric induction	19
1.6.2	The Zimmerman-Traxler transition state model.....	19
1.6.3	Enolate Formation and Geometry.....	20
1.6.4	Enantioselectivity of aldol condensations	23
1.7	Natural product targets	27
2	NOCAPYRONE AND VIOLAPYRONE NATURAL PRODUCTS AS POTENTIAL SYNTHETIC TARGET.....	28
2.1	Isolation and characterisation of Nocapyrone natural products	28
2.2	Biological studies on Nocapyrones	32
2.3	Nocapyrone as targets for synthesis	33
2.4	Previous work towards Nocapyrone C	33
2.5	Isolation and characterisation of Violapyrone natural products	37
2.6	Biological activity studies on Violapyrones.....	39
2.7	Violapyrones as targets for synthesis	40
2.8	Previous synthetic directions for Violapyrones.....	40
2.9	General synthetic strategy	41
2.10	Strategy and Tactics	42
3	INITIAL SYNTHETIC ATTEMPTS AT NOCAPYRONE NATURAL PRODUCTS .44	
3.1	Introduction	44
3.2	General synthetic strategy	45
3.3	First-generation synthetic strategy towards Nocapyrone C.....	46
3.4	Developing methods for dianion addition	47
3.5	Acquisition of pyrone bromide 135 in pursuit of Nocapyrone C	50
3.6	Synthesis of Nocapyrone H.....	55
3.7	Development of the Second Generation Synthetic Strategy.....	55
4	ASYMMETRIC ALDOL STEREOINDUCTION	57
4.1	Introduction	57
4.2	Crimmins aldol protocol utilising thiazolidinethione chiral auxiliaries	59

4.3	Preparation of thiazolidinethione chiral auxiliaries	60
4.4	Crimmins Aldol Protocol for <i>Syn</i> Stereoinduction	62
4.5	Stereochemical revision of 73 from 2013 Honours work	68
4.6	Acquisition of aldehyde 164	68
4.7	Acquisition of aldehyde 168	69
4.8	Paterson Aldol Protocol for <i>anti</i> Stereoinduction	71
4.9	Lactate derived (<i>S</i>)-ketone 173 preparation	73
4.10	Acquisition of <i>R,R</i> aldehyde 180	73
5	LINKER DEVELOPMENT AND NATURAL PRODUCT SYNTHESIS	76
5.1	Introduction.....	76
5.2	Development of Linker 187	76
5.3	Synthesis of Nocapyrone H and Violapyrone I natural products.....	80
5.4	Concluding Linker Functionality	83
5.5	Screening of Addition to β -Keto Esters and attempts at Violapyrone E.....	85
5.6	Synthetic directions towards Violapyrone C.....	88
5.7	Conclusion	89
6	DESYMMETRISATION OF α,α'-DIMETHOXY-γ-PYRONE	91
6.1	Introduction.....	91
6.2	Optimisation and preparation of α,α' -dimethoxy- γ -pyrone 203.....	93
6.3	Side chain preparation.....	99
7	CONCLUSION AND FUTURE DIRECTIONS	102
7.1	Summary and Conclusion of Nocapyrone and Violapyrone Synthesis	102
7.2	Summary and Conclusion of α,α' -Dimethoxy- γ -pyrone Desymmetrization.....	109
7.3	Future directions	110
8	EXPERIMENTAL PROCEDURES	113
8.1	General experimental procedures.....	113

List of Figures

Figure 1.1	Representative clinically approved pharmaceuticals derived directly from polyketide natural products.....	2
Figure 1.2	Model of Fatty Acid Biosynthesis. MAT malonyl-acetyl transferase, ACP acyl carrier protein, KS ketosynthase, KR ketoreductase, DH dehydratase, ER enol-reductase and TE thioesterase. ²⁵	3
Figure 1.3	Basic mechanisms involved in polyketide biosynthesis. (KS, β -keto acyl synthase; AT, acyl transferase; ACP, acyl carrier protein; DH, dehydratase; ER, enoyl reductase; KR, β -keto reductase; TE, thioesterase). ^{28,29}	5
Figure 1.4	Aureothin biosynthetic pathway through non-colinear modular type I PKS, including post-PKS tailoring steps. (KS, β -keto acyl synthase; AT, acyl transferase; ACP, acyl carrier protein; DH, dehydratase; ER, enoyl reductase; KR, β -keto reductase; TE, thioesterase). ^{23,36,38-40}	6

Figure 1.5 Tetraketide cyclisation modes resulting in either heterocyclic α and γ pyrones or hydroxylated aromatic chalcones and stilbenes.....	7
Figure 1.6 The comparison between α - and γ -pyrones.....	8
Figure 1.7 Comparison between internal and terminal biosynthetic pyrone formation in natural polyketide systems	8
Figure 1.8 Examples of isolated α and γ pyrone natural products.....	9
Figure 1.9 Harris <i>et al.</i> preparation of α -pyrone from metallated amine induced carboxylation of diketone. ⁴³	10
Figure 1.10 Suzuki <i>et al.</i> preparation of β,γ -diketo ester through crucial hydroamination and hydrolysis. ^{44,45}	10
Figure 1.11 Osman <i>et al.</i> preparation of hydroxy- α -pyrones utilizing β -lactone dimer intermediate. ⁵⁸	11
Figure 1.12 The Huckin-Weiler protocol for acylation and aldol type condensation of β -keto ester dianions. ⁵⁵⁻⁵⁷	11
Figure 1.13 Literature examples of aldol-like alkylation through Huckin-Weiler protocols in the preparation of β -keto esters. ⁶¹⁻⁶⁴	12
Figure 1.14 Undesired deprotonation of acylated β,γ -diketo ester, quenching	12
Figure 1.15 Literature examples of the use of Huckin-Weiler acylation protocols in the preparation of β -keto esters. ^{65-67,69-72,74,75}	13
Figure 1.16 Literature examples of ethyl methylmalonyl chloride in β,γ -diketo ester preparation. ⁷⁷⁻⁷⁹	14
Figure 1.17 Omura synthesis of Verticpyrone utilizing dioxinone aldol like alkylation. ⁸⁸	14
Figure 1.18 DBU mediated cyclisation to γ -hydroxy- α -pyrone.	15
Figure 1.19 Gold- or Silver-Catalyzed Syntheses of Pyrones from the Lee review. ⁹⁸	15
Figure 1.20 Yamamura's mild cyclisation protocol for the preparation of alkyl-substituted γ -pyrones from β -triketo with $\text{PPh}_3\text{-CCl}_4$. ¹⁰⁴	15
Figure 1.21 Conversion of 4-hydroxy-6-methyl-2-pyrone (37) to 2-methoxy-6-methyl-4-pyrone (38) ^{117,118}	16
Figure 1.22 Examples of methyl fluorosulfonate used as the methylating agent for the formation of α -methoxy- γ -pyrone. ^{61,67,74,75,88}	17
Figure 1.23 The preparation of (<i>E</i>)- and (<i>Z</i>)-iodovinyl pyrone towards Cyercene A and Placidenes natural products. ⁶⁰	18
Figure 1.24 Divergent Stille cross-coupling between vinyl stannanes for the completion of cyercene A and placidenes natural products.....	18
Figure 1.25 An aldol reaction of preformed enolate and aldehyde, with new stereocenters highlighted in red.....	19
Figure 1.26 Zimmerman-Traxler transition state model of the aldol reaction. ¹²¹	20
Figure 1.27 LDA enolisation giving (<i>E</i>)- <i>O</i> -enolate 55 and addition of DMPU reverses the selectivity to give (<i>Z</i>)- <i>O</i> -enolate 56. ¹²³	21
Figure 1.28 Enolate geometric selectivity during soft enolisation.	22
Figure 1.29 The relative topicity of closed transition state aldol reaction of ethyl ketones and aldehydes. ¹³⁸	23
Figure 1.30 Patterson's use of (-)-(Ipc) ₂ BOTf boron Lewis acids in reagent controlled aldol. ¹⁴¹⁻¹⁴³	24

Figure 1.31 Example of chiral aldehyde induced diastereoface selectivity.	25
Figure 1.32 Carreira's total synthesis of Bafilomycin A ₁ utilising an Evans auxiliary in boron mediated aldol. ¹⁴⁴	26
Figure 2.1 Proposed biosynthetic pathway for Nocapyrone natural products in <i>Nocardiopsis sp.</i> ¹⁵⁰	31
Figure 2.2 Nocapyrone L (75) co-isolated with Nocapyrone A-C from <i>Nocardiopsis alba</i> CR167 isolated from the venom duct of <i>Conus rolani</i> shelled mollusc. ¹⁵⁰	32
Figure 2.3 Nocapyrone B, H, and L reported calcium channel modulation. ¹⁵⁰	32
Figure 2.4 Summary of Nocapyrone C synthesis as reported in 2013. ¹⁵¹	33
Figure 2.5 α -methoxy- γ -pyrone (82) intermediate preparation.	34
Figure 2.6 Installation of <i>syn</i> stereochemistry with thiazolidinethione chiral auxiliary, followed by chain extension through olefination and functional group manipulation to form the allyl aldehyde 101.	35
Figure 2.7 Olefination, reduction and deprotection final steps of Nocapyrone C total synthesis.. 35	
Figure 2.8 Comparison between the synthetic product 73 and the isolated Nocapyrone C natural product, with green arrows indicating to the possibility of a relative isomer in the original isolate. ^{147,148}	36
Figure 2.9 ¹ H NMR spectrum of isolated natural product Violapyrone E with focus on the C-12 stereocentre. ¹⁴⁶	39
Figure 2.10 Noacpyrone C (73) ^{147,148} and Violapyrone E (105) ¹⁴⁶ as examples of potential synthetic targets.	40
Figure 2.11 Lee <i>et al.</i> synthesis of Violapyrone C. ¹⁶⁹	41
Figure 2.12 Gold(I) catalysed 6- <i>endo-dig</i> intramolecular cyclisation forming an α -pyrone ring and completing the synthesis of (+)-Violapyrone C. ¹⁶⁹	41
Figure 2.13 Shared retrosynthesis of Nocapyrone C and Violapyrone E natural products.....	42
Figure 3.1 Summary of the synthesis of Nocapyrone C through divergent strategy completed in 2013. ¹⁵¹	44
Figure 3.2 The preparation of γ -pyrone 80 from the 2013 Nocapyrone C synthesis. ¹⁵¹	45
Figure 3.3 General synthetic strategy for the construction of Nocapyrone and Violapyrone natural products.....	46
Figure 3.4 Synthetic strategy for Nocapyrone C through early-stage pyrone formation.....	47
Figure 3.5 The Huckin-Weiler protocol for acylation and aldol type condensation of β -keto ester dianions. ⁵⁵⁻⁵⁷	48
Figure 3.6 Preparation of pyrone bromide 135 via key aldol like alkylation.....	50
Figure 3.7 Conversion from hydroxy pyrone 134 to pyrone bromide 135 through an Appel reaction including the characteristic conversion of C-9 ¹³ C NMR signal.....	51
Figure 3.8 Failed conversion of bromide pyrone 135 to Wittig salt 136	52
Figure 3.9 Failed conversion of bromide 139 to Wittig salt 140.	52
Figure 3.10 Synthetic strategy with early-stage stereoinduction, chain extension, and late-stage pyrone formation.....	53
Figure 3.11 Methyl triflate test methylation on 4-Hydroxy-6-methyl-2-pyrone 143	54
Figure 3.12 Test methylation with methyl triflate on 4-Hydroxy-3,5,6-trimethyl-2-pyrone (80). 54	
Figure 3.13 Retrosynthesis of Nocapyrone H.....	54
Figure 3.14 Synthesis of Nocapyrone H including methyl triflate regio-methylation.....	55

Figure 3.15 General retrosynthetic strategy with early-stage stereinduction, chain extension, and late-stage pyrone installation.....	56
Figure 4.1 The general synthetic strategy visualising the differences between first and second synthetics strategies.....	57
Figure 4.2 General retrosynthetic strategy with early-stage stereinduction, chain extension, and late-stage pyrone installation.....	58
Figure 4.3 The acquisition of <i>anti</i> and <i>syn</i> stereochemistry through asymmetric aldol reaction. ..	59
Figure 4.4 Crimmins chlorotitanium enolate protocols for producing both non-Evans <i>syn</i> and Evans <i>syn</i> adducts. ^{154,180,181}	60
Figure 4.5 The preparation of thiazolidinedione via two pathways	60
Figure 4.6 proposed mechanism for the formation of oxazolidinethiones and thiazolidinethiones from β -amino alcohol in strong alkaline KOH solution and CS ₂ . ¹⁸⁵	61
Figure 4.7 Initial attempts at <i>syn</i> stereinduction and comparison of thin-layer chromatographic retention between isomers 159 and 160	62
Figure 4.8 ¹ H NMR spectrum of 159 diastereomer.....	63
Figure 4.9 ¹ H NMR spectrum of 160 diastereomer.....	64
Figure 4.10 The structures of aldol adducts 159 and 160 displaying the ¹ H NMR chemical shifts for installed stereogenic protons.....	64
Figure 4.11 The conversion between non-Evans <i>syn</i> and Evans <i>syn</i> adducts through implementation of different Crimmins chlorotitanium enolate protocols. ^{154,180,181}	66
Figure 4.12 The proposed thiocarbonyl decoordination due to interruption by excess acetaldehyde during the aldol transition state, forcing the Evans <i>syn</i> -aldol adduct.	66
Figure 4.13 X-ray crystal structure of 159 displaying (2 <i>R</i> ,3 <i>S</i>)-1-((<i>S</i>)-4-benzyl-2-thioxothiazolidin-3-yl)-3-hydroxy-2-methylbutan-1-one non-Evans <i>syn</i> stereochemistry.....	67
Figure 4.14 Revision of synthetic work 2013 Honours including stereochemical reassignment of intermediates and final synthetic compound 228. ¹⁵¹	68
Figure 4.15 Acquisition of aldehyde 164	69
Figure 4.16 ¹ H NMR spectrum of aldehyde 164.....	69
Figure 4.17 Optimised Crimmins Evans-aldol protocol and acquisition of aldehyde 168.....	70
Figure 4.18 Comparison of ¹ H NMR spectroscopic data between 162 (green) and 165 (red) TBS ethers.	71
Figure 4.19 Access to <i>anti</i> -aldol adducts through Mg-catalyzed reactions with chiral auxiliaries	72
Figure 4.20 The access of either <i>syn</i> or <i>anti</i> aldol adducts through substrate control of (<i>S</i>)-ethyl lactate derived ketones in boron mediated aldol reactions ¹⁸⁹⁻¹⁹¹	72
Figure 4.21 Preparation of (<i>S</i>)-ketone 173 from (<i>S</i>)-ethyl lactate 172	73
Figure 4.22 Boron-mediated aldol reaction with acetaldehyde resulting in <i>anti</i> -stereinduction and 174.....	73
Figure 4.23 ¹ H NMR spectroscopic data of aldol adduct 174	74
Figure 4.24 Acquisition of aldehyde 180 from <i>anti</i> -aldol adduct 174	75
Figure 5.1 Attempted preparation of Wittig salt 182 from butanediol 130.....	76
Figure 5.2 Preparation of benzothiazole sulfide 184 from benzyl protected butanediol 131.....	77
Figure 5.3 ¹ H NMR spectroscopic data of vinyl protons from isolated olefination 186 products.	79
Figure 5.4 The optimised preparation of saturated alcohol 187	79

Figure 5.5 ¹ H NMR spectroscopic data of saturated alcohol 187	80
Figure 5.6 The optimised reaction conditions for Violapyrone I and Nocapyrone H relevant triketo units.....	81
Figure 5.7 Synthesis of Nocapyrone H 76 including methyl triflate regio-methylation.....	82
Figure 5.8 Synthesis of Violapyrone I through optimised protocol.....	82
Figure 5.9 Imidazolide 192 and Aldehyde 190.....	84
Figure 5.10 Conversion of hydroxy-keto ester 193 to α -pyrone 197.....	86
Figure 5.11 Overlaid spectral comparison of synthetic α -pyrone 197 (green) against Violapyrone E 105 (black) ¹⁴⁶	87
Figure 5.12 Synthesis of γ -pyrone 202	88
Figure 6.1 Approach to Nocapyrone C from 2013 synthetic research. ¹⁵¹	91
Figure 6.2 The symmetrical α,α' -dimethoxy- γ -pyrone 203 and the desymmetrisation through nucleophilic substitution.	91
Figure 6.3 Proposed acid catalysed dehydrative cyclisation.....	92
Figure 6.4 De Paolis preparation of γ -pyrone 203. ¹⁷⁶	92
Figure 6.5 Desymmetrisation of α,α' -dimethoxy- γ -pyrone demonstrated by De Paolis ¹⁷⁶	93
Figure 6.6 Proposed mechanism for sulfur trioxide mediated dehydrative cyclisation of diester 205 to symmetrical γ -pyrone 203.....	95
Figure 6.7 Screening of reaction conditions for suitable 1,4-addition to symmetrical γ -pyrone 203	96
Figure 6.8 Possible functional group modification and utilisation of dithiane pyrone 216.	97
Figure 6.9 Comparison between the new α,α' -dimethoxy- γ -pyrone derived route (top) and the 2013 biomimetic lactone route ¹⁵¹ (bottom) towards γ -pyrone 80 preparation.	98
Figure 6.10 Conversion of α -methyl- α' -methoxy- γ -pyrone 80 to phosphonate 82.....	99
Figure 6.11 Preparation of stereocontrolled side chains 223, 225 and 227	100
Figure 6.12 Formal synthesis of Nocapyrone C integrating new preparation of γ -pyrone 80.....	101
Figure 7.1 Natural Products Nocapyrone C and Violapyrone E as identified synthetic targets. .	102
Figure 7.2 The general retrosynthetic analysis of the construction of Nocapyrone and Violapyrone natural products.....	103
Figure 7.3 First generation of synthetic strategy towards pyrone natural products.	103
Figure 7.4 The first generation synthetic route towards Nocapyrone natural products	104
Figure 7.5 The 4 step synthesis of Nocapyrone H 76	104
Figure 7.6 The 2 step synthesis of Violapyrone I	105
Figure 7.7 Proposed second-generation synthetic strategy.....	105
Figure 7.8 Crimmins aldol chemistry utilising thiazolidinethione chiral auxiliaries.	105
Figure 7.9 The proposed coordination between excess acetaldehyde and titanium during aldol transition state.	106
Figure 7.10 The preparation of 4-carbon linker.	106
Figure 7.11 The prepared side-chain aldehydes 190 and 230.....	107
Figure 7.12 Violapyrone E isomer 197 synthetic route end-game.....	107
Figure 7.13 The end-game synthetic route of (-)-Nocapyrone C 202.....	108
Figure 7.14 Preparation of α -methoxy- γ -pyrone 80 through the refined De Paolis protocol.	109

Figure 7.15 The asymmetrically prepared allyl alcohol side chain fragments 225, 227 and 223.	109
Figure 7.16 Screening of reaction conditions for suitable 1,4-addition to symmetrical γ -pyrone 203.	110
Figure 7.17 Osman <i>et al</i> preparation of 6-ethyl-3,5-dimethyl-4-hydroxy- α -pyrones utilizing β -lactone dimer intermediate. ⁵⁸	111

List of Tables

Table 1.1 Pyrone natural products Violapyrone A-G and Nocapyrone A-D. ^{144,145}	27
Table 2.1 NMR Spectroscopic Data (500 MHz, methanol- d_4) of Nocapyrone A (71). ^{146,147}	28
Table 2.2 NMR Spectroscopic Data (500 MHz, methanol- d_4) of Nocapyrone C (73). ^{146,147}	29
Table 2.3 NMR Spectroscopic Data (500 MHz, methanol- d_4) of Nocapyrone D (74). ^{146,147}	30
Table 2.4 NMR Spectroscopic Data (600 MHz, CDCl ₃) of Violapyrone D (104). ¹⁴⁵	37
Table 2.5 NMR Spectroscopic Data (600 MHz, DMSO- d_6) of Violapyrone E (105). ¹⁴⁵	38
Table 2.6 Reported Violapyrones A-J natural products. ^{145,156,157}	39
Table 3.1 Screening of reaction conditions on dianion addition with succinic anhydride	48
Table 3.2 Screening substrate scope for coupling reaction	49
Table 3.3 Comparison between major regioisomer 133 and previously reported α -methoxy and γ -methoxy pyrones. ¹¹¹	51
Table 4.1 Comparison of ¹³ CNMR Spectroscopic Data (150 MHz, CDCl ₃) of 159 and 160.	65
Table 4.2 Effect of reaction conditions on stereochemical outcome of Crimmins aldol.	65
Table 4.3 ¹³ CNMR comparison of 160 to that of (2 <i>R</i> ,3 <i>S</i>)-1-((<i>R</i>)-4-benzyl-2-thioxothiazolidin-3-yl)-3-hydroxy-2-methylbutan-1-one (161). ¹⁵⁴	67
Table 4.4 Optical rotation measurements of enantiomers 163, 164 and 167, 168	71
Table 5.1 Oxidation reactions examined for the preparation of sulfone 185	78
Table 5.2 Screening of reaction condition for Julia olefination.	78
Table 5.3 Screening reaction conditions for efficient production of triketo precursors.	81
Table 5.4 NMR Spectroscopic Data (600 MHz, CDCl ₃) of synthetic methoxy-pyrone 76.	82
Table 5.5 NMR Spectroscopic Data (600 MHz, methanol- d_4) of synthetic 106 with comparison to Violapyrone I ¹⁵⁶	83
Table 5.6 Reaction condition screening of oxidation and activation of alcohol 187.	84
Table 5.7 Reaction condition screening of coupling between β -keto ester and side chain	85
Table 5.8 NMR Spectroscopic Data (600 MHz, DMSO- d_6) of synthetic 197 with comparison to Violapyrone E ¹⁴⁵	87
Table 5.9 NMR Spectroscopic Data (600 MHz, CDCl ₃) of synthetic γ -pyrone 202.	89
Table 6.1 Reaction screening for optimal dehydrative cyclisation.	94

1 Introduction: Natural products, Polyketides, Pyrones, and the Aldol reaction

1.1 Natural products and Drug Discovery

Natural products can be broadly defined as molecules originating from living organisms.¹⁻⁵ The term is more commonly reserved specifically to small organic molecules, with molecular weights (MW) below approximately 1500-2000 Daltons, which are generated from secondary metabolic pathways.^{1,5} Metabolites can be categorised into either primary or secondary metabolites.⁶ Primary metabolites are those essential for the continued survival of the organism. Their roles involve the intrinsic processes such as normal growth, development, and reproduction of the organism.³ An organism lacking any primary metabolite would immediately undergo the process of death. Primary metabolites such as amino acids, fatty acids, nucleic acids and saccharides are common and conserved, throughout essentially all forms of life.⁷ Secondary metabolites in contrast to primary metabolites are non-essential metabolites performing functions and providing advantages other than those directly involved in the normal growth, development, and reproduction of the organism and their absence will not cause the immediate death of the organism.⁵ Secondary metabolites are more likely to be species-specific and interact in unique or niche ways with the organism or with other organisms. The most common secondary metabolites are characterised as alkaloids, terpenoids, glycosides, phenazines, polyketides and peptides.^{8,9} All are derived from primary metabolic pathways but are evolutionarily differentiated. The roles that different secondary metabolites can play include those of signalling, fragrance, flavour, pigment, protective (against radiation) or defensive (against predators or herbivores), anti-infectious (anti-microbial or anti-viral), or co-operative (with other organisms).^{8,10} These diverse and interesting properties are those usually found in natural products, and it is secondary metabolites which make up the majority of isolated natural products.^{6,7} This is due to the tendency that primary metabolites have been built into polymeric macromolecules such as proteins, phospholipids, DNA/RNA, and carbohydrates, which add to the macroscopic structure of higher organisms and are commonly separated during isolation procedures.^{3,11}

The properties of natural products did not go unnoticed by human history and eventually developed into a major portion of traditional medicines throughout the world.¹²⁻¹⁴ Medicines derived from natural sources were dominant until the advent of modern synthetic and combinational chemistry, and they still contribute heavily in modern western and eastern medicine. Natural products, natural product derivatives, synthetic drugs containing natural product pharmacophores, and natural product mimics made up the majority of all small-molecule approved pharmaceutical drugs between 1981 and 2014.¹⁵ Natural products' utility and advantage

over synthetic and combinatorial compounds has always been attributed to the evolutionary optimisation taking place in living organisms, which provide diversified and complex secondary metabolites capable of imparting selective advantage over their environments and competing organisms, ensuring continued survival.^{4,16-18}

Polyketides are a family of natural products which present diverse and complex chemical structure and featuring heavily as therapeutics. Clinically important as antibiotic, immunosuppressant and anti-tumour agents, polyketide drugs examples are displayed in Figure 1.1. These polyketide drugs include Tacrolimus (immunosuppressant), Erythromycin A (antibiotic), Lovastatin (Cholesterol-lowering agent), Amphotericin B (anti-fungal), Monensin A (antibiotic) and Pederin (anti-cancer).¹⁹ Polyketide secondary metabolites are evolutionarily derived from the fatty acid biosynthesis pathway where modifications have allowed for the retention of oxygen functionality, unsaturation and the creation of new carbon sp^3 stereocentres. These factors contribute to the increase of diversity and complexity in orders of magnitudes above that of the primary metabolic fatty acids. Providing credence to the consideration of polyketides as a privileged family of structures for bioactive novel chemical entities.^{8,20,21}

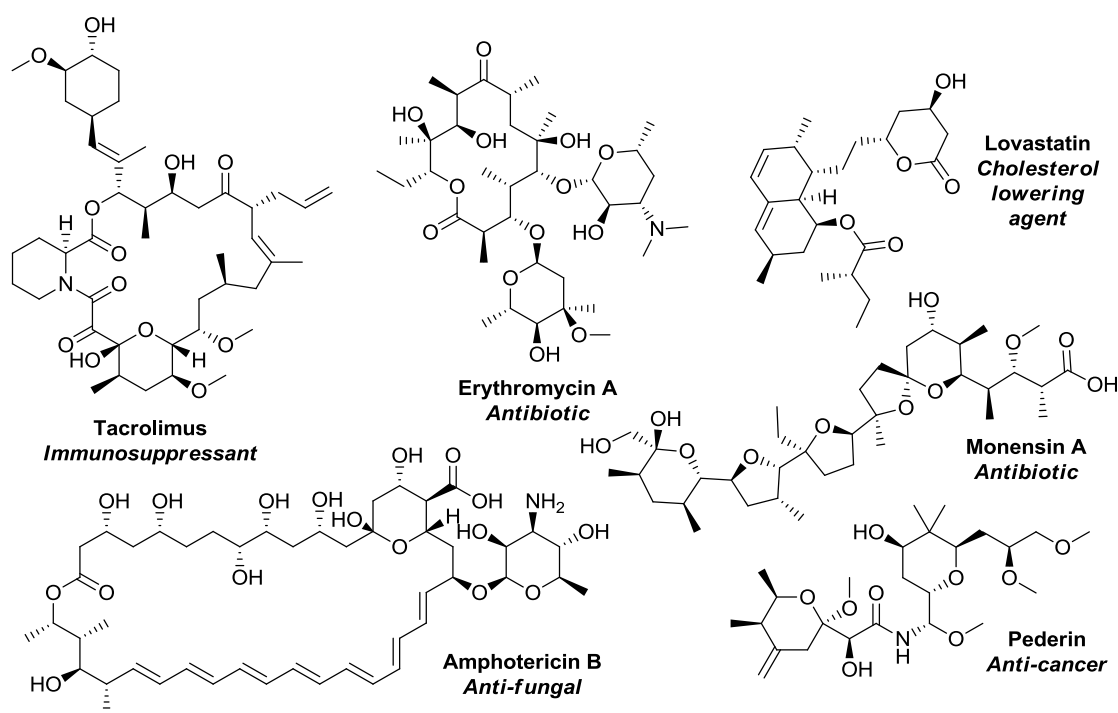


Figure 1.1 Representative clinically approved pharmaceuticals derived directly from polyketide natural products.

1.2 Polyketide biosynthesis relevant to pyrones

Polyketide metabolites are found in plants, fungi, and bacteria, and account for an appreciable percentage of isolated and studied natural products.^{22,23} These polyketide metabolites have the

ability to form very diverse chemical structures and can exhibit a wide array of biological functions, making them interesting targets and scaffolds for drug discovery. The function and structure of polyketides are a result of essentially simple but elegant biosynthetic pathways and are so defined due to their repeating β -keto (polyketomethylene) foundation. Polyketide synthase (PKS) is responsible for their construction through consecutive decarboxylative Claisen condensations which form an alternating pattern of *methylene* and keto functional groups into a long chain.²⁴ The structure undergoes functional group manipulation forming complexity in primary, secondary, and sometimes tertiary structures.

To more comprehensively understand polyketide biosynthesis, it is advantageous to examine the analogous biosynthetic pathway for fatty acid synthesis (Figure 1.2) from which it is evolutionarily derived. The biosynthetic pathways of both fatty acids and polyketides share strong homologies, including similar feedstock for chain extension and similarities in the chemical processes of chain extension itself. Fatty acid synthesis is ubiquitous among all life and involves enzyme-mediated assembly-line chain extension of thioester derived acetyl units with the total reduction to fully saturated carbon chains.²⁵

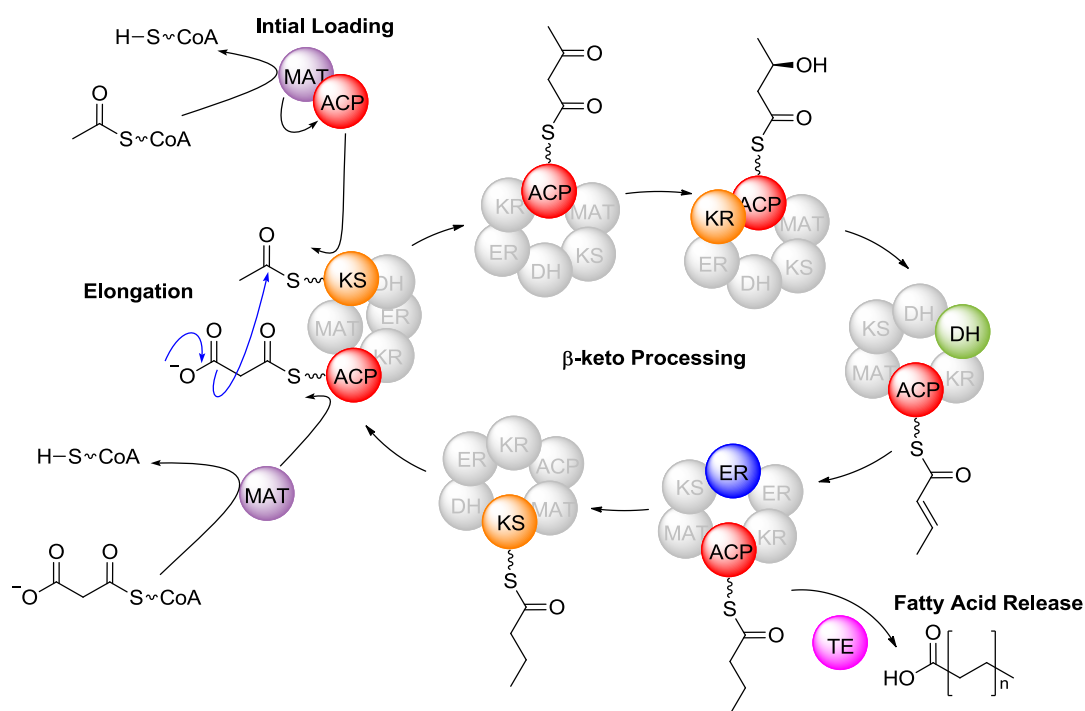


Figure 1.2 Model of Fatty Acid Biosynthesis. MAT malonyl-acetyl transferase, ACP acyl carrier protein, KS ketosynthase, KR ketoreductase, DH dehydratase, ER enol-reductase and TE thioesterase.²⁵

Fatty acid synthases are responsible for the biosynthetic process of polyketides, which can vary slightly between types of organisms but essentially function in the same way. The process (Figure 1.2) initiates with the attachment of an acetyl starter unit, derived from Acetyl CoA, onto the

cysteine thiol ketosynthase (KS). It is transferred by malonyl-acetyl transferase (MAT) and acyl carrier protein (ACP) enzymes. The KS is responsible for catalysing chain extension through decarboxylative condensation between the chain and the extender malonate unit. In the extension step, a malonyl CoA derived malonate thioester bound to ACP undergoes concerted decarboxylative condensation and carbon-carbon bond formation with the thioester chain bound to the KS. The resulting β -keto ester is carried by the ACP through consecutive enzymatic ketone reduction to the alcohol through ketoreductase (KR), followed by dehydration to an alkene through dehydratase (DH). Finally, reduction of the alkene to the alkane by enol-reductase (ER) garners a fully saturated carbon chain. The process is repeated from the extension with malonate and continues through reductive and extension cycles until a suitable chain length (usually 14, 16, or 18 carbons) is reached before the chain is transferred to thioesterase (TE) for release. It is then released as either the free acid or an acyl ester.²⁵

Polyketide synthesis (Figure 1.3) progresses through an analogous process to that of fatty acid biosynthesis but has diverged evolutionarily in both the feedstock and β -keto processing transformations. Polyketide biosynthesis is undertaken in large, complex, and multifunctional enzyme clusters called polyketide synthases (PKS).^{25,26} The synthases are categorised into three main groups of type I, type II, and type III polyketide synthases, which are defined by large multifunctional enzymes, aggregates of monofunctional enzymes and enzymes omitting the APC domains, respectively.^{27,28} Each type of these synthase enzymes have some subtle differences between species and organism types but generally function in a similar manner. Unlike fatty acid synthesis, polyketide biosynthesis is not limited to malonyl/acetyl CoA feedstock of starting material and can delve into a plethora of Coenzyme A thioesters, extending primary structural diversity much further. However, most polyketides limit themselves to malonyl and methyl-malonyl CoA feedstock and simply form polyacetates and polypropionates.^{25,26}

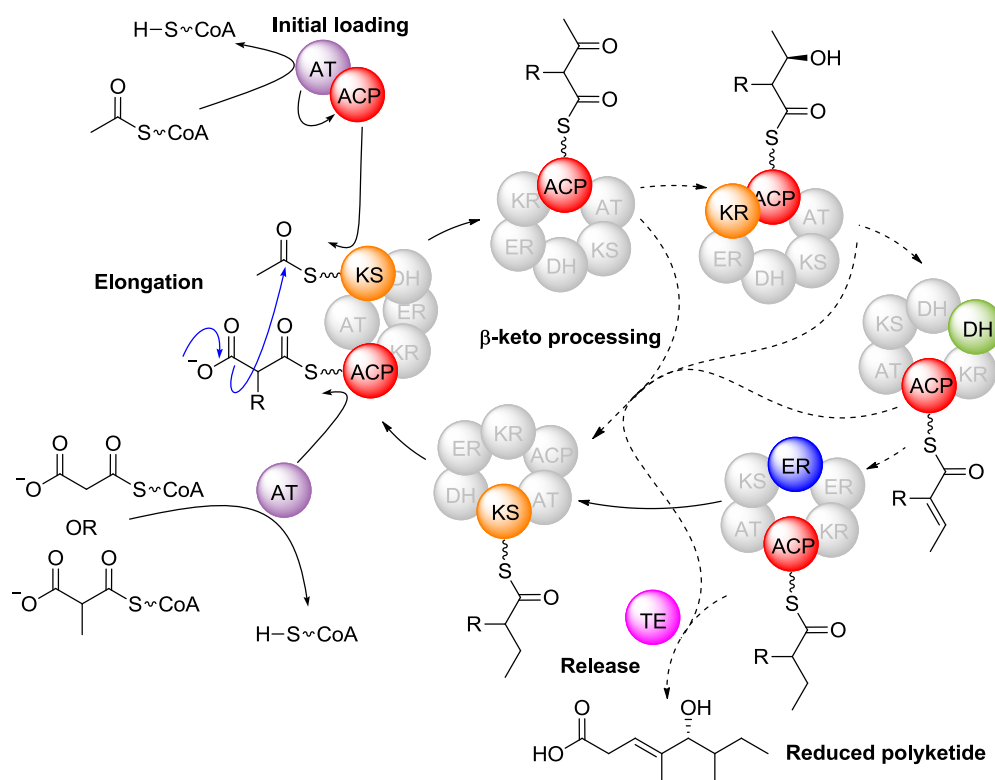


Figure 1.3 Basic mechanisms involved in polyketide biosynthesis. (KS, β -keto acyl synthase; AT, acyl transferase; ACP, acyl carrier protein; DH, dehydratase; ER, enoyl reductase; KR, β -keto reductase; TE, thioesterase).^{28,29}

The other contrasting difference between polyketide and fatty acid biosynthesis is found in the β -keto processing of polyketides. Where fatty acids are compelled to undertake full reduction to saturated hydrocarbon chains, polyketides are able to diversify the primary structure by omitting some or all reductive and dehydrative steps in any given cycle. If all β -keto processing steps were omitted, then post Claisen condensation elongation, the extended chain would be transferred to the KS for further elongation with malonyl-CoA derived feedstock producing pure polyketide chains. If only some steps were omitted, then polyketide chains of varying degrees of reduction would result in a primary structure of functional group diversity, including alcohols, ketones, methylenes, and unsaturation.

To illustrate the versatility and diversity possible through the polyketide biosynthetic pathway an example can be made of the biosynthesis of Aureothin (aur), a heterocycle-containing polyketide natural product isolated from *Streptomyces thioluteus* soil-born bacteria.³⁰ Antifungal³¹, anti-tumour²³, pesticidal,³² and anti-bacterial³³ properties have been attributed to Aureothin, which is a part of a structural class of polyketides which contain post-linear cyclisation modes named pyrones. The lactone cyclisation modes arise from the condensation of three ketide units within the linear backbone structure. Biosynthesis of Aureothin occurs in non-colinear modular type I PKS encoded by the 27 kb aur gene cluster.³⁰ The biosynthesis is initiated with the loading of an unusual *p*-nitrobenzoate-CoA thioester, itself derived from *p*-aminobenzoic acid, on to the first

PKS module.^{34,35} The backbone linear chain elongates through 5 catalysed cycles, over 4 modules, with selective amounts of reduction, as can be seen in Figure 1.4. Initially, the PKS module AurA adds 2 propionyl units selectively reduced to the alkene, producing a conjugated unsaturated system to the *p*-nitrobenzene. This is followed by the addition of one acyl unit by the PKS module AurB, reduced to full saturation, and 2 final propionyl units by the PKS module AurC without reduction, terminating the chain with a diketo thioester. Thioesterase (TE) unloads the linear chain with a signature lactonisation which forms a pyrone ring. Aureothin is completed after a set of post-PKS tailoring reactions which methylate the pyrone ring through AurI, fixing the γ -pyrone configuration and a tetrahydrofuran formation step with AurH.^{23,30,34,36–39}

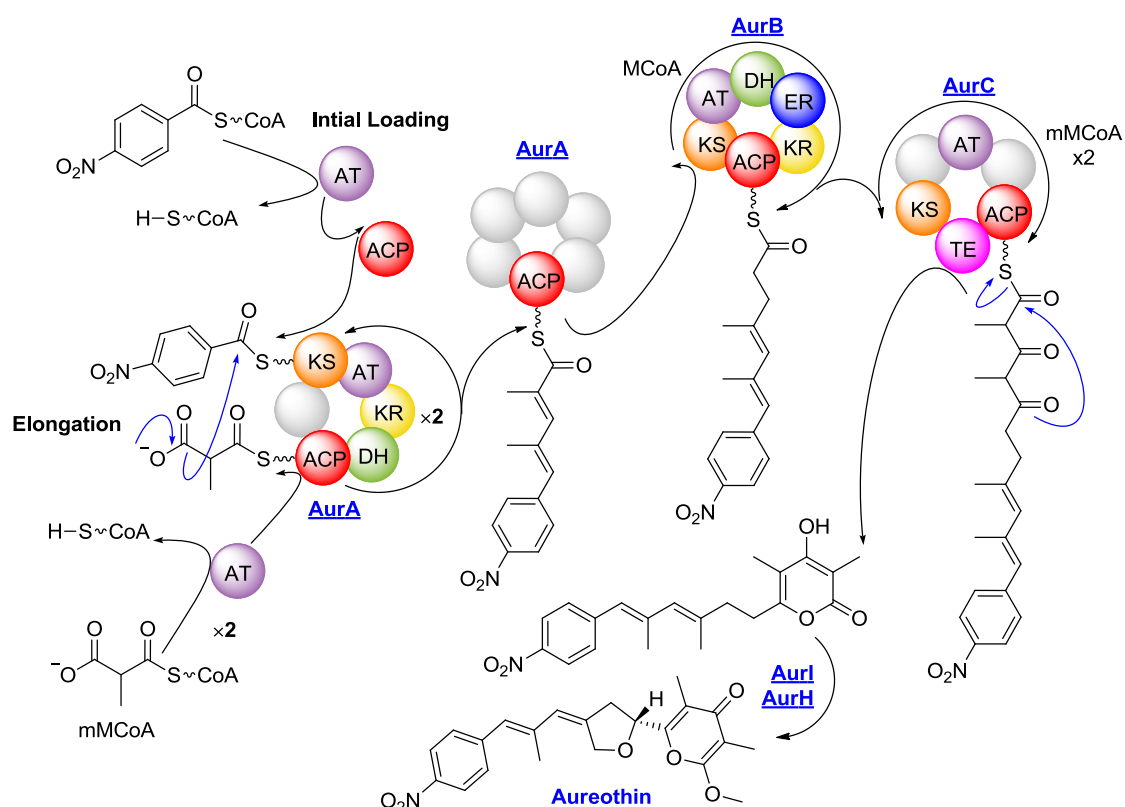


Figure 1.4 Aureothin biosynthetic pathway through non-colinear modular type I PKS, including post-PKS tailoring steps. (KS, β -keto acyl synthase; AT, acyl transferase; ACP, acyl carrier protein; DH, dehydratase; ER, enoyl reductase; KR, β -keto reductase; TE, thioesterase).^{23,36,38–}

40

The Aureothin biosynthesis exemplifies the structural diversity and functional group complexity which is possible through the polyketide biosynthetic pathway. The diversity in the feedstock of both malonyl and methyl-malonyl CoA, as well as the *p*-aminobenzoic acid derived *p*-nitrobenzoate-CoA starting unit, displays that the linear structure can differ in the branching R groups. The application of varying amounts of reduction through β -keto processing provides a variety of functional groups throughout the linear chain. The formation of new sp^3 stereocentres through reductive β -keto processing installs controlled stereochemistry which provides chirality

and extends the structural complexity an extra degree, which continues with cyclisation and post-PKS transformations.

1.3 From polyketide backbone to primary core structures

As shown in the biosynthesis of Aureothin (Figure 1.4), the linear polyketide backbone is not the final structure and extra layers of manipulation can add further architectural complexity. In addition to the β -keto processing and installation of stereochemistry, the polyketide backbone can be diversified with *in situ* alkylation, branching, as well as the possibility of pre or post-release cyclisation.

A relevant set of transformations which govern primary core polyketide structure are those of various cyclisation modes, including those occurring before and after release from the PKS. Most cyclisations occur when a repeating carbonyl primary structure present undergoes intramolecular nucleophilic attack on a carbonyl, either from the lone pair of the carbonyl oxygen or the enol tautomer. Cyclisation will normally form an energetically favoured 6 membered ring, either an unsaturated pyrone or aromatise into a substituted aryl ring. The longer the carbonyl repeats, the more degrees of freedom and a larger possible complexity of cyclisation modes.

An important example is one given for the cyclisation modes of tetraketides as they are able to undergo 4 important cyclisation modes, 2 of which develop into pyrones: α -pyrone and γ -pyrone motifs, as well as 2 hydroxylated aromatic motifs (chalcones and stilbenes), as seen in Figure 1.5.

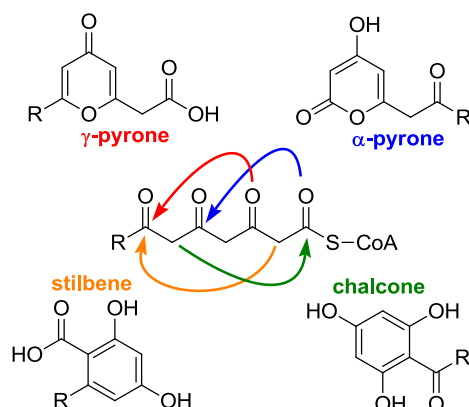


Figure 1.5 Tetraketide cyclisation modes resulting in either heterocyclic α and γ pyrones or hydroxylated aromatic chalcones and stilbenes.

1.4 Pyrones as structural motifs in polyketides natural products.

Pyrones are common structural features within polyketide natural products, occurring when triketide units undergo cyclisation. They are characterised as six-membered oxygen heterocycles bearing carbonyl functionality at either the 2- or 4-position and are categorised as either α -

pyrones (**1**) or γ -pyrones (**2**). The α -pyrones (**1**) are considered chemically closer to conjugated lactones and the γ -pyrone (**2**) to vinylogous lactones and less so to aromatic systems.⁴¹

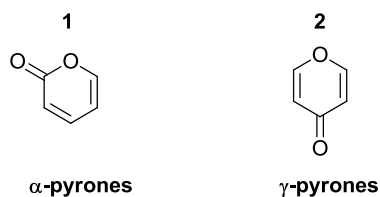


Figure 1.6 The comparison between α - and γ -pyrones

Pyrones appear in natural products in either the α or γ form depending on if the cyclisation mode arises at the terminating end or internally of the linear polyketide chain (Figure 1.7). Terminating α -pyrones (**5**) appear when β,δ -diketoacids (**3**) condense to form the unsaturated lactone (**4**), while γ -pyrones (**8**) appear internally through nucleophilic cyclisation and deoxygenation of an internal triketide (**7**), forming the vinylogous heterocycle. The terminating pyrones are able to interconvert between their tautomeric α (**5**) or γ (**6**) forms but reside as the more favoured α -pyrone (**5**) tautomer. Internal pyrones are locked in the γ (**8**) configuration due to the lack of α carbonyl for the exchange of tautomers (Figure 1.7).

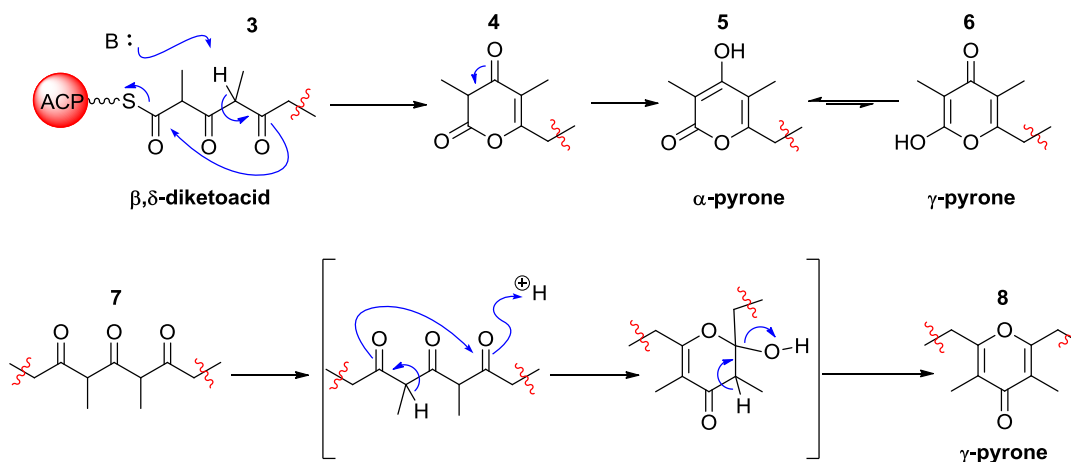


Figure 1.7 Comparison between internal and terminal biosynthetic pyrone formation in natural polyketide systems

Pyrone natural products are commonly found with post-PKS methylation locking the configuration of terminal pyrone features into either the α or γ position. These post-polyketide synthase modifications are expected to be crucial to a natural products' specific activity within its natural environment. Combinatorial studies have shown that the activity profiles and pharmacokinetics are influenced when post-PKS modifications are altered.^{36,42} Some important pyrone containing natural products can be seen in Figure 1.8, including examples of α - and γ -pyrones and examples of post-PKS methylation.

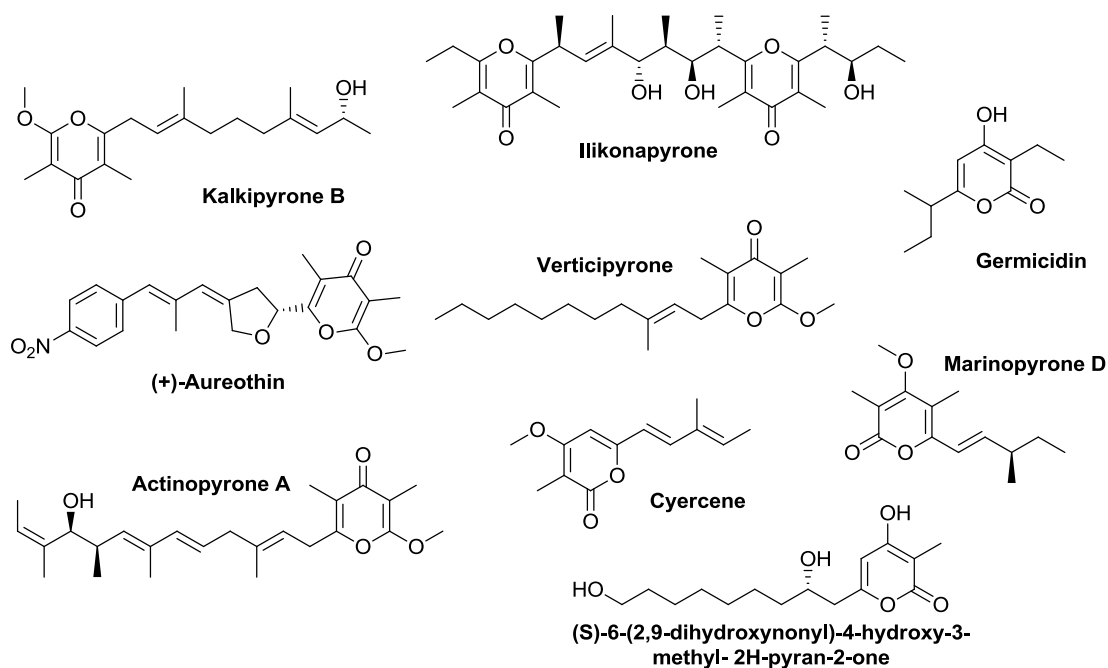


Figure 1.8 Examples of isolated α and γ pyrone natural products.

It has been shown through mutational analysis that aureothin-tailoring reactions of pyrone α -O-methylation occurs post-PKS transformation of the backbone polyketide structure and following thioester cleavage with formation of the pyrone ring. The methylation results from SAM-dependent pyrone methyltransferase specific to the γ -pyrone, with the methyl sub-unit transferred from methionine.³⁶

1.5 Synthetic approaches to pyrones motifs

The structural diversity, variety of substitutions, and methoxy derivatives combine to make pyrones in both α and γ configurations interesting synthetic challenges. A reasonable collection of literature has accumulated on the subject of synthetic preparation of pyrone motifs and review of the literature would illuminate the fundamental requirements for the pyrone construction.

This review will be limited to synthetic approaches, mainly derived from natural product synthetic studies, of monocyclic substituted pyrone preparation. Specifically, the investigation will focus on the preparation of hydroxy- α -pyrones and their α -methoxy derivatives (α -methoxy- γ -pyrones) containing side-chain substitutions extending from the C-6 and including minor substitutions (commonly methyl) at the C-3 and C-5 positions. This literature review will omit the synthetic approaches towards multicyclic pyrones such as 4-hydroxycoumarin type pyrone motifs, and will also exclude pyrone motifs which do not include oxygen functionality at both the C-2 and C-4 positions, as they are ultimately less relevant to this thesis and the synthetic targets discussed and pursued in chapter 2.

In the biomimetic approach towards pyrones are prepared through condensative lactone cyclisation of β,γ -diketo ester precursors when terminal α -pyrones are desired and the dehydrative deoxygenation of a triketone for internal vinylogous γ -pyrones. Irrespective of the desired final product, a precursory tricarbonyl linear structure is required. Although focus will be on hydroxy- α -pyrone and therefore the synthetic construction of β,γ -diketo ester precursors, most approaches are also applicable towards triketone preparation. With the increased degrees of freedom, the possible synthetic paths towards β,γ -diketo esters are wide and varied and reflected through past literature efforts towards them. Pioneering and prominently cited work is displayed by Harris⁴³ and Suzuki^{44,45} each showing unique and enduring approaches to hydroxy- α -pyrone via β,γ -diketo esters pathways.

Harris *et al.* demonstrated the utility of carboxylic acid formation from a strong amine base induced dianion addition to carbon dioxide (Figure 1.9). The diketone 3-methylpentane-2,4-dione (**9**) was exposed to sodium amide to form the dianion which reacted carbon dioxide to form the carboxylic acid **10** and acidic treatment with HF forced cyclisation to pyrone **11**.⁴³ This example along with precursory work⁴⁶⁻⁵⁴ was an important influence on the further developed of dianion chemistry relevant to pyrone preparation, including the work by Huckin and Weiler.⁵⁵⁻⁵⁷

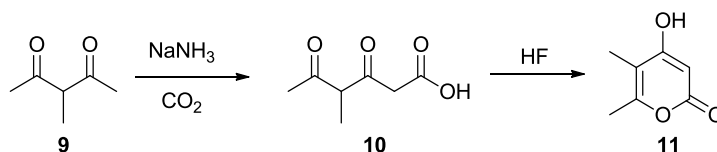


Figure 1.9 Harris *et al.* preparation of α -pyrone from metallated amine induced carboxylation of diketone.⁴³

The first synthetic examples of 3,5,6-trialkyl pyrone were reported synthesised by Suzuki *et al.* (Figure 1.10) using alkynyl Grignard addition over the ethyl methylmalonyl chloride (**12**) to give a γ,δ -acetylenic β -keto-ester **13**, which were converted to enamine- β -keto ester **14** through hydroamination across the alkyne with ethylamine. Heating the enamine with methyl iodide alkylates the γ -position and hydrolysis with hydrochloric acid gives the desired β,γ -diketo ester **15** precursor. Cyclisation to 3,5,6-trialkyl pyrone was conducted under acidic conditions with polyphosphoric acid (PPA).^{44,45}

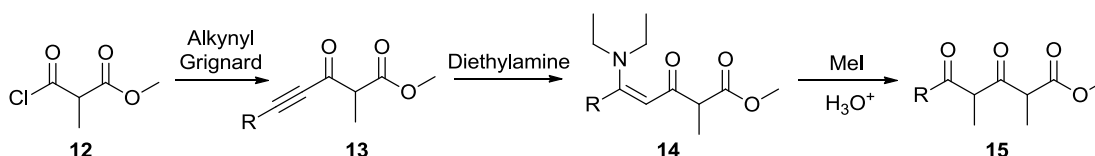


Figure 1.10 Suzuki *et al.* preparation of β,γ -diketo ester through crucial hydroamination and hydrolysis.^{44,45}

Compared to both of the above, the approaches that intersect β,γ -diketo esters on the way to pyrone formation, Osman *et al.*,⁵⁸ also pioneering authors in hydroxy- α -pyrones preparation, reported a one-step procedure to fully substituted pyrones. The procedure utilises the condensation of three molecules of propanoyl chloride (**16**) to a short-lived intermediate β -lactone **17**, presumably through a ketene (Figure 1.11).⁵⁸ This specific approach is limited to the formation of 6-ethyl-3,5-dimethyl-4-hydroxy- α -pyrones (**18**), but could become very useful if the pyrone fragments were to be expanded.

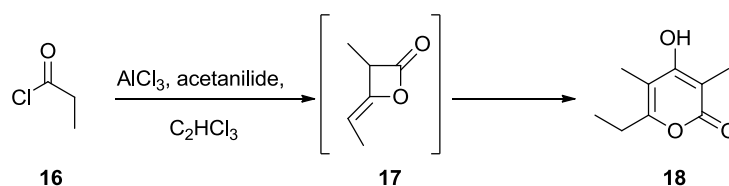


Figure 1.11 Osman *et al.* preparation of hydroxy- α -pyrones utilizing β -lactone dimer intermediate.⁵⁸

From the pioneering examples, the approaches by Harris⁴³ and Suzuki^{44,45} and derivatives of their work constitute the majority of procedures for pyrone formation until the widespread adoption of dianion protocols, as demonstrated by Huckin and Weiler.⁵⁵⁻⁵⁷ The dianion protocols deprotonate β -keto esters (**19**) with either two equivalents of lithium diisopropylamide (LDA) or with one equivalent of sodium hydride and one equivalent of *n*-butyllithium (Figure 1.12). The delocalised anion of the central α -proton protects the ester and ketone carbonyls from nucleophilic attack while the second equivalents of strong base deprotonates the γ -proton and directs electrophilic addition to the γ -position. Both aldol-like alkylations and acylation (as well as direct alkylation) were demonstrated and continue to be utilised for β,γ -diketo ester **22** preparation.⁵⁵⁻⁵⁷

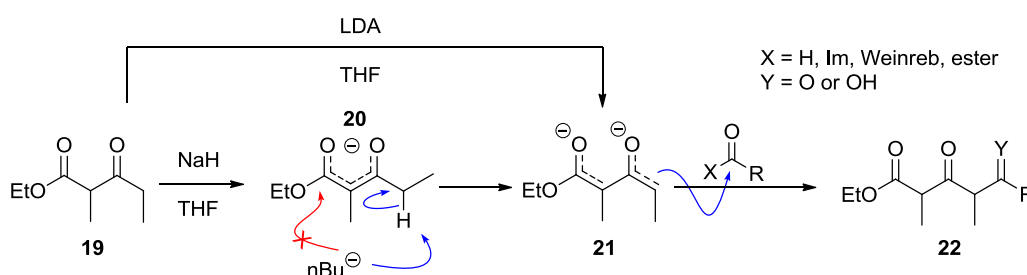


Figure 1.12 The Huckin-Weiler protocol for acylation and aldol type condensation of β -keto ester dianions.⁵⁵⁻⁵⁷

The aldol-like alkylations display the advantage of providing a strong electrophile in the way of the aldehyde substrate which can be consumed to full conversion relatively quickly at the reaction conditions without the requirement for an excess of either the aldehyde or dianion β -keto ester. As a disadvantage, the aldol product from alkylation requires oxidation before forming the desired β,γ -diketo ester and although demonstrated to be achieved through an array of oxidation methods, some conditions are less optimal, with harsh or acidic conditions resulting in undesired side-

products. A five-membered 3-oxofurane side product was characterised by Onda *et al.* when the relatively mild Swern conditions are used.⁵⁹ Acidic oxidation conditions are suspected of catalysing premature lactone cyclisation or dehydration and therefore reducing the overall β,γ -diketo ester yield. The contemporary oxidation method of choice has been dominated by Dess Martin periodinane (DMP)^{60–63} due to its mild reaction conditions (Figure 1.13).

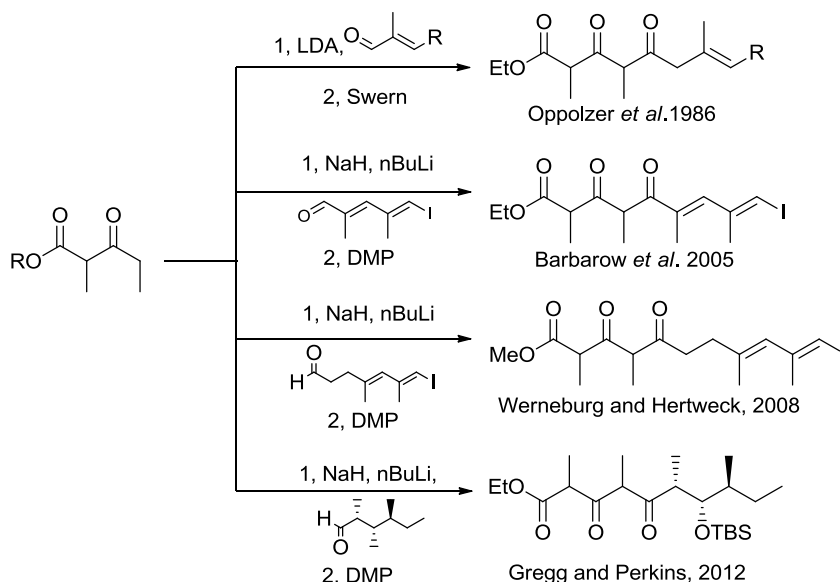


Figure 1.13 Literature examples of aldol-like alkylation through Huckin-Wieler protocols in the preparation of β -keto esters.^{61–64}

More prominently, the use of acylations with the Huckin-Wieler protocol has been seen for the preparation of β,γ -diketo esters. The acylating agents vary from simple methyl or ethyl esters^{65–68} with Weinreb amide^{69–71} and imidazole^{72–76} also featuring prominently (Figure 1.15). The apparent advantages of acylation are that the ketone oxidation state is pre-formed and cyclisation can proceed directly after. The disadvantage being that the resulting β,γ -diketo ester condensation product **23** contains a more acidic proton in the γ -position than that of the monoanion **20** of the starting β -keto ester and proton exchange between the dianion **21** and β,γ -diketo ester **23** results in quenching of any further acylation (Figure 1.14).⁵⁶ This can result in diminished yields unless extra equivalents of β -keto ester dianion are used, as the alkoxide formed from condensation is rarely strong enough to deprotonate the starting β -keto ester.⁵⁶

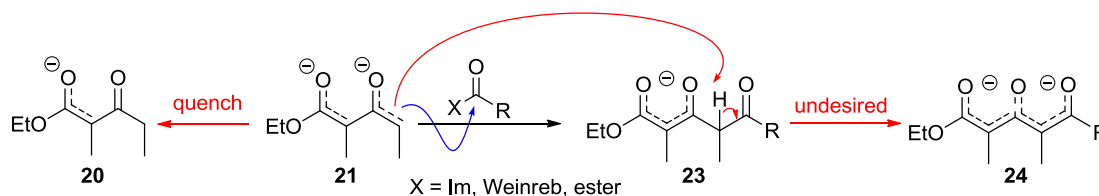


Figure 1.14 Undesired deprotonation of acylated β,γ -diketo ester, quenching

Extra equivalents are not always desirable when the β -keto ester is of higher synthetic value than that of commercially available β -keto esters. Extra equivalents of metallated amine base have not been shown to improvement in yield.⁵⁶ The most effective approaches have seen the use of efficient acylation agents such as imidazoles^{72–76} and Weinreb amides^{69–71}, which presumably either provide condensation products capable of deprotonating the monoanion (metallated imidazole) or in the case of Weinreb amide, not convert to the ketone until after protonation through treatment with acidic aqueous solution (Figure 1.15).

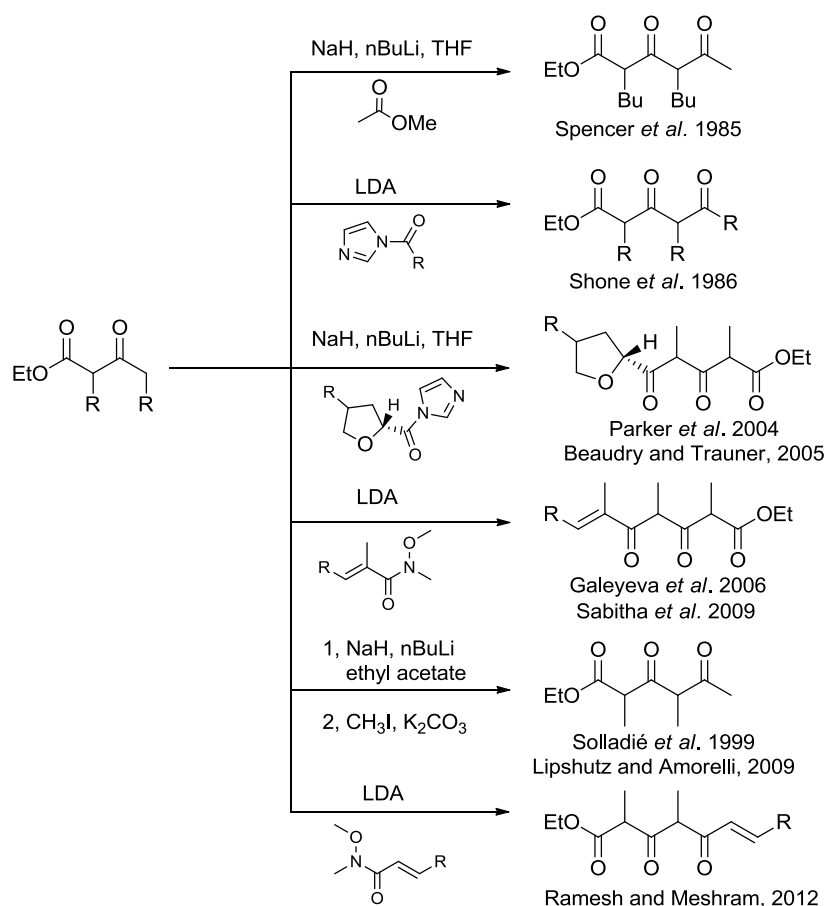


Figure 1.15 Literature examples of the use of Huckin-Weiler acylation protocols in the preparation of β -keto esters.^{65–67,69–72,74,75}

There have been a few examples of β,γ -diketo ester preparation^{77–79} which reused the ethyl 2-methylmalonyl chloride (**12**) from previously demonstrated Suzuki protocols^{44,45} but with the modification which saw the acid chloride **12** electrophile directly acylating a ketone enolate (Figure 1.16). A lithium enolate is generated on the terminating ketone of the synthetically precious side-chain before the addition of ethyl 2-methylmalonyl chloride (**12**). Peña developed the acylation protocol on a model system⁷⁷ before applying it to the synthesis of Phenoxan.⁷⁸ Trauner emulated this protocol on the synthesis of (\pm)-Photodeoxytridachione after many unsuccessful attempts at cross-Claisen condensation onto the β -keto ester dianion.⁷⁹

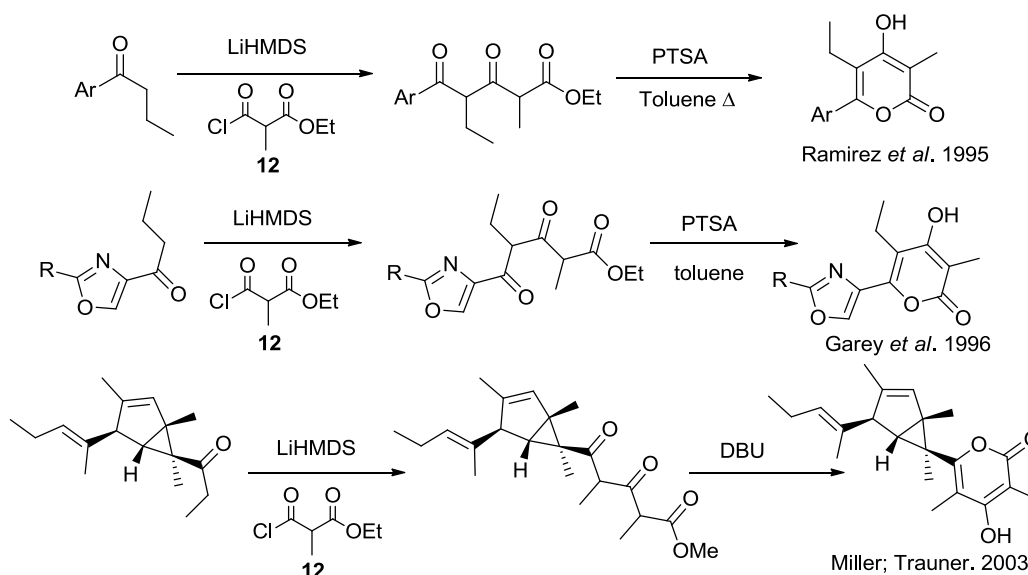


Figure 1.16 Literature examples of ethyl methylmalonyl chloride in β,γ -diketo ester preparation.⁷⁷⁻⁷⁹

Another important method for triketo preparation has been through the utilisation of β -keto ester protection via dioxinone, then lithium or titanium enolates allow for C-alkylation or acylation.⁸⁰⁻⁸⁷ The most relevant of which was demonstrated by Omura (Figure 1.17),⁸⁸ where dioxinone **26** was converted to γ -keto-dioxinone **27** through lithium enolate aldol-like alkylation with acetaldehyde, followed by Swern oxidation. Cyclisation was achieved with sodium methoxide treatment allowing for deprotection and condensation to the α -pyrone **28** in excellent yield.

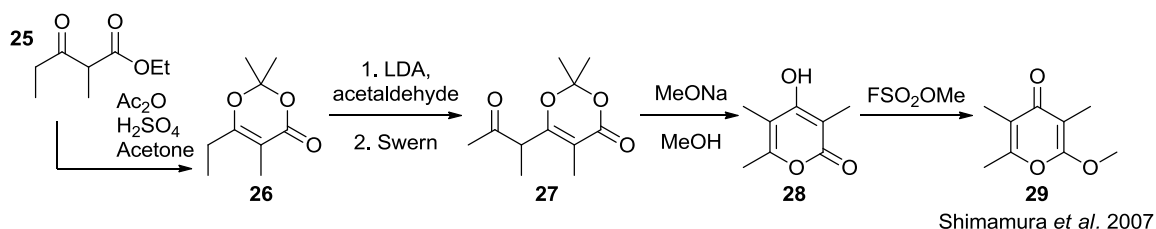


Figure 1.17 Omura synthesis of Verticpyrone utilizing dioxinone aldol like alkylation.⁸⁸

The next stage in the biomimetic preparation of α -methoxy- γ -pyrones is the condensative lactone cyclisation of the terminal β,γ -diketo ester **30** to the hydroxy- α -pyrone **5**, followed by methylation. The cyclisation is thermodynamically driven by the loss of the ester alkoxide. It is most commonly undertaken through DBU (**31**) organic-base mediated enol lactonization (Figure 1.18),^{60-62,67,69-71,73-76,79,89-95} but was originally and still occasionally carried out under acidic conditions^{44,45,65,77,78,96,97}.

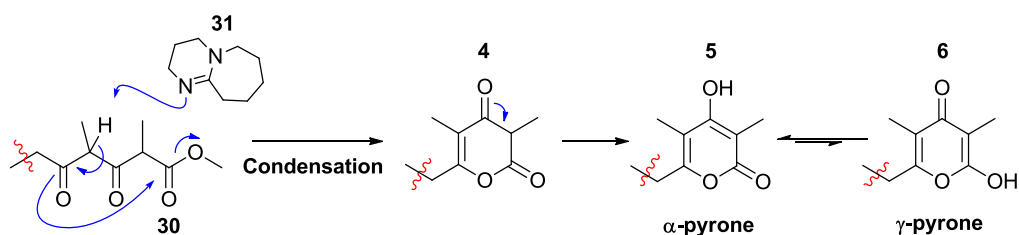


Figure 1.18 DBU mediated cyclisation to γ -hydroxy- α -pyrone.

Construction of the α -pyrone ring can be mediated through transition metal cyclisation of unsaturated substrates which have recently had much elegant advancement and have been covered in detail through a review by Lee.⁹⁸ Predominantly, these approaches displayed the utilisation of 3-oxo-5-alkynoic acid ester (**32**) substrates but lack the ability to substitute at the C-5 position of the ring, resulting in lower diversity of substitution patterns due to the presence of the alkyne moiety (Figure 1.19).

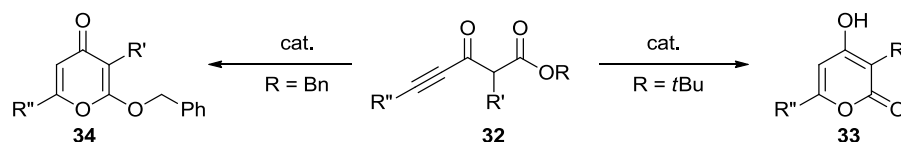


Figure 1.19 Gold- or Silver-Catalyzed Syntheses of Pyrones from the Lee review.⁹⁸

Less directly related to this work but still relevant are 2,6-alkyl substituted γ -pyrones **36**, which are also found prominently within polyketide natural products. These pyrones are found internally within the polyketide skeleton and are commonly constructed through dehydrative cyclisation of a linear 1,3,5-triketone **35**. Early examples^{72,99–103} used harsh conditions including strong acids and high temperatures to force dehydrative cyclisation, resulting in low yields and uncertain product mixtures with the possible loss of stereocontrolled stereocentres or sensitive functional groups. Milder protocols have since been developed¹⁰⁴ which employ dimethyl sulfoxide with oxalyl chloride or triphenylphosphine with carbon tetrachloride as dehydrative cyclisation agents. These protocols described by Yamamura *et al.* (Figure 1.20)¹⁰⁴ have been the prevailing methods for alkyl-substituted internal pyrones with many examples in the natural synthesis.^{105–110}

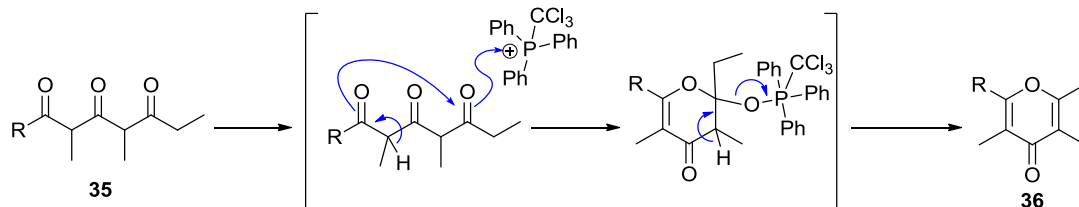


Figure 1.20 Yamamura's mild cyclisation protocol for the preparation of alkyl-substituted γ -pyrones from β -triketone with $\text{PPh}_3\text{-CCl}_4$.¹⁰⁴

The methylated methoxy-pyrones can be considered the most advanced form of the pyrone motif with the relevant α -methoxy- γ -pyrone almost exclusively achieved through *O*-methylation of

precursory hydroxy- α -pyrone. Many procedures have been utilised for their preparation including non-selective methylation such as methyl iodide, diazomethane, and dimethyl sulfate, requiring separation of the desired product from the mixture of methylated α - and γ -pyrones. The dominant contemporary protocols pursue regio-selective *O*-methylation, reducing or eliminating the loss of substrate to side-products of the regio-isomer. Methodology examples include use of dimethyl sulfate in combination with Li_2CO_3 ¹¹¹ or CaCO_3 ^{76,112,113} allowing for regio-selectivity in favour of the γ -pyrone as opposed to that of K_2CO_3 ^{114–116} which provides the opposite selectivity (γ -methoxy- α -pyrone). The use of trimethyloxonium tetrafluoroborate⁷⁸ demonstrated selective α -methoxy- γ -pyrone methylation but only when coupled with selective silyl protection of the γ -hydroxyl group. One reagent which has been considered a standout in regio-selective methylation towards γ -pyrones has been methyl fluorosulfonate (MeOSO_2F), originally reported by Beak *et al.*¹¹⁷ The very strong electrophilic nature of MeOSO_2F is reported to exploit the ground-state energies of the α - and γ -hydroxy pyrone tautomers and have an influence on the transition states, resulting in selective methylation. Indeed, the conversion of 4-hydroxy-6-methyl-2-pyrone (**37**) to 2-methoxy-6-methyl-4-pyrone (**38**) was reported to proceed in 98% yield (Figure 1.21).¹¹⁷

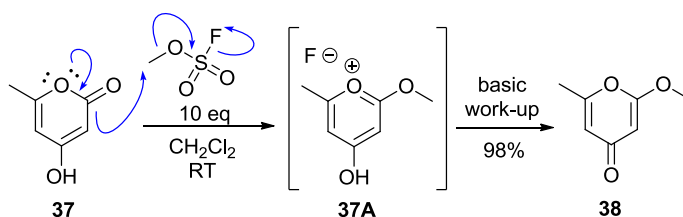


Figure 1.21 Conversion of 4-hydroxy-6-methyl-2-pyrone (37**) to 2-methoxy-6-methyl-4-pyrone (**38**)**^{117,118}

The reports by Beak *et al.*¹¹⁷ resulted in methyl fluorosulfonate being used substantially throughout the literature for the installation of α -methoxy-functionality to pyrones through regioselective methylation. Major examples (Figure 1.22) are seen by Trauner^{60,63,75,79,119,120}, Omura⁸⁸, Lipshutz⁶⁷, Hertweck⁶¹, Ishibashi⁷³ and Parker⁷⁴.

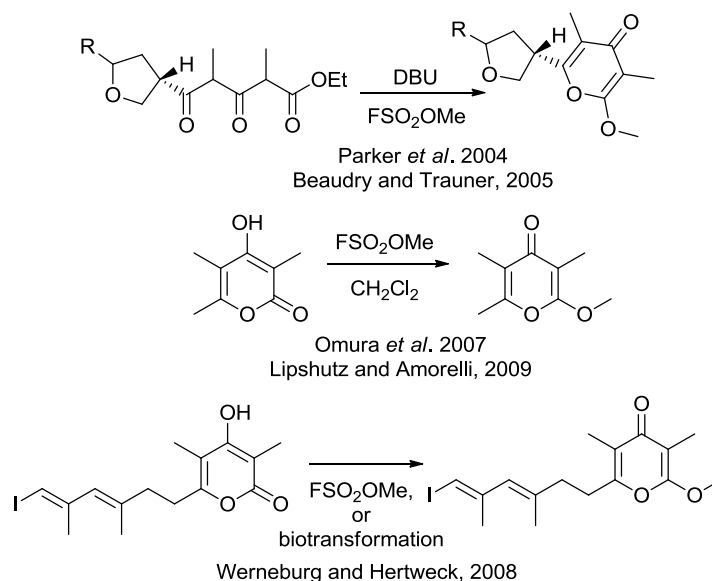


Figure 1.22 Examples of methyl fluorosulfonate used as the methylating agent for the formation of α -methoxy- γ -pyrone.^{61,67,74,75,88}

To exemplify the preparation of α -methoxy- γ -pyrones an example can be found in the stereoselective synthesis of Cyercene A and Placidenes natural products by Liang, Miller, and Trauner (Figure 1.23).⁶⁰ The divergent strategy prepared both (*E*)- and (*Z*)-iodovinyl pyrones through a shared protocol. The (*E*)-iodovinyl pyrone **44** construction beginning with Huckin-Wieler aldol-like alkylations between β -keto ester **39** and (*E*)-iodovinyl aldehyde **40** followed by DMP oxidation of the hydroxy-keto ester intermediate to the β,γ -diketo ester **42**. DBU mediated cyclisation of **42** provided the hydroxy- α -pyrone **43**, with the three step procedure converting in 53 % yield. The preparation was concluded with regio-selective methylation to the (*E*)-iodovinyl α -methoxy- γ -pyrone **44** in 95 % yield. An analogous approach was taken for the (*Z*)-iodovinyl pyrone **47**, with a Huckin-Wieler aldol-like alkylation with (*Z*)-iodovinyl aldehyde **41** and β -keto ester **39**. This was followed by DMP oxidation and DBU cyclisation to give hydroxy- α -pyrone **46** in 52 % yield over the 3 steps. Methylation gave the (*Z*)-iodovinyl pyrone **47** in 81 % yield.

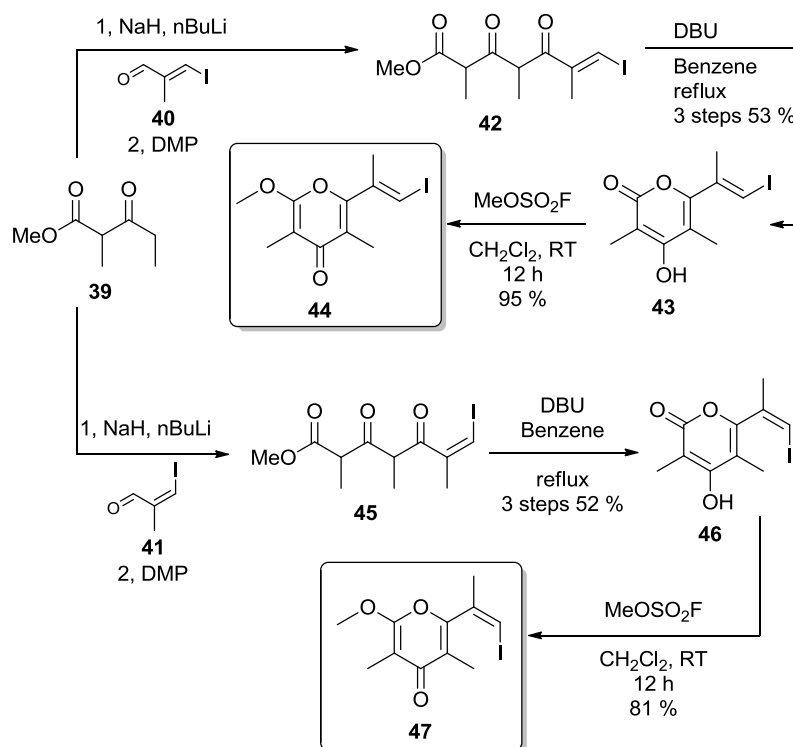


Figure 1.23 The preparation of (*E*)- and (*Z*)-iodovinyl pyrone towards Cyercene A and Placidenes natural products.⁶⁰

The iodovinyl pyrones **44** and **47** were used in divergent Stille cross-coupling between a collection of vinyl stannanes (**48**, **49**, **50**) which allowed the completion of cyercene A, placidenes A and B, and isoplacidenes A and B (Figure 1.24).

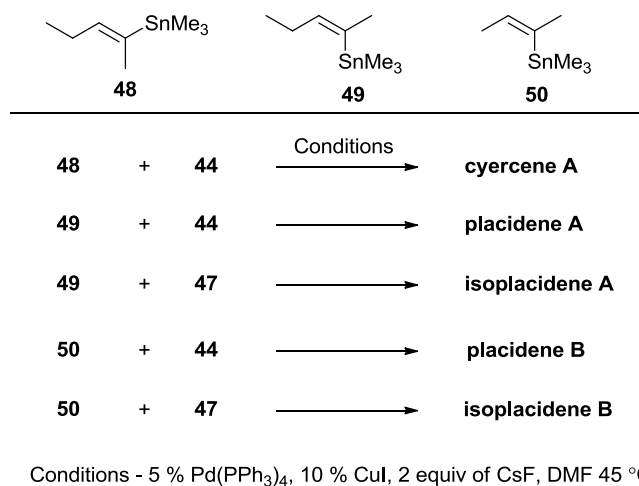


Figure 1.24 Divergent Stille cross-coupling between vinyl stannanes for the completion of cyercene A and placidenes natural products

1.6 Asymmetric Aldol and Chiral Auxiliaries

1.6.1 The aldol reaction in polyketide chain construction and asymmetric induction

Following from description of synthetic methods towards pyrone polyketides, it is important to highlight the aldol reaction and discuss its utility in polyketide chemistry. Despite the versatility from the plethora of carbon-carbon bond-forming reactions, including the Claisen condensations and olefinations which both have analogy to that of polyketide biosynthesis, the aldol reaction is a particular standout. This section will discuss the importance of the aldol reaction and the use of chiral auxiliaries with relevance to polyketide and specifically polypropionate polyketides. The focus will be set on propionate aldol substrates (three-carbon units) and their asymmetric outcomes.

In the absence of dehydrating conditions, the aldol reaction yields β -hydroxy carbonyl compounds, where two new contiguous stereocenters are created, making it perfect for installing and controlling absolute and relative stereochemistry in a synthetic pathway. Modern aldol reactions are conducted through the pre-formation of an enolate over a carbonyl compound (usually a ketone) either with the use of a strong base or through the combination of Lewis acid coordination and a weak base. The enolate **51** then nucleophilically adds across the electrophilic carbonyl substrate (commonly an aldehyde) **52** causing the carbon-carbon bond formation. Through the course of the reaction, there is a conversion from two sp^2 hybridised carbons to two sp^3 hybridised carbons during the bond formation, which gives rise to two new stereocenters in an α, β arrangement **53** (Figure 1.25).

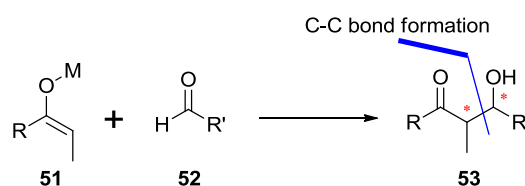


Figure 1.25 An aldol reaction of preformed enolate and aldehyde, with new stereocenters highlighted in red.

1.6.2 The Zimmerman-Traxler transition state model

The stereoselectivity of the aldol reaction is dependent on two factors: the enolate geometry being either (*E*) or (*Z*), and the facial nucleophilic attack being either *re* or *si*. This is most commonly rationalised by the Zimmerman-Traxler transition state model,¹²¹ where the distribution of ancillary side chain and enolate geometry over the equatorial and axial positions of the closed, six-membered transition state dictates the stereochemical outcome. The six-membered transition state itself comes together in from the coordination of the metal, the oxygen of enolate and the

oxygen of the aldehyde, and takes on the lower energy chair conformation. It can be seen in Figure 1.26 that preformed (*Z*)-*O*-enolates result in *syn* products when their methyl groups are directed axially, and (*E*)-*O*-enolates result in *anti* products when their methyl groups are directed equatorially.

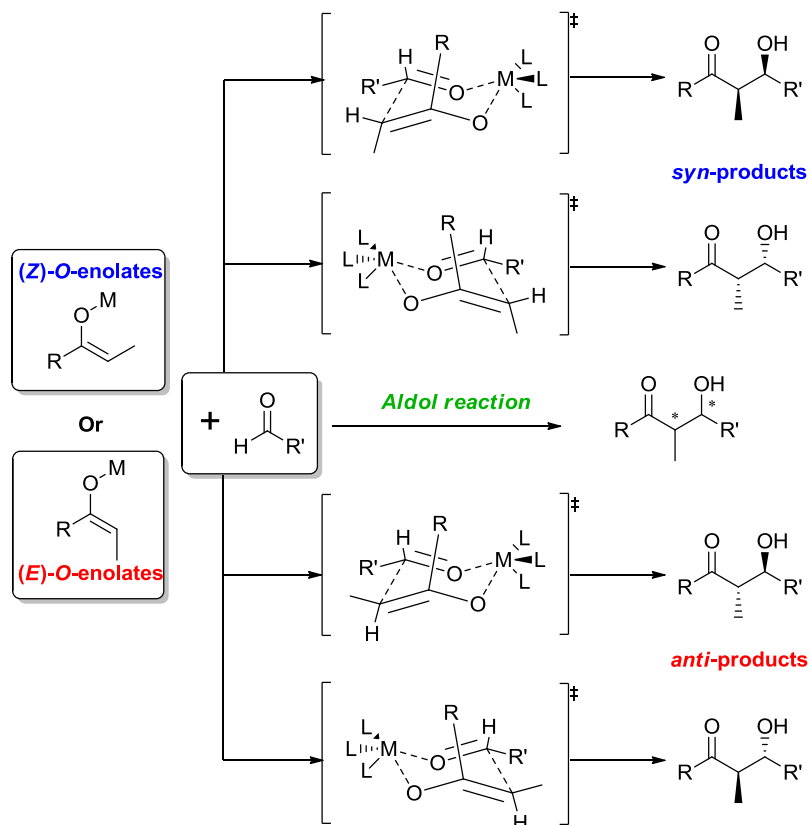


Figure 1.26 Zimmerman-Traxler transition state model of the aldol reaction.¹²¹

1.6.3 Enolate Formation and Geometry

The enolate geometry is crucial in the relative topology and the stereoselectivity of the aldol reaction. The stereo definition of the enolate geometry is dependent on the mode of deprotonation of the α -hydrogen to the carbonyl. Two methods are commonly employed for the preformation of kinetic enolates: either through hard enolisation, where a strong base deprotonates the α -hydrogen directly, or through soft enolisation, where a Lewis acid activates the α -hydrogen for deprotonation by an amine base.

In the case of hard enolisation through deprotonation of the α -position on ethyl ketones, metallated amide bases are usually employed for this purpose with lithium diisopropyl amide (LDA) being the most common strong non-nucleophilic base used. Generally, LDA treatment of ethyl ketone induces the (*E*)-*O*-enolate **55** as the stereochemical outcome when THF is used as the solvent; the selectivity has been seen to reverse to the (*Z*)-*O*-enolate **56** when a coordinating solvent is present such as HMPA or DMPU. These results were originally rationalised by Ireland

*et al.*¹²² through the use of a closed chair-like six-membered transition state (**55-TS**) during α -proton deprotonation, where the carbonyl oxygen is coordinated to an amide base via the lithium cation. The stereochemical outcomes are a result of the steric interactions of the enolate alkyl side chain and the ligands on the amide base. The large 1,3-diaxial interactions between the methyl group in the axial position and that of isopropyl groups of the amide make the transition state unfavourable. Transition states where the methyl group is equatorial are found to be more favourable, giving rise to the (*E*)-*O*-enolate **55**. If the alkyl side chain on the carbonyl is much larger, however, the result can be reversed as the steric interactions make the (*Z*)-*O*-enolate **56** more favourable. The inclusion of HMPA or DMPU is said to disrupt the six-membered transition state due to its ability to solvate the lithium cation (**56-TS**), removing the 1,3-diaxial interaction and favouring the (*Z*)-*O*-enolate **56**, as shown in Figure 1.27.¹²³

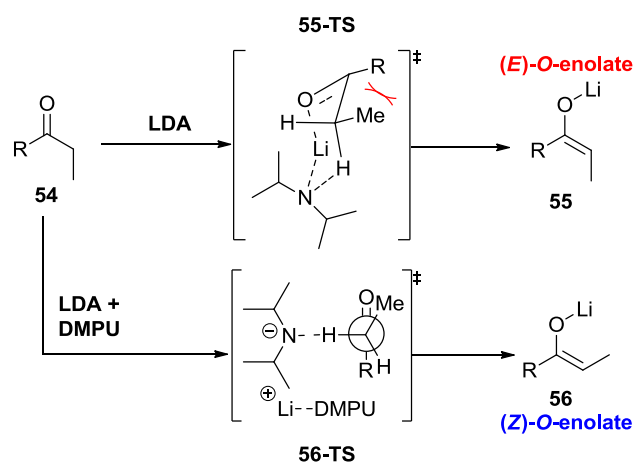


Figure 1.27 LDA enolisation giving (*E*)-*O*-enolate **55** and addition of DMPU reverses the selectivity to give (*Z*)-*O*-enolate **56**.¹²³

The soft enolisation of ethyl-type ketones is typically achieved through complexation of the carbonyl oxygen with a Lewis acid (boron^{124–127}, titanium(VI)^{128–132}, tin(II)^{133–136} being commonly used), activating the α -carbon making it susceptible to deprotonation from a weaker tertiary amine base. The enolate geometry is, again, dependent on the steric interactions of the methyl group against the side chain of the carbonyl, the ligands of the Lewis acid, and the size of the amine base. As displayed in Figure 1.28, large interactions between the carbonyl side chain and the α -methyl group give unfavourable conditions for (*E*)-*O*-enolate **59** formation and large interactions between the Lewis acid ligands and the methyl group make for unfavourable conditions for (*Z*)-*O*-enolate **60** formation. The influence of large amine bases typically favours the formation of (*Z*)-*O*-enolates **60**.

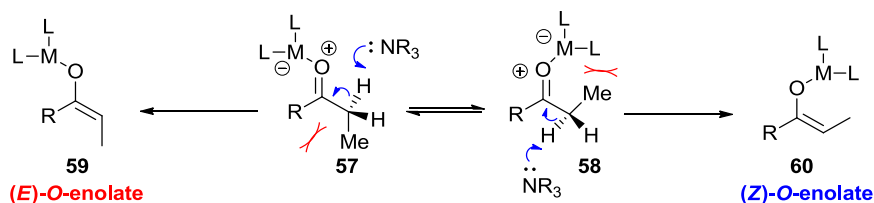


Figure 1.28 Enolate geometric selectivity during soft enolisation.

When considering the aldol reaction of ethyl-type ketones with aldehydes, the relative topicity factors into the stereochemical outcome with both the enolate geometry and steric interaction during the transition state dictating the result. The relative topicity is the facial selectivity of nucleophilic or electrophilic attack, and since both the enolate and aldehyde contain π -bond environments, they are essentially flat plains susceptible to facial attack. The *re* and *si* faces of a trigonal planar feature such as an enolate or carbonyl are defined by the Cahn-Ingold-Prelog priority order protocol, with the *re* face having a decreasing priority in a clockwise direction and the *si* face having a decreasing priority in an anti-clockwise direction.¹³⁷

The relative topicity of aldol reactions of ethyl-type ketones can be separated into eight distinct reactions and transition states resulting in four possible products, as shown in Figure 1.29. The (*E*)-*O*-enolate can undergo facial attack from either the *re* or *si* face of the enolate, or the *re* or *si* face of an aldehyde, to give four possible transition states (*re-re*, *re-si*, *si-si* or *si-re*). Steric 1,3-diaxial interactions between the side chain of the enolate and aldehyde make the *si-re* and *re-si* transition states disfavoured. This results in the formation of *anti* products from favourable *re-re* and *si-si* facial selectivity. The opposite selectivity is seen when a (*Z*)-*O*-enolate is used, where the *re-re* and *si-si* transition states are found to have the unfavoured 1,3-diaxial interaction. This leaves the *si-re* and *re-si* transition states favoured and result in *syn* products.¹³⁸

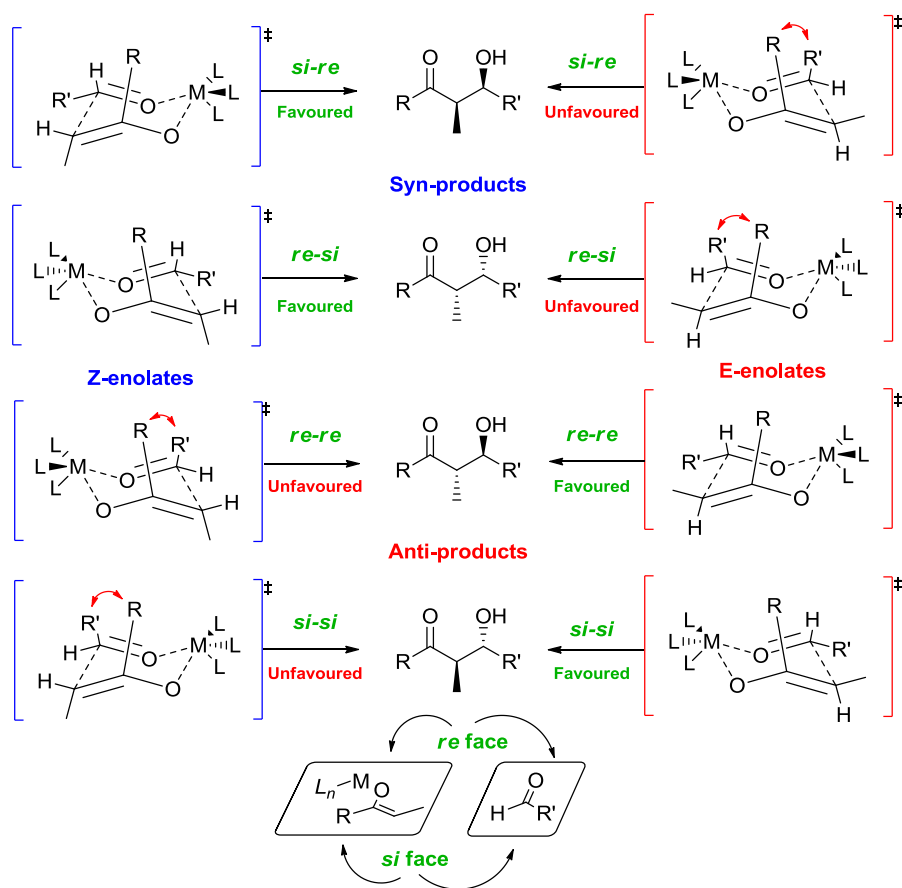


Figure 1.29 The relative topicity of closed transition state aldol reaction of ethyl ketones and aldehydes.¹³⁸

It can be seen that the 1,3-diaxial and ligand interaction in Zimmerman-Traxler transition states during aldol reactions can be used as a tool to exploit stereoselectivity. Selectivity between *syn* or *anti* relative stereochemistries could be tuned through the use of either (*E*)-*O* or (*Z*)-*O*-enolates but an extra layer of control would have to be in place to give enantiomeric purity or control over the absolute stereochemistry. This next layer of control requires to differentiate and disfavour one of the two transition states (*re-re* or *si-si* in the case of (*E*)-*O*-enolates, or *re-si* or *si-re* in the case of (*Z*)-*O*-enolates), leaving only one favoured product.¹³⁸ The most common approach to achieve this is through the introduction of chiral steric bulk at either: the enolate, aldehyde or Lewis acid ligand.

1.6.4 Enantioselectivity of aldol condensations

The absolute stereochemistry of aldol reactions can be controlled through three different tactics: the addition of chiral enolates to achiral aldehydes, the addition of achiral enolates to chiral aldehydes, and the use of chiral ligands or chiral catalysts.

These tactics are themselves separated into substrate and reagent control. Chiral enolates or chiral aldehydes provide the substrate control, while chiral ligands or chiral catalysts provide the reagent

control, which imparts asymmetry into the aldol condensation. Each tactic involves the use of a chiral element which will disrupt one of the two ordinarily favoured Zimmerman-Traxler transition states through steric interaction, inducing a single isomeric outcome.

Before discussing reagent control, organocatalysis should be mentioned. Efforts in recent years have expanded the organocatalytic toolkit with application in asymmetric aldol reactions. Even when limited to proline derived enamine catalysis, the currently proposed mechanisms and transition states do not commonly conform to the Zimmerman-Traxler six-membered transition states discussed above.¹³⁹ A disservice would be done to the field by a truncated summary of a single organocatalytic reaction and therefore a discussion on the topic will be omitted here. Heravi *et al.* has presented a recent review¹⁴⁰ into the subject of asymmetric aldol reaction through organocatalysis and provide thorough insight into the field.

Reagent control employs a chiral reagent to induce diastereoselectivity between both achiral enolates and achiral aldehydes through increased chiral steric bulk interactions with axial side chains. Common approaches utilise chiral ligands in conjunction with Lewis acids or metal catalysts.

A classic example of ligand-induced stereoinduction comes from Patterson's use of (-)-(Ipc)₂BOTf boron Lewis acids (Figure 1.30).¹⁴¹⁻¹⁴³ The boron oxygen bond lengths are shorter compared to other Lewis acids and therefore allow for an exacerbated 1,3 diaxial interaction during the transition state **63-TS** between the chiral α -pinene ligands and the side chain of the substrates. This interaction reduces the favoured *si-re* and *re-si* transition states to only one *re-si* transition state **63-TS**, providing an enantioselective approach through reagent control.

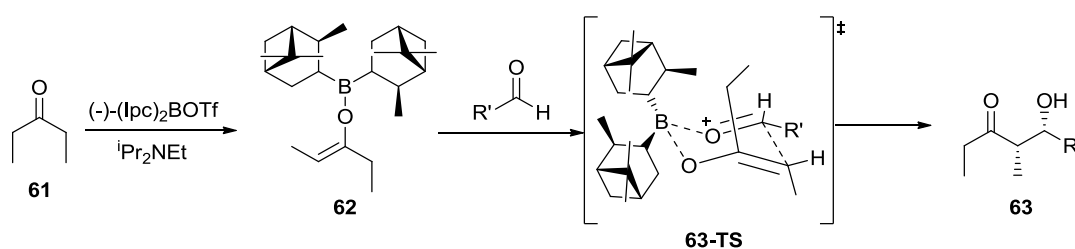


Figure 1.30 Patterson's use of (-)-(Ipc)₂BOTf boron Lewis acids in reagent controlled aldol.¹⁴¹⁻¹⁴³

Substrate-controlled diastereoface selectivity can be achieved through the use of chiral reacting species, being either a chiral aldehyde or chiral enolate. When a chiral aldehyde is used, a *syn* pentane interaction is induced in one of the otherwise favoured transition states for that given enolate which consequently renders it unfavoured leaving only one favoured transition state. In the example in Figure 1.31 it can be seen that the application of chiral aldehyde **65** with the achiral enolate **64** gives the *si-si* transition state **66-TS** which induces a *syn* pentane interaction,

reducing the favourability of this transition state. This renders only the *re-re* transition state **67-TS** favourable and therefore provides selective access to adduct **67**.

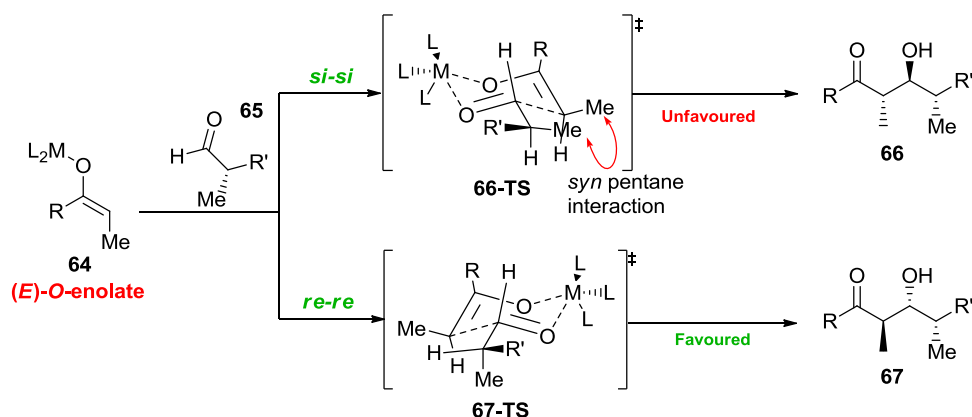


Figure 1.31 Example of chiral aldehyde induced diastereoface selectivity.

The application of chiral aldehyde induced diastereoface selectivity is seen less often, mainly because it is not as effective as chiral enolate induced diastereoface selectivity. The effect of a chiral enolate will have similar interaction with the transition state as that of the chiral aldehyde, with chiral bulk interactions into the interior of the transition state reducing the likelihood of carbon-carbon bond formation.

To utilise a chiral enolate, chirality must be imparted on an enolate through some means. Either the enolate derives from a biological source of enzymatic synthesis or from a previous synthetic stereoinduction. One highly utilised method for inducing chirality is through the use of cleavable chiral auxiliaries, which are attached to substrates before stereoselective reactions and then cleaved and recycled after the reaction. Oxazolidinones are one type of chiral auxiliary highly utilised for stereoinduction. The five-membered heterocycles were introduced by Evans¹²⁷ as chiral auxiliaries in aldol condensations and have continued to be utilised and derived. Oxazolidinone auxiliaries are generally prepared from precursory amino acids and retain the natural enantiopurity, which is important for enantioselectivity of the aldol products. A recent example by Carreira and co-workers¹⁴⁴ of chiral oxazolidinone use in asymmetric aldol during the total synthesis of Bafilomycin A₁ can be seen in Figure 1.32. The (*R*)-4-Benzyl-2-oxazolidinone **68** is originally derived from the unnatural (*R*)-phenylalanine, and the auxiliary is acylated to the propionyl imide. The boron mediated aldol proceeds with addition to acetaldehyde through Zimmerman-Traxler transition states **69-TS** where the auxiliary interacts least with the other constituents as well as minimising dipole interactions. The optimal arrangement sees the carbonyl group of the oxazolidinone auxiliary point in the opposite direction to that of the enolate oxygen. The benzylic group of the auxiliary is the directing feature, with all transition states where the group faces into the centre of the transition state are disfavoured. Due to the single stereoisomer, only one transition state exists where the benzylic group extends away from the centre of the

transition state and is therefore favoured and selective. The combination of the auxiliary directing group and dipole minimisation results in an “Evans *syn*” adduct **69**, which Carreira brings through a further 28 steps to Bafilomycin A₁.¹⁴⁴

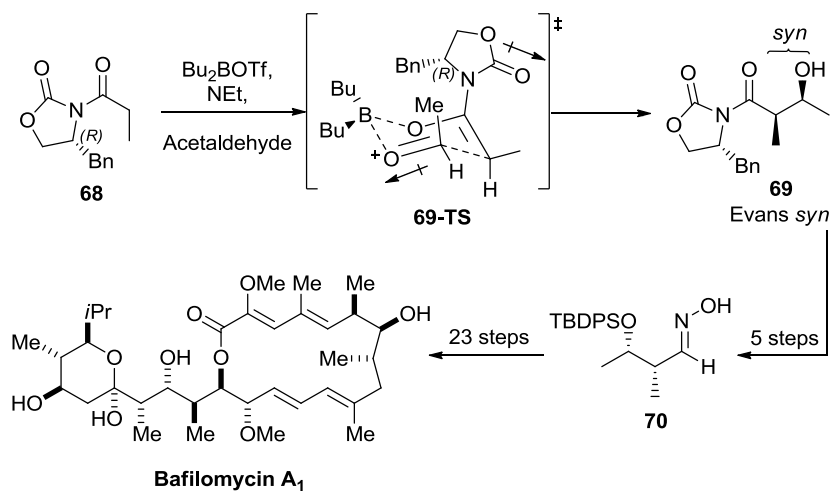


Figure 1.32 Carreira's total synthesis of Bafilomycin A₁ utilising an Evans auxiliary in boron mediated aldol.¹⁴⁴

The aldol reaction with strong diastereoselectivity and enantioselectivity can be an invaluable tool for the construction of complex asymmetric polyketide and polypropionate natural products.

1.7 Natural product targets

The literature has recently produced reports of two different families of novel polyketide pyrone-containing natural products, Nocapyrones and Violapyrones (Table 1.1). Nocapyrones A-D were first isolated from marine sponge *Halichondria panacea* from the Baltic Sea¹⁴⁵ and Violapyrones A-G were first isolated from *Streptomyces violascens*,¹⁴⁶ associated with *Hylobates hoolock* faeces. Opportunities exist for the development of shared synthetic methodologies for these structurally similar pyrone natural products which could allow for structural and stereo-elucidation and the possibility of derivatization into a suite of potentially bioactive analogues. Chapter 2 will discuss the isolation and characterisation of Nocapyrone C and D, as well as the structurally similar Violapyrone D and E natural products, and the analysis (structural potential, previous synthetic attempts, and retrosynthetic analysis) leading up to the decision to pursue them as synthetic targets.

Table 1.1 Pyrone natural products Violapyrone A-G and Nocapyrone A-D.^{145,146}

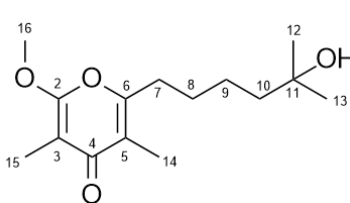
Violapyrone		Nocapyrone	
R'	R	R	
A	H	A	
B	H	B	
C	H	C	
D	H	D	
E	H		
F	H		
G	Me		

2 Nocapyrone and Violapyrone Natural Products as Potential Synthetic Target

2.1 Isolation and characterisation of Nocapyrone natural products

In 2010, a set of 4 novel γ -pyrones were isolated from the symbiotically associated *Nocardopsis* strain HB383 Actinobacteria, isolated from the marine sponge *Halichondria panicea* from the Baltic Sea.^{147,148} The pyrone natural products were allocated the names Nocapyrone (A-D) and their structures elucidated through one- and two-dimensional NMR experiments with supporting HPLC-UV/MS and HRESIMS analyses. The characterisation of Nocapyrone A (**71**) gave a high-resolution molecular ion $[M + H]^+$ at a m/z 269.1847, corresponding to a chemical formula of $C_{15}H_{24}O_4$ (calculated 269.1847), suggesting four degrees of unsaturation and/or a ring. The ^{13}C NMR presented 14 discrete signals. Evidence of a carbonyl group was seen with a chemical shift of 183.4 ppm, and four olefinic quaternary signals were observed at 164.8, 161.4, 119.3 and 100.2 ppm, with the signals from 164.8, 161.4 ppm carbons resulting from proximity to oxygens. A set of 4 NMR signals (δC 31.7, δH 2.72 (t, $J = 7.5$ Hz, 2H); δC 28.8, δH 1.71 (tt, $J = 7.5, 7.5$ Hz, 2H); δC 25.0, δH 1.46 (m); and δC 44.5, δH 1.50 (m)), indicated to a chain of four methylene groups. Three signals indicating to three individual methyl groups (δC 56.5, δH 4.03), (δC 10.3, δH 1.94) and (δC 7.2, δH 1.81), and two overlapping signals indicating to two equivalent methyl groups (δC 29.4, δH 1.17). The 2D NMR experiments were able to assist in the correlation of these conclusions as displayed in Table 2.1. The spectral results and mass measurements were in agreement to that of previously reported γ -pyrones¹⁴⁹ and the assigned structure of Nocapyrone A (**71**) was later confirmed by independent isolation and characterisation.¹⁵⁰

Table 2.1 NMR Spectroscopic Data (500 MHz, methanol- d_4) of Nocapyrone A (71**).**^{147,148}

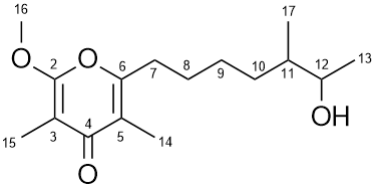
Nocapyrone A		position	δ_c	multi	δ_H (J in Hz)	HMBC
 <p style="text-align: center;">71</p>	2	164.8	C			
	3	100.2	C			
	4	183.4	C			
	5	119.3	C			
	6	161.4	C			
	7	31.7	CH ₂	2.72, t (7.5)	5, 6, 8, 9	
	8	28.8	CH ₂	1.71, tt (7.5, 7.5)	6, 7, 9, 10	
	9	25.0	CH ₂	1.46, m	7, 8, 10	
	10	44.5	CH ₂	1.50, m	9, 11, 12/13	
	11	71.4	C			
	12/13	29.4	CH ₃	1.17, s	10, 11, 12/13	
	14	10.3	CH ₃	1.94, s	4, 5, 6	
	15	7.2	CH ₃	1.81, s	2, 3, 4	
	16	56.5	CH ₃	4.03, s	2	

The Nocapyrones B to D were sequentially structurally elucidated, with strong similarity to that of Nocapyrone A. Nocapyrone B (**72**) was found to contain the same carbon structure to that of Nocapyrone A with the omission of the hydroxy functionality at the C-11 position. This was evidenced by the molecular ion $[M + H]^+$ at a m/z 253.1805 (calculated for $C_{15}H_{25}O_3$, 253.1798)

which differed by the mass of an oxygen atom and was further supported by spectral data.^{147,148} The Nocapyrone C (**73**) and D (**74**) isolates also provided strong correlations to Nocapyrone A, with the biggest structural differences found on the side chains. Evidence was found for a longer side chain containing stereochemical diversity from both the increased measured mass, C₁₆H₂₆O₄ for Nocapyrone C and C₁₆H₂₄O₄ for D, and from optical rotation measurements. Nocapyrone C provided a $[\alpha]_D^{20} +11$ (c 0.07, MeOH) rotation and Nocapyrone D a $[\alpha]_D^{20} +120$ (c 0.005, MeOH) rotation, indicating chirality in the structure, potentially from an enzymatic installed stereocentre.

Nocapyrone C (**73**) was isolated as a possible mixture of isomers due to the presence of doubled peaks in the spectral NMR data but without discrepancy in the MS or IR spectra. The molecular formula of C₁₆H₂₆O₄ was determined from a molecular ion $[M + H]^+$ at a m/z 283.1903 (calculated 283.1903), which suggested the presence of a similar pyrone ringed structure to Nocapyrone A. The ¹H and ¹³C NMR matched the assigned substructure of a γ -pyrone ring, with the methyl shifts (δ C 10.1, δ H 1.93; δ C 7.0, δ H 1.93), methoxy shifts (δ C 56.4, δ H 4.03) and sp² carbons (δ C 183.2, 164.6, 161.3, 119.2, 100.1) analogous to those of Nocapyrone A. The sidechain also saw similarities through the 4 carbon methylene chain (δ C 31.5, δ H 2.72 (t, $J = 7.5$ Hz, 2H); δ C 27.7, δ H 1.71 (m, $J = 7.5$ Hz, 2H; δ C 33.5, δ H 1.3-1.5 (m, 2H); δ C 33.3, δ H 1.3-1.5 (m, 2H)) correlating to the side chain seen with Nocapyrone A albeit differing at the terminating end. The terminating end of the sidechain displayed a pronounced functional group divergence, including the presence of two methyl groups (δ C 20.0, δ H 1.11 (d, $J = 6.2$ Hz, 3H); δ C 14.9, δ H 0.88 (d, $J = 6.9$ Hz, 3H)) and two tertiary stereocentres (δ C 40.8, δ H 1.45 (m, 1H); δ C 71.8, δ H 3.62 (dq, $J = 6.2, 4.6$ Hz, 1H)) with the latter geminal to a free hydroxy group. The full spectroscopic data and assigned structure can be examined in Table 2.2.

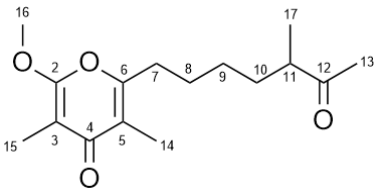
Table 2.2 NMR Spectroscopic Data (500 MHz, methanol-d₄) of Nocapyrone C (73**).**^{147,148}

Nocapyrone C		position	δ_c	multi	δ_H (J in Hz)	HMBC	COSY
 <p style="text-align: center;">73</p>	2	164.6	C				
	3	100.1	C				
	4	183.2	C				
	5	119.2	C				
	6	161.3	C				
	7	31.5	CH ₂	2.72, t (7.5)	5, 6,	8	
	8	27.7	CH ₂	1.71, m (7.5)	7	7, 9	
	9	33.5	CH ₂	1.3-1.5, m			
	10	33.3	CH ₂	1.3-1.5, m			
	11	40.8	CH	1.45, m		12, 17	
	12	71.8	CH	3.62, dq (6.2)		11, 12	
	13	20.0	CH ₃	1.11, d (6.2)	11, 12	12	
	14	10.1	CH ₃	1.93, s	4, 5, 6		
	15	7.0	CH ₃	1.81, s	2, 3, 4		
	16	65.4	CH ₃	4.03, s	2		
	17	14.9	CH ₃	0.88, d (6.9)	10, 11, 12	11	

Nocapyrone D (**74**) provided an almost identical spectral analysis (Table 2.3) to that of Nocapyrone C albeit omitting the lone hydroxyl signal which has been replaced with a carbonyl group signal (δ C 215.3) and a migration of the tertiary proton (δ C 47.4, δ H 2.59 (sextet, $J = 6.8$

Hz, 1H) and the terminal methyl group (δC 28.3, δH 2.14 (s, 3H) which are under more severe electronic influence of the adjacent (vicinal) carbonyl group. The correlation to the Nocapyrone C isolate began with the γ -pyrone ring, with the methyl shifts (δC 10.1, δH 1.93 (s, 3H); δC 7.0, δH 1.93 (s, 3H)), methoxy shifts (δC 56.3, δH 4.03 (s, 3H)) and sp^2 carbons (δC 183.2, 164.6, 161.3, 119.2, 100.1). The correlation continued with the 4 carbon methylene chain (δC 31.4, δH 2.70 (t, $J = 7.5$ Hz, 2H); δC 27.7, δH 1.71 (quint, $J = 7.5$ Hz, 2H); δC 31.2, δH 1.28-1.45 (m, 2H); δC 33.3, δH 1.7, 1.4 (m, 2H)) which is directly connected to the pyrone ring. The other terminating methyl group (δC 16.5, δH 1.08 (d, $J = 7.0$ Hz, 3H) completes the structural similarity and it was determined that the Nocapyrone D was a structural analogue to that of Nocapyrone C but with the replacement of the C-12 hydroxy with a carbonyl functionality.

Table 2.3 NMR Spectroscopic Data (500 MHz, methanol- d_4) of Nocapyrone D (74).^{147,148}

Nocapyrone D		position	δc	multi	δH (J in Hz)	HMBC	COSY
 <p style="text-align: center;">74</p>	2	164.8	C				
	3	99.8	C				
	4	182.7	C				
	5	119.0	C				
	6	161.0	C				
	7	31.4	CH ₂	2.70, t (7.5)	5, 6, 8	8	
	8	27.7	CH ₂	1.71, quint (7.5)	6, 9, 10	7, 9	
	9	31.2	CH ₂	1.28-1.45, m			
	10	33.4	CH ₂	1.70, 1.40, m	8		
	11	47.4	CH	2.59, sext (6.8)		10, 17	
	12	215.3	C				
	13	28.3	CH ₃	2.14, s	11, 12		
	14	10.1	CH ₃	1.93, s	4, 5, 6		
	15	7.0	CH ₃	1.81, s	2, 3, 4		
	16	56.3	CH ₃	4.03, s	2		
	17	16.5	CH ₃	1.08, d (7.0)	10, 11, 12	11	

Studies by Lin *et al.* of *Nocardiopsis alba* CR167 isolated from the venom duct of *Conus rolani* shelled mollusc also isolated the natural product Nocapyrone C, along with novel Nocapyrones H-Q.¹⁵⁰ These studies investigated the genome of *N. alba* CR167 and compared it to the previously sequenced genome of *Nocardiopsis alba* ATCC BAA-2165, identifying the ncp gene cluster as a possible candidate for the possible biosynthetic pathway (Figure 2.1) of Nocapyrone natural products within *Nocardiopsis sp* bacteria.

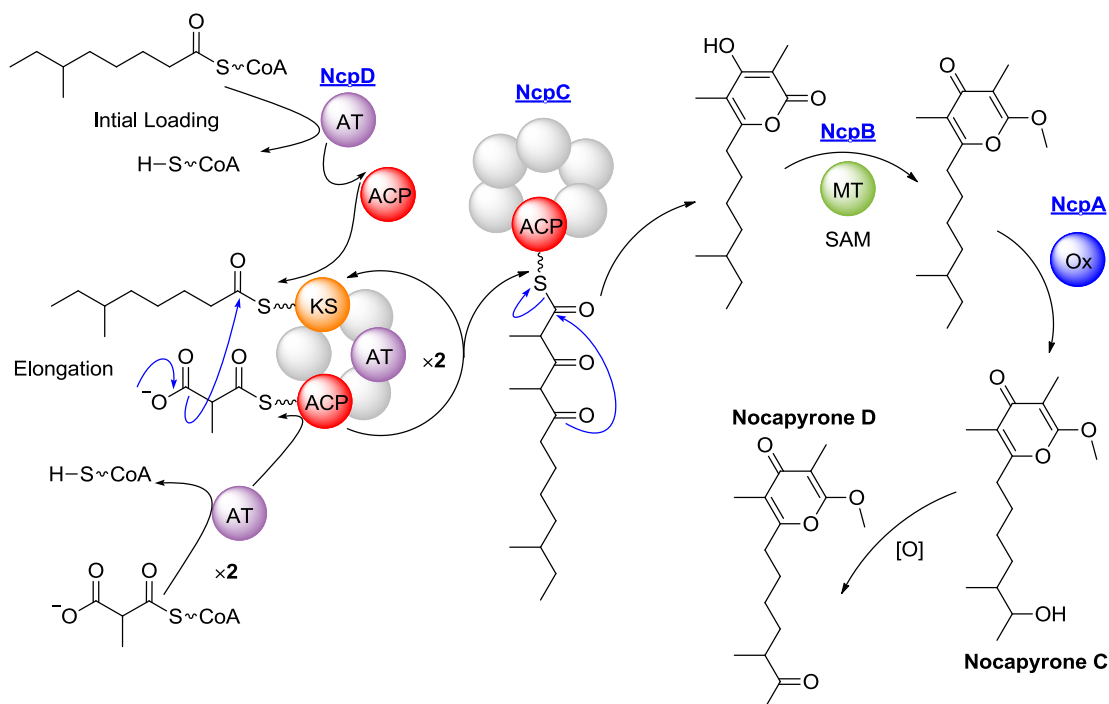


Figure 2.1 Proposed biosynthetic pathway for Nocapyrone natural products in *Nocardiopsis* sp.¹⁵⁰

From three possible PKS gene clusters, the *npc* cluster was identified from the sequenced genomic data as being most likely responsible for the biosynthesis of the various Nocapyrones due to possessing the correct domains for pyrone construction and the crucial methyltransferase required for post-linear *O*-methylation. The *npc* comprises a cluster of four genes, *NcpA* the oxidoreductase, *NcpB* the methyltransferase, *NcpC* the PSK, and *NcpD*, the putative free-standing acyltransferase. The proposed biosynthetic pathway as seen in Figure 2.1 begins with a fatty acid CoA thioester, expected to be extracted from a primary metabolic pathway, being loaded onto the *NcpC*. The *NcpC* PKS elongates the chain through two additions of methylmalonyl CoA. Pyrone cyclisation releases the chain from the *NcpC* PKS and the substrate undergoes *O*-methylation by *NcpB* forming the γ -pyrone motif. It is not clear from current data but speculation points to the *NcpA* being responsible for *C*-oxidation and providing the functionality to the linear fatty acid chain.¹⁵⁰

If the *NcpA* module was responsible for the *C*-oxidation, the co-isolated Nocapyrone L (**75**) (Figure 2.2)¹⁵⁰ could be suggested as a potential biosynthetic precursor to Nocapyrone C (**73**) through *C*-oxidation at the C-12 carbon, and itself could also be a possible precursor to Nocapyrone D (**74**) through the sequential oxidation of the hydroxyl functionality. As of yet no such evidence has been obtained to confirm these suggestions but could serve in future studies.

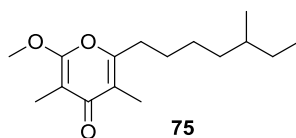


Figure 2.2 Nocapyrone L (75) co-isolated with Nocapyrone A-C from *Nocardiosis alba* CR167 isolated from the venom duct of *Conus rolani* shelled mollusc.¹⁵⁰

Nocapyrones C and D were originally reported by Imhoff¹⁴⁷ without assigned stereochemistries, but following independent isolation of Nocapyrone C by Schmidt,¹⁵⁰ Mosher's ester derivatisation analysis was performed to determine the stereocenters at C-12 OH, and C-11. The C-12 OH was able to be directly assigned as *S* but literature comparison of *O*-methine chemical shifts and coupling constants were used for C-11 with the assignment of *R* for the major isomer. In both isolation studies, Nocapyrone C was isolated as a mixture of diastereomers but with only two enantiomers present. Schmidt¹⁵⁰ reported the isolation of 11*S*,12*S* configuration along with 11*R*,12*S* at a 1.3:1 ratio while Imhoff¹⁴⁷ reported an optically active mixture at a higher ratio of major diastereomer. Racemisation upon isolation was deemed inconsistent with these results and was expected to be intentionally biosynthesised as a diastereomeric mixture.

2.2 Biological studies on Nocapyrones

As with many natural product isolation studies, only Nocapyrones isolated in sufficient quantity were subjected to biological assays. From the current reports of γ-pyrone Nocapyrone natural products, Nocapyrones B (72), H (76), and L (77) (Figure 2.3) have shown modulation of calcium channels, with B and H being moderately cytotoxic to cancer cell lines as well.¹⁵⁰

Imhoff's¹⁴⁷ original product extract exhibited activity against Gram-positive bacteria *Staphylococcus lentus* and *Bacillus subtilis* but analysis of isolated Nocapyrone A and B were unable to show any meaningful biological activity in either bacteriostatic or bactericidal assays.¹⁴⁷ These studies did not, however, report any antimicrobial assays of Nocapyrone C or D, which were also present in the original extract.

Despite the structural diversity of isolated and characterised Nocapyrone natural products, only a select few were actually subjected to thorough biological testing. There is potential that with a larger quantity of product, more meaningful analyses could be conducted.

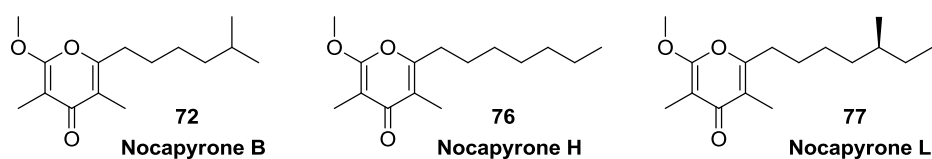


Figure 2.3 Nocapyrone B, H, and L reported calcium channel modulation.¹⁵⁰

2.3 Nocapyrone as targets for synthesis

The two studies showed that the isolation and characterisation of Nocapyrone natural products provide a valuable and interesting insight into the diverse variety of structures possible with pyrone secondary metabolites. From these two studies, Nocapyrones C and D stood out as potential targets for synthetic studies towards total synthesis. These natural products share a γ -pyrone motif, a structure which appears with many biologically active natural products; a fatty acid side chain, which shows functionality in many positions; and displays controlled stereochemistries. A rigorous exploration of possible methodologies for the simple and reliable synthesis of pyrone structures with easy and stereoselective differentiation could allow for the construction of a potential library of novel compounds. These analogues would be ready for extensive biological testing and allow for structural and stereo elucidation and verification of recently isolated natural products.

2.4 Previous work towards Nocapyrone C

Previous work towards the synthesis and stereochemical elucidation of Nocapyrone natural products was done by myself within the Perkins group in 2013. The Honours thesis¹⁵¹ culminated in the preparation of the desired target Nocapyrone C (**73**). The synthesis utilised a convergent strategy which saw the pyrone motif and stereocontrolled side-chain prepared separately and combined towards the final steps to form the final structure. The total synthesis spanned 11 steps from thiazolidinethione and resulted in an overall yield of 2.9% (Figure 2.4).

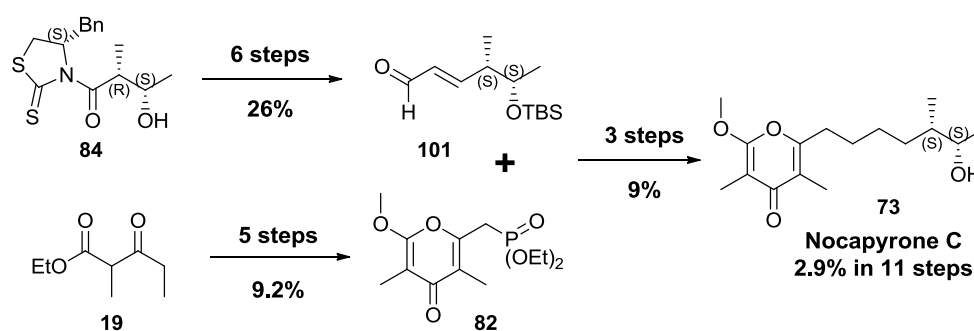


Figure 2.4 Summary of Nocapyrone C synthesis as reported in 2013.¹⁵¹

The synthetic strategy centred on minimising the influence of undesired methylation during the regioselective methylation of hydroxy- α -pyrone. The most prominent reagent for regio-selective methylation in pyrone literature has been *methyl fluorosulfonate*,^{67,73,75,117,152} but due to its high acute toxicity,¹⁵³ commercial availability is increasingly being phased out so its use in late-stage methylation was practically unattainable. Therefore a less selective method of *O*-methylation was implemented and required methylation to occur at an early stage of synthesis. This approach allowed for undesired γ -methylation to have a marginal effect on the overall synthesis. The

synthetic strategy incorporated the example demonstrated by Hecht *et al.*⁷⁶ for the construction of 2-Methoxy-3,5,6-trimethyl-4-pyrone, which was compatible for use in a convergent approach and cumulated from the choice methods of the wider literature.

The forward synthesis (Figure 2.5) started with the pyrone preparation and the notoriously unreliable step of tricarbonyl formation. Many different conditions for diketo ester formation were screened, including variations of Huckin-Weiler dianion acylation conditions as well as Solladié⁶⁶ protocol for dianion regeneration, using both ester and imidazole acetylating agents. These screenings found only minimal production of hydroxy α -pyrone **79**, with the reliable method seeing β -keto ester **19** subject to dianion conditions with LDA and condensation via N-acetylimidazole to give the tricarbonyl intermediate **78**, which was directly cyclised with DBU to garner hydroxy α -pyrone **79** as per Hecht *et al.*⁷⁶ but with only 20% from the β -keto ester **19**. The unreliability of tricarbonyl formation was attributed to the documented instability⁷⁶ of the diketo ester intermediate **78**.

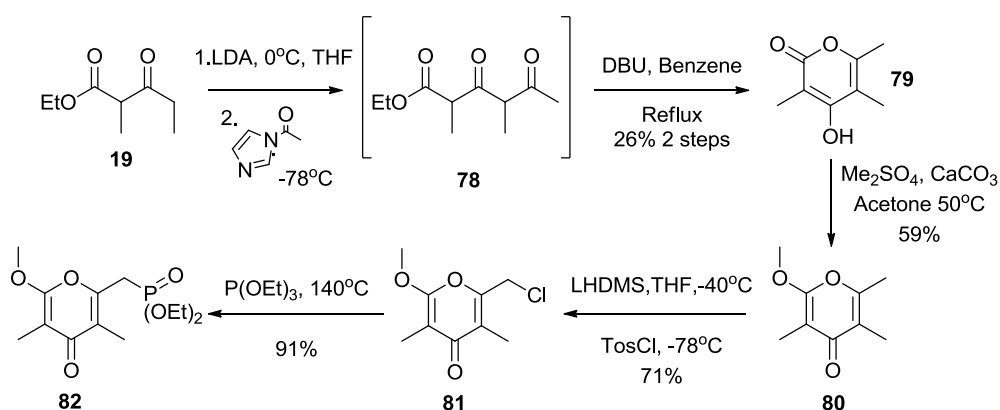


Figure 2.5 α -methoxy- γ -pyrone (82**) intermediate preparation.**

The hydroxy α -pyrone **79** was then subjected to methylation conditions demonstrated by Hosokawa^{112,113} for regioselective pyrone methylation through the use of CaCO₃/ Me₂SO₄. The α -methoxy pyrone **80** was produced in 59% yield after cycling unreacted starting material two times. This protocol allowed for this transformation without the use of methyl fluorosulfonate. The methylating conditions were successful at giving good selectivity but were unable to provide good conversion; with 3-4 day reaction time gave a maximum of 70% conversion with only 59% yield of the desired product. The pyrone was transformed further to the pyrone phosphite **82** required for a Horner–Wadsworth–Emmons coupling to the side chain fragment. This preparation was done through the intermediate chloride **81** which was accessed with the use of tosyl chloride as demonstrated by Lipshutz in 71 % yield.⁶⁷ The phosphite functionality was installed through heating the pyrone chloride **81** in neat triethyl phosphite and providing the pyrone phosphite **82** in 91 % yield.

The side chain preparation (Figure 2.6) was initiated with the controlled installation of *syn* stereochemistry through aldol reaction and at that time was reported as the non-Evans adduct **84** in 94% yield and >90% diastereoselectivity, following the Crimmins protocol.^{154,155} The aldehyde **88** was prepared through three steps in 81% from **84** then taken through two-carbon chain extension via Wittig olefination with (Carbethoxymethylene)triphenylphosphorane giving the ethyl ester **100** in 66%. The allyl ester **100** was then transformed to the aldehyde **101** in two steps and 65% yield ready for olefination with the pyrone fragment.

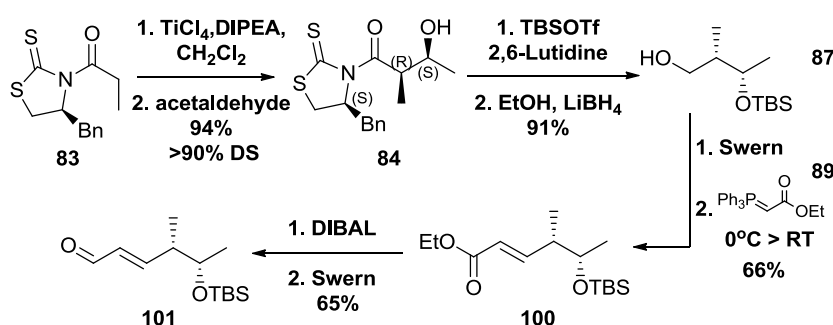


Figure 2.6 Installation of *syn* stereochemistry with thiazolidinethione chiral auxiliary, followed by chain extension through olefination and functional group manipulation to form the allyl aldehyde **101**.

The aldehyde **101** and phosphite pyrone **82** fragments were brought together (Figure 2.7) through a Horner–Wadsworth–Emmons coupling reaction providing **102** in reasonable *Z* selectivity, but this was of no consequence as the following step saw hydrogenation to give a saturated **103**. Deprotection of the silyl ether **103** provided the free hydroxyl **73** which matched the spectroscopic data^{147,148} and was reported as the natural product Nocapyrone C.

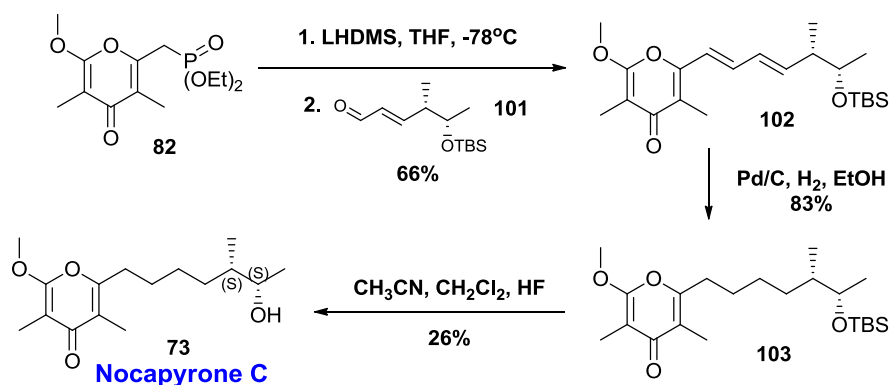


Figure 2.7 Olefination, reduction and deprotection final steps of Nocapyrone C total synthesis.

The reported total synthesis of Nocapyrone C demonstrated a possible route to Nocapyrone natural products through methods derived considerably from recent literature.⁷⁶ The comparison of spectroscopic data of the synthetic **73** to that of the natural product Nocapyrone C indicated a match with both ^1H and ^{13}C NMR. Comparison of the optical rotations found correlation in the

sign and intensity of the measurements ($[\alpha]_{\text{D}}^{20} +16.8$ (c 0.375, MeOH) against lit. $[\alpha]_{\text{D}}^{20} +11$ (c 0.07, MeOH)^{147,148}). The NMR spectral data indicated to the structure and relative stereochemistry matching that of the natural product and optical rotation provided enough evidence to suggest a match in the absolute stereochemistry. With these results, it was with some confidence that **73** was reported as Nocapyrone C and at that time, stereoelucidation assigned 11*S* and 12*S* stereochemical configuration. Although, in the subsequent chapters of this work an investigation and discussion will provide evidence of the erroneous stereochemical assignment of the aldol adduct **84** and therefore the propagation into erroneous assignment of C11 and C12 of the final synthetic in this 2013 Honours work.

An interesting detail was also encountered during ^1H NMR comparison of the synthetic compound against that of the isolated natural product (Figure 2.8). It was found that the isolated natural product contained peaks which did not correspond with that of Nocapyrone C and it was suggested that it could have been caused by a co-isolated isomer.¹⁴⁷

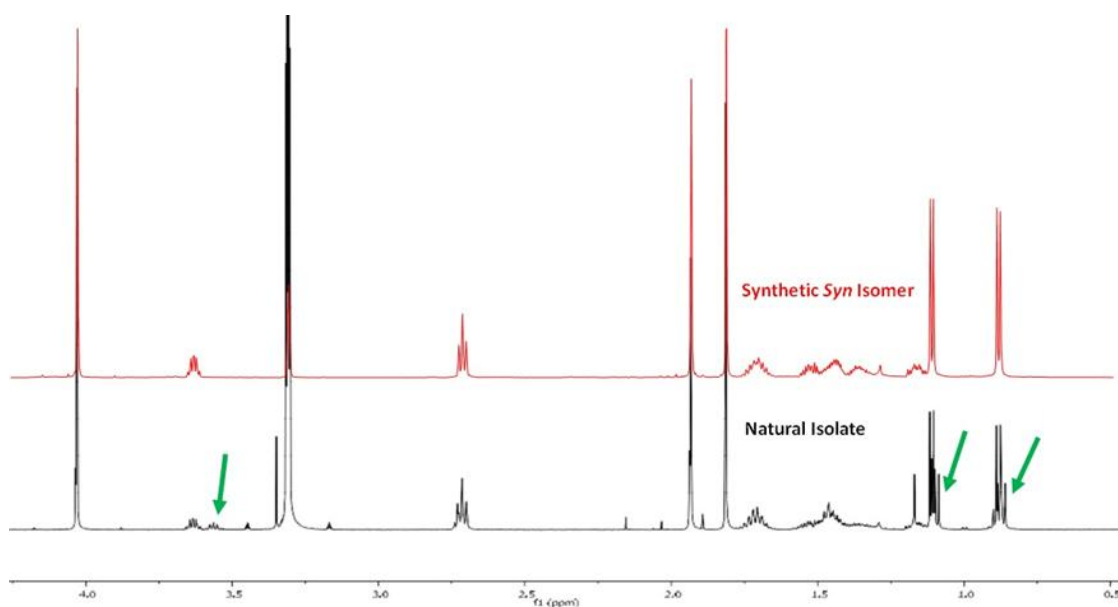


Figure 2.8 Comparison between the synthetic product **73 and the isolated Nocapyrone C natural product, with green arrows indicating to the possibility of a relative isomer in the original isolate.**^{147,148}

A critical review of the previous attempt at Nocapyrone C highlights that challenges still exist in the synthesis and mainly revolve around the γ -pyrone substructure preparation. The poor yield and poor reproduction of the initial tricarbonyl formation and subsequent cyclisation to the α -pyrone **79** is not optimal in an ideal or efficient synthesis sense and may require tactical revision or strategic replacement. The short tricarbonyl intermediate was reported⁷⁶ as being unstable and the extension of the acylated chain could see an increase in stability and yield.

The presence of a possible diastereomer in the isolated natural product sample warrants further investigation and the synthesis of a relative isomer to that of the reported 11*S* and 12*S*

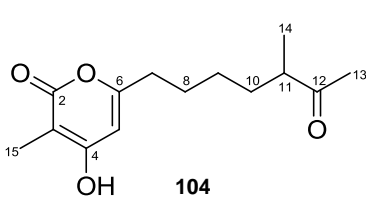
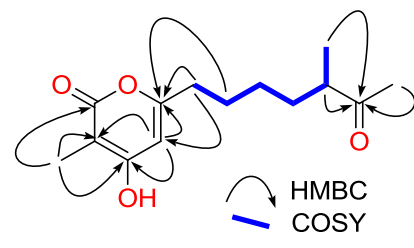
stereochemical configuration of **73** would allow for further stereo-elucidation of the natural products. Significant production of isomers, both natural and novel, could allow for derivation to the oxidised Nocapyrone D and allow for biological testing beyond that reached by the isolation team.

2.5 Isolation and characterisation of Violapyrone natural products

Violapyrones were first isolated from *Streptomyces violascens* associated with *Hylobates hoolock* faeces.¹⁴⁶ The fermentation broth of *Streptomyces violascens* YIM 100525 exhibited antimicrobial activity and 7 novel α -pyrone natural products were isolated with the designated names of Violapyrone A-G. These pyrones were characterised through the use of HRESIMS, 1D and 2D NMR, IR, UV vis, and optical rotation.¹⁴⁶

Violapyrone D (**104**) was determined to have a molecular formula of $C_{14}H_{22}O_4$ from the HRESIMS molecular ion $[M + H]^+$ at a m/z 254.1517 (calculated at 253.1440), indicating to 5 degrees of unsaturation. The IR signals 3423, 1631, and 1584 cm^{-1} and UV max of 290.3 nm along with NMR spectra closely correlated to that of the co-isolated Violapyrone A¹⁴⁶ and other previously reported 3,4,6-trisubstituted α -pyrone natural products.¹⁵⁶ This indicated strongly to the presence of an α -pyrone motif within the structure. The pyrone ring was determined to contain trisubstitution with the C-3 (δ_C 98.8) bonded to methyl group C3-Me (δ_C 8.4, δ_H 1.96 (*s*, 3H)); the C-4 (δ_C 166.4) bonded to hydroxyl; and C-6 (δ_C 162.9) the oxygen heteroatom of the ring. The ring was completed with the lactone carbonyl C-2 (δ_C 168.0) and with the unsaturated and unsubstituted C-5 (δ_C 100.8, δ_H 6.13 (*s*, 1H)). This provided the elucidated structure of 3-methyl-4-hydroxypyran-2-one with a side chain extending from the C-6 position. The side chain was determined to extend by four methylene groups C-7 to C-10 (δ_C 33.4, δ_H 2.45 (*t*, $J = 7.5$ Hz, 2H); δ_C 26.9, δ_H 1.64 (*m*, 2H); δ_C 26.6, δ_H 1.30 (*m*, 2H); and δ_C 32.5, δ_H 1.36, 1.69 (*m*, 2H)), followed by one tertiary carbon stereocentre; C-11 (δ_C 47.2, δ_H 2.52 (*m*, 1H)) bonded to C11-Me (δ_C 16.7, δ_H 1.09 (*d*, $J = 7.0$ Hz, 3H)); and ketone carbonyl C-12 (δ_C 214.1) bonded to C12-Me (δ_C 28.4, δ_H 2.17 (*s*, 3H)). The full structure of Violapyrone D (**104**) was assigned as 4-hydroxy-3-methyl-6-(5-methyl-6-oxoheptyl)-2H-pyran-2-one, and supported by all spectroscopic data (Table 2.4).

Table 2.4 NMR Spectroscopic Data (600 MHz, $CDCl_3$) of Violapyrone D (**104**).¹⁴⁶

Violapyrone D	position	δ_C	multi	δ_H (J in Hz)	COSY & HMBC
	2	168.0	C		
	3	98.8	C		
	4	166.4	C		
	5	100.8	CH	6.13, <i>s</i>	
	6	162.9	C		
	7	33.4	CH ₂	2.45, <i>t</i> (7.5)	
	8	26.9	CH ₂	1.64, <i>m</i>	
	9	26.6	CH ₂	1.30, <i>m</i>	
	10	32.5	CH ₂	1.69, 1.36, <i>m</i>	
	11	47.2	CH	2.52, <i>m</i>	
	12	214.1	C		
	13	28.4	CH ₃	2.14, <i>s</i>	
	14	16.7	CH ₃	1.93, <i>d</i> (7.0)	
	15	8.4	CH ₃	1.81, <i>s</i>	

Violapyrone E (**105**) produced an HRESIMS molecular ion $[M]^+$ at m/z 254.1517 and a molecular formula of $C_{14}H_{22}O_4$ (calculated for $C_{14}H_{22}O_4$, 254.1518) was determined, indicating 4 degrees of unsaturation. The structure was determined to be analogous to that of Violapyrone D, with the dialkyl substituted pyrone ring assigned with C-3 (δ_C 96.3) bonded to methyl group C3-Me (δ_C 8.5, δ_H 1.74 (*s*, 3H)); the C-4 (δ_C 162.6) bonded to hydroxyl; and C-6 (δ_C 165.3) the oxygen heteroatom of the ring. The ring was completed with the lactone carbonyl C-2 (δ_C 165.3) and with the unsaturated and unsubstituted C-5 (δ_C 99.4, δ_H 5.96 (*s*, 1H)). The C-6 side chain was determined to extend by four methylene groups (δ_C 32.6, δ_H 2.41 (*t*, $J = 7.0$ Hz, 2H); δ_C 26.8, δ_H 1.50 (*m*, 2H); δ_C 26.1, δ_H 1.19, 1.33 (*m*, 2H); and δ_C 32.0, δ_H 1.00, 1.41 (*m*, 2H)), followed by two tertiary carbon stereocentres; C-11 (δ_C 39.5, δ_H 1.34 (*m*, 1H)) bonded to C11-Me (δ_C 14.6, δ_H 0.76 (*d*, $J = 6.7$ Hz, 3H)); and C-12 (δ_C 69.4, δ_H 3.42 (*m*, 1H)) bonded to C12-Me (δ_C 19.4, δ_H 0.97 (*d*, $J = 6.4$ Hz, 3H)). The full structure of Violapyrone E was assigned as 4-hydroxy-3-methyl-6-(5-methyl-6-hydroxyheptyl)-2*H*-pyran-2-one, and details can be seen in Table 2.5.¹⁴⁶

Table 2.5 NMR Spectroscopic Data (600 MHz, DMSO- d_6) of Violapyrone E (**105**)¹⁴⁶

Violapyrone E		position	δ_C	multi	δ_H (J in Hz)
	2	165.3	C		
	3	96.5	C		
	4	165.3	C		
	5	99.4	CH		5.96, <i>s</i>
	6	162.6	C		
	7	32.6	CH ₂		2.41, <i>t</i> (7.0)
	8	26.8	CH ₂		1.50, <i>m</i>
	9	26.1	CH ₂		1.19, 1.33, <i>m</i>
	10	32.0	CH ₂		1.00, 1.41, <i>m</i>
	11	39.5	CH		1.34, <i>m</i>
	12	69.4	CH		3.42, <i>m</i>
	3-Me	8.5	CH ₃		1.74, <i>s</i>
	11-Me	14.6	CH ₃		0.76, <i>d</i> (6.7)
	12-Me	19.4	CH ₃		0.97, <i>d</i> (6.4)

The absolute stereochemistry of C-12 was determined to be *S* through Mosher's ester analysis but C-11 was left undetermined.¹⁴⁶ An optical rotation of $[\alpha]_D^{20} +17.2$ (c 0.65, MeOH) suggests a degree of enantiomeric excess but it is not certain if the natural product is enantiopure or if the peak at δ_H 3.47(*m*) (Figure 2.9) is an indication of co-isolated diastereomer.¹⁴⁶

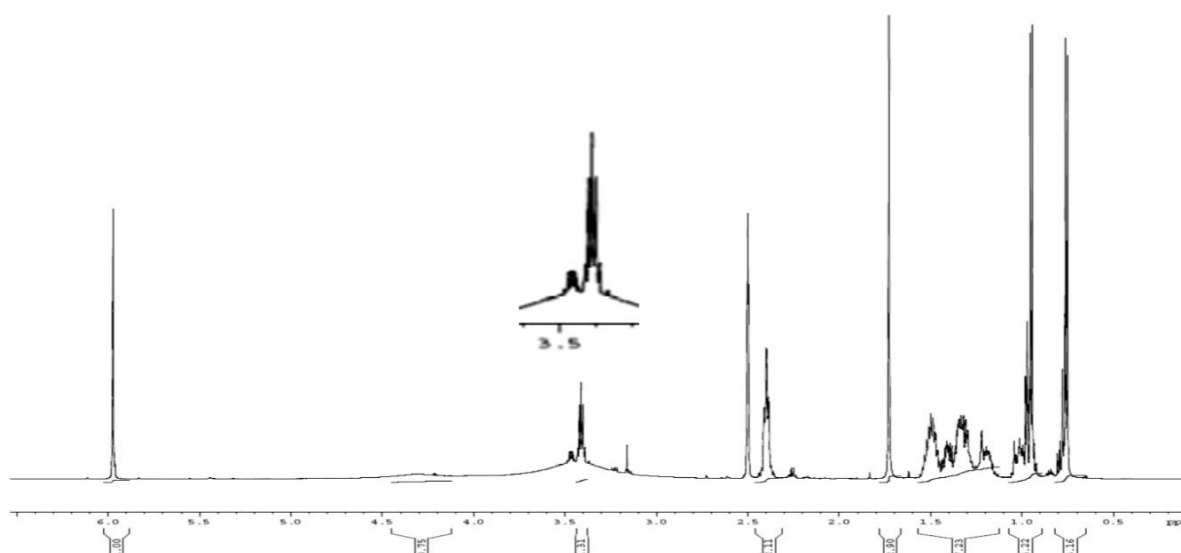


Figure 2.9 ^1H NMR spectrum of isolated natural product Violapyrone E with focus on the C-12 stereocentre.¹⁴⁶

The Violapyrone family (Table 2.6) has been expanded further with isolations of Violapyrone H-I¹⁵⁷ and J¹⁵⁸, all sharing the underlying 3,4,6-trisubstituted α -pyrone substructure with an aliphatic side chain extending from the C-6 position. The side chain continued over at least four contiguous methylene units directly after the pyrone ring and extended by five to seven carbons, with functionalization at the terminating end.

Table 2.6 Reported Violapyrones A-J natural products.^{146,157,158}

	R'	R	R'	R		
	A	H		F	H	
	B	H		G	Me	
	C	H		H	H	
	D	H		I	H	
	E	H		J	H	

2.6 Biological activity studies on Violapyrones

Many different biological activities have been attributed to previously isolated α -pyrones including antimicrobial,^{159,160} antifungal,^{161,162} anti HIV,¹⁶³ anticancer,¹⁶⁴ and antioxidant^{165–167} activities. The novel Violapyrones were all tested for biological activities, where moderate antibacterial activities were shown by Violapyrone A-C against *Bacillus subtilis* and *Staphylococcus aureus*, with MIC values of 4–32 $\mu\text{g/mL}$.¹⁴⁶ Cytotoxicity was reported against

human cancer cell lines in concentrations below 26.12 $\mu\text{g/mL}$ in assays of Violapyrone H, I, B, and C.¹⁵⁷ It is suggested that the length of the side chain and the position and makeup of constituent groups can greatly affect the activity.^{146,157} Unsaturation of the side chain was suggested to increase the cytotoxicity and antibacterial activities¹⁴⁶ but this raised the question about the role of these pyrone natural products and if assays for other biological activities would show different results.

2.7 Violapyrones as targets for synthesis

Violapyrones exhibit the same characteristics to Nocapyrones which make them both interesting and valuable targets for synthesis (Figure 2.10), as both include a substituted pyrone substructure (methyl substitution at both the C-3 and C-5, or just the C-3 position) with extended aliphatic side chain from the C-6 position, terminating with methyl and oxygen functionality (C-11 and C-12). Both families of pyrones have shown some biological activity and could still uncover other untested activities.

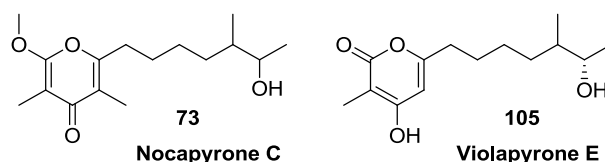


Figure 2.10 Nocapyrone C (73)^{147,148} and Violapyrone E (105)¹⁴⁶ as examples of potential synthetic targets.

From the Violapyrone family of natural products, Violapyrone D (**104**) and E (**105**) stand out as valuable synthetic targets mainly due to their similarities in structure, especially in the 7 membered aliphatic side chain which exhibits identical functionality (11-Me and 12-OH) at the same C-11 and C-12 positions. Violapyrone I (**106**)¹⁵⁷ and Nocapyrone H (**76**)^{150,168} exhibit fully saturated 7-carbon side chains which could allow for model studies into pyrone preparation protocols.

2.8 Previous synthetic directions for Violapyrones

Violapyrone C (**73**) was synthesised and absolute stereochemistry determined to be *S* at C-12 position by comparison of optical rotation,¹⁶⁹ with a rotation of $[\alpha]_D^{20} +49.0$ (c 0.1, MeOH) in agreement with that of the isolated natural product, $[\alpha]_D^{20} +50.0$ (c 0.1, MeOH).¹⁴⁶ The synthesis utilised gold(I)-catalyzed intramolecular 6-endo-dig cyclizations in the formation of α -pyrone motifs from tert-butyl alkynyl ester precursors. As displayed in Figure 2.11, commercially available (*S*)-(-)-2-methyl-1-butanol was used as the chiral feedstock, beginning the synthesis with conversion to the corresponding Wittig salt **108** through Mitsunobu reaction to iodide and reaction with triphenylphosphine. Wittig reaction was conducted with aldehyde **107** derived from

1,4-butanediol, to form the extended unsaturated chain which was promptly hydrogenated to provide the deprotected 8 carbon saturated alcohol **109**. Long-chain alcohol **109** was then transformed to the alkyne **110** through Swern oxidation and Corey-Fuchs single-carbon homologation. A lithium acetylide was generated from alkyne **110** for nucleophilic addition over methyl chloroformate, and Claisen condensation with LDA and tert-butyl propionate concluded with the installation of desired β -keto ester **111**.

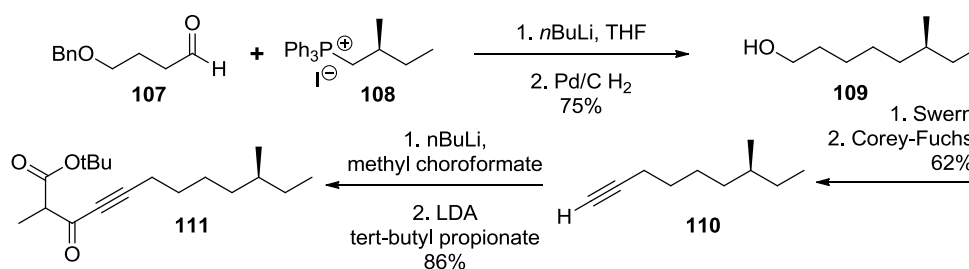


Figure 2.11 Lee *et al.* synthesis of Violapyrone C.¹⁶⁹

The β -keto ester **111** was subjected to gold(I) catalysed 6-endo-dig intramolecular cyclisation forming the installation of the α -pyrone ring and completing the synthesis of (+)-Violapyrone C (Figure 2.12). This cyclisation procedure was building on previous work done by Fürstner *et al.* which used similar gold(I) catalysis in the formation of 4-hydroxy-2-pyrones and subsequent use in the synthesis of Neurymenolide A.¹⁷⁰

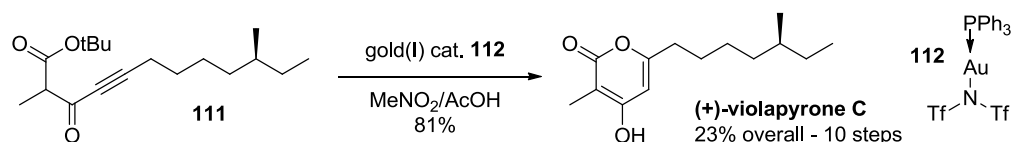


Figure 2.12 Gold(I) catalysed 6-endo-dig intramolecular cyclisation forming an α -pyrone ring and completing the synthesis of (+)-Violapyrone C.¹⁶⁹

Of the currently identified members of the Nocapyrone and Violapyrone natural product families, Nocapyrone C and Violapyrone E would make for interesting combined initial synthetic targets taking advantage of their structural similarities. Both natural products contain a terminating pyrone motif, and a 12-carbon linear backbone with stereocontrolled branching functionalisation at the C-11 (methyl) and C-12 (hydroxyl) positions. A combined general synthetic approach to both natural products could allow for the synthesis of reported natural products and their stereoelucidation, as well as the ability for structural derivation providing novel analogues in quantities sufficient enough for thorough biological testing.

2.9 General synthetic strategy

In the pursuit of synthesising Nocapyrone and Violapyrone natural products, a general synthetic strategy should be developed which allows for the easy and efficient interception of numerous natural products, isomers, and derivatives.

A general synthetic strategy would initially focus on Nocapyrone C and Violapyrone E, with future opportunities for derivation. The retrosynthetic analysis (Figure 2.13) of both Nocapyrone C (**73**) and Violapyrone E (**105**) revealed that a shared structure existed in the form of an α -pyrone (**117**). The precursory linear 12-carbon skeletal substructure (**116**) would consist of a β,γ -diketo ester extended through a 7-carbon aliphatic side chain terminating with branched methyl and hydroxyl functionality. The acquisition of the linear skeletal substructure could be envisioned to constitute three components with two critical disconnections; a β,γ -diketo ester from a precursory β -keto ester (**113**), a 4-carbon saturated linker chain (**114**), and a stereocontrolled branched hydroxy functionalised tail (**115**). A convergent strategy utilising common intermediates could be implemented where each fragment is prepared separately and combined appropriately to give many natural products, isomers, and derivatives. The order of combination would be the more important question, as there are advantages and disadvantages to each.

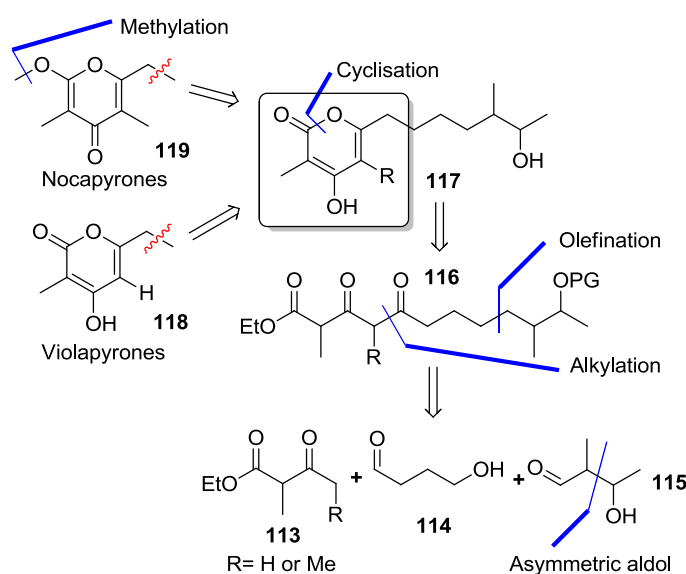


Figure 2.13 Shared retrosynthesis of Nocapyrone C and Violapyrone E natural products.

The order of crucial carbon-carbon bond forming reactions has advantages and disadvantages in the larger scope of the synthetic route and must be taken into account accordingly.

2.10 Strategy and Tactics

In the following chapters, the discussion will delve into the synthetic pursuit of the target Nocapyrone and Violapyrone natural products and their derivatives through the development and review of synthetic routes. It is important to define two terms, Strategies and Tactics, which will feature heavily in the following chapters. These two terms are sometimes used interchangeably as plans, but this is not strictly correct. In the context of total synthesis, Strategy can be defined as the macroscopic plan to achieve a goal, for example, a convergent strategy to Nocapyrone C. A strategic feature can refer to specific disconnections, the order of coupling, interception of key

Chapter 2

intermediates, or key reactions (eg. cyclisations or rearrangements). In contrast, Tactics refer to the specific approach utilised in fulfilling strategic objectives. An example could be the protective groups used during the synthesis route, the oxidation state of functional groups at particular stages, or the specific reactions used (eg. Wittig vs Julia). This thesis will continue to refer to macroscopic decisions as strategic, and discreet or microscopic decisions as tactical.

3 Initial synthetic attempts at Nocapyrone natural products

3.1 Introduction

This chapter aimed to build upon work previously done during my honours research within the Perkins group, on the synthesis of Nocapyrone C.¹⁵¹ The development of a new synthetic strategy was determined as the way forward to address the underperforming reactions in the previous synthesis which reduced its suitability as a general protocol for the preparation of Nocapyrone isomers and derivatives.

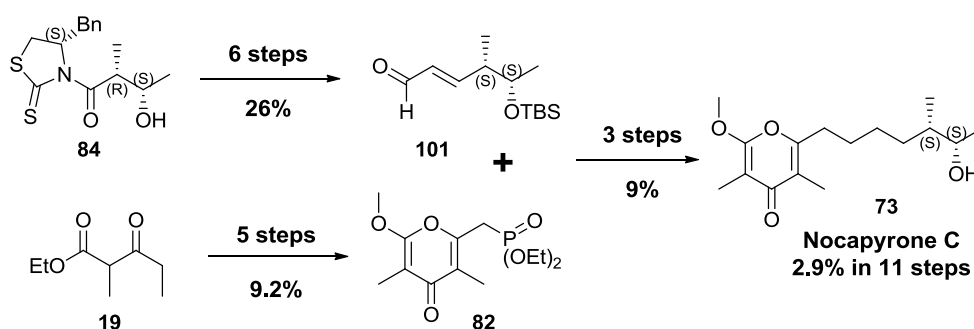


Figure 3.1 Summary of the synthesis of Nocapyrone C through divergent strategy completed in 2013.¹⁵¹

A critical review of the 2013 Nocapyrone C synthesis¹⁵¹ (Chapter 2) shows that γ -pyrone **80** substructure preparation was underperforming in its tactical approach (Figure 3.2), with both poor yield and poor reproducibility. Reactions involving the β,γ -diketo ester **78** preparation where β -keto ester **19** substrates were extended by the addition of short-chain ethyl reagents (ethyl acetate, N-acylimidazole), and then subsequently cyclised to the hydroxy- α -pyrone **79**, were found to be low yielding and only sporadically successful (Figure 3.2).¹⁵¹ The review in Chapter 2 suggested that increasing the chain length of the addition species to the β -keto ester could possibly remedy for the instability of the triketo intermediates,⁷⁶ and provide the added benefit of combined side-chain extension.

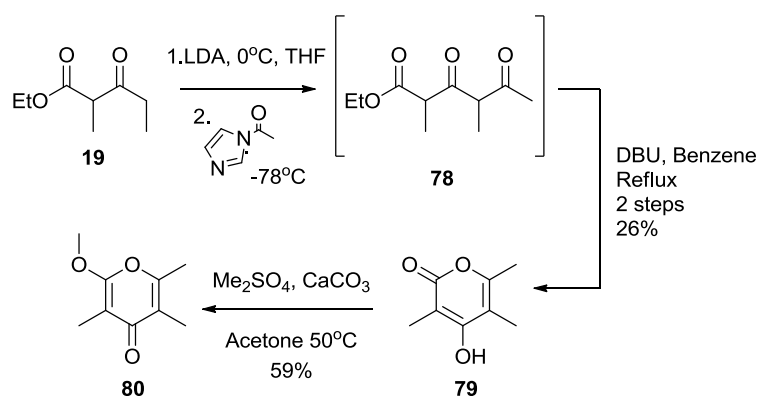


Figure 3.2 The preparation of γ -pyrone **80** from the 2013 Nocapyrone C synthesis.¹⁵¹

It was recognised that a new synthesis directed towards Nocapyrone C and related isomers could benefit from longer chain addition to the β -keto ester, as well as an investigation into alternatives to the acylation reaction conditions used during β,γ -diketo esters preparation. A new synthetic strategy which retains a convergent connectivity strategy, similar to the one used in the 2013 synthesis, could take advantage of the interchange between separately prepared pyrone and side-chain fragments. For example, separately prepared pyrones could include or omit methylation or substitution at C-3 and C-5 positions and be coupled to side chains of varying lengths and functionality. Stereocontrolled side chain functionality could also be separately prepared and allow for the creation of numerous isomers and derivatives. The coupling strategy implemented in the new synthetic strategy would have to be synthetically facile for both fragments and have strong fidelity, especially during the concluding steps of the synthesis.

3.2 General synthetic strategy

The development of a general strategy for the preparation of both Nocapyrone C (**73**) and Violapyrone E (**105**) natural products began with a thorough retrosynthetic analysis (Figure 3.3). Both natural products could be said to share an α -pyrone foundational structure which contains methyl substitution at C-3 and C-5 positions (or just C-3 as with Violapyrones) with a major skeletal side chain extending from the C-6 position. The aliphatic side chain extends 7 carbons and terminates with functionalised branching at C-11 (methyl) and C-12 (hydroxyl) positions. The functionalisation at these positions would be controlled in its stereochemistry for the natural products. Nocapyrone natural products require the α -pyrone **117** to be further methylated to the α -methoxy- γ -pyrone **119** but otherwise, the substructure is shared. The α -pyrone substructure **117** can be formed from a β,γ -diketo ester linear precursor **116**. The linear skeleton comprises a 12 carbon long chain with three major components with two critical disconnections; a tricarbonyl from precursory β -keto ester **113**, a 4-carbon saturated linker chain from 1,4 butanediol **114**, and a stereocontrolled branched hydroxy functionalised tail in the manner of an β -hydroxy aldol adduct **115**. A good general convergent synthetic strategy would utilise different substitution,

functionality, and stereochemistry in the separately prepared fragments to provide a variety of final products. These could include the reported Violapyrone and Nocapyrone natural products but also their stereoisomers and other non-natural derivatives.

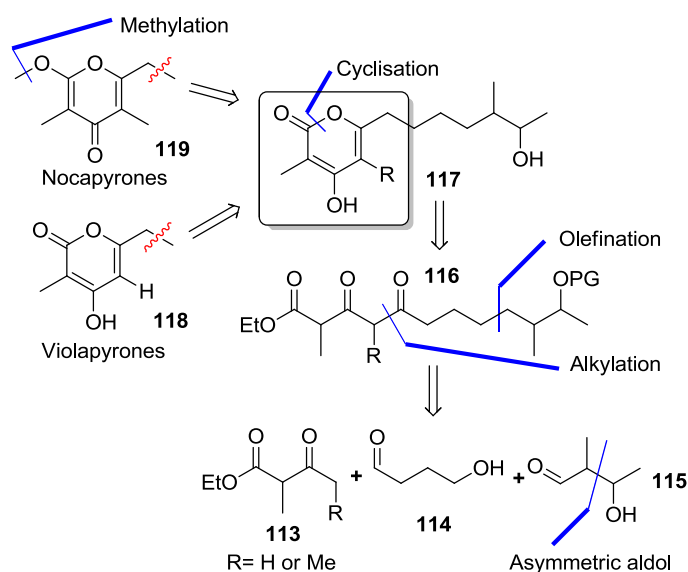


Figure 3.3 General synthetic strategy for the construction of Nocapyrone and Violapyrone natural products

The order of connection between each fragment (β -keto ester and linker first, or stereocontrolled fragment and linker first) would have to be taken into consideration as this could be influential in the efficiency and fidelity to the tactical approaches towards the final product.

3.3 First-generation synthetic strategy towards Nocapyrone C

A synthetic strategy (Figure 3.4) was devised which takes advantage of a convergent coupling between a pre-prepared pyrone fragment and a functionalised stereocontrolled terminating fragment. The crucial connection between a 4-carbon linker **114** derived from 1,4 butanediol and the β -keto ester **113** was determined to be a necessary initial step allowing for early pyrone formation and methylation (to **120**). As the previous 2013 attempts¹⁵¹ at pyrone preparation resulted in poor yield and reproducibility it was decided that pyrone preparation would also be retained as early in the synthesis. This, in combination with convergent strategy, could allow for mitigation of any low yielding steps. The incorporation of the 4-carbon linker **114** in the pyrone preparation would test the influence of longer chain addition via dianion conditions on the stability of the intermediate β,γ -diketo ester formation and allow for combined chain extension in fewer steps.

A generalised version of the strategy (Figure 3.4) could incorporate variation in the pyrone substitution and omission of methylation, with the combination of divergence through various

terminating functionalities accommodating Violapyrone natural products as well as other derivatives.

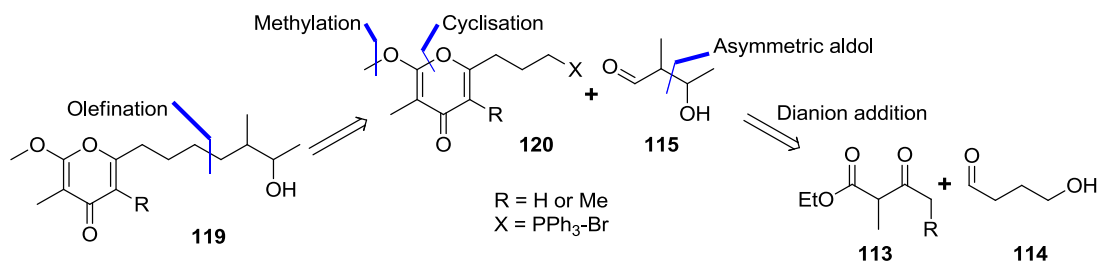


Figure 3.4 Synthetic strategy for Nocapyrone C through early-stage pyrone formation

The tactical approaches for stereoiduction to be implemented during functionalisation of the terminus of the side-chain could include an asymmetric aldol reaction between aldehyde and ketone, but could also potentially be substituted with alternatives such as asymmetric epoxidations of an alkene or asymmetric ketone reduction. The final crucial coupling between the pyrone **120** and terminal fragment **115** in the final stages of synthesis would require high fidelity reactions and in this case, a Wittig type olefination may be a suitable candidate.

3.4 Developing methods for dianion addition

To begin the synthesis, a suitable set of reactions had to be devised for the tactical approach towards the pyrone fragment and, by extension, the preparation of β,γ -diketo ester intermediate **116** through the crucial side chain **114** and β -keto ester **113** connection. As discussed in Chapter 1 dianion conditions are commonly utilised in the alkylation of β -keto esters, and most protocols are derived from those demonstrated by Huckin and Weiler (Figure 3.5).⁵⁵⁻⁵⁷ Deprotonation of β -keto esters requires subjection to either two molar equivalents of non-nucleophilic LDA or the sequential addition of one molar equivalent of NaH and one molar equivalent of *n*-BuLi. The initial molar equivalent of alkali metal base forms a delocalised anion through the deprotonation of the more acidic α -proton of the β -keto ester. The subsequent molar equivalent of strong lithium base is required to deprotonate the γ -proton. The delocalised anion prevents nucleophilic attack on the carbonyl functional groups and directs electrophilic addition to the γ -carbon position, inducing carbon-carbon bond formation.

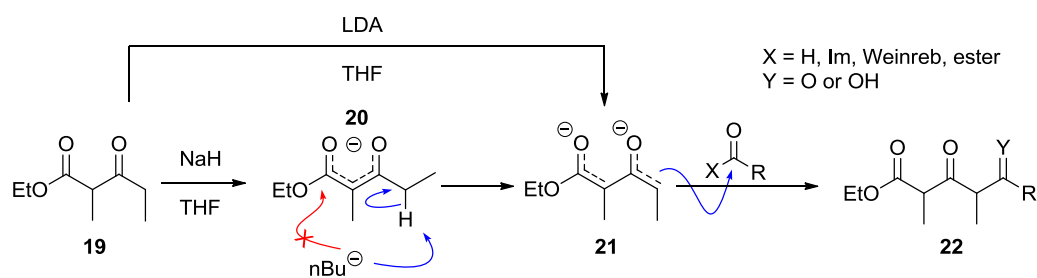
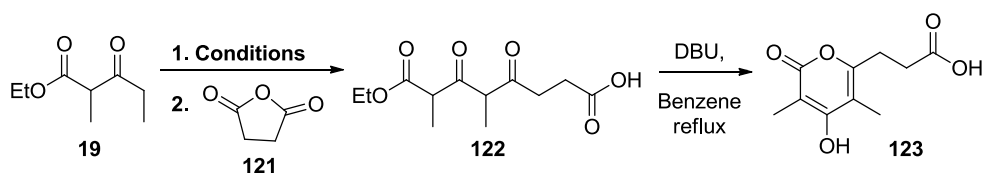


Figure 3.5 The Huckin-Weiler protocol for acylation and aldol type condensation of β -keto ester dianions.⁵⁵⁻⁵⁷

The β -keto ester, ethyl-2-methyl-3-oxopentanoate (**19**), was best suited for preparing the β,γ -diketo ester for Nocapyrone natural products as it provided the C-3 and C-5 methyl substitutions of the final ring. Ethyl 2-methylacetoacetate would be suitable for Violapyrone natural product ring preparation. The appropriate electrophiles for the β,γ -diketo ester preparations were still to be determined but 4-carbon chain, possibly derived from 1,4-butanediol, would allow for direct connection to a 4-carbon stereocontrolled fragment, possibly a 3-hydroxy-2-methylbutanal fragment from an asymmetric aldol reaction.

Initial screening reactions aimed to determine the best dianion reaction conditions suitable for further substrate screening. The reaction screening study (Table 3.1) investigated the formation of dianions of the β -keto ester, ethyl-2-methyl-3-oxopentanoate (**19**), through common conditions including the LDA and sodio-lithio dianion conditions described by Huckin-Weiler,⁵⁷ as well as screening the influence of coordinating co-solvents. The addition of coordinating co-solvents such as Tetramethylethylenediamine (TMEDA) or Dimethylpropyleneurea (DMPU) were utilised as ligands for lithium ions, as selective coordination of the cation increases the reactivity of enolisation and organolithium nucleophiles.^{171,172} The formed dianions were reacted with the readily available succinic anhydride (**121**) electrophile and carried through cyclisation to the α -pyrone **123** to investigate yield and reliability.

Table 3.1 Screening of reaction conditions on dianion addition with succinic anhydride



Conditions	Temp	Yield
LDA, THF	-78 \rightarrow 0 °C	25%
LDA, TMEDA, THF	-78 \rightarrow 0 °C	23%
LDA, DMPU, THF	-78 \rightarrow 0 °C	23%
NaH, n-BuLi, THF	-78 \rightarrow 0 °C	29%

The screening study (Table 3.1) found that dianions formed through LDA produced a similar result regardless of whether a coordinating co-solvent was present or not. Best results were

3.5 Acquisition of pyrone bromide 135 in pursuit of Nocapyrone C

It was determined that the forward synthesis towards (Figure 3.6), initially, Nocapyrone C would utilise the aldol like alkylation between the β -keto ester ethyl 2-methyl-3-oxopentanoate **19** and the aldehyde 4-(benzyloxy)butanal **124** as the key coupling step in the preparation of the pyrone fragment. The coupling reaction to be conducted between the pyrone fragment and the separately prepared stereocontrolled terminating fragment would be a Wittig or Wittig-type olefination and would require a pyrone halide as a precursor. The pyrone bromide **135** was prepared for this purpose.

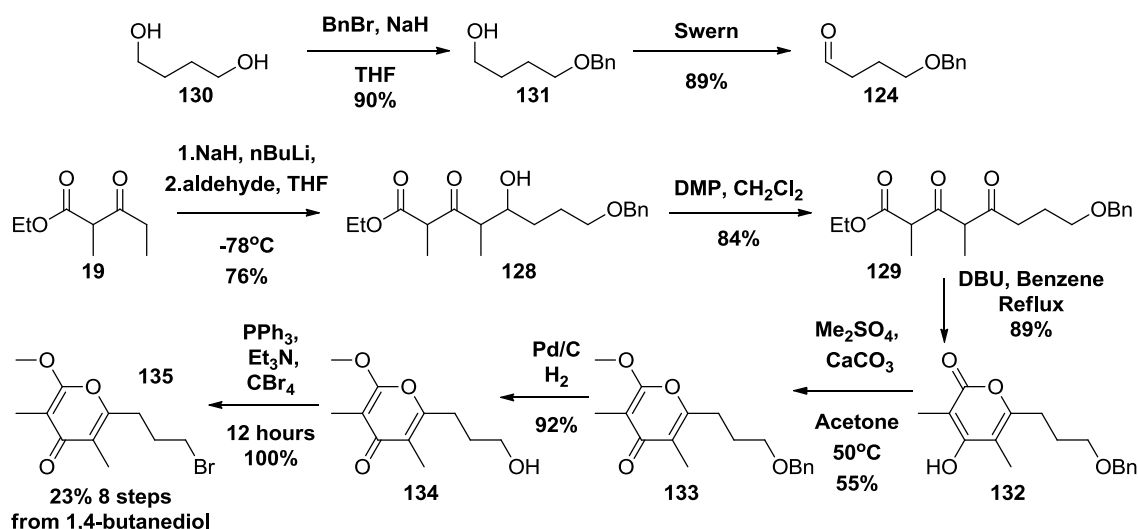
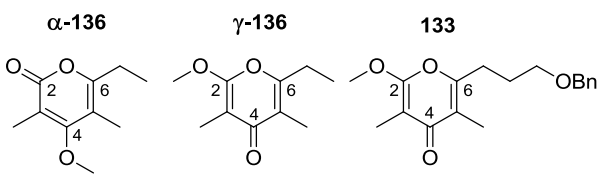


Figure 3.6 Preparation of pyrone bromide **135** via key aldol like alkylation

Initially, the intermediate 4-(benzyloxy)butanal **124** was prepared from butanediol **130** with mono-benzyl protection carried out with benzyl bromide and NaH in THF cooled to 0°C . The mono-protected diol **131** was then Swern oxidised to obtain the aldehyde **124** in 80% over two steps. A Huckin-Weiler dianion enolate of ethyl 2-methyl-3-oxopentanoate **19** was obtained by subjecting the substrate to the addition of NaH followed by $n\text{-BuLi}$ in THF at 0°C . The enolate then had aldehyde **124** added in an aldol reaction to provide the β -keto- γ -hydroxyl ester **128** as a mixture of stereoisomers in 76%. The β -keto- γ -hydroxyl ester **128** was oxidised with Dess–Martin periodinane (DMP) over a couple of days at room temperature in CH_2Cl_2 to afford the triketone **129** in 84%. Cyclisation to the subsequent α -pyrone **132** was conducted through standard DBU conditions in excellent yield (89%). Regio-selective methylation was performed in the conditions developed by Hosokawa,^{112,113} with the use of calcium carbonate and dimethyl sulfate, supplying the α -methoxy- γ -pyrone **133** in 55% yield. The pyrone regioisomers were determined through NMR comparisons to previously reported α -methoxy and γ -methoxy pyrones (Table 3.3),¹¹¹ with the major α -methoxy- γ -pyrone **133** regioisomer determined by the important tertiary C-2 (δC 162.3) and methoxy C-10 (δC 55.46, δH 3.95 (*s*, 3H)) characteristic of the α -methoxy.

Additionally, contributions from the C-4 carbonyl (δ_C 181.16) and tertiary C-6 (δ_C 157.8) indicate the γ -pyrone configuration. Good correlation was found with the major regioisomer and that of α -methoxy- γ -pyrone γ -**136** (2-Ethyl-6-methoxy-3,5-dimethyl-4H-pyran-4-one) reported by Rodriguez *et al.* in their synthesis of cyercene A. 2D NMR data of **133** was also able to confirm the regioselective α -methylation.¹¹¹

Table 3.3 Comparison between major regioisomer 133 and previously reported α -methoxy and γ -methoxy pyrones.¹¹¹



Pyrone	Methoxy δ_H, δ_C	C-2 δ_C	C-4 δ_C	C-6 δ_C
133	3.95; 55.46	162.3	181.16	157.8
γ - 136	3.94; 55.2	162.1	181.1	159.1
α - 136	3.73; 60.1	166.2	168.4	160.0

The preparation concluded with debenzoylation of the hydroxyl protecting group through hydrogenolysis conditions giving access to the free alcohol **134** in 92%, and subsequent conversion to bromide **135** through standard Appel conditions in quantitative yield.

The pyrone bromide **135** structure was confirmed through NMR spectral analysis. The α -methoxy- γ -pyrone moiety was characterised the C-10 methoxy (δ_C 55.54, δ_H 3.95 (s, 3H)), the methyl substations at C-11 (δ_C 6.99, δ_H 1.84 (s, 3H)) and C-12 (δ_C 10.13, δ_H 1.96 (s, 3H)), the sp^2 ring carbons C-2 to C-6 (δ_C 162.25, 99.73, 119.28, 156.50) including the C-4 carbonyl (δ_C 180.87). The side chain was characterised by the 3 contiguous methylene carbons C-7 to C-9 (δ_C 29.22, δ_H 2.78 (t, J = 7.3 Hz, 2H), δ_C 30.05, δ_H 2.25 – 2.16 (m, 2H), δ_C 32.20, δ_H 3.43 (t, J = 6.3 Hz, 2H)). The conversion from the pyrone **134** to the bromide **135** was characterised by the shift from the hydroxy C-9 displaying a NMR signal of δ_C 61.71, δ_H 3.70 (t, J = 6.2 Hz, 2H) to **135** with bromide C-9 displaying a signal of δ_C 32.20, δ_H 3.43 (t, J = 6.3 Hz, 2H).

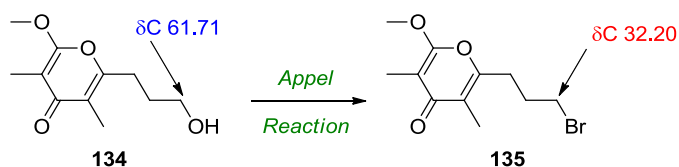


Figure 3.7 Conversion from hydroxy pyrone 134 to pyrone bromide 135 through an Appel reaction including the characteristic conversion of C-9 ^{13}C NMR signal

This newly developed approach was able to achieve two things over the previous synthetic preparation of a pyrone fragment.¹⁵¹ Firstly, it combined the chain extension through addition of the 4-carbon linker and secondly, prepared the pyrone fragment in high yield (23% in 8 steps) through a reliable procedure. The results from this preparation suggested that the use of a longer

carbon chain in combination with aldol conditions contributed to reducing any possible instability in the intermediate tricarbonyl, as opposed to reports for shorter tricarbonyl precursors.⁷⁶

The pyrone bromide **135** was utilised in a number of attempts towards conversion to the phosphonium bromide Wittig salt, but all attempts were unsuccessful (Figure 3.8). The reaction of **135** with triphenyl phosphine in THF with both heating to reflux or stirring at room temperature resulting in complex mixtures of products and full consumption of starting material. This unexpected result left no opportunity to test the subsequent Wittig coupling with any aldehyde substrates and terminated this tactic for completion of the synthetic route.

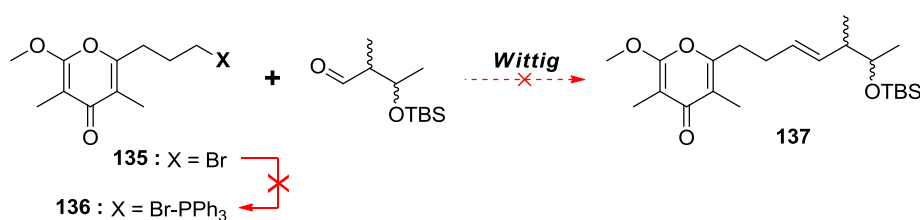


Figure 3.8 Failed conversion of bromide pyrone **135** to Wittig salt **136**

A tactical revision was attempted of the Wittig coupling reaction, with the attempt aimed at reversing the coupling functional groups between the pyrone and stereocontrolled substrates (Figure 3.9). Although the pyrone aldehyde **138** was able to be easily prepared through Swern oxidation of pyrone alcohol **134**, the Wittig salt formation on the TBS ether **139** was again unsuccessful and denied any attempts at Wittig olefination.

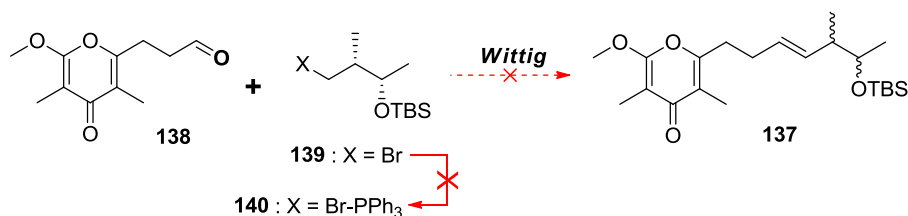


Figure 3.9 Failed conversion of bromide **139** to Wittig salt **140**.

These results brought up the question of whether exhaustive efforts should be conducted into discovering a tactical remedy for this strategy through screening of reaction conditions and alternative olefination methods, or if the strategy itself required revision.

There was a concern that even after extensive screening a suitable coupling reaction could not be found, or would require the addition of extra synthetic steps, resulting in a cumbersome or suboptimal outcome. The question was asked whether strategic revision of the synthetic route could produce a better overall outcome compared to a tactical one.

The major strategic alternative (Figure 3.10) to the current approach would see the order of disconnection reversed and reserve pyrone preparation until the concluding steps of the synthesis

with the stereoinduction and chain extension initiating the synthetic route. An example of a late-stage pyrone formation strategy can be seen in Figure 3.10, where the common α -pyrone **117** from the general synthetic strategy (Figure 3.3) can also be achieved through the coupling of β -keto ester **113** and a linear 8-carbon fragment **142** followed by cyclisation. The linear side chain fragment **142** would be constructed from a 4-carbon linker **141** and a stereocontrolled fragment **115**.

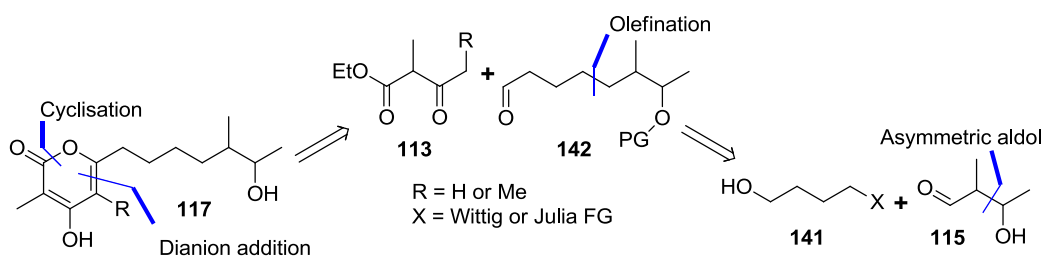


Figure 3.10 Synthetic strategy with early-stage stereoinduction, chain extension, and late-stage pyrone formation.

In comparison with the current early-stage pyrone formation strategy (first-generation synthetic strategy) (Figure 3.4), the alternative strategy would reverse the coupling priorities and therefore also the justifications for their original order. Late-stage pyrone formation (Figure 3.10) brings up two crucial challenges which are inherently mitigated in the current strategy and would have to be sufficiently addressed before they could be justified in their implementation; these include late-stage triketo preparation, pyrone cyclisation, and late-stage regio-selective methylation of the ring. To confront the concerns surrounding this crucial sequence of reactions, a set of tests were devised to determine if the alternative strategy had validity.

In the original 2013 attempts at Nocapyrone C,¹⁵¹ as well as the current initial strategy (Figure 3.6), the Hosokawa dimethyl sulfide/calcium carbonate methylation protocol^{112,113} was implemented, and intentionally retained in the early stages of synthesis due to the expectation of only modest conversion. Optimised methylation from α -pyrone **132** was able to provide regioselective yields of 55% of the desired α -methoxy- γ -pyrone **133**, with a return of starting material (~ 25-30 %) and only minimal conversion to the γ -methoxy- α -pyrone (< 15 %). This implementation was a compromise due to the inability to source and reluctance to handle the most common regioselective methylating agent, methyl fluorosulfonate.^{60,61,120,63,67,73-75,79,88,119} Commonly referred to as “magic methyl”, methyl fluorosulfonate is currently disfavoured due to its high toxicity, and its phasing out increases the requirement for better alternatives. A literature search revealed that despite its similarity to methyl fluorosulfonate, methyl trifluorosulfonate (methyl triflate) has not been implemented in the methylation of pyrones. A prudent course of action was to conduct a test to gauge the utility of methyl triflate as an alternative for regioselective methylation.

Commercially available 4-hydroxy-6-methyl-2-pyrone (**143**) was subject to methyl triflate while stirring at 0 °C in CH₂Cl₂ (Figure 3.11). The reaction progressed quickly and within the hour a spot conversion of starting material to product was observed using TLC. The fast full conversion was encouraging and NMR analysis of the crude mixture showed a single product, but a comparison to the methoxy α -pyrone **145**, produced through selective K₂CO₃ dimethyl sulfate γ -methylation,^{173,174} gave a direct correlation. This result displayed that triflate could be used for fast selective methylation, but to the undesired γ -methoxy- α -pyrone **144**.

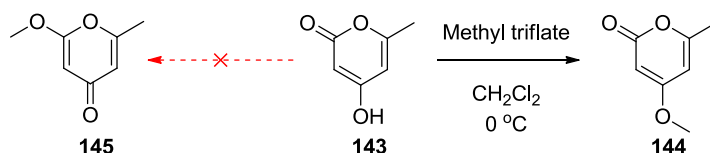


Figure 3.11 Methyl triflate test methylation on 4-Hydroxy-6-methyl-2-pyrone **143**

Despite the undesired regioselective methylation of **143** to the γ -methoxy- α -pyrone **144**, the same methyl triflate reaction conditions (methyl triflate, CH₂Cl₂, 0 °C) were subjected to the trisubstituted 4-Hydroxy-3,5,6-trimethyl-2-pyrone (**79**) and conversion to a single product was also observed (Figure 3.12). The NMR of the isolated product on this attempt showed reversed selectivity, and conversion to the α -methoxy- γ -pyrone **80** was seen as the exclusive product with the resulting NMR correlating to that of previous syntheses.^{67,76,88,112,113,175-177}

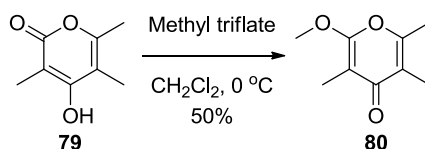


Figure 3.12 Test methylation with methyl triflate on 4-Hydroxy-3,5,6-trimethyl-2-pyrone (**80**).

The methylation reaction was suspected to have been quenched prematurely as starting material was recovered, and it was suggested that extended reaction time, increased temperature, or recycling of starting material could be utilised to increase conversion. With this positive result, it was important to also test if larger side chain fragments retain the reaction fidelity of the crucial dianion aldol alkylation required for triketo formation. A model system was devised to investigate these parameters as well as testing later stage methylation with the synthesis of Nocapyrone H, a natural product Nocapyrone featuring an unbranched saturated 7-carbon sidechain.^{150,168,178} A simple 4 step synthesis can be envisaged as per retrosynthesis in Figure 3.13.

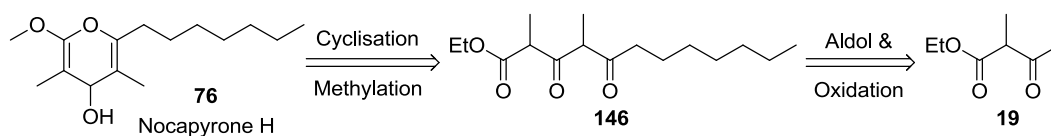


Figure 3.13 Retrosynthesis of Nocapyrone H

3.6 Synthesis of Nocapyrone H

The synthesis was initiated with the optimised dianion aldol reaction between β -keto ester ethyl 2-methyl-3-oxopentanoate **19** and octanal providing a mixture of β -keto- γ -hydroxyl isomers (Figure 3.14). The crude mixture was subsequently oxidised with DMP to form the triketo **146** as an inseparable mixture of isomers. The triketo **146** mixture was subjected to DBU mediated cyclisation in refluxing benzene and yielded the α -pyrone **147** in 32 % over the three steps. The methylation was conducted with methyl triflate in CH_2Cl_2 at 0 °C and warming to room temperature over an hour, providing the α -methoxy- γ -pyrone **76** as the single regioisomer in 52% yield. NMR analysis of the crude mixture shows unreacted starting material. NMR analysis of the desired product showed strong structural correlation to the data from the natural product isolation.^{150,168} The full characterisation and comparison to the isolated natural product is covered in Chapter 5 and confirmed as a successful synthesis of Nocapyrone H.

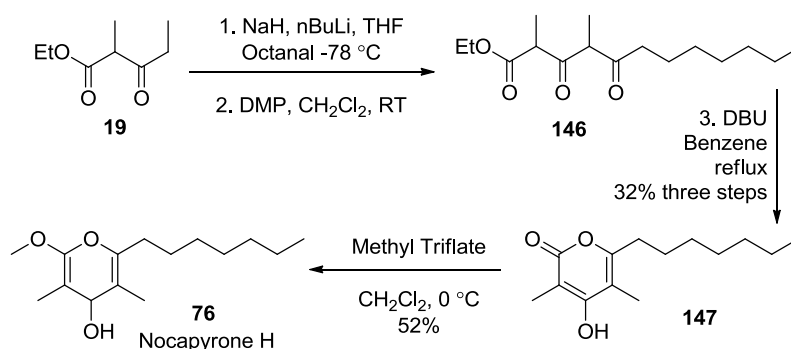


Figure 3.14 Synthesis of Nocapyrone H including methyl triflate regio-methylation

The successful synthesis of Nocapyrone H allowed for the implementation and scrutiny of reaction conditions that are crucial in the development of an alternative synthetic pathway to Nocapyrone natural products. Specifically, late-stage methylation with methyl triflate was seen to exclusively yield the α -methoxy- γ -pyrone regioisomer in reasonable yield, with room for optimisation and possible full conversion. Dianion aldol addition of lengthier side chain fragments to β -keto esters was also shown not only to be viable but superior to any of the tested acylation methods in both the first generation synthetic strategy and Nocapyrone H synthesis. To build upon these successes, a synthetic strategy was developed which could incorporate all of these features in an early-stage stereoinduced side-chain preparation and late-stage pyrone preparation.

3.7 Development of the Second Generation Synthetic Strategy

The second-generation strategy aimed to approach the synthesis from the opposite direction to that of the first, with pyrone installation left until the concluding steps of the synthesis and beginning with the asymmetric induction of stereochemical functionality of the side chain. This

approach can be visualised in the general retrosynthesis (Figure 3.15), where pyrone methylation is included in the final steps and can be utilised for Nocapyrone, and pyrone methylation can be omitted for Violapyrone, natural products and isomers.

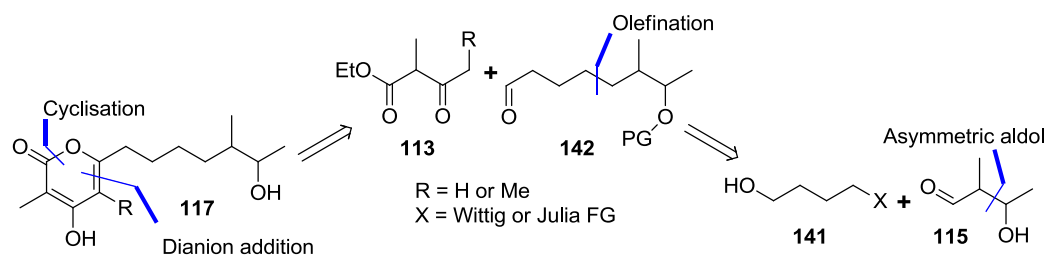


Figure 3.15 General retrosynthetic strategy with early-stage stereinduction, chain extension, and late-stage pyrone installation

The forward synthetic direction was proposed to start with the preparation of the side chain **142** and the stereocontrolled terminating fragment **115**, with chain extension through olefination of a 4-carbon linker **141**. After the side chain **142** has been completed, the second crucial connection would take place between the side chain **142** and β -keto ester **113** during β,γ -diketo ester preparation via dianion addition. The synthesis would conclude with pyrone **117** cyclisation and possible regioselective methylation.

The terminating fragment would have the stereocenters installed through the use of asymmetric aldol reactions, controlling for both *syn* and *anti* relative stereochemistry which are important for the stereoelucidation of Nocapyrone and Violapyrone natural products, as well as for the production of various isomers. To be able to discuss the development of the second generation synthetic strategy, it would be important to discuss the tactical approaches for stereocenter installation and the importance of the asymmetric aldol addition. Chapter 4 will explore the utilisation of Crimmins chiral auxiliaries in mediating asymmetric aldol carbon-carbon bond forming reactions for the installation of C-11 and C-12 stereocenters.

4 Asymmetric Aldol Stereoinduction

4.1 Introduction

As discussed in Chapter 3, revision of the synthetic strategy into a second generation was considered to be more advantageous solution than tactical amendment to the synthetic deadlock experienced with the first generation strategy towards Nocapyrone C, where crucial coupling between the pyrone fragment and the terminal stereocontrolled fragment was still unrealised. The decision to opt for strategic revision stemmed from 3 factors; tactical amendment may be more challenging than anticipated and could lead to a suboptimal outcome, the synthetic limiting factors rationalising first generation strategy had become less compelling with recent experimental results and opened potential to intercept Violapyrone natural products with less effort.

Strategic revision would see the second generation reverse the order of disconnection between the crucial synthetic fragments (the β -keto ester **113**, the 4-carbon linker **114**, and the terminal stereocontrolled fragment **115**) (Figure 4.1) of the general synthetic strategy, where the β -keto ester **113** and the 4-carbon linker **114** were coupled first in the early stage pyrone preparation of the first generation, the possible alternative lies in the initial coupling of the terminal stereocontrolled fragment **115** and the 4-carbon linker prior to addition to β -keto **114** fragment for late-stage pyrone preparation.

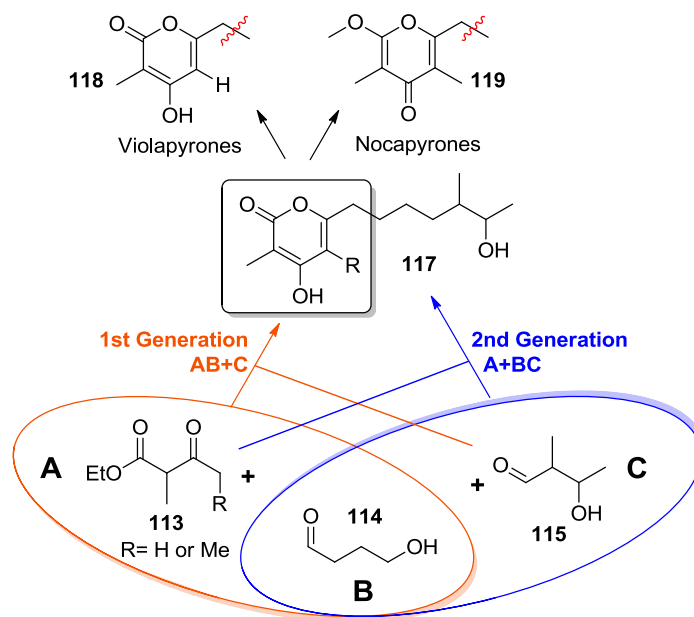


Figure 4.1 The general synthetic strategy visualising the differences between first and second synthetic strategies.

The proposed secondary synthetic strategy aimed to build upon the lessons learnt in the first generation strategy and the optimised approaches to β -keto dianion addition, coupling this with the advances demonstrated with successful synthesis of Nocapyrone H. The synthesis of Nocapyrone H (Figure 3.14) was used as a model synthesis to simulate late-stage pyrone preparation through long side-chain dianion addition to β -keto esters, cyclisation, and regioselective methylation, producing an advanced α -methoxy- γ -pyrone in a short synthesis. The critical lessons learnt from Nocapyrone H synthesis was that late-stage pyrone preparation could be pursued along with the use of methyl triflate in regioselective methylation.

The second-generation synthetic strategy (Figure 4.2) proposed to initiate the synthesis with the establishment of controlled stereochemistry with a separately prepared fragment (**115**) which is to be coupled to an extending fragment (**141**). This would provide the side chain **142** and would build the skeleton towards the pyrone functionality. The linear skeleton would be completed with coupling between β -keto ester **113** and side-chain **142**. The strategy would conclude with the pyrone cyclisation (to **117**) and post-cyclisation methylation (for Nocapyrone natural products) reserved until concluding stages of the route.

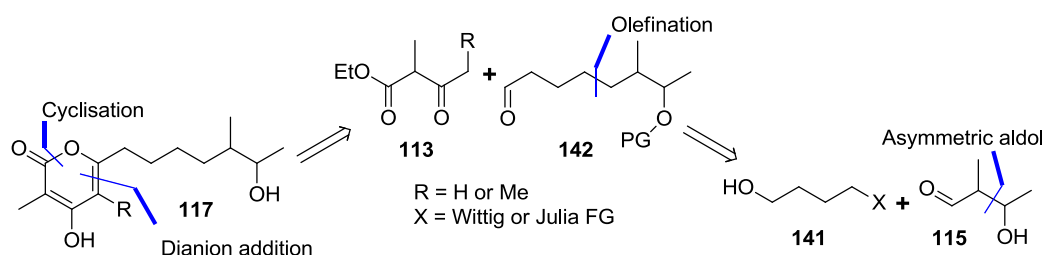


Figure 4.2 General retrosynthetic strategy with early-stage stereoinduction, chain extension, and late-stage pyrone installation

The strategy for stereoelucidation of Violapyrone and Nocapyrone natural products asked for a terminating fragment with controlled tertiary α -methyl and β -hydroxyl stereocenters. A set of fragments which resemble 3-hydroxy-2-methylbutanal **115** would best suit olefination type coupling between the 4-carbon central linker **141** (Figure 4.3). The stereochemistry of this 3-hydroxy-2-methylbutanal **115** intermediate fragment would be required to persist through the synthesis to the final products and would be used for stereo elucidation of the final products. To facilitate the elucidation of two stereocenters at C-11 and C-12 of Nocapyrone and Violapyrone natural products, at least two diastereomers would be required to determine relative and absolute stereochemistries.

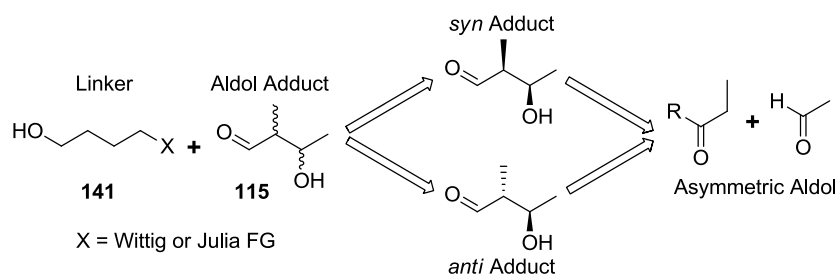


Figure 4.3 The acquisition of *anti* and *syn* stereochemistry through asymmetric aldol reaction.

The most suitable protocol for the installation of the desired stereochemistry could be accomplished through the correct application of an asymmetric aldol. The aldol reaction is uniquely positioned to install both α -methyl and β -hydroxyl stereocenters in combination with the carbon-carbon bond formation in one single step.

Asymmetric aldol reactions mediated by chiral auxiliaries are important synthetic tactics which often draw upon the versatility of cleavable chiral auxiliaries in enolate driven stereinduction.¹⁷⁹ Most cleavable chiral auxiliary mediated aldol adducts can simply be converted to a 3-hydroxy-2-methylbutanal-type **115** fragment required in olefination coupling with the 4-carbon linker **141**. Oxazolidinones, oxazolidinethiones, and thiazolidinethiones are well established and among the most common classes of chiral auxiliaries, with their utility deriving from their facile installation and cleavage, easy preparation, and ability to provide reliable diastereoselectivity in aldol reactions.

4.2 Crimmins aldol protocol utilising thiazolidinethione chiral auxiliaries

It was envisaged that the synthetic strategy would deploy the protocols developed by Crimmins^{154,180,181} which make use of thiazolidinethiones and titanium enolate conditions to provide versatile access to *syn* stereochemistry of the 3-hydroxy-2-methylbutanal **115** intermediate (Figure 4.4). The acylated thiazolidinethione chiral auxiliary **83** is interestingly positioned to be able to selectively access either Evans *syn* **149** or non-Evans *syn* **148** aldol adducts during stereinduction through the variation of input reagents. The enolisation protocols utilise titanium tetrachloride and one equivalent of amine base to form chelated chlorotitanium enolates which can coordinate to the thiocarbonyl of the auxiliary (**148-TS**), resulting in reversed *syn* selectivity (non-Evans *syn*) compared to the boron oxazolidinone enolates (Evans *syn*) from Chapter 1 (Figure 1.32).^{124,127,182-184} Alteration of the reaction mixture to include 2 equivalents of an amine base (typically (–)-sparteine) or the addition of 1-methyl-2-pyrrolidinone (NMP) disrupts the thiocarbonyl coordination **149-TS** and provides the well established Evans *syn* stereoselectivity.

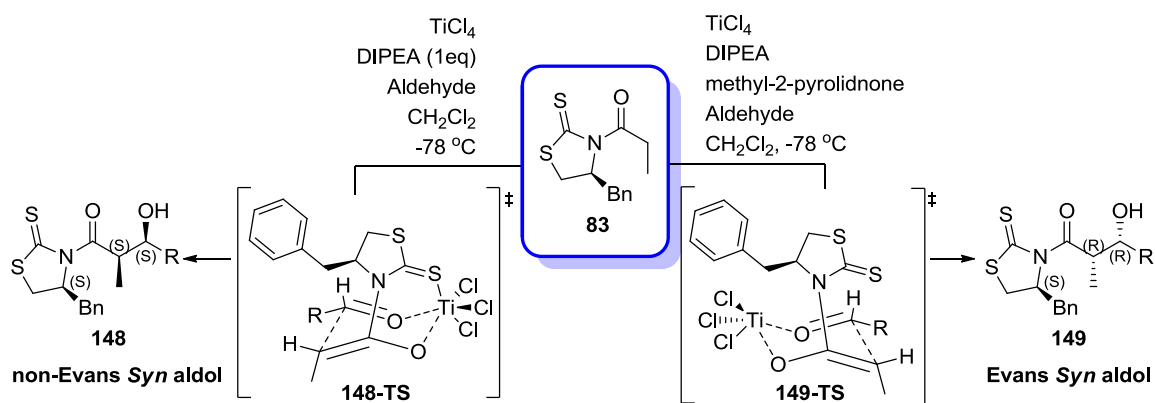


Figure 4.4 Crimmins chlorotitanium enolate protocols for producing both non-Evans *syn* and Evans *syn* adducts.^{154,180,181}

This ability for the Crimmins chlorotitanium enolates to convert between stereoselectivity, coupled with the redundancy of oxidative workup when compared with boron aldol protocols^{124,127,182–184} provides for versatile access to enantiomers without the need for redevelopment of synthetic pathways. The bright yellow colour of thiazolidinethione aldol adducts also aids in ease of purification during chromatography, as separation of diastereomeric products can easily be visualised.

4.3 Preparation of thiazolidinethione chiral auxiliaries

The thiazolidinedione chiral auxiliaries were prepared from enantiopure amino alcohols derived from phenylalanine amino acids. L-phenylalanine **150** was reduced under LiAlH_4 in THF and cyclisation to the thiazolidinedione **151** through extended heating with carbon disulfide in alkaline solution, yielding the five-membered heterocycle **151** in 64% over 2 steps (Figure 4.5). Alternatively, the commercially available Evans oxazolidinones **152** was converted via the similar reaction conditions, but increasing the alkalinity to 2.5 molar KOH attained the thiazolidinethione **151** in 64 % yield. Acylation was conducted by subjecting thiazolidinedione **151** to deprotonation with $n\text{-BuLi}$ in THF at $-78\text{ }^\circ\text{C}$ and reacting with propanoyl chloride, producing propanoyl thiazolidinedione amide **83** in 91% yield.

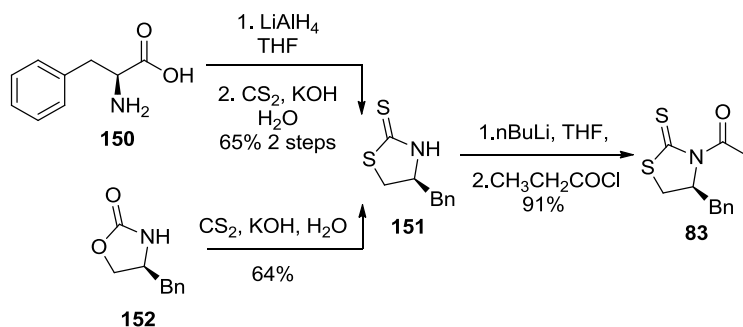


Figure 4.5 The preparation of thiazolidinedione via two pathways

The conversion of oxazolidinethione **152** to thiazolidinethione **151** has not previously been reported in literature, and the initial justification for the attempt was from the successful conversion of oxazolidinethiones to thiazolidinethiones via hydroxy induced ring-opening.¹⁸⁵ The proposed mechanism of the formation of oxazolidinethiones (**156**) and thiazolidinethiones (**151**) from β -amino alcohols (**153**) in strong alkaline KOH solution with excess carbon disulfide is shown in Figure 4.6. Under mild basic conditions and stoichiometric CS₂, allows for majority access to oxazolidinethione **156**. Under stronger alkaline conditions with excess CS₂ and longer reaction times, it allows for ring-opening of the oxazolidinethione **156** and regeneration of initial β -amino alcohol **153** via degradation of an unstable intermediate **157**. If the first intermediate **154** can be intercepted with a second addition of carbon disulfide (**158**), the resulting ring-closing elimination will provide thiazolidinethione **151**, and with longer reaction times will become the dominant product.

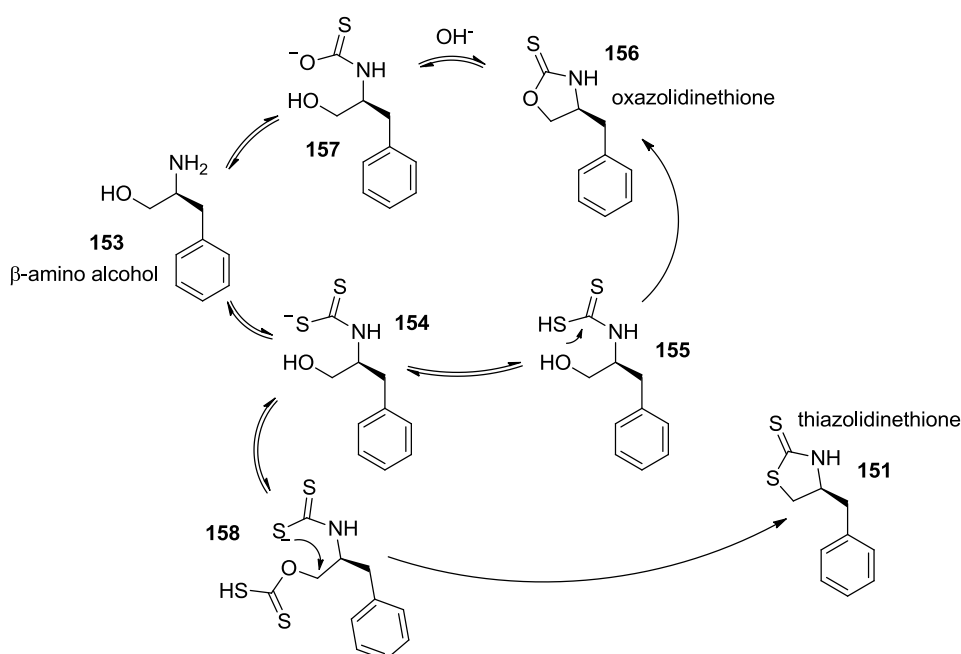


Figure 4.6 proposed mechanism for the formation of oxazolidinethiones and thiazolidinethiones from β -amino alcohol in strong alkaline KOH solution and CS₂.¹⁸⁵

Similar strong alkaline conditions have been used to induce ring-opening and regenerate β -amino alcohols from oxazolidinones in previous reports¹⁸⁶ and it was expected that in the presence of excess carbon disulfide, direct conversion to thiazolidinethione **151** could be possible. Small scale test reactions showed direct conversion using TLC from (*S*)-4-benzyl oxazolidinone **152** to (*S*)-4-benzyl thiazolidinethione **151** and larger scale provided 60% yield of thiazolidinethione **151**.

This conversion could be seen as lucrative, as commercially available oxazolidinones have decreased in price and can usually be found at cheaper prices from suppliers than the precursory β -amino alcohols. The commercial arbitrage would be the main justification for the

cannibalisation of such an advanced reagent over the processing of starting materials, especially since the starting materials are abundant amino acids.

4.4 Crimmins Aldol Protocol for *Syn* Stereoinduction

The Crimmins aldol protocol^{154,180} was utilised with the intention of preparing non-Evans *syn* aldol adducts for the terminal end side chain functionality. The preprepared propionyl thiazolidinedione amide **83** was treated with titanium tetrachloride and diisopropylethylamine to form the titanium enolate, and then was reacted with large excess (~8 equivalents) of acetaldehyde via slow addition (over 15 minutes). It was evident immediately that the aldol reaction had not progressed as previously reported in earlier work from 2013,¹⁵¹ as TLC showed a significantly more pronounced spot for the previously assigned minor isomer. Initial results saw the reaction proceed within 76 % yield, with the less polar diastereomer (R_f = 0.38 (30% EtOAc/X4) on TLC) **159** isolated in 53 % against the more polar diastereomer (R_f = 0.32 (30% EtOAc/X4) on TLC) **160** isolated in 46 %. This provided a diastereomeric ratio of 53:46, an almost non-selective reaction compared to a previously reported dr of 1:3.¹⁵¹ Repeated reaction saw selectivity return to 1:6 dr (by NMR) when similarly large excess of acetaldehyde was added to the titanium enolate reaction mixture in a relatively fast rate (full addition in under 2 minutes). These results brought into question the effects of the aldehyde rate of addition and reaction equivalents on the stereoselective outcome of the Crimmins aldol protocol. It must be mentioned that under normal circumstances, the aldehyde equivalents of a Crimmins aldol is kept almost universally at a 1:1 ratio and the deviation from this standard is only due to the high volatility and low boiling point of acetaldehyde (20.2 °C), requiring a large excess to overcome loss to evaporation.

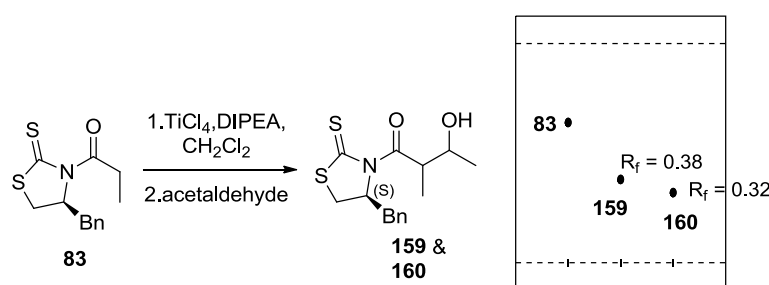


Figure 4.7 Initial attempts at *syn* stereoinduction and comparison of thin-layer chromatographic retention between isomers 159 and 160

To investigate the influence of aldehyde addition rate and reaction equivalents on the diastereoselectivity of the Crimmins aldol protocol, the diastereomers needed to be characterised through the spectroscopic data of the isolated adducts and compared. The ¹H NMR spectra of crude aldol adduct mixtures could be utilised to determine diastereomeric ratios of various reaction conditions and could make suggestions to the influencing factors.

The ^1H NMR acquired for diastereomer **159** (Figure 4.8) distinguished the thiazolidinedione structure from the 5 aromatic protons seen as a multiplet at δ 7.37 – 7.26, the ddd at δ 5.37 from the tertiary proton on the five-membered ring, the doublet of doublets at δ 3.38 and the doublet at δ 2.89 accounting for the a,b diastereotopic methylene protons on the ring, and the doublet of doublets at δ 3.24 and 3.05 produced by the benzylic protons.

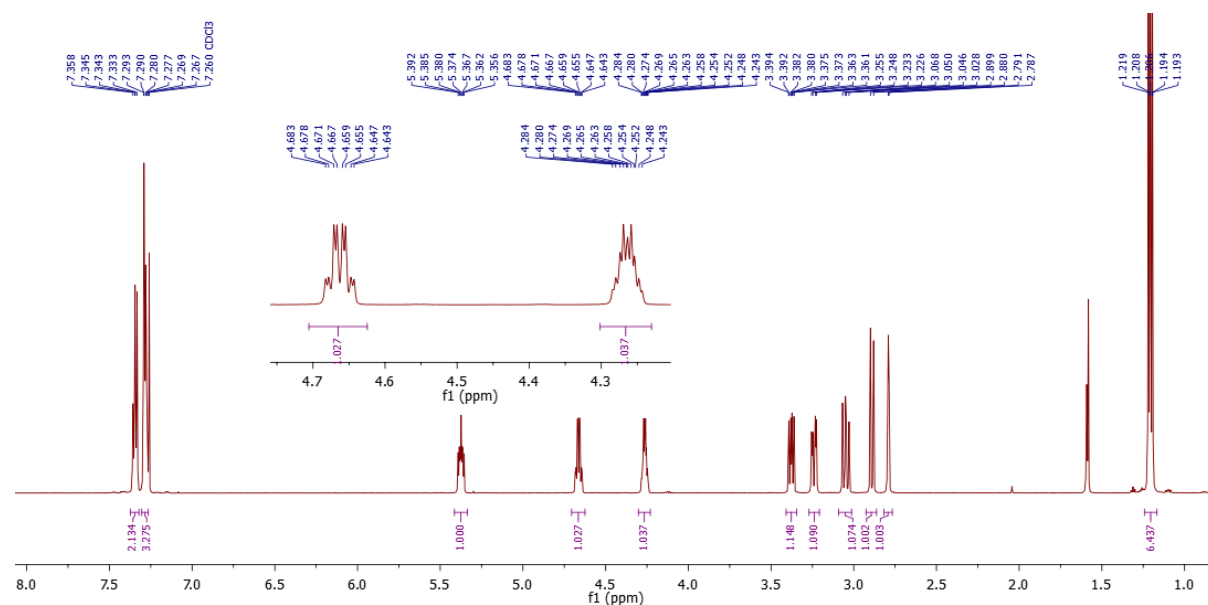


Figure 4.8 ^1H NMR spectrum of **159** diastereomer

The quartet of doublets at δ 4.66 accounts for the tertiary proton α between the carbonyl and alcohol, and the multiplet at δ 4.30-4.23 was the tertiary proton of the alcohol. The signal for the alcohol was seen as a singlet at δ 2.79. The methyl signals are found as an overlapping multiplet at δ 1.21 accounting for 6 protons.

The corresponding spectroscopic data for that of diastereomer **160** differed only at the expected stereogenic tertiary α and tertiary β -hydroxy positions in reference to the amide functional group. The ^1H NMR spectrum (Figure 4.9) showed similarly the signals for the thiazolidinedione starting with the multiplet for the 5 aromatic protons at δ 7.37 – 7.26, the ddd of the stereogenic tertiary ring proton at δ 5.35, the ddd and the doublets of doubles at δ 3.40 and 2.91 responsible for the a,b diastereotopic methylene protons on the ring, and the two sets of doublets of doublets at δ 3.21 and 3.05 respectively from the two benzylic protons.

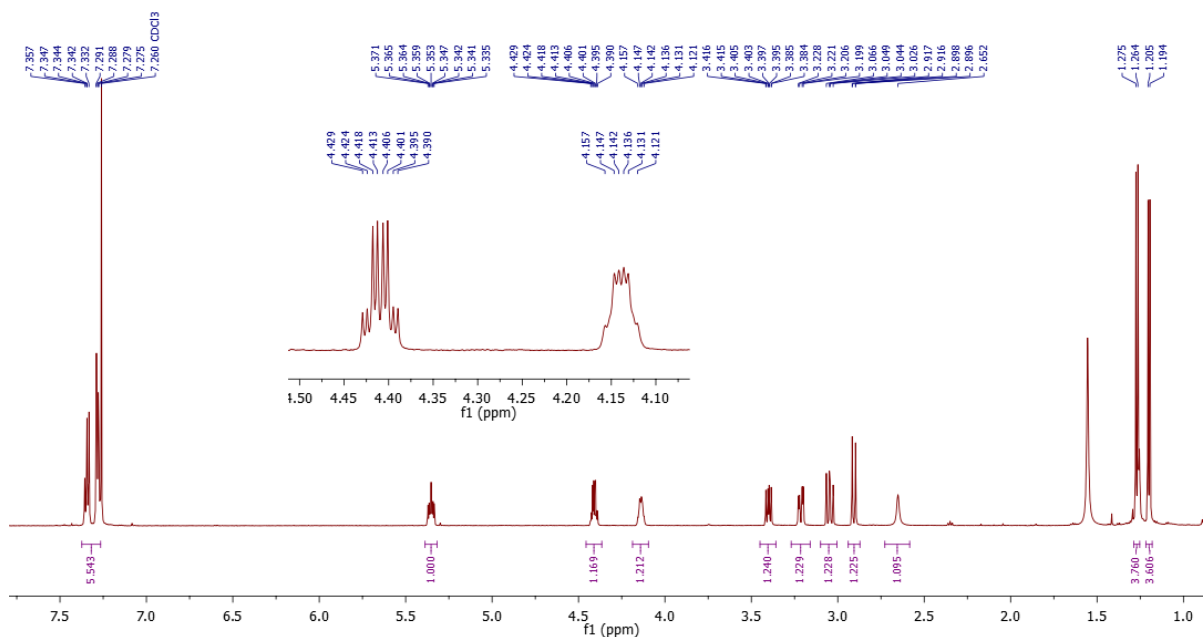


Figure 4.9 ¹H NMR spectrum of 160 diastereomer.

A deviation from the spectrum of **159** was seen with the tertiary stereogenic proton of the α position found as a quartet of doublets at δ 4.41 and the β -hydroxy proton exhibiting a doublet of triplets at δ 4.14 (Figure 4.10). The stereogenic methyl groups also showed a marked difference from that of **159**, in that they are not overlapping and are distinctly forming two doublet peaks at δ 1.27 and 1.20 for three protons respectively. The single hydroxy proton signal was also visible as a singlet at δ 2.65. This spectral data matched previous 2013 work conducted in the Perkins group¹⁵¹

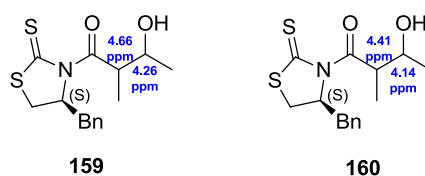
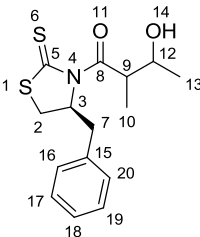


Figure 4.10 The structures of aldol adducts **159** and **160** displaying the ¹H NMR chemical shifts for installed stereogenic protons.

The comparison of ¹³C NMR data between **159** and **160** correlated with the results of the ¹H NMR comparison (Table 4.1), with the methyl, tertiary α , and tertiary β -hydroxy stereogenic carbons all deviating in comparative chemical shift. It was evident that a diastereomeric relationship existed between the two samples.

Table 4.1 Comparison of ^{13}C NMR Spectroscopic Data (150 MHz, CDCl_3) of **159** and **160**

Aldol Adduct	Carbon	159 δ_c	160 δ_c
	5	201.88	201.56
	8	178.34	178.51
	15	136.54	136.50
	17,19	129.60	129.59
	16,20	129.08	129.09
	18	127.44	127.44
	3	69.07	68.91
	12	67.53	68.59
	9	43.62	44.53
	3	37.14	36.94
	7	31.99	32.28
	13	19.57	20.37
	10	10.68	10.58

To investigate the relationship between the influence of aldehyde addition rate and reaction equivalents on the diastereoselectivity of the Crimmins aldol protocol, the repeated aldol reactions were tabulated (Table 4.2) and the diastereomeric ratio was determined from the ^1H NMR integration of stereogenic protons at 4.66 ppm (from **159**) and 4.41 ppm (from **160**). The aldol reactions (Table 4.2) 3-8 were conducted with acetaldehyde in mole equivalents of 2:1 against that of the titanium enolate and was added dropwise as a precooled (ice bath) solution in CH_2Cl_2 via cannula. The tabulated (Table 4.2) results were only able to provide a general trend in changes of reaction conditions although, this was to be expected to some degree due to variations in stirring and reaction scale. The deduced trend indicated to better selection towards **159** with addition of lower molar equivalents of acetaldehyde and slow addition, and fast addition of excess equivalents of acetaldehyde gave better selection for **160** diastereomer. This suggests that the molar equivalents of acetaldehyde in the reaction mixture at any given time may have an influence on the transition state of aldol reaction.

Table 4.2 Effect of reaction conditions on stereochemical outcome of Crimmins aldol

Entry	Reaction Conditions ^a	Add rate ^b	Yield	159:160 ^c
1	TiCl_4 , DIPEA, Acetaldehyde (8 eq)	15 min	76 %	1:1
2	TiCl_4 , DIPEA, Acetaldehyde (8 eq)	3 min	90 %	1:6
3	TiCl_4 , DIPEA, Acetaldehyde (2 eq)	15 min	54 %	8:1
4	TiCl_4 , DIPEA, Acetaldehyde (2 eq)	15 min	51 %	4:1
5	TiCl_4 , DIPEA, Acetaldehyde (2 eq)	10 min	48 %	7:1
6	TiCl_4 , DIPEA, Acetaldehyde (2 eq)	5 min	70 %	9:1
7	TiCl_4 , DIPEA, Acetaldehyde (2 eq)	5 min	79 %	9:1
8	TiCl_4 , DIPEA, NMP, Acetaldehyde (2 eq)	5 min	84 %	1:19

^a estimated eq of acetaldehyde ^b estimated rate of addition ^c comparison of 4.66 ppm and 4.41 ppm NMR peak integration

The reported stereochemical induction from the use of Crimmins protocol^{154,180} is that of a non-Evans *syn*-aldol adduct but which can undergo reversion to the Evans *syn*-aldol adduct through the application of the second equivalents of amine base or the inclusion of 1-methyl-2-pyrrolidinone (NMP), as seen in Figure 4.11.¹⁸¹

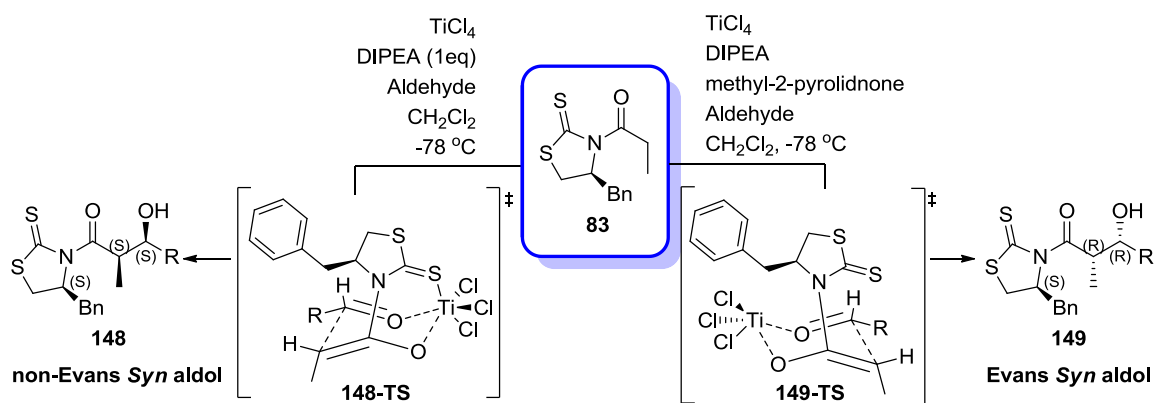


Figure 4.11 The conversion between non-Evans *syn* and Evans *syn* adducts through implementation of different Crimmins chlorotitanium enolate protocols.^{154,180,181}

It is reported that in the 6-membered transition state of the aldol reaction, the thiocarbonyl coordination to the titanium metal centre is less favoured than that of coordination to the diamine.¹⁵⁴ The ability of these chlorotitanium enolate aldol conditions to reverse diastereomeric selectivity through competitive coordination of auxiliary reagents posed the question if excess aldehyde was inducing similar coordination and diastereoselectivity (Figure 4.12).

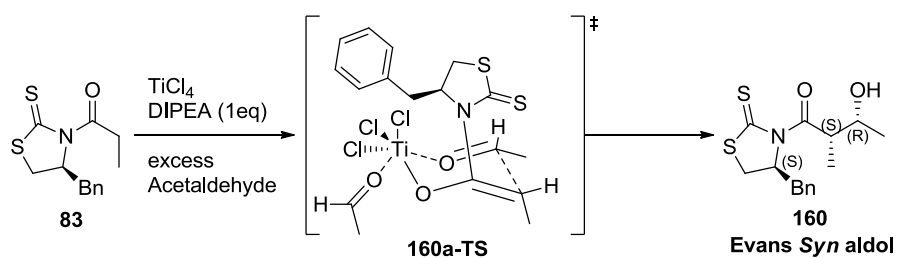


Figure 4.12 The proposed thiocarbonyl decooordination due to interruption by excess acetaldehyde during the aldol transition state, forcing the Evans *syn*-aldol adduct.

These results called into question the originally assigned absolute stereochemistry of both **159** and **160**.¹⁵¹ The aldol adduct **159** had no precedent in the literature and the spectroscopic data could not be directly compared, but the enantiomer of **160**, (2*R*,3*S*)-1-((*R*)-4-benzyl-2-thioxothiazolidin-3-yl)-3-hydroxy-2-methylbutan-1-one (**161**) had been previously reported in a doctoral thesis from the Crimmins group.¹⁵⁵ The enantiomeric *R*-thiazolidinedione chiral auxiliary was used to prepare the Evans *syn* aldol product through the Crimmins Evans *syn*-aldol protocol¹⁸¹ and both the reported ^{13}C and ^1H NMR spectra agreed with that of **160**.¹⁵⁵ The ^{13}C NMR comparison can be seen in Table 4.3, with a focus on the stereogenic carbons of the α -methyl and the β -hydroxy.

Table 4.3 ^{13}C NMR comparison of **160** to that of **(2*R*,3*S*)-1-((*R*)-4-benzyl-2-thioxothiazolidin-3-yl)-3-hydroxy-2-methylbutan-1-one (161)**.¹⁵⁵

160

161

Aldol Adduct	Carbon	160 δ_c	161 δ_c
	5	201.56	201.44
	8	178.51	178.55
	15	136.50	136.37
	17,19	129.59	129.46
	16,20	129.09	128.95
	18	127.44	127.30
	3	68.91	68.79
	12	68.59	68.45
	9	44.53	44.41
	3	36.94	36.78
	7	32.28	32.14
	13	20.37	20.25
	10	10.58	10.48

The optical rotation was found to be the opposite sign but similar magnitude to that of **160** (Lit enti¹⁵⁵: $[\alpha]^{22}_D = -110$ ($c = 16.5$ g/100 mL, CH_2Cl_2); **160**: $[\alpha]^{20}_D = 150$ ($c = 0.19$ g/100 mL, CHCl_3)).¹⁵⁵ These comparisons indicated that **160** was the enantiomer of **161** and the Evans *syn*-aldol adduct, possessing the *S,S,R* absolute stereochemistry. The **159** diastereomer was then implied to contain the non-Evans *syn*-aldol configuration. This finding was contrary to that reported in previous work from 2013¹⁵¹ and was further supported after an X-ray crystal structure was collected from a recrystallised **159** sample. The crystallography data (Figure 4.13) confirmed **159** as **(2*R*,3*S*)-1-((*S*)-4-benzyl-2-thioxothiazolidin-3-yl)-3-hydroxy-2-methylbutan-1-one**, and the non-Evans *syn*-aldol adduct with the *R,S,S* absolute stereochemistry. These results indicated to the ability of excess aldehyde in the reaction mixture to interfere with the thiocarbonyl coordination to the titanium metal centre and allow for unselective or complete reversal of diastereomeric selectivity.

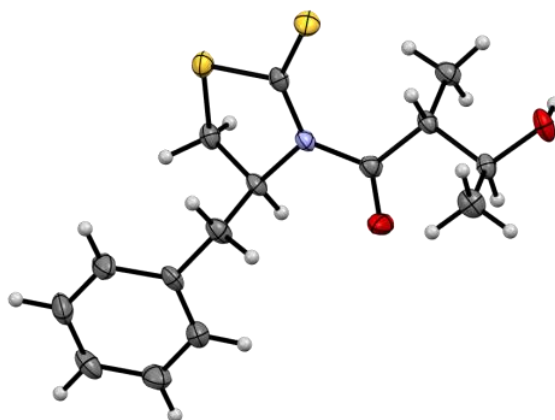


Figure 4.13 X-ray crystal structure of **159** displaying **(2*R*,3*S*)-1-((*S*)-4-benzyl-2-thioxothiazolidin-3-yl)-3-hydroxy-2-methylbutan-1-one** non-Evans *syn* stereochemistry.

4.5 Stereochemical revision of 73 from 2013 Honours work

The thorough investigation into the impact of differing molar equivalents of acetaldehyde in the Crimmins chlorotitanium enolate aldol protocol with thiazolidinedione chiral auxiliary, specifically in the preparation of **159** and **160** has concluded that the aldehyde competes for coordination to the titanium metal atom with the sulfur atom of the chiral auxiliary. In situations of excess aldehyde the chiral auxiliary is crowded out and is no longer involved in complexation with titanium metal atom, favouring Evans aldol adduct products. The major diastereomeric adduct is therefore dependent on the molar equivalent of aldehyde, with non-Evans adducts given when one equivalent is present and Evans adducts resulting from excess aldehyde. As previous work from 2013¹⁵¹ utilised excess amounts (*ca.* 10 molar equivalents) the resulting major diastereomeric adduct did not conform with that expected from the Crimmins protocol (non-Evans *syn*-aldol adduct) and instead provided the Evans *syn*-aldol adduct. The investigation provided matching analytical data to support this as a result the previous work from 2013¹⁵¹ had to have the assignment for adduct **84** and subsequent synthetic products converted to the corrected stereochemistry. This included a stereochemical revision of the final compound **228** from *S,S* to *R,R* at positions C11 and C12 and in turn revising the stereochemical assignment for the Nocapyrone C natural product.

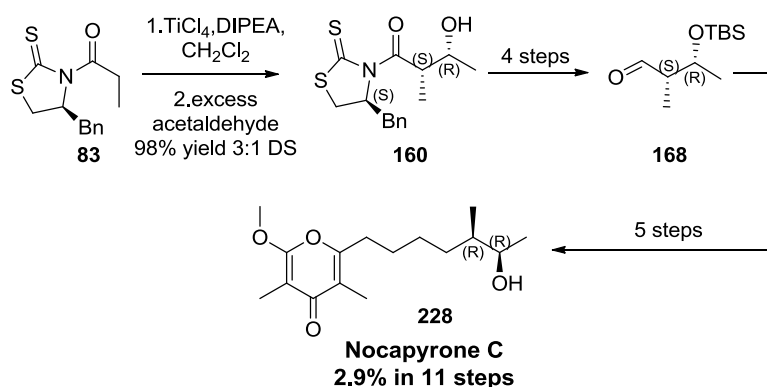
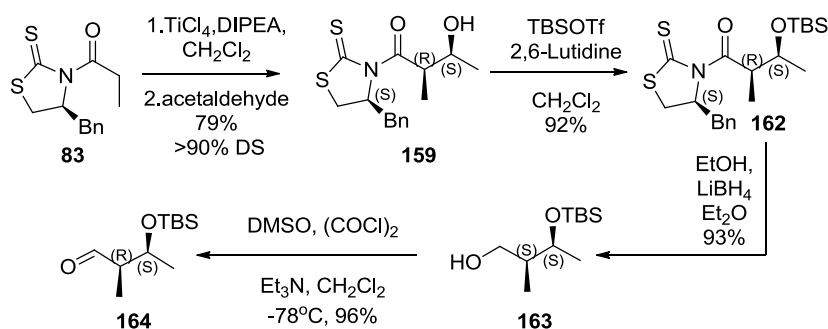


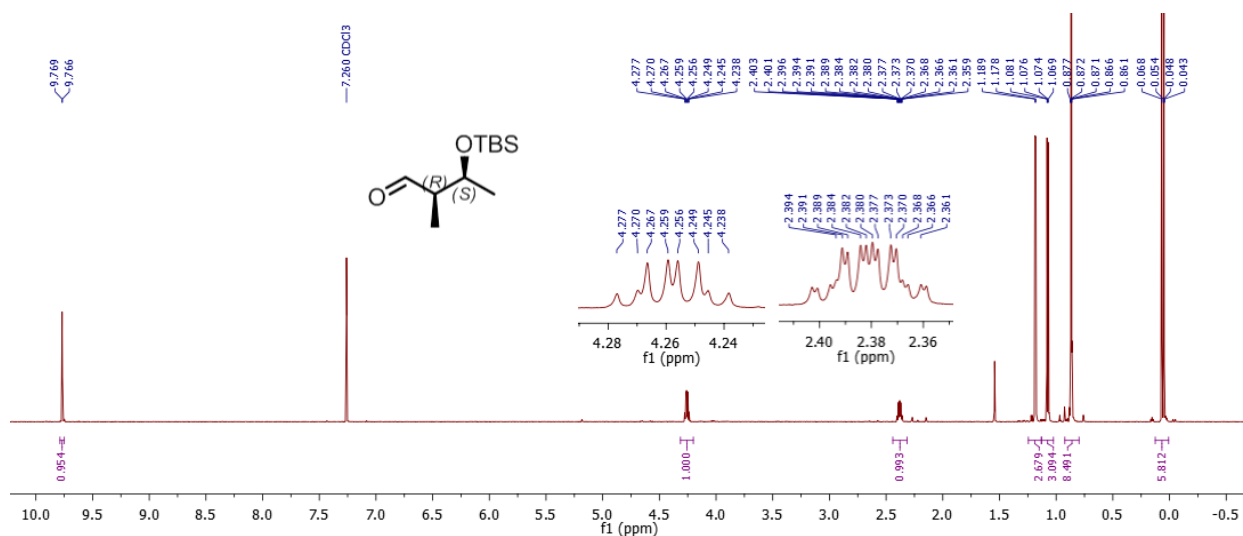
Figure 4.14 Revision of synthetic work 2013 Honours including stereochemical reassignment of intermediates and final synthetic compound **228**.¹⁵¹

4.6 Acquisition of aldehyde 164

Taking into account the recent understanding of aldehyde requirements, the Crimmins protocol was performed with slow addition of cold acetaldehyde to give **159** as the non-Evans aldol adduct in 79 % with 9:1 dr. Then, the free hydroxyl of **159** was protected with TBS triflate in the presence of 2,6-Lutidine to give the TBS ether **162** in excellent yield. The thiazolidinedione chiral auxiliary was reductively cleaved with LiBH_4 to give the primary alcohol **163** (92 %) and Swern oxidation afforded the aldehyde **164** ready for coupling and chain extension (Figure 4.15).

Figure 4.15 Acquisition of aldehyde **164**

The ^1H NMR spectrum of aldehyde **164** (Figure 4.16) exhibited interesting coupling signals at the tertiary stereogenic protons as with the signal at δ 4.26, displaying a quartet of doublets from coupling between the methyl at δ 1.18 and the α stereogenic proton at δ 2.38, concluding its positions as a tertiary proton under the TBS ether. The signal at δ 2.38 showed a quartet of doublets of doublets from coupling with both the aldehyde at δ 9.77 and the methyl at δ 1.07 and the tertiary proton at δ 4.26, giving its position as the single stereogenic proton α relative to the aldehyde functional group. The TBS protecting group is characterised by the shielded signals from the singlet at δ 0.87 from the 9 protons of the tetrabutyl terminating end and the strongly shielded signal at δ 0.06 attributed to the 6 protons from both methyl groups connected to the silicon atom.

Figure 4.16 ^1H NMR spectrum of aldehyde **164**

4.7 Acquisition of aldehyde **168**

Since Evans aldol adduct **160** was isolated in significant quantities (3.21 g) from previous under-selective aldol reactions, it was feasible to incorporate this material in route development and final structural elucidation of either Nocapyrone or Violapyrone natural products. Therefore it was decided to optimise the alternative protocol for the Evans aldol product.

The aldol reaction used the optimised parameters reported by Crimmins¹⁵⁵ for the selective induction of *S,R* stereochemistry through the use of *N*-methyl-2-pyrrolidinone as a competitive chelator of the chlorotitanium enolate during the aldol reaction. The preparation of **160** was able to be optimised to 84 % yield and 94 % ds. The Evans aldol adduct **160** was consolidated and then TBS protected to the TBS ether **165** in 94 % yield. Reductive cleavage and Swern oxidation progress to aldehyde **168** (88 %, over two steps) under the same protocols as with **164** (Figure 4.17).

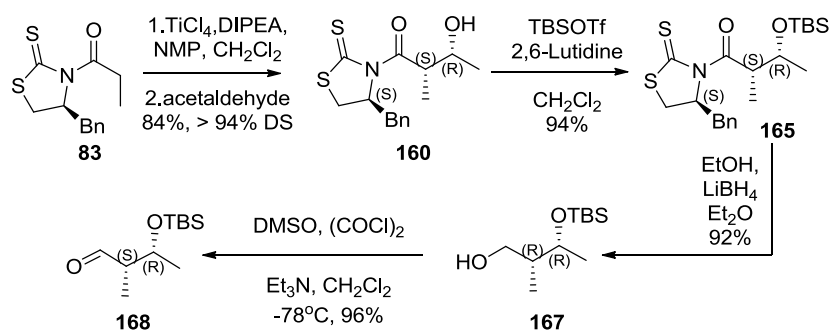


Figure 4.17 Optimised Crimmins Evans-aldol protocol and acquisition of aldehyde 168

The aldol adduct diastereomers **159** and **160** differ both spectroscopically at the tertiary α stereogenic and tertiary β -hydroxy protons, and the methyl peaks within the ^1H NMR. The comparisons are shown in above in Figure 4.8, Figure 4.9 and Figure 4.10. The diastereomers are also easily physically separated over a generous chromatographic column and a relatively non-polar mobile phase (5-10% EtOAc/hexane). Unlike the aldol adducts the TBS ethers **162** and **165** are unable to be separated physically through column chromatography and require separation in the previous step. The spectral data (Figure 4.18) between the **162** and **165** TBS ethers differs significantly enough for easy distinction, specifically between the methyl groups (**162**: δH 1.21 (dd, $J = 6.5, 5.6$ Hz, 6H); **165**: δH 1.21 (d, $J = 6.8$ Hz, 3H), 1.17 (d, $J = 6.2$ Hz, 3H)), tertiary α (**162**: δH 4.62 (qd, $J = 6.8, 5.7$ Hz, 1H); **165**: δH 4.53 (qd, $J = 6.8, 5.2$ Hz, 1H)), and tertiary β -hydroxy (**162**: δH 4.24 (p, $J = 6.0$ Hz, 1H); **165**: δH 4.15 – 4.08 (m, 1H)) stereogenic centres.

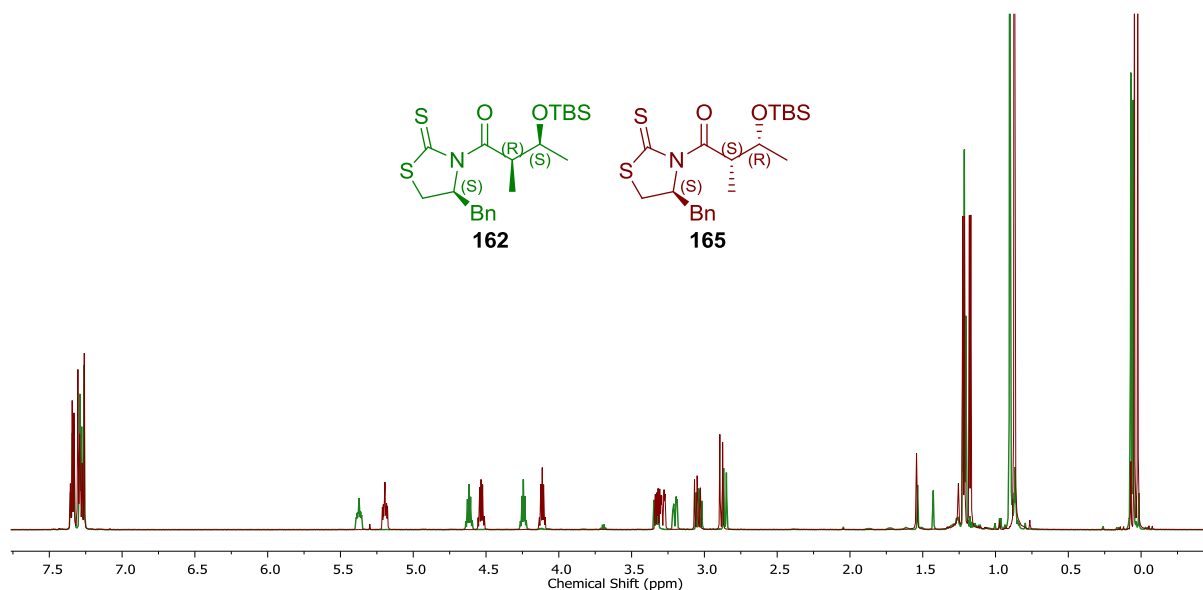


Figure 4.18 Comparison of ^1H NMR spectroscopic data between **162 (green) and **165** (red) TBS ethers.**

Spectroscopically, alcohol **167** and aldehyde **168** did not differ to that of **163** and **164** respectively as they were enantiomers of each other and only displayed the opposite sign but similar magnitude in optical rotation experiments, as would be expected of enantiomers (Table 4.4).

Table 4.4 Optical rotation measurements of enantiomers **163, **164** and **167**, **168****

non-Evans	Evans
<p>163 $[\alpha]_{\text{D}}^{20} = 13.8$</p>	<p>167 $[\alpha]_{\text{D}}^{20} = -5.5$</p>
<p>164 $[\alpha]_{\text{D}}^{20} = -37.9$</p>	<p>168 $[\alpha]_{\text{D}}^{20} = 42.2$</p>

With both **164** and **168** aldehydes available, the development of coupling and chain extension protocols could progress. The linker had a requirement to span 4-carbons in length and be incorporated in two coupling reactions at opposite ends, so a mixture of functionality and protection were required.

4.8 Paterson Aldol Protocol for *anti* Stereinduction

With *syn* stereo-induced aldol fragments available, a protocol had to be established for the production of *anti* relative stereochemistry to ensure the utility of stereoelucidation. Access to *anti*-aldol adducts has been achieved through the use of oxazolidinone and thiazolidinethione chiral auxiliaries, with catalytic magnesium metal chelation (Figure 4.19). However, the protocols

invoke the use of non-enolisable aldehydes as substrates.^{187,188} Unfortunately, these approaches are incompatible with the current system requirements.

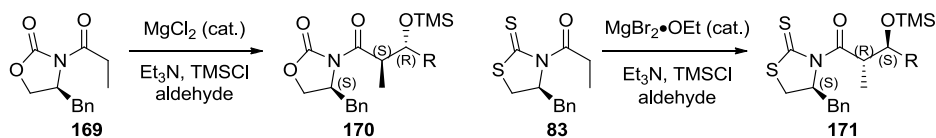


Figure 4.19 Access to *anti*-aldol adducts through Mg-catalyzed reactions with chiral auxiliaries

Unlike the installation of *syn* stereochemistry through asymmetric aldol, *anti*-stereoinduction can be more challenging. It was decided that pursuing the well established Paterson aldol^{189–191} protocols, utilising boron enolates of chiral lactate-derived ketones for *anti*-stereoinduction, would be ideal (Figure 4.20). A combination of enolate geometry and auxiliary steric bulk protecting the latent lactone hydroxyl influences the transitional state into the desired stereochemical outcome. The ketone reagents were derived from the preceding (*S*)-ethyl (**172**) or (*R*)-isobutyl lactate esters and protected as either the sterically bulky benzyl ether (**175**) or the benzoate ester (**173**). The inclusion of 4 variables allows for a variation between 4 absolute stereochemistries of the two newly formed stereocenters from the asymmetric aldol reaction. The hydroxy protecting groups direct the relative stereochemistry of either *syn* or *anti*, with benzyl protection resulting in *syn* and benzoyl protection resulting in *anti*. The relative stereochemistries are further enantiomerically controlled by the directing influence of the latent hydroxy stereocenter carried through from the original lactate ester. The *S* ketones provide access to 2*S*, 4*R*, 5*S* *syn*-aldol adducts (**176**) when benzyl protected, and 2*S*, 4*R*, 5*S* *anti*-aldol adducts (**174**) when benzoyl protected, with *R* ketones providing their enantiomers.

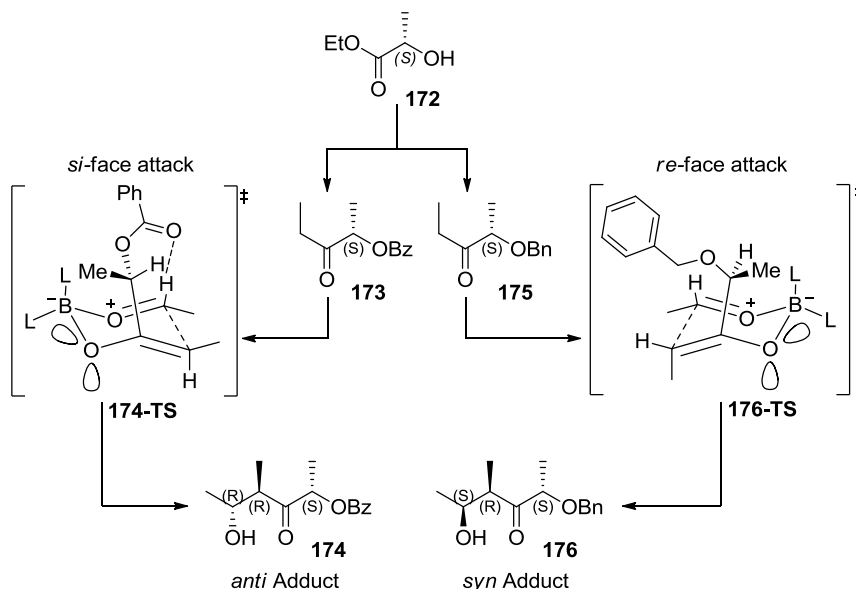


Figure 4.20 The access of either *syn* or *anti* aldol adducts through substrate control of (*S*)-ethyl lactate derived ketones in boron mediated aldol reactions^{189–191}

The rationale for *anti*-aldol stereinduction is proposed to be through *si*-face selectivity during the 6 membered transition state (**174-TS**), with both the sterics and electronics of substituents contributing to the result (Figure 4.20). The transition state is expected to limit configurations which reduce axial 1,3 allylic strain. To reduce destabilising electronics of lone-pair repulsions, it is proposed that the benzoate carbonyl oxygen participates in hydrogen bonding with the aldehyde hydrogen.¹⁹¹

4.9 Lactate derived (*S*)-ketone **173** preparation

The ketones required for *anti* stereinduction were prepared through the protocol set out by Paterson^{189–191} (Figure 4.21) with the (*S*)-ketone **173** derived from (*S*)-ethyl lactate **172** via conversion to Weinreb amide **177** in 71% yield. Ketone conversion proceeded by subjection to ethyl Grignard and protection of free hydroxyl with DMAP, DIPEA, and benzoic anhydride over 16 hours, providing the (*S*)-ketone **173** in 40%. Smaller scale preparation saw better conversion rates than those of larger scale reactions but was consistent with attempts conducted in literature.^{192,193}

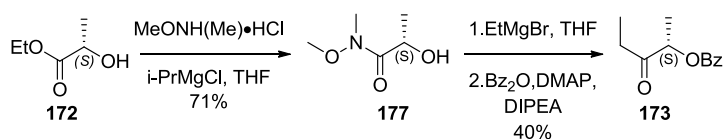


Figure 4.21 Preparation of (*S*)-ketone **173** from (*S*)-ethyl lactate **172**

4.10 Acquisition of *R,R* aldehyde **180**

The chlorodicyclohexylborane Lewis acid required for the aldol reaction was prepared through the addition of cyclohexene to a solution of monochloroborane-methyl sulfide complex and distillation of pure dicyclohexylboron chloride in 96% yield.¹⁹⁴ With the (*S*)-ketone **173** available, the *E*-enolate was induced through dicyclohexylboron chloride and dimethylethylamine and subjected to acetaldehyde garnished the *anti*-aldol adduct **174** in 98% yield and excellent diastereomeric selectivity (Figure 4.22).

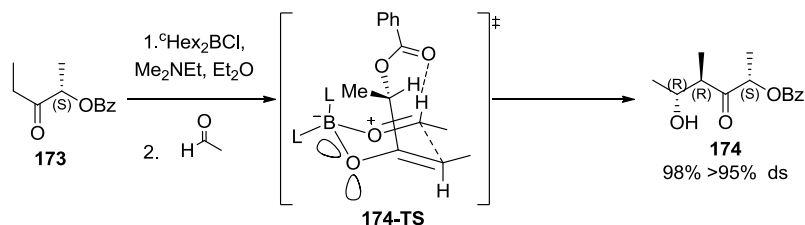


Figure 4.22 Boron-mediated aldol reaction with acetaldehyde resulting in *anti*-stereinduction and **174**

The spectroscopic data (Figure 4.23) for the aldol adduct **174** provided evidence of a 1,2-*anti* relationship from the diagnostic large vicinal coupling constant ($J_{1,2} = 6.4\text{--}7.2$ Hz) between the

diastereotopic protons.^{191,195,196} The ¹H NMR data showed a clean single diastereomer, displaying the aromatic protons at δ 8.12 – 8.06 (m, 2H), δ 7.59 (t, $J = 7.4$ Hz, 1H), and δ 7.46 (t, $J = 7.7$ Hz, 2H) corresponding to the benzylic protecting group. The quartet at δ 5.45 is produced by the stereogenic proton of the protected hydroxyl which couples ($J = 7.1$ Hz) to the methyl at δ 1.58 (d, $J = 7.1$ Hz, 3H), and both originate from the (*S*)-ketone substrate. The heptet at δ 3.99 accounts for the diastereotopic proton of the installed β -hydroxy which couples ($J = 6.4$ Hz) to the methyl at δ 1.24 (d, $J = 6.4$ Hz, 3H). The pentet at δ 2.81 accounts for the diastereotopic proton of the installed α -methyl which couples ($J = 7.2$ Hz) to the methyl at δ 1.26 (d, $J = 7.2$ Hz, 3H). The hydroxyl proton is seen at δ 2.38.

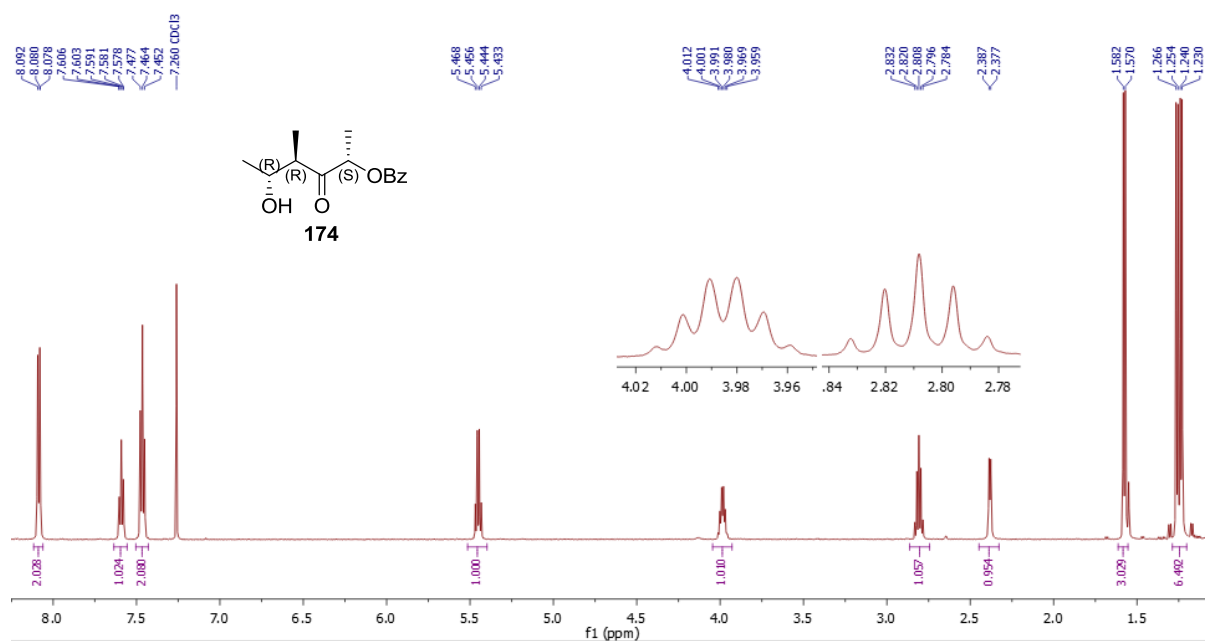


Figure 4.23 ¹H NMR spectroscopic data of aldol adduct **174**

The *anti*-aldol adduct **174** had the newly installed β -hydroxyl protected with TBS chloride and imidazole to give the TBS ether **178** in 95% yield. The TBS ether **178** was treated with reductive deprotecting conditions with LiBH₄, providing the diastereomeric mixture of diol **179** in 87% yield. This same reductive deprotection was also pursued with LiAlH₄ in 85% yield. The final step saw the diol oxidatively cleaved with sodium periodate in aqueous methanol providing the TBS protected aldehyde **180** in 92% yield (Figure 4.24). Aldehyde **180** was documented as unstable^{197,198} and prolonged reaction or storage resulted in degradation of the aldehyde. The reaction pathway was halted at the diol **179** and only converted to the aldehyde through oxidative cleavage prior to immediate use in the next synthetic step.

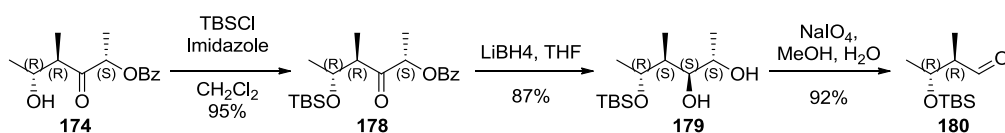


Figure 4.24 Acquisition of aldehyde 180 from *anti*-aldol adduct 174

The implementation of asymmetric aldol mediated with chiral auxiliaries allowed for the preparation of the *syn*-aldol **164** and **168** aldehydes, as well as the *anti*-aldol **174** aldehyde fragments. The *syn*-aldol fragments, **164** and **168**, were accessed through the implementation of thiazolidinethione chiral auxiliaries in combination with titanium enolates, with protocols developed by Crimmins.^{154,180,181} The *anti*-aldol fragment, **180**, was accessed through lactate derived ketone aldol protocols developed by Paterson.^{189–191} Progression through the synthetic route seeks to couple these stereocontrolled terminating fragments with the proposed 4-carbon linker fragment to complete the side chain prior to addition to a β -keto ester and finalising the full linear structural skeleton. The linear skeleton would be further progressed through cyclisation to the pyrone heterocycle and pyrone natural products. Chapter 5 will discuss the development of the 4-carbon linker and the protocols for coupling as well as the progression to β -keto addition and cyclisation. The attempts towards Nocapyrone and Violapyrone natural products and accompanying spectral analysis will also be discussed.

5 Linker Development and Natural Product Synthesis

5.1 Introduction

With both *syn* and *anti* aldehydes (**159**, **160** and **180**) successfully acquired, the next stage in forward synthesis development would include the crucial side-chain coupling and chain extension protocols. The linker had a requirement to span 4-carbons in length and be incorporated in two coupling reactions at opposite ends so the establishment of a mixture of functional groups and protecting tactics were called upon. The optimal functional group variation would be incorporated into coupling between the stereocontrolled aldehydes (**159**, **160** and **180**) and dianion addition to β -keto esters variants (ethyl 2-methyl-3-oxopentanoate **19** and ethyl 2-methylacetoacetate **188**) to form the precursory tricarbonyl units required for pyrone cyclisation. The model natural product systems of Nocapyrone H and Violapyrone I would be pursued as a way to optimise the coupling, β - γ -diketo ester preparation, and cyclisation protocols.

5.2 Development of Linker 187

The synthetic strategy aimed to utilise a butanediol derivative for the foundation of the linker fragment, with robust mono protection on one hydroxyl functionality while conversion to Wittig-type reagent occurred on the other end. Preparation began with selective protection of butanediol with BnBr in strong alkaline conditions and provided the benzyl protected mono-alcohol **131** in 90% yield (Figure 5.1). Conducting the selective protection with the benzyl bromide as the limiting reagent allowed for full consumption of starting material and removed any adverse workup conditions and simpler purification. **131** was then converted to the bromide via Mitsunobu reaction giving bromide **181** in 75% yield. However, the conversion to the Wittig salt **182** was found to be problematic and, after a number of attempts, insignificant amounts of reagent were produced to be able to conduct proper olefination tests with aldehyde substrates.

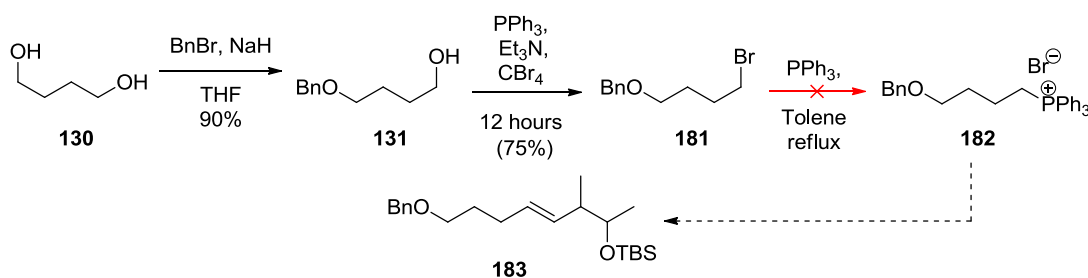


Figure 5.1 Attempted preparation of Wittig salt 182 from butanediol 130.

With the inability to prepare a Wittig salt **182** for an olefination, it was decided to install sulfone functionality for a Julia-type olefination. With a number of different reagent types to choose from, including phenyl sulfone (classic Julia), benzothiazole sulfone (modified Julia), and tetrazole sulfone (Julia-Kocienski), a suitable reaction setup could be developed to deliver an optimal coupling.

The first attempt utilised the mercaptobenzothiazole auxiliary group for attachment to the butanediol linker (**131**) which was prepared through Mitsunobu reaction, substituting the mono-alcohol for the sulfide **184** in 96% yield (Figure 5.2).

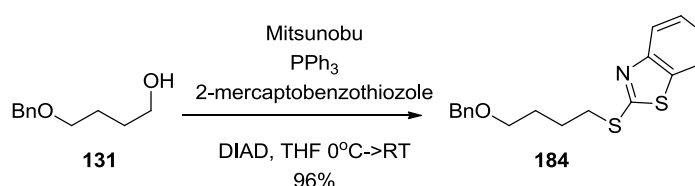
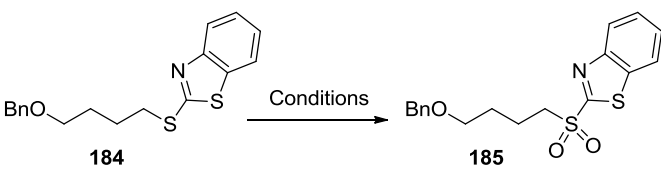


Figure 5.2 Preparation of benzothiazole sulfide **184 from benzyl protected butanediol **131**.**

The oxidation from sulfide to sulfone is commonly performed with mCPBA^{199–204} and the protocol was utilised on the oxidation of sulfide **184**. However, even after overnight reaction, the conversion only extended to the sulfoxide in 75 % yield. Other oxidation tactics were examined to rectify the under oxidation, with a preference towards protocols suitable for scale-up (Table 5.1). Protocols which would require expensive or hazardous reagents lower in utility as the scale of reaction increases and are especially evident with organic peroxides which pose an explosive hazard. A test was carried out to see if the auto-oxidation of aldehydes to peroxy acids²⁰⁵ would assist in the oxidation to sulfone, with the oxygen being provided by compressed air bubbling through a heating mixture of isobutyraldehyde in acetonitrile at 80 °C overnight. The reaction was successful in oxidising the sulfide, although a mixture of sulfide, sulfoxide, and sulfone were observed by TLC even after overnight reaction. This reaction showed promise with the use of oxygen (from compressed air) as the stoichiometric oxidant, but it was found that the reaction apparatus resulted in excessive evaporation of isobutyraldehyde which contributed to poor performance.

Potassium peroxymonosulfate, commercially known as Oxone®, was also tested as a stoichiometric oxidant for the oxidation to sulfide. When used in a methanolic solution in water, a 90% yield was seen exclusively to the sulfone after overnight reaction, with slow warming from 0 to 24 °C. When catalytic amounts of NaCl are added into the reaction mixture, the decomposition of Oxone® increased, as did the rate of oxidation.²⁰⁶ The Oxone® oxidation of sulfide **184** to sulfone **185** was carried out in a suitably simple, cheap, and efficient manner, confirming it as the reaction which would be carried through to larger scales.

Table 5.1 Oxidation reactions examined for the preparation of sulfone 185



Conditions	Temp	Time (h)	Yield
mCPBA, DCM	0 → 24 °C	18	Sulfoxide 75 %
(CH ₃) ₂ CHCHO, CH ₃ CN, Air	80 °C	18	mixture
Oxone, H ₂ O/MeOH	0 → 24 °C	18	90 %
Oxone, cat NaCl, H ₂ O/MeOH	0 → 24 °C	5	90 %

With both the sulfone **184** and stereocontrolled aldehyde fragments (**159**, **160** and **180**) now available, the olefination reaction condition could be properly investigated and optimised (Table 5.2).

Table 5.2 Screening of reaction condition for Julia olefination.



Conditions	Aldehyde	Temp	Time (h)	Result
Pre-metallation, LDA, THF	2-methylbutyraldehyde	-78 → 26 °C	3	complex
Pre-metallation, LDA, THF	2-methylbutyraldehyde	0 → 26 °C	16	mixture
Barbier, LDA, THF	2-methylbutyraldehyde	-78 → 26 °C	3	Self condensation
Barbier, LDA, THF	2-methylbutyraldehyde	0 → 26 °C	16	Self condensation
Pre-metallation, LHMDS, THF	benzaldehyde	0 → 24 °C	5	Single product
Barbier, LHMDS, THF	159	0 °C	1	186 >95% yield

The optimisation saw both pre-metallated and Barbier conditions tested at a range of reduced temperatures (-78 → 26 °C and 0 °C to RT), while being subjected to model aldehydes (2-methylbutyraldehyde and benzaldehyde). Conclusion of tested reaction conditions found that pre-metallation of the sulfone before submission to aldehyde generally resulted in poor conversion. Initially it was suspected that the cold temperature conditions (-78 °C) were not allowing for correct deprotonation and resulting in side-product formation. Warmer temperatures (0 °C) coupled with prolonged metalation and reaction time showed little to no improvement. It was suspected that a self-condensation side product of the sulfone could be at fault. Even when the pre-metallation was replaced with Barbier conditions, where LDA was added to a mixture of sulfone **185** and 2-methylbutyraldehyde, the reactions gave inconclusive results with either temperature range. The results only resolved when the base (LDA) was exchanged for LHMDS, with short pre-metallation conditions (10 minutes) and reaction with benzaldehyde, where a single product was seen on TLC after 10 minutes. The best results were found with the use of Barbier

conditions with combination of LHMDS and optimisation with **159**, which provided a mixture of olefination isomers **186** in > 95% yield in under an hour at 0 °C.

The olefination was found to be non-selective towards neither E nor Z isomers, as was evidenced by a 1:1 ratio between the vinyl protons in the ¹H NMR (Figure 5.3). The olefination with benzothiazole sulfone **185** substrate was not expected to provide any selectivity towards any specific olefin isomer and there appeared to be no directing effects from the stereochemically pure aldehyde **159**. As the next synthetic step sought to saturate and debenzylate the chain, the olefin isomers were of no consequence and require no further separation. These optimised olefination reaction conditions were utilised for the chain extension of **159**, **160** and **180** stereoisomers without alteration.

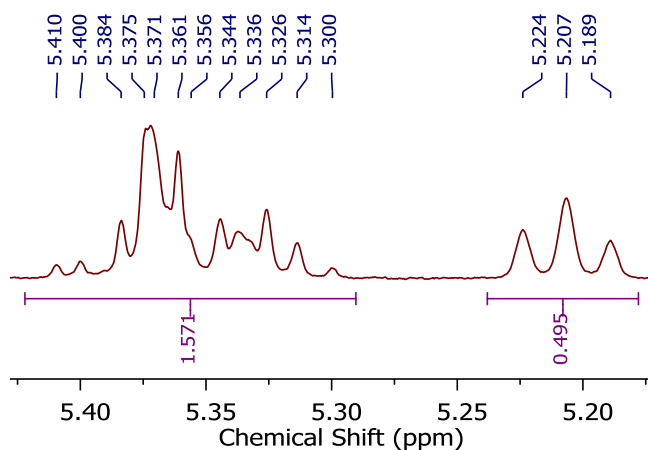


Figure 5.3 ¹H NMR spectroscopic data of vinyl protons from isolated olefination **186** products.

The reduction and debenzylation of **186** to the saturated alcohol **187** was done through hydrogenation. Initially, the hydrogenation of **186** was conducted with 10% Pd/C and in ethanol, but the yield was recorded between 70-77% and reaction time could be between 1-3 days until TLC showed consumption of starting material. Some batches showed partial loss of the TBS protecting group and residual moisture and acidity was suggested as contributing to the loss. The hydrogenation was optimised to use ethyl acetate as the solvent and the addition of molecular sieves to the reaction mixture saw yield climb to 94% of the saturated alcohol **187**, with only overnight reaction. The optimised preparation of saturated alcohol **187** from propionyl thiazolidinethione **83** was able to reach 59 % overall yield (Figure 5.4).

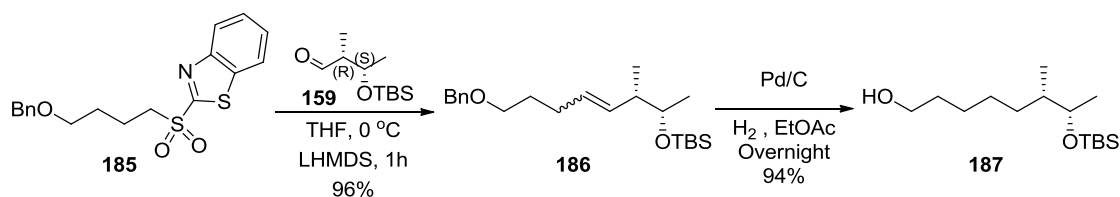


Figure 5.4 The optimised preparation of saturated alcohol **187**

The spectroscopic data of **187** (Figure 5.5) was able to characterise it as the desired saturated alcohol. The NMR data evidenced the stereogenic oxygen-bearing carbon (δC 71.79, δH 3.70 – 3.66 (m, 1H)), the primary alcohol bearing carbon (δC 63.27, δH 3.64 (t, $J = 6.7$ Hz, 2H)), the 4 contiguous methylene carbons (δC 40.40, 33.00, 32.66, 27.48; δH 1.57 (ddt, $J = 8.4, 6.7, 3.6$ Hz, 3H), 1.51 – 1.17 (m, 5H)), the methyl groups (δC 20.67, δH 1.05 (d, $J = 6.3$ Hz, 3H); δC 14.76, δH 0.82 (d, $J = 6.8$ Hz, 3H)) and the TBS ether (δC 26.23, 26.04, δH 0.88 (s, 9H); δC -4.09, -4.66, δH 0.03 (d, $J = 7.1$ Hz, 6H)).

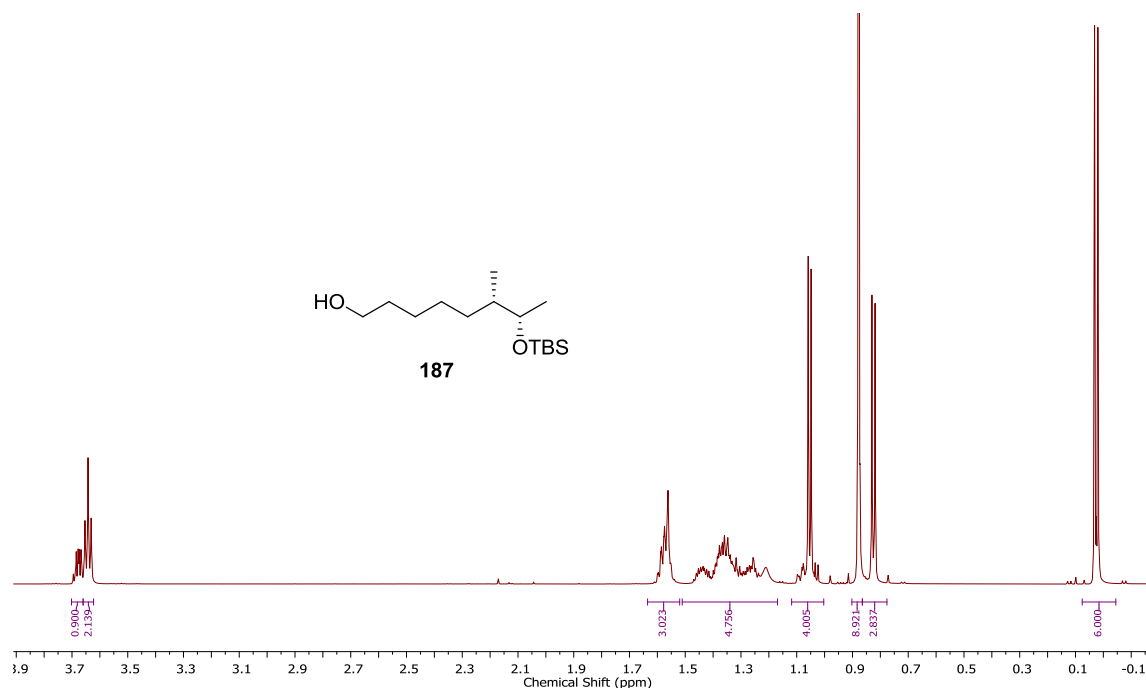


Figure 5.5 ^1H NMR spectroscopic data of saturated alcohol **187**

With the saturated alcohol **187** obtained, the hydroxyl would have to be oxidised to an activated form suitable for, and coupled to, the β -keto ester in anticipation of the prerequisite triketo unit required for pyrone cyclisation. To ensure both oxidation and addition conditions are optimised, the model natural product systems of Nocapyrone H and Violapyrone I were pursued.

5.3 Synthesis of Nocapyrone H and Violapyrone I natural products

The synthesis of both Nocapyrone H and Violapyrone I relied on suitable and functional addition to the β -keto ester as a cornerstone of their synthesis. To address this, optimisation screened the Huckin-Weiler dianion addition of octane imidazolide and octanal to ethyl 2-methyl-3-oxopentanoate **19** and ethyl 2-methylacetoacetate **188** β -keto esters to determine the most efficient coupling method (Table 5.3).

Table 5.3 Screening reaction conditions for efficient production of triketo precursors.

19: R = Me
188: R = H

Y = OH
Y = O

Conditions A	R	X	Temp	Conditions B	product	Yield
NaH, nBuLi, THF, 16h	H	Im	-78 → 20 °C	-	189	65%
NaH, nBuLi, THF, 3h	H	Im	-78 → 20 °C	-	189	-
NaH, nBuLi, THF, 3h	H	H	RT	DMP, 16 h	189	49%
NaH, nBuLi, THF, 3h	Me	H	RT	DMP, 16 h	146	46%
NaH, nBuLi, THF, 16h	Me	Im	RT	-	146	31%

The screening showed that even though octane imidazolide was effective in forming the Violapyrone relevant triketo **189** in 65 % yield through overnight reaction, the method did not translate well to the Nocapyrone relevant triketo **146** (Figure 5.6). It was found that the acylating conditions of Huckin-Weiler dianion addition of octane imidazolide with ethyl 2-methyl-3-oxopentanoate **19** only produced modest at 31 %. The dianion additions performed best on aldehyde substrate, preparing the triketo **146** in 46 % yield after oxidation of the γ -hydroxy keto ester. These results correlated similarly to the previous results (Table 3.2) conducted in the first generation synthetic strategy (Chapter 3). The resulting γ -hydroxy keto esters from the aldol-type additions require oxidation before they can be subjected to cyclisation. The oxidation was conducted with the use of the mild Dess-Martin periodinane (DMP) reagent with reasonable results.

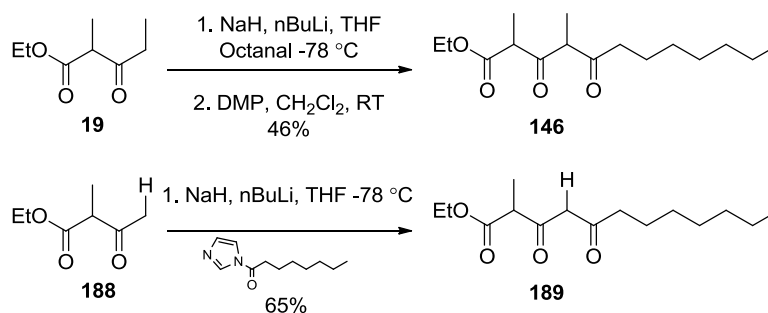


Figure 5.6 The optimised reaction conditions for Violapyrone I and Nocapyrone H relevant triketo units

The optimised reaction conditions, previously discussed in Chapter 3, were utilised for the successful synthesis of Nocapyrone H (Figure 5.7). The 4 step synthesis of Nocapyrone H **76** was completed in 17 % yield and spectral analysis showed a strong structural correlation to that of the natural product isolating data (Table 5.4).^{150,168,178} The late-stage regio-selective methylation with methyl triflate was an important development which can be carried through to other Nocapyrone natural products and derivatives.

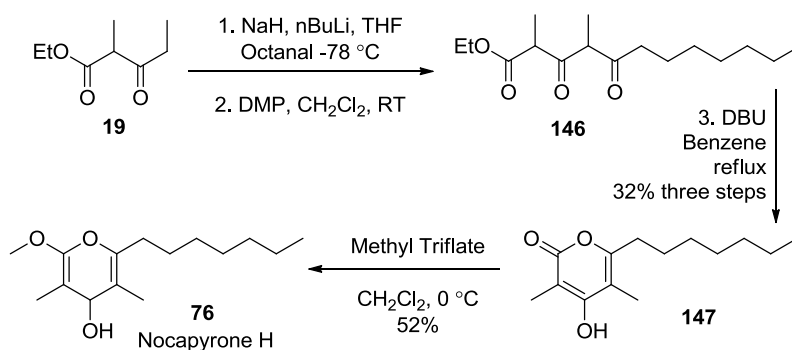


Figure 5.7 Synthesis of Nocapyrone H 76 including methyl triflate regio-methylation

The NMR Spectroscopic Data for the synthetic Nocapyrone H was consolidated in Table 5.4 and provided a good comparison to the reported structure of Nocapyrone H.^{150,168,178}

Table 5.4 NMR Spectroscopic Data (600 MHz, CDCl₃) of synthetic methoxy-pyrone 76.

Nocapyrone H	position	δ_c	multi	δ_H (J in Hz)	COSY & HMBC
	2	162.26	C		
	3	99.47	C		
	4	181.22	C		
	5	118.38	C		
	6	158.57	C		
	7	30.84	CH ₂	2.58, t (7.5)	
	8	27.20	CH ₂	1.64, p (7.5)	
	9	29.20	CH ₂	1.40-1.17, m	
	10	29.15	CH ₂	-	
	11	31.86	CH ₂	-	
	12	22.76	CH ₂	-	
	13	14.21	CH ₃	0.89, t (6.9)	
	14	10.11	CH ₃	1.85, s	
	15	7.02	CH ₃	1.94, s	
	16	55.39	CH ₃	3.95, s	

The spectroscopic structural analysis provided evidence of a γ -pyrone through the characteristic carbon chemical shifts of C-2 to C-6 (δ_C 162.26, 99.47, 181.22, 118.38, 158.57), with the γ -methoxy characterised by both C-2 and C-16 (δ_C 162.26; δ_C 55.39, δ_H 3.95 (s, 3H)). The methyl substitutions C-14 and C-15 (δ_C 10.11, δ_H 1.85 (s, 3H); δ_C 7.02, δ_H 1.94 (s, 3H)) on the pyrone ring were also confirmed by HMBC correlations. The C-6 substituted sidechain correlated well with 2D NMR experiments and all characteristics are consistent to similar α -methoxy- γ -pyrone structures in literature.^{88,111,115,116,207-212} The spectroscopic analysis determined that the structure was consistent with the reported structure of Nocapyrone H.^{150,168,178}

The synthesis of Violapyrone I utilised the Huckin-Weiler dianion acylation of ethyl 2-methylacetoacetate **188** β -keto ester with octane imidazolide in 66% yield and DBU mediated cyclisation of triketo **189** garnered pyrone **106** in 75% yield (Figure 5.8).

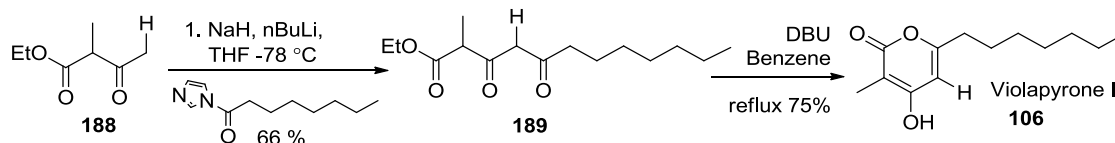


Figure 5.8 Synthesis of Violapyrone I through optimised protocol

The spectroscopic analysis (Table 5.5) of α -pyrone **106** displayed the signals characteristic of α -pyrone chemical structures^{158,159,162,213} beginning with the ring carbon environments of C-2 to C-6 (δ_C 169.4; 98.84; 168.24; 101.19; 164.87), and the methyl C-14 (δ_C 8.23, δ_H 1.85 (*s*, 3H)) and C-5 (δ_C 101.19, δ_H 5.98 (*s*, 1H)) ring substitutions. The C-6 (δ_C 164.87) position was confirmed to host the 7 membered saturated sidechain of C-7 to C-13 (δ_C 34.24, δ_H 2.47 (*t*, $J = 7.6$ Hz, 2 H); δ_C 27.95, δ_H 1.70 - 1.60 (*m*, 2 H); δ_C 30.06, δ_H 1.42 - 1.23 (*m*, 8 H); δ_C 29.94, δ_H 1.42 - 1.23 (*m*, 8 H); δ_C 32.85, δ_H 1.42 - 1.23 (*m*, 8 H); δ_C 23.66, δ_H 1.42 - 1.23 (*m*, 8 H)). The structure of 6-heptyl-4-hydroxy-3-methyl-2*H*-pyran-2-one was confirmed for the final product **106**.

Table 5.5 NMR Spectroscopic Data (600 MHz, methanol-*d*₄) of synthetic **106 with comparison to Violapyrone I¹⁵⁷**

COSY & HMBC	position	δ_C	multi	δ_H (J in Hz)	Comparison Isolated & Synthetic δ_C
		2	169.4	C	
	3	98.84	C		
	4	168.24	C		
	5	101.19	CH	5.98, <i>s</i>	
	6	164.87	C		
	7	34.24	CH ₂	2.47, <i>t</i> (7.6)	
	8	27.95	CH ₂	1.70-1.60, <i>m</i>	
	9	30.06	CH ₂	1.42-1.23, <i>m</i>	
	10	29.94	CH ₂	"	
	11	32.85	CH ₂	"	
	12	23.66	CH ₂	"	
	13	14.38	CH ₃	0.90, <i>t</i> (6.9)	
	14	8.23	CH ₃	1.85, <i>s</i>	

The spectroscopic comparison with the synthetic product **106**, confirmed correlation with the isolated natural product Violapyrone I,¹⁵⁷ with ¹H NMR data matching closely and deviation of the ¹³C NMR between the synthesised and isolated products were found to be no more than $\delta_C \pm 0.66$ ppm. Therefore, it was determined that Violapyrone I was successfully synthesised in 2 steps and 50 % yield from octane imidazolide.

With both natural products, Violapyrone I and Nocapyrone H, successfully synthesised, the optimised model systems can be implemented onto the functionalization of future linkers.

5.4 Concluding Linker Functionality

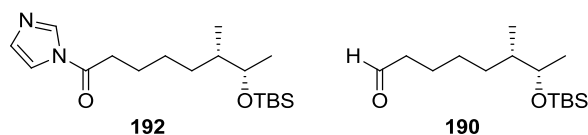
The model systems of Violapyrone I **106** and Nocapyrone H **76** confirmed that Huckin-Weiler dianion aldol additions with aldehydes are compatible reactions with both ethyl 2-methyl-3-oxopentanoate **19** and ethyl 2-methylacetoacetate **188** β -keto esters, correlating to results from early synthetic strategies (Chapter 3). It was also revealed that acylation though imidazolide activated carboxylic acids are more successful with ethyl 2-methylacetoacetate **188** β -keto esters which are relevant to Violapyrone derivatives. The functionalization to both aldehydes and activated imidazolides were conducted on **187** (Table 5.6).

Table 5.6 Reaction condition screening of oxidation and activation of alcohol **187**

Conditions	Temp	Time (h)	R	Product	Yield
Swern	-78 → 20 °C	2	H	190	77%
Swern ^a	-78 → 20 °C	2	H	190	86-98%
TEMPO	RT	0.20	H	190	53-90% ^b
TEMPO	RT	1	OH	191	68%
CDI, THF ^c	RT	1	Im	192	95%

^a Conducted with extra dry reagents ^b Results were not reproducible ^c Reaction on the carboxylic acid **191**

The initial attempts with a Swern reaction resulted with some deprotection of TBS functionality; it was suspected that the DMSO used for the reaction may have absorbed too much moisture and allowed the formation of an acidic solution capable of deprotection. When the Swern reaction was repeated with redistilled DMSO stored on molecular sieves, providing extremely dry DMSO, the reaction delivered an optimised yield of 86-98% of the aldehyde **190**. Conversion of **187** to the aldehyde under TEMPO mediated oxidation was possible at high conversion (~90 %) if reaction timing was exactly right, quenching prior to over oxidation, but was difficult to control and resulted in inconsistent results. Despite this, the TEMPO oxidation was a convenient protocol for access to carboxylic acid **191** under mildly basic conditions (NaHCO₃). This approach was advantageous in preserving the TBS protecting group as compared to acidic oxidation protocols. The carboxylic acid was directly converted to imidazolide **192** with CDI and used in addition reactions without further purification. The protocols were able to prepare the activated side chains as the imidazolide **192** and Aldehyde **190** (Figure 5.9).

Figure 5.9 Imidazolide **192** and Aldehyde **190**

196 were not very successful, with attempts including stirring in HF-pyridine and aqueous HF in CH₂Cl₂, both of which displaying little consumption of starting material or degradation of the product. The bilayer of α -pyrone **196** in CH₂Cl₂ and aqueous HF was then subjected to shaking on a vortex pad at high speed. It was found that the bilayers homogenised and resulted in quick consumption of starting material and conversion. The resulting α -pyrone **197** was isolated in 24 % yield.

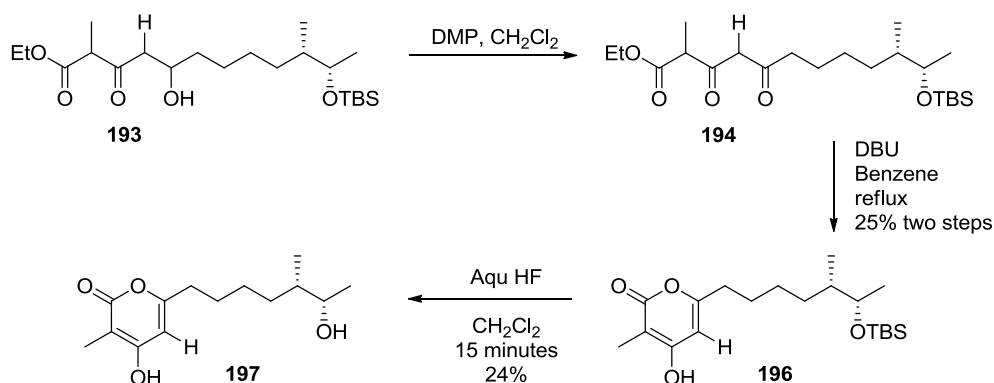


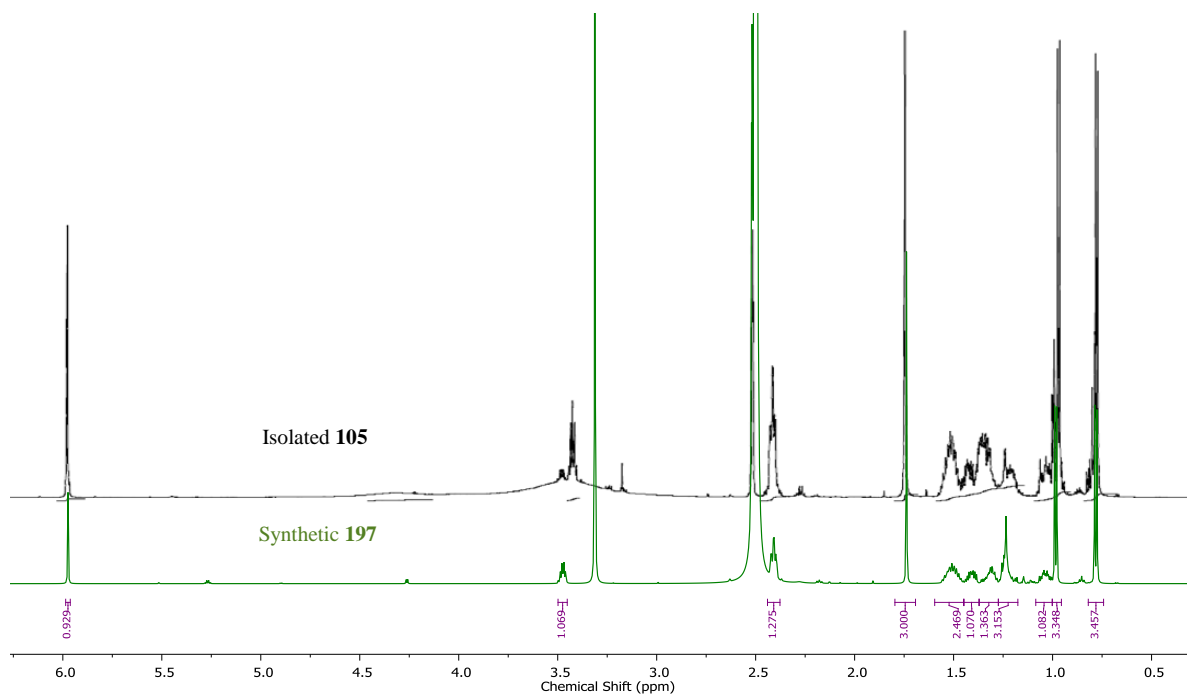
Figure 5.10 Conversion of hydroxy-keto ester 193 to α -pyrone 197

The structure of α -pyrone **197** was characterised as per Table 5.8 and provided the characteristic carbon chemical shifts of C-2 to C-6 of an α -pyrone (δ C 165.07, 96.48, 164.81, 99.15, 162.57). The pyrone ring contained a single methyl substitution at C-14 (δ C 8.35, δ H 1.74 (s, 3H)) and unsubstituted on C-5 (δ C 99.15, δ H 5.97 (s, 1H)). The side chain was located on C-6 (δ C 162.57), with four methylene carbons C-7 to C-10 (δ C 32.58, δ H 2.41 (td, $J = 7.5, 2.7$ Hz, 2H); δ C 26.66, δ H 1.57 – 1.45 (m, 2H); δ C 26.11, δ H 1.45 – 1.20 (m, 4H); δ C 31.72, δ H 1.45 – 1.20 (m, 4H)), followed by stereogenic C-11 and hydroxy-containing C-12 (δ C 39.52, δ H 1.45 – 1.20 (m, 4H); δ C 68.88, δ H 3.47 (dtd, $J = 10.8, 6.4, 4.5$ Hz, 1H)) and finished with branching C-13 and C-15 (δ C 20.23, δ H 0.98 (d, $J = 6.3$ Hz, 3H); δ C 14.5, δ H 0.78 (d, $J = 6.8$ Hz, 3H)). Unfortunately, mass spectroscopy and optical rotation experiments were unable to provide definitive results due to lack of prepared material. However, the precursory TBS ether **196** was fully characterised from full spectroscopic data and the structure was determined as 6-((5*S*,6*S*)-6-((tert-butyl)dimethylsilyl)oxy)-5-methylheptyl)-4-hydroxy-3-methyl-2*H*-pyran-2-one. Due to the full characterisation of the precursory TBS ether **196** and the correlation with NMR data the structure of 4-hydroxy-6-((5*S*,6*S*)-6-hydroxy-5-methylheptyl)-3-methyl-2*H*-pyran-2-one was assigned to the synthesised α -pyrone **197**.

Table 5.8 NMR Spectroscopic Data (600 MHz, DMSO-*d*₆) of synthetic **197** with comparison to Violapyrone E¹⁴⁶

Synthetic 197	position	δ_c	multi	δ_H (<i>J</i> in Hz)	Comparison Isolated & Synthetic δ_c	
					Difference (ppm)	Carbon position
	2	165.07	C			
	3	96.48	C			
	4	164.81	C			
	5	99.15	CH	5.97, <i>s</i>		
	6	162.57	C			
	7	32.58	CH ₂	2.41, <i>td</i> (7.5, 2.7)		
	8	26.66	CH ₂	1.57 - 1.45, <i>m</i>		
	9	26.11	CH ₂	1.45 - 1.20, <i>m</i>		
	10	31.72	CH ₂	1.45 - 1.20, <i>m</i>		
	11	39.52	CH	1.45 - 1.20, <i>m</i>		
	12	68.88	CH	3.47, <i>dtd</i> (10.8, 6.4, 4.5)		
	13	20.23	CH ₃	0.98, <i>d</i> (6.3)		
	14	8.35	CH ₃	1.74, <i>s</i>		
	15	14.5	CH ₃	0.78, <i>d</i> (6.8)		

When the spectroscopic data from Table 5.8 was compared to that of reported natural product Violapyrone E **105**¹⁴⁶ the difference in carbon shifts differed by less than 0.83 of a chemical shift (ppm). The most deviation was seen in the stereogenic hydroxy bearing C-12 and methyl C-13, suggesting an inconsistency with the stereocenter at C-12. A comparison of the reported natural product (**105**) and the synthesised α -pyrone **197** through overlay of ¹H NMR spectra (Figure 5.11) showed that the peaks for the stereogenic C-12 did not align between the synthetic (δ_c 68.88, δ_H 3.47 (*dtd*, *J* = 10.8, 6.4, 4.5 Hz, 1H)) and the isolated (δ_c 69.4, δ_H 3.42 (*quin*, *J* = 6.0 Hz, 1H)). It could be suggested that the synthetic C-12 peak was aligned to a suspected *anti* minor isomer present in the isolated natural product.

Figure 5.11 Overlaid spectral comparison of synthetic α -pyrone **197** (green) against Violapyrone E **105** (black)¹⁴⁶

It was determined that a relative *syn* stereoisomer of Violapyrone E was synthesised and that the natural product was present as the major isomer in the *anti* relative stereochemical configuration at the C-12 and C-12 stereogenic carbons of the side chain.

5.6 Synthetic directions towards Violapyrone C

Following the optimised synthesis of Nocapyrone H through aldol addition over β -keto ester and late-stage methylation, the protocols could be applied to the synthesis of Nocapyrone C (Figure 5.12) and its derivatives.

Ethyl 2-methyl-3-oxopentanoate **19** was subject to Huckin-Weiler dianion conditions before the addition of aldehyde **190**. The resulting hydroxy-keto ester **198** was oxidised to the γ - β -diketo ester **199** with DMP and then immediately carried through to DBU mediated cyclisation to the α -pyrone **200** in 21 % yield over the three steps. The α -pyrone **200** was subject to regioselective methylation conditions through the use of methyl triflate and resulted in the γ -pyrone **201** in 51 % yield. Subsequent deprotection with aqueous HF with vortex agitation provided the γ -pyrone **202** in 70 % yield.

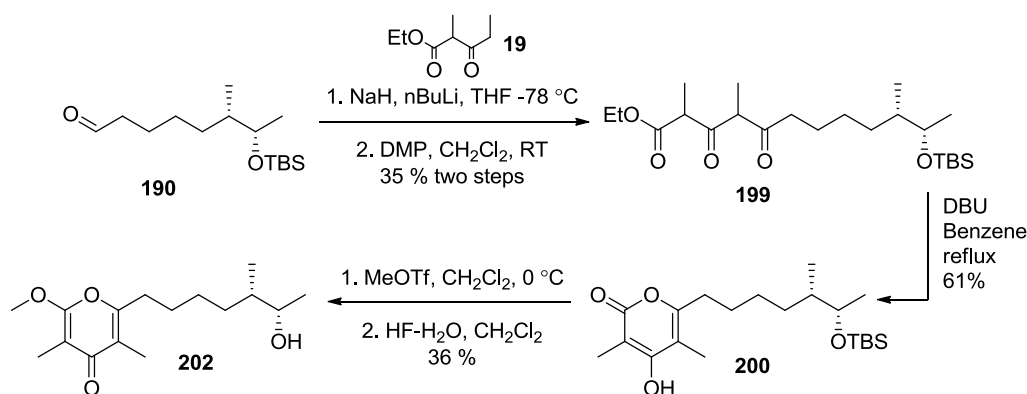
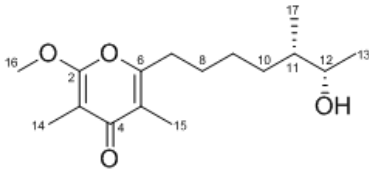
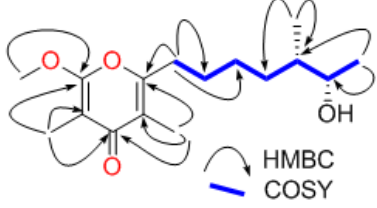


Figure 5.12 Synthesis of γ -pyrone **202**

The synthetic γ -pyrone **202** was characterised through NMR as per Table 5.9 and the structure provided the characteristic chemical signals of C-2 to C-6 of a γ -pyrone (δ C 162.26, 99.52, 181.17, 118.43, 158.38). The methoxy substitution at C-16 (δ C 55.42, δ H 3.95 (s, 3H)) and the ring substitution of C-14 and C-15 (δ C 10.13, δ H 1.84 (s, 3H); δ C 7.02, δ H 1.94 (s, 3H)) were observed within the expected characteristic shifts. The substitution at C-6 (δ C 158.38) contained the sidechain characterised by C-7 (δ C 30.86, δ H 2.59 (t, $J = 7.6$ Hz, 2H)) and the three methylene carbons C-8 to C-10 (δ C 27.53, δ H 1.71 – 1.58 (m, 2H); δ C 27.12, δ H 1.54 – 1.22 (m, 4H); δ C 32.44, δ H 1.54 – 1.22 (m, 4H)). The stereogenic C-11 (δ C 39.82, δ H 1.54 – 1.22 (m, 4H)) and hydroxy bound C-12 (δ C 71.33, δ H 3.71 (td, $J = 6.4, 4.3$ Hz, 1H)) were connected to C-17 (δ C 14.28, δ H 0.88 (d, $J = 6.7$ Hz, 3H)) and C-13 (δ C 20.42, δ H 1.15 (d, $J = 6.3$ Hz, 3H)) respectively. The optical rotation found a measurement of $[\alpha]_D^{20} = -16.5$. Atmospheric pressure chemical ionization mass spectrometry provided a mass measurement of m/z 283.1902 $[M + H]^+$ corresponding to a chemical formula of $C_{16}H_{27}O_4$.

Table 5.9 NMR Spectroscopic Data (600 MHz, CDCl₃) of synthetic γ -pyrone **202**

(-) Nocapyrone C	position	δ_c	multi	δ_H (J in Hz)	COSY & HMBC
	2	162.26	C		
	3	99.52	C		
	4	181.17	C		
	5	118.43	C		
	6	158.38	C		
	7	30.86	CH ₂	2.59, t (7.6)	
	8	27.53	CH ₂	1.71 – 1.58, m	
	9	27.12	CH ₂	1.54 – 1.22, m	
	10	32.44	CH ₂	-	
	11	39.82	CH	-	
	12	71.33	CH	3.71, td (6.4, 4.3)	
	13	20.42	CH ₃	1.15, d (6.3)	
	14	10.13	CH ₃	1.84, s	
	15	7.02	CH ₃	1.94, s	
	16	55.42	CH ₃	3.95, s	
	17	14.28	CH ₃	0.88, s (6.7)	

The structural analysis was able to confirm that the synthesised γ -pyrone **202** consisted of absolute structure of 2-((5*S*,6*S*)-6-hydroxy-5-methylheptyl)-6-methoxy-3,5-dimethyl-4*H*-pyran-4-one. When this structure was compared to that described for Nocapyrone C by Schneemann¹⁴⁵, it was found to be a structural match apart from the optical rotation which was in the opposite sign. This indicated to the natural product being the enantiomeric form of this *syn* product which correlated with corrected results from the 2013 previous synthesis.¹⁵¹

As described earlier, the previous successful synthesis of Nocapyrone C¹⁵¹ incorrectly assigned C-11 and C-12 stereocenters as 11*S* and 12*S*, but upon further investigation in this work (Chapter 4), the installed stereochemistry was corrected to 11*R* and 12*R*, with complete structural assignment as 2-((5*R*,6*R*)-6-hydroxy-5-methylheptyl)-6-methoxy-3,5-dimethyl-4*H*-pyran-4-one.

A recent paper by Lin *et al.* provided a competing analysis and stereochemical assignment to Nocapyrone C natural products isolated from *Nocardiosis alba* CR167 bacterial culture.¹⁵⁰ Lin *et al.* assigned 2-((5*S*,6*S*)-6-hydroxy-5-methylheptyl)-6-methoxy-3,5-dimethyl-4*H*-pyran-4-one as the absolute structure for the *syn* isomer after Mosher's ester analysis (both *S*-MTPA and *R*-MTPA) of the Nocapyrone C isolated compounds. The Mosher's ester analysis however, utilised comparison to the analogous (2*R**,3*S**)- and (2*R**,3*R**)-3-methyltridecan-2-ol compounds previously reported in literature.²¹⁴ This approach could be viewed as problematic in determining the absolute stereochemistry of the isolated *syn* isolated natural products due to the indirect nature of the comparison. If the results are to be believed the Nocapyrone C isolated Lin *et al.* must undergo a slightly different biosynthetic pathway to that encountered by Schneemann *et al.* and potentially presents future research opportunities.

5.7 Conclusion

The linear synthetic strategy found some success in the production of natural products and related isomers of Nocapyrone H and C, as well as Violapyrone I and E. The model systems used for optimising the addition, cyclisation, and methylation of the pyrone rings provided the correctly

correlating natural products Nocapyrone H, in 4 steps and 17 % yield, and Violapyrone I, in 2 steps and 50 % yield. The optimised addition conditions did not translate directly into the synthesis of Nocapyrone C (**202**) or Violapyrone E (**197**) pathways, with an aldol addition being used for both α and γ -pyrone production. The (6*S*,7*S*)-7-((tert-butyl)dimethylsilyloxy)-6-methyloctan-1-ol **187** side chain was progressed through the linear synthetic route to produce **202** in 6 steps and 6 % yield of the γ -pyrone and with an overall yield from propionyl thiazolidinethione **83** optimised to 3.5 % over 12 steps.. The structural characterisation presented the same structure as described in isolation but with the opposite sign in optical rotation. The side chain **187** was also progressed towards Violapyrone E over 4 steps resulting in 4 % yield of the α -pyrone and with an overall yield from propionyl thiazolidinethione **83** optimised to 2% over 11 steps. The structural analysis presented a structure correlating to that described from the isolated product but with discrepancy in the relative stereochemistry of the C-12 stereocenter, suggesting the isolated natural product has *anti* stereochemistry in the major isomer.

With the optimised preparation of saturated aldehyde **190** from propionyl thiazolidinethione **83** able to reach 59% overall yield, this linear strategy provided many merits in its pursuit. Although, even after many attempts at optimisation of late-stage reactions, critical reactions failed to yield results required for robust and efficient pyrone synthesis, providing modest yields at best. For the single pursuit of natural product synthesis and structural elucidation, this strategic approach can be said to suffice. However, for routine construction of pyrone libraries, much is left to be desired. Chapter 6 will investigate an alternative route for potentially effective access towards the α -methoxy- γ -pyrone synthon with intentions of pursuing Nocapyrone and other γ -pyrone natural products.

6 Desymmetrisation of α,α' -Dimethoxy- γ -pyrone

6.1 Introduction

The linear second-generation synthetic strategy was able to provide a completed synthesis of Nocapyrone H and C, as well as Violapyrone I and E, but it was determined that it could be prudent to revisit the synthetic strategy from 2013 research (Figure 6.1).¹⁵¹ The 2013 research which culminated with the synthesis of Nocapyrone C¹⁵¹ was confronted with particularly challenging preparation of the α -methoxy- γ -pyrone synthon resulting in poor conversion rates and instability and was found to be the main limiting factor in utilising that strategy for routine pyrone synthesis.

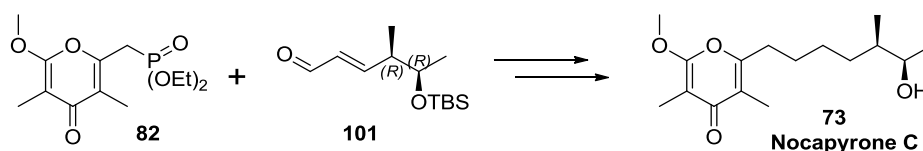


Figure 6.1 Approach to Nocapyrone C from 2013 synthetic research.¹⁵¹

In recent years a novel approach was developed by De Paolis and co-workers in regards to the construction of the α -methoxy- γ -pyrone synthon.^{152,176,177,215} Originally structurally elucidated by Woodward,²¹⁶ from an earlier report by Schroeter,²¹⁷ the symmetrical α,α' -dimethoxy- γ -pyrone **203** was revived as a possible simplified route to α -methoxy- γ -pyrones (**204**) which bypasses the precursory γ -hydroxy- α -pyrone and any potentially unselective or inefficient methylation. The symmetrical α,α' -dimethoxy- γ -pyrone **203** is reported to allow for desymmetrisation through nucleophilic attack and substitution of a single methoxy functional group providing C-6 substitution while preserving α -methoxy functionality (Figure 6.2).

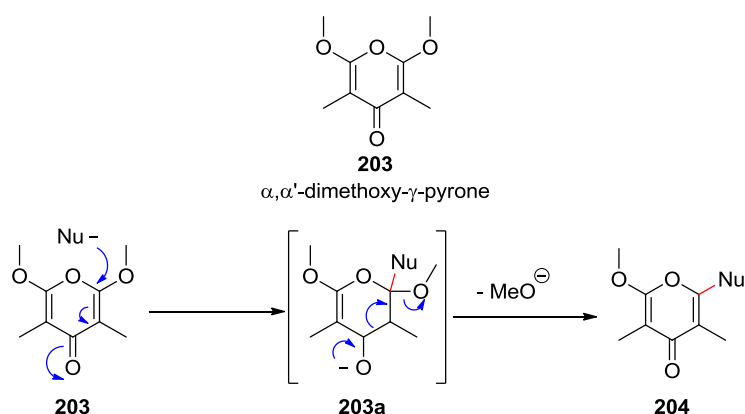


Figure 6.2 The symmetrical α,α' -dimethoxy- γ -pyrone **203** and the desymmetrisation through nucleophilic substitution.

This approach goes against the typical biomimetic approaches which sees a β,γ -diketo ester undergo lactone cyclisation in a γ -hydroxy- α -pyrone followed by methylation to provide the desired product α -methoxy- γ -pyrone. In contrast, the De Paolis protocol installs the methylation prior to cyclisation and retains it after cyclisation.^{118,176,218} The methoxy functional groups originate from the dimethyl- α,α' -dimethylacetonedicarboxylate **205** symmetrical precursor ester, and are retained post cyclisation. An unconventional dehydrative cyclisation is required where the carbonyl oxygen is displaced instead of the ester methoxide. This type deoxygenation of carbonyl oxygen in favour of alkoxide loss has little precedent in literature and is expected to be an extremely unfavourable reaction. A mechanism is proposed in Figure 6.3 of a potential acid catalysed dehydrative cyclisation reaction which could result in the symmetrical α,α' -dimethoxy- γ -pyrone **203**.

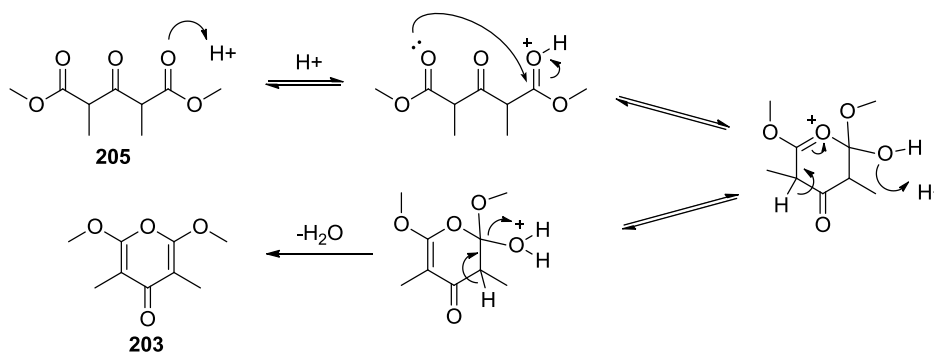


Figure 6.3 Proposed acid catalysed dehydrative cyclisation

Initial synthetic preparation of α,α' -dimethoxy- γ -pyrone **203** from the dimethyl- α,α' -dimethylacetonedicarboxylate **205** precursor utilised the dehydrative power of sulfuric acid but to only limited yield, and increased sulfuric acid concentration with excess sulfur trioxide saw marginally higher yields but still low.^{216,217} Efforts to improve yield and efficiency of the cyclisation reaction investigated some strong acids (H_3PO_4 and $\text{CF}_3\text{SO}_3\text{H}$) and the strong dehydrating agent P_2O_5 but no improvement was found.¹⁷⁶ Investigations into even stronger concentrations of sulfuric acid lead to the use of neat oleum (fuming sulfuric acid) and resulted in reliable production of γ -pyrone **203** in yields reaching 55-60% (Figure 6.4).^{118,176,218} The increase in yield was attributed to the removal of water and prevention of possible hydrolysis and allowed for multi-gram scale-up of preparation.²¹⁸ The only drawback apart from the use of hazardous oleum was that the optimised cyclisation requires 4 days of reaction time.^{118,176,218}

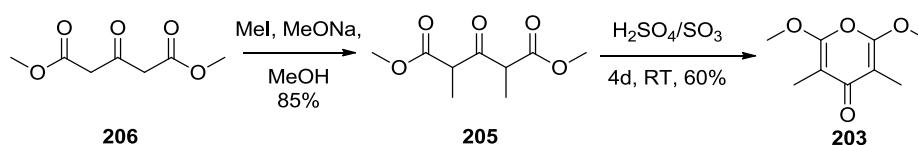


Figure 6.4 De Paolis preparation of γ -pyrone **203.**¹⁷⁶

The desymmetrisation of γ -pyrone **203** was an important development which would eventually allow for the access of a useful selection of methoxy-pyrone derivatives. Initial screenings by De Paolis for a suitable protocol of conjugate 1,4-addition reagents demonstrated that weak amine or thiol nucleophiles were not favourable and were unable to provide desired products even under high pressure (16 kbar) reaction conditions.¹¹⁸ Reactions with common 1,4-addition nucleophiles such as vinyl cuprate (from vinylmagnesium bromide and $\text{CuBr}\cdot\text{SMe}_2$) and vinyltrimethylsilane (in combination with Lewis acids) were also unable to provide 1,4-addition products.¹¹⁸ Reactions with organolithium reagents ($n\text{-BuLi}$, PhLi) or Grignard reagents both provided undesired 1,2-addition products. The screening was eventually able to find successful a 1,4-addition product (**208**) with the implementation of umpolung nucleophile 2-lithio-1,3-dithiane **207**.^{219,220} The addition reaction was able to be optimised to provide a reliable 75 % yield. A similar set of 1,4-addition products were able to be prepared with the use of allyl lithium (generated from allyltributylstannane and $n\text{-BuLi}$), which provided a mixture of two isomers (**209** & **210**) in 60-65 % yield (Figure 6.5).

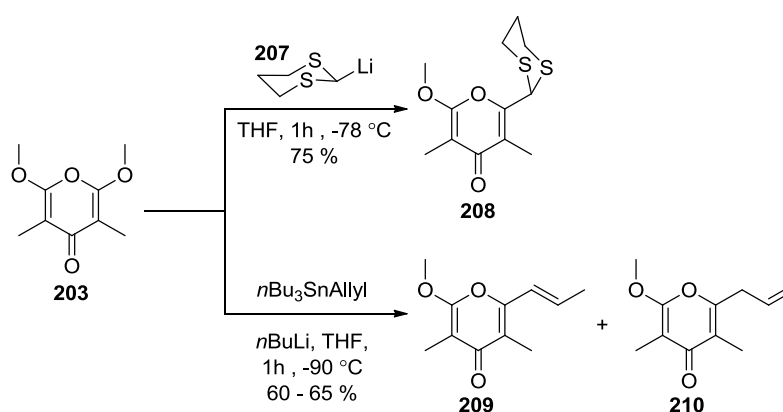


Figure 6.5 Desymmetrisation of α, α' -dimethoxy- γ -pyrone demonstrated by De Paolis¹⁷⁶

The utilisation 2-lithio-1,3-dithiane and allyl lithium for desymmetrisation protocols of γ -pyrone **203**, were eventually able to be utilised in the synthesis of Aureothin^{118,152,177,218} and Verticipyrene^{118,176,215} natural products.

6.2 Optimisation and preparation of α, α' -dimethoxy- γ -pyrone **203**

Our motivation was to optimise the preparation and incorporate the α, α' -dimethoxy- γ -pyrone **203** into the synthetic strategies towards accessing Nocapyrones and other α -methoxy- γ -pyrone containing natural products, isomers, and derivatives.

Attempts were made towards α, α' -dimethoxy- γ -pyrone **203** initiating with the preparation of the dimethyl ester precursor **205** through the methylation of dimethyl-1,3-acetonedicarboxylate **206** as per the literature protocol.¹¹⁸ The protocol utilised methyl iodide as the methylating agent in the

alkaline conditions provided by MeONa, MeOH. The literature conditions, however, were found to be not as successful as reported and the reaction conditions were changed. Subsequent reaction condition screening provided a protocol using MeI with K_2CO_3 in THF which progressed to **205** in an optimised yield of up to 99%. Screening of potential dehydrative cyclisation conditions were also carried out to investigate if conditions other than neat oleum could provide the symmetrical γ -pyrone **203** (Table 6.1).

Table 6.1 Reaction screening for optimal dehydrative cyclisation

Conditions	Yield
H_2SO_4/SO_3 (oleum) 84 hours ¹	60 %
DBU, Benzene	NR
$Na_2S_2O_7$, conc H_2SO_4	0-6%
MeOH, AcCl	NR
$Na_2S_2O_7$, MeOH	NR
TFAA, DCM	Undesired product
$BF_3 \cdot O(Et)_2$, THF	polymerisation
$PPh_3 \cdot CCl_4$	NR
Mitsunobu	Undesired product
SO_3 -pyr, conc H_2SO_4	NR
Triflic anhydride (neat)	24-30 %
P_4O_{10} , con H_2SO_4 12 hours	64 %
P_4O_{10} , $K_2S_2O_7$, conc H_2SO_4 12 hours	60 – 78%

1. De Paolis *et al.* *J. Chem. - A Eur. J.* 2010, 16 (37), 11229.

The screening of dehydrative cyclisation conditions investigated both dry acidic and dehydrating conditions (Table 6.1). Non-anhydrous acidic conditions usually resulted in the hydrolysis and loss of starting material but when anhydrous production of acid (MeOH, AcCl) was utilised, there was also no conversion to the desired product. A different attempt investigated the possibility of incorporating Swern ylides or phosphonium salts in an analogous protocol to that set out by Yamamura *et al.*, who utilised the mild cyclisation conditions for the preparation of 2,6-alkyl- γ -pyrones **36** as seen in Figure 1.20 from Chapter 1.¹⁰⁴ Unfortunately, these conditions were not able to translate to the diester system and returned only starting material. Interestingly, the use of neat triflic anhydride was dehydrative enough to be able to induce the dehydrative conditions required to cyclise the diester in modest yields of between 24-30%. The most successful conditions were found when phosphorous pentoxide was used in combination with concentrated sulfuric acid; the dehydrating strength of P_4O_{10} is able to dehydrate mineral acids to their anhydrides, providing an oleum alternative. Initially, the dehydration of concentrated sulfuric acid with phosphorous pentoxide was able to provide the cyclised γ -pyrone **203** in yields of up to 64% but when the mixture was supplemented with potassium pyrosulfate the conversion of γ -pyrone **203** increased to 60 - 78%. Both of these protocols outperformed the literature^{118,176,218} in both the higher yield as well as through shorter reaction time. The reaction mixture was able to show consumption of starting material by TLC within the first few minutes of diester **205** addition. Reactions were, however, continued to stir overnight to ensure the viscous mixture had completely homogenised before the reactions were quenched and worked up.

The successful conversion of diester **205** to symmetrical γ -pyrone **203** appeared to require anhydrous and desiccating conditions, and the conversion was found to perform best in the presence of *in situ* sulfur trioxide. From this inference a mechanism was proposed for the conversion of diester **205** to symmetrical γ -pyrone **203**, through sulfur trioxide mediated dehydrative cyclisation (Figure 6.6).

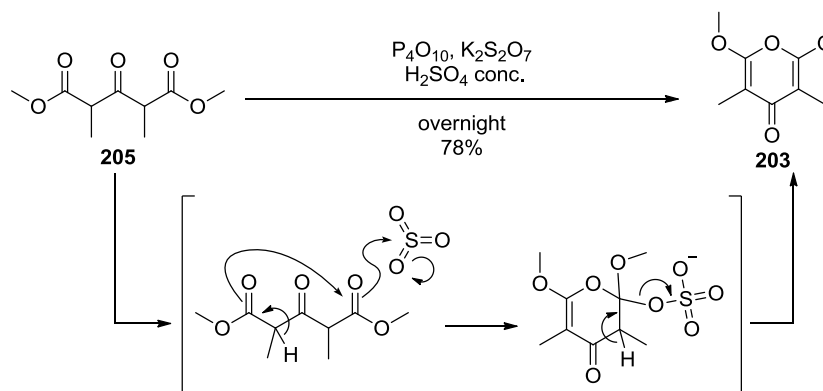


Figure 6.6 Proposed mechanism for sulfur trioxide mediated dehydrative cyclisation of diester **205** to symmetrical γ -pyrone **203**.

With the symmetrical γ -pyrone **203** available, a regime of reaction condition screenings was implemented to investigate potential side-chain insertion through nucleophilic desymmetrisation (Figure 6.7). A number of possible organolithium nucleophiles were envisaged as possible contenders for conjugate addition to symmetrical γ -pyrone **203** with preference to those capable of facile coupling with side chain fragments. Initial attempts aimed to emulate the success of the Horner–Wadsworth–Emmons phosphonium substrate **82** from the Actinopyrone A synthesis by Hosokawa *et al.*¹¹³ and which was also utilised in the Nocapyrone C synthesis from 2013.¹⁵¹ The utilisation of metallated methyl sulfones of benzothiazoles (**211**) and tetrazoles (**212**) could allow for fast access to Julia-type olefination fragments able to couple to aldehyde terminating side chains. These substrates were tested against the γ -pyrone **203** but even rigorous condition screening (variation in temperature, time, lithium base, or co-solvent) was unable to find any substitution to the pyrone substrate. Even though these sulfone nucleophiles (**211** & **212**) were unable to induce addition into the pyrone ring, there would have to be other favourable candidates.

The utilisation of methyl lithium was considered and implemented for the conjugate addition role as desymmetrisation of **203** would intercept the α -methyl- α' -methoxy- γ -pyrone **80**, but the reactions tested also did not result in any of the desired 1,4-addition products. It was envisaged that lithiated propargyl benzyl ether **213** could be used as a potential nucleophile and was also tested, but provided only undesired addition products. The screening resolved to progress through the proven protocol with both allyl lithium nucleophiles **214** derived from allyl stannanes and 2-lithio-1,3-dithiane nucleophiles **215**.¹⁷⁶ However, attempts with the allyl lithium nucleophiles

were unsuccessful and no addition products were observed. Progression with the dithianes was hampered in producing reliable and reproducible results while using *n*-BuLi or even *t*-BuLi during preparation of the 2-lithio-1,3-dithiane nucleophiles under either pre-metalation or Barbier conditions. Reliable and reproducible results were only found after the deprotonation conditions were ornamented through the use of Schlosser's base (*n*-BuLi and *t*-BuOK)^{221,222} and the 1,4-addition was able to reach as high as 54 % yield (Figure 6.7).

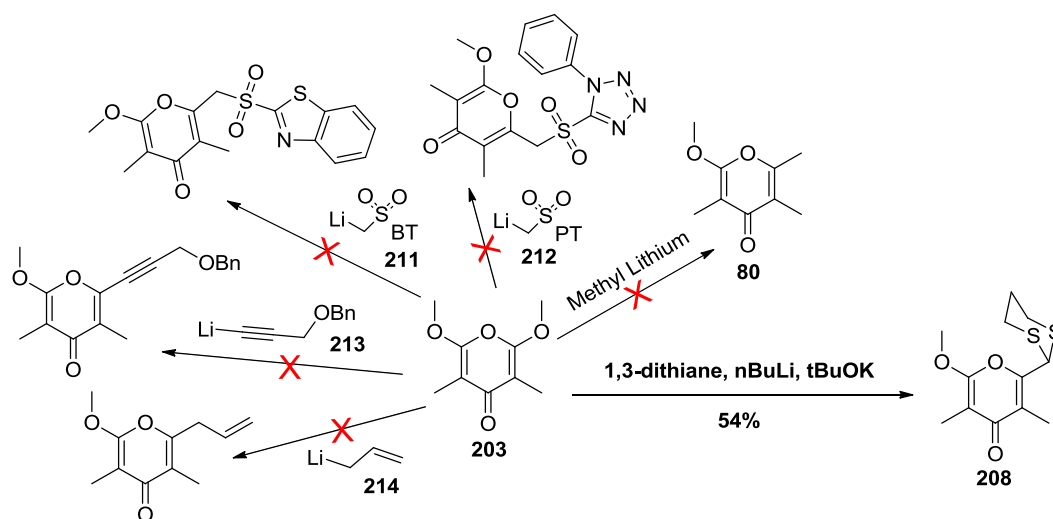


Figure 6.7 Screening of reaction conditions for suitable 1,4-addition to symmetrical γ -pyrone **203**

With the optimisation of nucleophilic 1,4-addition of 1,3-dithiane to γ -pyrone **203** providing the desymmetrised γ -pyrone **208**. This **208** dithiane pyrone fragment could progress to coupling with potential side-chain partners, in its current form or after functional group modification through a selection of possible reaction options (Figure 6.8). The dithiane γ -pyrone **208** could be deprotonated and utilised directly as a nucleophile against a suitable side chain electrophilic group (to give **217**), or utilised in a one-pot telescoping system as previously displayed in approaches to Aureothin.^{118,152,177,218} The dithiane γ -pyrone **208** could be reductively demasked with a slurry of Raney nickel to form the α -methyl- α' -methoxy- γ -pyrone **80** and then progressed through either direct alkylation or further modification for coupling (to give **220**). Otherwise, an oxidative demasking could be used to provide aldehyde functionality (**218**), allowing the pyrone fragment to be used as an electrophile in olefination coupling with the side chain (to give **219**).

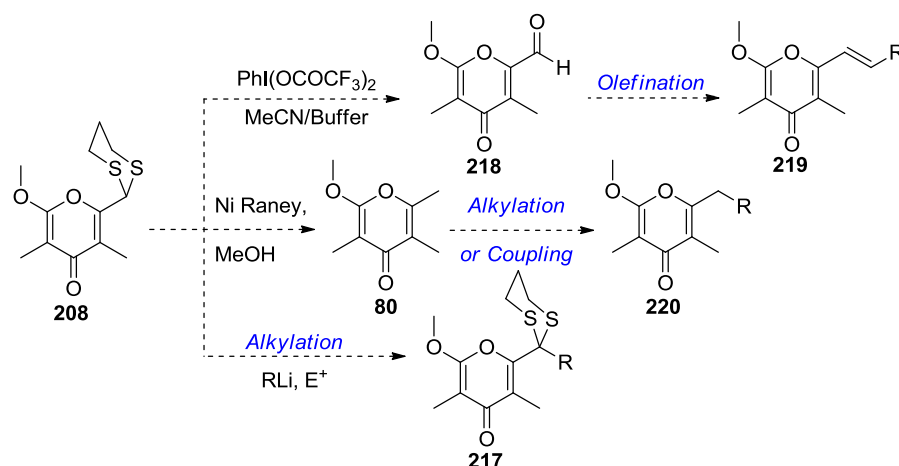


Figure 6.8 Possible functional group modification and utilisation of dithiane pyrone 216.

Initial attempts investigated the interception of the Horner–Wadsworth–Emmons phosphonate substrate **82** previously utilised in the 2013 synthesis of Nocapyrone C.¹⁵¹ For the preparation of the phosphonium substrate, the α -methyl- α' -methoxy- γ -pyrone **80** was required. The pyrone **80** was produced in 92 % through demasking of the dithiane with Raney nickel. Characterisation provided the expected α -methyl- α' -methoxy- γ -pyrone **80** with strong correlation to that of previous 2013 preparation; the methoxy C-10 at δC 55.47, δH 3.93 (s, 3H); the tertiary sp^2 C-2 and C-6 at δC 162.21 and δC 154.93; the tertiary sp^2 C-3 and C-5 at δC 99.52 and δC 118.60; the carbonyl C-4 at δC 180.95; the methyl substitutes at C-8 and C-9 at δC 10.23, δH 1.91 (s, 3H) and δC 6.97, δH 1.83 (s, 3H); and finally the demasked C-7 at δC 17.02, δH 2.25 (s, 3H).¹⁵¹

A comparison between the De Paolis derived route towards γ -pyrone **80** to that of the route used in the previous 2013 synthesis¹⁵¹ (Figure 6.9) shows that the new route was able to provide the γ -pyrone **80** in a superior yield of 39 % in 4 synthetic steps. The previous 2013 route,¹⁵¹ as discussed in Chapter 2, was plagued with irreproducibility and the highest produced yield could only be found at 10-15 % over 3 synthetic steps. If the yield calculation of the 2013 route also includes the formation of ethyl-2-methyl-3-oxo-pentanoate **19**, through the self-condensation of ethyl propionate, the yield over 4 steps can reduce to around 4 %.

Desymmetrisation of α,α' -Dimethoxy- γ -pyrone

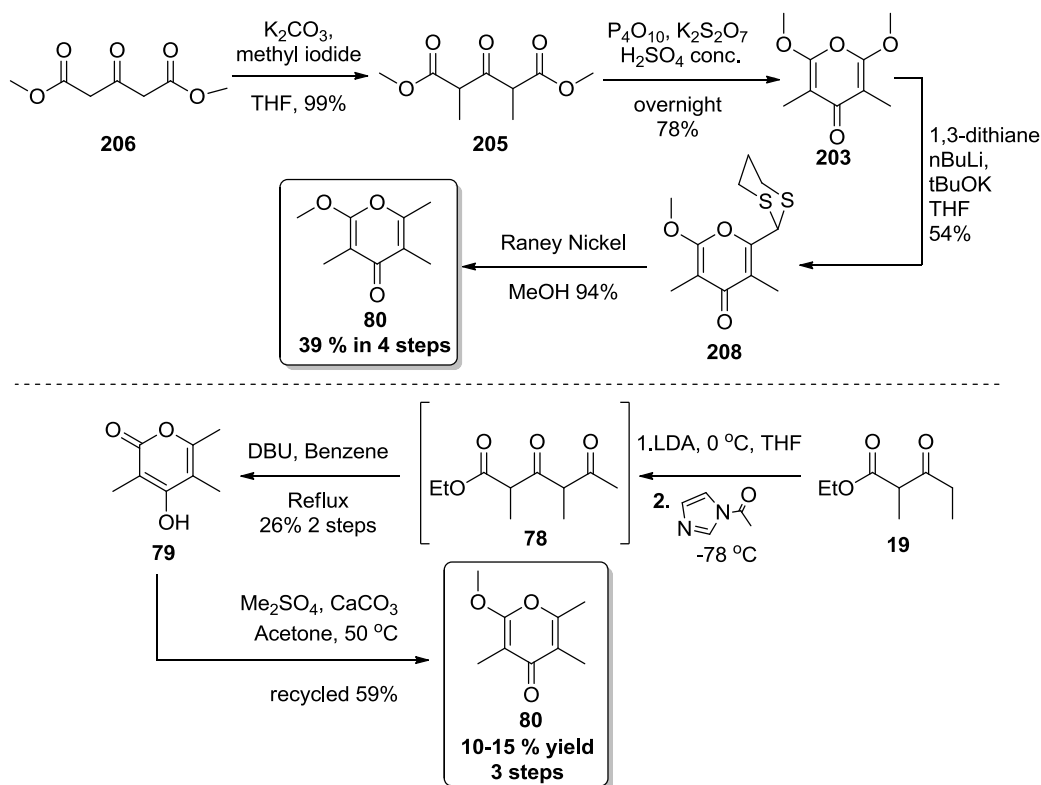


Figure 6.9 Comparison between the new α,α' -dimethoxy- γ -pyrone derived route (top) and the 2013 biomimetic lactone route¹⁵¹ (bottom) towards γ -pyrone **80** preparation.

The newly refined route demonstrated a superior synthetic approach to α -methyl- α' -methoxy- γ -pyrone **80**, and if incorporated to the previous 2013 synthetic strategy¹⁵¹ through the Horner–Wadsworth–Emmons phosphonate coupling fragment **82** as originally reported by Hosokawa *et al.*,¹¹³ could allow for a very convenient approach to Nocapyrone natural products.

For the α -methyl- α' -methoxy- γ -pyrone **80** to be utilised in the coupling olefination it would have to be converted to the phosphonate **82** via conversion of the C-7 position to an electrophile before the addition of the phosphonate functional group. Previously¹⁵¹ the conversion to electrophile was performed through chlorination via tosyl chloride of the pyrone lithium anion. The γ -pyrone was subjected to LHMDS to form the lithium anion and tosyl chloride was used to provide the Cl⁺ cation required for chlorination. This approach was not as successful as expected, providing the chlorinated pyrone **81** but from a reaction mixture prone to impurities and in unreliable fashion. An alternative approach used NCS as the chlorinating agent to give a cleaner chlorinated γ -pyrone **81** in 50% yield (Figure 6.10). To conclude the pyrone coupling fragment, the γ -pyrone chloride would have to be converted to the phosphonate **82** by substitution with ethyl phosphite.

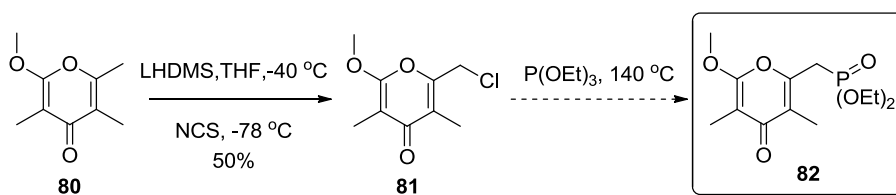


Figure 6.10 Conversion of α -methyl- α' -methoxy- γ -pyrone **80** to phosphonate **82**.

6.3 Side chain preparation

To fulfil a foundational motivation for pursuing the preparation of the α -methoxy- γ -pyrone synthon through desymmetrisation of α,α' -dimethoxy- γ -pyrone **203**, a side chain fragment was required to complete the synthesis of Nocapyrone natural products. A stereocontrolled side chain fragment would allow for the completion of the synthesis and also allow for stereoelucidation of the target natural products. The combination of pyrone **80** and side-chain fragments provides for a convergent synthetic strategy which allows for increased efficiency of fragment preparation. The interconversion between different pyrones or side chain fragments imparts a divergent component to the synthetic strategy, allowing for the preparation of a larger amount of final products. In this case coupling of a variety of side-chain partners to the prepared pyrone **80** fragment with allow of the constructed of the reported Nocapyrone natural products, their isomers, and possible derivatives.

The stereocontrolled side chain fragments were to utilise the asymmetric aldehydes fragments **164**, **168** and **180** previously prepared and discussed in Chapter 4. An appropriate chain extension would have to be implemented to elongate the carbon chain to the required length. Unlike in both the first and second-generation synthetic strategies, the linker need not be 4 carbons long as preparation of α,α' -dimethoxy- γ -pyrone and dithiane desymmetrisation to γ -pyrone **80** have provided two extra carbons on the pyrone fragment. A more suitable chain extension would follow the example from the previous 2013 Nocapyrone C synthesis¹⁵¹ with the utilisation of stabilised ylide (Carbomethoxymethylene)triphenylphosphorane for the installation of the 2 required carbons (Figure 6.11). This approach would install a simple ethyl ester and olefin which can undergo easy functional group manipulation to whichever coupling tactics are implemented between the side chain and pyrone fragments. Simple protocols exist for the reduction to a terminal hydroxyl and hydrogenation to aliphatic carbon chain. When these modifications are done under basic or mild conditions, they are compatible with the existing TBS protecting group.

The chain extension to the allyl alcohols **225** and **226** were progressed through Wittig coupling with stabilised ylide **221** and the corresponding aldehydes **164** and **168**, followed by reduction with DIBALH to a yield of 66 % and 82 % respectively over the 2 steps. The anti-stereocontrolled fragment required that the diol **179** be converted to the aldehyde **180** through oxidative cleavage

with NaIO_4 and then used immediately in Wittig coupling due to its instability. The resulting allyl ester was reduced with DIBALH to allyl alcohol **223** in 69 % yield and 3 steps.

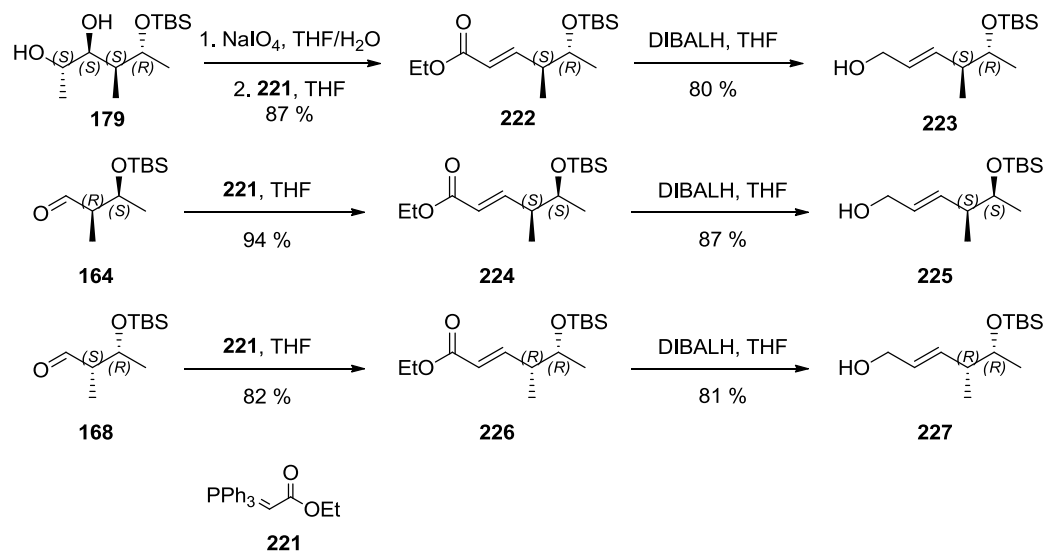


Figure 6.11 Preparation of stereocontrolled side chains **223**, **225** and **227**

With the refined synthesis of the crucial fragments of the α -methyl- α' -methoxy- γ -pyrone **80** and the *syn* allyl alcohols **225** & **227** and the *anti* allyl alcohol **223**, the original convergent synthetic strategy for Nocapyrone C from 2013¹⁵¹ research could be implemented. In fact, with the De Paolis derived preparation of γ -pyrone **80**, formal synthesis of Nocapyrone C could be recorded with the intersection of previous work (Figure 6.12).¹⁵¹

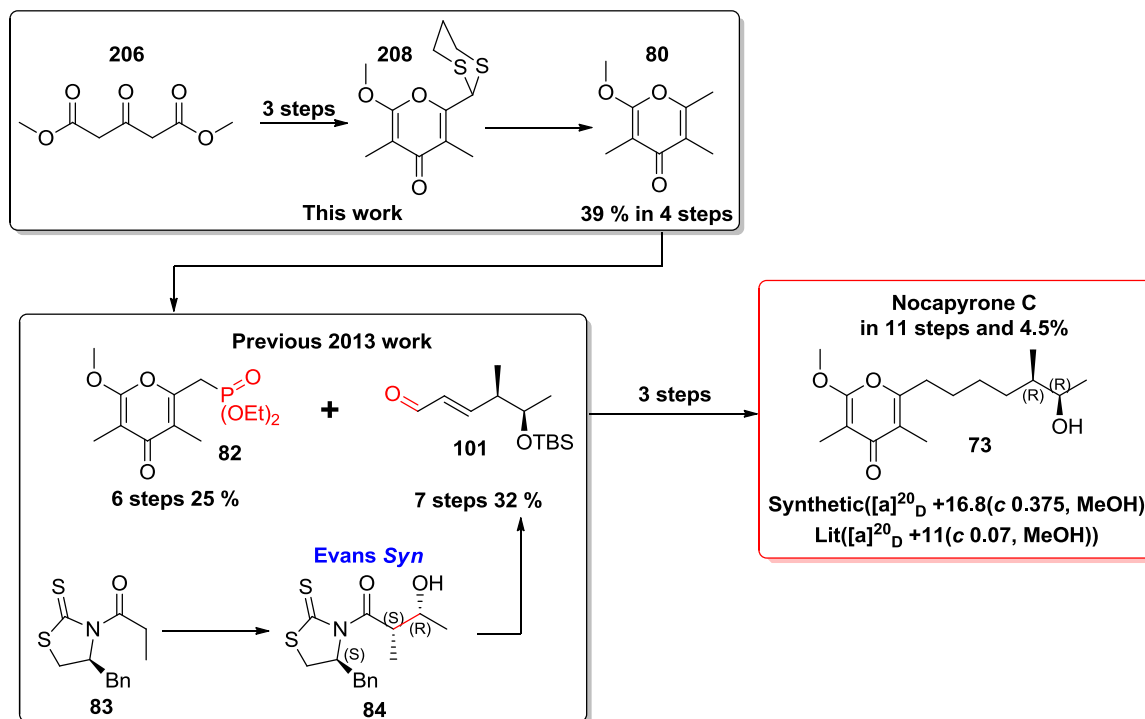


Figure 6.12 Formal synthesis of Nocapyrone C integrating new preparation of γ -pyrone 80

7 Conclusion and Future Directions

7.1 Summary and Conclusion of Nocapyrone and Violapyrone Synthesis

Pyrone containing natural products have been prominent features in isolated polyketide extracts from terrestrial and marine organisms from the earliest investigations. The synthetic construction of substituted terminating pyrones really became more prominent after the pioneering work by Harris⁴³, Suzuki^{44,45} and Osman⁵⁸, but even after many successfully natural product syntheses, a robust, reliable, and widely adopted protocol towards these oxygenated heterocycles has not persisted throughout the literature.

This thesis aimed to analyse and develop strategic and tactical approaches to hydroxy- α -pyrone and α -methoxy- γ -pyrone synthons by the practical pursuit of a set of similarly structured pyrone natural products.

The natural products Nocapyrone C **73**^{147,148} and Violapyrone E **105**¹⁴⁶ (Figure 7.1) were identified as interesting targets for total synthesis, as they possessed shared structural features, including pyrone cyclisation modes and specifically a 7-carbon side chain extending from the C-6 substitution of the ring which included enzyme-installed stereocenters at C-11 and C-12. It was envisioned that a well designed convergent synthetic strategy would be able to intersect both natural products while a potential divergent strategy could allow for the construction of many derivatives, isomers, and analogues (Figure 7.2).

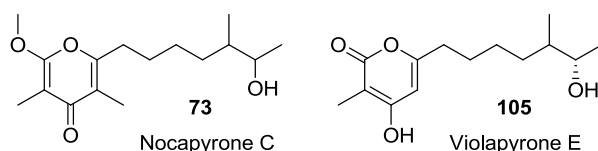


Figure 7.1 Natural Products Nocapyrone C and Violapyrone E as identified synthetic targets.

Two generations of synthetic strategy were developed derived from a general retrosynthetic analysis of the natural products (Figure 7.2), with the first strategy (Figure 7.3) built off of the lesson learnt from synthetic studies of Nocapyrone C construction conducted in 2013,¹⁵¹ while the second strategy (Figure 7.7) modified the disconnection approach from the first.

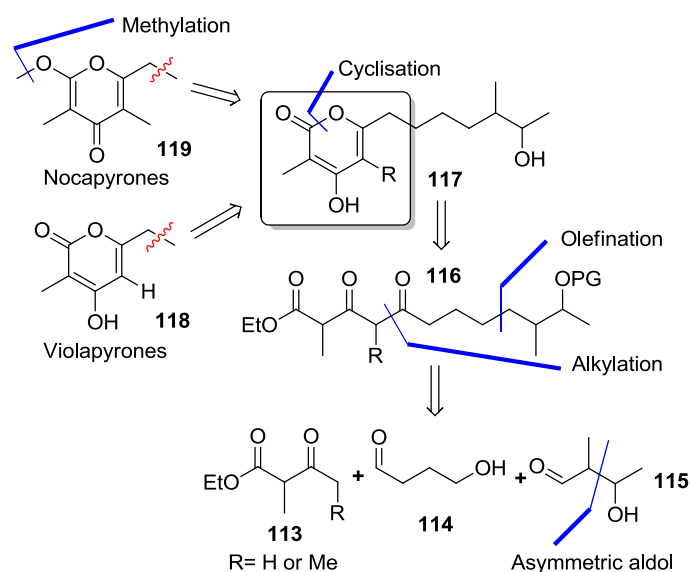


Figure 7.2 The general retrosynthetic analysis of the construction of Nocapyrone and Violapyrone natural products.

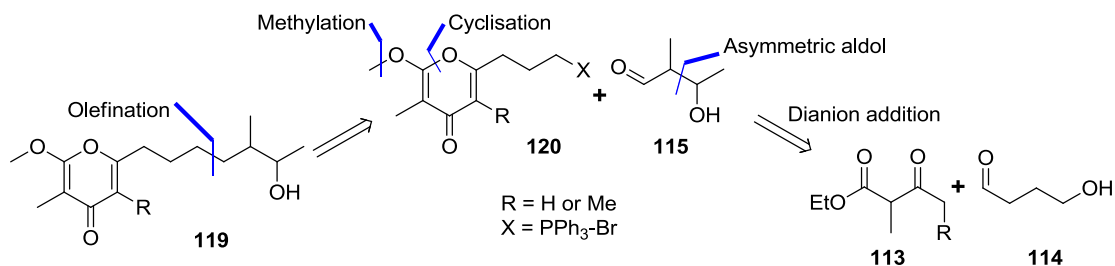


Figure 7.3 First generation of synthetic strategy towards pyrone natural products.

The implementation of the first generation synthetic strategy progressed through the majority of the route to Nocapyrone C and provided important results in the preparation of the pyrone ring, but was ultimately unable to realise crucial coupling to the terminal side chain fragment. The pyrone ring fragment **135** was realised in 23 % over 8 steps (Figure 7.4) including a 3-carbon side chain. The crucial features included the extended 4-carbon aldol addition to β-keto ester, DMP oxidation to triketo, cyclisation, and regioselective methylation. All of these features allowed for an increase in both yield and route progression, enabling the construction of an 8-carbon linear fragment constructed out of the total 12-carbon linear chain, and 23 % yield over 8 steps compared to 15 % yield over 3 steps (to α-methoxy-γ-pyrone) from the 2013 study.¹⁵¹ Ultimately, the attempts at olefin coupling were unsuccessful and the completion of the synthetic route was not realised, and a decision had to be made if extra tactical attempts were to be made at achieving the coupling or to pursue an alternative synthetic approach.

Conclusion and Future Directions

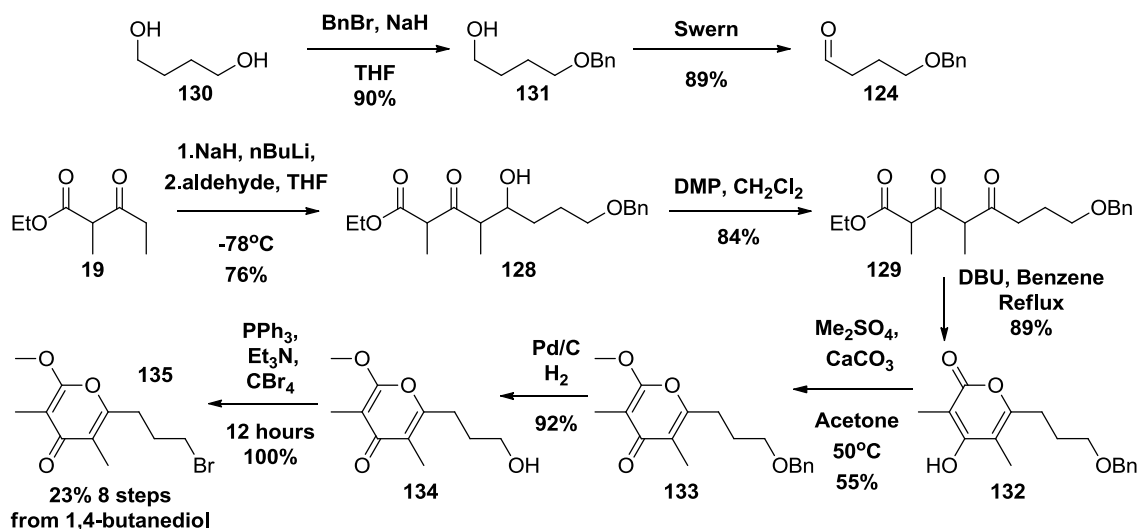


Figure 7.4 The first generation synthetic route towards Nocapyrone natural products

To allow for a clear decision to be made on regarding a change to the synthetic strategy, the developments made in the first generation strategy were implemented in the exploratory synthesis of Nocapyrone H **76** (Figure 7.5). This synthesis tested the important long side-chain addition, cyclisation, as well as testing a novel methylation tactic geared towards use in late-stage regioselective methylation.

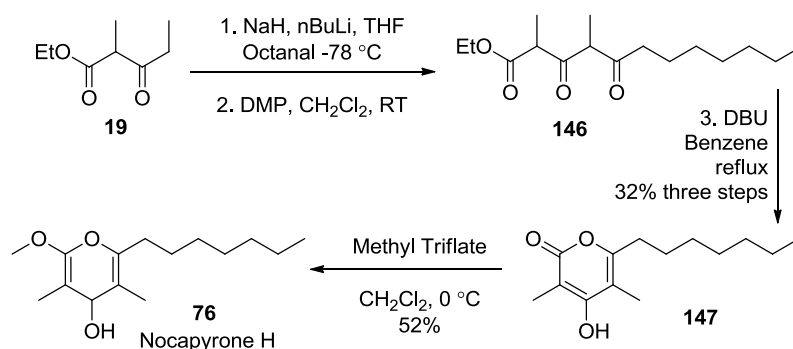


Figure 7.5 The 4 step synthesis of Nocapyrone H **76**

The successful synthesis of Nocapyrone H **76** displayed the successful application of long side-chain addition, DMP oxidation, cyclisation, and especially the application of methyl triflate regioselective methylation. The successful application of these concepts paved the way for the potential pursuit of a revised synthetic strategy in a second generation, with a side-chain first preparation approach.

To complement the exploratory synthesis, Violapyrone I **106** (Figure 7.6) was also synthesised through an analogous two-step approach, providing a natural product while further validating the proposed late-stage cyclisation and long side-chain addition of the second generation strategy.

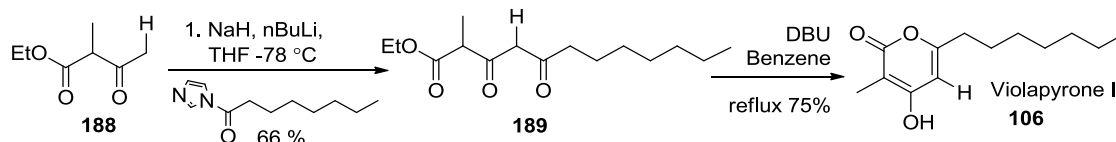


Figure 7.6 The 2 step synthesis of Violapyrone I

The decision to opt for strategic revision for the synthesis of Nocapyrone and Violapyrone natural products stemmed from 3 factors; tactical amendment to coupling could potentially be more challenging than anticipated and could lead to suboptimal outcome (increased amount of steps), the synthetic limiting factors (poor regiomeylation and low yielding pyrone preparation) rationalising first generation strategy had become less compelling with recent experimental results, and opened potential to intercept Violapyrone natural products with less effort.

A second generation synthetic strategy (Figure 7.7) was pursued which implemented a change in the order of coupling and disconnection, seeking to prepare the side chain **142** prior to addition to the β -keto ester **113** and cyclisation to pyrone.

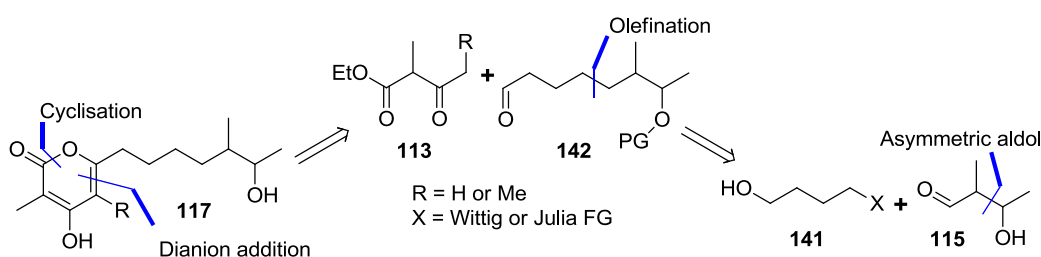


Figure 7.7 Proposed second-generation synthetic strategy.

The second-generation synthetic strategy relied upon the installation of stereochemistry (at C-11 and C-12) at the beginning of the route and relied on an asymmetric aldol to provide reliable access to a stereocontrolled fragment. Crimmins aldol chemistry and thiazolidinethione cleavable chiral auxiliary were utilised for the installation of stereocenters C-11 and C-12 (Figure 7.8).

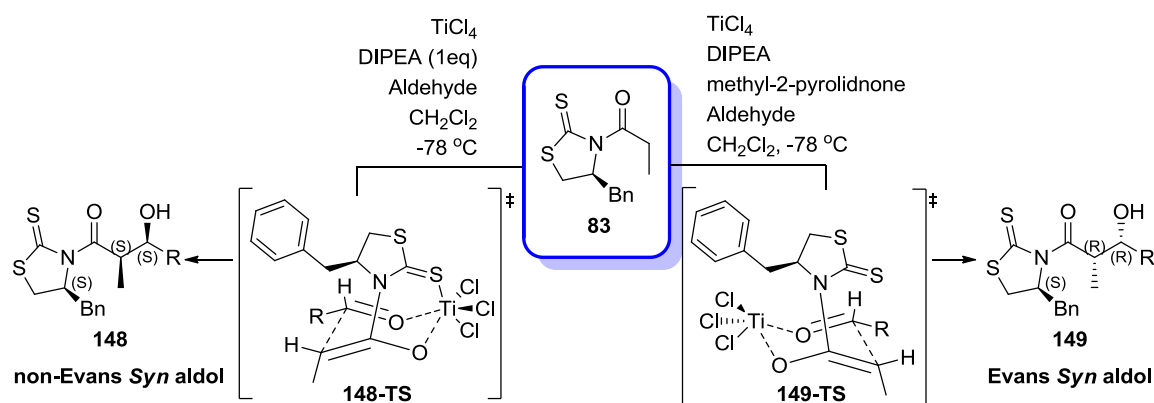


Figure 7.8 Crimmins aldol chemistry utilising thiazolidinethione chiral auxiliaries.

During stereochemical installation, a discovery was made regarding the Crimmins aldol reaction stereoselectivity and the reagent composition and addition schedule. It was found that excessive aldehyde in the reaction mixture interrupted the titanium metal complexation during the reaction transition state (**160a-TS**), resulting in the opposite (Evans *syn*) stereochemical outcome to that predicted (non-Evans *syn*) (Figure 7.9). This had an impact on the previously reported Nocapyrone C synthesis from 2013,¹⁵¹ with the reported installed stereochemistry as *S,S* being overturned and to the actual *R,R* stereochemistry in the final synthesised natural product.

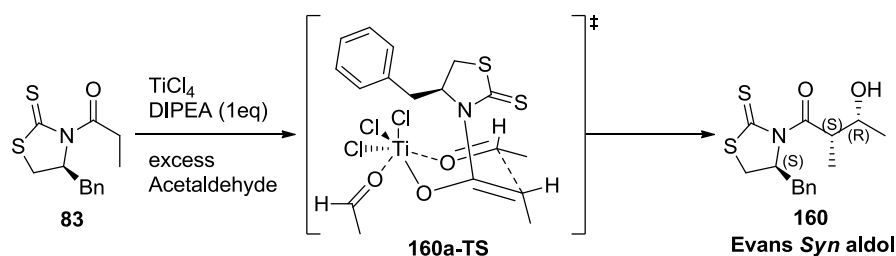


Figure 7.9 The proposed coordination between excess acetaldehyde and titanium during aldol transition state.

After stereochemical installation, the second-generation strategy progressed through the development of the side chain and olefination extension coupling. A linker fragment **185** was developed through the functionalization of both ends of 1,4 butanediol (**131**), with one end benzyl protected and the other end serving as a modified-Julia olefination partner with a benzothiazole sulfone functional group (Figure 7.10). This versatile linker **185** could be utilised for a 4-carbon extension between the terminal stereocontrolled fragment and β -keto esters, regardless of the natural product targets.

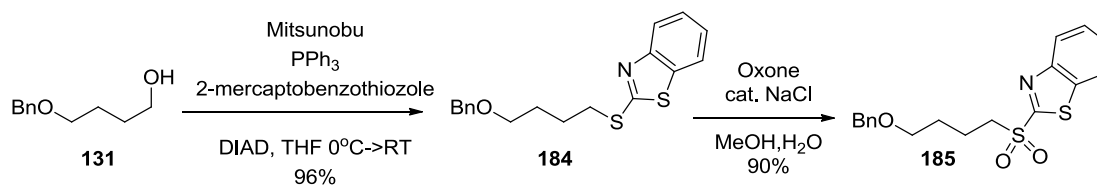


Figure 7.10 The preparation of 4-carbon linker.

The benzothiazole sulfone linker **185** was utilised in the modified-Julia olefination chain extension of the *syn* stereocontrolled aldol fragments, **164** and **168**. These side chains were then progressed through hydrogenation and oxidation to the 8-carbon straight-chain saturated aldehydes, **190** and **230**. The linear synthetic route from the asymmetric aldol was well optimised, providing the aldehyde **190** in 57% over 7 steps and aldehyde **230** in 61%, also in 7 steps (Figure 7.11).

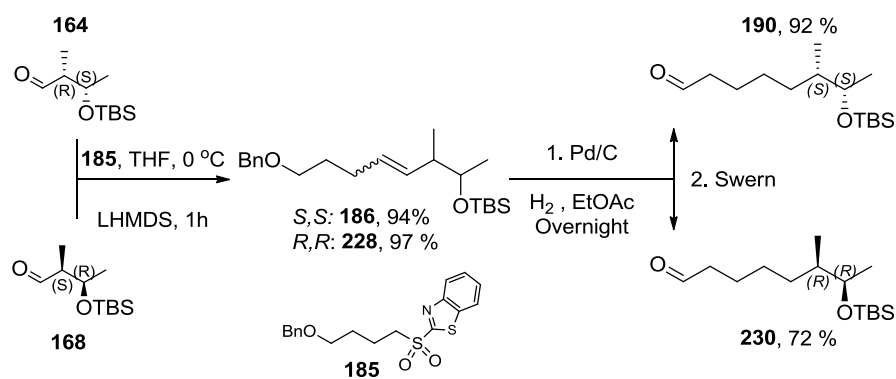


Figure 7.11 The prepared side-chain aldehydes **190** and **230**

The saturated aldehyde side chains **190** and **230** were able to be progressed through to dianion addition with β -keto esters and cyclisation in the process of pyrone preparation. The refined dianion addition, oxidation, and cyclisation conditions were partially determined through Nocapyrone H **76** and Violapyrone I **106** synthesis but still required optimisation. The aldehyde side chain, **190**, was added to the β -keto ester ethyl 2-methylacetoacetate **188**, oxidised, and cyclised to the α -pyrone **196**, and after deprotection, the resulting product was characterised as anti-relative stereoisomer of Violapyrone E (**197**) and the successful synthesis provided the natural product isomer in 2 % yield over 11 steps (Figure 7.12).

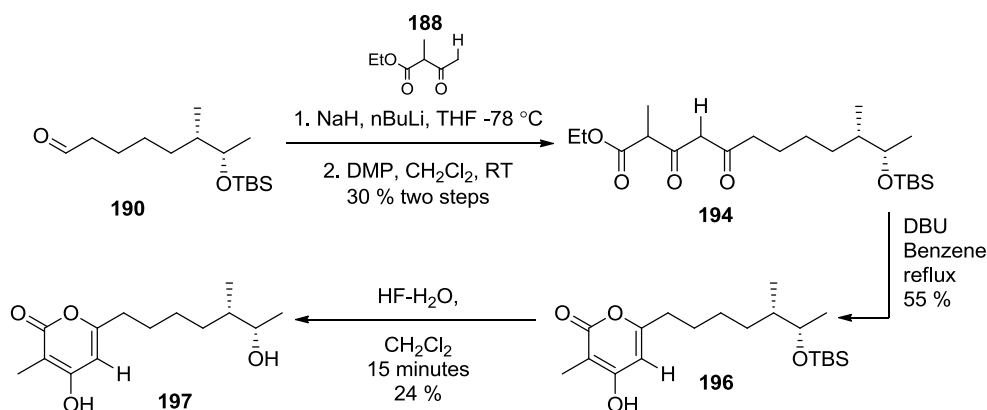


Figure 7.12 Violapyrone E isomer **197** synthetic route end-game

The most influential steps of the synthesis were those at the tail end of the route; the oxidation, cyclisation, and TBS deprotection were all found to be only low to moderate yielding (7.8% over three steps) at best. These low conversions impacted on the final yield of the route, with the overall yield after dianion addition reduced from 33 % over 8 steps to 2 % after the 3 final steps (11 steps overall). The final steps of the synthesis have much room to improve through optimisation, particularly with the final deprotection step (24 % yield). Future investigations would have to pay attention to the deprotection conditions and determine if they have any influence on the stability of the pyrone structure, as no starting material was isolated from the low

yielding (24 %) reaction. It could be possible that the pyrone ring undergoes ring-opening or another type of decomposition.

The pursuit for the natural product Nocapyrone C saw the utilisation of ethyl-2-methyl-3-oxo-pentanoate β -keto ester as the coupling partner with aldehyde side chain **190** for the triketo preparation. The end-game of the synthetic route was brought together in an analogous fashion to the Violapyrone route, with addition, oxidation, cyclisation, and TBS deprotection, but with the inclusion of regioselective methylation. The synthetic route was completed in 3.4 % yield in 12 steps from asymmetric aldol, and spectroscopic analysis determined the products as the (-)-Nocapyrone C (**202**), the enantiomer of the natural product. The route was found to be relatively better yielding than that of the Violapyrone isomer **197** end-game but still moderate, with yields ranging 40-87 % and totalling 6 % for the final 5 steps (Figure 7.13).

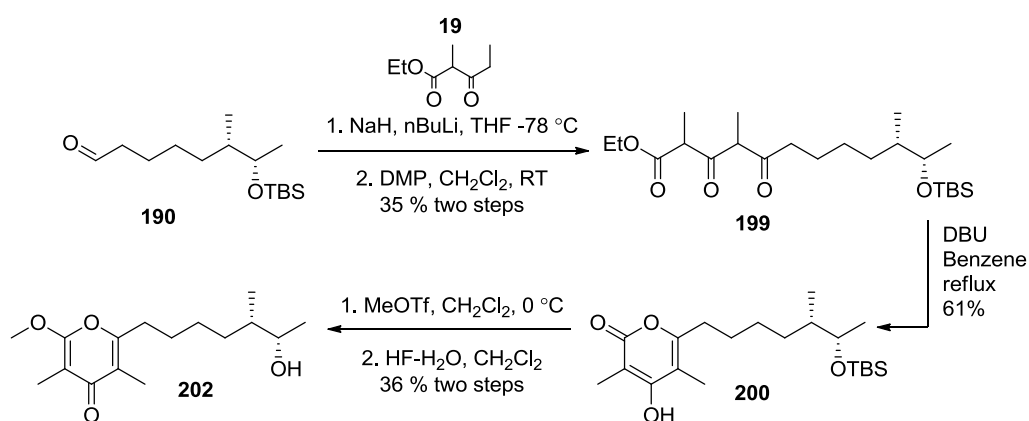


Figure 7.13 The end-game synthetic route of (-)-Nocapyrone C **202**

The second-generation synthetic strategy allowed for the synthesis of both Violapyrone E isomer **197** and (-)-Nocapyrone C **202**. When the synthetic route for (-)-Nocapyrone C **202** directly was compared to the synthesis of Nocapyrone C from research conducted in 2013,¹⁵¹ which was able to provide the natural product in 11 linear steps with a final 2.9% yield, the current strategy delivered (-)-Nocapyrone C **202** in 11 linear steps with a final yield of 2 %. The major difference between the two strategies is that the 2013 route is convergent in relation to pyrone and side-chain preparation, with the α -methoxy- γ -pyrone synthon being prepared to an advanced stage before coupling with the side chain fragment. This convergent approach allows for the low yielding steps of pyrone preparation and methylation to be mitigated from the overall synthetic yield. In contrast, the second-generation strategy can be considered linear as pyrone preparation is conducted after coupling with the side chain. Even though the steps leading up to the pyrone preparation steps are of high yield, the pyrone preparation steps have a more direct impact on overall yield than the convergent strategy of 2013.

7.2 Summary and Conclusion of α,α' -Dimethoxy- γ -pyrone Desymmetrisation

To build upon the recently demonstrated preparation and desymmetrisation of α,α' -dimethoxy- γ -pyrone developed by De Paolis and co-workers^{152,176,177,215} this thesis set out to investigate more efficient and more effective approaches to both preparation and desymmetrisation. The preparation was refined through intensive reaction screening to provide the α,α' -dimethoxy- γ -pyrone **203** at elevated yield (77 % over 2 steps) (Figure 7.14) and reduced time frame (2 days) to that of the original reports (55 % over +4 days).^{152,176,177,215} This refined protocol allowed for fast access to α -methoxy- γ -pyrone **80** synthon through dithiane addition and subsequent demasking which could be utilised in convergent synthesis towards Nocapyrone natural products.

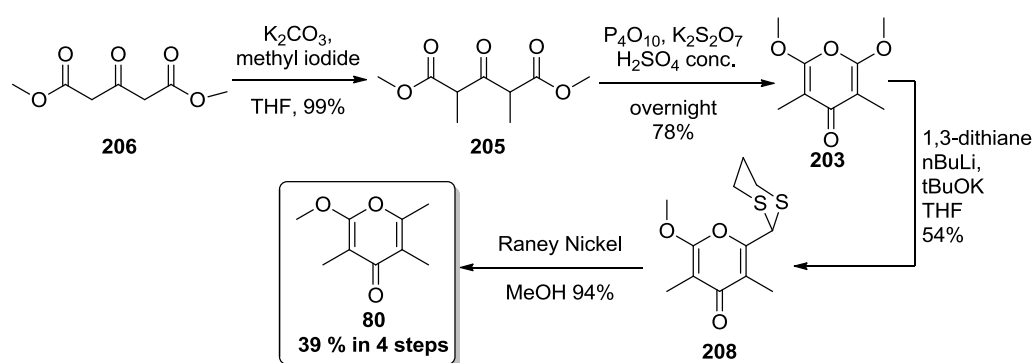


Figure 7.14 Preparation of α -methoxy- γ -pyrone **80** through the refined De Paolis protocol.

Sidechain fragments were prepared to allow for the intersection of the convergent synthetic pathway demonstrated in the 2013 synthetic strategy.¹⁵¹ The *syn* allyl alcohols **225**, **227** and *anti* allyl alcohol **223** isomeric derivatives were prepared to investigate the stereochemistry of Nocapyrone natural products and to prepare isomers and derivatives (Figure 7.15). Future work would see the allyl alcohols converted to the corresponding aldehydes and allow for coupling with the Horner–Wadsworth–Emmons phosphonate pyrone **82** fragment.

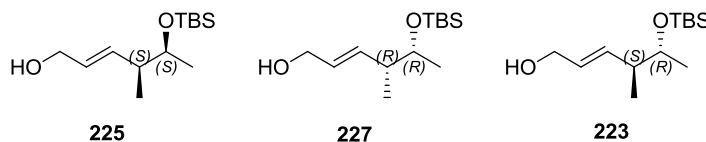


Figure 7.15 The asymmetrically prepared allyl alcohol side chain fragments **225**, **227** and **223**.

The nucleophilic 1,4-addition is able to facilitate the desymmetrisation of the α,α' -dimethoxy- γ -pyrone **203** and was realised through the use of the 1,3-dithiane lithium nucleophile, as demonstrated previously by De Paolis and co-workers.^{152,176,177,215} Even though a selection of 5 other lithium nucleophiles (Figure 7.16) were tested under various reaction conditions, no alternative 1,4-addition partner was discovered. The addition of 1,3-dithiane allowed for preparation of α -methoxy- γ -pyrone **80** and it was envisioned that different nucleophiles could

provide access to different 6-C substitution and possibly a truncated protocol to a suitable coupling fragment.

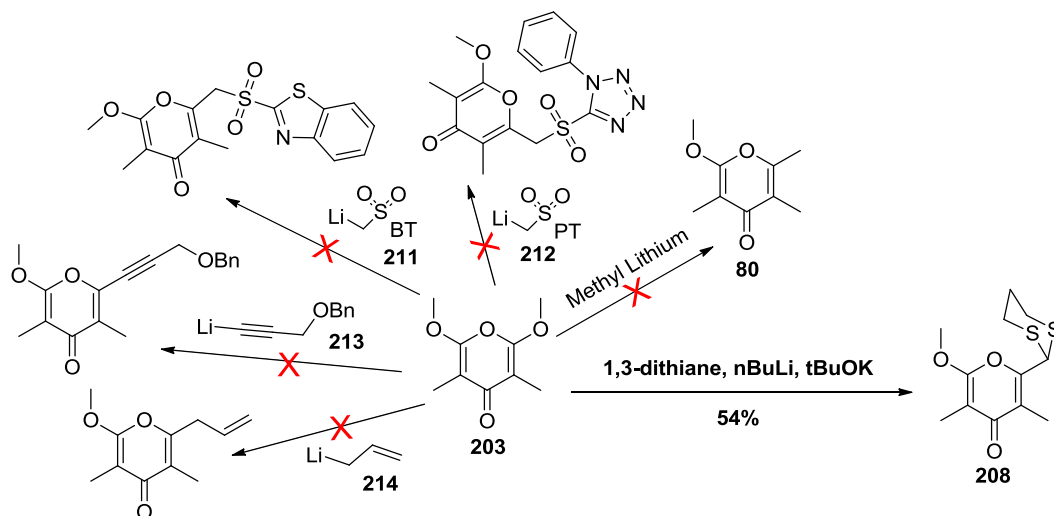


Figure 7.16 Screening of reaction conditions for suitable 1,4-addition to symmetrical γ -pyrone **203**.

The preparation of α -methoxy- γ -pyrone **80** from demasking of dithiane pyrone **208** provided the shared intermediate with the 2013 synthetic strategy¹⁵¹ and could be regarded as a formal synthesis of Nocapyrone C if the same route is imposed. Although, claiming this formal synthesis would not contribute to increasing the key performance indicator of overall yield, as the convergent strategy excludes the pyrone preparation from the longest linear steps and therefore the yield calculation. It would be found that the end-game steps influence the overall yield more considerably and the final poor yielding deprotection step has the most impact. These circumstances, however, do not diminish the impact of pyrone preparation optimisation and in fact, was required to allow for the production of enough pyrone intermediate to be able to conduct coupling and end-game steps.

The end-game steps in both Nocapyrone C and Violapyrone E synthetic routes were found to be less than optimal and resulted in the erosion of overall yield, indicating that more work would have to be required in the future towards mitigating end-game impact.

7.3 Future directions

The most important parts of future directions are the development of more robust protocols for pyrone preparation, be it from the existing first or second-generation synthetic strategies or through the development of the De Paolis desymmetrisation pathway. All three approaches have unrealised potential and if developed further could allow for good synthetic routes towards pyrone natural products, isomers, and derivatives. The first generation failed to undergo the originally

planned olefination coupling reaction, but if coupling reaction alternatives were thoroughly re-examined there could be a possible protocol to reach the final compounds. The second-generation synthetic strategy saw very good progress through most of the synthetic route and only finding limitation at the coupling between side chain and β -keto ester and the following protocols to pyrone preparation. If these steps were more thoroughly investigated there could be solutions which could allow for higher yielding and more reliable access to the functionalised pyrone natural products.

Both first and second-generation synthetic strategies have lengthy step counts and rely on high fidelity of all synthetic steps to provide reliable access to the pyrone motif. An optimal future outcome would see a movement away from the lengthy dianion addition, oxidation, and cyclisation methodologies that were refined within the first and second-generation synthetic strategies but provided only incremental developments over those previously utilised in the literature. Meaningful innovation would see pyrone preparation completed in less than 3 steps ready for coupling to a side chain, increasing the convergent and divergent utility of a multi-fragment strategy. The De Paolis desymmetrisation approach investigated in Chapter 6 could allow for such a fast, reliable, and high yielding access to α -methoxy- γ -pyrone natural products. The main obstacle yet to overcome is the stubborn 1,4-addition reaction to the pyrone ring which, if a reliable alternative nucleophile could be found, a novel set of approaches could be incorporated into a functional synthetic strategy. Another interesting approach which has seen little development is the single pot preparation of 6-ethyl-3,5-dimethyl-4-hydroxy- α -pyrones through the condensation of three propionyl chloride units demonstrated by Osman (Figure 7.17),⁵⁸ originally demonstrated in 1977 and utilised in a number of early pyrone syntheses but has seen limited protocol application.

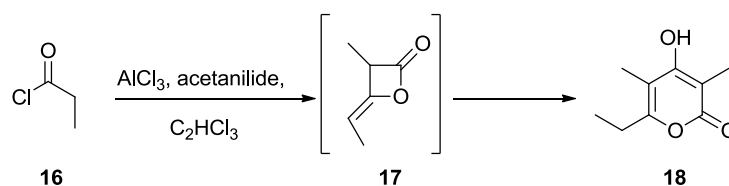


Figure 7.17 Osman *et al* preparation of 6-ethyl-3,5-dimethyl-4-hydroxy- α -pyrones utilizing β -lactone dimer intermediate.⁵⁸

The alkyl ketene dimer, specifically the methylketene dimer, approach shows underutilised potential for pyrone preparation and a greater understanding of the mechanism and reagent contributors could allow the discovery of novel and short preparations of substituted pyrone synthons.

Conclusion and Future Directions

8 Experimental Procedures

8.1 General experimental procedures

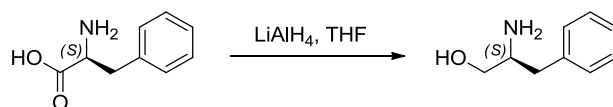
All reactions were carried out in flame-dried glassware and reactions took place under nitrogen or argon atmosphere unless otherwise indicated. Laboratory solvents: CH₂Cl₂ distilled over CaH₂ and THF, Et₂O were distilled over sodium and benzophenone prior to use. Reagents: Diisopropylamine (HDA), triethylamine (NEt₃), DMPU, were distilled over CaH₂. DMSO was distilled under vacuum and stored over 4A MS. Other reagents and solvents were used as provided by commercial supplier. Analytical thin-layer chromatography was performed on Merck TLC Silica gel 60 F²⁵⁴ alumina backed sheets, visualised with an ultraviolet lamp and developed with KMnO₄ solution (3.0 g KMnO₄, 20 g K₂CO₃, 5 mL 5% NaOH, 300 mL H₂O). Column chromatography was performed on Merck Silicagel (0.04 – 0.06 mm) 230 – 400 mesh silica.

¹H NMR spectra were produced on Bruker Avance III NMR Spectrometers at either 400 MHz or 600 MHz. The same instruments were utilised for analysis of ¹³C NMR spectra, using either 100 MHz or 150 MHz. The internal lock was calibrated to Chloroform-*d* solvent used in all samples and referenced to CHCl₃ (δ 7.26) for ¹H NMR and CHCl₃ (δ 77.16) for ¹³C NMR. Abbreviations: *s* = singlet, *d* = doublet, *t* = triplet, *m* = multiplet. Structural and stereochemical assignments of synthetic compounds, where required, were made using COSY, HMQC and HMBC 2D NMR experiments.

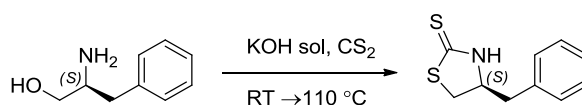
Optical rotation of compounds was determined by polarimetry on a PolA AR21 polarimeter referenced to the sodium D line (589 nm) at 20 °C. Electrospray Ionisation (ESI) mass spectra were recorded using a Waters Synapt HDMS or LC/MS equipped with a time-of-flight mass analyser. Atmospheric pressure chemical ionization (APCI) mass spectra were recorded using a Perkin Elmer AxION DSA-ToF and calibrated through infusion of Agilent Technologies APCI/APPI Tuning mix, P/N: G2432A. The mass spectra data were reported as the observed molecular ion.

Infrared spectra were recorded on an FTIR spectrometer with the absorptions reported in wavenumbers (cm⁻¹).

Experimental Procedures

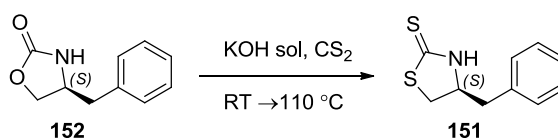


(S)-2-Amino-3-phenyl-1-propanol (L-Phenylalaninol) LiAlH₄ (4.36 g, 0.11 mol) was weighed out and diluted with slow addition of THF (150 mL) with evolution of hydrogen. The mixture was heated to reflux before portioned addition of L-phenylalanine (9.5 g, 57.5 mmol) over 30 minutes where vigorous liberation of hydrogen was observed. This mixture was allowed to react for 48 hours before addition of ethyl acetate (10 mL) to destroy excess LiAlH₄. Then an aqueous Rochelle's salt solution (60 g in 60 mL) was added to break up the eventual slurry. This mixture was allowed to stir for an hour before the organic phase was separated and the aqueous extracted with ethyl acetate (3×100 mL). The organic extracts were combined, dried with Na₂SO₄ and concentrated under vacuum. Giving a crude orange oil which after recrystallisation (ether:hexane) give the *title compound* (6.94 g, 79%) as white crystals. ¹H NMR (600 MHz, Chloroform-*d*) δ 7.30 - 7.27 (m, 2H), 7.23 - 7.20 (m, 1H), 7.19 - 7.17 (m, 2H), 3.63 (dd, J = 10.8, 3.6 Hz, 1H), 3.40 (dd, J = 10.8, 7.2 Hz, 1H), 3.13 (m, 1H), 2.78 (dd, J = 13.8, 5.4 Hz, 1H), 2.72 (br s, 3H), 2.55 (dd, J = 13.2, 8.4 Hz, 1H); ¹³C NMR (101 MHz, Chloroform-*d*) δ 138.5, 129.3, 128.7, 126.6, 65.9, 54.3, 40.5. The analytical data matched that of literature.^{223,224}



(S)-4-benzylthiazolidine-2-thione (151) To a stirring suspension of *L-Phenylalaninol* (6.10 g, 40.3 mmol) in KOH solution (2.5M, 161 mL) was added carbon disulfide (9.71 mL, 0.161 mol), dropwise over 5 minutes. The resulting orange solution was then heated to reflux (110 °C) overnight, then cooled to RT and extracted with CH₂Cl₂ (3 × 50 mL). The combined organic extracts were dried (Na₂SO₄) and concentrated under vacuum, yielding the thiazolidinethione (6.943 g, 82%) as clear amorphous solid giving crystals over time. Further purification was conducted through column chromatography (CH₂Cl₂)

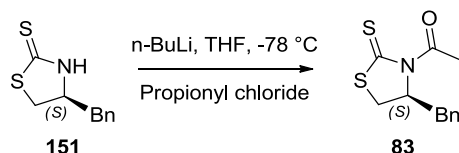
Alternative route from oxazolidinone:



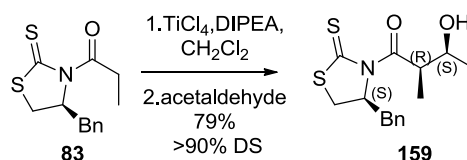
To a stirring suspension of the oxazolidinone **152** (12 g, 67.7 mmol) in KOH solution (2.5M, 226 mL) was added carbon disulfide (20 mL, 338 mmol), slowly over 5 minutes. The resulting orange solution was then heated to reflux (110 °C) overnight, then cooled to RT and extracted with

Experimental Procedures

CH₂Cl₂ (3 × 100 mL). The combined organic extracts were dried (Na₂SO₄) and concentrated under vacuum, yielding the thiazolidinethione **151** (8.51 g, 60 %) as clear amorphous solid. Further purification was conducted through column chromatography. ¹H NMR (600 MHz, Chloroform-*d*) δ 7.37 (t, *J* = 7.4 Hz, 2H), 7.30 (t, *J* = 7.3 Hz, 1H), 7.21 (d, *J* = 7.4 Hz, 2H), 6.94 (s, 1H), 4.45 (p, *J* = 7.3 Hz, 1H), 3.64 (dd, *J* = 11.2, 7.6 Hz, 1H), 3.35 (dd, *J* = 11.2, 7.0 Hz, 1H), 3.05 – 2.96 (m, 2H); ¹³C NMR (151 MHz, Chloroform-*d*) δ 200.8, 135.7, 129.0, 128.9, 127.4, 65.0, 39.9, 38.1 Characterisation matched that of the literature.²²⁵



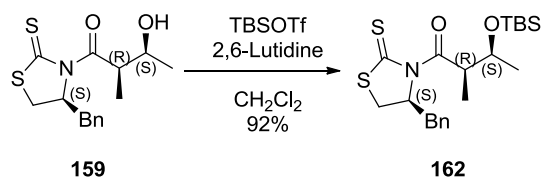
1-[(4*S*)-4-benzyl-2-thioxo-1,3-thiazolidin-3-yl]propan-1-one (83) To a stirred solution of thiazolidinethione (227 mg, 1.08 mmol) in THF (10 mL) n-BuLi (0.75mL; 1.2mmol from 1.6 M solution in THF) was added dropwise at -78 °C. The solution stirred for 30 minutes before Propionyl chloride (0.20 mL, 2.3 mmol) was added dropwise. The reaction was stirred for a further 30 minutes at -78 °C. The reaction was allowed to warm to RT over 2 hours and then quenched with 10% K₂CO₃ (100 mL). The aqueous layer was extracted with CH₂Cl₂ (3 x 50 mL). The combined organic layers were dried (Na₂SO₄) and concentrated under vacuum. Purification through column chromatography (CH₂Cl₂) afforded the *title compound* **3** (260.4 mg, 90.8%) as yellow solid. *R_f* = 0.475 (20% EtOAc/ X4). ¹H NMR (600 MHz, Chloroform-*d*) δ 1.20 (t, *J* = 7.2 Hz, 3H), 2.88 (d, *J* = 11.5 Hz, 1H), 3.05 (dd, *J* = 13.2, 10.6 Hz, 1H), 3.09 – 3.18 (m, 1H), 3.22 (dd, *J* = 13.2, 3.9 Hz, 1H), 3.41 (ddd, *J* = 24.7, 11.1, 7.2 Hz, 2H), 5.39 (ddd, *J* = 10.8, 7.2, 3.8 Hz, 1H), 7.27 – 7.31 (m, 3H), 7.34 (t, *J* = 7.5 Hz, 2H); ¹³C NMR (151 MHz, Chloroform-*d*) δ 201.15, 174.99, 136.62, 129.48, 128.93, 127.23, 68.70, 36.81, 32.37, 31.94, 8.83; **IR** (thin film) ν 3147, 2941, 1602, 1495, 1294, 1265, 1043, 1007, 952, 746, 701, 499;



(2*S*,3*R*)-1-[(4*S*)-4-benzyl-2-thioxo-thiazolidin-3-yl]-3-hydroxy-2-methyl-butan-1-one (non-Evans *syn*) (159) To a solution of propionyl thiazolidinethione **83** (0.4595 g, 1.73 mmol) in CH₂Cl₂ (6 mL), at -40 °C, was added TiCl₄ (1.9 mL of a 1M soln. in CH₂Cl₂) The solution was stirred at -40 °C for 40 mins. iPr₂NEt (0.30 mL, 1.73 mmol) was then added at -40 °C and the solution was stirred for 30 min, the reaction mixture was then cooled to -78 °C. Cold Acetaldehyde (0.20 mL, 3.46 mmol) was added via cannula with 2 mL CH₂Cl₂. The solution was

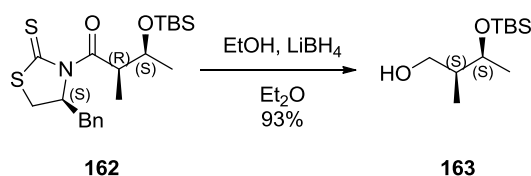
Experimental Procedures

stirred at $-78\text{ }^{\circ}\text{C}$ over a 1 hour period. When TLC showed consumption of starting material, the reaction was quenched with NH_4Cl (8 mL) and diluted with brine. The organic layer was separated and the aqueous layer extracted with CH_2Cl_2 (3×10 mL). The organic extracts were combined, dried with Na_2SO_4 and concentrated under vacuum. The product was purified through Column Chromatography (10% EtOAc/X4) affording the *title compound* as the major isomer (0.3829 g, 1.24 mmol) and minor isomer (0.0438 g, 0.14 mmol)(79% yield 9:1 dr) as yellow solids. $R_f = 0.38$ (30% EtOAc/X4); $^1\text{H NMR}$ (600 MHz, Chloroform-*d*) δ 7.37 – 7.32 (m, 2H), 7.30 – 7.26 (m, 3H), 5.37 (ddd, $J = 10.9, 7.1, 4.1$ Hz, 1H), 4.66 (qd, $J = 7.1, 2.6$ Hz, 1H), 4.30 – 4.23 (m, 1H), 3.38 (ddd, $J = 11.5, 7.2, 1.1$ Hz, 1H), 3.24 (dd, $J = 13.3, 4.1$ Hz, 1H), 3.05 (dd, $J = 13.2, 10.4$ Hz, 1H), 2.89 (d, $J = 11.5$ Hz, 1H), 2.79 (s, $J = 2.8$ Hz, 1H), 1.21 (dd, $J = 8.1, 6.7$ Hz, 6H); $^{13}\text{C NMR}$ (151 MHz, Chloroform-*d*) δ 201.88, 178.34, 136.54, 129.60, 129.08, 127.44, 69.07, 67.53, 43.62, 37.14, 31.99, 19.57, 10.68; **IR** (thin film) ν 3402, 3027, 2925, 1688, 1495, 1454, 1341, 1292, 1258, 1192, 1164, 1136, 1033, 912, 849, 797, 742, 702, 455; $[\alpha]_D^{20} = 166.3$ ($c = 0.445$ g/100 mL, CHCl_3); **MS** (APCI) calculated for $\text{C}_{15}\text{H}_{20}\text{NO}_2\text{S}_2$ $[\text{M}+\text{H}]^+$: 310.0935, found 310.0924.

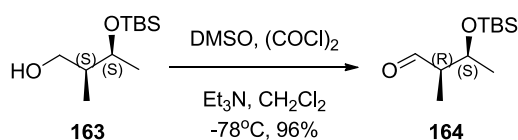


(2*S*,3*R*)-1-[(4*S*)-4-benzyl-2-thioxo-thiazolidin-3-yl]-3-tertbutyldimethylsilyloxy-2-methyl-butan-1-one (162) To a stirring solution of the major aldol product **159** (1.47 g, 4.75 mmol) in CH_2Cl_2 (24 mL), 2,6-lutidine (1.1 mL, 9.5 mmol) was added at $-78\text{ }^{\circ}\text{C}$, followed by TBSOTf (1.96 mL, 8.55 mmol). The solution was stirred at $-78\text{ }^{\circ}\text{C}$ for 2.5 hours. The reaction was warmed slowly to $0\text{ }^{\circ}\text{C}$ and quenched with 5% NaHCO_3 (50 mL). The organic layer was separated and the aqueous layer extracted with CH_2Cl_2 (3×30 mL). The organic extracts were combined, dried (Na_2SO_4) and concentrated under reduced pressure. Column Chromatography (10% EtOAc/X4) afforded the TBS ether (1.859 g, 92%) as a thick, yellow oil. $R_f = 0.61$ (20% EtOAc/ X4); $^1\text{H NMR}$ (600 MHz, Chloroform-*d*) δ 7.34 (dd, $J = 8.1, 6.8$ Hz, 2H), 7.28 (dd, $J = 7.7, 2.0$ Hz, 3H), 5.37 (dddd, $J = 10.9, 7.3, 3.7, 1.2$ Hz, 1H), 4.62 (qd, $J = 6.8, 5.7$ Hz, 1H), 4.24 (p, $J = 6.0$ Hz, 1H), 3.33 (ddd, $J = 11.5, 7.3, 1.1$ Hz, 1H), 3.20 (dd, $J = 13.2, 3.7$ Hz, 1H), 3.04 (dd, $J = 13.2, 10.7$ Hz, 1H), 2.86 (dd, $J = 11.5, 1.2$ Hz, 1H), 1.21 (dd, $J = 6.5, 5.6$ Hz, 6H), 0.90 (s, 9H), 0.06 (d, $J = 8.9$ Hz, 6H); $^{13}\text{C NMR}$ (151 MHz, Chloroform-*d*) δ 201.33, 176.75, 136.76, 129.55, 129.08, 127.37, 69.74, 69.20, 45.78, 37.31, 31.75, 26.02, 22.21, 18.24, 13.64, -3.94, -4.56; **IR** (thin film) ν 3027, 2928, 2855, 1701, 1604, 1496, 1460, 1361, 1341, 1293, 1254, 1190, 1162, 1137, 1101, 1029, 962, 835, 805, 775, 743, 701, 455; $[\alpha]_D^{20} = 128.6$ ($c = 0.35$ g/100 mL, CHCl_3); **MS** (ESI) calculated for $\text{C}_{21}\text{H}_{34}\text{NO}_2\text{S}_2\text{Si}$ $[\text{M}+\text{H}]^+$: 424.1800, found 424.1804.

Experimental Procedures



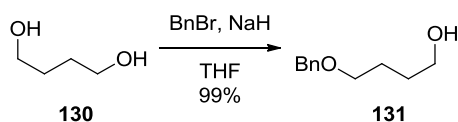
(2*S*,3*S*)-3-((*tert*-butyldimethylsilyl)oxy)-2-methylbutan-1-ol (163) A solution of the TBS ether **162** (1 g, 2.36 mmol) in 12 mL Et₂O was cooled to -10 °C and had EtOH (0.69 mL, 11.8 mmol) added dropwise, followed by LiBH₄ (2.95 mL 5.9 mmol, of a 2M solution in THF). Gas was seen to evolve. The solution was stirred at -10 °C for 4 hours and colour change was observed from yellow to white. When TLC showed consumption of starting material, the reaction was quenched at -10 °C with NaOH solution (3M, 10 mL), followed by stirring at -10 °C for a further 10 min. The solution was poured onto brine, with the brine layer extracted with Et₂O (3 × 20 mL). The organic extracts were combined, dried (Na₂SO₄) and concentrated under reduced pressure. Selectively dissolving the liquid in X4, followed by purification via column chromatography (10% EtOAc/X4 on buffered silica), yielding the *title compound* (0.479 g, 93%) as a clear liquid. **R_f** = 0.4 (20% EtOAc/ X4); **¹H NMR** (600 MHz, Chloroform-*d*) δ 4.00 (qd, *J* = 6.3, 3.5 Hz, 1H), 3.72 (ddd, *J* = 10.7, 8.9, 2.8 Hz, 1H), 3.51 (ddd, *J* = 11.1, 7.1, 4.5 Hz, 1H), 2.97 (dd, *J* = 7.2, 3.0 Hz, 1H), 1.95 (dqdd, *J* = 14.1, 7.1, 4.6, 3.5 Hz, 1H), 1.15 (d, *J* = 6.3 Hz, 3H), 0.89 (s, 9H), 0.79 (d, *J* = 7.1 Hz, 3H), 0.08 (d, *J* = 4.2 Hz, 6H); **¹³C NMR** (151 MHz, Chloroform-*d*) δ 72.38, 65.81, 40.96, 25.93, 18.39, 18.10, 12.51, -4.37, -4.92; **IR** (thin film) ν 3367, 2957, 2929, 2857, 1472, 1463, 1373, 1253, 1157, 1092, 1042, 1006, 958, 902, 836, 775, 455; **[α]_D²⁰** = 13.8 (*c* = 0.58 g/100 mL, CHCl₃); **MS** (APCI) calculated for C₁₁H₂₇O₂Si [M+H]⁺: 219.1780, found 219.1773.



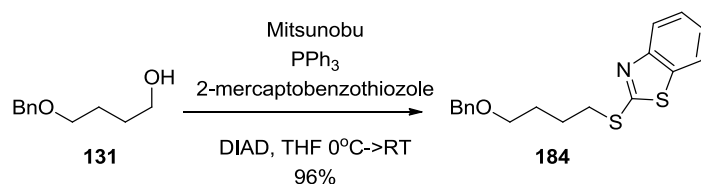
(2*R*,3*S*)-3-((*tert*-butyldimethylsilyl)oxy)-2-methylbutanal (164) (*Swern*) To a stirring solution of DMSO (0.85 ml 12 mmol) in CH₂Cl₂ (16 ml), was added oxalyl chloride (2.7 ml; 5.4 mmol of 2 M solution in CH₂Cl₂). This mixture was stirred for 30 minutes at -78 °C. Then a solution of alcohol **163** (0.655 g; 3 mmol, in 4 mL of CH₂Cl₂) was added dropwise and stirred for 40 minutes at -78 °C. To this mixture was added Et₃N (2.93 ml; 20 mmol) and allowed for 40 minutes until TLC showed consumption of starting material. The reaction was quenched with sat. NH₄Cl sol. and diluted with brine. The organic layer was separated and the aqueous layer extracted with CH₂Cl₂ (2 × 20 mL). The organic extracts were combined, dried with Na₂SO₄ and concentrated under vacuum. The product was purified through Column Chromatography (5% EtOAc/X4 on buffered silica), yielded the *title compound* as a clear liquid (0.62 g, 96%). The aldehyde was not stored but used immediately for the next step. **R_f** = 0.659 (20% EtOAc/ X4); **¹H NMR** (600 MHz,

Experimental Procedures

Chloroform-*d*) δ 9.77 (d, $J = 1.3$ Hz, 1H), 4.26 (qd, $J = 6.3, 4.3$ Hz, 1H), 2.38 (qdd, $J = 7.0, 4.2, 1.3$ Hz, 1H), 1.18 (d, $J = 6.3$ Hz, 3H), 1.07 (d, $J = 6.9$ Hz, 3H), 0.87 (s, 8H), 0.06 (d, $J = 11.8$ Hz, 6H); ^{13}C NMR (151 MHz, Chloroform-*d*) δ 205.43, 68.36, 53.59, 25.86, 21.34, 18.11, 8.33, -4.12, -4.85; $[\alpha]_{\text{D}}^{20} = -37.9$ ($c = 0.225$ g/100 mL, CHCl_3);

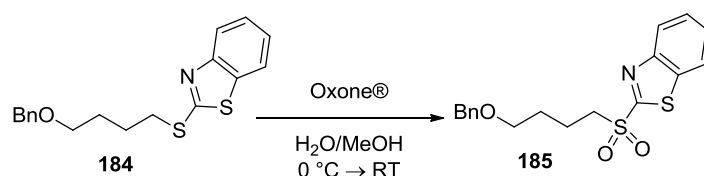


4-(benzyloxy)butan-1-ol (131) To a solution of sodium hydride (4.91 g of 60% dispersion in mineral oil, 0.122 mol) in THF (173 ml) was added dropwise a solution of 1,4-butanediol **130** (29 ml, 0.327 mol) in THF (100 ml) at 0 °C, hydrogen was evolved. The mixture was stirred overnight and then quenched slowly with sat NH_4Cl sol and diluted with brine. The organic layer was separated and the aqueous layer extracted with Et_2O (3×20 mL). The organic extracts were combined, dried with Na_2SO_4 and concentrated under vacuum. The product was purified through flash chromatography (10% $\text{EtOAc}/\text{X4}$) to give the *title compound* (14.65, 99 % yield) as a clear liquid; $R_f = 0.317$ (50% $\text{EtOAc}/\text{X4}$); ^1H NMR (600MHz, Chloroform-*d*) $\delta = 7.38 - 7.27$ (m, 5 H), 4.53 (s, 2 H), 3.65 (t, $J = 6.0$ Hz, 2 H), 3.53 (t, $J = 5.8$ Hz, 2 H), 1.77 - 1.64 (m, 4 H); ^{13}C NMR (151 MHz, Chloroform-*d*) δ 138.3, 128.6, 127.9, 127.8, 73.2, 70.5, 62.9, 30.3, 26.9. Spectral data matched that of literature.²²⁶

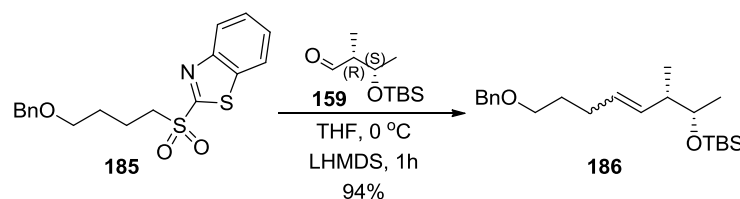


2-((4-(benzyloxy)butyl)thio)benzo[d]thiazole (184) To a solution of benzyl ether **131** (4.75 g, 26.35 mmol) in THF was added PPh_3 (9.63 g, 36.9 mmol), 2-Mercaptobenzothiazole (6.61 g, 39.5 mmol) and DIAD (8.53 ml, 42.2 mmol) at 0 °C. The mixture was allowed to mix overnight and then quenched with water (30 ml). The aqueous extracted with EtOAc . The organic extracts were combined, dried with Na_2SO_4 and concentrated under vacuum. The product was purified through flash chromatography (10% $\text{EtOAc}/\text{X4}$) affording the *title compound* **184** (8.30 g, 95%) as a clear light yellow liquid; $R_f = 0.561$ (30% $\text{Et}_2\text{O}/\text{X4}$); ^1H NMR (600MHz, Chloroform-*d*) $\delta = 7.90$ (d, $J = 8.3$ Hz, 1 H), 7.77 (d, $J = 8.1$ Hz, 1 H), 7.44 (t, $J = 7.7$ Hz, 1 H), 7.36 (d, $J = 4.2$ Hz, 3 H), 7.32 (t, $J = 7.1$ Hz, 1 H), 7.34 - 7.27 (m, $J = 5.5$ Hz, 1 H), 4.54 (s, 2 H), 3.56 (t, $J = 6.2$ Hz, 2 H), 3.41 (t, $J = 7.3$ Hz, 2 H), 1.98 (quin, $J = 7.4$ Hz, 2 H), 1.89 - 1.80 (m, 2 H); ^{13}C NMR (151 MHz, Chloroform-*d*) δ 138.3, 128.6, 127.9, 127.8, 73.2, 70.5, 62.9, 30.3, 26.9; IR (thin film) ν 3062, 3029, 2938, 2857, 1495, 1361, 1309, 1361, 1309, 1275, 1206, 1158, 1044, 935, 852, 800, 672.

Experimental Procedures



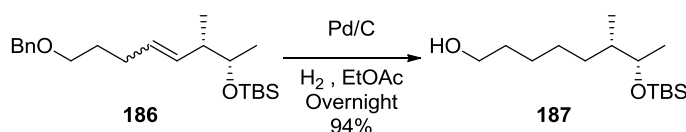
2-((4-(benzyloxy)butyl)sulfonyl)benzo[d]thiazole (185) To a solution of Oxone® (2.37 g, 3.8 mmol) in equal parts water/methanol (10 mL) was added sulfide **184** (317 mg, 0.96 mmol) and brine (1 mL) at 0 °C. The mixture was stirred for 30 minutes and then allowed to warm to room temperature and stirred overnight. The reaction was then quenched with 1M HCl (10 mL) was added and the mixture was extracted with CH₂Cl₂ (3 × 10 mL). The organic extracts were combined, dried with Na₂SO₄ and concentrated under vacuum. The product was purified through flash chromatography (10% EtOAc/X4) affording the *title compound* **185** (316 mg, 91 %) as a clear liquid; *R_f* = 0.362 (30% Et₂O/X4); ¹H NMR (600MHz, Chloroform-*d*) δ = 8.22 (d, *J* = 8.3 Hz, 1 H), 8.02 (d, *J* = 8.1 Hz, 1 H), 7.67 - 7.57 (m, 2 H), 7.33 - 7.23 (m, 5 H), 4.46 (s, 2 H), 3.59 - 3.53 (m, 2 H), 3.48 (t, *J* = 6.0 Hz, 2 H), 2.06 - 1.97 (m, 2 H), 1.81 - 1.73 (m, 2 H); ¹³C NMR (151 MHz, Chloroform-*d*) δ 166.0, 152.9, 138.3, 136.9, 128.5, 128.1, 127.8, 127.8, 125.6, 122.5, 73.2, 69.2, 54.7, 28.4, 19.9; IR (thin film) ν 3164, 1674, 1470, 1211, 1043, 746, 635.



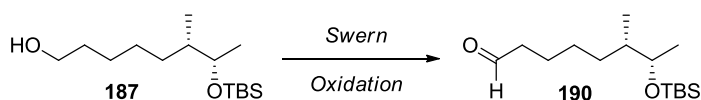
((2*S*,3*S*)-8-(benzyloxy)-3-methyloct-4-en-2-yl)oxy)(*tert*-butyl)dimethylsilane (186) To a stirring solution of aldehyde **164** (0.485 g, 2.24 mmol) and sulfone **185** (1.62 g, 4.48 mmol, 2 eq) in THF (6.80 mL) at 0 °C, was added LHMDS (4.48 mL, 1 mol/L in toluene). The reaction mixture was stirred at 0 °C for 30 minutes, when TLC showed consumption of SM, the reaction mixture was quenched with sat NH₄Cl solution. The organic layer was separated and the aqueous layer extracted with Et₂O (3 × 10 mL). The organic extracts were combined, dried with Na₂SO₄ and concentrated under vacuum. The crude mixture was purified through column chromatography (10% EtOAc/X4) giving a mixture *cis* and *trans* isomers as a colourless liquid (0.7629g; 94%). *R_f* = 0.65 (20% EtOAc/X4); ¹H NMR (600MHz, Chloroform-*d*) δ = 7.34 (dd, *J* = 4.6, 0.7 Hz, 4H), 7.28 (qd, *J* = 4.6, 1.1 Hz, 1H), 5.44 - 5.17 (m, 2H), 4.50 (s, 2H), 3.59 - 3.49 (m, 1H), 3.47 (td, *J* = 6.6, 2.4 Hz, 2H), 2.46 - 2.37 (m, 1H), 2.21 - 2.03 (m, 3H), 1.68 (tq, *J* = 8.5, 6.6 Hz, 2H), 1.08 (d, *J* = 6.1 Hz, 2H), 1.04 (d, *J* = 6.1 Hz, 2H), 0.94 (dd, *J* = 6.8, 1.8 Hz, 3H), 0.89 (d, *J* = 4.6 Hz, 9H), 0.04 (dd, *J* = 6.1, 2.8 Hz, 6H); ¹³C NMR (151 MHz, Chloroform-*d*) δ 138.71, 138.65, 133.84, 133.76, 129.23, 128.51, 128.36, 127.65, 127.50, 127.49, 72.95, 72.90, 72.55, 72.34, 69.98, 69.84, 44.68, 40.01, 29.85, 29.63, 29.28, 25.95, 25.93, 24.31, 21.95, 21.23, 18.18, 18.16, 17.18, 16.28, -

Experimental Procedures

4.21, -4.28, -4.72; **IR** (thin film) ν 3031, 2956, 2930, 2857, 1723, 1496, 1472, 1463, 1361, 1313, 1252, 1109, 1079, 1029, 1006, 957, 940, 836, 814, 774, 734, 697, 666; **MS** (APCI) calculated for $C_{22}H_{39}O_2Si$ $[M+H]^+$: 363.2714, found 363.2712.



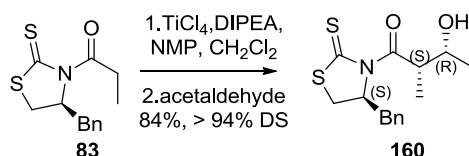
(6S,7S)-7-((tert-butyldimethylsilyl)oxy)-6-methyloctan-1-ol (187) A mixture of *cis* and *trans* isomers **186** (2.56 g; 7.06 mmol) in dry ethyl acetate with 10% Pd/C (0.750 g, 0.71 mmol) was stirred under a hydrogen atmosphere at room temperature for 24 h. The reaction mixture was filtered through a plug of silica and the solvent evaporated *in vacuo* to give the crude product, which was purified by flash chromatography (10% EtOAc/X4) affording the *title compound* **187** (1.80 g, 6.57 mmol 93%) as a clear liquid; $R_f = 0.312$ (20% Et₂O/X4); **¹H NMR** (600MHz, Chloroform-*d*) δ 3.70 – 3.66 (m, 1H), 3.64 (t, $J = 6.7$ Hz, 2H), 1.57 (ddt, $J = 8.4, 6.7, 3.6$ Hz, 3H), 1.51 – 1.17 (m, 5H), 1.12 – 1.00 (m, 1H), 1.05 (d, $J = 6.3$ Hz, 3H), 0.88 (s, 9H), 0.82 (d, $J = 6.8$ Hz, 3H), 0.03 (d, $J = 7.1$ Hz, 6H); **¹³C NMR** (151 MHz, Chloroform-*d*) δ 71.79, 63.27, 40.40, 33.00, 32.66, 27.48, 26.23, 26.04, 20.67, 18.27, 14.76, -4.09, -4.66; **IR** (thin film) ν 3392, 2931, 2858, 1642, 1472, 1380, 1251, 1108, 1072, 955, 836, 773; $[\alpha]_D^{20} = 0.0$ (unable to detect rotation); **MS** (APCI) calculated for $C_{15}H_{34}O_2Si$ $[M+H]^+$: 275.2401, found 275.2401.



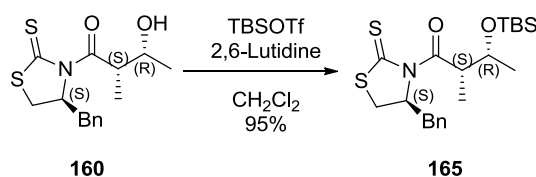
(6S,7S)-7-((tert-butyldimethylsilyl)oxy)-6-methyloctanal (190) (Swern oxidation) To a solution of DMSO (0.124 mL, 1.75 mmol) in CH₂Cl₂ (4 mL), was added oxalyl chloride (0.35 mL 0.69 mmol of 2 M solution in CH₂Cl₂), This mixture was stirred for 30 minutes at -78 °C. Then a solution of alcohol **187** (120 mg, 0.44 mmol, in 1 mL of CH₂Cl₂) was added dropwise and stirred for 40 minutes at -78°C. To this mixture was added Et₃N (0.45 mL, 3.2 mmol) and allowed for 40 minutes until TLC showed consumption of starting material. The reaction was quenched with sat NH₄Cl sol and diluted with brine. The organic layer was separated and the aqueous layer extracted with CH₂Cl₂ (2 × 8 mL). The organic extracts were combined, dried with Na₂SO₄ and concentrated under vacuum. The product was purified through Column Chromatography to give the *title compound* **190** (0.118 g, 0.43 mmol, 99%) as a clear liquid; $R_f = 0.3125$ (20% Et₂O/X4); **¹H NMR** (600MHz, Chloroform-*d*) δ 9.76 (t, $J = 1.8$ Hz, 1H), 3.67 (qd, $J = 6.2, 3.9$ Hz, 1H), 2.42 (td, $J = 7.5, 1.9$ Hz, 2H), 1.61 (tddd, $J = 13.6, 12.3, 8.6, 6.2$ Hz, 3H), 1.49 – 1.41 (m, 1H), 1.42 – 1.33 (m, 2H), 1.32 – 1.23 (m, 1H), 1.12 – 1.06 (m, 1H), 1.04 (d, $J = 6.2$ Hz, 3H), 0.87 (s, 10H), 0.81 (d, $J = 6.7$ Hz, 5H), 0.02 (d, $J = 8.6$ Hz, 7H); **¹³C NMR** (151 MHz, Chloroform-*d*) δ 203.04,

Experimental Procedures

77.16, 71.66, 44.07, 40.25, 32.36, 32.35, 27.25, 26.02, 22.55, 20.55, 18.25, 14.70, -4.10, -4.68; **IR** (thin film) ν 3838, 2957, 2930, 2858, 2711, 1729, 1473, 1463, 1380, 1252, 1106, 1072, 1005, 957, 836, 774, 666, 646, 618, 614, 609, 606, 602; $[\alpha]_D^{20} = 0.0$ (unable to detect rotation); **MS** (APCI) calculated for $C_{15}H_{32}O_2Si$ $[M+H]^+$: 271.2088, found 271.2082.

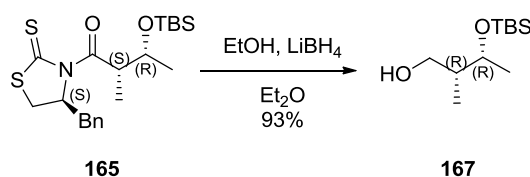


(2R,3S)-1-[(4S)-4-benzyl-2-thioxo-thiazolidin-3-yl]-3-hydroxy-2-methyl-butan-1-one (Evans syn) (160) To a solution of thiazolidinethione **83** (0.212 g, 0.8 mmol) in CH_2Cl_2 (3 mL), at 0 °C, was added TiCl_4 (0.84 mL of a 1M soln. in CH_2Cl_2) The solution was stirred at 0 °C for 40 minutes. $i\text{Pr}_2\text{NEt}$ (0.14 mL, 0.8 mmol) was then added at 0 °C and the solution was stirred for 30 min, then *N*-methyl-2-pyrrolidinone (0.15 mL, 1.6 mmol) was added and stirred for a further 30 minutes. The reaction mixture was then cooled to -78 °C and acetaldehyde (0.18 mL, 3.2 mmol) was added via cannula with 1 mL CH_2Cl_2 . The solution was stirred at -78 °C over a 1 hour period until TLC showed consumption of SM. The reaction was allowed to warm to -40 °C, then quenched with NH_4Cl aqueous solution and diluted with brine. The organic layer was separated and the aqueous layer extracted with CH_2Cl_2 (4 \times 10 mL). The organic extracts were combined, dried with Na_2SO_4 and concentrated under vacuum. The product was purified through Column Chromatography (20% EtOAc/X4) affording the *title compound* as the major isomer (0.2079 g, 0.67 mmol, 84% yield 94% ds) as yellow pungent oil and minor isomer (0.011 g, 0.48 mmol) as yellow solid. $R_f = 0.313$ (30% EtOAc/X4). **$^1\text{H NMR}$** (600 MHz, Chloroform-*d*) δ 7.38 – 7.31 (m, 2H), 7.31 – 7.26 (m, 3H), 5.35 (ddd, $J = 10.7, 7.0, 3.9$ Hz, 1H), 4.41 (qd, $J = 6.9, 3.1$ Hz, 1H), 4.14 (dd, $J = 6.5, 3.2$ Hz, 1H), 3.40 (ddd, $J = 11.6, 7.1, 1.1$ Hz, 1H), 3.21 (dd, $J = 13.3, 4.0$ Hz, 1H), 3.05 (dd, $J = 13.2, 10.5$ Hz, 1H), 2.91 (d, $J = 11.5$ Hz, 1H), 1.27 (d, $J = 6.9$ Hz, 4H), 1.20 (d, $J = 6.4$ Hz, 3H); **$^{13}\text{C NMR}$** (151 MHz, Chloroform-*d*) δ 201.56, 178.51, 136.50, 129.59, 129.09, 127.44, 68.91, 68.59, 44.53, 36.94, 32.28, 20.37, 10.58; **IR** (thin film) ν 3393, 3064, 3028, 2955, 2929, 2856, 1699, 1604, 1496, 1472, 1455, 1361, 1341, 1319, 1292, 1257, 1192, 1165, 1137, 1103, 1078, 1031, 964, 889, 835, 803, 775, 744, 702, 451; $[\alpha]_D^{20} = 150$ ($c = 0.19$ g/100 mL, CHCl_3); **MS** (APCI) calculated for $C_{15}H_{20}NO_2S_2$ $[M+H]^+$: 310.0935, found 310.0926.

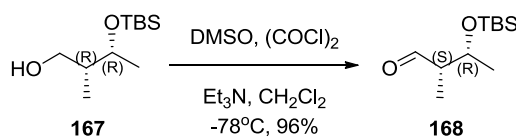


Experimental Procedures

(2*S*,3*R*)-1-[(4*S*)-4-benzyl-2-thioxo-thiazolidin-3-yl]-3-tertbutyldimethylsilyloxy-2-methyl-butan-1-one (165) To a stirring solution of the aldol adduct **160** (1.27 g, 4.12 mmol) in CH₂Cl₂ (21 mL), 2,6-lutidine (0.86 mL, 7.4 mmol) was added at -78°C, followed by TBSOTf (1.32 mL, 5.77 mmol). The solution was stirred at -78 °C for 2.5 hours. The reaction was warmed slowly to 0 °C and quenched with 5% NaHCO₃ (50 mL). The organic layer was separated and the aqueous layer extracted with CH₂Cl₂ (3 × 30 mL). The organic extracts were combined, dried (Na₂SO₄) and concentrated under reduced pressure. Column Chromatography (10% EtOAc/X4) afforded the TBS ether (1.6541 g, 94.7%) as a thick yellow oil. **R_f** = 0.61 (20% EtOAc/ X4); **¹H NMR** (600 MHz, Chloroform-*d*) δ 7.36 – 7.31 (m, 2H), 7.26 (s, 3H), 5.22 – 5.15 (m, 1H), 4.53 (qd, *J* = 6.8, 5.2 Hz, 1H), 4.15 – 4.08 (m, 1H), 3.35 – 3.24 (m, 2H), 3.03 (dd, *J* = 13.2, 10.7 Hz, 1H), 2.87 (dd, *J* = 11.5, 0.7 Hz, 1H), 1.21 (d, *J* = 6.8 Hz, 3H), 1.17 (d, *J* = 6.2 Hz, 3H), 0.90 – 0.81 (m, 11H), 0.06 – -0.02 (m, 8H); **¹³C NMR** (151 MHz, Chloroform-*d*) δ 201.35, 176.79, 136.84, 129.64, 129.05, 127.33, 70.78, 69.64, 46.44, 36.70, 32.19, 25.92, 21.58, 18.17, 12.34, -4.24, -4.83. **IR** (thin film) ν 3027, 2928, 2855, 1701, 1604, 1496, 1460, 1361, 1341, 1293, 1254, 1190, 1162, 1137, 1101, 1029, 962, 835, 805, 775, 743, 701, 455; [α]_D²⁰ = 160.7 (*c* = 0.585 g/100 mL, CHCl₃); **MS** (APCI) calculated for C₂₁H₃₄NO₂S₂Si [M+H]⁺: 424.1800, found 424.1790.



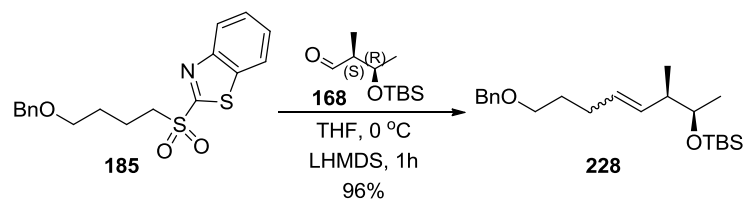
(2*R*,3*R*)-3-tertbutyldimethylsilyloxy-2-methyl-butan-1-ol (167). Experimental followed the same procedure as that used for **163**. Afforded the *title compound* (0.479 g, 93%) as a clear liquid. **R_f** = 0.4 (20% EtOAc/ X4); **¹H NMR** (600 MHz, Chloroform-*d*) δ 4.00 (qd, *J* = 6.3, 3.5 Hz, 1H), 3.72 (ddd, *J* = 10.7, 8.9, 2.8 Hz, 1H), 3.51 (ddd, *J* = 11.1, 7.1, 4.5 Hz, 1H), 2.97 (dd, *J* = 7.2, 3.0 Hz, 1H), 1.95 (dqdd, *J* = 14.1, 7.1, 4.6, 3.5 Hz, 1H), 1.15 (d, *J* = 6.3 Hz, 3H), 0.89 (s, 9H), 0.79 (d, *J* = 7.1 Hz, 3H), 0.08 (d, *J* = 4.2 Hz, 6H); **¹³C NMR** (CDCl₃, 151 MHz) δ 72.38, 65.81, 40.96, 25.93, 18.39, 18.10, 12.51, -4.37, -4.92; **IR** (thin film) ν 3367, 2957, 2929, 2857, 1472, 1463, 1373, 1253, 1157, 1092, 1042, 1006, 958, 902, 836, 775, 455; [α]_D²⁰ = -5.5 (*c* = 1.085 g/100 mL, CHCl₃); **MS** (APCI) calculated for C₁₁H₂₇O₂Si [M+H]⁺: 219.1780, found 219.1775.



(2*R*,3*S*)-3-((tert-butyl dimethylsilyl)oxy)-2-methylbutanal (168) Experimental followed the same procedure as that used for **164**. Yielded the *title compound* (0.62 g, 96%) as a clear liquid. **R_f** =

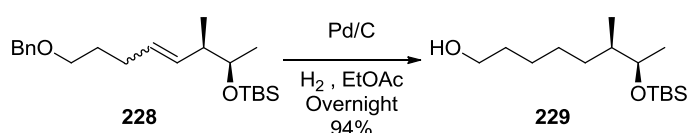
Experimental Procedures

0.659 (20% EtOAc/ X4); $^1\text{H NMR}$ (600 MHz, Chloroform-*d*) δ 9.77 (d, $J = 1.3$ Hz, 1H), 4.26 (qd, $J = 6.3, 4.3$ Hz, 1H), 2.38 (qdd, $J = 7.0, 4.2, 1.3$ Hz, 1H), 1.18 (d, $J = 6.3$ Hz, 3H), 1.07 (d, $J = 6.9$ Hz, 3H), 0.87 (s, 8H), 0.06 (d, $J = 11.8$ Hz, 6H); $^{13}\text{C NMR}$ (151 MHz, Chloroform-*d*) δ 205.43, 68.36, 53.59, 25.86, 21.34, 18.11, 8.33, -4.12, -4.85; $[\alpha]_D^{20} = 42.2$ ($c = 0.64$ g/100 mL, CHCl_3);



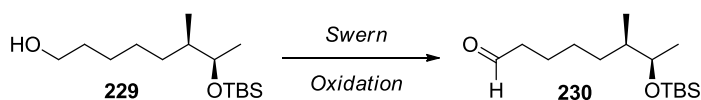
(((2R,3R)-8-(benzyloxy)-3-methyloct-4-en-2-yl)oxy)(tert-butyl)dimethylsilane (228)

Experimental followed the same procedure as that used for **186**. Yielded the *title compound* as a mixture of isomers (0.172 g, 96%) and a clear liquid. $R_f = 0.65$ (20% EtOAc/X4); $^1\text{H NMR}$ (600MHz, Chloroform-*d*) $\delta = 7.34$ (d, $J = 4.4$ Hz, 3H), 7.30 – 7.26 (m, 1H), 5.43 – 5.30 (m, 2H), 5.25 – 5.17 (m, 0.5H), 4.50 (s, 2H), 3.54 (dp, $J = 23.9, 6.3$ Hz, 1H), 3.47 (td, $J = 6.6, 2.4$ Hz, 2H), 2.41 (dp, $J = 10.0, 6.8$ Hz, 0.5H), 2.22 – 2.02 (m, 3H), 1.73 – 1.61 (m, 2H), 1.08 (d, $J = 6.1$ Hz, 1H), 1.04 (d, $J = 6.1$ Hz, 2H), 0.94 (dd, $J = 6.8, 1.8$ Hz, 3H), 0.89 (d, $J = 4.6$ Hz, 9H), 0.04 (dd, $J = 6.1, 2.8$ Hz, 6H); $^{13}\text{C NMR}$ (151 MHz, Chloroform-*d*) δ 138.84, 138.77, 133.97, 133.89, 129.36, 128.64, 128.49, 127.78, 127.64, 127.62, 73.09, 73.03, 72.69, 72.48, 70.11, 69.97, 44.81, 40.14, 29.98, 29.75, 29.41, 26.08, 26.06, 26.04, 24.44, 22.08, 21.36, 18.31, 18.29, 17.31, 16.41, -4.08, -4.15, -4.59; **IR** (thin film) ν 3031, 2956, 2930, 2857, 1723, 1496, 1472, 1463, 1361, 1313, 1252, 1109, 1079, 1029, 1006, 957, 940, 836, 814, 774, 734, 697, 666; **MS** (APCI) calculated for $\text{C}_{22}\text{H}_{39}\text{O}_2\text{Si}$ $[\text{M}+\text{H}]^+$: 363.2714, found 363.2709.

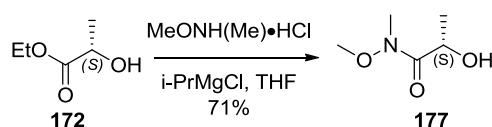


(6R,7R)-7-((tert-butyldimethylsilyl)oxy)-6-methyloctan-1-ol (229) Experimental followed the same procedure as that used for **187**. Yielded the *title compound* (0.62 g, 94%) as a clear liquid. $R_f = 0.312$ (20% Et₂O/X4); $^1\text{H NMR}$ (600MHz, Chloroform-*d*) $\delta = 3.71 - 3.66$ (m, 1 H), 3.64 (t, $J = 6.6$ Hz, 2 H), 1.62 - 1.50 (m, 2 H), 1.49 - 1.18 (m, 7 H), 1.05 (d, $J = 6.2$ Hz, 3 H), 0.88 (s, 6 H), 0.85 - 0.80 (m, 3 H), 0.05 - 0.00 (m, 6 H) **NMR** (151 MHz, Chloroform-*d*) $\delta = 71.8, 63.3, 40.4, 33.0, 32.7, 27.5, 26.2, 26.0, 20.7, 18.3, 14.8, -4.1, -4.7$; **IR** (thin film) ν 3342, 2930, 2857, 1463, 1380, 1252, 1106, 1072, 957, 836, 774, 666, 506, 493, 469, 459, 453; $[\alpha]_D^{20} = 0.0$ (unable to detect rotation); **MS** (APCI) calculated for $\text{C}_{15}\text{H}_{34}\text{O}_2\text{Si}$ $[\text{M}+\text{H}]^+$: 275.2401, found 275.2389.

Experimental Procedures



(6R,7R)-7-((tert-butyl dimethylsilyl)oxy)-6-methyloctanal (230) Experimental followed the same procedure as that used for **190**. Yielded the *title compound* (0.095 g, 76%) as a clear liquid. $R_f = 0.3125$ (20% Et₂O/X4); $^1\text{H NMR}$ (600MHz, Chloroform-*d*) $\delta = 3.71 - 3.66$ (m, 1 H), 3.64 (t, $J = 6.6$ Hz, 2 H), 1.62 - 1.50 (m, 2 H), 1.49 - 1.18 (m, 7 H), 1.05 (d, $J = 6.2$ Hz, 3 H), 0.88 (s, 6 H), 0.85 - 0.80 (m, 3 H), 0.05 - 0.00 (m, 6 H); $^{13}\text{C NMR}$ (151 MHz, Chloroform-*d*) δ 71.8, 63.3, 40.4, 33.0, 32.7, 27.5, 26.2, 26.0, 20.7, 18.3, 14.8, -4.1, -4.7; **IR** (thin film) ν 3838, 2957, 2930, 2858, 2711, 1729, 1473, 1463, 1380, 1252, 1106, 1072, 1005, 957, 836, 774, 666, 646, 618, 614, 609, 606, 602; $[\alpha]_D^{20} = 0.0$ (unable to detect rotation); **MS** (APCI) calculated for C₁₅H₃₂O₂Si $[\text{M}+\text{H}]^+$: 271.2088, found 271.2090.



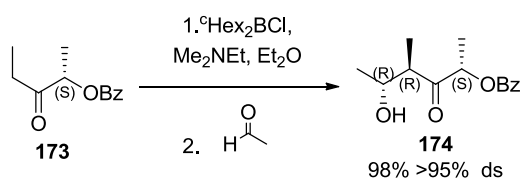
(S)-2-hydroxy-N-methoxy-N-methylpropionamide (177) To a mixture of ethyl (*S*)-lactate (8.4 mL, 71 mmol) and *N,O*-dimethylhydroxylamine hydrochloride (13.87 g, 0.14 mol) in THF (237 mL, 0.3 mol/L) at -10 °C was added *i*-PrMgCl (142 mL of a 2 M solution in THF, 0.28 mol) dropwise over 20 minutes. The mixture stirred for 2 hours warming slowly to 0 °C and when consumption was seen by TLC the reaction was quenched by slow addition of NH₄Cl solution. The mixture was diluted with ether and organic phase separated. The aqueous phase was extracted with ether (2 × 100 mL) and CH₂Cl₂ (3 × 100 mL), The organic extracts were combined, dried with Na₂SO₄ and concentrated under vacuum. The product was purified through distillation under high vacuum to give the *title compound* (6.68 g, 71 %) as a clear liquid; **b.p.** 62-65 °C at 0.5 Torr (lit. 63-65 °C at 0.5 Torr); $^1\text{H NMR}$ (600MHz, Chloroform-*d*) δ 4.48 (quin, $J = 6.8$ Hz, 1 H), 3.72 (s, 3 H), 3.32 (d, $J = 7.7$ Hz, 1 H), 3.25 (s, 3 H), 1.36 (d, $J = 6.8$ Hz, 4 H); $^{13}\text{C NMR}$ (151 MHz, Chloroform-*d*) δ 175.5, 64.8, 61.2, 32.3, 20.8; **IR** (thin film) ν 3797, 3735, 3447, 2938, 2349, 1651, 1448, 1366, 1086, 1038, 991, 913, 886, 743, 668, 617; $[\alpha]_D^{20} = -41$ ($c = 1.075$ g/100 mL, CHCl₃); **MS** (ESI) calculated for C₅H₁₂NO₃ $[\text{M}+\text{H}]^+$: 134.0812, found 134.0817.



(S)-3-oxopentan-2-yl benzoate (173) To a stirring of Weinreb amide **177** (12 g, 0.1 mol) in THF (500 mL) at 0 °C was added EtMgBr (68 mL of a 1 M solution in THF, 0.2 mol) and the reaction

Experimental Procedures

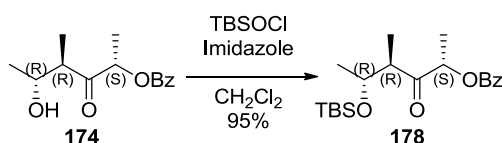
mixture was allowed to warm to room temperature. After 1 hour, saturated aqueous NH_4Cl (200 mL) was carefully added and the mixture was extracted with Et_2O (300 mL) and CH_2Cl_2 (2 x 300 mL). The combined organic extracts were dried (MgSO_4) and concentrated in vacuo to ca. 100 mL. To this solution was added benzoic anhydride (34.47 g, 0.152 mol), DMAP (1.24 mg, 10 mmol) and $i\text{Pr}_2\text{NEt}$ (26.54 mL, 0.152 mol) and the resulting solution stirred at room temperature for 14 hours. Excess Bz_2O was removed by addition of ethylenediamine (1 mL). H_2O (100 mL) was added and the mixture was extracted with Et_2O (3 x 80 mL), then the combined organic extracts were dried (Na_2SO_4) and concentrated in vacuo. Purification of the crude oil by column chromatography (20% EtOAc /hexanes) afforded the ketone **173** (5.48 g, 40%) as a colourless oil. $R_f = 0.45$ (20% EtOAc /hexanes); $^1\text{H NMR}$ (600 MHz, Chloroform- d) δ 8.12 – 8.07 (m, 2H), 7.63 – 7.57 (m, 1H), 7.50 – 7.44 (m, 2H), 5.36 (q, $J = 7.0$ Hz, 1H), 2.66 (dq, $J = 18.3, 7.3$ Hz, 1H), 2.53 (dq, $J = 18.3, 7.2$ Hz, 1H), 1.53 (d, $J = 7.0$ Hz, 3H), 1.10 (t, $J = 7.3$ Hz, 3H); $^{13}\text{C NMR}$ (151 MHz, Chloroform- d) δ 208.66, 166.07, 133.51, 129.94, 129.65, 128.62, 75.29, 31.63, 16.66, 7.39; **IR** (thin film) ν 3425, 3064, 2983, 2941, 1717, 1602, 1585, 1492, 1452, 1411, 1380, 1316, 1269, 1177, 1110, 1097, 1071, 1027, 974, 898, 855, 801, 712, 688 ; $[\alpha]_D^{20} = +24.8$ ($c = 1.09$ g/100 mL, CHCl_3); **MS** (ESI) calculated for $\text{C}_{12}\text{H}_{15}\text{O}_3$ $[\text{M}+\text{H}]^+$: 207.1016, found 207.1012.



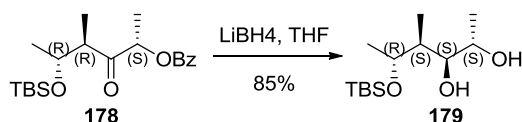
(2S,4R,5R)-5-hydroxy-4-methyl-3-oxohexan-2-yl benzoate (174) To a stirring solution of dicyclohexylboron chloride (4.47 mL, 15.8 mmol) in Et_2O (40 mL) at -78 °C was added Me_2NEt (1.76 mL, 16.8 mmol) followed by ketone **173** (2.18 g, 10.5 mmol) in Et_2O (13 mL). The reaction mixture was warmed to 0 °C and stirred for 2 hours, before being re-cooled to -78 °C. Then acetaldehyde (6.0 mL, 0.1 mol) was added at -78 °C for 2 hours then at -23 °C for 14 hours. The reaction was quenched at 0 °C with the addition of pH 7 buffer solution (40 mL), diluted with ether and then aqueous was extracted with ether (2 x 20 mL) and CH_2Cl_2 (3 x 20 mL). The organic phase was concentrated under reduced pressure leaving a clear oil. The crude oil was suspended in methanol (50 mL) and pH 7 buffer solution (40 mL), which was cooled to 0 °C. The suspension had hydrogen peroxide (12 mL of 30% w/w solution) added dropwise over 10 minutes and the mixture was allowed to stir for 2 hours at 0 °C. The mixture was partitioned between H_2O (150 mL) and CH_2Cl_2 (3 x 100 mL). The combined organic extracts were dried (Na_2SO_4) and concentrated under reduced pressure. The crude was purified by column chromatography (10% EtOAc /X4) to give the *title compound* (2.58 g, 97 %) as a clear liquid; $R_f = 0.25$ (20%

Experimental Procedures

EtOAc/hexanes); $^1\text{H NMR}$ (600 MHz, Chloroform-*d*) δ 8.12 – 8.06 (m, 2H), 7.59 (t, $J = 7.4$ Hz, 1H), 7.46 (t, $J = 7.7$ Hz, 2H), 5.45 (q, $J = 7.1$ Hz, 1H), 3.99 (h, $J = 6.4$ Hz, 1H), 2.81 (p, $J = 7.2$ Hz, 1H), 2.38 (d, $J = 5.7$ Hz, 1H), 1.58 (d, $J = 7.1$ Hz, 3H), 1.25 (dd, $J = 15.0, 6.8$ Hz, 6H); $^{13}\text{C NMR}$ (151 MHz, Chloroform-*d*) δ 211.87, 166.02, 133.52, 129.95, 129.59, 128.67, 128.62, 74.66, 69.66, 50.11, 21.04, 16.08, 14.60; **IR** (thin film) ν 3286, 2975, 2918, 1733, 1721, 1602, 1451, 1380, 1351, 1315, 1288, 1265, 1175, 1149, 1120, 1069, 1047, 1029, 1006, 917, 827, 731, 709, 687, 616 ; $[\alpha]_D^{20} = 35.4$ ($c = 1.075$ g/100 mL, CHCl_3); **MS** (ESI) calculated for $\text{C}_{14}\text{H}_{19}\text{O}_4$ $[\text{M}+\text{H}]^+$: 251.1278, found 251.1287.



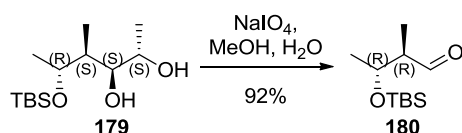
(2S,4R,5R)-5-((tert-butylidimethylsilyl)oxy)-4-methyl-3-oxohexan-2-yl benzoate (178) To a stirring solution of **174** (3.7455 g; 14.97 mmol) in CH_2Cl_2 (50 mL, 0.3 mol/L) at 0 °C was added imidazole (2.24 g; 32.9 mmol) and TBS-Cl (3.61 g; 23.9 mmol). The mixture was allowed to stir overnight warming to room temperature. When TLC showed consumption of starting material the reaction was quenched with addition of NH_4Cl sat solution and extracted with CH_2Cl_2 (4 x 50 mL). The combined organic extracts were dried (Na_2SO_4) and concentrated under reduced pressure. The crude was purified by column chromatography (10% EtOAc/X4) to give the *title compound* (5.20 g, 14.3 mmol, 95 %) as a clear liquid; $R_f = 0.8$ (20% EtOAc/hexanes); $^1\text{H NMR}$ (600MHz , Chloroform-*d*) δ 8.08 (d, $J = 7.1$ Hz, 2H), 7.62 – 7.54 (m, 1H), 7.45 (t, $J = 7.7$ Hz, 2H), 5.41 (q, $J = 7.0$ Hz, 1H), 4.06 (dq, $J = 8.2, 6.1$ Hz, 1H), 2.90 – 2.81 (m, 1H), 1.52 (d, $J = 7.0$ Hz, 3H), 1.15 (d, $J = 5.9$ Hz, 3H), 1.11 (d, $J = 7.1$ Hz, 3H), 0.84 (s, 7H), 0.01 (d, $J = 42.9$ Hz, 6H); $^{13}\text{C NMR}$ (151 MHz, Chloroform-*d*) δ 209.54, 165.91, 133.34, 129.96, 129.90, 128.55, 75.24, 70.28, 50.73, 25.98, 21.32, 18.04, 15.41, 13.93, -4.52, -4.67; **IR** (thin film) ν 2957, 2931, 2885, 2857, 1722, 1603, 1586, 1472, 1462, 1452, 1380, 1361, 1316, 1268, 1176, 1117, 1069, 1027, 1012, 975, 949, 838, 810, 777, 711, 687, 665; $[\alpha]_D^{20} = -14.4$ ($c = 1.045$ g/100 mL, CHCl_3); **MS** (ESI) calculated for $\text{C}_{20}\text{H}_{33}\text{O}_4\text{Si}$ $[\text{M}+\text{H}]^+$: 365.2143, found 365.2152.



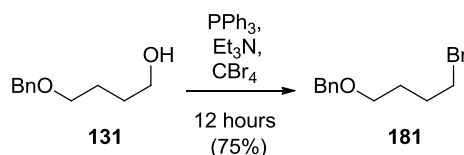
(2S,3S,4S,5R)-5-((tert-butylidimethylsilyl)oxy)-4-methylhexane-2,3-diol (179) To a stirring slurry of LiAlH_4 (0.190 g; 0.5 mmol) in Et_2O (3 mL) at -78 °C was added **178** (0.457 g, 1.25 mmol) in Et_2O (3 mL) dropwise over 10 minutes. The mixture was allowed to stir for 3 hours at -78 °C then allowed to warm to 0 °C. When TLC showed full conversion of the starting material the mixture

Experimental Procedures

was quenched first with slow addition of ethyl acetate (8 mL) over 10 minutes, the subsequent slurry was broken up with a solution of potassium sodium tartrate (Rochelle's salt) (20 mL) and allowed to stir until two clear layer were visible. The aqueous was extracted with EtOAc (4 x 10 mL), then the combined organic extracts were dried (Na_2SO_4) and concentrated under vacuum. The resulting crude was purified through column chromatography (20% EtOAc/hexanes) to afford the *title compound* (0.2802 g, 85.1 %) as a clear liquid; $R_f = 0.3$ (30% Et₂O/X4); $^1\text{H NMR}$ (600MHz, Chloroform-*d*) δ 3.89 (p, $J = 6.2$ Hz, 1H), 3.81 (td, $J = 6.6, 4.0$ Hz, 1H), 3.58 (ddd, $J = 8.3, 4.0, 2.4$ Hz, 1H), 3.40 (d, $J = 2.6$ Hz, 1H), 2.59 (t, $J = 6.9$ Hz, 1H), 1.64 – 1.53 (m, 1H), 1.19 (dd, $J = 22.3, 6.2$ Hz, 6H), 0.91 (s, 9H), 0.82 (d, $J = 6.9$ Hz, 3H), 0.11 (d, $J = 2.6$ Hz, 6H); $^{13}\text{C NMR}$ (151 MHz, Chloroform-*d*) δ 77.22, 73.37, 68.14, 43.16, 25.97, 21.61, 18.11, 16.43, 12.47, -4.04, -4.70; **IR** (thin film) ν 3404, 2957, 2931, 2858, 1472, 1386, 1255, 1108, 1061, 985, 965, 938, 899, 838, 775, 666; $[\alpha]_D^{20} = -6.6$ ($c = 1.06$ g/100 mL, CHCl_3); **MS** (ESI) calculated for $\text{C}_{13}\text{H}_{31}\text{O}_3\text{Si}$ $[\text{M}+\text{H}]^+$: 263.2037, found 263.2038



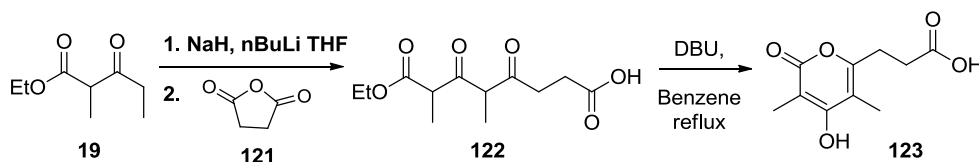
(2R,3R)-3-((tert-butyldimethylsilyl)oxy)-2-methylbutanal (180) To a stirring solution of **179** (0.105 g; 0.4 mmol) in THF (2 mL) was added an aqueous solution of NaIO_4 (0.26 g; 1.2 mmol) in 2 mL of water. This biphasic mixture was stirred vigorously until TLC showed consumption of starting material. The mixture was then diluted with water and extracted with CH_2Cl_2 (3 x 5 mL), combined organic extracts were dried (Na_2SO_4) and concentrated under vacuum. The resulting crude was purified through column chromatography (20% EtOAc/hexanes) to afford the *title compound* (0.080 g, 0.37 mmol 92 %) as an unstable^{197,198} clear liquid which was not stored and used immediately in the next step; $R_f = 0.75$ (20% Et₂O/X4); $^1\text{H NMR}$ (600 MHz, Chloroform-*d*) δ 9.75 (d, $J = 2.6$ Hz, 1H), 4.03 (p, $J = 6.2$ Hz, 1H), 2.37 (pd, $J = 7.0, 2.6$ Hz, 1H), 1.22 (d, $J = 6.3$ Hz, 3H), 1.07 (d, $J = 7.1$ Hz, 3H), 0.87 (s, 9H), 0.06 (d, $J = 8.5$ Hz, 6H);



benzyl 4-bromobutyl ether (181) To a 0.25 mol/L aqueous NaOH solution (1.4g, 100ml) at room temperature was added benzyl alcohol (3.74mL, 36 mmol) and stirred for 10 minutes before addition of dibromobutane (3.32 mL, 27.8 mmol) and tetrabutylammonium hydrogensulfate (10

Experimental Procedures

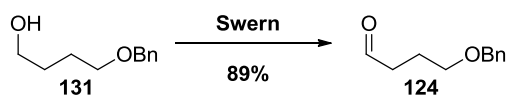
mg), the reaction was heated to 80 °C and allowed to stir over night. The mixture was then cooled to RT and aqueous extracted with ether (3×40 mL) combined organic layers were dried (Na₂SO₄) and concentrated under reduced pressure. **R_f** = 0.89 (20% EtOAc/X4); **¹H NMR** (600 MHz, Chloroform-*d*) δ 1.70–1.82 (m, 2H), 1.91–2.06 (m, 2H), 3.43 (t, *J* = 6.7 Hz, 2H), 3.50 (t, *J* = 6.2 Hz, 2H), 4.50 (s, 2H), 7.23–7.40 (m, 5H); **¹³C NMR** (300 MHz, Chloroform-*d*) δ 28.4, 29.7, 33.8, 69.3, 73.0, 127.7, 128.4, 138.5. The spectroscopic data were in accordance with those in the literature.⁴



3-(4-hydroxy-3,5-dimethyl-2-oxo-2H-pyran-6-yl)propanoic acid (123) Dianion Addition – To a stirring solution of NaH (0.76 g; 18.9 mmol, 60% dispersion in oil) in dry THF (60 mL) was added ethyl-2-methyl-3-oxo-pentanoate **19** (2 g; 12.6 mmol) slowly dropwise at 0 °C over five minutes. The mixture was stirred until the evolution of hydrogen bubbles had subsided, and then freshly titrated *n*-BuLi (9.5 mL, 1.6 mol/L in hexanes) was added dropwise with colour change to yellow. The mixture was cooled to -78 °C before addition of succinic anhydride (1.27 g, 12.6 mmol) and allowed to react for 3 hours until TLC showed consumption of starting material. The reaction mixture was slowly warmed to 0 °C before quenching with aqueous NaHCO₃ solution. Aqueous was washed with ether and organic extracted with NaHCO₃ solution (3 × 10 mL), the aqueous extracts acidified and extracted with EtOAc (3 × 20 mL). The reaction mixture cooled to room temperature, worked up by addition of NH₄Cl sat solution and extracted with CH₂Cl₂ (3 × 20 mL). The combined organic extracts were dried (Na₂SO₄) and concentrated under reduced pressure. The crude was used directly in the cyclisation step.

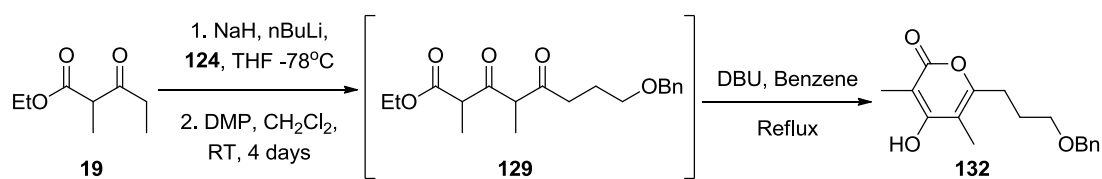
DBU Cyclisation - The partially purified extract (1.75 g) was dissolved in benzene (50 mL) and had DBU (1.6 mL) added. The reaction mixture was heated to reflux and stirred overnight. Reaction was cooled to room temperature before quenching with aqueous NaHCO₃ solution organic extracted with NaHCO₃ solution (3 × 10 mL), the aqueous extracts acidified and extracted with EtOAc (3 × 10 mL). The combined organic extracts were dried (Na₂SO₄) and concentrated under reduced pressure. The crude was purified through column chromatography (10 →100 % MeOH/CH₂Cl₂) to afford the *title compound* (0.973 g, 3.7 mmol 29 %) as white amorphous solid. **R_f** = baseline (CH₂Cl₂); **¹H NMR** (600MHz, DMSO-*d*₆) δ 2.71 (t, *J* = 7.3 Hz, 2H), 2.50 (m, 2H), 1.88 (s, 3H), 1.82 (s, 3H); **¹³C NMR** (151 MHz, DMSO-*d*₆) δ 173.11, 164.77, 164.29, 156.02, 107.10, 97.24, 39.52, 30.89, 25.58, 9.76, 9.20;

Experimental Procedures



4-Benzyloxy-1-butanol (124) PCC Oxidation - To a stirring solution of **131** (4 g, 22 mmol) in CH_2Cl_2 (150 mL) was added celite (6.7 g) and PCC (6.7 g, 31 mmol). This mixture was stirred at room temperature until TLC showed consumption of starting material. The reaction mixture was then passed through a plug of celite and fractions combined and concentrated under reduced pressure. The resulting crude mixture was further purified through either column chromatography (20% EtOAc/X4) or distillation to remove PCC residue impurities, affording the *title compound* as clear oil (3.201 g, mol, 81%);

Swern Oxidation - To a stirring solution of DMSO (4.75 mL 66.5 mmol) in CH_2Cl_2 (140 mL), was added oxalyl chloride (22 mL; 44.3 mmol of 2 M solution in CH_2Cl_2), This mixture was stirred for 30 minutes at -78°C . Then a solution of alcohol **131** (4 g; 22.2 mmol, in 4 mL of CH_2Cl_2) was added dropwise and stirred for 40 minutes at -78°C . To this mixture was added Et_3N (18.6 mL; 0.13 mol) and allowed for 40 minutes until TLC showed consumption of starting material. The reaction was quenched with sat. NH_4Cl sol. and diluted with brine. The organic layer was separated and the aqueous layer extracted with CH_2Cl_2 (3×50 mL). The organic extracts were combined, dried with Na_2SO_4 and concentrated under vacuum. The product was purified through column chromatography (10% EtOAc/X4 on buffered silica), yielded the *title compound* (3.536 g, 89%) as a clear liquid. The aldehyde was not stored but used immediately for the next step. $R_f = 0.8$ (20% EtOAc/hexanes); $^1\text{H NMR}$ (600MHz, Chloroform-*d*) δ 9.79 (q, $J = 1.4$ Hz, 1H), 7.32 (tt, $J = 13.9, 7.6$ Hz, 5H), 4.49 (s, 2H), 3.51 (t, $J = 6.1$ Hz, 2H), 2.55 (tt, $J = 7.1, 1.3$ Hz, 2H), 1.95 (p, $J = 6.5$ Hz, 2H); $^{13}\text{C NMR}$ (151 MHz, Chloroform-*d*) δ 202.39, 138.40, 128.54, 127.76, 73.10, 69.28, 41.10, 22.72;



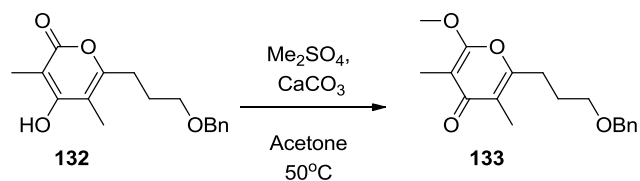
6-[2-(benzyloxy)ethyl]-4-hydroxy-3,5-dimethyl-2H-pyran-2-one (132) Dianion Addition - To a stirring solution of NaH (0.66 g; 16.5 mmol, 60% dispersion in oil) in dry THF (50 mL) was added ethyl-2-methyl-3-oxo-pentanoate **19** (1.74 g; 11 mmol) slowly dropwise at -10°C over five minutes. The mixture was stirred until the evolution of hydrogen bubbles had subsided, and then freshly titrated *n*-BuLi (8.25 mL, 1.6 mol/L in hexanes) was added dropwise with colour change to yellow. This reaction mixture was stirred for 15 minutes before cooling to -30°C where aldehyde **124** (2.35 g; 13.2 mmol) was added. The reaction was stirred at -30°C until TLC

Experimental Procedures

showed consumption of aldehyde. The reaction was quenched with addition of NH_4Cl sat solution and extracted with ether (3 x 50 mL). The combined organic extracts were dried (Na_2SO_4) and concentrated under reduced pressure. The crude was purified by column chromatography (10 % EtOAc/X4) giving mixture of isomers (2.8082 g).

DMP Oxidation - These isomers were combined together and oxidised to give the triketo ester. To a stirring solution of mixed isomers (2.8042 g) in CH_2Cl_2 (80 mL) was added DMP (6 g, 14.1 mmol). The reaction was stirred at room temperature in darkness until TLC showed consumption of starting material (2 days). The reaction mixture was worked up by dilution with ether then with addition of NaHCO_3 solution and sodium thiosulfate sat solution. When the mixture cleared it was extracted with CH_2Cl_2 , dried with Na_2SO_4 and concentrated under reduced pressure providing mixture of isomers (2.34 g).

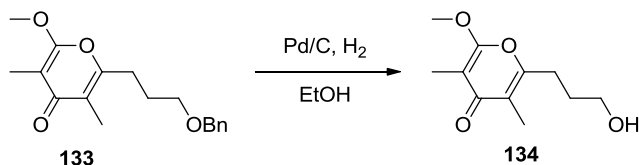
DBU Cyclisation - The crude mixture was dissolve in benzene (35 mL) and had DBU (0.53 mL, 3.5 mmol) added before warming the mixture up to reflux temperature and allowed to stir overnight. The reaction mixture cooled to room temperature, worked up by addition of NH_4Cl sat solution and extracted with CH_2Cl_2 (3 x 20 mL). The combined organic extracts were dried (Na_2SO_4) and concentrated under reduced pressure. The crude was purified by column chromatography (10 % EtOAc/X4) to afford the *title compound* as white amorphous solid (1.8 g, 6.2 mmol, 57 % from β -keto ester); $R_f = 0.665$ (20% EtOAc/ CH_2Cl_2); $^1\text{H NMR}$ (600MHz, Chloroform-*d*) δ 7.39 - 7.27 (m, 5 H), 4.49 (s, 2 H), 3.48 (t, $J = 6.0$ Hz, 2 H), 2.64 (t, $J = 7.4$ Hz, 2 H), 1.97 (s, 3 H), 1.96 (s, 3 H), 1.99 - 1.92 (m, 2 H); $^{13}\text{C NMR}$ (151 MHz, Chloroform-*d*) δ 165.7, 164.1, 158.7, 138.4, 128.5, 127.8, 106.6, 98.3, 73.1, 69.0, 27.6, 27.5, 9.8, 8.5;



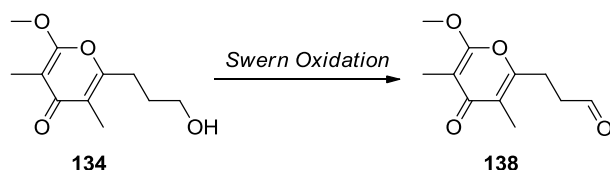
2-(3-(benzyloxy)propyl)-6-methoxy-3,5-dimethyl-4H-pyran-4-one (133) To a stirring solution of **132** (0.8848 g, 3.07 mmol) and CaCO_3 (6.14 g) in acetone (31 ml, 0.1 mol/L) was added dimethyl sulfate (2.90 mL, 30 mmol). The reaction mixture was heated to 40 °C and stirred for two days. The reaction was diluted with water and allowed to stir for 30 minutes. The mixture was filtered and extracted with EtOAc (3 x 10 mL). The combined organic extracts were washed with water, then brine and then dried (Na_2SO_4) and concentrated under reduced pressure. The crude was purified by column chromatography (50% EtOAc/X4) to afford the *title compound* as white crystals (0.512 g, mol, 55 %); $R_f = 0.52$ (10% MeOH/ CH_2Cl_2); $^1\text{H NMR}$ (600MHz, Chloroform-*d*) δ 7.37 - 7.27 (m, 5 H), 4.50 (s, 2 H), 3.91 (s, 3 H), 3.50 (t, $J = 6.1$ Hz, 2 H), 2.71 (t, $J = 7.4$ Hz,

Experimental Procedures

2 H), 1.99 - 1.92 (m, 2 H), 1.94 (s, 3 H), 1.84 (s, 3 H); $^{13}\text{C NMR}$ (151 MHz, Chloroform-*d*) δ 181.1, 162.3, 157.8, 138.3, 128.6, 127.9, 127.8, 118.8, 99.6, 73.3, 69.0, 55.4, 27.7, 27.3, 10.1, 7.0;

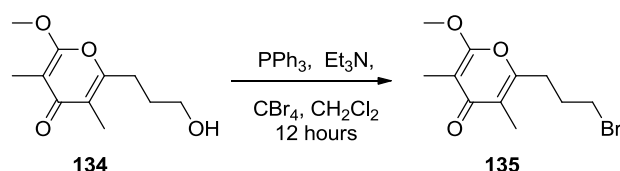


2-(3-hydroxypropyl)-6-methoxy-3,5-dimethyl-4H-pyran-4-one (134) To a stirring solution of **133** (0.3789 g; 1.25 mmol) in dry ethanol with 10% Pd/C (0.07 g, 0.063 mmol) was stirred under a hydrogen atmosphere at room temperature for 24 h. The reaction mixture was filtered through a plug of silica and the solvent evaporated *in vacuo* to give the crude product, which was purified by flash chromatography (50% EtOAc/X4) affording the *title compound* **134** (0.2463 g, 1.16 mmol 92%) as a clear crystals; $R_f = 0.263$ (10% MeOH/CH₂Cl₂); $^1\text{H NMR}$ (600MHz, Chloroform-*d*) δ 3.95 (s, 3H), 3.70 (t, $J = 6.2$ Hz, 2H), 2.77 – 2.68 (m, 2H), 1.94 (d, $J = 0.5$ Hz, 3H), 1.93 – 1.88 (m, 2H), 1.83 (s, 3H); $^{13}\text{C NMR}$ (151 MHz, Chloroform-*d*) δ 181.12, 162.30, 157.80, 118.74, 99.60, 61.71, 55.46, 29.91, 27.33, 10.06, 7.01;

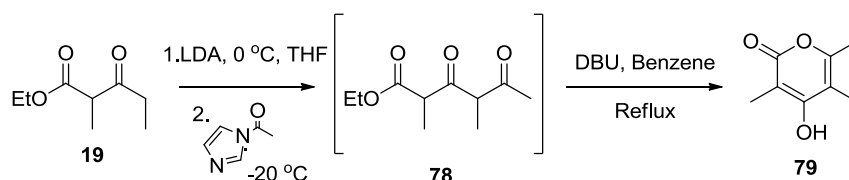


3-(6-methoxy-3,5-dimethyl-4-oxo-4H-pyran-2-yl)propanal (138) To a stirring solution of DMSO (0.16 mL, 2.3 mmol) in CH₂Cl₂ (11 mL), was added oxalyl chloride (1.16 mL; 2.3 mmol of 2 M solution in CH₂Cl₂), This mixture was stirred for 30 minutes at -78 °C. Then a solution of alcohol **134** (246 mg; 1.16 mmol, in 1 mL of CH₂Cl₂) was added dropwise and stirred for 40 minutes at -78°C. To this mixture was added Et₃N (1 mL; 7 mol) and allowed for 40 minutes until TLC showed consumption of starting material. The reaction was quenched with sat. NH₄Cl sol. and diluted with brine. The organic layer was separated and the aqueous layer extracted with CH₂Cl₂ (3 × 10 mL). The organic extracts were combined, dried with Na₂SO₄ and concentrated under vacuum. The crude was purified through column chromatography (10% EtOAc/X4 on buffered silica), yielded the *title compound* (0.127 g, 52 %) as a clear liquid. $R_f = 0.314$ (10% MeOH/CH₂Cl₂); $^1\text{H NMR}$ (600MHz, Chloroform-*d*) δ 9.86 (t, $J = 1.0$ Hz, 1H), 3.93 (s, 3H), 2.98 – 2.90 (m, 2H), 2.83 (tt, $J = 7.2, 0.9$ Hz, 2H), 1.96 (d, $J = 0.6$ Hz, 3H), 1.84 (s, 3H); $^{13}\text{C NMR}$ (151 MHz, Chloroform-*d*) δ 199.56, 180.80, 162.21, 156.02, 119.04, 99.91, 55.63, 40.73, 23.34, 10.04, 7.02;

Experimental Procedures



2-(3-bromopropyl)-6-methoxy-3,5-dimethyl-4H-pyran-4-one (135) To a stirring solution of pyrone **134** (0.089 g, 0.42 mmol) in CH₂Cl₂ (3 mL) was added PPh₃ (0.33 g, 1.2 mmol) and CBr₄ (0.42, 1.2 mmol) at -30 °C. The reaction was allowed to stir overnight warming slowly to RT. The reaction mixture was worked up with an aqueous saturated solution of NH₄Cl and extracted CH₂Cl₂. The organic fractions were washed with brine, dried with Na₂SO₄ and concentrated under vacuum. The crude was purified through column chromatography (100 % CH₂Cl₂ on buffered silica), yielded the *title compound* (0.115 g, 99 %) as a clear liquid. *R_f* = 0.256 (20% EtOAc/CH₂Cl₂); ¹H NMR (600MHz, Chloroform-*d*) δ 3.95 (s, 3H), 3.43 (t, *J* = 6.3 Hz, 2H), 2.78 (t, *J* = 7.3 Hz, 2H), 2.25 – 2.16 (m, 2H), 1.96 (s, 3H), 1.84 (s, 3H); ¹³C NMR (151 MHz, Chloroform-*d*) δ 180.87, 162.25, 156.50, 119.28, 99.73, 55.54, 32.20, 30.05, 29.22, 10.13, 6.99;

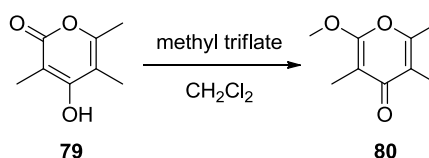


4-hydroxy-3,5,6-trimethyl-2H-pyran-2-one (79) To a stirring solution of NaH (454 mg, 11.3 mmol of 60% dispersion in mineral oil) in THF (28 mL) was added ethyl-2-methyl-3-oxo-pentanoate **19** (1.83 mL, 11.3 mmol) at 0 °C. The solution was stirred for 30 minutes until hydrogen bubbles stop evolving. Then *n*-BuLi (5.67 mL, 11.3 mmol of 2M solution in cyclohexane) was added drop-wise 0 °C, the solution turning a light yellow colour. This mixture was stirred for 45 minutes before the addition of ethyl acetate (0.55 mL, 56.7 mmol) at 0 °C, this mixture was stirred for a further hour before being transferred to the freezer (-20 °C) to react overnight. TLC showed a significant spot for the product and the reaction was quenched with sat. NH₄Cl sol. The organic layer was separated and the aqueous layer extracted with CH₂Cl₂ (2 × 10 mL). The organic extracts were combined, dried with Na₂SO₄ and concentrated under vacuum. The product was purified through column chromatography (10% EtOAc/X4) to remove excess beta keto ester. Giving a complex mixture of isomers as a clear liquid (*ethyl 2,4-dimethyl-3,5-dioxohexanoate 78*) (545 mg, 48%), which was immediately used in next step.

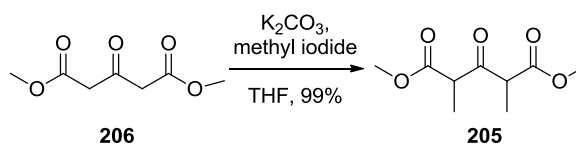
To a stirring solution of diketo-ester **78** (545 g, 2.7 mmol) benzene (14 mL) was added DBU (0.4 mL, 2.7 mmol). This mixture was heated to reflux and allowed to react overnight. The reaction mixture was diluted with sat NaHCO₃ solution and ether (10 mL). Ether layer was partitioned and discarded. The aqueous was acidified with conc HCl until a pH of 2 was reached. The aqueous

Experimental Procedures

was then extracted with EtOAc (3 × 15 mL) the organic extracts were combined, dried with Na₂SO₄ and concentrated under vacuum. This gave essentially pure α-pyrone **79** which was further purified through column chromatography (5% MeOH/CH₂Cl₂) to give a clear crystalline solid (345 mg, 82%) (39 % from β-keto ester). $R_f = 0.34$ (10% MeOH/CH₂Cl₂); ¹H NMR (600MHz, Chloroform-*d*) δ 1.93 (s, 3 H) 1.97 (s, 3 H) 2.17 (s, 3 H); ¹³C NMR (151 MHz, Chloroform-*d*) δ 167.30, 155.35, 98.44, 17.23, 10.18, 8.73; IR (thin film) ν 3224, 2983, 2935, 1674, 1570, 1452, 1412, 1389, 1354, 1236, 1178, 1127, 1070, 1035, 1009, 915, 864, 758, 680, 644, 606, 476, 464, 452; The spectroscopic data were in accordance with those in the literature.⁷⁶



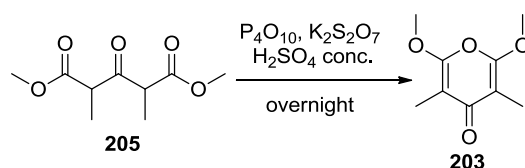
2-methoxy-3,5,6-trimethyl-4H-pyran-4-one (80) To a stirring solution of pyrone (**79**) (0.2345 g, 1.5 mmol) in CH₂Cl₂ (8 mL) at 0 °C was added methyl triflate (0.50 mL, 4.56 mmol) and the reaction mixture was allowed to stir and warm slowly over an hour. Quenched with sat NaHCO₃ solution and extracted with CH₂Cl₂. The organic extracts were combined, dried with Na₂SO₄ and concentrated under vacuum. Giving essentially pure α-methoxy-γ-pyrone which was further purified through column chromatography (5% MeOH/CH₂Cl₂) to give a clear crystalline solid (128 mg 50 %). $R_f = 0.4$ (100% EtOAc); ¹H NMR (600MHz, Chloroform-*d*) δ 3.93 (s, 3H), 2.25 (s, 3H), 1.91 (s, 2H), 1.83 (s, 3H); ¹³C NMR (151 MHz, Chloroform-*d*) δ 180.95, 162.21, 154.93, 118.60, 99.52, 55.47, 17.02, 10.23, 6.97; IR (thin film) ν 3357, 3261, 1527, 1302, 1161, 1098, 904, 817, 704, 534; MS (APCI) calculated for C₉H₁₃O₃ [M+H]⁺: 169.0855, found 169.0859. The spectroscopic data were in accordance with those in the literature.¹⁷⁶



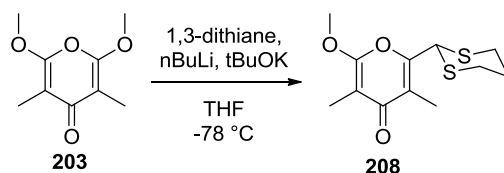
dimethyl 2,4-dimethyl-3-oxopentanedioate (205) To a slurry of dimethyl-1,3-acetonedicarboxylate **206** (10 g, 57 mmol) and K₂CO₃ (15.9 g, 114 mmol) in THF (191 ml) was added methyl iodide (7.15 mL, 114 mmol) at 0 °C and allowed to stir overnight warming slowly to room temperature. The reaction was quenched with NH₄Cl sat solution and aqueous was extracted with ether. The combined organic extracts were dried (Na₂SO₄) and concentrated under

Experimental Procedures

reduced pressure. The crude was purified by column chromatography (50 % EtOAc/X4) to give the *title compound* (11.51 g, 99 %) as a clear liquid; $R_f = 0.313$ (30 % EtOAc/hexanes); $^1\text{H NMR}$ (600MHz, Chloroform-*d*) δ 3.85 (q, $J = 7.1$ Hz, 1H), 3.78 (q, $J = 7.3$ Hz, 1H), 3.73 (s, 6H), 1.37 (t, $J = 7.5$ Hz, 6H); $^{13}\text{C NMR}$ (151 MHz, Chloroform-*d*) δ 201.23, 170.68, 170.39, 52.70, 52.66, 51.88, 51.64, 13.30, 12.91;



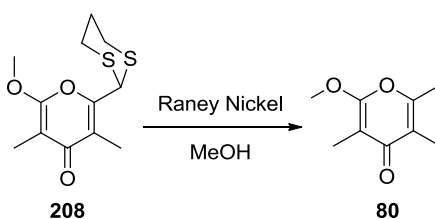
2,6-dimethoxy-3,5-dimethyl-4H-pyran-4-one (203) To an anhydrous amount of phosphorous pentoxide (1.89 g, 6.68 mmol) under a nitrogen atmosphere was added diester **205** (1 g, 4.95 mmol) dropwise and allowed to stir for five minutes to allow for even distribution. Then was added concentrated H_2SO_4 (2.47 mL) dropwise at 0 °C and allowed to warm to RT and stir overnight. When TLC showed consumption of starting material the reaction was quenched with slow addition of solid NaHCO_3 then addition of NaHCO_3 saturated solution until the solution was basic. The aqueous was diluted with addition of water and extracted with CH_2Cl_2 (3×50 mL), dried and evaporation of solvent gave essentially pure pyrone (0.71 g, 78 %) as white crystals, further purification through column chromatography (100% EtOAc). $R_f = 0.351$ (100% EtOAc); $^1\text{H NMR}$ (600MHz, Chloroform-*d*) δ 3.98 (s, 6H), 1.84 (s, 6H); $^{13}\text{C NMR}$ (151 MHz, Chloroform-*d*) δ 182.65, 158.80, 99.38, 56.21, 7.20.; **IR** (thin film) ν 2960, 1683, 1591, 1471, 1448, 1403, 1365, 1329, 1259, 1241, 1187, 1161, 990, 903, 761, 683, 657, 487, 466, 453; **MS** (APCI) calculated for $\text{C}_9\text{H}_{13}\text{O}_4$ $[\text{M}+\text{H}]^+$: 185.0808, found 185.0814. The spectroscopic data were in accordance with those in the literature.¹⁷⁶



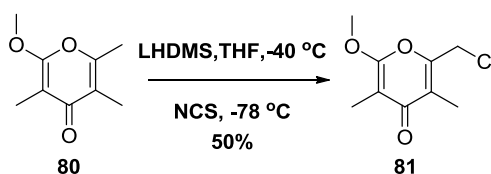
2-(1,3-dithian-2-yl)-6-methoxy-3,5-dimethyl-4H-pyran-4-one (208) To a stirring solution of $t\text{BuOK}$ (730 mg, 6.52 mmol) and dithiane (783 mg, 6.52 mmol) in THF (16 mL) was added $t\text{BuLi}$ (3.832 mL, 1.7 mol/L in hexanes) at -78 °C and stirred for 15 minutes before addition of symmetrical pyrone **203** (0.6 g, 3.2 mmol). This mixture was stirred at -78 °C until TLC showed

Experimental Procedures

consumption of SM. The reaction was quenched through addition of MeOH at $-78\text{ }^{\circ}\text{C}$ and allowed to warm to $0\text{ }^{\circ}\text{C}$ before diluted with ether and NH_4Cl solution. The aqueous was extracted with CH_2Cl_2 ($3 \times 20\text{ mL}$), dried with Na_2SO_4 and concentrated under vacuum. Purification preformed through column chromatography (100% EtOAc). $R_f = 0.28$ (100% EtOAc); $^1\text{H NMR}$ (600MHz, Chloroform-*d*) δ 5.30 (s, 1H), 4.04 (s, 3H), 3.07 (ddd, $J = 14.5, 12.0, 2.5\text{ Hz}$, 2H), 2.97 (ddd, $J = 14.3, 4.5, 2.9\text{ Hz}$, 2H), 2.05 (s, 3H), 2.04 – 1.93 (m, 1H), 1.85 (s, 3H); $^{13}\text{C NMR}$ (151 MHz, Chloroform-*d*) δ 180.43, 162.32, 153.01, 119.62, 100.22, 55.99, 46.67, 31.47, 25.25, 10.17, 7.10; **IR** (thin film) ν 2924, 1660, 1592, 1466, 1408, 1375, 1321, 1256, 1158, 978, 913, 765, 699, 469, 452; **MS** (APCI) calculated for $\text{C}_{13}\text{H}_{21}\text{O}_3$ $[\text{M}+\text{H}]^+$: 273.0614, found 273.0604. The spectroscopic data were in accordance with those in the literature.¹⁷⁶



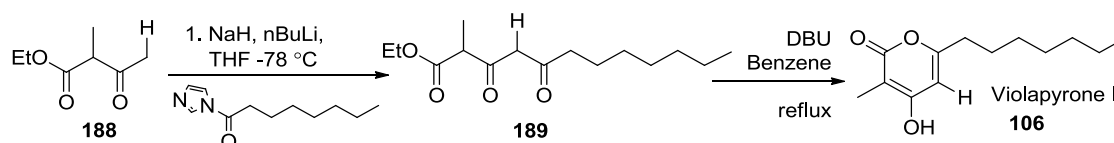
2-methoxy-3,5,6-trimethyl-4H-pyran-4-one (80) Desulfurisation – To a stirring solution of dithiane pyrone **208** (0.702 g, 2.58 mmol) in MeOH (6 mL) was added Raney nickel aqueous solution (6 mL) and stirred for 15 minutes. When TLC showed consumption of starting material the reaction was flushed through a plug of silica or celite with MeOH and dried with Na_2SO_4 and concentrated under vacuum. This gave essentially pure α -methoxy- γ -pyrone **80** which was further purified through column chromatography (100% EtOAc) to give a clear crystalline solid (0.40 g, 2.38 mmol, 92 %) $R_f = 0.4$ (100% EtOAc); $^1\text{H NMR}$ (600MHz, Chloroform-*d*) δ 3.93 (s, 3H), 2.25 (s, 3H), 1.91 (s, 2H), 1.83 (s, 3H); $^{13}\text{C NMR}$ (151 MHz, Chloroform-*d*) δ 180.95, 162.21, 154.93, 118.60, 99.52, 55.47, 17.02, 10.23, 6.97; **IR** (thin film) ν 3357, 3261, 1527, 1302, 1161, 1097, 904, 817, 704, 534; **MS** (APCI) calculated for $\text{C}_9\text{H}_{13}\text{O}_3$ $[\text{M}+\text{H}]^+$: 169.0855, found 169.0859. The spectroscopic data were in accordance with those in the literature.¹⁷⁶



2-(chloromethyl)-6-methoxy-3,5-dimethyl-4H-pyran-4-one (81) To a stirring solution of γ -pyrone **80** (0.22 g, 1.3 mmol) in THF (6 mL) at $-78\text{ }^{\circ}\text{C}$ was added LHMDS (1.44 mL, 1 mol/L) and allowed to stir for 15 minutes. The reaction was allowed to stir for 15 minutes until the colour of the solution changed to orange. The reaction was retained at $-78\text{ }^{\circ}\text{C}$ during the addition of NCS (0.19 g) solution in THF (0.5 mL). The reaction was stirred until the colour returned to colourless

Experimental Procedures

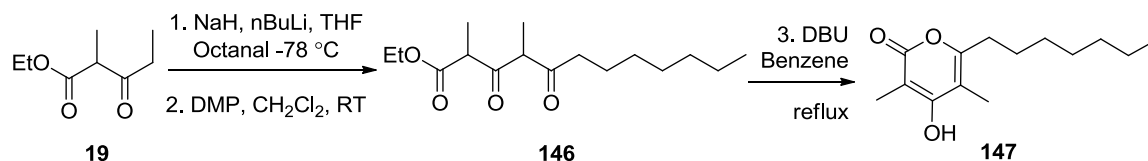
and TLC showed consumption of SM, at which point the reaction was quenched by addition of NaHCO_3 sat solution. The aqueous was extracted with CH_2Cl_2 (4×10 mL). The organic extracts were combined, dried with Na_2SO_4 and concentrated under vacuum. The product was purified through column chromatography (50% EtOAc/X4) affording the *title compound* (0.135 g, 50 %) as white solid. $R_f = 0.66$ (100% EtOAc); $^1\text{H NMR}$ (600MHz, Chloroform-*d*) δ 4.45 (s, 2H), 4.01 (s, 3H), 2.04 (s, 3H), 1.86 (s, 3H); $^{13}\text{C NMR}$ (151 MHz, Chloroform-*d*) δ 180.38, 162.35, 151.81, 121.53, 100.57, 55.79, 39.53, 9.99, 7.11; **IR** (thin film) ν 3040, 1667, 1600, 1465, 1417, 1384, 1332, 1277, 1255, 1208, 1149, 985, 765, 735, 685, 484; **MS** (APCI) calculated for $\text{C}_9\text{H}_{12}\text{O}_3$ $[\text{M}+\text{H}]^+$: 203.0470, found 203.0472.



6-heptyl-4-hydroxy-3-methyl-2H-pyran-2-one (Violapyrone I) (106) Dianion Addition - To a stirring solution of NaH (80 g; mol, 60% dispersion in oil) in dry THF (6 mL) was added ethyl 2-methylacetoacetate **188** (296 mg; 2 mmol) slowly dropwise at 0 °C over five minutes. The mixture was stirred until the evolution of hydrogen bubbles had subsided; the solution will have become gelatinous. Then freshly titrated *n*-BuLi (1 mL, 2 mol/L in hexanes) was added dropwise with colour change to yellow. This reaction mixture was stirred for 15 minutes before cooling to -20 °C where a THF solution of freshly prepared octane imidazolide (0.27 g; 1.39 mmol) was added. The reaction was moved to the freezer (-20 °C) to stir over night. The reaction was quenched with addition of NH_4Cl sat solution and extracted with ether (3×10 mL). The combined organic extracts were dried (Na_2SO_4) and concentrated under reduced pressure. The crude was purified by column chromatography (10% EtOAc/X4) to give a mixture of isomers **189** (249 mg, 0.9 mmol, 66 %).

DBU Cyclisation - The mixture of isomers **189** (249 mg, 0.9 mmol) was dissolve in benzene (6 mL) and had DBU (0.14 mL, 0.9 mmol) added before warming the mixture up to reflux temperature and allowed to stir overnight. The reaction mixture cooled to room temperature, worked up by addition of NH_4Cl sat solution and extracted with CH_2Cl_2 (3×10 mL). The combined organic extracts were dried (Na_2SO_4) and concentrated under reduced pressure. The crude was purified by column chromatography (50% EtOAc/X4) to afford the *title compound* as white amorphous solid (154 mg, mol, 75 %); $R_f = 0.15$ (40 % EtOAc/hexanes); $^1\text{H NMR}$ (600MHz, Methanol-*d*₄) δ 5.98 (s, 1 H), 2.47 (t, $J = 7.6$ Hz, 2 H), 1.85 (s, 3 H), 1.70 - 1.60 (m, 2 H), 1.42 - 1.23 (m, 8 H), 0.90 (t, $J = 6.9$ Hz 3 H); $^{13}\text{C NMR}$ (151 MHz, Methanol-*d*₄) δ 169.19, 168.24, 164.87, 101.19, 98.84, 34.24, 32.85, 30.06, 29.94, 27.95, 23.66, 14.38, 8.23; **IR** (thin

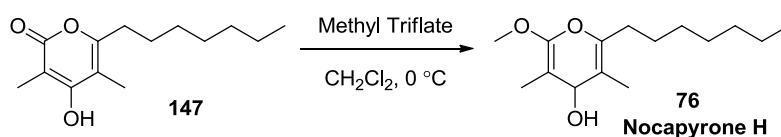
film) v 2954, 2924, 2854, 2672, 1634, 1575, 1511, 1409, 1253, 1177, 1129, 1069, 1003, 860, 751, 598, 529; **MS** (APCI) calculated for C₁₃H₂₁O₃ [M+H]⁺: 225.1485, found 225.1475.



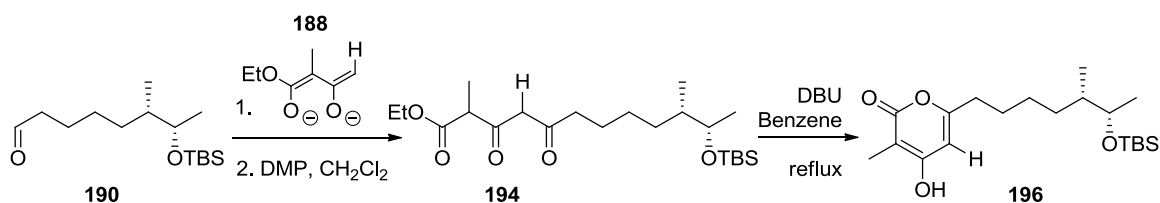
6-heptyl-4-hydroxy-3,5-dimethyl-2H-pyran-2-one (147) Dianion Addition - To a stirring solution of NaH (213 mg ; 5.3 mmol, 60% dispersion in oil) in dry THF (10 mL) was added ethyl-2-methyl-3-oxo-pentanoate **19** (0.42 g; 2.67 mmol) slowly dropwise at 0 °C over five minutes. The mixture was stirred until the evolution of hydrogen bubbles had subsided, and then freshly titrated *n*-BuLi (1.33 mL, 2 mol/L in hexanes) was added dropwise with colour change to yellow. This reaction mixture was stirred for 15 minutes before cooling to -20 °C where a THF solution of freshly prepared Octanal (0.19 g; 1.48 mmol) was added. The reaction was moved to the freezer (-20 °C) to stir over night. The reaction was quenched with addition of NH₄Cl sat solution and extracted with ether (3 x 10 mL). The combined organic extracts were dried (Na₂SO₄) and concentrated under reduced pressure. The crude was purified by column chromatography (10% EtOAc/X4) to give a mixture of isomers (0.279 g, 67 %). These isomers were combined together to be oxidised to the triketo ester.

DMP Oxidation - To a stirring solution of mixed isomers (0.279 g) in CH₂Cl₂ was added DMP (0.279 g, mol). The reaction was stirred at room temperature in darkness until TLC showed consumption of starting material. The reaction mixture was worked up by dilution with ether then with addition of NaHCO₃ solution and sodium thiosulfate sat solution. When the mixture cleared it was extracted with CH₂Cl₂ (3 x 10 mL), dried with Na₂SO₄ and concentrated under reduced pressure.

DBU Cyclisation - The crude mixture was dissolve in benzene (4.6 mL) and had DBU (0.1 mL, mol) added before bringing the mixture up to reflux temperature and allowed to stir overnight. The reaction mixture cooled to room temperature, worked up by addition of NH₄Cl sat solution and extracted with CH₂Cl₂ (3 x 10 mL). The combined organic extracts were dried (Na₂SO₄) and concentrated under reduced pressure. The crude was purified by column chromatography (50% EtOAc/X4) to afford the *title compound* as white amorphous solid (114 mg, 0.4 mmol, 32%); **R_f** = 0.167 (40% EtOAc/hexanes); **¹H NMR** (600MHz, Chloroform-*d*) δ 5.91 (s, 1H), 2.50 (t, *J* = 7.7 Hz, 2H), 1.98 (s, 3H), 1.96 (s, 3H), 1.63 (p, *J* = 7.4 Hz, 2H), 1.29 (ddd, *J* = 20.9, 10.4, 5.4 Hz, 8H), 0.88 (t, *J* = 6.9 Hz, 3H); **¹³C NMR** (151 MHz, Chloroform-*d*) δ 165.65, 164.02, 159.65, 105.91, 98.06, 31.85, 31.00, 29.29, 29.15, 27.55, 22.75, 14.21, 9.82, 8.42;



2-heptyl-6-methoxy-3,5-dimethyl-4H-pyran-4-one (Nocapyrone H) (76) To a stirring solution of pyrone (**147**) (113 mg, 0.47 mmol) in CH₂Cl₂ (5 mL) at 0 °C was added methyl triflate (62 μL, 0.57 mmol) and the reaction mixture was allowed to stir until TLC showed consumption of SM. Quenched with sat NaHCO₃ solution and extracted with CH₂Cl₂. The organic extracts were combined, dried with Na₂SO₄ and concentrated under vacuum. This gave essentially pure α-methoxy-γ-pyrone which was further purified through column chromatography (50% EtOAc/X4) to give a clear crystalline solid (62 mg, 0.25 mmol, 52%); *R_f* = 0.353 (40% EtOAc/hexanes); ¹H NMR (600MHz, Chloroform-*d*) δ 3.95 (s, 3H), 2.58 (t, *J* = 7.5 Hz, 2H), 1.94 (s, 3H), 1.85 (s, 3H), 1.64 (p, *J* = 7.5 Hz, 2H), 1.40 – 1.17 (m, 8H), 0.89 (t, *J* = 6.9 Hz, 3H); ¹³C NMR (151 MHz, Chloroform-*d*) δ 181.22, 162.26, 158.57, 118.38, 99.47, 55.39, 31.86, 30.84, 29.20, 29.15, 27.20, 22.76, 14.21, 10.11, 7.02; IR (thin film) ν 2926, 2856, 1670, 1604, 1464, 1410, 1379, 1320, 1248, 1167, 769, 566, 562, 558; MS (APCI) calculated for C₁₅H₂₄O₃ [M+H]⁺ : 253.1798, found 253.1804.



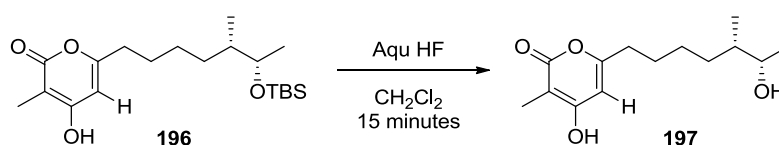
6-((5S,6S)-6-((tert-butyl dimethylsilyloxy)-5-methylheptyl)-4-hydroxy-3-methyl-2H-pyran-2-one (196) *Dianion Addition* – To a stirring solution of NaH (27.9 mg; 70 μmol, 60% dispersion in oil) in dry THF (3.5 mL, 0.1 mol/L) was added ethyl 2-methylacetoacetate **188** (100 mg; 0.7 μmol) slowly dropwise at 0 °C over five minutes. The mixture was stirred until the evolution of hydrogen bubbles had subsided; the solution will have become gelatinous. Then freshly titrated n-BuLi (436 μL, 1.6 mol/L in hexanes) was added dropwise with colour change to yellow. This reaction mixture was stirred for 15 minutes before cooling to -20 °C where a THF solution of aldehyde **190** (95.1 mg; 0.35 μmol) was added. The reaction was moved to the freezer (-20 °C) to stir over night. The reaction was quenched with addition of NH₄Cl sat solution and extracted with ether (3 x 50 mL). The combined organic extracts were dried (Na₂SO₄) and concentrated under reduced pressure. The crude was purified by column chromatography (10 % EtOAc/X4) to give a

Experimental Procedures

mixture of isomers (84.5 mg, 58 %). These isomers were combined together oxidised to give the triketo ester.

DMP Oxidation - To a stirring solution of mixed isomers (84 mg) in CH₂Cl₂ (2 mL, 0.1 mol/L) was added DMP (171 mg, 0.4 μmol). The reaction was stirred at room temperature in darkness until TLC showed consumption of starting material. The reaction mixture was worked up by dilution with ether then with addition of NaHCO₃ solution and sodium thiosulfate sat solution. When the mixture cleared it was extracted with CH₂Cl₂, dried with Na₂SO₄ and concentrated under reduced pressure giving crude mixture (43 mg, 51 %).

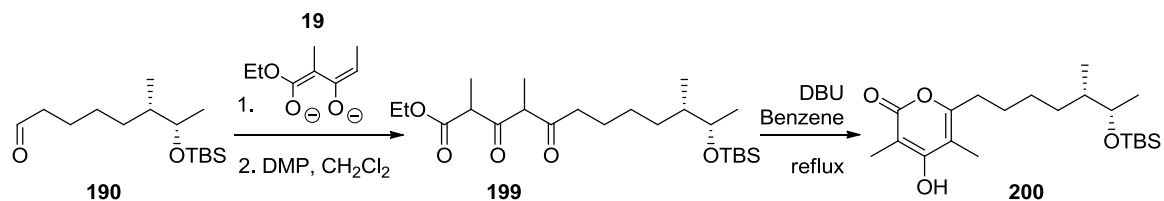
The crude mixture was dissolve in benzene (1 mL) and had DBU (15.8 μL, mol) added before bringing the mixture up to reflux temperature and allowed to stir overnight. The reaction mixture cooled to room temperature, worked up by addition of NH₄Cl sat solution and extracted with CH₂Cl₂ (3 x 20 mL). The combined organic extracts were dried (Na₂SO₄) and concentrated under reduced pressure. The crude was purified by column chromatography (10 % Et₂O/CH₂Cl₂) to afford the *title compound* **196** as yellow amorphous solid (21 mg, 16 % from aldehyde **190**); **R_f** = 0.338 (10 % Et₂O/CH₂Cl₂); **¹H NMR** (600MHz, Chloroform-*d*) δ 5.95 (s, 1H), 3.67 (qd, *J* = 6.1, 3.9 Hz, 1H), 2.45 (t, *J* = 7.7 Hz, 2H), 1.96 (s, 3H), 1.62 (th, *J* = 21.0, 6.9 Hz, 3H), 1.50 – 1.20 (m, 3H), 1.09 (dt, *J* = 7.4, 4.6 Hz, 1H), 1.05 (d, *J* = 6.2 Hz, 3H), 0.81 (d, *J* = 6.7 Hz, 3H), 0.87 (s, 9H), 0.02 (d, *J* = 10.9 Hz, 6H); **¹³C NMR** (151 MHz, Chloroform-*d*) δ 167.06, 164.81, 163.85, 99.80, 98.59, 71.73, 40.29, 33.69, 32.27, 27.25, 27.09, 26.04, 20.55, 18.26, 14.76, 8.20, -4.09, -4.67; **IR** (thin film) ν 2930, 2858, 1635, 1575, 1409, 1251, 1174, 1126, 1056, 1005, 836, 774; **[α]_D²⁰** = 0 (*c* = 0.23 g/100 mL, CHCl₃); **MS** (ESI) calculated for C₂₀H₃₆O₄SiNa [M+Na]⁺ : 391.2281, found 391.2276.



4-hydroxy-6-((5*S*,6*S*)-6-hydroxy-5-methylheptyl)-3-methyl-2*H*-pyran-2-one (197) To a solution of TBS ether pyrone (**196**) (12 mg, 33 μmol) in CH₂Cl₂ (300 μL), HF was added (160 μL, 40 % w/w aqu. solution). The reaction mixture was shaken on a vortex pad inside a centrifuge tube for 10 minutes. Then mixture was diluted with water, quenched with aqueous NaHCO₃ solution, extracted with EtOAc (3 x 4 mL). The solvent was removed under reduced pressure and purification through column chromatography (100% EtOAc) afforded the *title compound* **197** as yellow amorphous solid (2 mg, 24 %); **R_f** = 0.508 (100% EtOAc); **¹H NMR** (600MHz, DMSO-*d*₆) δ 11.07 (s, 1H), 5.97 (s, 1H), 3.47 (dtd, *J* = 10.8, 6.4, 4.5 Hz, 1H), 2.41 (td, *J* = 7.5, 2.7 Hz, 2H), 1.74 (s, 3H), 1.57 – 1.45 (m, 2H), 1.45 – 1.20 (m, 4H), 1.08 – 1.00 (m, 1H), 0.98 (d, *J* = 6.3

Experimental Procedures

Hz, 3H), 0.78 (d, $J = 6.8$ Hz, 3H); ^{13}C NMR (151 MHz, DMSO- d_6) δ 165.07, 164.83, 162.57, 99.15, 96.48, 68.88, 40.06, 32.58, 31.72, 26.66, 26.11, 20.23, 14.50, 8.35; **IR** (thin film) ν 2927, 2856, 1712, 1590, 1463, 1378, 1251, 1095, 836, 774.62; Insufficient material was available for optical rotation or mass spectroscopic analysis.

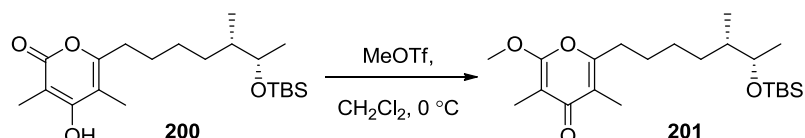


6-((5*S*,6*S*)-6-((*tert*-butyldimethylsilyl)oxy)-5-methylheptyl)-4-hydroxy-3,5-dimethyl-2*H*-pyran-2-one (200**) Dianion Addition** – To a stirring solution of NaH (56 mg; mol, 60% dispersion in oil) in dry THF (2.6 mL) was added ethyl-2-methyl-3-oxo-pentanoate **19** (146 mg; 0.92 mmol) slowly dropwise at 0 °C over five minutes. The mixture was stirred until the evolution of hydrogen bubbles had subsided, and then freshly titrated *n*-BuLi (514 μL , 2 mol/L in hexanes) was added dropwise with colour change to yellow. This reaction mixture was stirred for 15 minutes before cooling to -20 °C where a THF solution of aldehyde **190** (140 mg; 0.51 mmol) was added. The reaction was moved to the freezer (-20 °C) to stir 4 hours. After TLC showed consumption of starting material the reaction was quenched with addition of NH_4Cl sat solution and extracted with ether (3 x 10 mL). The combined organic extracts were dried (Na_2SO_4) and concentrated under reduced pressure. The crude was purified by column chromatography (20% EtOAc/X4) to give a mixture of isomers. These isomers were combined together oxidised to give the triketo ester.

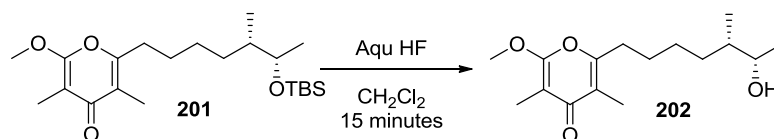
DMP Oxidation - To a stirring solution of mixed isomers (88 mg, 0.2 mmol) in CH_2Cl_2 (2 mL) was added DMP (260 mg, 0.61 mmol). The reaction was stirred at room temperature in darkness until TLC showed consumption of starting material. The reaction mixture was worked up by dilution with ether then with addition of NaHCO_3 solution and sodium thiosulfate sat solution. When the mixture cleared it was extracted with CH_2Cl_2 (3 x 5 mL), dried with Na_2SO_4 and concentrated under reduced pressure. The crude mixture was dissolve in benzene (1.8 mL) and had DBU (27 mL, 0.18 mmol) added before bringing the mixture up to reflux temperature and allowed to stir overnight. The reaction mixture cooled to room temperature, worked up by addition of NH_4Cl sat solution and extracted with CH_2Cl_2 (3 x 5 mL). The combined organic extracts were dried (Na_2SO_4) and concentrated under reduced pressure. The crude was purified by column chromatography (20 % EtOAc/X4) to afford the *title compound* **200** as white amorphous solid (76 mg, 0.18 mmol, 21 % from aldehyde **190**); $R_f = 0.26$ (40 % EtOAc/hexanes); ^1H NMR (600MHz, Chloroform-*d*) δ 3.66 (qd, $J = 6.2, 4.0$ Hz, 1H), 2.50 (t, $J = 7.7$ Hz, 2H), 1.99 (s, 3H),

Experimental Procedures

1.97 (s, 3H), 1.65 – 1.54 (m, 2H), 1.42 (ddd, $J = 12.2, 10.2, 5.1$ Hz, 1H), 1.35 (tdd, $J = 7.3, 5.6, 3.5$ Hz, 1H), 1.31 – 1.21 (m, 1H), 1.11 – 1.00 (m, 1H), 1.04 (d, $J = 6.2$ Hz, 3H), 0.86 (s, 9H), 0.80 (d, $J = 6.7$ Hz, 3H), 0.01 (d, $J = 11.3$ Hz, 6H); $^{13}\text{C NMR}$ (151 MHz, Chloroform- d) δ 166.67, 165.45, 159.32, 107.10, 98.36, 71.68, 40.31, 32.44, 31.00, 27.85, 27.26, 26.01, 20.64, 14.64, 10.00, 8.72, -4.10, -4.70; **IR** (thin film) ν 2957, 2931, 2858, 1800, 1667, 1568, 1463, 1372, 1250, 1055, 957, 837, 774, 666, 570; $[\alpha]_{\text{D}}^{20} = -1.6$ ($c = 0.155$ g/100 mL, CHCl_3); **MS** (APCI) calculated for $\text{C}_{21}\text{H}_{39}\text{O}_4\text{Si}$ $[\text{M}+\text{H}]^+$: 383.2612, found 383.2596



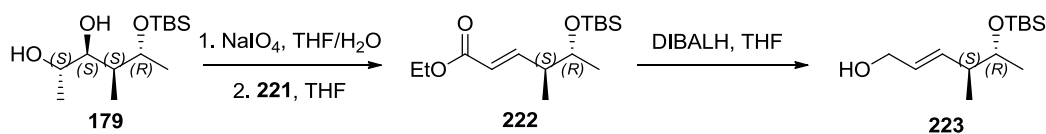
2-((5S,6S)-6-((tert-butyl dimethylsilyl)oxy)-5-methylheptyl)-6-methoxy-3,5-dimethyl-4H-pyran-4-one (201) To a stirring solution of pyrone (**200**) (14 mg, 37 μmol) in CH_2Cl_2 (5 mL) at 0 $^\circ\text{C}$ was added methyl triflate (45 μL of 0.89 mol/L solution in CH_2Cl_2) and the reaction mixture was allowed to stir until TLC showed consumption of SM. Quenched with sat NaHCO_3 solution and extracted with CH_2Cl_2 . The organic extracts were combined, dried with Na_2SO_4 and concentrated under vacuum. This gave essentially pure α -methoxy- γ -pyrone which was further purified through column chromatography (50% EtOAc/X4) to give a clear crystalline solid (7.4 mg, mol, 51%); $R_f = 0.38$ (30 % EtOAc/hexanes); $^1\text{H NMR}$ (600MHz, Chloroform- d) δ 3.94 (s, 3H), 3.68 (dt, $J = 10.1, 5.2$ Hz, 1H), 2.58 (t, $J = 7.6$ Hz, 2H), 1.94 (s, 3H), 1.85 (s, 3H), 1.73 – 1.07 (m, 7H), 1.05 (d, $J = 6.3$ Hz, 3H), 0.87 (s, 9H), 0.82 (d, $J = 6.7$ Hz, 3H), 0.02 (d, $J = 13.0$ Hz, 6H); $^{13}\text{C NMR}$ (151 MHz, Chloroform- d) δ 165.62, 164.01, 159.56, 105.92, 98.07, 71.70, 40.32, 32.45, 31.02, 27.88, 27.29, 26.03, 20.65, 18.26, 14.66, 9.84, 8.45, -4.08, -4.69; $[\alpha]_{\text{D}}^{20} = 0$ ($c = 0.135$ g/100 mL, CHCl_3); **MS** (APCI) calculated for $\text{C}_{22}\text{H}_{41}\text{O}_4\text{Si}$ $[\text{M}+\text{H}]^+$: 397.2769, found 397.2775.



2-((5S,6S)-6-hydroxy-5-methylheptyl)-6-methoxy-3,5-dimethyl-4H-pyran-4-one (202) To a solution of TBS ether pyrone (**201**) (4 mg, 10 μmol) in CH_2Cl_2 (300 μL), HF was added (500 μL , 40 % w/w aqu. solution). The reaction mixture was shaken on a vortex pad inside a centrifuge tube for 10 minutes. Then mixture was diluted with water, quenched with aqueous NaHCO_3 solution, extracted with EtOAc (3 x 4 mL). The solvent was removed under reduced pressure and purification through column chromatography (50% EtOAc/hexanes) afforded the *title compound* as yellow amorphous solid (1.6 mg, 56 %); $R_f = 0.332$ (100% EtOAc); $^1\text{H NMR}$ (600 MHz, Chloroform- d) δ 3.95 (s, 3H), 3.71 (td, $J = 6.4, 4.3$ Hz, 1H), 2.59 (t, $J = 7.6$ Hz, 2H), 1.94 (s, 3H),

Experimental Procedures

1.84 (s, 4H), 1.71 – 1.58 (m, 2H), 1.54 – 1.22 (m, 4H), 1.15 (d, $J = 6.3$ Hz, 3H), 0.88 (d, $J = 6.7$ Hz, 3H); ^{13}C NMR (151 MHz, Chloroform- d) δ 181.17, 162.26, 158.37, 118.42, 99.51, 71.33, 55.42, 39.82, 32.44, 30.86, 27.53, 27.12, 20.42, 14.28, 10.13, 7.02. ; IR (thin film) ν 3411, 2926, 1667, 1586, 1465, 1416, 1379, 1322, 1251, 1168, 984, 770 ; $[\alpha]_{\text{D}}^{20} = -16.5$ ($c = 0.055$ g/100 mL, MeOH); MS (APCI) calculated for $\text{C}_{16}\text{H}_{27}\text{O}_4$ $[\text{M}+\text{H}]^+$: 283.1904, found 283.1902



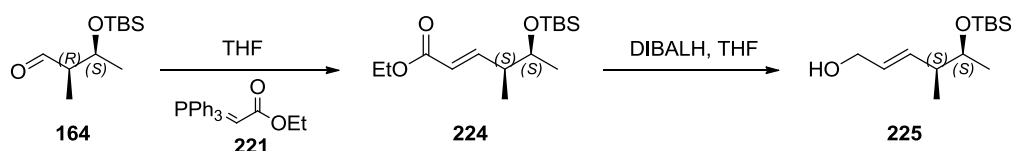
(4S,5R,E)-5-((tert-butyldimethylsilyl)oxy)-4-methylhex-2-en-1-ol (223) To a stirring solution of **179** (0.105 g; 0.4 mmol) in THF (2 mL) was added an aqueous solution of NaIO_4 (0.26 g; 1.2 mmol) in 2 mL of water. This biphasic mixture was stirred vigorously until TLC showed consumption of starting material. The mixture was then diluted with water and extracted with CH_2Cl_2 (3 x 5 mL), combined organic extracts were dried (Na_2SO_4) and concentrated under vacuum to afford crude (2R,3R)-3-((tert-butyldimethylsilyl)oxy)-2-methylbutanal **180** (0.080 g, 0.37 mmol 92 %) ($R_f = 0.75$ (20% $\text{Et}_2\text{O}/\text{X4}$) as an unstable^{197,198} clear liquid which was not stored and used immediately in the next step;

Witting reaction – To a stirring solution of **180** (0.08 g; 0.37 mmol) in THF (1 mL) was added THF solution (1 mL) of (Carbethoxymethylene)triphenylphosphorane **221** (0.39 g, 1.1 mmol) and the solution was stirred at room temperature overnight. The reaction was worked up with brine solution and extracted with CH_2Cl_2 (3 x 5 mL), combined organic extracts were dried (Na_2SO_4) and concentrated under vacuum. The crude mixture was purified through column chromatography (20% $\text{EtOAc}/\text{X4}$) to afford (4S,5R,E)-ethyl 5-((tert-butyldimethylsilyl)oxy)-4-methylhex-2-enoate **222** (0.1 g, 0.37 mmol) and then used directly in the next reaction. $R_f = 0.727$ (20% $\text{EtOAc}/\text{X4}$)

DIBALH reduction - To a stirring solution of **222** (0.1 g; 0.37 mmol) in THF (1 mL) was added DIBALH solution (1.05 mL, 1 mol/L in THF, 3 equ) at 0 °C. The addition of DIBALH solution released small amounts of hydrogen gas as bubbles. The reaction mixture was stirred at 0 °C for an hour until TLC showed consumption of starting material. The mixture was warmed to room temperature and ethyl acetate (5 mL) was added slowly to the reaction mixture to destroy excess DIBALH. Then an aqueous Rochelle's salt solution (5 mL) was added to break up the eventual slurry. This mixture was allowed to stir for an hour before the organic phase was separated and the aqueous extracted with ethyl acetate (3 x 5 mL). The organic extracts were combined, dried (Na_2SO_4) and concentrated under vacuum. The crude mixture was purified through column chromatography (20 % $\text{EtOAc}/\text{X4}$) to afford *title compound* **223** (0.0680 g, 0.278 mmol, 75 %) as a clear liquid. $R_f = 0.384$ (20% $\text{EtOAc}/\text{X4}$); ^1H NMR (600 MHz, Chloroform- d) δ 5.69 – 5.59

Experimental Procedures

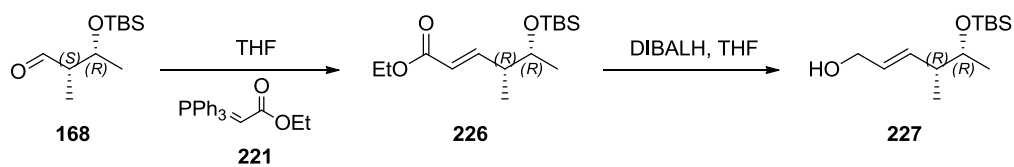
(m, 2H), 4.11 (d, $J = 5.0$ Hz, 2H), 3.69 (qd, $J = 6.2, 4.5$ Hz, 1H), 2.18 (pd, $J = 6.8, 4.4$ Hz, 1H), 1.05 (d, $J = 6.2$ Hz, 3H), 0.99 (d, $J = 6.9$ Hz, 3H), 0.88 (s, 9H), 0.03 (d, $J = 3.8$ Hz, 6H); ^{13}C NMR (151 MHz, Chloroform- d) δ 135.54, 128.97, 71.78, 64.01, 44.04, 25.87, 20.77, 18.13, 15.95, -4.31, -4.80; IR (thin film) ν 3322, 2959, 2930, 2858, 1463, 1375, 1254, 1083, 1036, 1006, 972, 836, 774, 667; $[\alpha]_D^{20} = -10.3$ ($c = 0.78$ g/100 mL, CHCl_3); MS (APCI) calculated for $\text{C}_{13}\text{H}_{28}\text{O}_2\text{Si}$ $[\text{M}+\text{H}]^+$: 287.2037, found 287.2027.



(4S,5S,E)-5-((tert-butyldimethylsilyl)oxy)-4-methylhex-2-en-1-ol (225) *Wittig reaction* – To a stirring solution of **164** (0.2140 g, 0.989 mmol) in THF (5 mL) was added (Carbethoxymethylene)triphenylphosphorane **221** (1 g, 2.9 mmol) and the solution was stirred at room temperature overnight. The reaction was worked up with brine solution and extracted with CH_2Cl_2 (3 x 5 mL), combined organic extracts were dried (Na_2SO_4) and concentrated under vacuum. The crude mixture was purified through column chromatography (20% EtOAc/X4) to afford *(4S,5S,E)-ethyl 5-((tert-butyldimethylsilyl)oxy)-4-methylhex-2-enoate* **224** (0.2649 g, 0.925 mmol) and then used directly in the next reaction. $R_f = 0.652$ (20% EtOAc/X4)

DIBALH reduction - To a stirring solution of **224** (0.2567g, 0.896 mmol) in THF (5 mL) was added DIBALH solution (2.7 mL, 1 mol/L in THF, 3 equ) at 0 °C. The addition of DIBALH solution released small amounts of hydrogen gas as bubbles. The reaction mixture was stirred at 0 °C for 2 hours until TLC showed consumption of starting material. The mixture was warmed to room temperature and ethyl acetate (5 mL) was added slowly to the reaction mixture to destroy excess DIBALH. Then an aqueous Rochelle's salt solution (5 mL) was added to break up the eventual slurry. This mixture was allowed to stir for an hour before the organic phase was separated and the aqueous extracted with ethyl acetate (3 x 5 mL). The organic extracts were combined, dried (Na_2SO_4) and concentrated under vacuum. The crude mixture was purified through column chromatography (20 % EtOAc/X4) to afford *title compound* **225** (0.1902 g, 0.778 mmol, 80 %) as a clear liquid. $R_f = 0.302$ (20% EtOAc/ X4); ^1H NMR (600 MHz, Chloroform- d) δ 5.73 – 5.56 (m, 2H), 4.11 (t, $J = 4.8$ Hz, 2H), 3.64 (p, $J = 6.1$ Hz, 1H), 2.18 (h, $J = 6.7$ Hz, 1H), 1.07 (d, $J = 6.2$ Hz, 3H), 0.99 (d, $J = 6.8$ Hz, 3H), 0.89 (s, 9H), 0.04 (d, $J = 4.8$ Hz, 6H); ^{13}C NMR (151 MHz, Chloroform- d) δ 135.99, 128.85, 72.09, 64.14, 44.22, 26.03, 21.10, 18.28, 15.77, -4.18, -4.62; IR (thin film) ν 3326, 2958, 2930, 2858, 1463, 1373, 1256, 1097, 1006, 972, 836, 774, 666; $[\alpha]_D^{20} = -10.8$ ($c = 0.835$ g/100 mL, CHCl_3); MS (APCI) calculated for $\text{C}_{13}\text{H}_{28}\text{O}_2\text{Si}$ $[\text{M}+\text{H}]^+$: 287.2037, found 245.1923.

Experimental Procedures



(4R,5R,E)-5-((tert-butyl dimethylsilyl)oxy)-4-methylhex-2-en-1-ol (227) The reaction procedure was conducted as per the preparation of the enantiomer **(4S,5S,E)-5-((tert-butyl dimethylsilyl)oxy)-4-methylhex-2-en-1-ol 225** but initiating from the aldehyde **168**. The spectroscopic data was the same as that of **225** with the exception of the optical rotation analysis which provided the same magnitude but opposite sign of rotation.

Bibliography

- (1) Walsh, C. T.; Tang, Y. *Natural Product Biosynthesis*; The Royal Society of Chemistry, 2017.
- (2) Editorial. *Nat. Chem. Biol.* **2007**, 3 (7), 351.
- (3) Cooper, R.; Nicola, G. *Natural Products Chemistry: Sources, Separations and Structures*; CRC Press, 2014.
- (4) Firm, R. D.; Jones, C. G. *Nat. Prod. Rep.* **2003**, 20 (4), 382.
- (5) Sarker, S. D.; Nahar, L. In *Natural Products Isolation*; Sarker, S. D., Nahar, L., Eds.; Methods in Molecular Biology; Humana Press: Totowa, NJ, 2012; Vol. 864.
- (6) Hanson, J. R. *Natural Products: The Secondary Metabolites*; Royal Society of Chemistry: Cambridge, 2003; Vol. 17.
- (7) Herbert, R. B. *The Biosynthesis of Secondary Metabolites*; Springer Netherlands, 2012.
- (8) Dewick, P. M. *Medicinal Natural Products*; John Wiley & Sons, Ltd: Chichester, UK, 2009.
- (9) Laursen, J. B.; Nielsen, J. *Chem. Rev.* **2004**, 104 (3), 1663.
- (10) David E. Wedge, N. D. C. In *Biologically Active Natural Products*; Cutler, S. J., Cutler, H. G., Eds.; CRC Press, 1999; p 15.
- (11) Satyajit D. Sarker, Zahid Latif, A. I. G. In *Natural Products Isolation*; Sarker, S. D., Latif, Z., Gray, A. I., Eds.; Humana Press: Totowa, NJ, 2005.
- (12) Cragg, G. M.; Newman, D. J. *Biochim. Biophys. Acta* **2013**, 1830 (6), 3670.
- (13) David, B.; Wolfender, J.-L.; Dias, D. A. *Phytochem. Rev.* **2014**, 14 (2), 299.
- (14) *Natural Products as Source of Molecules with Therapeutic Potential*; Cechinel Filho, V., Ed.; Springer International Publishing: Cham, 2018.
- (15) Newman, D. J.; Cragg, G. M. *J. Nat. Prod.* **2016**, 79 (3), 629.
- (16) Young, D. W. Bittker, J. A., Ross, N. T., Eds.; *Chemical Biology*; Royal Society of Chemistry: Cambridge, 2016; pp 16–36.

Bibliography

- (17) Zhang, L.; Demain, A. L. *Natural products: Drug discovery and therapeutic medicine*; 2005.
- (18) Koehn, F. E.; Carter, G. T. *Nat. Rev. Drug Discov.* **2005**, *4* (3), 206.
- (19) Weissman, K. J. *Philos. Trans. A. Math. Phys. Eng. Sci.* **2004**, *362* (1825), 2671.
- (20) Taylor, R. E.; Chen, Y.; Galvin, G. M.; Pabba, P. K. *Org. Biomol. Chem.* **2004**, *2* (1), 127.
- (21) Evans, B. E.; Rittle, K. E.; Bock, M. G.; DiPardo, R. M.; Freidinger, R. M.; Whitter, W. L.; Lundell, G. F.; Veber, D. F.; Anderson, P. S.; Chang, R. S. L.; Lotti, V. J.; Cerino, D. J.; Chen, T. B.; Kling, P. J.; Kunkel, K. A.; Springer, J. P.; Hirshfield, J. *J. Med. Chem.* **1988**, *31* (12), 2235.
- (22) Jenke-Kodama, H.; Sandmann, A.; Müller, R.; Dittmann, E. *Mol. Biol. Evol.* **2005**, *22* (10), 2027.
- (23) Busch, B.; Hertweck, C. *Phytochemistry*. Elsevier Ltd 2009, pp 1833–1840.
- (24) Demain, A. L.; Lancini, G. In *The Prokaryotes*; Springer New York: New York, NY, 2006; pp 812–833.
- (25) Staunton, J.; Weissman, K. J. *Nat. Prod. Rep.* **2001**, *18* (4), 380.
- (26) Hertweck, C. *Angew. Chemie Int. Ed.* **2009**, *48* (26), 4688.
- (27) Khosla, C.; Gokhale, R. S.; Jacobsen, J. R.; Cane, D. E. *Annu. Rev. Biochem.* **1999**, *68*, 219.
- (28) Weissman, K. J. *Methods Enzymol.* **2009**, *459* (B), 3.
- (29) Hopwood, D. A. *Chem. Rev.* **1997**, *97* (7), 2465.
- (30) Hirata, Y.; Nakata, H.; Yamada, K.; Okuhara, K.; Naito, T. *Tetrahedron* **1961**, *14* (3–4), 252.
- (31) Friedrich, T.; Van Heek, P.; Leif, H.; Ohnishi, T.; Forche, E.; Kunze, B.; Jansen, R.; Trowitzsch-Kienast, W.; Höfle, G.; Reichenbach, H.; Weiss, H. *Eur. J. Biochem.* **1994**, *219* (1–2), 691.
- (32) Oishi, H.; Hosokawa, T.; Okutomi, T.; Suzuki, K.; Ando, K. *Agric. Biol. Chem.* **1969**, *33* (12), 1790.

Bibliography

- (33) Taniguchi, M.; Watanabe, M.; Nagai, K.; Suzumura, K.; Suzuki, K.; Tanaka, A. *J. Antibiot. (Tokyo)*. **2000**, *53* (8), 844.
- (34) He, J.; Hertweck, C. *J. Am. Chem. Soc.* **2004**, *126* (12), 3694.
- (35) Busch, B.; Ueberschaar, N.; Behnken, S.; Sugimoto, Y.; Werneburg, M.; Traitcheva, N.; He, J.; Hertweck, C. *Angew. Chemie - Int. Ed.* **2013**, *52* (20), 5285.
- (36) Müller, M.; He, J.; Hertweck, C. *ChemBioChem* **2006**, *7* (1), 37.
- (37) Ziehl, M.; He, J.; Dahse, H. M.; Hertweck, C. *Angew. Chemie - Int. Ed.* **2005**, *44* (8), 1202.
- (38) Cardillo, R.; Fuganti, C.; Ghiringhelli, D.; Giangrasso, D.; Grasselli, P.; Santopietro-Amisano, A. *Tetrahedron* **1974**, *30* (3), 459.
- (39) Werneburg, M.; Busch, B.; He, J.; Richter, M. E. A.; Xiang, L.; Moore, B. S.; Roth, M.; Dahse, H. M.; Hertweck, C. *J. Am. Chem. Soc.* **2010**, *132* (30), 10407.
- (40) He, J.; Hertweck, C. *Chem. Biol.* **2003**, *10* (12), 1225.
- (41) Dewick, P. M. In *Essentials of Organic Chemistry: For Students of Pharmacy, Medicinal Chemistry and Biological Chemistry*; 2013; pp 403–462.
- (42) Rix, U.; Fischer, C.; Remsing, L. L.; Rohr, J. *Nat. Prod. Rep.* **2002**, *19* (5), 542.
- (43) Harris, T. M.; Harris, C. M. *J. Org. Chem.* **1966**, *31* (4), 1032.
- (44) Suzuki, E.; Sekizaki, H.; Inoue, S. *J. Chem. Soc. Chem. Commun.* **1973**, 6 (16), 568.
- (45) SUZUKI, E.; Sekizaki, H.; INOUE, S. *J. Chem. Res.* **1977**, No. 3, 200.
- (46) Hauser, C. R.; Harris, T. M. *J. Am. Chem. Soc.* **1958**, *80* (23), 6360.
- (47) Work, S. D.; Hauser, C. R. *J. Org. Chem.* **1963**, *28* (3), 725.
- (48) LIGHT, R. J.; HAUSER, C. R. *J. Org. Chem.* **1960**, *25* (4), 538.
- (49) Kirby, F. B.; Harris, T. M.; Hauser, C. R. *J. Org. Chem.* **1963**, *28* (9), 2266.
- (50) Miles, M. L.; Harris, T. M.; Hauser, C. R. *J. Org. Chem.* **1965**, *30* (4), 1007.
- (51) Harris, T. M.; Carney, R. L. *J. Am. Chem. Soc.* **1967**, *89* (25), 6734.

Bibliography

- (52) Hampton, K. G.; Harris, T. M.; Harris, C. M.; Hauser, C. R. *J. Org. Chem.* **1965**, *30* (12), 4263.
- (53) Harris, T. M.; Boatman, S.; Hauser, C. R. *J. Am. Chem. Soc.* **1965**, *87* (14), 3186.
- (54) Harris, T. M.; Murphy, G. P. *J. Am. Chem. Soc.* **1971**, *93* (24), 6708.
- (55) Huckin, S. N.; Weiler, L. *J. Am. Chem. Soc.* **1974**, *96* (1970), 1082.
- (56) Huckin, S. N.; Weiler, L. *Can. J. Chem.* **1973**, *52* (8), 1343.
- (57) Huckin, S. N.; Weiler, L. *Canadian Journal of Chemistry*. 1974, pp 2157–2164.
- (58) Osman, M. A.; Seibl, J.; Pretsch, E. *Helv. Chim. Acta* **1977**, *60* (8), 3007.
- (59) Onda, K.; Hayakawa, I.; Sakakura, A. *Synlett* **2017**, *28* (13), 1596.
- (60) Liang, G.; Miller, A. K.; Trauner, D. *Org. Lett.* **2005**, *7* (5), 819.
- (61) Werneburg, M.; Hertweck, C. *ChemBioChem* **2008**, *9* (13), 2064.
- (62) Gregg, C.; Perkins, M. V. *Org. Biomol. Chem.* **2012**, *10* (32), 6547.
- (63) Barbarow, J. E.; Miller, A. K.; Trauner, D. *Org. Lett.* **2005**, *7* (14), 2901.
- (64) Oppolzer, W.; Moretti, R.; Bernardinelli, G. *Tetrahedron Lett.* **1986**, *27* (39), 4713.
- (65) Spencer, R. W.; Copp, L. J.; Pfister, J. R. *J. Med. Chem.* **1985**, *28* (12), 1828.
- (66) Solladié, G.; Gehrold, N.; Maignan, J. *European J. Org. Chem.* **1999**, *1999* (9), 2309.
- (67) Lipshutz, B. H.; Amorelli, B. *Tetrahedron Lett.* **2009**, *50* (18), 2144.
- (68) Minassi, A.; Cicione, L.; Koeberle, A.; Bauer, J.; Laufer, S.; Werz, O.; Appendino, G. *European J. Org. Chem.* **2012**, *2012* (4), 772.
- (69) Galejeva, Y.; Helbig, S.; Morr, M.; Sasse, F.; Nimtz, M.; Laschat, S.; Baro, A. *Chem. Biodivers.* **2006**, *3* (8), 935.
- (70) Sabitha, G.; Gopal, P.; Yadav, J. S. *Tetrahedron Asymmetry* **2009**, *20* (19), 2205.
- (71) Ramesh, P.; Meshram, H. M. *Tetrahedron* **2012**, *68* (45), 9289.
- (72) Shone, R. L.; Deason, J. R.; Miyano, M. *J. Org. Chem.* **1986**, *51* (2), 268.

Bibliography

- (73) Ishibashi, Y.; Ohba, S.; Nishiyama, S.; Yamamura, S. *Tetrahedron Lett.* **1996**, *37* (17), 2997.
- (74) Parker, K. A.; Lim, Y. *J. Am. Chem. Soc.* **2004**, *126* (49), 15968.
- (75) Beaudry, C. M.; Trauner, D. *Org. Lett.* **2005**, *7* (20), 4475.
- (76) Leiris, S. J.; Khmour, O. M.; Segerman, Z. J.; Tsosie, K. S.; Chapuis, J.-C.; Hecht, S. M. *Bioorg. Med. Chem.* **2010**, *18* (10), 3481.
- (77) Ramirez, M.-L.; Garey, D.; Peña, M. R. *J. Heterocycl. Chem.* **1995**, *32* (5), 1657.
- (78) Garey, D.; Ramirez, M.; Gonzales, S.; Wertsching, A.; Tith, S.; Keefe, K.; Peña, M. R. *J. Org. Chem.* **1996**, *61* (14), 4853.
- (79) Miller, A. K.; Trauner, D. *Angew. Chemie Int. Ed.* **2003**, *42* (5), 549.
- (80) Patel, B. H.; Barrett, A. G. M. *J. Org. Chem.* **2012**, *77*, 11296.
- (81) De Rosa, M.; Acocella, M. R.; Rega, M. F.; Scettri, A. *Tetrahedron Asymmetry* **2004**, *15*, 3029.
- (82) Navarro, I.; Pöverlein, C.; Schlingmann, G.; Barrett, A. G. M. *J. Org. Chem.* **2009**, *74*, 8139.
- (83) Singer, R. a; Carreira, E. M. *J. Am. Chem. Soc.* **1995**, *117* (49), 12360.
- (84) Dalby, S. M.; Goodwin-Tindall, J.; Paterson, I. *Angew. Chemie Int. Ed.* **2013**, *52* (25), 6517.
- (85) Patel, B. H.; Mason, A. M.; Patel, H.; Coombes, R. C.; Ali, S.; Barrett, A. G. M. *J. Org. Chem.* **2011**, *76*, 6209.
- (86) Calo, F.; Richardson, J.; Barrett, A. G. M. *Org. Lett.* **2009**, *11* (21), 4910.
- (87) Cookson, R.; Barrett, T. N.; Barrett, A. G. M. *Acc. Chem. Res.* **2015**, *48* (3), 628.
- (88) Shimamura, H.; Sunazuka, T.; Izuhara, T.; Hirose, T.; Shiomi, K.; Ōmura, S. *Org. Lett.* **2007**, *9* (1), 65.
- (89) Banerjee, A. K.; Achari, B. *Tetrahedron Lett.* **1993**, *34* (7), 1209.
- (90) Hagiwara, H.; Kobayashi, K.; Miya, S.; Hoshi, T.; Suzuki, T.; Ando, M. *Org. Lett.* **2001**, *3*

Bibliography

- (2), 251.
- (91) Zhang, F.; Danishefsky, S. J. *Angew. Chemie* **2002**, *114* (8), 1492.
- (92) Kim, H.; Baker, J. B.; Lee, S. U.; Park, Y.; Bolduc, K. L.; Park, H. B.; Dickens, M. G.; Lee, D. S.; Kim, Y.; Kim, S. H.; Hong, J. *J. Am. Chem. Soc.* **2009**, *131* (9), 3192.
- (93) Oguchi, T.; Watanabe, K.; Ohkubo, K.; Abe, H.; Katoh, T. *Chem. - A Eur. J.* **2009**, *15* (12), 2826.
- (94) Shishido, K.; Yoshida, M.; Takai, H.; Mitsunashi, C. *Heterocycles* **2010**, *82* (1), 881.
- (95) Yokoe, H.; Mitsunashi, C.; Matsuoka, Y.; Yoshimura, T.; Yoshida, M.; Shishido, K. *J. Am. Chem. Soc.* **2011**, *133* (23), 8854.
- (96) Harris, T. M.; Harris, C. M.; Wachter, M. P. *Tetrahedron* **1968**, *24* (24), 6897.
- (97) Köster, G.; Hoffmann, R. W. *Liebigs Ann. der Chemie* **1987**, No. 11, 987.
- (98) Lee, J. *Mar. Drugs* **2015**, *13* (3), 1581.
- (99) Work, S. D.; Hauser, C. R. *J. Org. Chem.* **1963**, *28* (3), 725.
- (100) Light, R. J.; Hauser, C. R. *J. Org. Chem.* **1960**, *25* (4), 538.
- (101) Cavalieri, L. F. *Chem. Rev.* **1947**, *41* (3), 525.
- (102) Miles, M. L.; Hauser, C. R. *Org. Synth.* **1966**, *46* (September), 60.
- (103) Harris, T. M.; Murphy, G. P.; Poje, A. J. *J. Am. Chem. Soc.* **1976**, *98* (24), 7733.
- (104) Yamamura, S.; Nishiyama, S. *Bull. Chem. Soc. Jpn.* **1997**, *70* (9), 2025.
- (105) Arimoto, H.; Cheng, J.-F.; Nishiyama, S.; Yamamura, S. *Tetrahedron Lett.* **1993**, *34* (36), 5781.
- (106) Arimoto, H.; Nishiyama, S.; Yamamura, S. *Tetrahedron Lett.* **1994**, *35* (51), 9581.
- (107) Arimoto, H.; Yokoyama, R.; Nakamura, K.; Okumura, Y.; Uemura, D. *Tetrahedron* **1996**, *52* (44), 13901.
- (108) Paterson, I.; Franklin, A. S. *Tetrahedron Lett.* **1994**, *35* (37), 6925.
- (109) Paterson, I.; Chen, D. Y.-K.; Aceña, J. L.; Franklin, A. S. *Org. Lett.* **2000**, *2* (11), 1513.

Bibliography

- (110) Sharma, P.; Powell, K.; Burnley, J.; Awaad, A.; Moses, J. *Synthesis (Stuttg)*. **2011**, 2011 (18), 2865.
- (111) Rodriguez, R.; Adlington, R. M.; Eade, S. J.; Walter, M. W.; Baldwin, J. E.; Moses, J. E. *Tetrahedron* **2007**, 63 (21), 4500.
- (112) Hosokawa, S.; Yokota, K.; Imamura, K.; Suzuki, Y.; Kawarasaki, M.; Tatsuta, K. *Tetrahedron Lett.* **2006**, 47 (30), 5415.
- (113) Hosokawa, S.; Yokota, K.; Imamura, K.; Suzuki, Y.; Kawarasaki, M.; Tatsuta, K. *Chem. Asian J.* **2008**, 3 (8–9), 1415.
- (114) Patel, P.; Pattenden, G. *J. Chem. Soc. Perkin Trans. 1* **1991**, No. 8, 1941.
- (115) Hatakeyama, S.; Ochi, N.; Takano, S. *Chem. Pharm. Bull. (Tokyo)*. **1993**, 41 (8), 1358.
- (116) Zuidema, D. R.; Jones, P. B. *J. Photochem. Photobiol. B Biol.* **2006**, 83 (2), 137.
- (117) Beak, P.; Lee, J.; McKinnie, B. G. *J. Org. Chem.* **1978**, 43 (7), 1367.
- (118) De Paolis, M. *Soc. Chim. Ital.* **2017**, 20 (Scheme 1), 63.
- (119) Liang, G.; Seiple, I. B.; Trauner, D. *Org. Lett.* **2005**, 7, 2837.
- (120) Miller, A. K.; Byun, D. H.; Beaudry, C. M.; Trauner, D. *Proc Natl Acad Sci U S A* **2004**, 101 (33), 12019.
- (121) Zimmerman, H. E.; Traxler, M. D. *J. Am. Chem. Soc.* **1957**, 79 (8), 1920.
- (122) Ireland, R. E.; Mueller, R. H.; Willard, a K. *J. Am. Chem. Soc.* **1976**, 98 (4), 2868.
- (123) Rizzacasa, M.; Perkins, M. *Stoichiometric Asymmetric Synthesis*; Wiley-Blackwell, 2000.
- (124) Cowden, C. J.; Paterson, I. In *Organic Reactions*; John Wiley & Sons, Inc.: Hoboken, NJ, USA, 1997; pp 1–200.
- (125) Walker, M. A.; Heathcock, C. H. *J. Org. Chem.* **1991**, 56 (20), 5747.
- (126) Martin, S. F.; Guinn, D. E. *J. Org. Chem.* **1987**, 52 (25), 5588.
- (127) Evans, D. A.; Bartroli, J.; Shih, T. L. *J. Am. Chem. Soc.* **1981**, 103 (8), 2127.
- (128) Evans, D. A.; Rieger, D. L.; Bilodeau, M. T.; Urpi, F. *J. Am. Chem. Soc.* **1991**, 113 (3),

Bibliography

- 1047.
- (129) Nerz-Stormes, M.; Thornton, E. R. *J. Org. Chem.* **1991**, *56* (7), 2489.
- (130) Bonner, M. P.; Thornton, E. R. *J. Am. Chem. Soc.* **1991**, *113* (4), 1299.
- (131) Yan, T. H.; Tan, C. W.; Lee, H. C.; Lo, H. C.; Huang, T. Y. *J. Am. Chem. Soc.* **1993**, *115* (7), 2613.
- (132) Yan, T.-H.; Hung, A.-W.; Lee, H.-C.; Chang, C.-S.; Liu, W.-H. *J. Org. Chem.* **1995**, *60* (11), 3301.
- (133) Fujita, E.; Nagao, Y. In *Advances in Heterocyclic Chemistry*; 1989; Vol. 45, pp 1–36.
- (134) Nagao, Y.; Yamada, S.; Kumagai, T.; Ochiai, M.; Fujita, E. *J. Chem. Soc. Chem. Commun.* **1985**, *65* (20), 1418.
- (135) Nagao, Y.; Hagiwara, Y.; Kumagai, T.; Ochiai, M.; Inoue, T.; Hashimoto, K.; Fujita, E. *J. Org. Chem.* **1986**, *51* (12), 2391.
- (136) Hsiao, C. N.; Liu, L.; Miller, M. J. *J. Org. Chem.* **1987**, *52* (11), 2201.
- (137) Cahn, R. S.; Ingold, C.; Prelog, V. *Angew. Chemie Int. Ed. English* **1966**, *5* (4), 385.
- (138) Ward, D. E. In *Modern Methods in Stereoselective Aldol Reactions*; Wiley-VCH Verlag GmbH & Co. KGaA: Weinheim, Germany, 2013; pp 377–429.
- (139) Mukherjee, S.; Yang, J. W.; Hoffmann, S.; List, B. *Chem. Rev.* **2007**, *107* (12), 5471.
- (140) Heravi, M. M.; Zadsirjan, V.; Dehghani, M.; Hosseintash, N. *Tetrahedron Asymmetry* **2017**, *28* (5), 587.
- (141) Paterson, I.; Anne Lister, M. *Tetrahedron Lett.* **1988**, *29* (5), 585.
- (142) Paterson, I.; McClure, C. K. *Tetrahedron Lett.* **1987**, *28* (11), 1229.
- (143) Paterson, I.; Lister, M. A.; McClure, C. K. *Tetrahedron Lett.* **1986**, *27* (39), 4787.
- (144) Kleinbeck, F.; Fettes, G. J.; Fader, L. D.; Carreira, E. M. *Chem. - A Eur. J.* **2012**, *18* (12), 3598.
- (145) Schneemann, I.; Ohlendorf, B.; Zinecker, H.; Nagel, K.; Wiese, J.; Imhoff, J. F. *J. Nat. Prod.* **2010**, *73* (8), 1444.

Bibliography

- (146) Zhang, J.; Jiang, Y.; Cao, Y.; Liu, J.; Zheng, D.; Chen, X.; Han, L.; Jiang, C.; Huang, X. *J. Nat. Prod.* **2013**, *76*, 2126.
- (147) Schneemann, I.; Ohlendorf, B.; Zinecker, H.; Nagel, K.; Wiese, J.; Imhoff, J. F. *J. Nat. Prod.* **2010**, *73* (8), 1444.
- (148) Schneemann, I.; Nagel, K.; Kajahn, I.; Labes, A.; Wiese, J.; Imhoff, J. F. *Appl. Environ. Microbiol.* **2010**, *76* (11), 3702.
- (149) Yano, K.; Yokoi, K.; Sato, J.; Oono, J.; Kouda, T.; Ogawa, Y.; Nakashima, T. *J. Antibiot. (Tokyo)*. **1986**, *39* (1), 32.
- (150) Lin, Z.; Torres, J. P.; Ammon, M. A.; Marett, L.; Teichert, R. W.; Reilly, C. a; Kwan, J. C.; Hughen, R. W.; Flores, M.; Tianero, M. D.; Peraud, O.; Cox, J. E.; Light, A. R.; Villaraza, A. J. L.; Haygood, M. G.; Concepcion, G. P.; Olivera, B. M.; Schmidt, E. W. *Chem. Biol.* **2013**, *20* (1), 73.
- (151) Syta, P. Total Synthesis of Nocapyrone C and D for Stereochemical Elucidation, Flinders University of South Australia, 2013.
- (152) Henrot, M.; Richter, M. E. A.; Maddaluno, J.; Hertweck, C.; De Paolis, M. *Angew. Chemie Int. Ed.* **2012**, *51* (38), 9587.
- (153) Hite, M.; Rinehart, W.; Braun, W.; Peck, H. *Am. Ind. Hyg. Assoc. J.* **1979**, *40* (7), 600.
- (154) Crimmins, M. T.; Chaudhary, K. *Org. Lett.* **2000**, *2* (6), 775.
- (155) Crimmins, M. T.; Dechert, A. R. *Org. Lett.* **2012**, *14* (9), 2366.
- (156) Cutignano, A.; Fontana, A.; Renzulli, L.; Cimino, G. *J. Nat. Prod.* **2003**, *66* (10), 1399.
- (157) Shin, H.; Lee, H.-S.; Lee, J.; Shin, J.; Lee, M.; Lee, H.-S.; Lee, Y.-J.; Yun, J.; Kang, J. *Mar. Drugs* **2014**, *12* (6), 3283.
- (158) Leutou, A. S.; Yang, I.; Seong, C. N.; Ko, J.; Nam, S. *Nat. Prod. Sci.* **2015**, *21* (4), 248.
- (159) Jadulco, R.; Brauers, G.; Edrada, R. A.; Ebel, R.; Wray, V.; Sudarsono; Proksch, P. *J. Nat. Prod.* **2002**, *65* (5), 730.
- (160) Sitachitta, N.; Gadepalli, M.; Davidson, B. S. *Tetrahedron* **1996**, *52* (24), 8073.
- (161) Claydon, N.; Allan, M.; Hanson, J. R.; Avent, A. G. *Trans. Br. Mycol. Soc.* **1987**, *88* (4),

Bibliography

- 503.
- (162) Evidente, A.; Conti, L.; Altomare, C.; Bottalico, A.; Sindona, G.; Segre, A. L.; Logrieco, A. *Nat. Toxins* **1994**, *2* (1), 4.
- (163) Appendino, G.; Ottino, M.; Marquez, N.; Bianchi, F.; Giana, A.; Ballero, M.; Sterner, O.; Fiebich, B. L.; Munoz, E. *J. Nat. Prod.* **2007**, *70* (4), 608.
- (164) Liu, D.; Li, X. M.; Meng, L.; Li, C. S.; Gao, S. S.; Shang, Z.; Proksch, P.; Huang, C. G.; Wang, B. G. *J. Nat. Prod.* **2011**, *74* (8), 1787.
- (165) Hirota, A.; Nemoto, A.; Tsuchiya, Y.; Hojo, H.; Abe, N. *Biosci. Biotechnol. Biochem.* **1999**, *63* (2), 418.
- (166) Washida, K.; Abe, N.; Sugiyama, Y.; Hirota, A. *Biosci. Biotechnol. Biochem.* **2007**, *71* (4), 1052.
- (167) Sugiyama, Y.; Oya, A.; Kudo, T.; Hirota, A. *J. Antibiot. (Tokyo)*. **2010**, *63* (7), 365.
- (168) Ochoa, J. L.; Bray, W. M.; Lokey, R. S.; Linington, R. G. *J. Nat. Prod.* **2015**, *78* (9), 2242.
- (169) Lee, J. S.; Shin, J.; Shin, H. J.; Lee, H. S.; Lee, Y. J.; Lee, H. S.; Won, H. *European J. Org. Chem.* **2014**, *2014* (21), 4472.
- (170) Chaładaj, W.; Corbet, M.; Fürstner, A. *Angew. Chemie Int. Ed.* **2012**, *51* (28), 6929.
- (171) Sun, X.; Collum, D. B. *J. Am. Chem. Soc.* **2000**, *122* (11), 2452.
- (172) Reich, H. J. *J. Org. Chem.* **2012**, *77* (13), 5471.
- (173) Wadsworth, A.; Sperry, J.; Brimble, M. *Synthesis (Stuttg.)*. **2010**, *2010* (15), 2604.
- (174) Hansen, C. a.; Frost, J. W. *J. Am. Chem. Soc.* **2002**, *124* (21), 5926.
- (175) Suzuki, E.; Hamajima, R.; Inoue, S. *Synthesis (Stuttg.)*. **1975**, *1975* (03), 192.
- (176) De Paolis, M.; Rosso, H.; Henrot, M.; Prandi, C.; D'Herouville, F.; Maddaluno, J. *Chem. - A Eur. J.* **2010**, *16* (37), 11229.
- (177) Henrot, M.; Jean, A.; Peixoto, P. A.; Maddaluno, J.; De Paolis, M. *J. Org. Chem.* **2016**, *81* (12), 5190.
- (178) Kim, Y.; Ogura, H.; Akasaka, K.; Oikawa, T.; Matsuura, N.; Imada, C.; Yasuda, H.;

Bibliography

- Igarashi, Y. *Mar. Drugs* **2014**, *12* (7), 4110.
- (179) Ager, D. J.; Prakash, I.; Schaad, D. R. *Chem. Rev.* **1996**, *96* (2), 835.
- (180) Crimmins, M. T.; King, B. W.; Tabet, E. a; Chaudhary, K. *J. Org. Chem.* **2001**, *66* (3), 894.
- (181) Crimmins, M. T.; She, J. *Synlett* **2004**, *1997* (8), 1371.
- (182) Gage, J. R.; Evans, D. A. *Org. Synth.* **1990**, *68* (September), 83.
- (183) Martin, S. F.; Guinn, D. E. *J. Org. Chem.* **1987**, *52* (25), 5588.
- (184) Martin, S. F.; Dodge, J. A.; Burgess, L. E.; Hartmann, M. *J. Org. Chem.* **1992**, *57* (4), 1070.
- (185) Delaunay, D.; Toupet, L.; Corre, M. Le. *J. Org. Chem.* **1995**, *60* (20), 6604.
- (186) Cardillo, G.; Orena, M.; Sandri, S.; Tomasini, C. *Tetrahedron* **1985**, *41* (1), 163.
- (187) Evans, D. A.; Tedrow, J. S.; Shaw, J. T.; Downey, C. W. *J. Am. Chem. Soc.* **2002**, *124* (3), 392.
- (188) Evans, D. a; Downey, C. W.; Shaw, J. T.; Tedrow, J. S. *Org. Lett.* **2002**, *4* (7), 1127.
- (189) Paterson, I.; Wallace, D. J.; Velázquez, S. M. *Tetrahedron Lett.* **1994**, *35* (48), 9083.
- (190) Paterson, I.; Wallace, D. J. *Tetrahedron Lett.* **1994**, *35* (48), 9087.
- (191) Paterson, I. *Synthesis (Stuttg.)* **1998**, *1998* (S1), 639.
- (192) Scheeff, S.; Menche, D. *Org. Lett.* **2019**, *21* (1), 271.
- (193) Dias, L. C.; Polo, E. C. *J. Org. Chem.* **2017**, *82* (8), 4072.
- (194) Brown, H. C.; Dhar, R. K.; Ganesan, K.; Singaram, B. *J. Org. Chem.* **1992**, *57* (2), 499.
- (195) Heathcock, C. H. In *Asymmetric Synthesis, Volume 3*; 2014; pp 111–212.
- (196) Evans, D. A.; Nelson, J. V.; Taber, T. R. In *Topics in Stereochemistry, Volume 13*; 2007; pp 1–115.
- (197) Conway, J. C.; Quayle, P.; Regan, A. C.; Urch, C. J. *Tetrahedron* **2005**, *61* (50), 11910.

Bibliography

- (198) Marti, G. J. Studies toward the synthesis of bafilomycin A₁ and fusidilactone C, Eidgenössische Technische Hochschule, 2007.
- (199) Hussain, H.; Al-Harrasi, A.; Green, I. R.; Ahmed, I.; Abbas, G.; Rehman, N. U. *RSC Adv.* **2014**, *4* (25), 12882.
- (200) Tsui, G. C.; Lautens, M. *Angew. Chemie Int. Ed.* **2010**, *49* (47), 8938.
- (201) Banwell, M. G.; McRae, K. J. *J. Org. Chem.* **2001**, *66* (20), 6768.
- (202) Lin, G.; Chang, L.; Liu, Y.; Xiang, Z.; Chen, J.; Yang, Z. *Chem. - An Asian J.* **2013**, *8* (4), 700.
- (203) Micoine, K.; Fürstner, A. *J. Am. Chem. Soc.* **2010**, *132* (40), 14064.
- (204) Gu, J.; Ma, C.; Li, Q.-Z.; Du, W.; Chen, Y.-C. *Org. Lett.* **2014**, *16* (15), 3986.
- (205) Uhl, A.; Bitzer, M.; Wolf, H.; Hermann, D.; Gutewort, S.; Völkl, M.; Nagl, I. In *Ullmann's Encyclopedia of Industrial Chemistry*; American Cancer Society, 2018; pp 1–45.
- (206) Schulze, A.; Pagona, G.; Giannis, A. *Synth. Commun.* **2006**, *36* (9), 1147.
- (207) Eade, S. J.; Walter, M. W.; Byrne, C.; Odell, B.; Rodriguez, R.; Baldwin, J. E.; Adlington, R. M.; Moses, J. E. *J. Org. Chem.* **2008**, *73* (13), 4830.
- (208) Jacobsen, M. F.; Moses, J. E.; Adlington, R. M.; Baldwin, J. E. *Tetrahedron* **2006**, *62* (8), 1675.
- (209) Jacobsen, M. F.; Moses, J. E.; Adlington, R. M.; Baldwin, J. E. *Org. Lett.* **2005**, *7* (4), 641.
- (210) Wang, F.; Tian, X.; Huang, C.; Li, Q.; Zhang, S. *J. Antibiot. (Tokyo)*. **2011**, *64* (2), 189.
- (211) Davies-Coleman, M. T.; Garson, M. J. *Nat. Prod. Rep.* **1998**, *15* (5), 477.
- (212) Manzo, E.; Ciavatta, M. L.; Gavagnin, M.; Mollo, E.; Wahidulla, S.; Cimino, G. *Tetrahedron Lett.* **2005**, *46* (3), 465.
- (213) Tezuka, Y.; Huang, Q.; Kikuchi, T.; Nishi, A.; Tubaki, K. *Chem. Pharm. Bull. (Tokyo)*. **1994**, *42* (12), 2612.
- (214) Larsson, M.; Galandrin, E.; Högberg, H. E. *Tetrahedron* **2004**, *60* (47), 10659.

Bibliography

- (215) Rosso, H.; De Paolis, M.; Collin, V. C.; Dey, S.; Hecht, S. M.; Prandi, C.; Richard, V.; Maddaluno, J. *J. Org. Chem.* **2011**, *76* (22), 9429.
- (216) Woodward, R. B.; Small-Jr., G. *J. Am. Chem. Soc.* **1950**, *72* (1947), 1297.
- (217) Schroeter, G.; Stassen, C. *Berichte der Dtsch. Chem. Gesellschaft* **1907**, *40* (2), 1604.
- (218) Henrot, M.; De Paolis, M. In *Strategies and Tactics in Organic Synthesis, Volume 12*; Elsevier Ltd., 2017; Vol. 12, pp 119–142.
- (219) Corey, E. J.; Seebach, D. *Org. Synth.* **1970**, *50* (September), 72.
- (220) Seebach, D.; Corey, E. J. *J. Org. Chem.* **1975**, *40* (2), 231.
- (221) Schlosser, M. *J. Organomet. Chem.* **1967**, *8* (1), 9.
- (222) Schlosser, M. *Pure Appl. Chem.* **1988**, *60* (11), 1627.
- (223) McKennon, M. J.; Meyers, A. I.; Drauz, K.; Schwarm, M. *J. Org. Chem.* **1993**, *58* (13), 3568.
- (224) Wang, G. P.; Wang, L. P.; Qin, S. L.; Huang, F. F.; Huang, S. P.; Wang, X. J. *Adv. Mater. Res.* **2014**, *1033–1034*, 526.
- (225) Skaanderup, P. R.; Jensen, T. *Org. Lett.* **2008**, *10* (13), 2821.
- (226) Iyengar, R.; Schildknecht, K.; Morton, M.; Aubé, J. *J. Org. Chem.* **2005**, *70* (26), 10645.

Bibliography

Appendices

The appendix includes full copies of the 1D and 2D ^1H and ^{13}C NMR spectra for each of the synthesised final products and all unpublished synthetic intermediates. All raw data presented in this chapter is provided in support of the thesis body.

List of Appendices

1. ^1H NMR (600 MHz, CDCl_3) compound 159
2. COSY (600 x 600 MHz, CDCl_3) compound 159
3. ^{13}C NMR (151 MHz, CDCl_3) compound 159
4. HMQC (600 x 151 MHz, CDCl_3) compound 159
5. HMBC (600 x 151 MHz, CDCl_3) compound 159

6. ^1H NMR (600 MHz, CDCl_3) compound 162
7. COSY (600 x 600 MHz, CDCl_3) compound 162
8. ^{13}C NMR (151 MHz, CDCl_3) compound 162
9. HMQC (600 x 151 MHz, CDCl_3) compound 162
10. HMBC (600 x 151 MHz, CDCl_3) compound 162

11. ^1H NMR (600 MHz, CDCl_3) compound 163
12. COSY (600 x 600 MHz, CDCl_3) compound 163
13. ^{13}C NMR (151 MHz, CDCl_3) compound 163
14. HMQC (600 x 151 MHz, CDCl_3) compound 163
15. HMBC (600 x 151 MHz, CDCl_3) compound 163

16. ^1H NMR (600 MHz, CDCl_3) compound 164
17. COSY (600 x 600 MHz, CDCl_3) compound 164
18. ^{13}C NMR (151 MHz, CDCl_3) compound 164
19. HMQC (600 x 151 MHz, CDCl_3) compound 164
20. HMBC (600 x 151 MHz, CDCl_3) compound 164

21. ^1H NMR (600 MHz, CDCl_3) compound 184
22. ^{13}C NMR (151 MHz, CDCl_3) compound 184

23. ^1H NMR (600 MHz, CDCl_3) compound 185
24. ^{13}C NMR (151 MHz, CDCl_3) compound 185

25. ^1H NMR (600 MHz, CDCl_3) compound 186
26. ^{13}C NMR (151 MHz, CDCl_3) compound 186

27. ^1H NMR (600 MHz, CDCl_3) compound 187
28. COSY (600 x 600 MHz, CDCl_3) compound 187
29. ^{13}C NMR (151 MHz, CDCl_3) compound 187
30. HMQC (600 x 151 MHz, CDCl_3) compound 187
31. HMBC (600 x 151 MHz, CDCl_3) compound 187

32. ^1H NMR (600 MHz, CDCl_3) compound 190
33. ^{13}C NMR (151 MHz, CDCl_3) compound 190

34. ^1H NMR (600 MHz, CDCl_3) compound 160
35. COSY (600 x 600 MHz, CDCl_3) compound 160
36. ^{13}C NMR (151 MHz, CDCl_3) compound 160
37. HMQC (600 x 151 MHz, CDCl_3) compound 160
38. HMBC (600 x 151 MHz, CDCl_3) compound 160

39. ^1H NMR (600 MHz, CDCl_3) compound 165
40. COSY (600 x 600 MHz, CDCl_3) compound 165
41. ^{13}C NMR (151 MHz, CDCl_3) compound 165
42. HMQC (600 x 151 MHz, CDCl_3) compound 165
43. HMBC (600 x 151 MHz, CDCl_3) compound 165

44. ^1H NMR (600 MHz, CDCl_3) compound 228

Appendix

45. ^{13}C NMR (151 MHz, CDCl_3) compound 228
46. ^1H NMR (600 MHz, CDCl_3) compound 229
47. COSY (600 x 600 MHz, CDCl_3) compound 229
48. ^{13}C NMR (151 MHz, CDCl_3) compound 229
49. HMQC (600 x 151 MHz, CDCl_3) compound 229
50. HMBC (600 x 151 MHz, CDCl_3) compound 229

51. ^1H NMR (600 MHz, CDCl_3) compound 230
52. ^{13}C NMR (151 MHz, CDCl_3) compound 230

53. ^1H NMR (600 MHz, CDCl_3) compound 174
54. COSY (600 x 600 MHz, CDCl_3) compound 174
55. ^{13}C NMR (151 MHz, CDCl_3) compound 174
56. HMQC (600 x 151 MHz, CDCl_3) compound 174
57. HMBC (600 x 151 MHz, CDCl_3) compound 174

58. ^1H NMR (600 MHz, CDCl_3) compound 178
59. COSY (600 x 600 MHz, CDCl_3) compound 178
60. ^{13}C NMR (151 MHz, CDCl_3) compound 178
61. HMQC (600 x 151 MHz, CDCl_3) compound 178
62. HMBC (600 x 151 MHz, CDCl_3) compound 178

63. ^1H NMR (600 MHz, CDCl_3) compound 179
64. COSY (600 x 600 MHz, CDCl_3) compound 179
65. ^{13}C NMR (151 MHz, CDCl_3) compound 179
66. HMQC (600 x 151 MHz, CDCl_3) compound 179
67. HMBC (600 x 151 MHz, CDCl_3) compound 179

68. ^1H NMR (600 MHz, DMSO-d) compound 123
69. ^{13}C NMR (151 MHz, DMSO-d) compound 123

70. ^1H NMR (600 MHz, CDCl_3) compound 132
71. ^{13}C NMR (151 MHz, CDCl_3) compound 132

72. ^1H NMR (600 MHz, CDCl_3) compound 133
73. ^{13}C NMR (151 MHz, CDCl_3) compound 133

74. ^1H NMR (600 MHz, CDCl_3) compound 134
75. ^{13}C NMR (151 MHz, CDCl_3) compound 134

76. ^1H NMR (600 MHz, CDCl_3) compound 138
77. ^{13}C NMR (151 MHz, CDCl_3) compound 138

78. ^1H NMR (600 MHz, CDCl_3) compound 135
79. ^{13}C NMR (151 MHz, CDCl_3) compound 135

80. ^1H NMR (600 MHz, CDCl_3) compound 80
81. ^{13}C NMR (151 MHz, CDCl_3) compound 80

82. ^1H NMR (600 MHz, CDCl_3) compound 203
83. ^{13}C NMR (151 MHz, CDCl_3) compound 203

84. ^1H NMR (600 MHz, CDCl_3) compound 208
85. ^{13}C NMR (151 MHz, CDCl_3) compound 208

86. ^1H NMR (600 MHz, CDCl_3) compound 81
87. ^{13}C NMR (151 MHz, CDCl_3) compound 81

88. ^1H NMR (600 MHz, CDCl_3) compound 106
89. COSY (600 x 600 MHz, CDCl_3) compound 106
90. ^{13}C NMR (151 MHz, CDCl_3) compound 106
91. HMQC (600 x 151 MHz, CDCl_3) compound 106
92. HMBC (600 x 151 MHz, CDCl_3) compound 106

93. ^1H NMR (600 MHz, CDCl_3) compound 147
94. COSY (600 x 600 MHz, CDCl_3) compound 147

Appendix

95. ^{13}C NMR (151 MHz, CDCl_3) compound 147
96. ^1H NMR (600 MHz, CDCl_3) compound 76
97. COSY (600 x 600 MHz, CDCl_3) compound 76
98. ^{13}C NMR (151 MHz, CDCl_3) compound 76
99. HMQC (600 x 151 MHz, CDCl_3) compound 76
100. HMBC (600 x 151 MHz, CDCl_3) compound 76

101. ^1H NMR (600 MHz, CDCl_3) compound 196
102. COSY (600 x 600 MHz, CDCl_3) compound 196
103. ^{13}C NMR (151 MHz, CDCl_3) compound 196
104. HMQC (600 x 151 MHz, CDCl_3) compound 196
105. HMBC (600 x 151 MHz, CDCl_3) compound 196

106. ^1H NMR (600 MHz, DMSO-d) compound 197
107. ^1H NMR (600 MHz, DMSO-d) compound 197 comparison to Violapyrone E
108. ^{13}C NMR (151 MHz, DMSO-d) compound 197

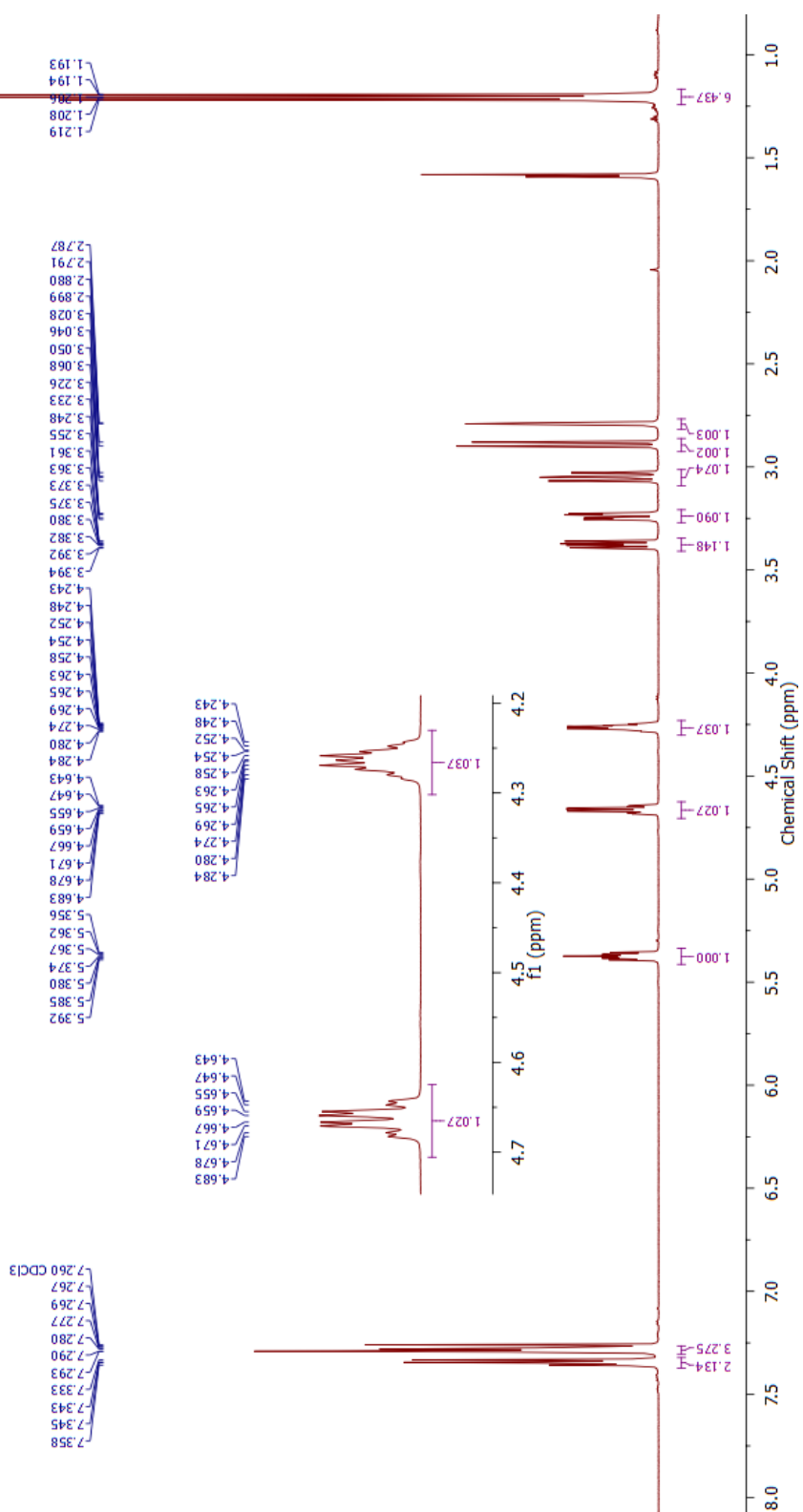
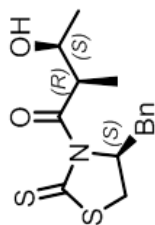
109. ^1H NMR (600 MHz, CDCl_3) compound 200
110. COSY (600 x 600 MHz, CDCl_3) compound 200
111. ^{13}C NMR (151 MHz, CDCl_3) compound 200
112. HMQC (600 x 151 MHz, CDCl_3) compound 200
113. HMBC (600 x 151 MHz, CDCl_3) compound 200

114. ^1H NMR (600 MHz, CDCl_3) compound 201
115. COSY (600 x 600 MHz, CDCl_3) compound 201
116. ^{13}C NMR (151 MHz, CDCl_3) compound 201
117. HMQC (600 x 151 MHz, CDCl_3) compound 201
118. HMBC (600 x 151 MHz, CDCl_3) compound 201

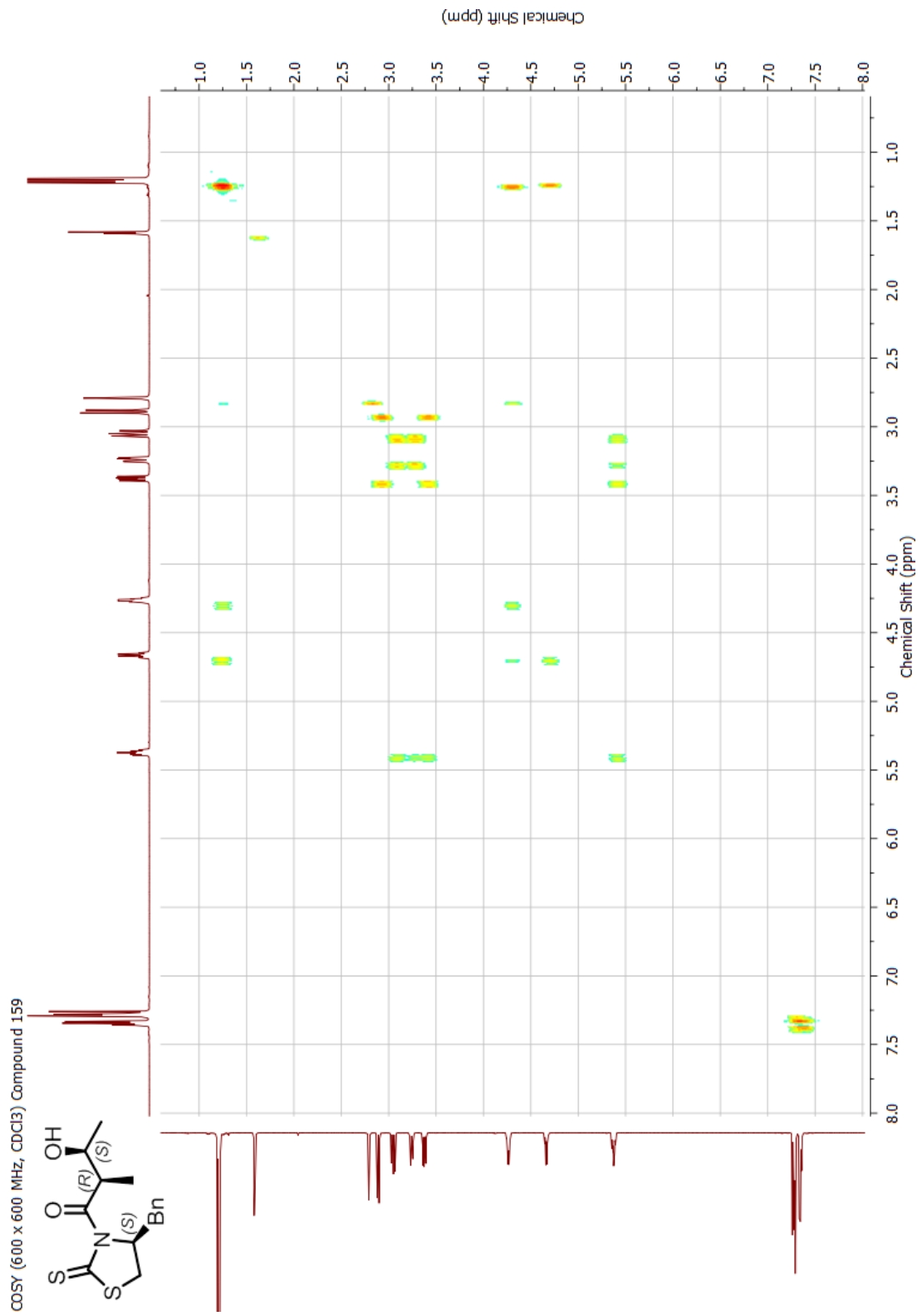
119. ^1H NMR (600 MHz, CDCl_3) compound 202
120. COSY (600 x 600 MHz, CDCl_3) compound 202
121. ^{13}C NMR (151 MHz, CDCl_3) compound 202
122. HMQC (600 x 151 MHz, CDCl_3) compound 202
123. HMBC (600 x 151 MHz, CDCl_3) compound 202

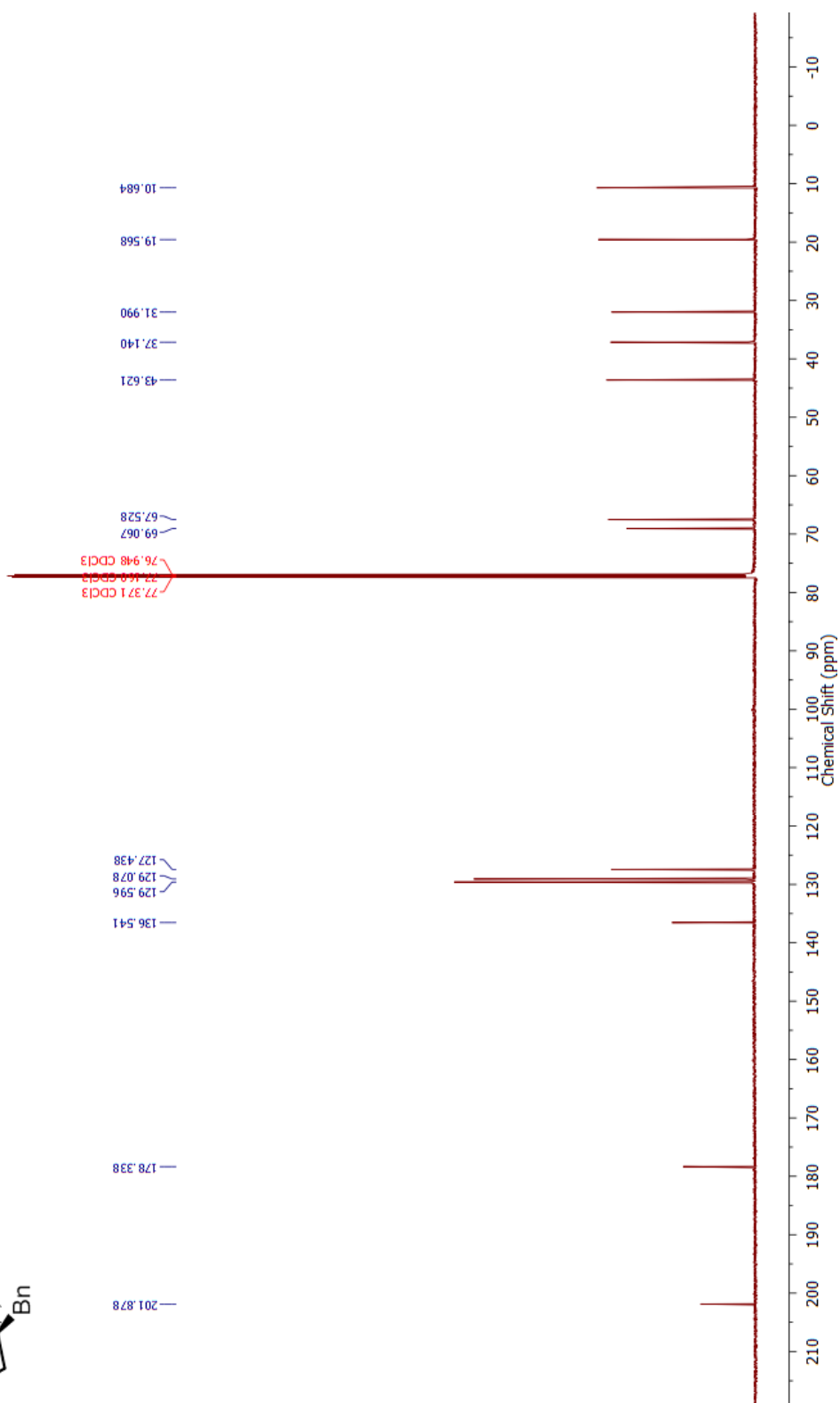
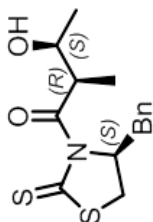
Appendix

¹H NMR (600 MHz, CDCl₃) compound 159

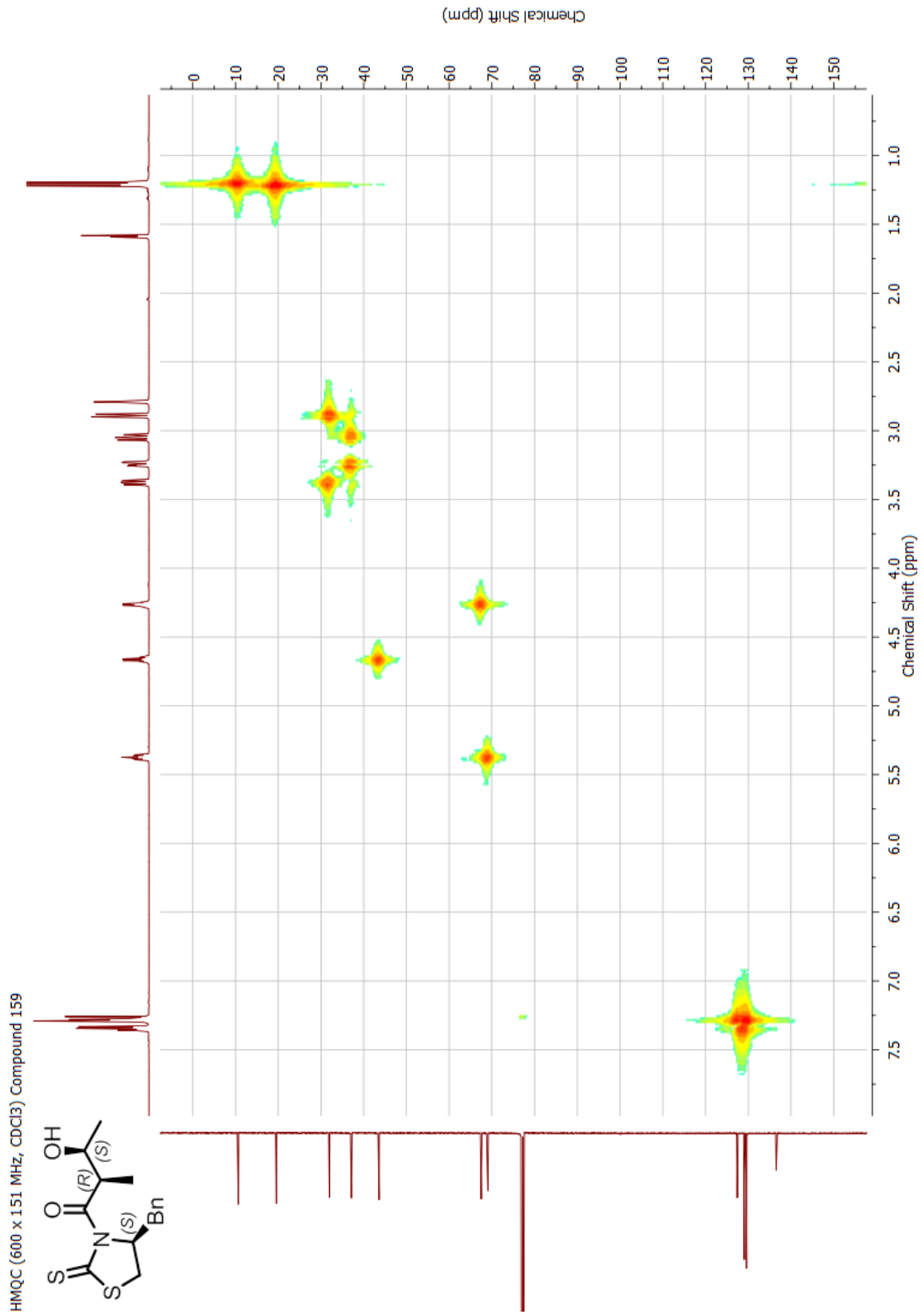


Appendix

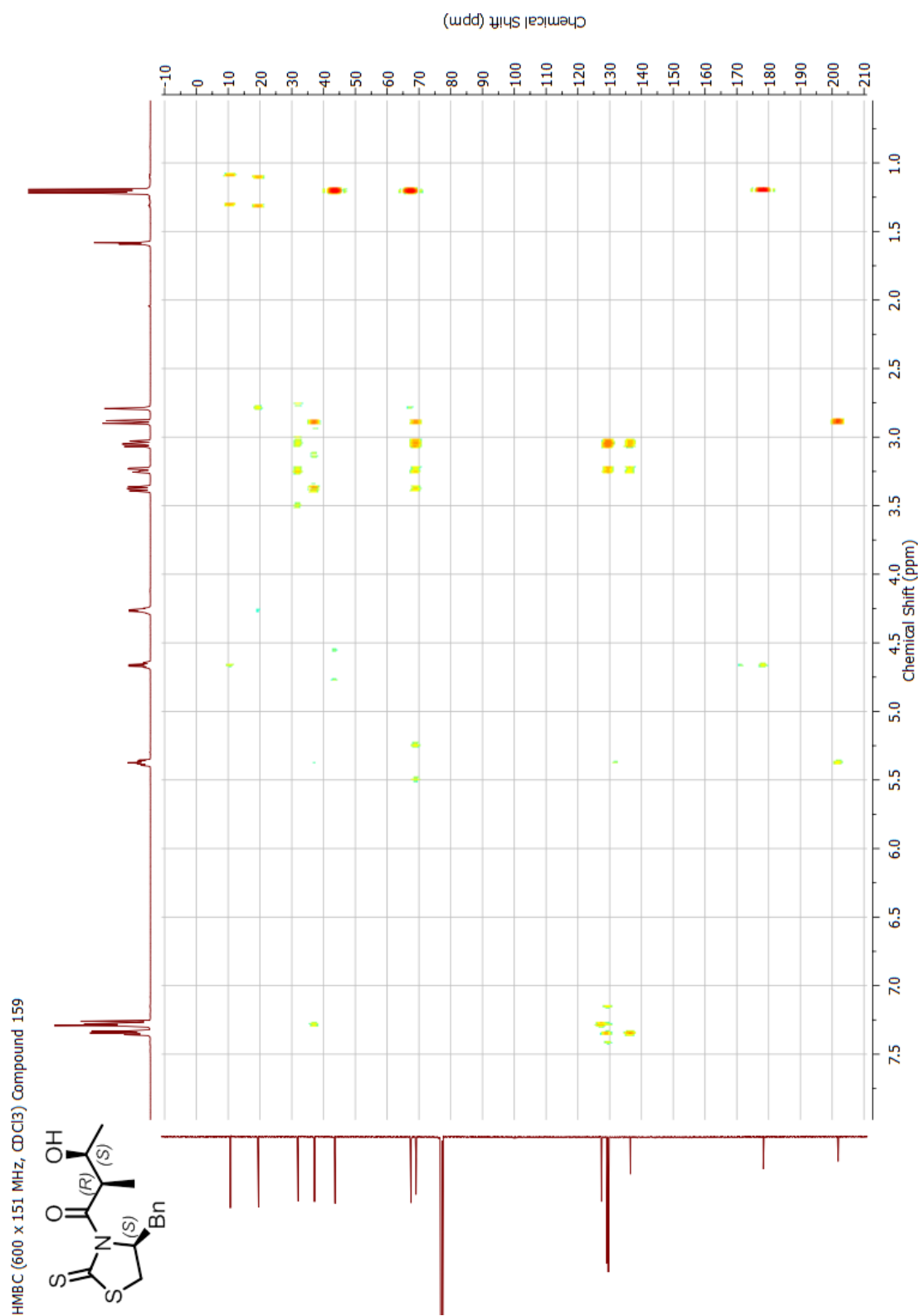


¹³C NMR (151 MHz, CDCl₃) Compound 159

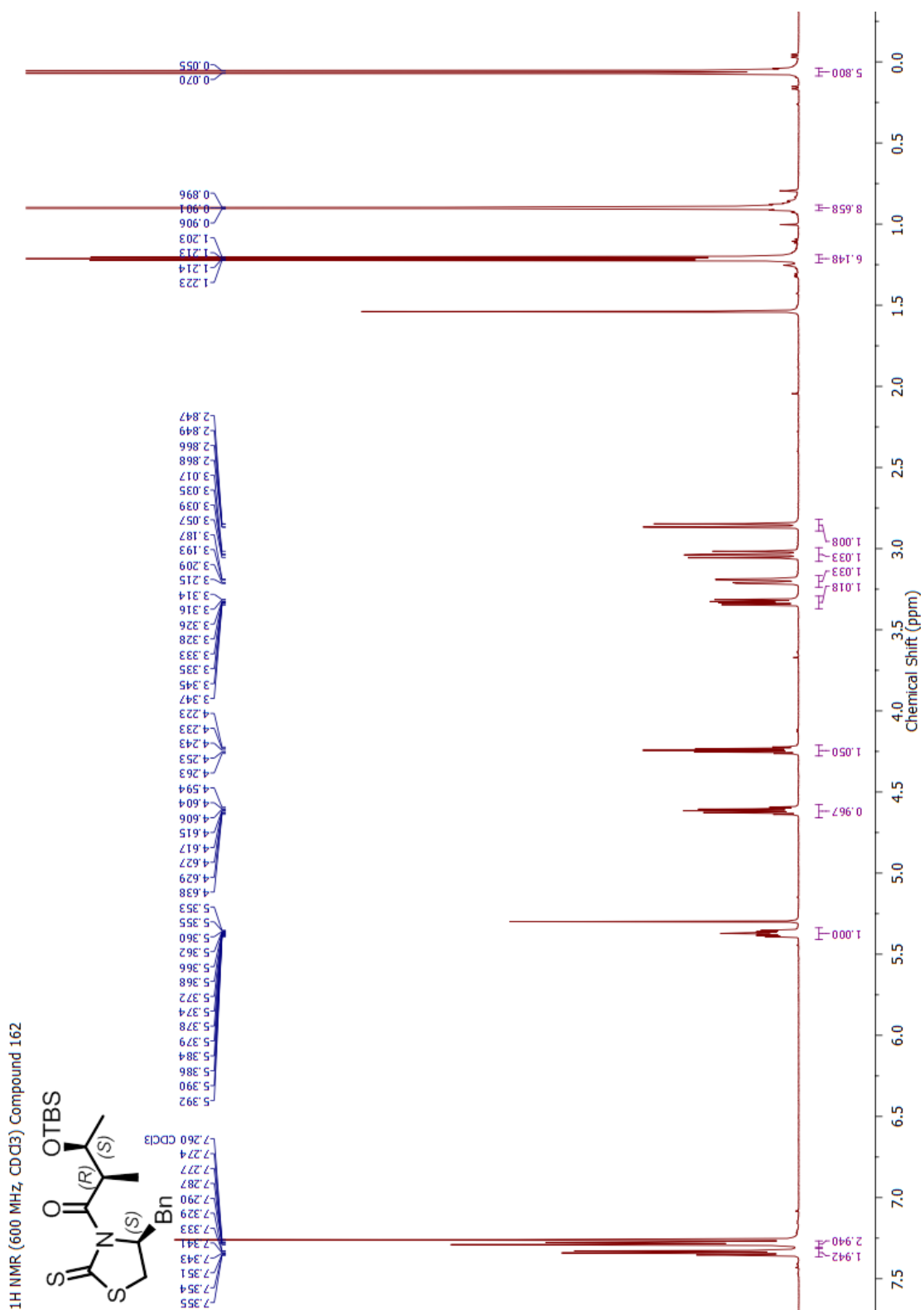
Appendix

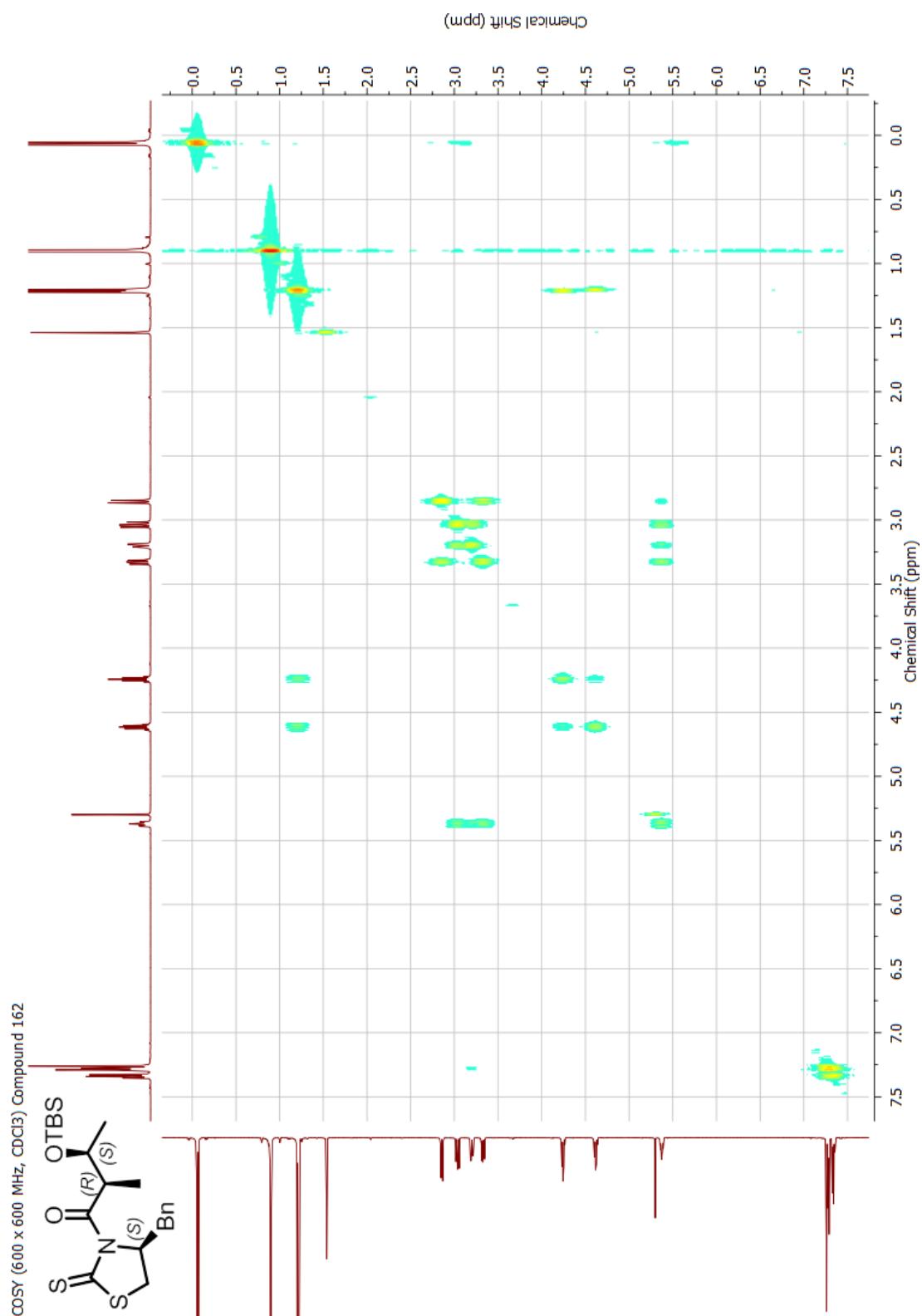


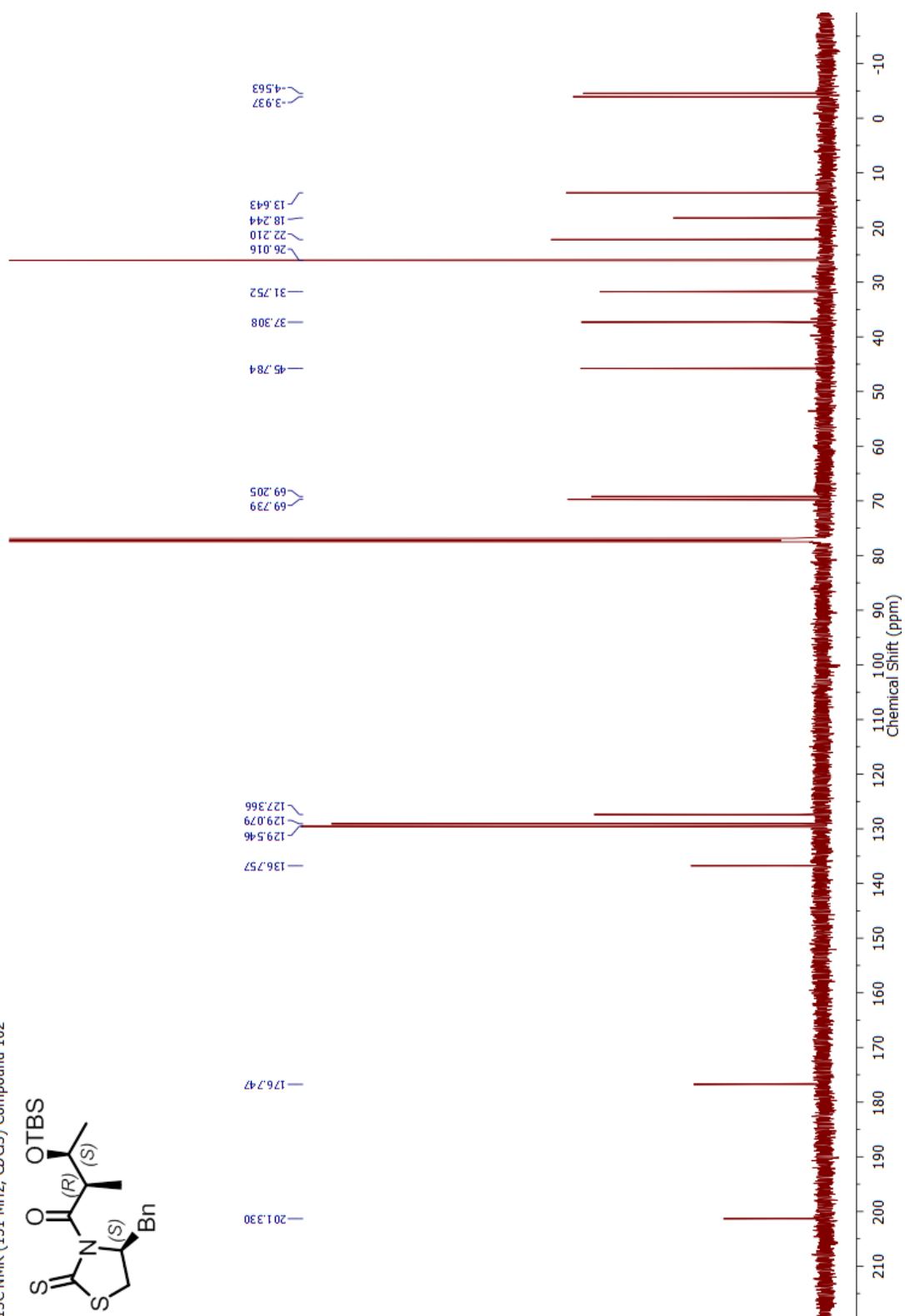
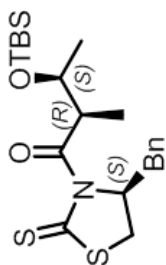
Appendix



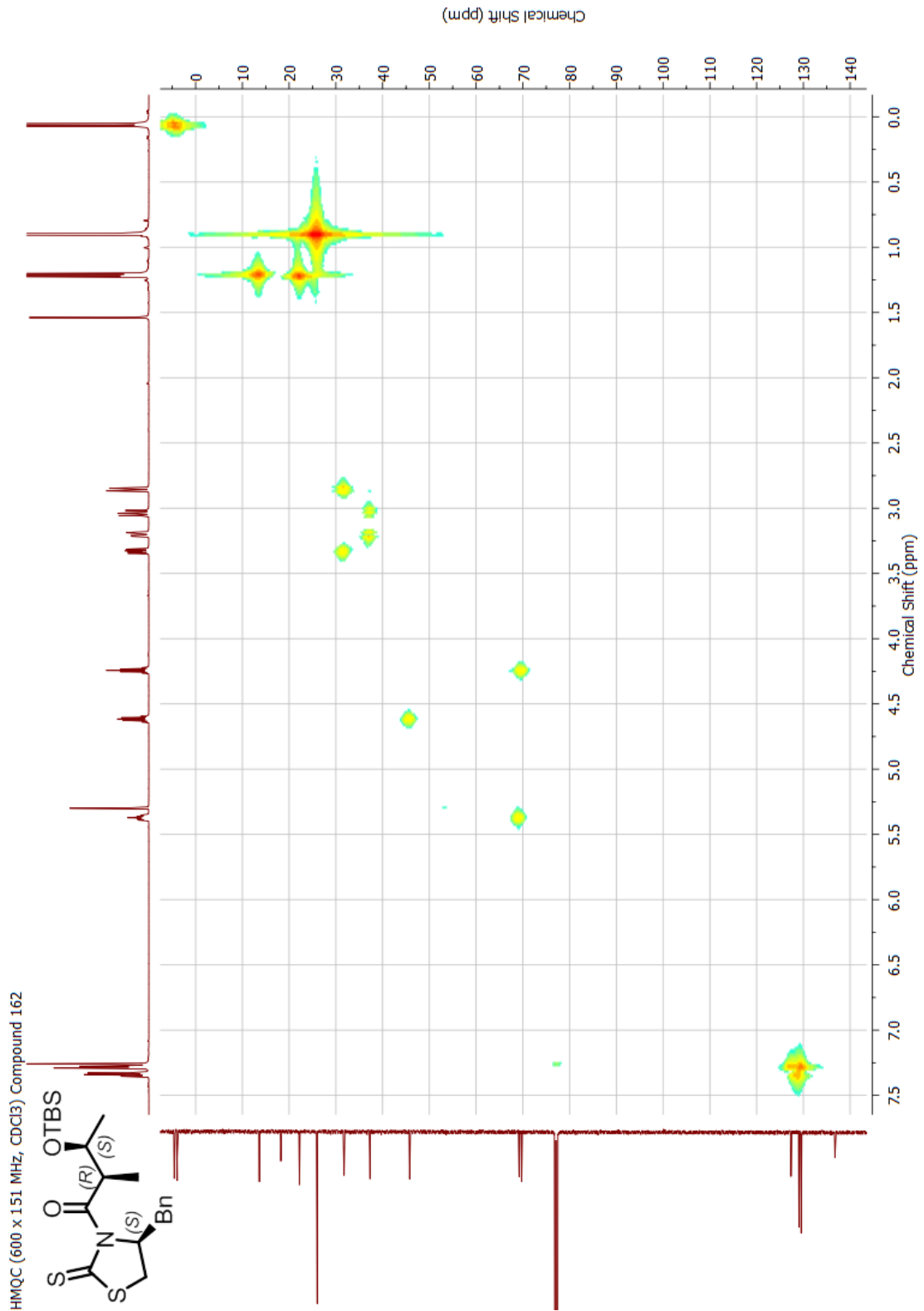
Appendix



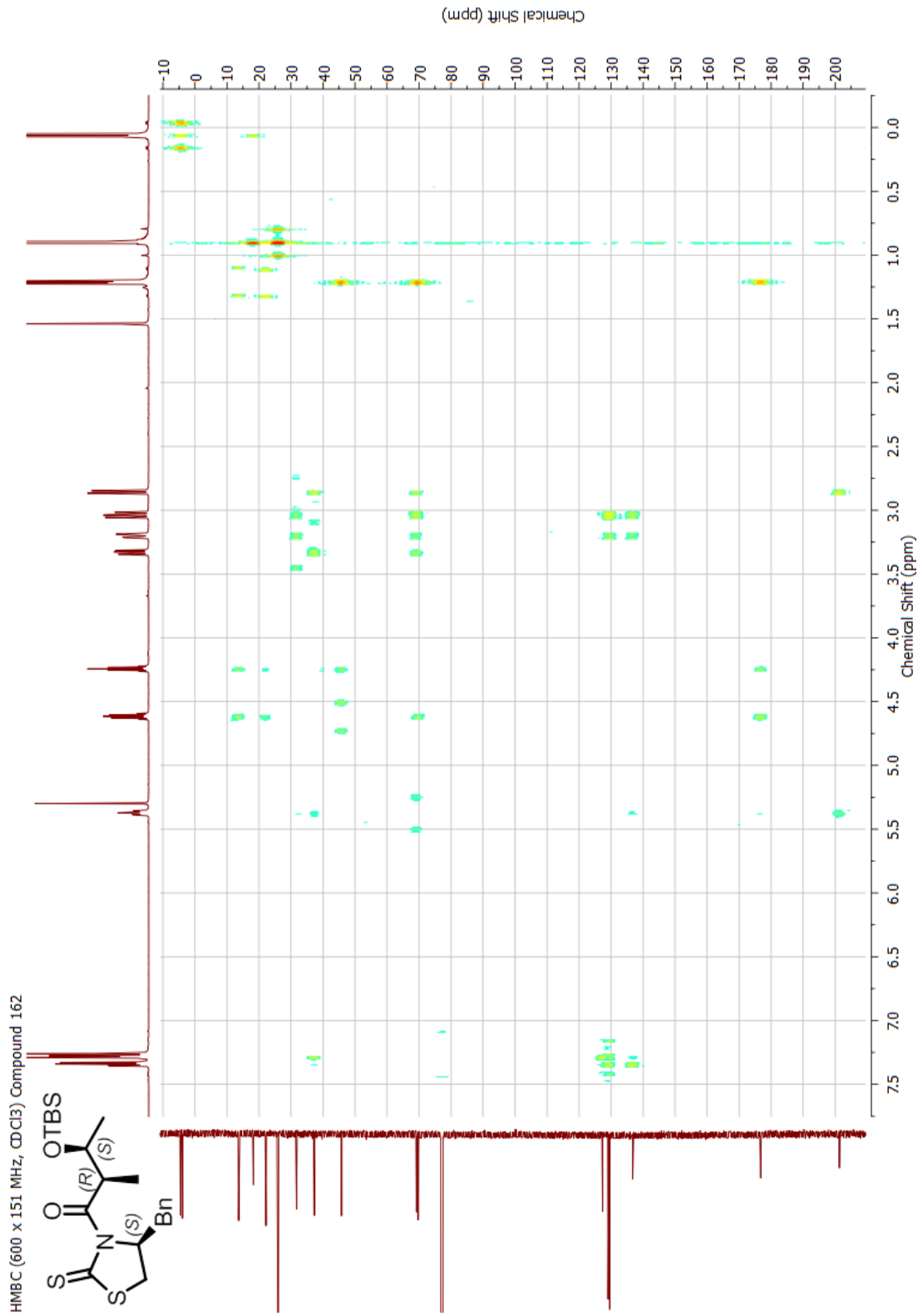


¹³C NMR (151 MHz, CDCl₃) Compound 162

Appendix

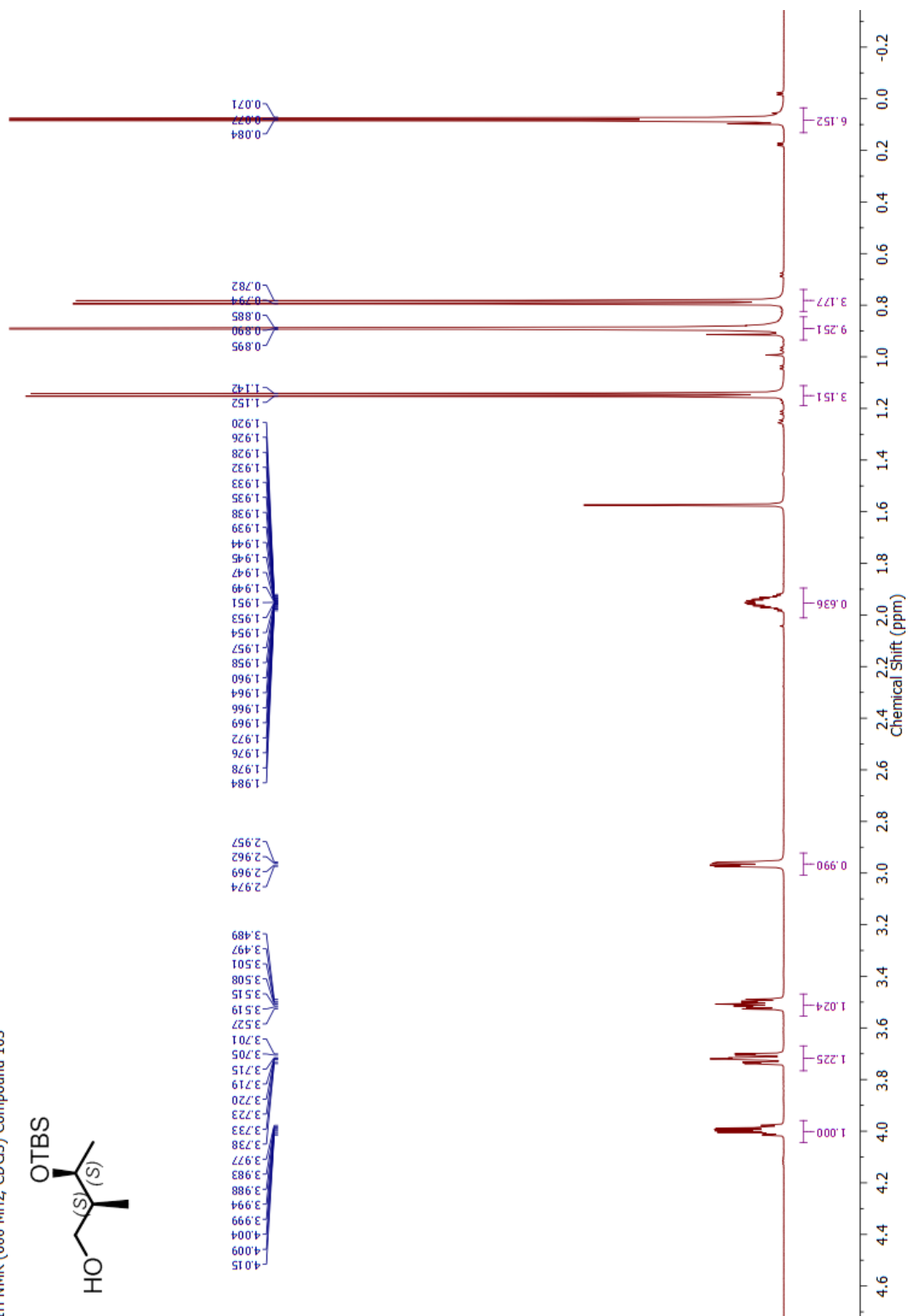
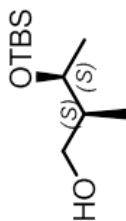


Appendix

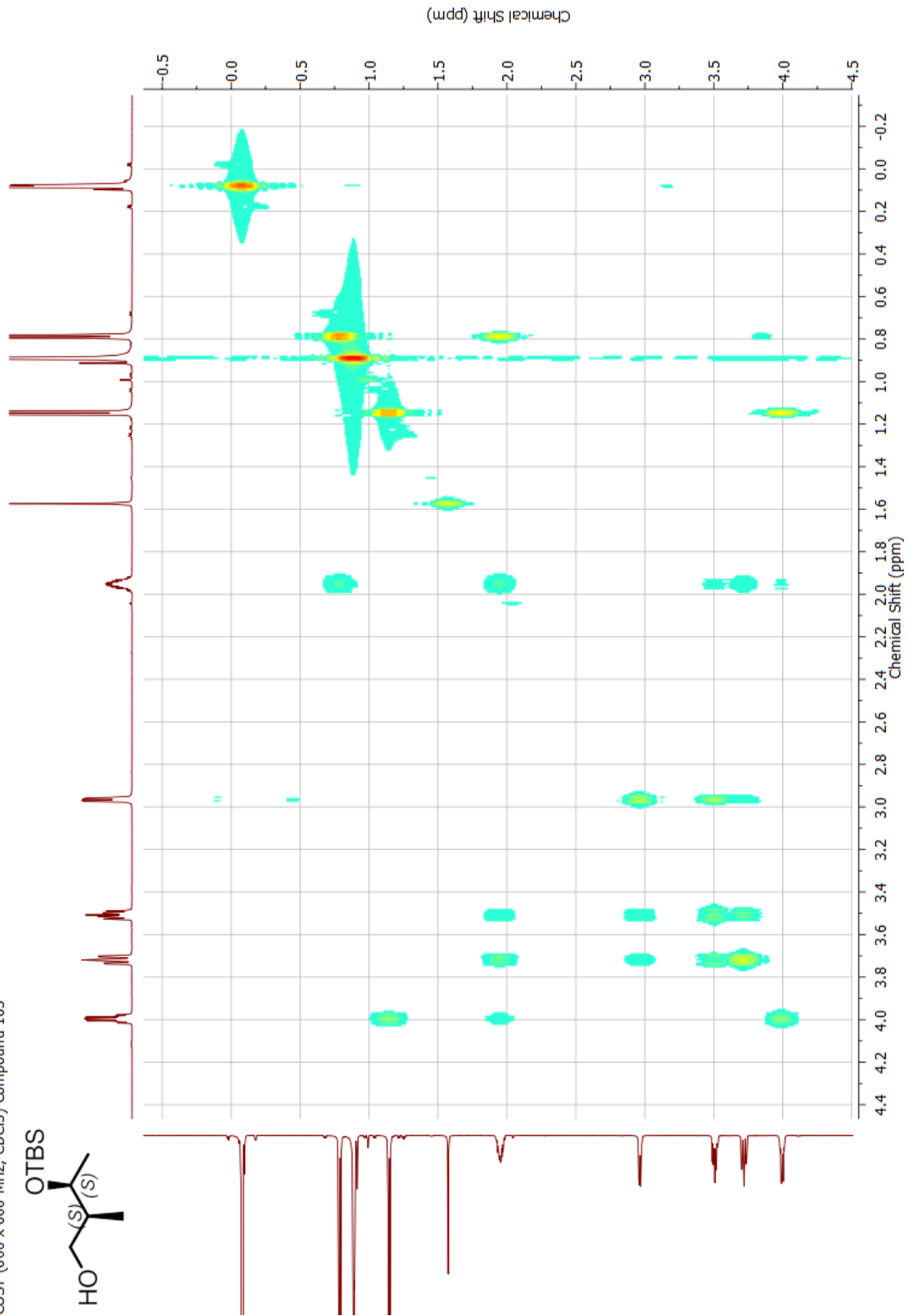
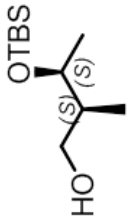


Appendix

¹H NMR (600 MHz, CDCl₃) Compound 163

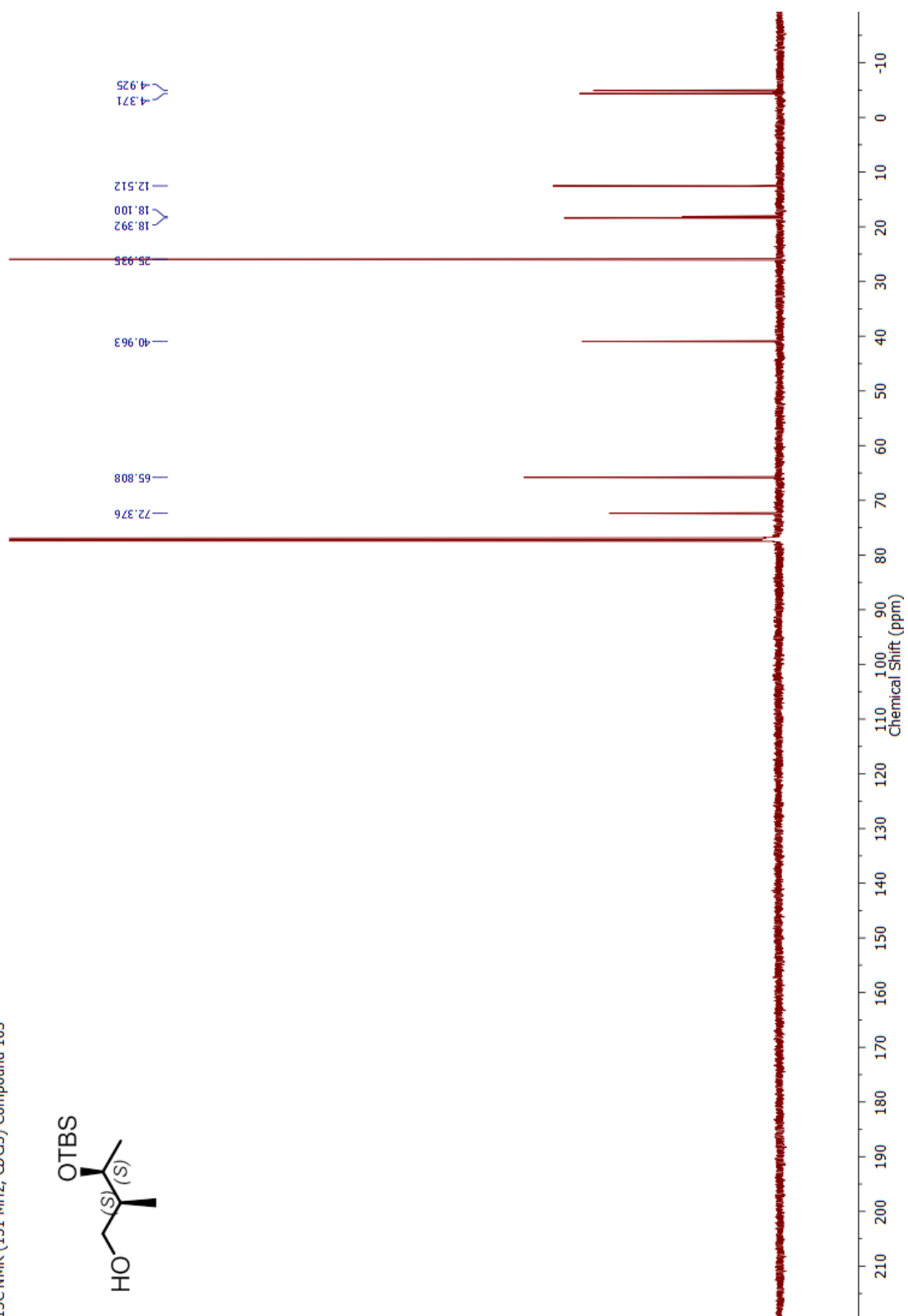
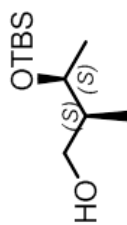


COSY (600 x 600 MHz, CDCl₃) Compound 163

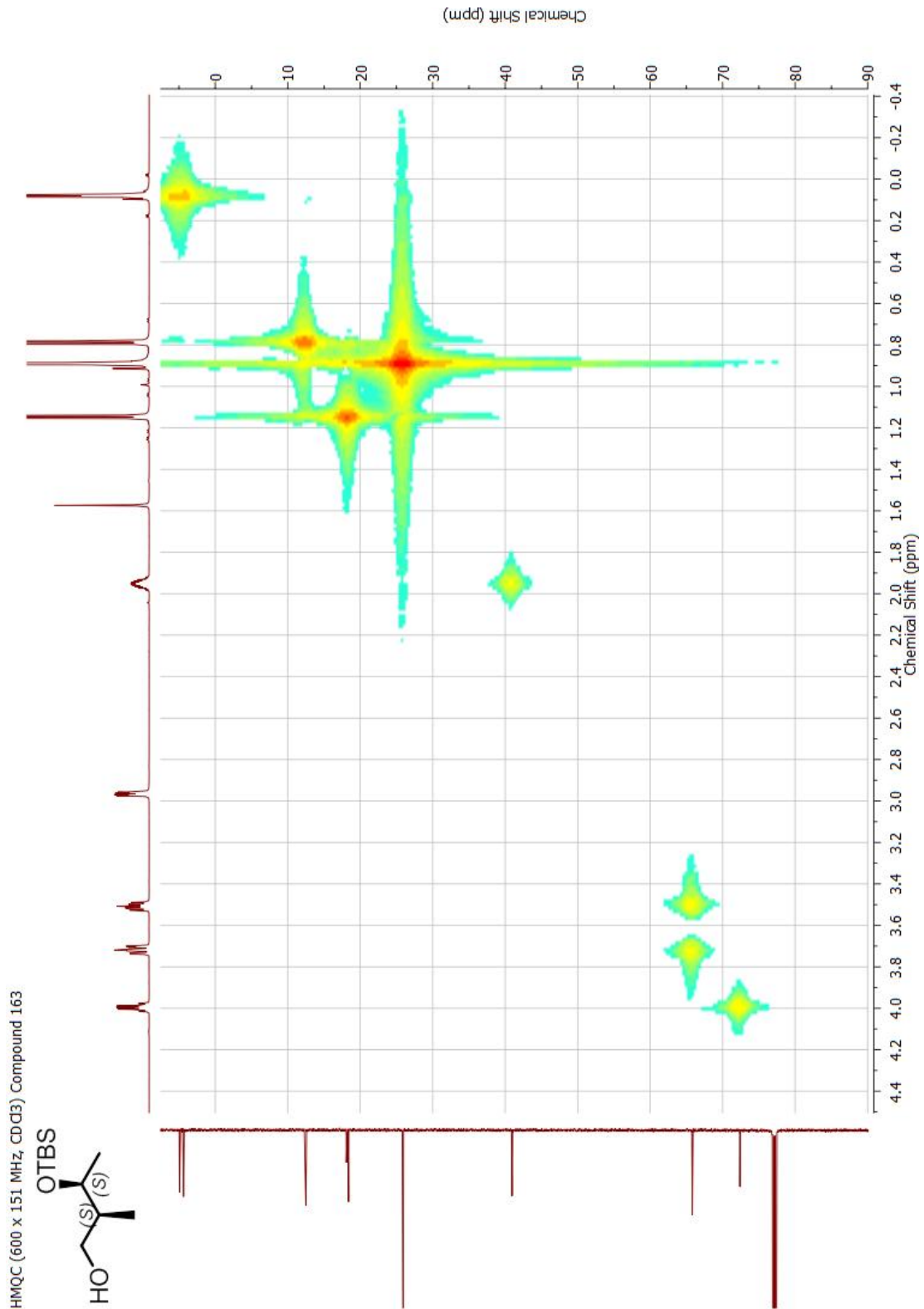


Appendix

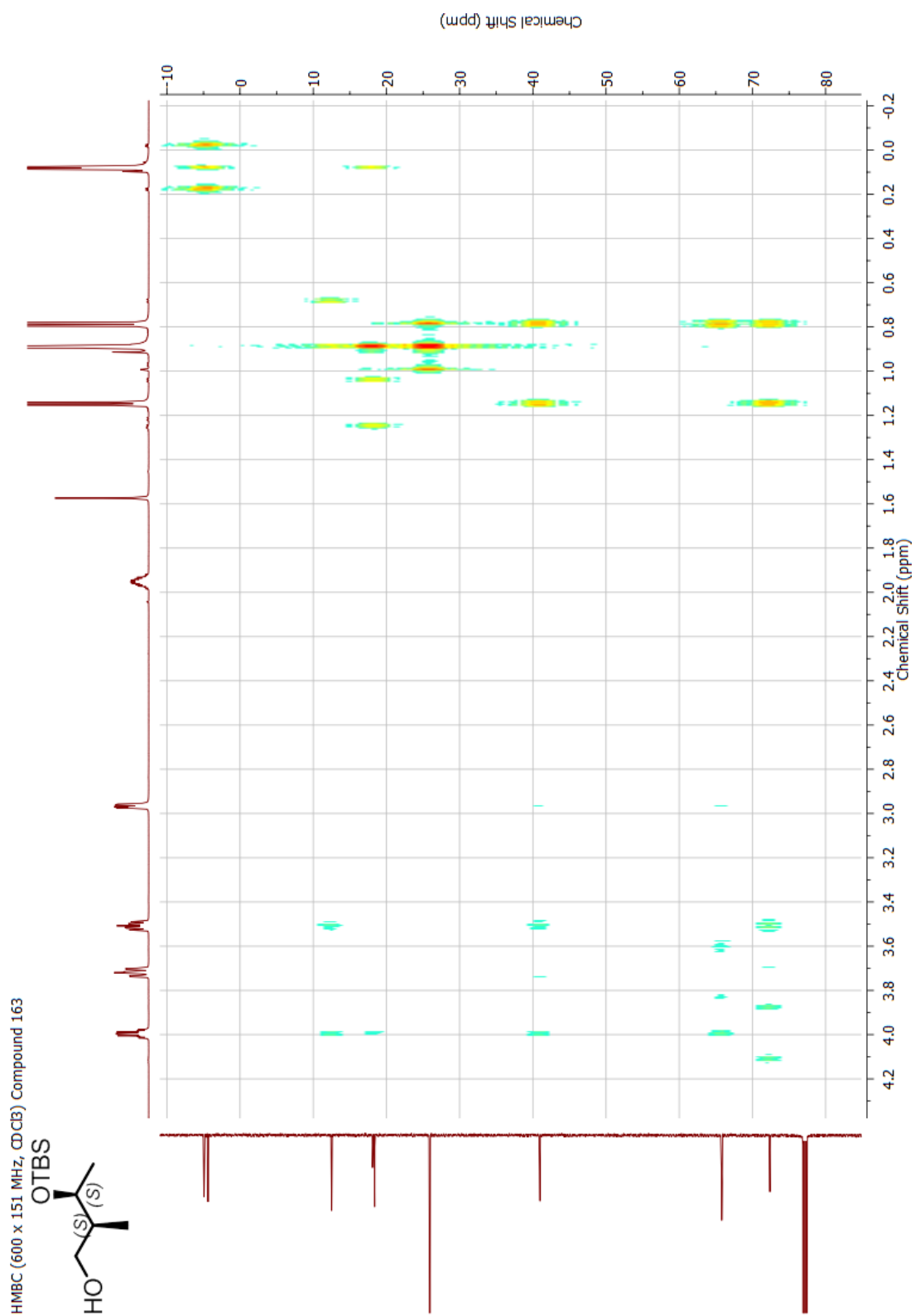
¹³C NMR (151 MHz, CDCl₃) Compound 163



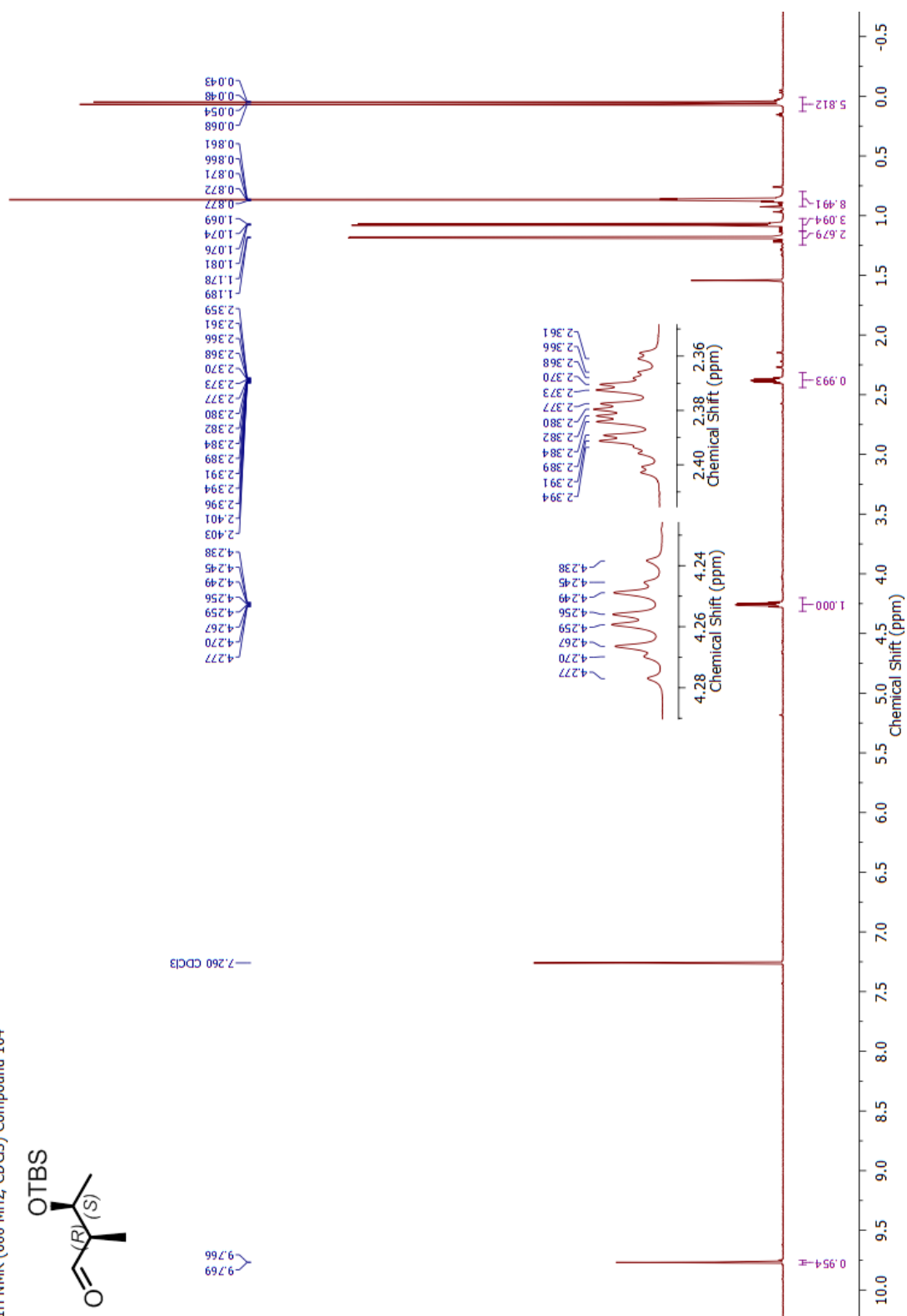
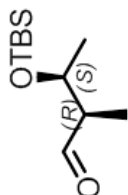
Appendix



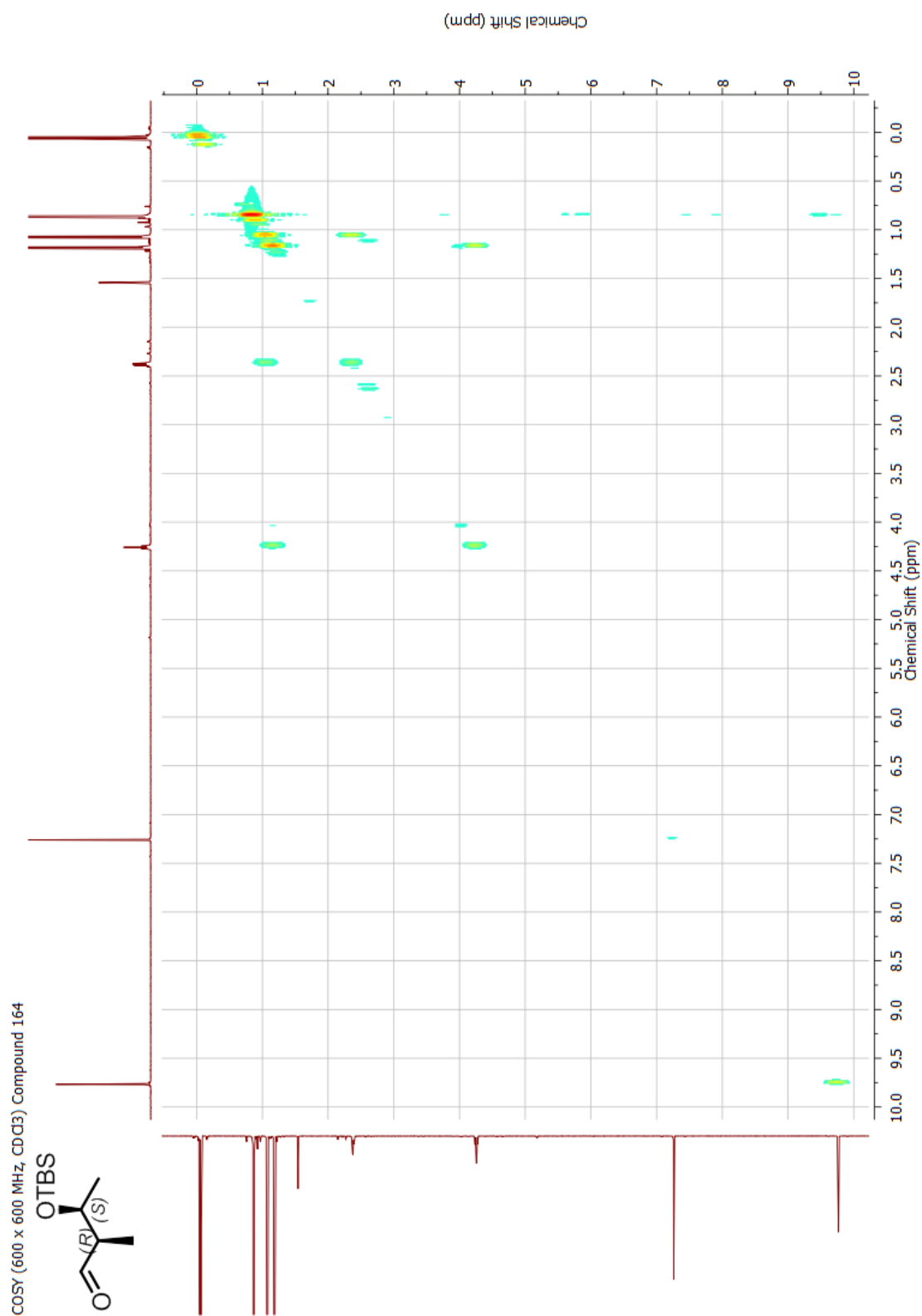
Appendix



¹H NMR (600 MHz, CDCl₃) Compound 164

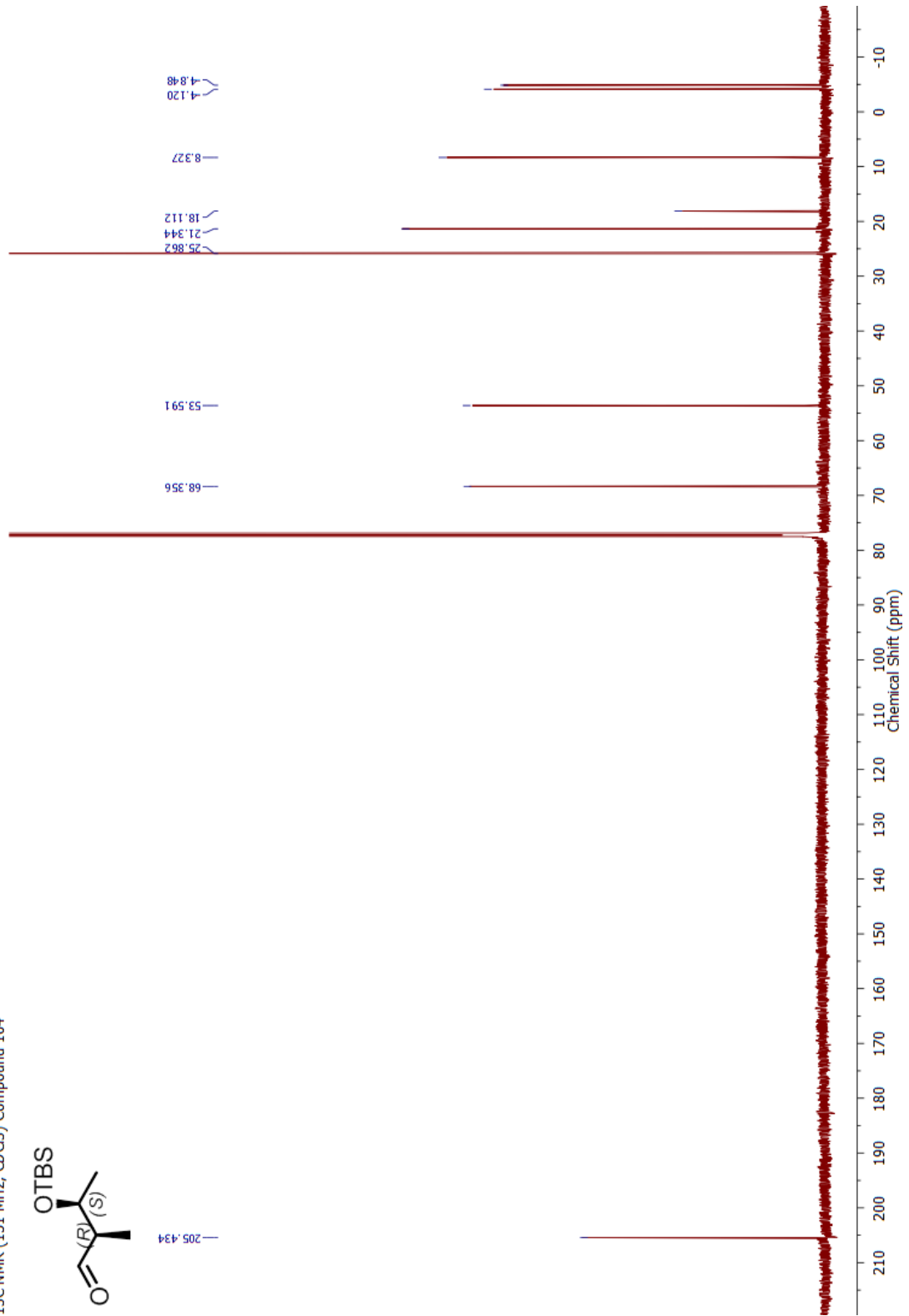
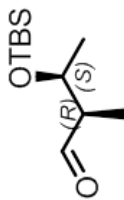


Appendix

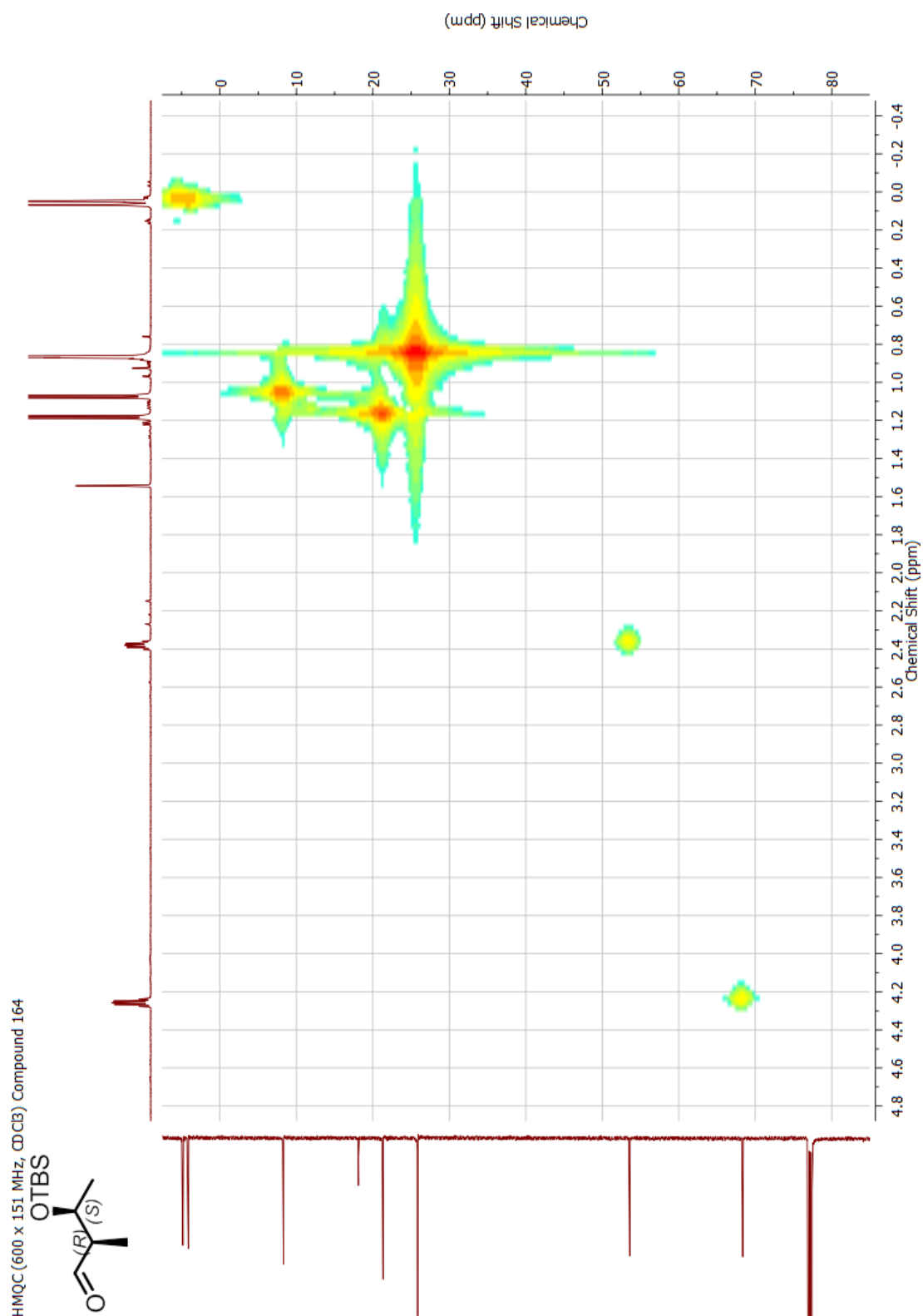


Appendix

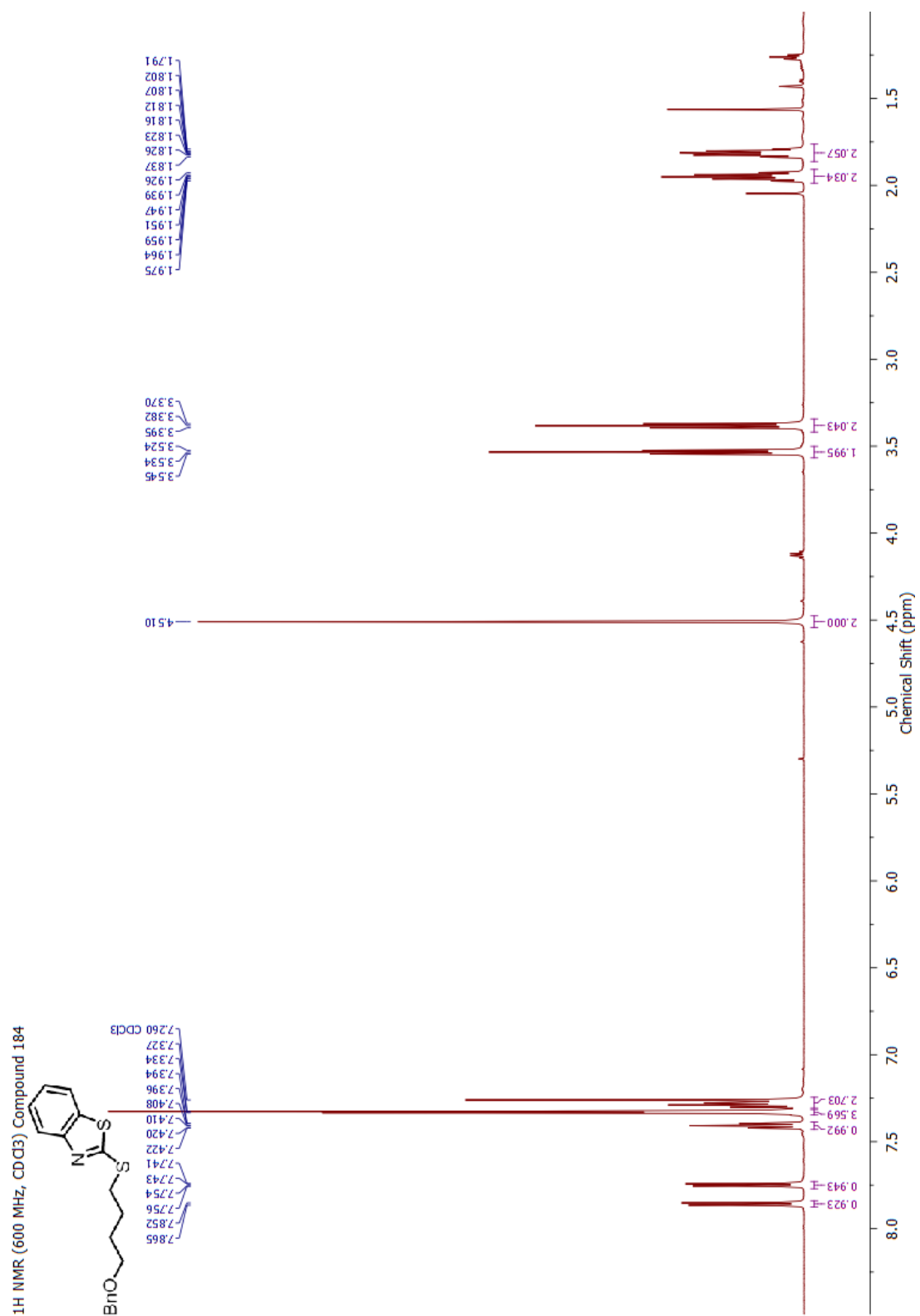
¹³C NMR (151 MHz, CDCl₃) Compound 164



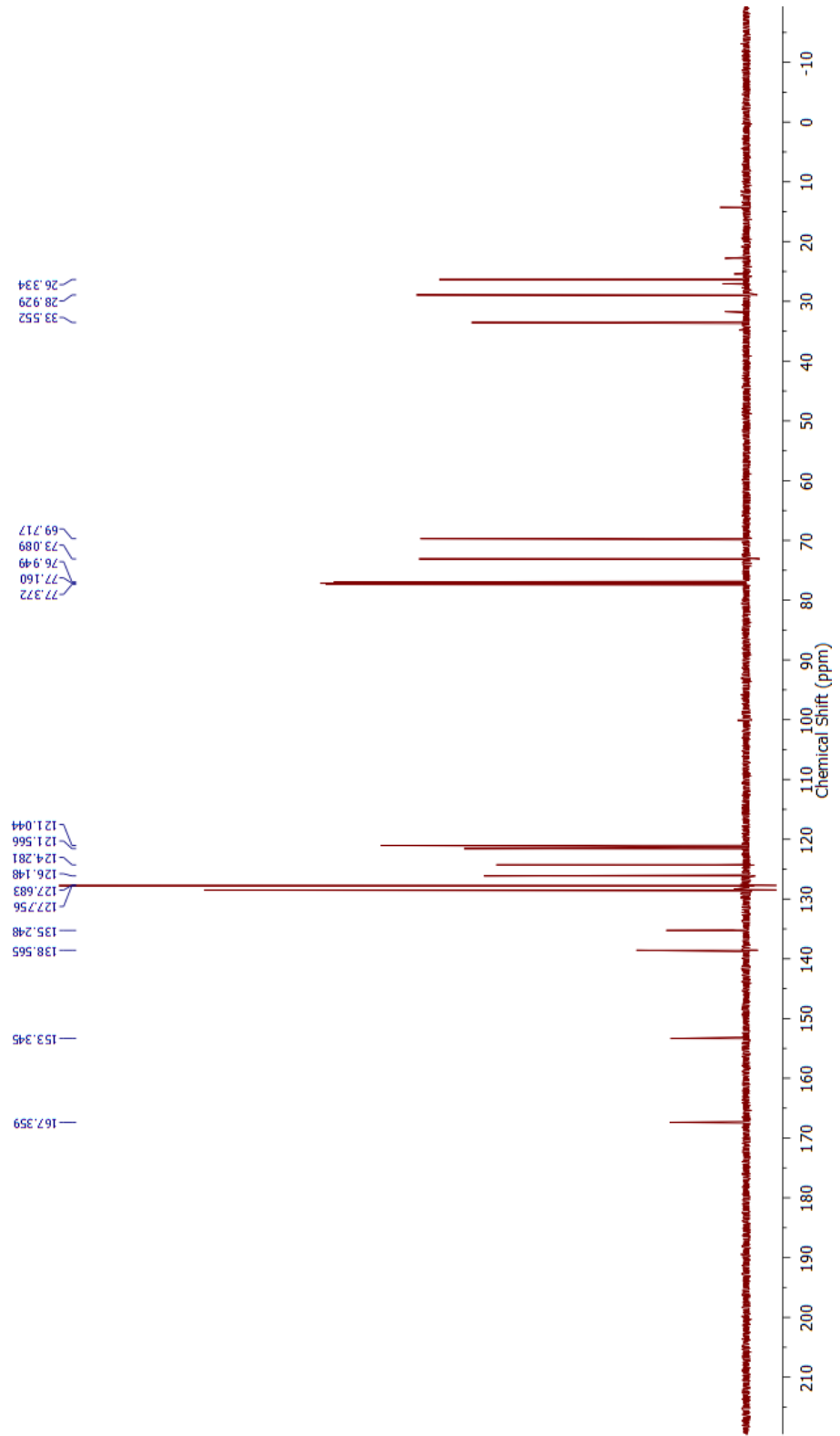
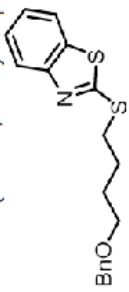
Appendix



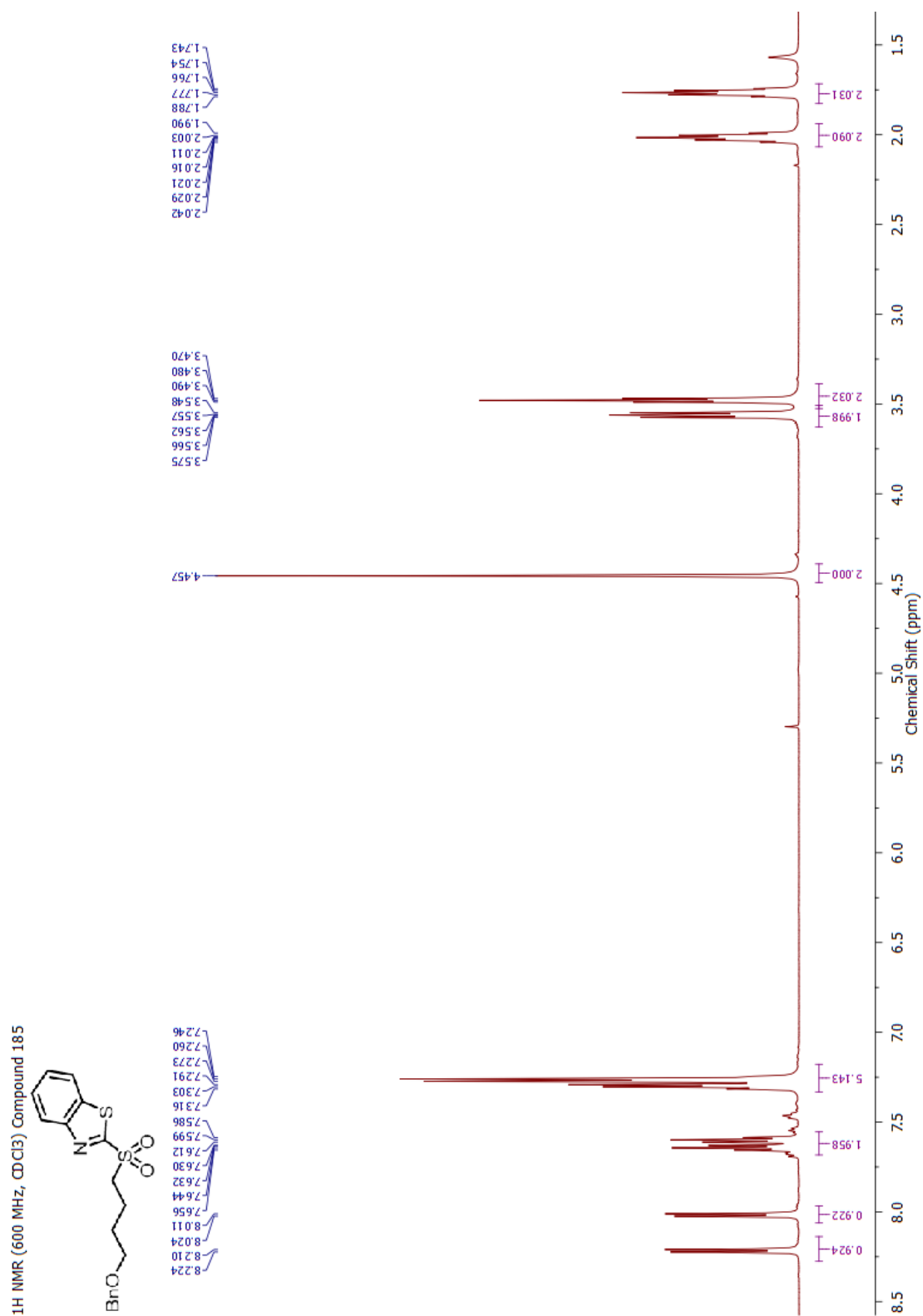
Appendix



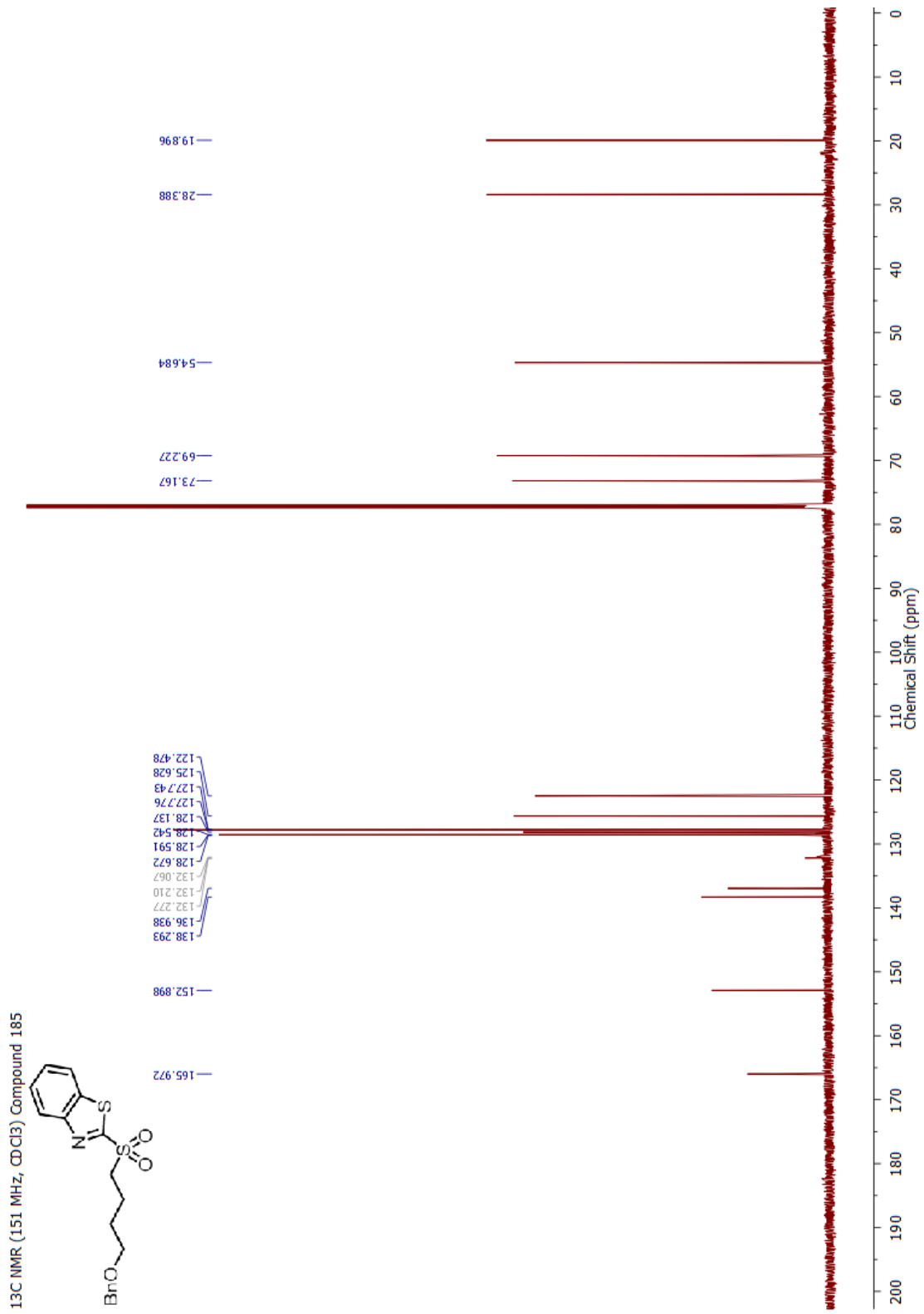
¹³C NMR (151 MHz, CDCl₃) Compound 184



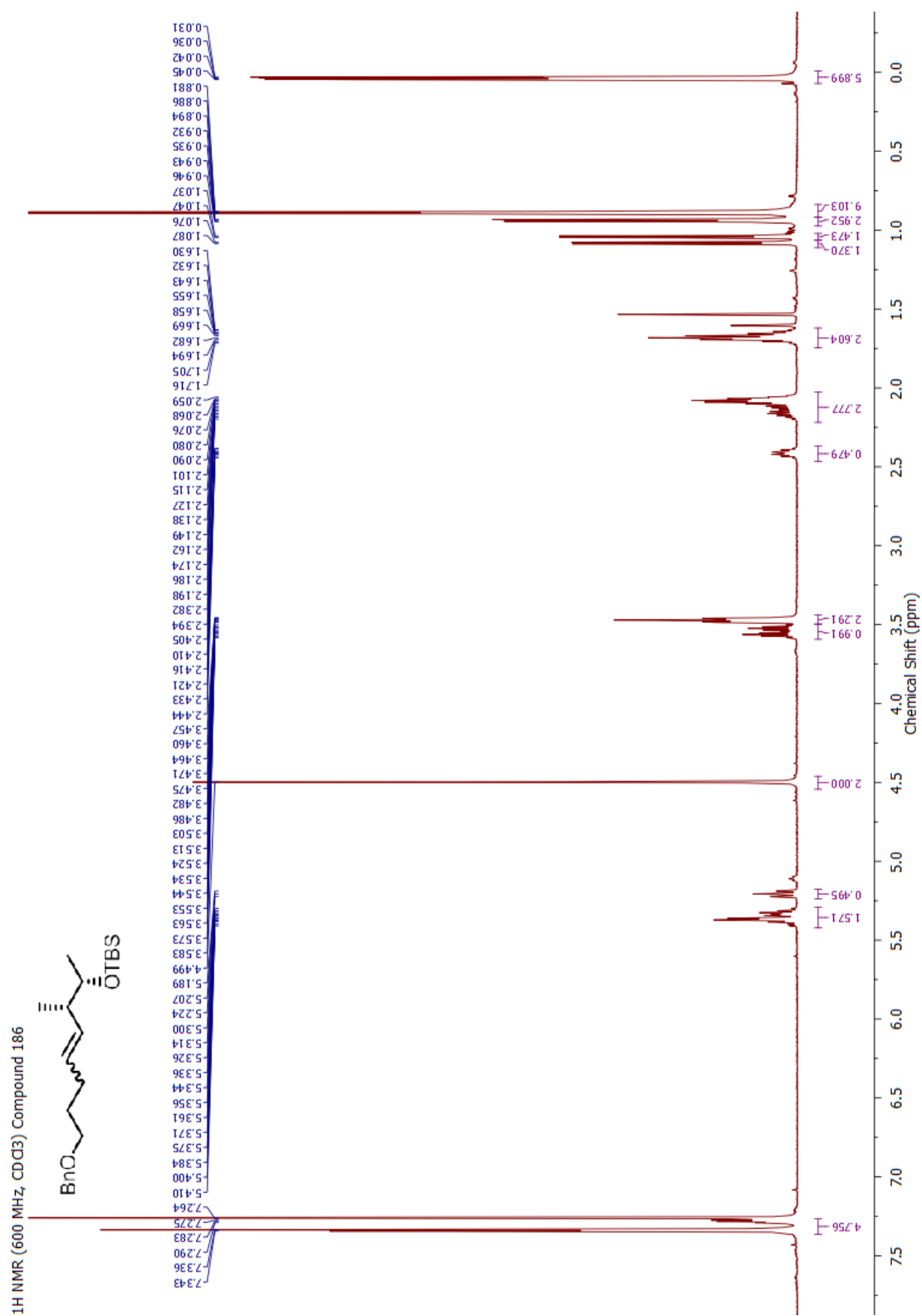
Appendix

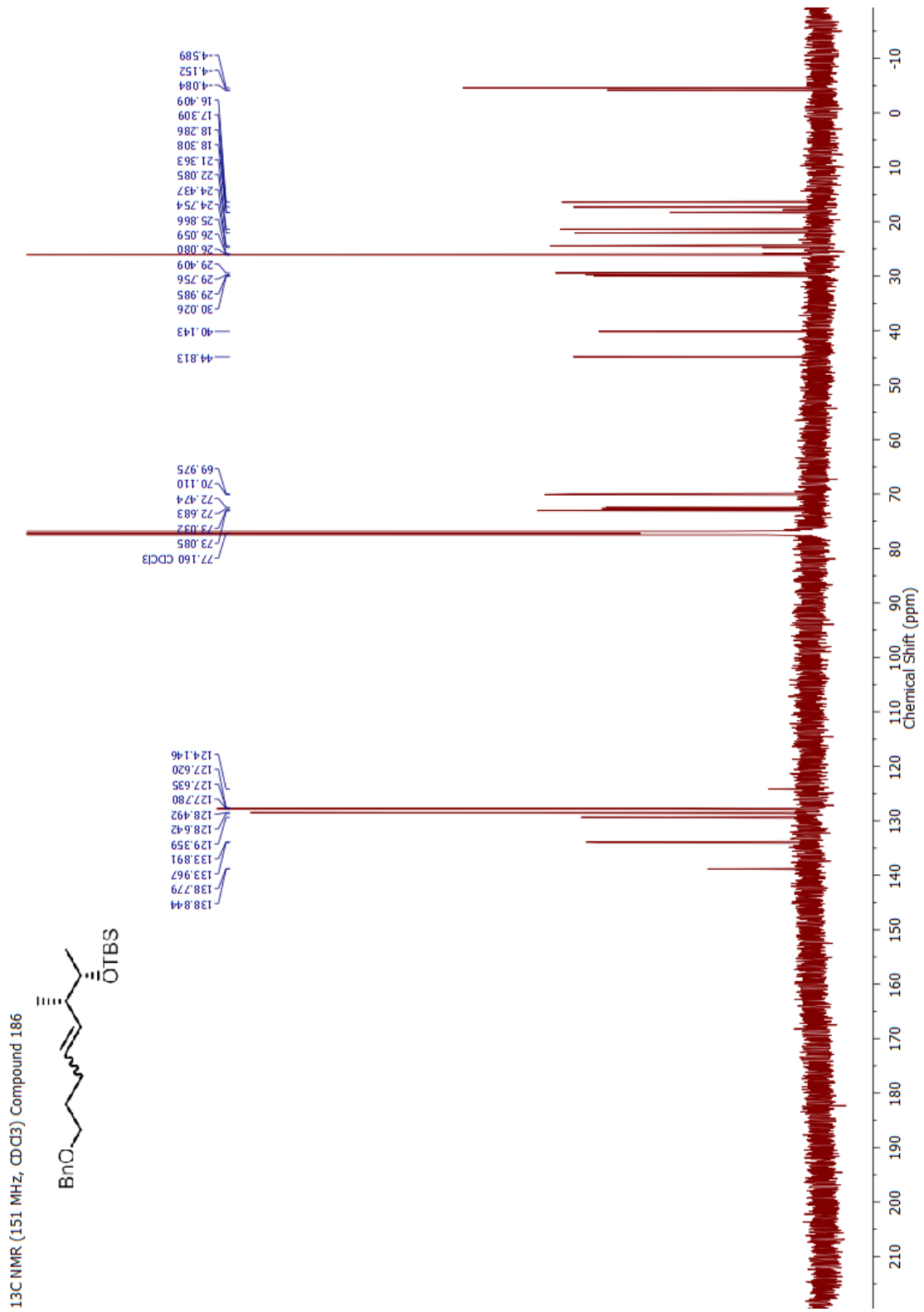


Appendix



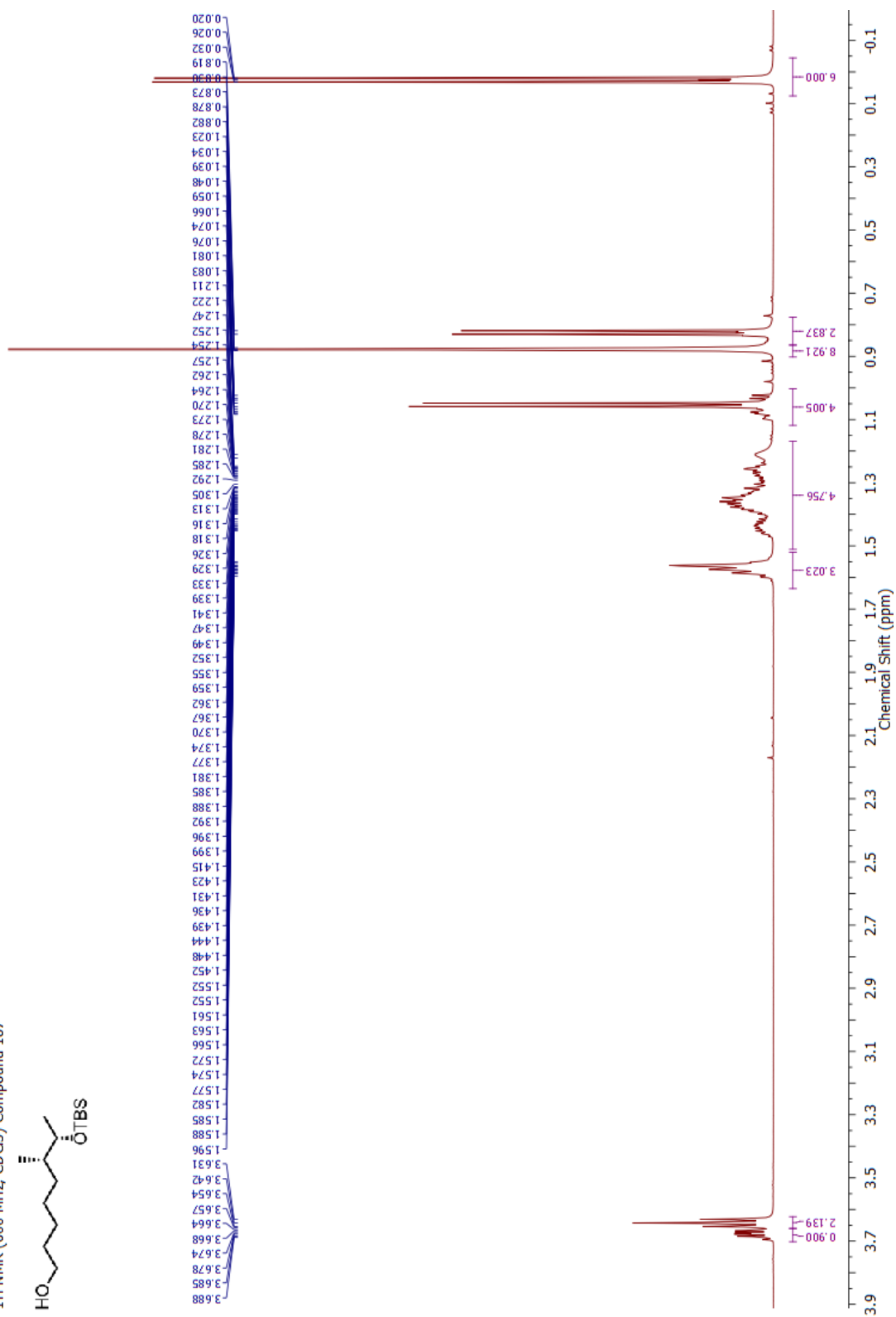
Appendix

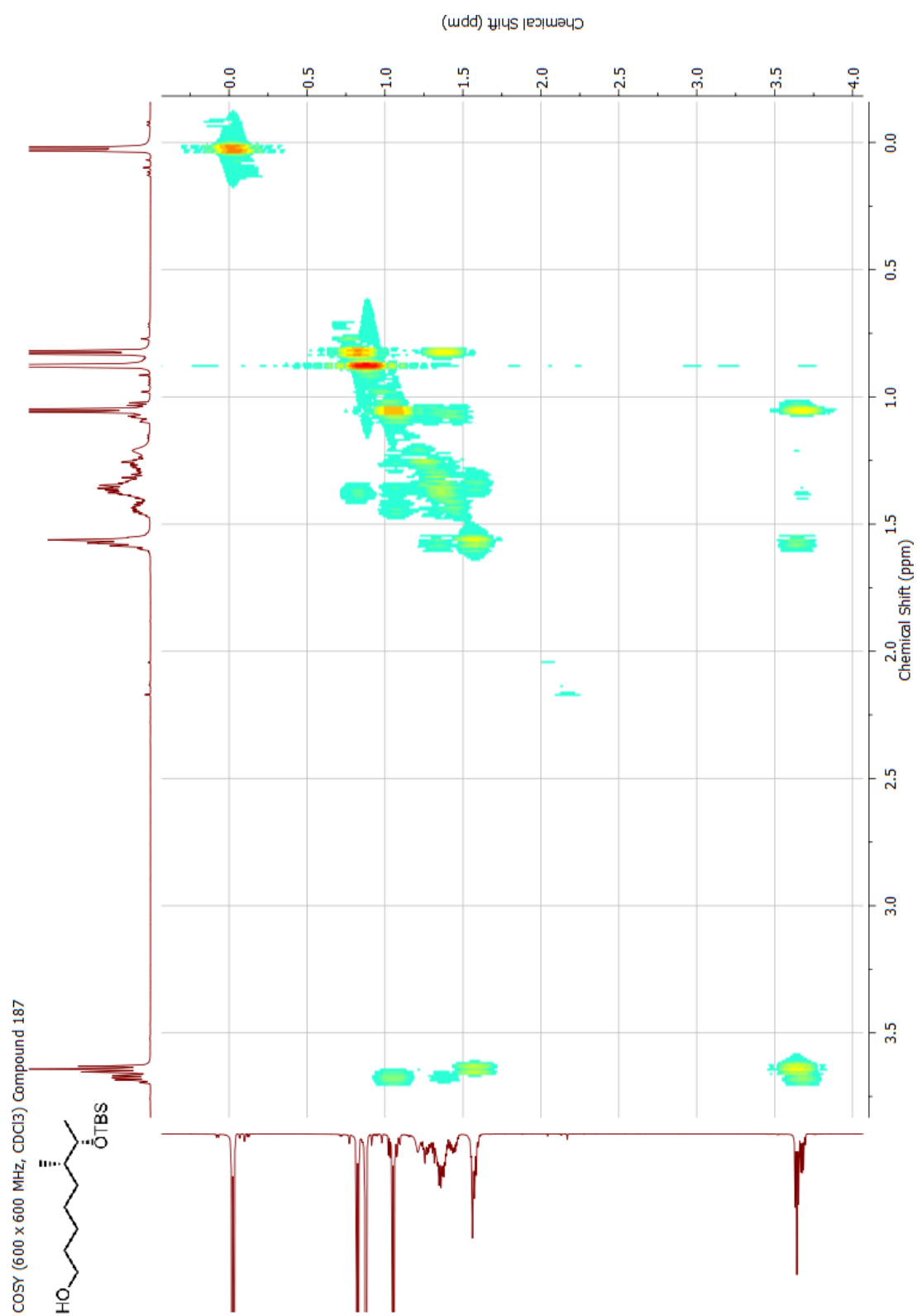




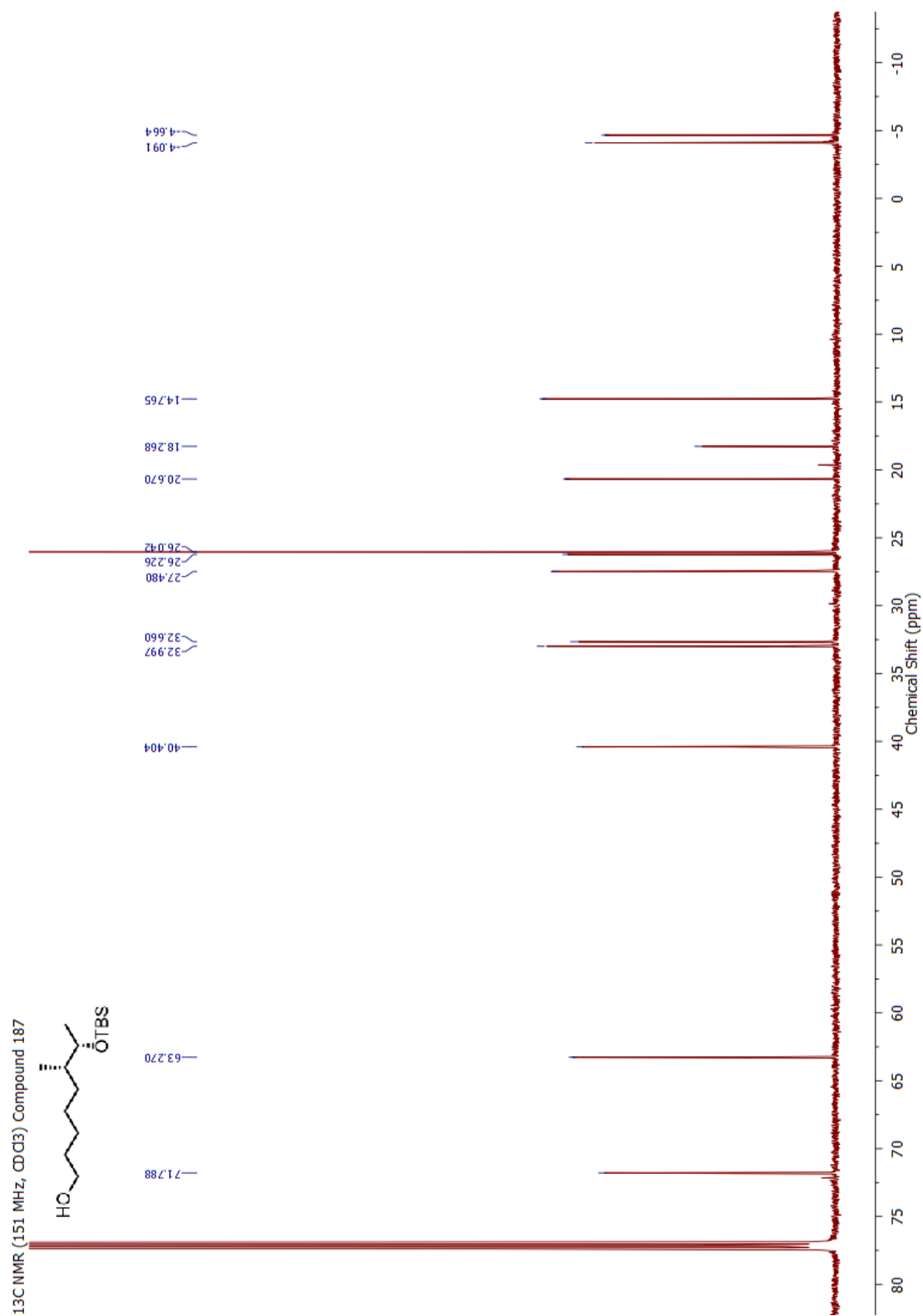
Appendix

¹H NMR (600 MHz, CDCl₃) Compound 187

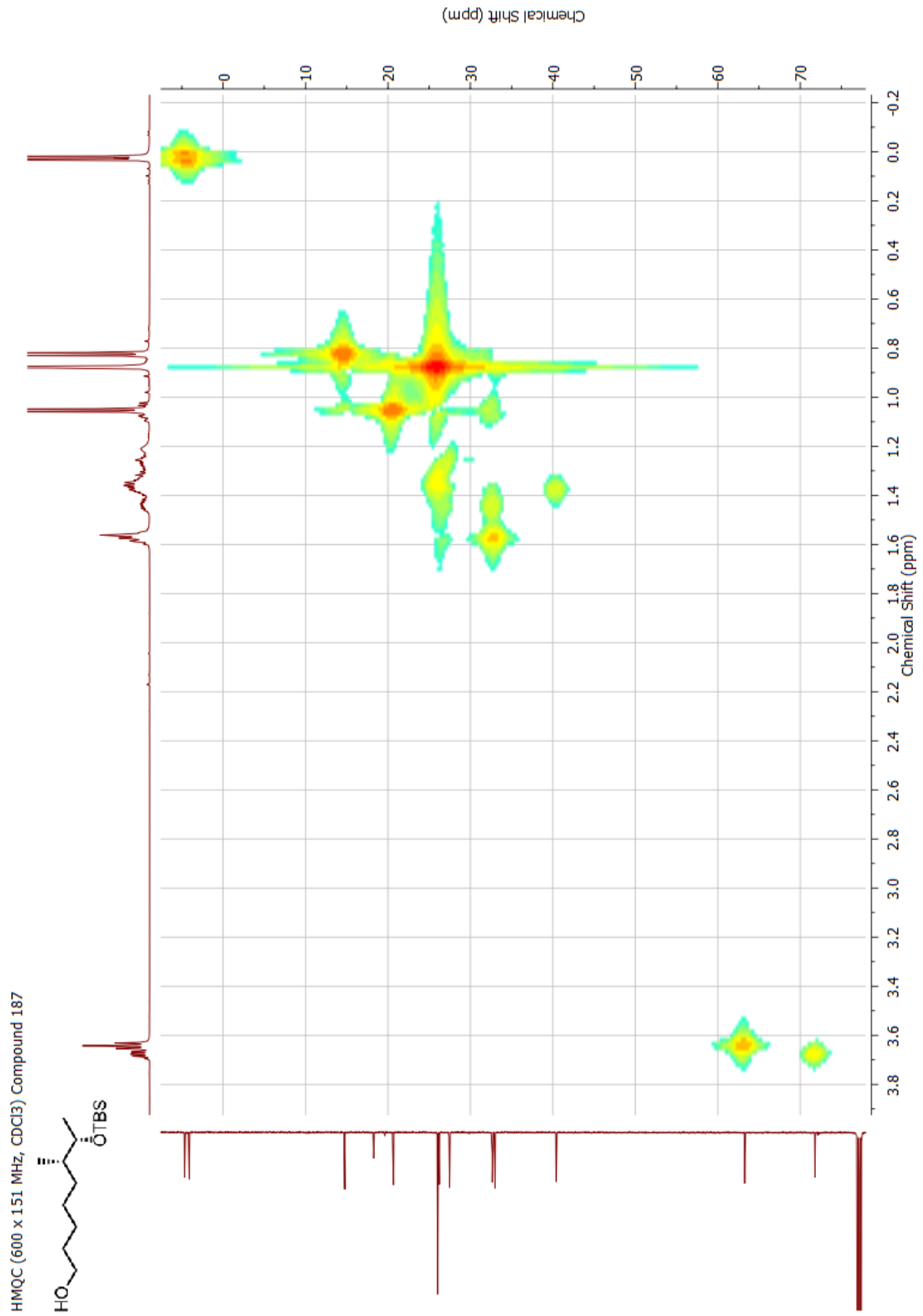




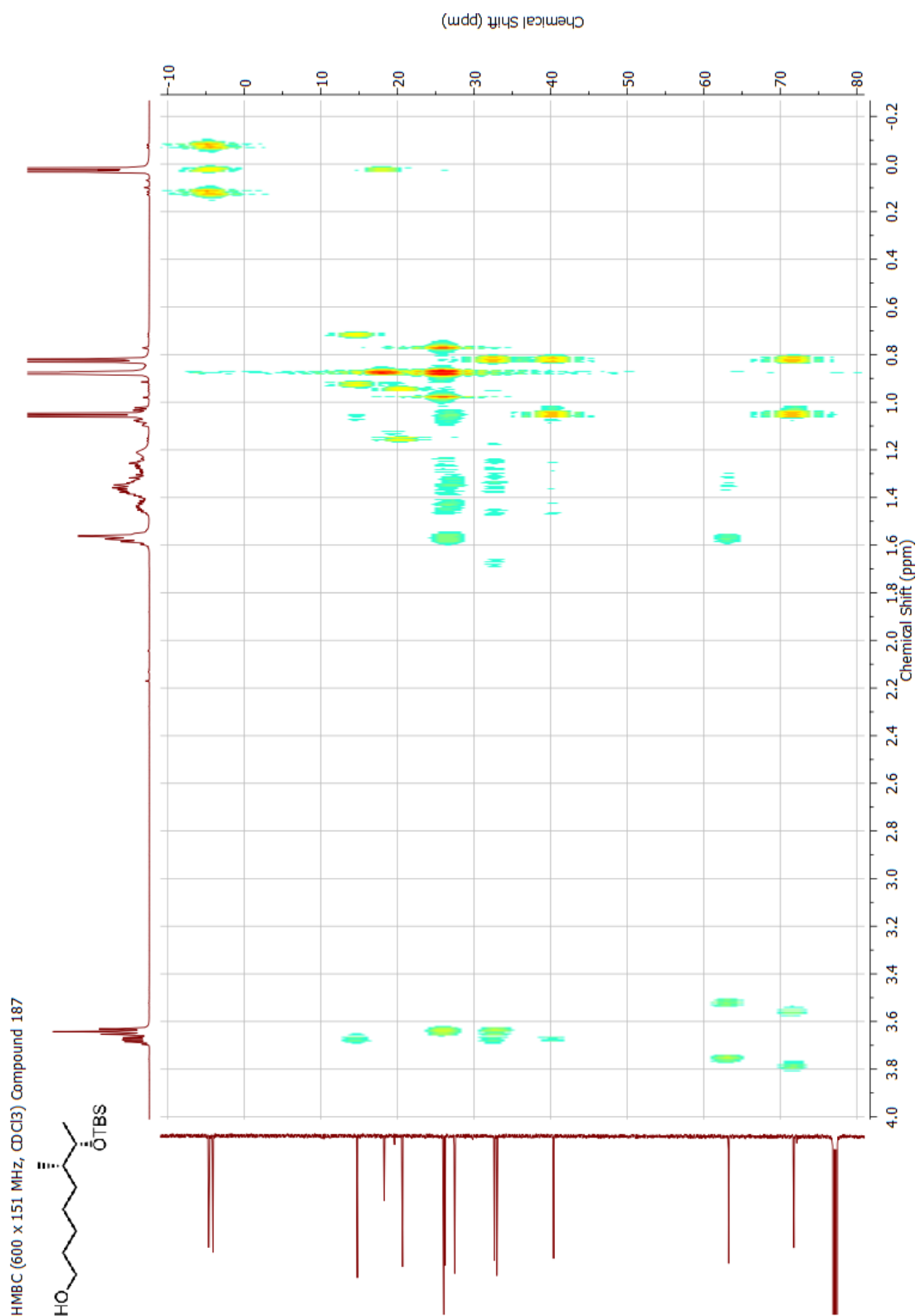
Appendix



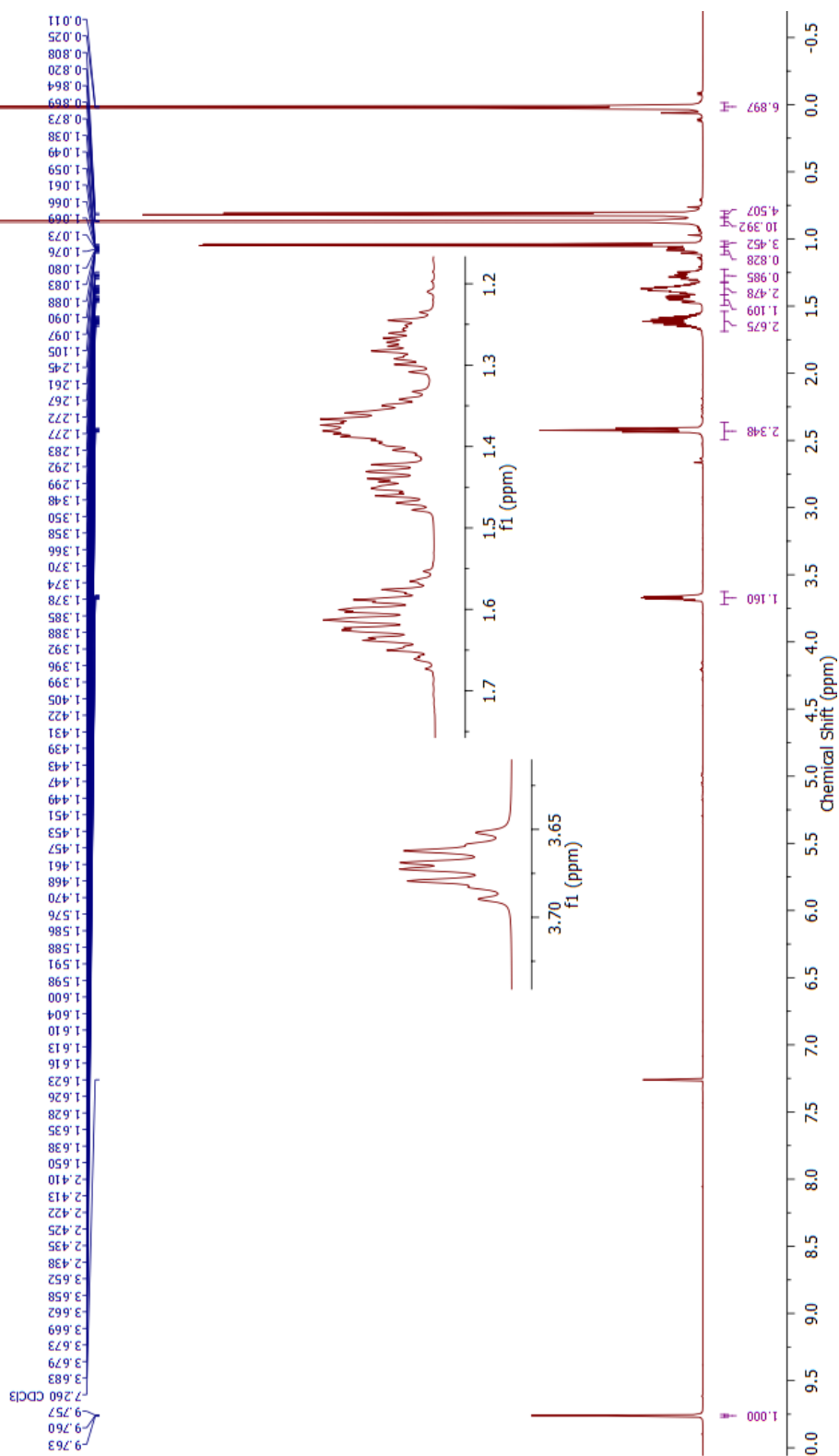
Appendix



Appendix

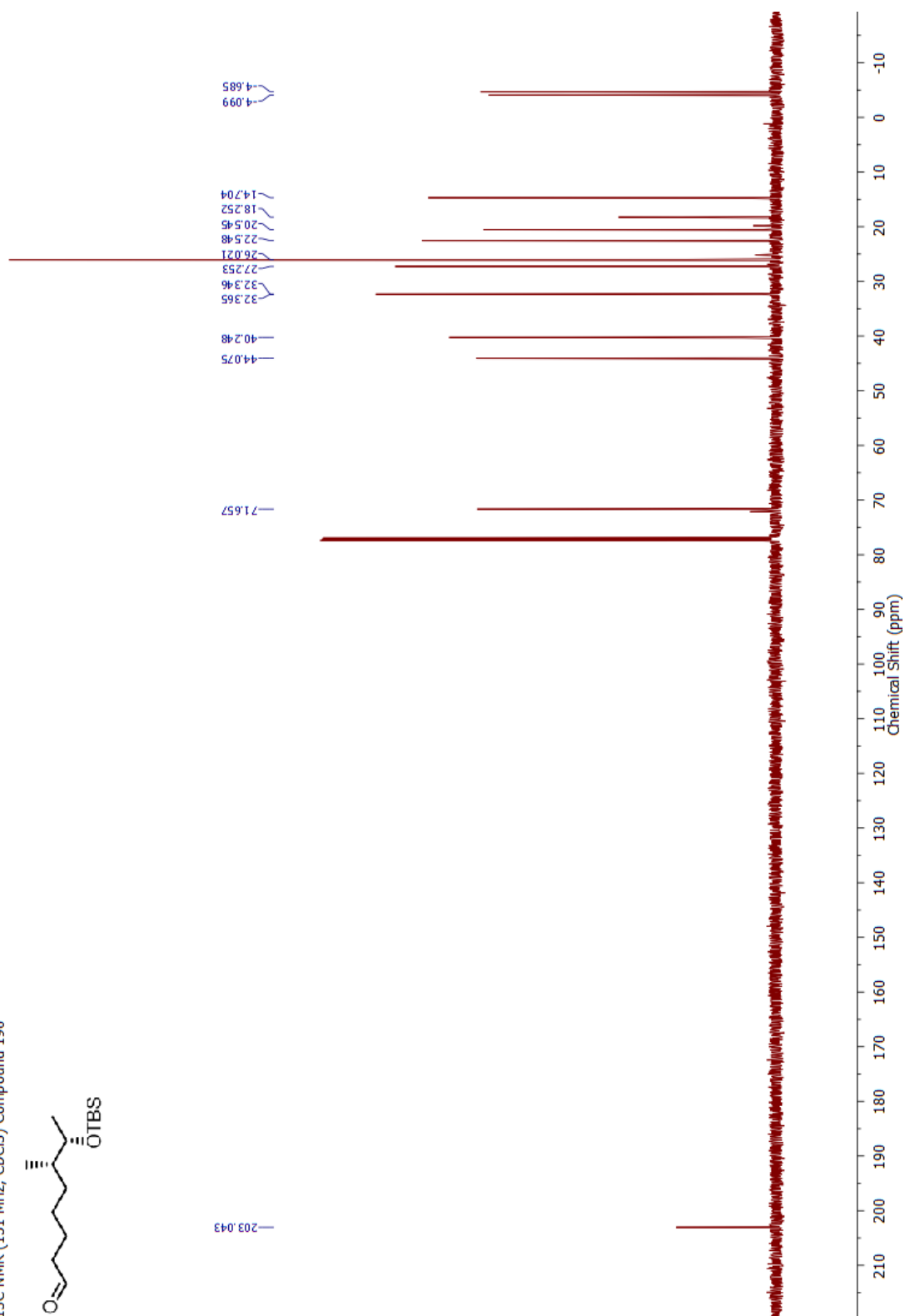


¹H NMR (600 MHz, CDCl₃) Compound 190



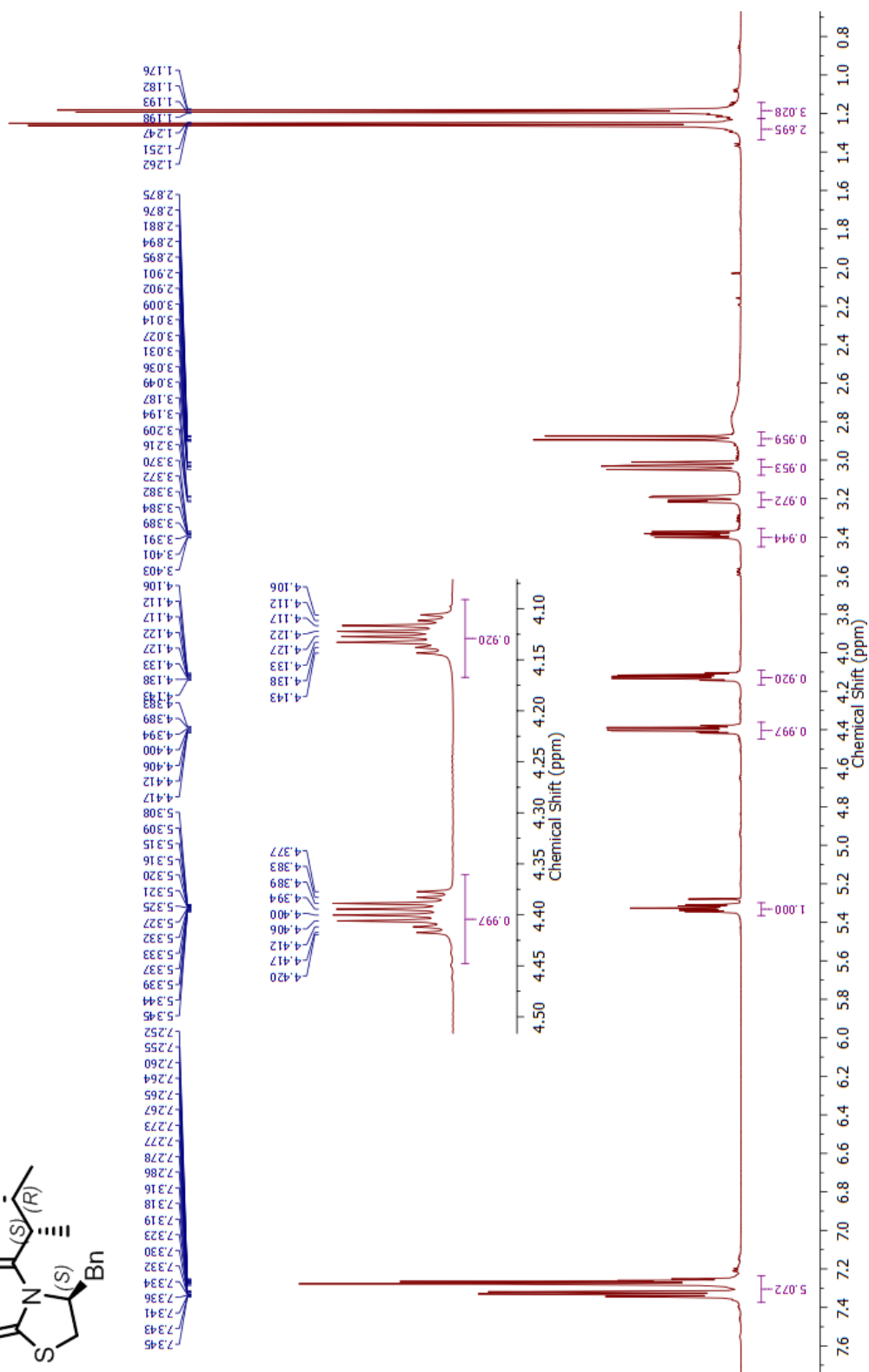
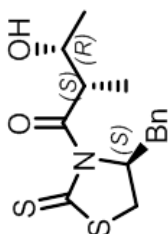
Appendix

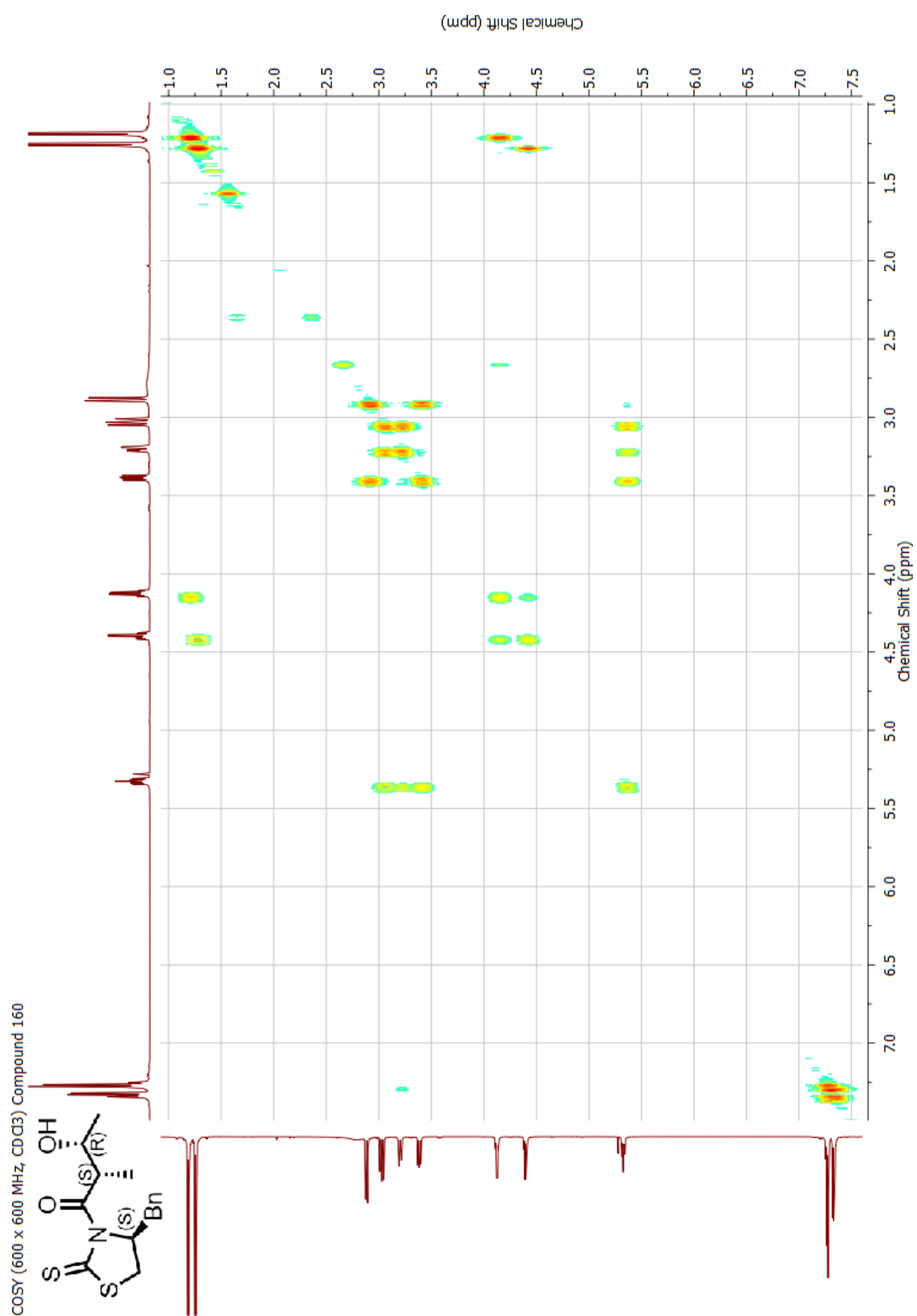
¹³C NMR (151 MHz, CDCl₃) Compound 190



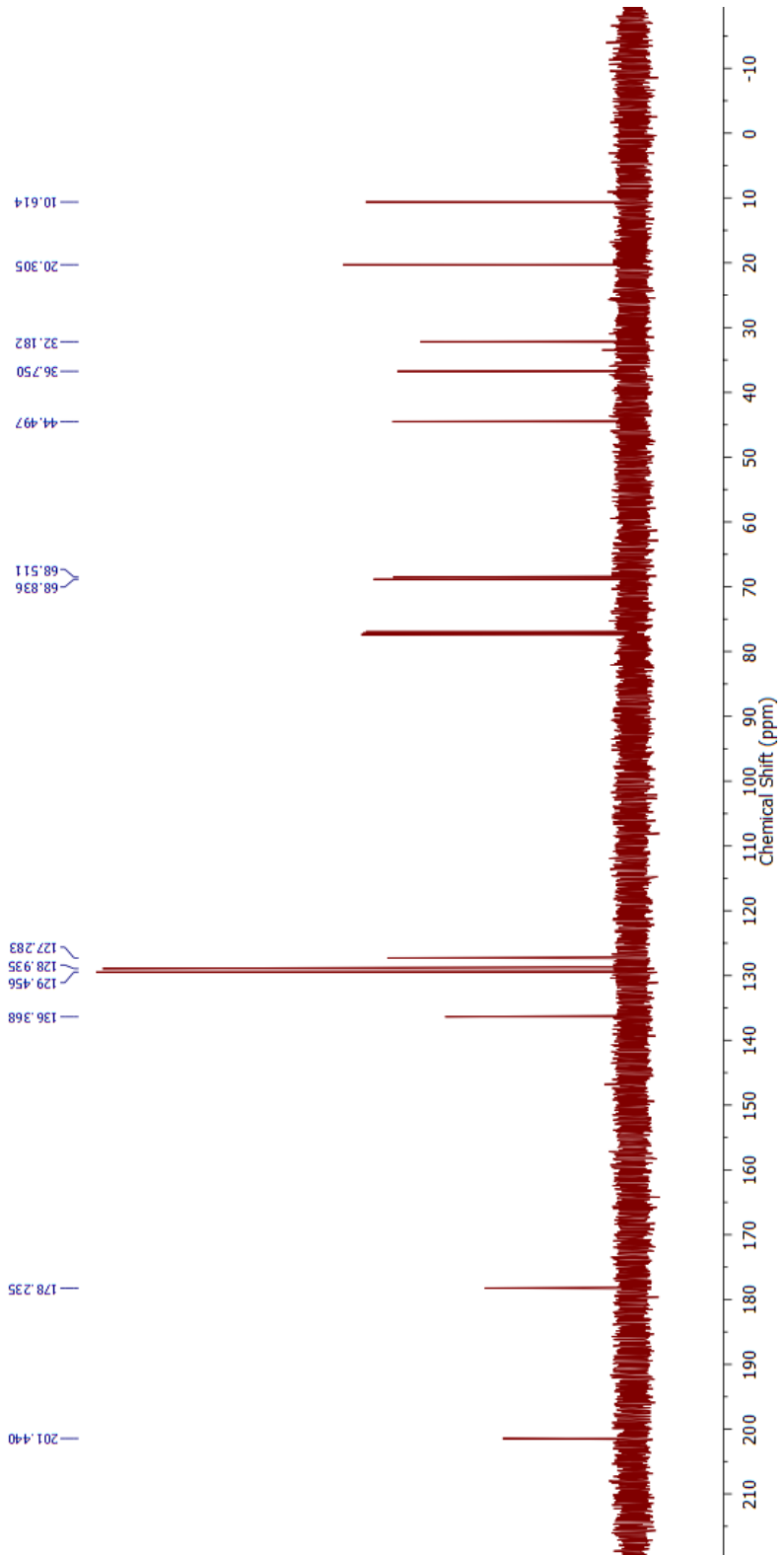
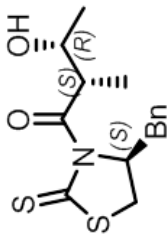
Appendix

¹H NMR (600 MHz, CDCl₃) Compound 160

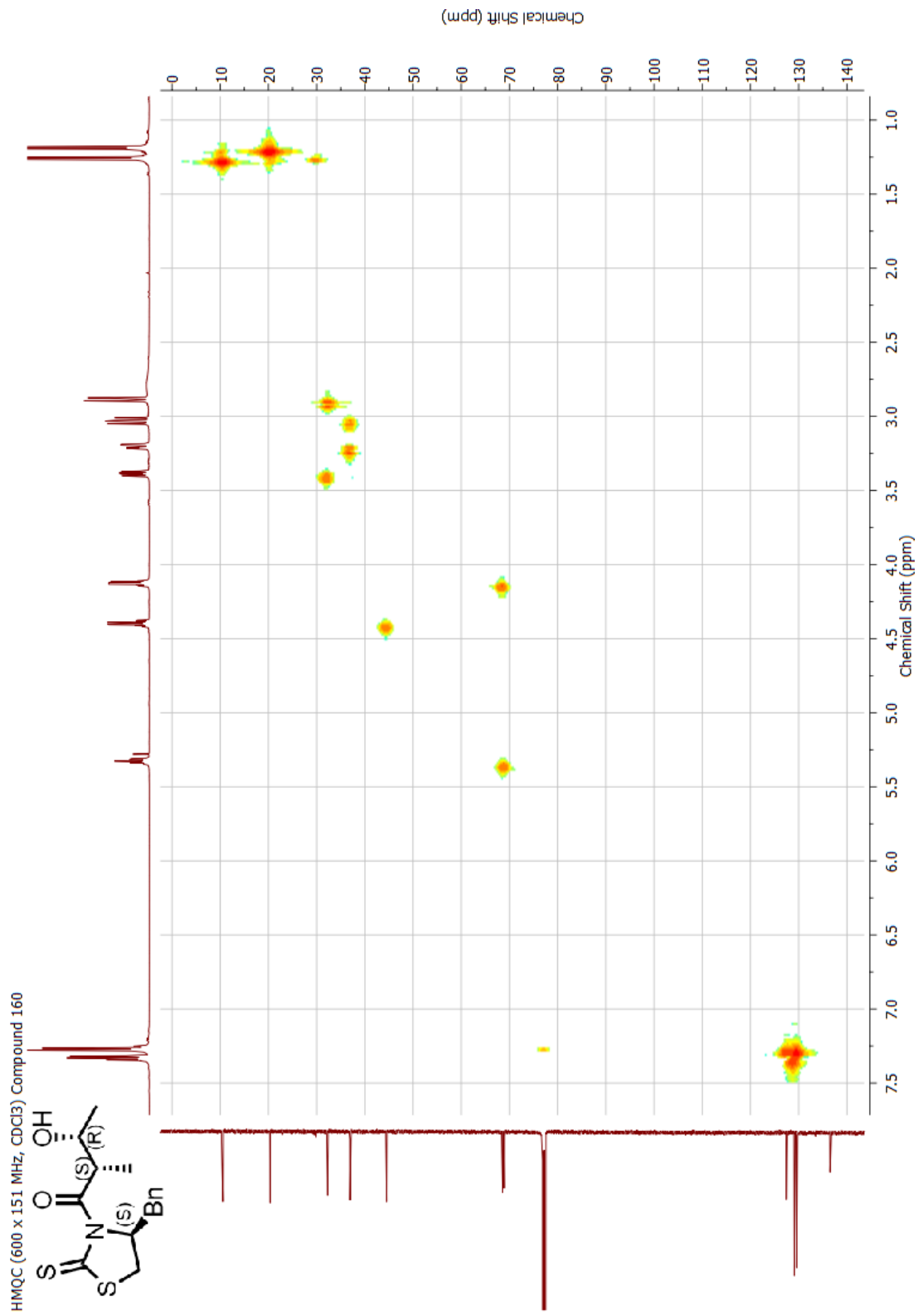




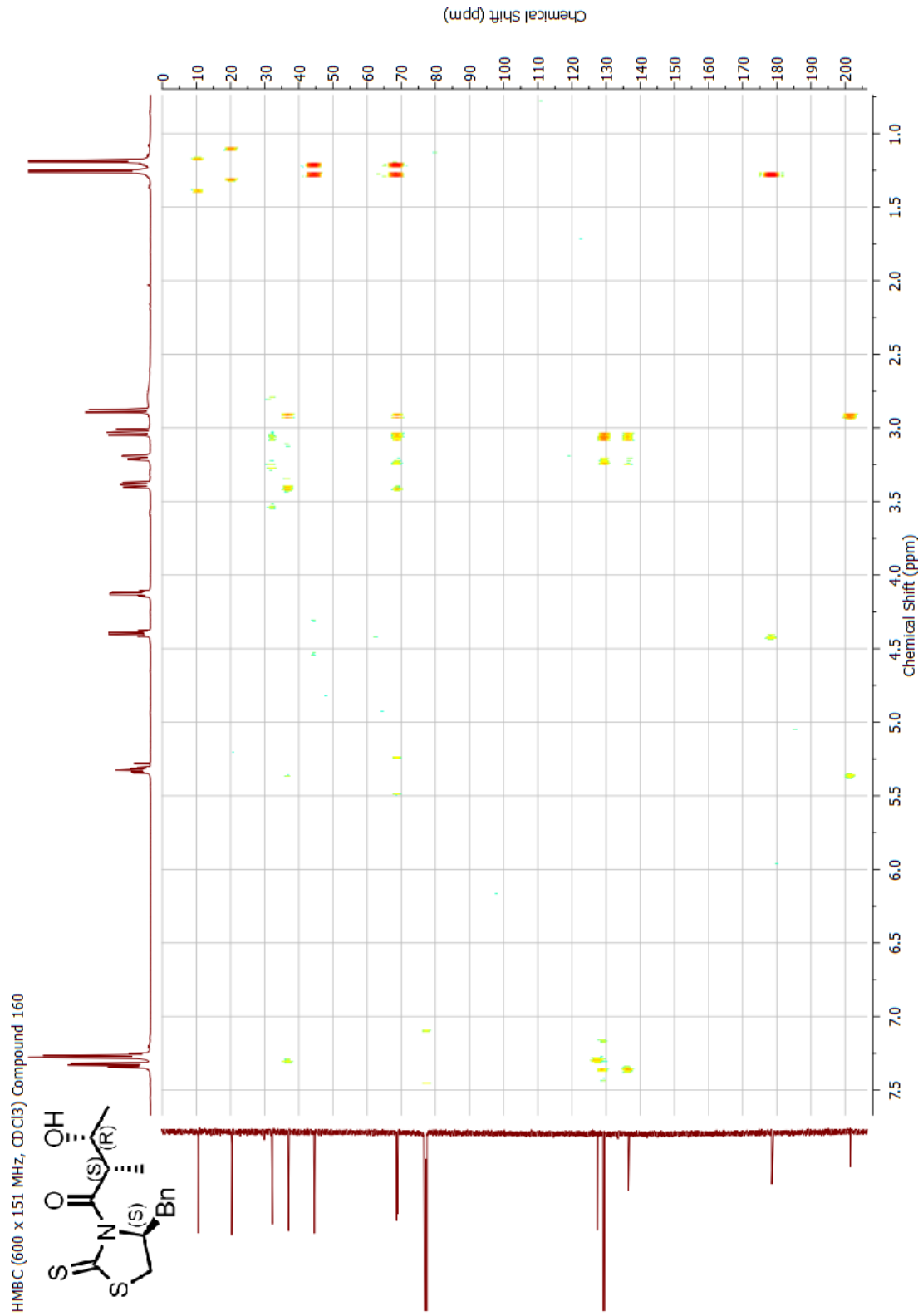
¹³C NMR (151 MHz, CDCl₃) Compound 160



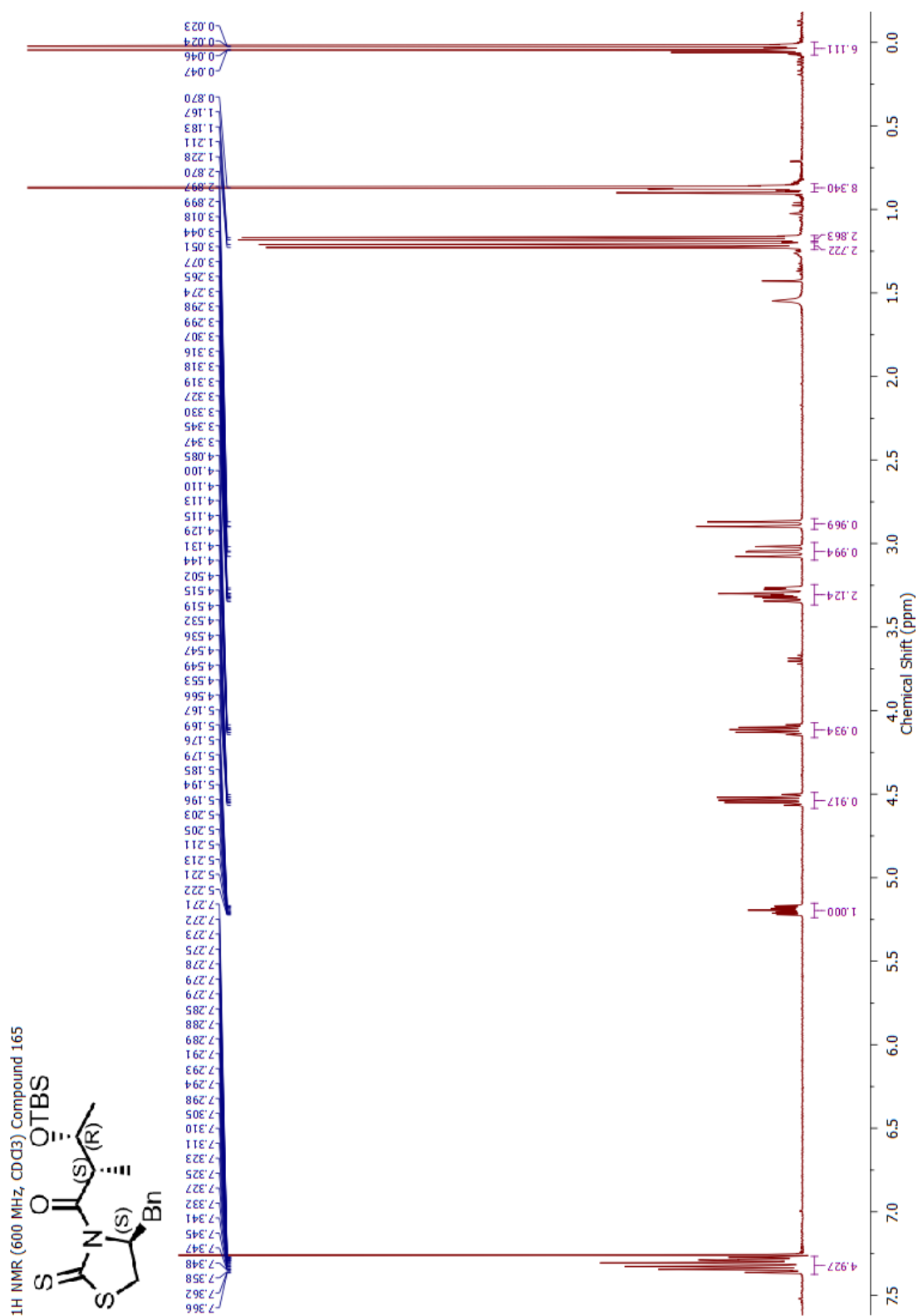
Appendix



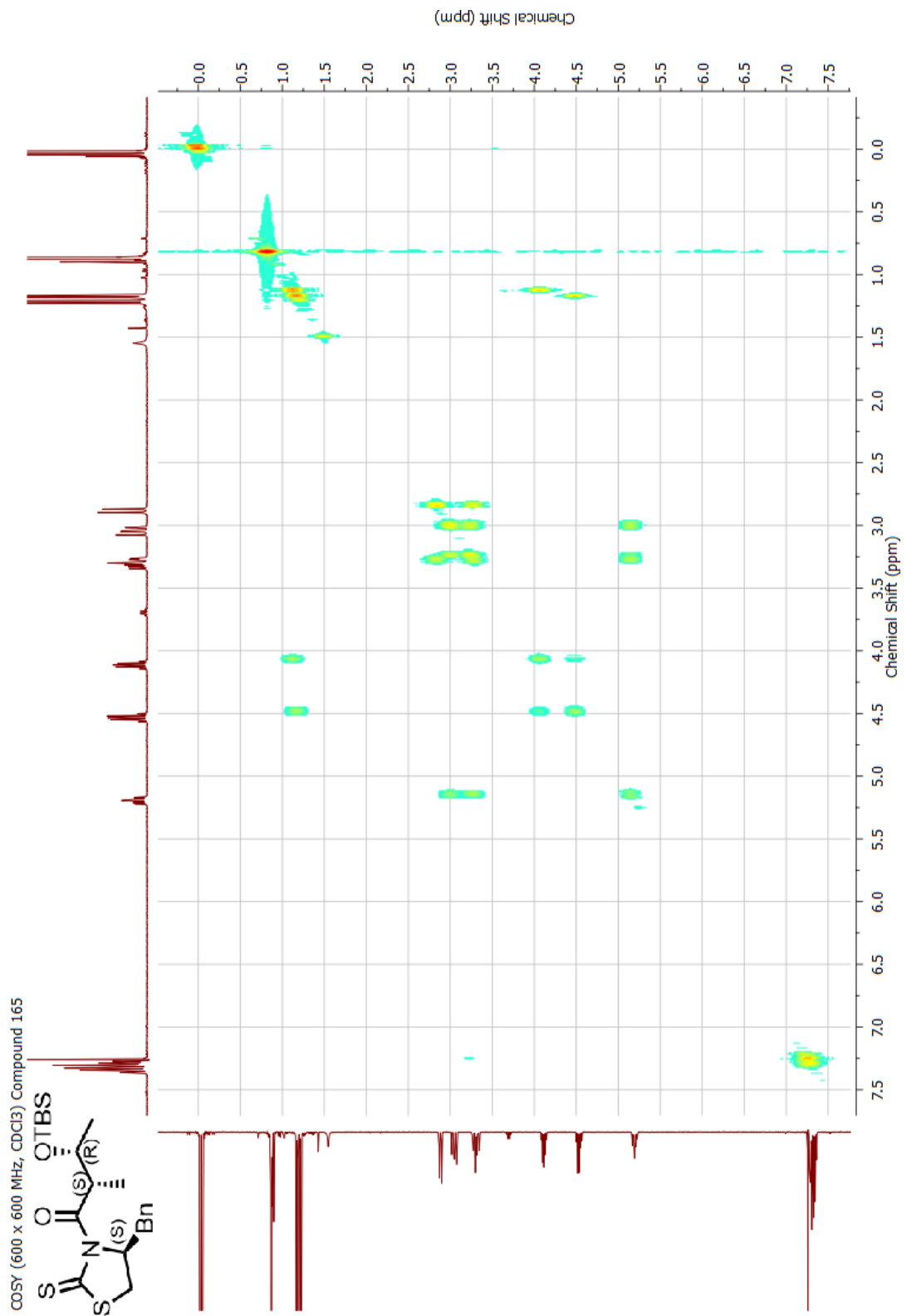
Appendix



Appendix

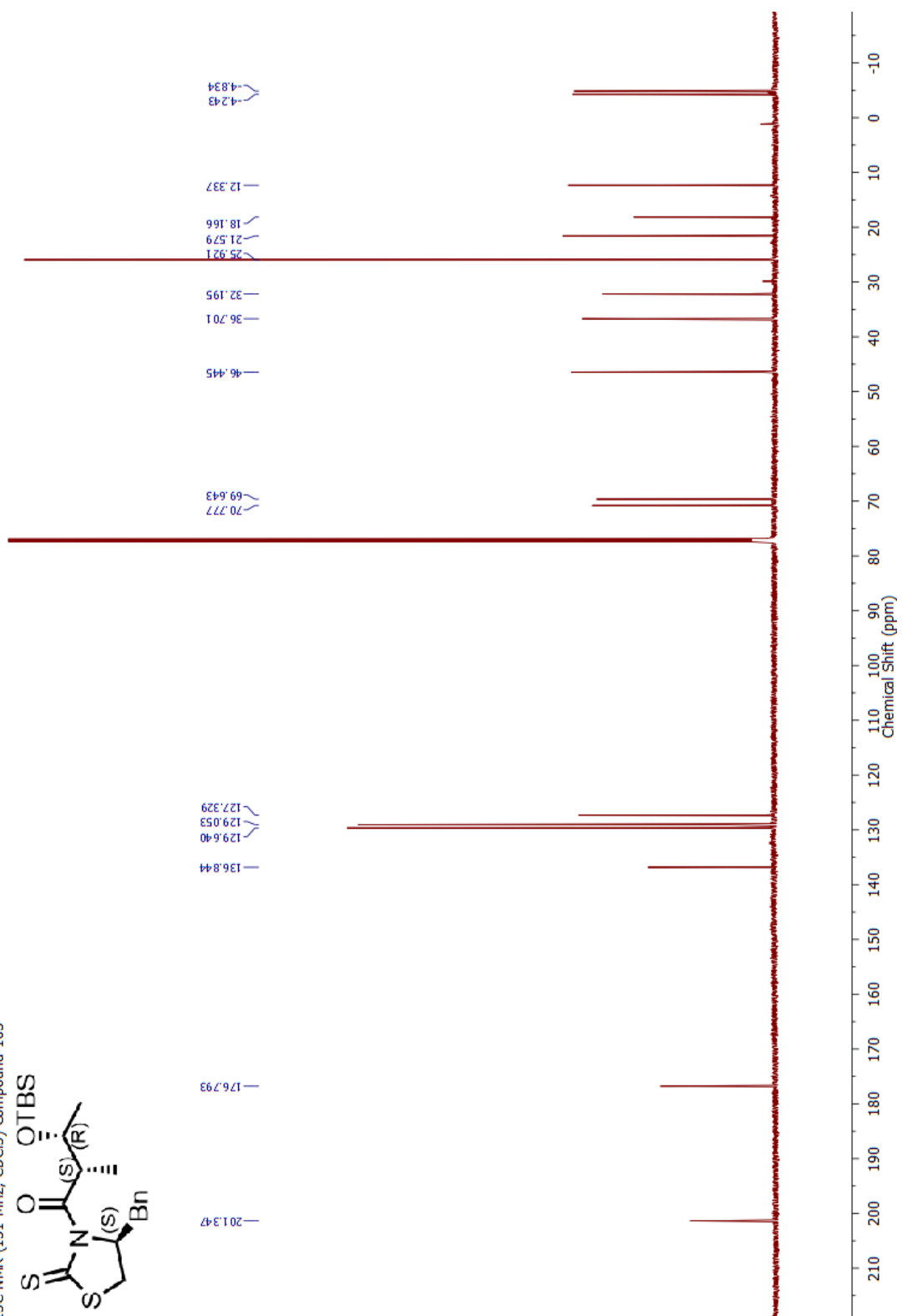
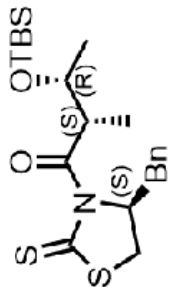


Appendix

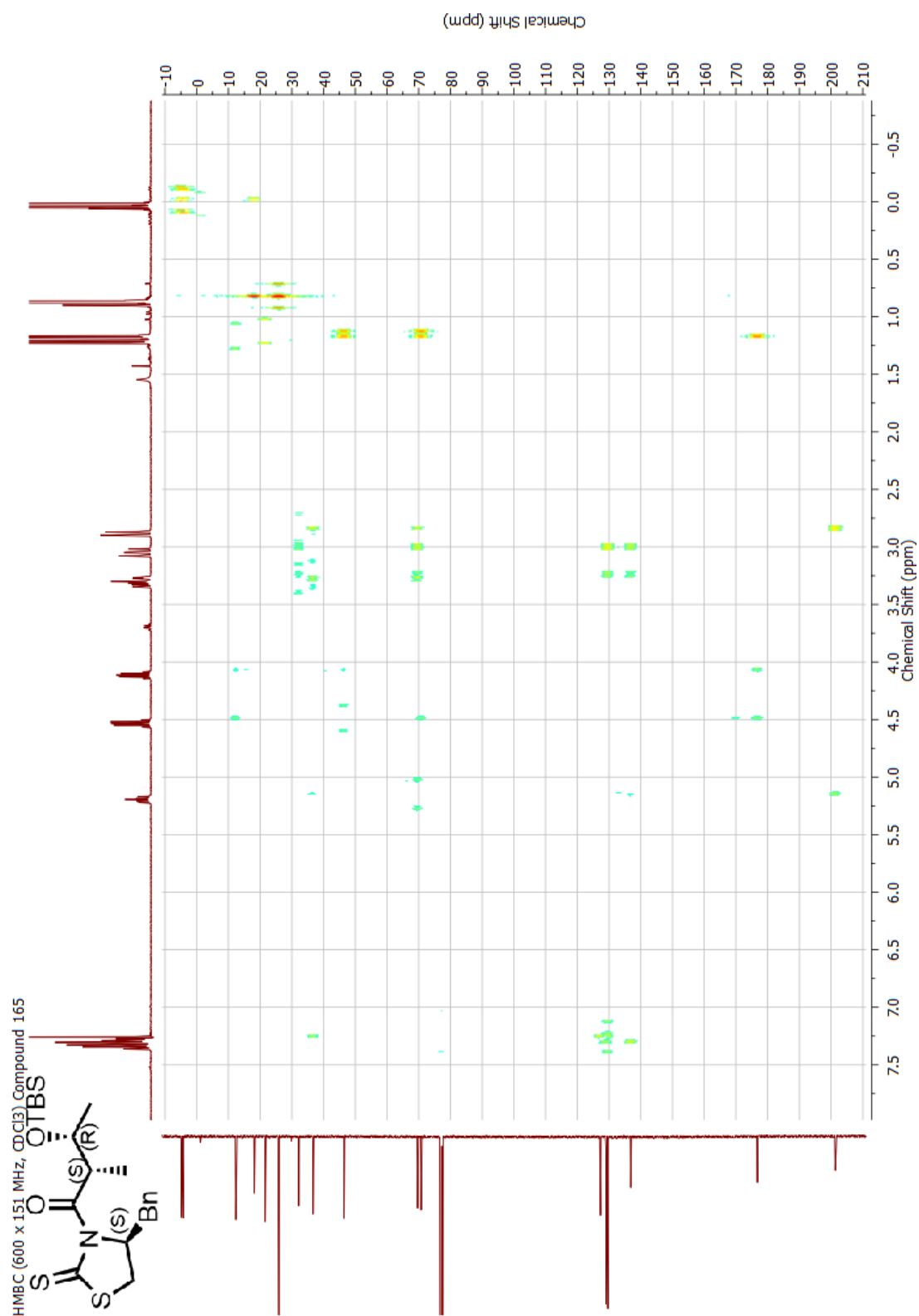


Appendix

¹³C NMR (151 MHz, CDCl₃) Compound 165

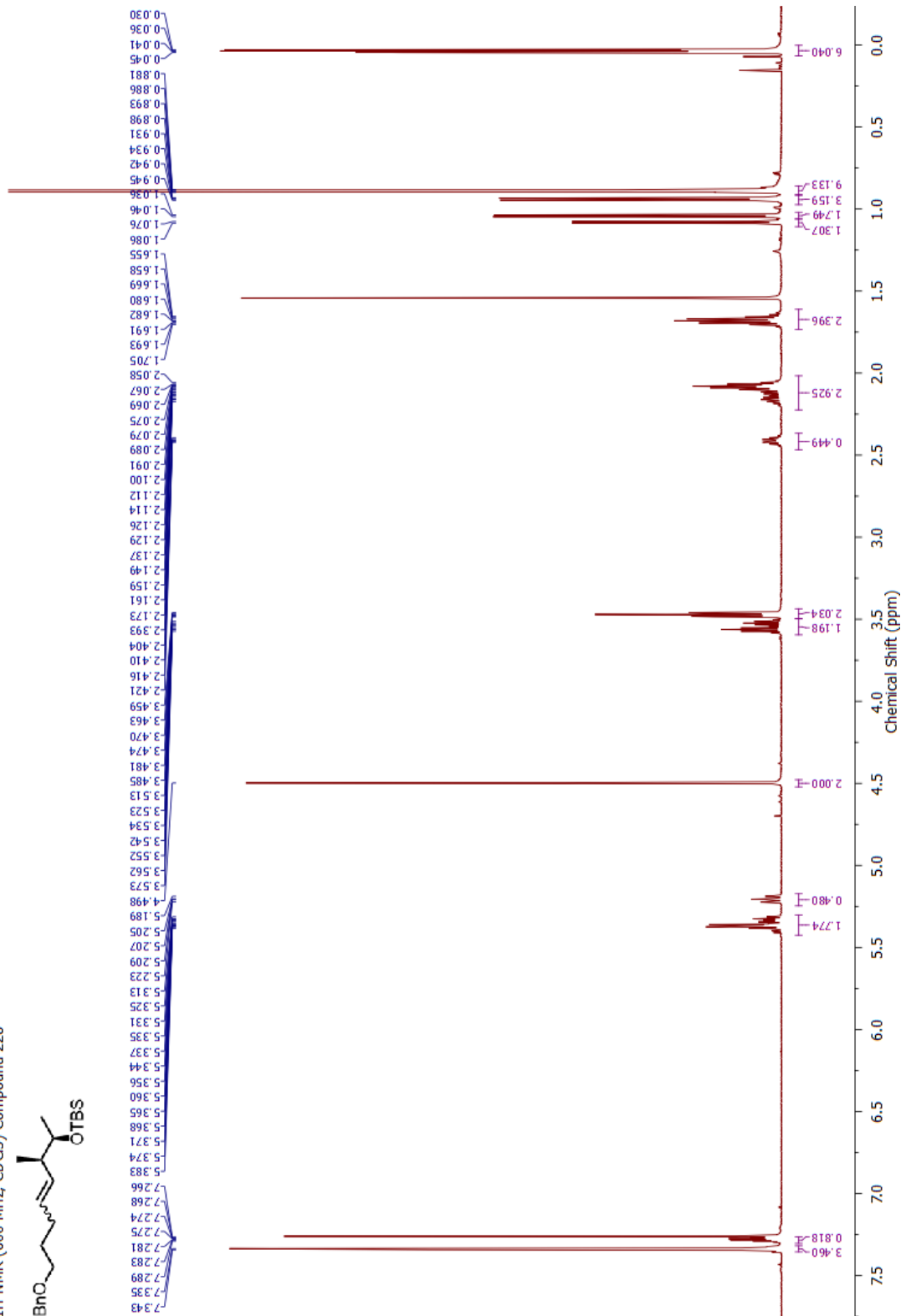


Appendix



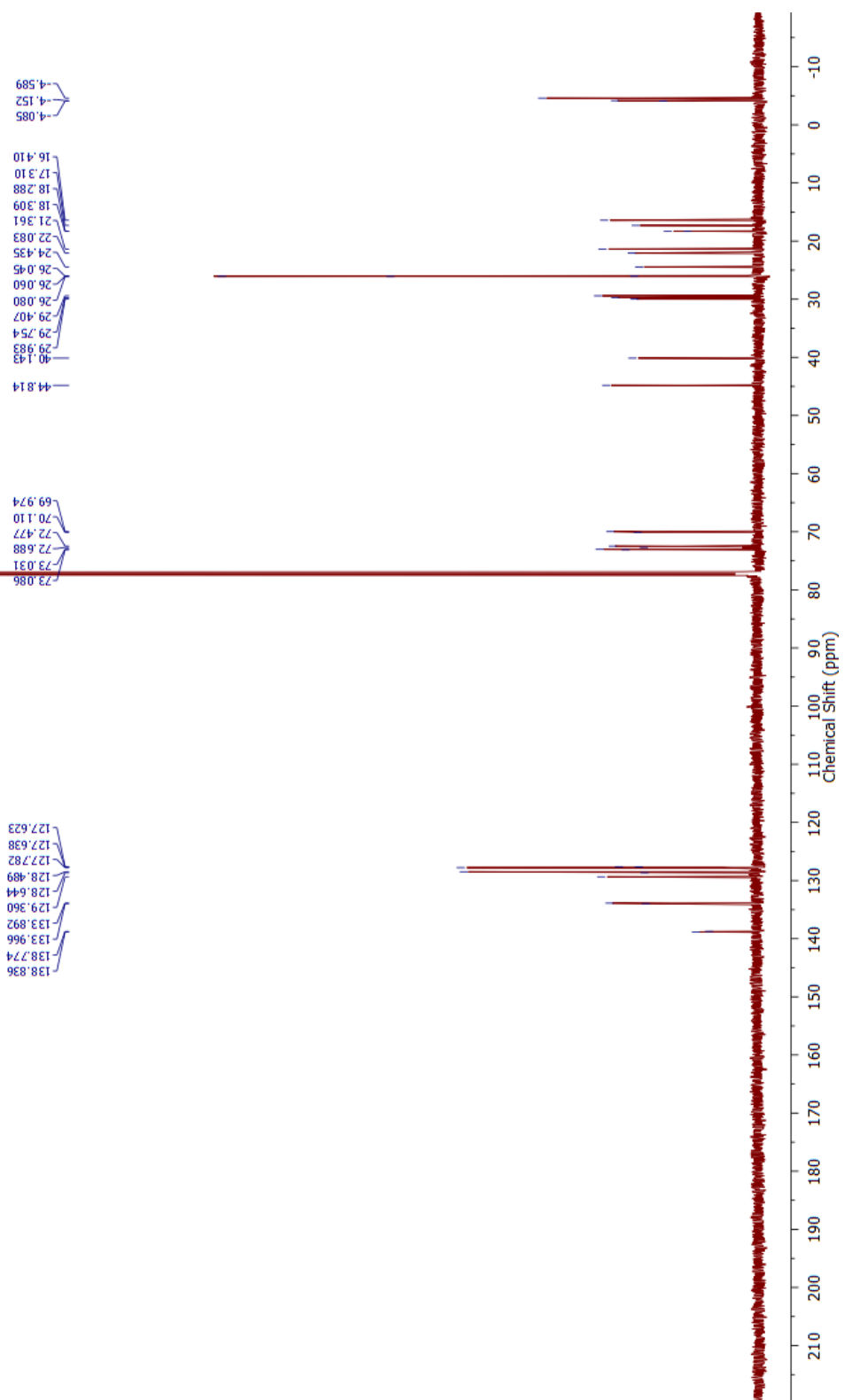
Appendix

¹H NMR (600 MHz, CDCl₃) Compound 228

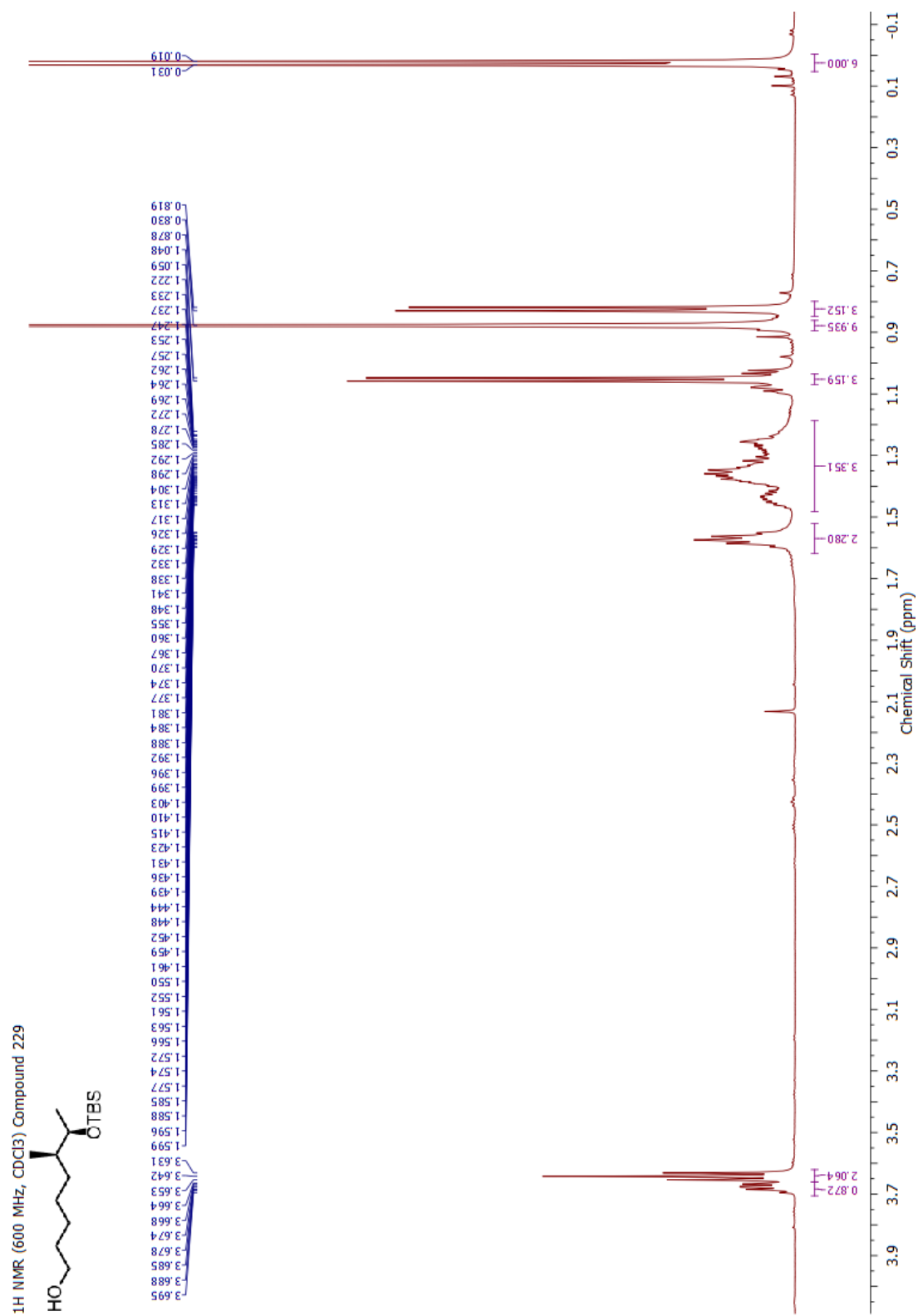


Appendix

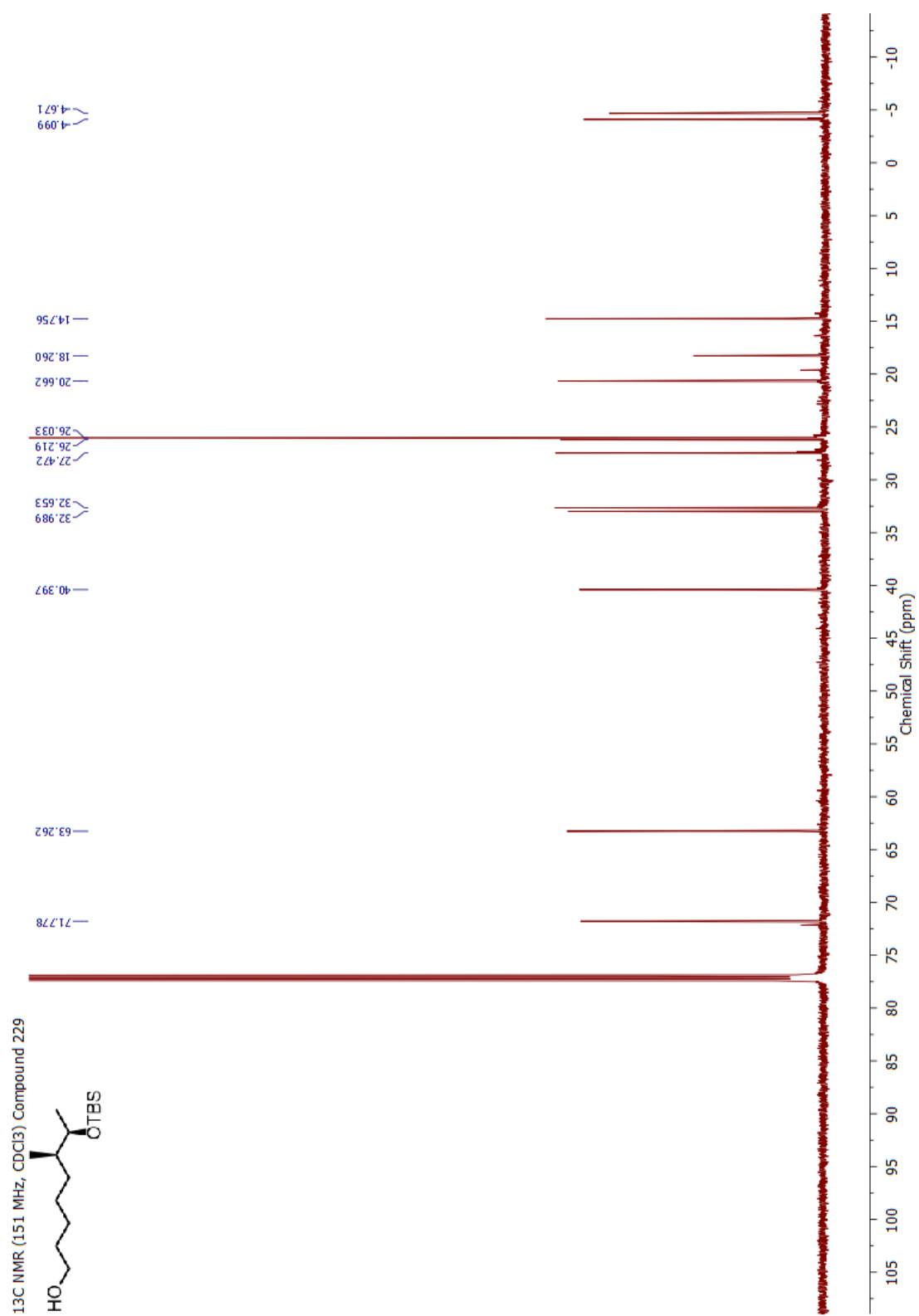
¹³C NMR (151 MHz, CDCl₃) Compound 228



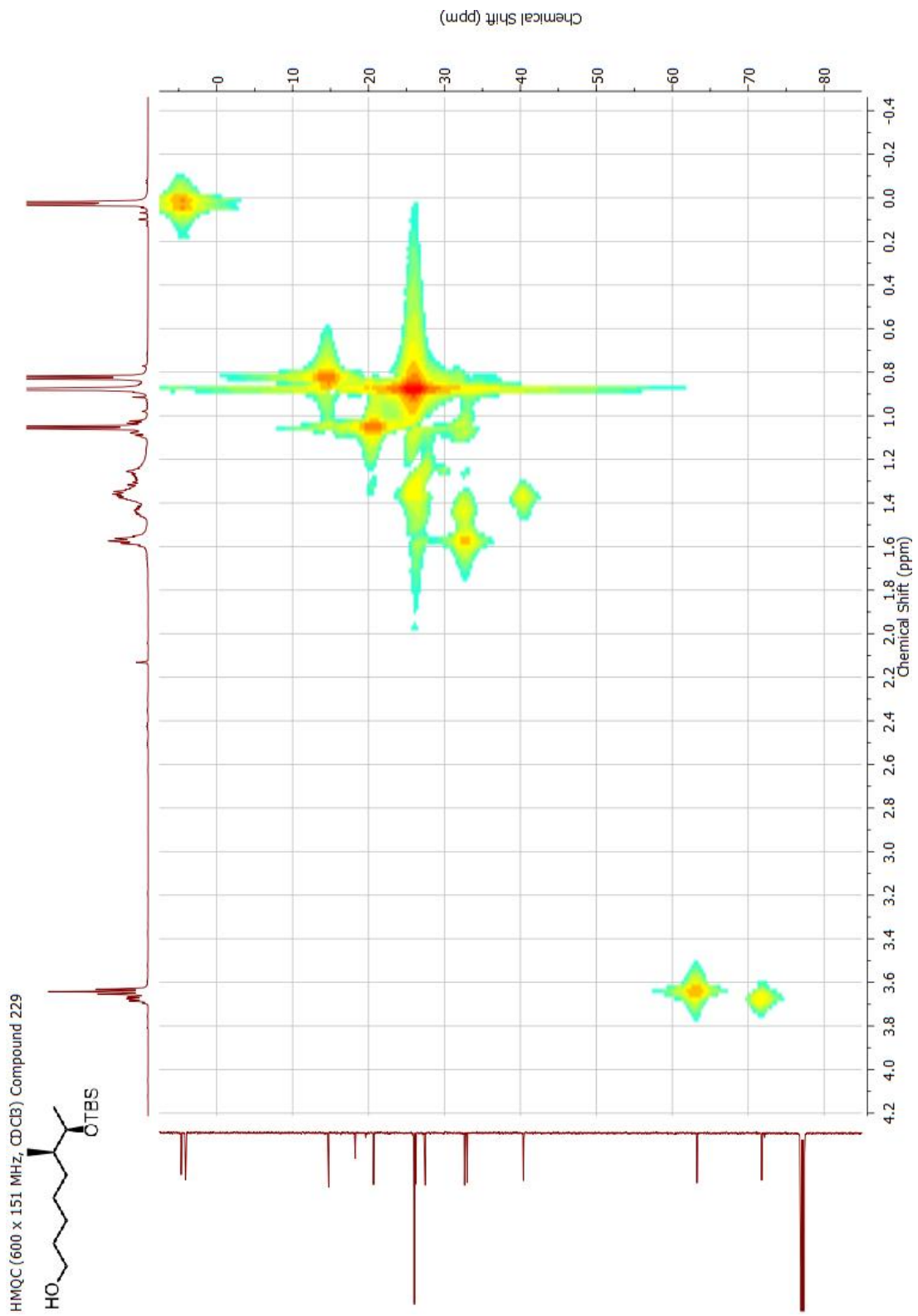
Appendix



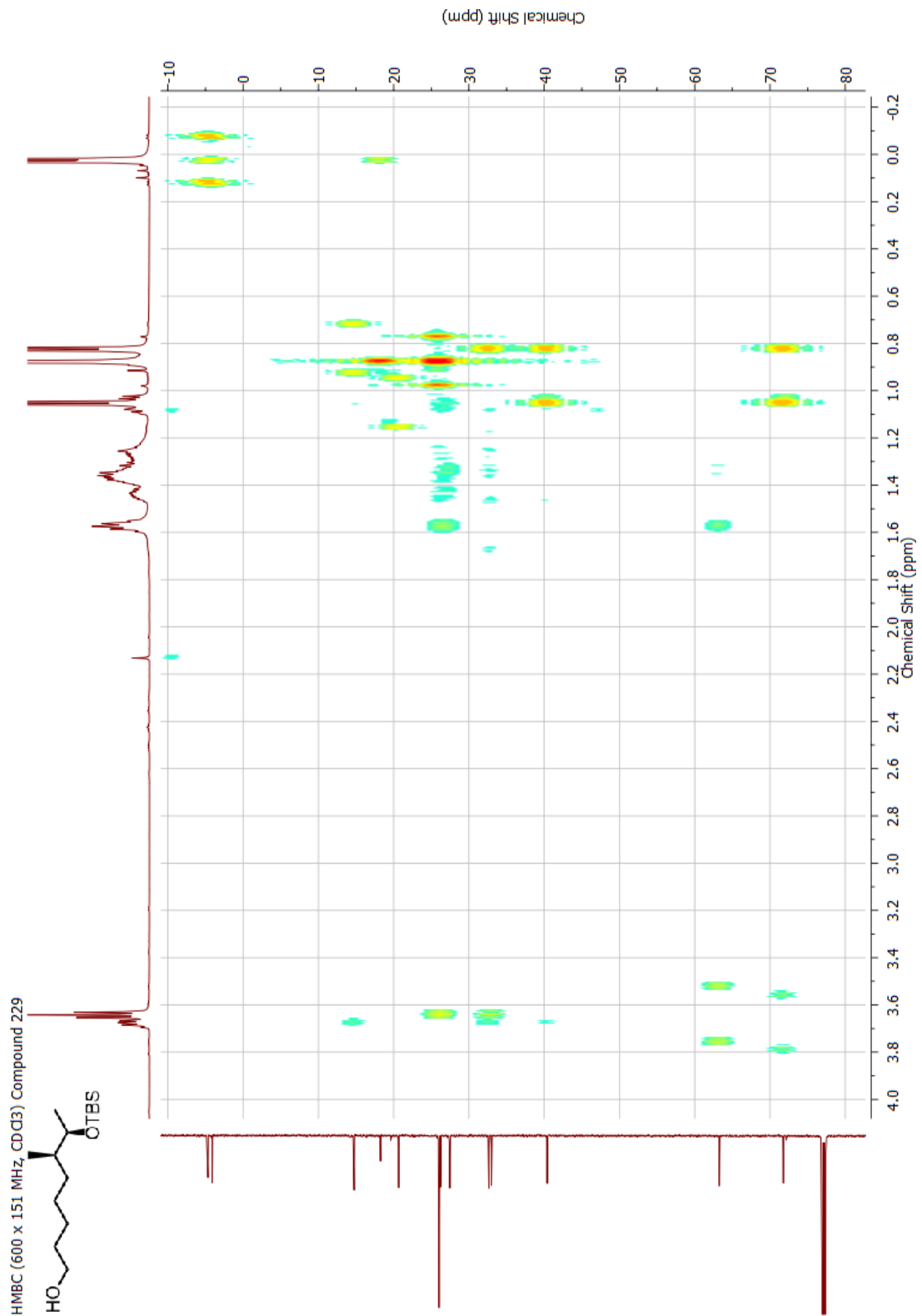
Appendix



Appendix

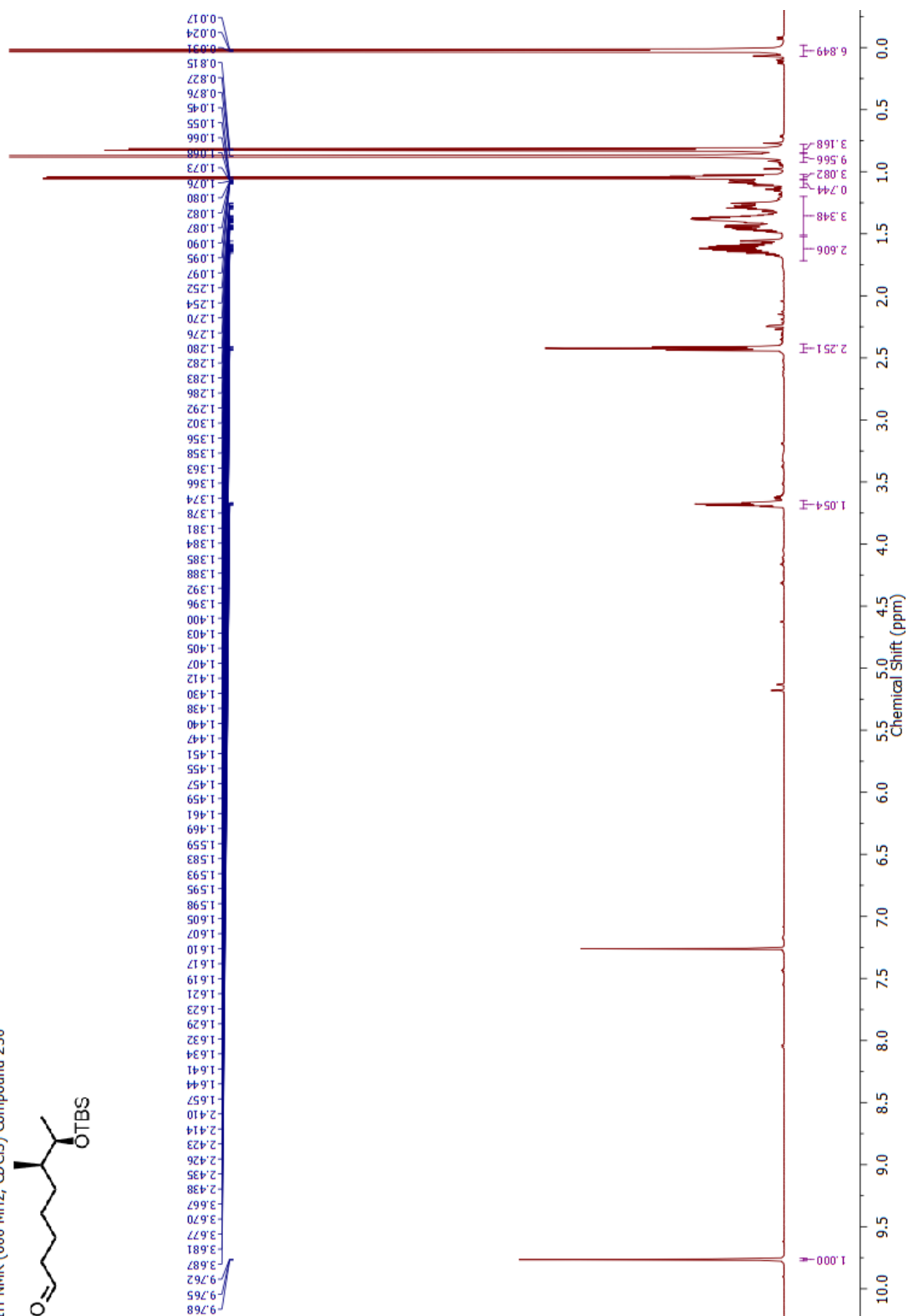


Appendix

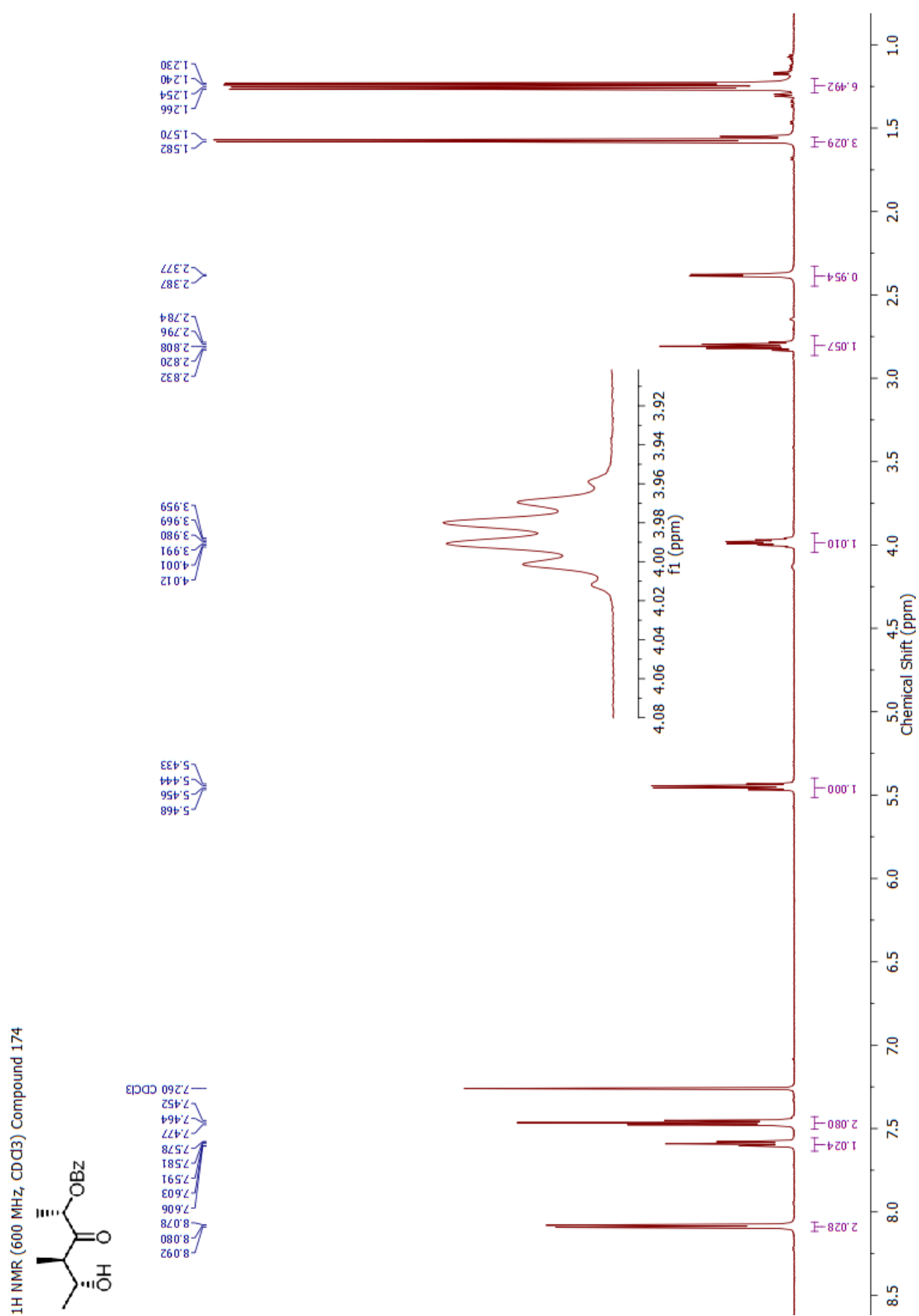


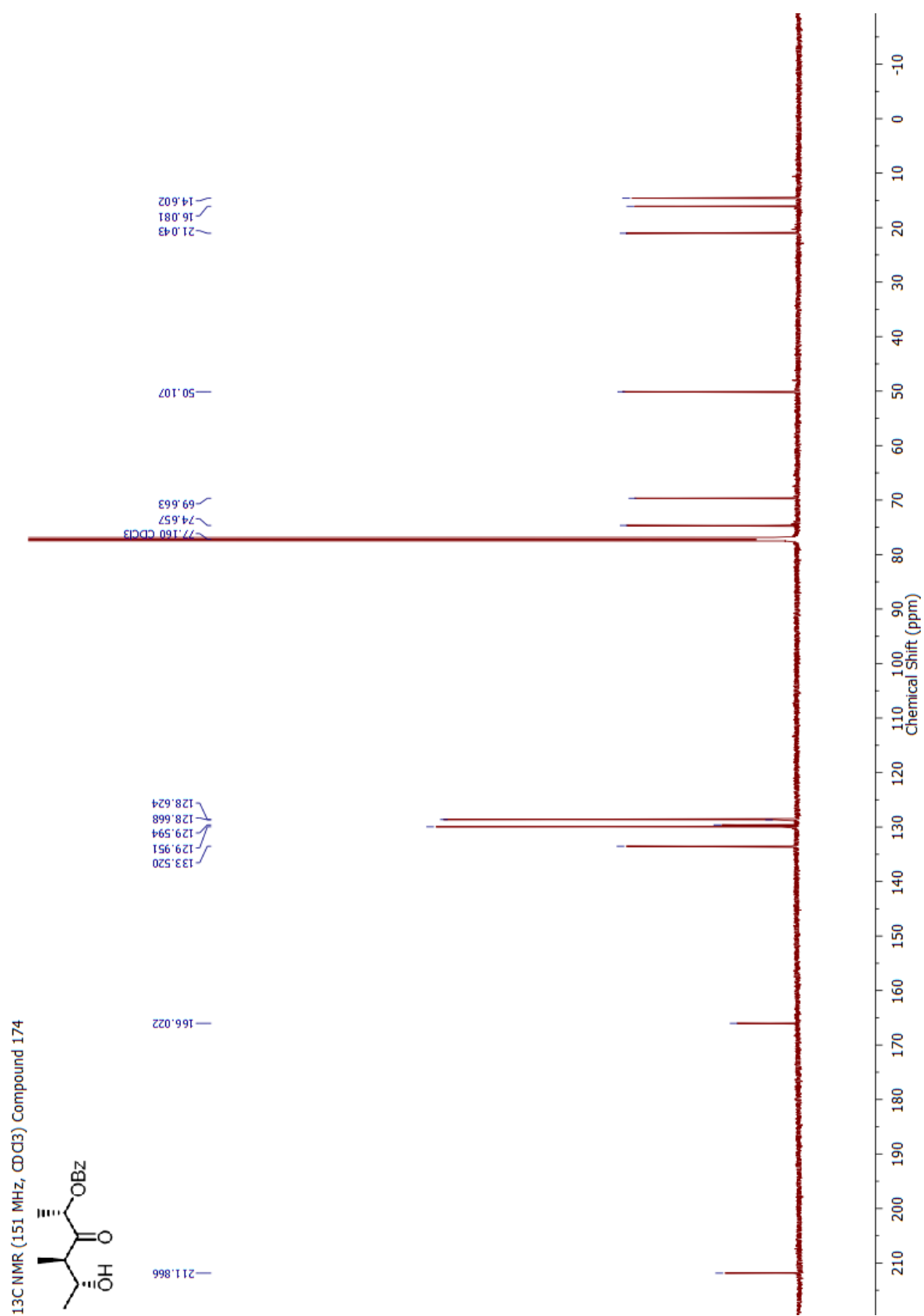
Appendix

¹H NMR (600 MHz, CDCl₃) Compound 230

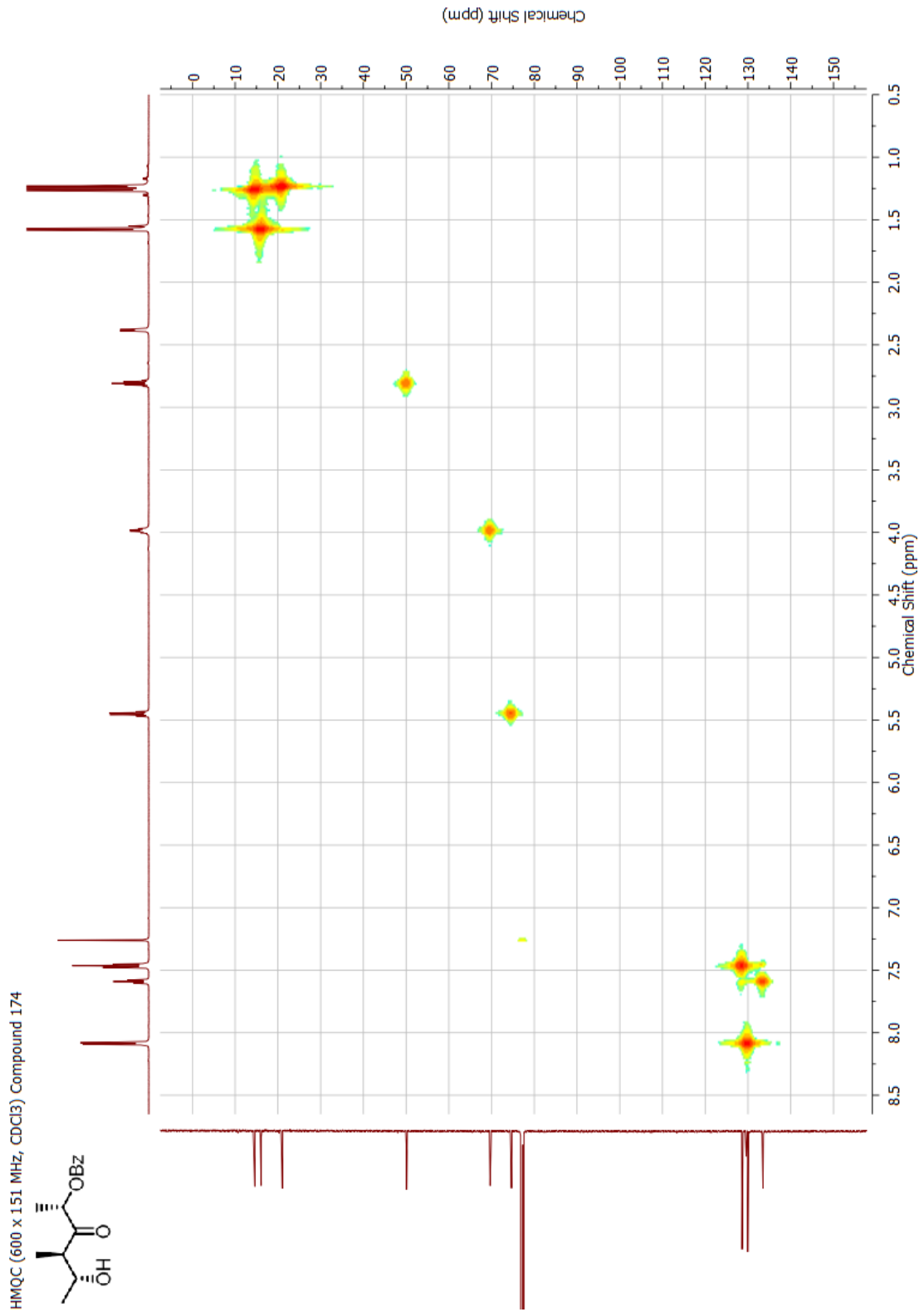


Appendix

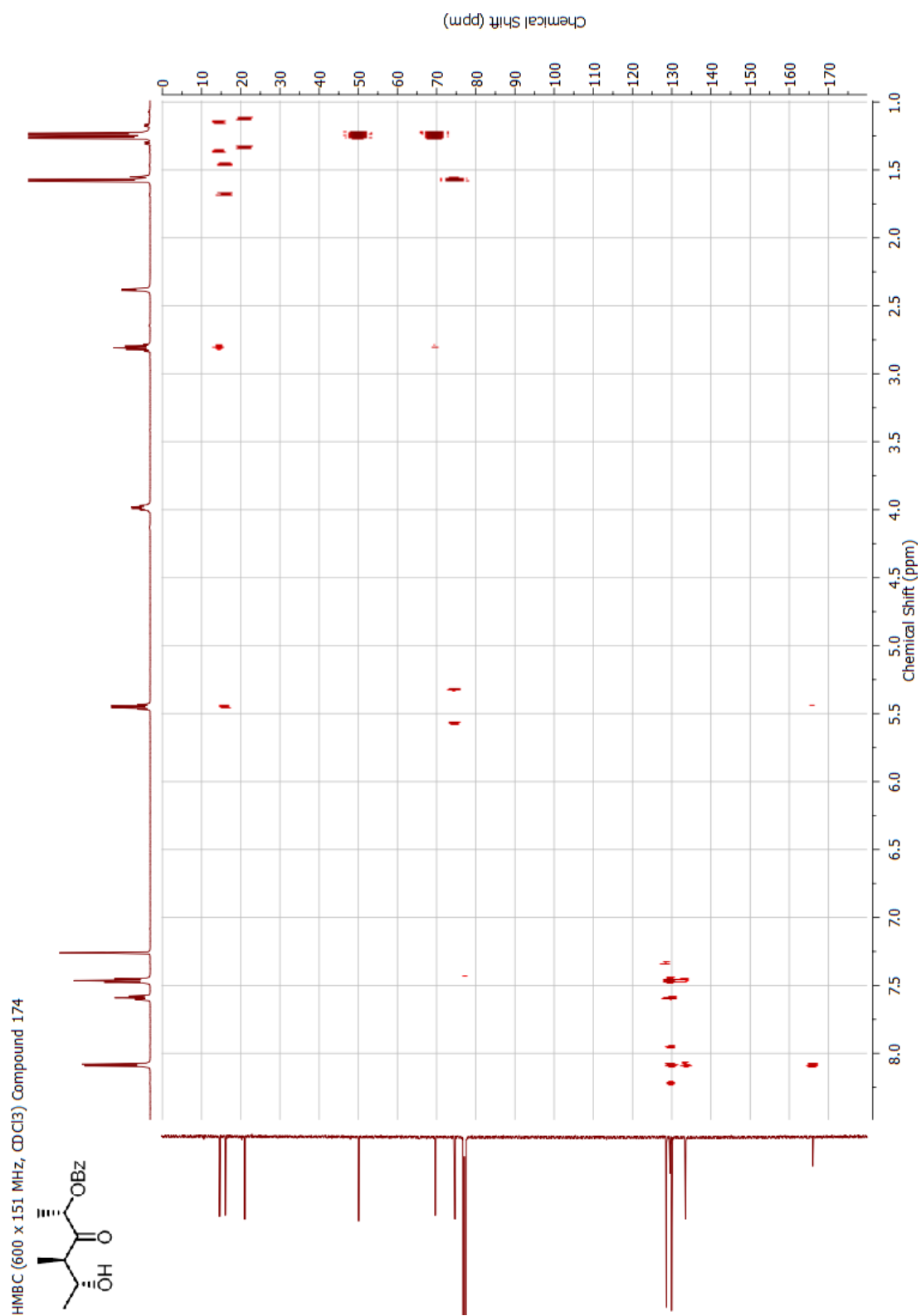




Appendix

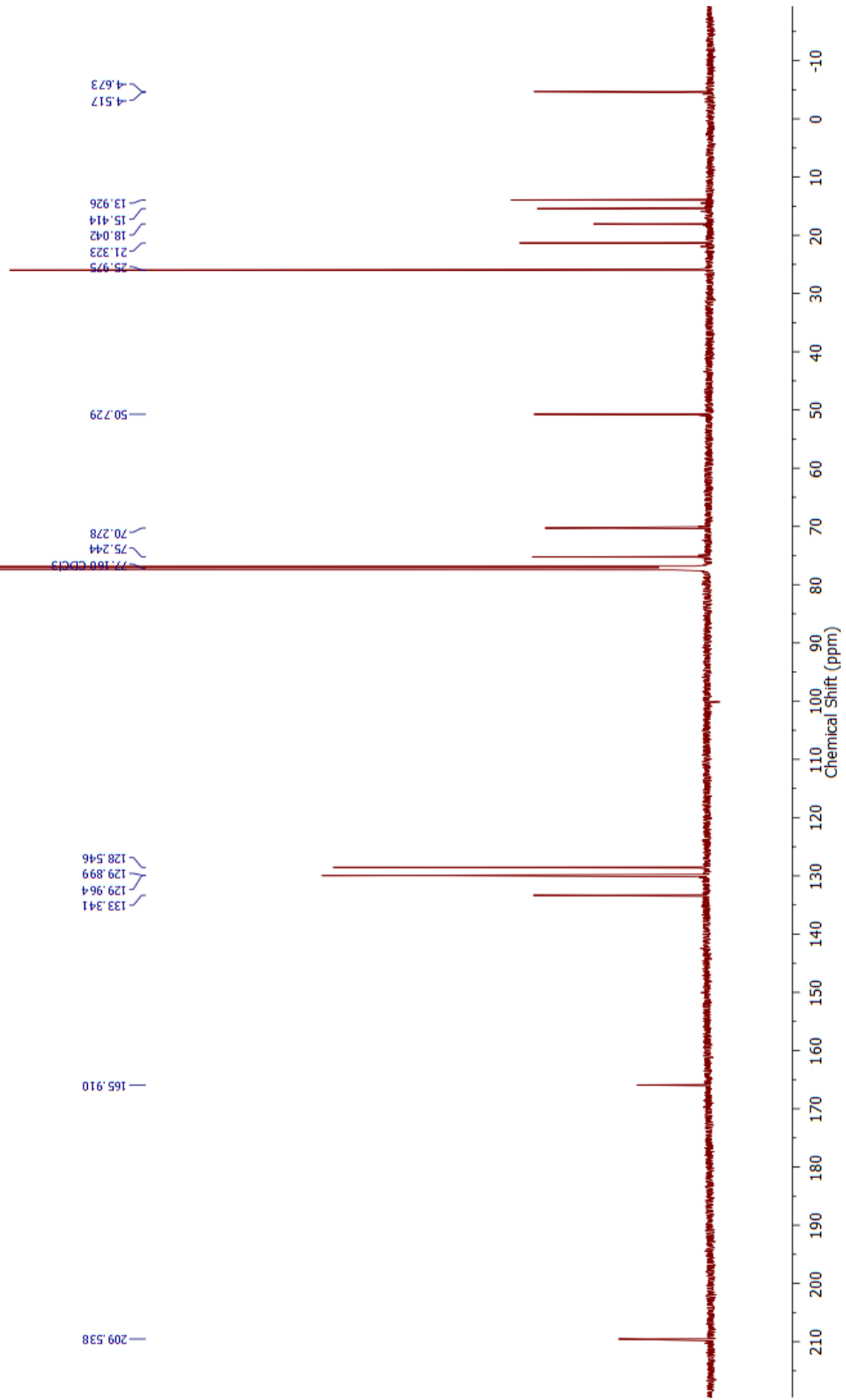
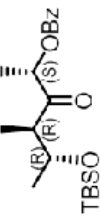


Appendix

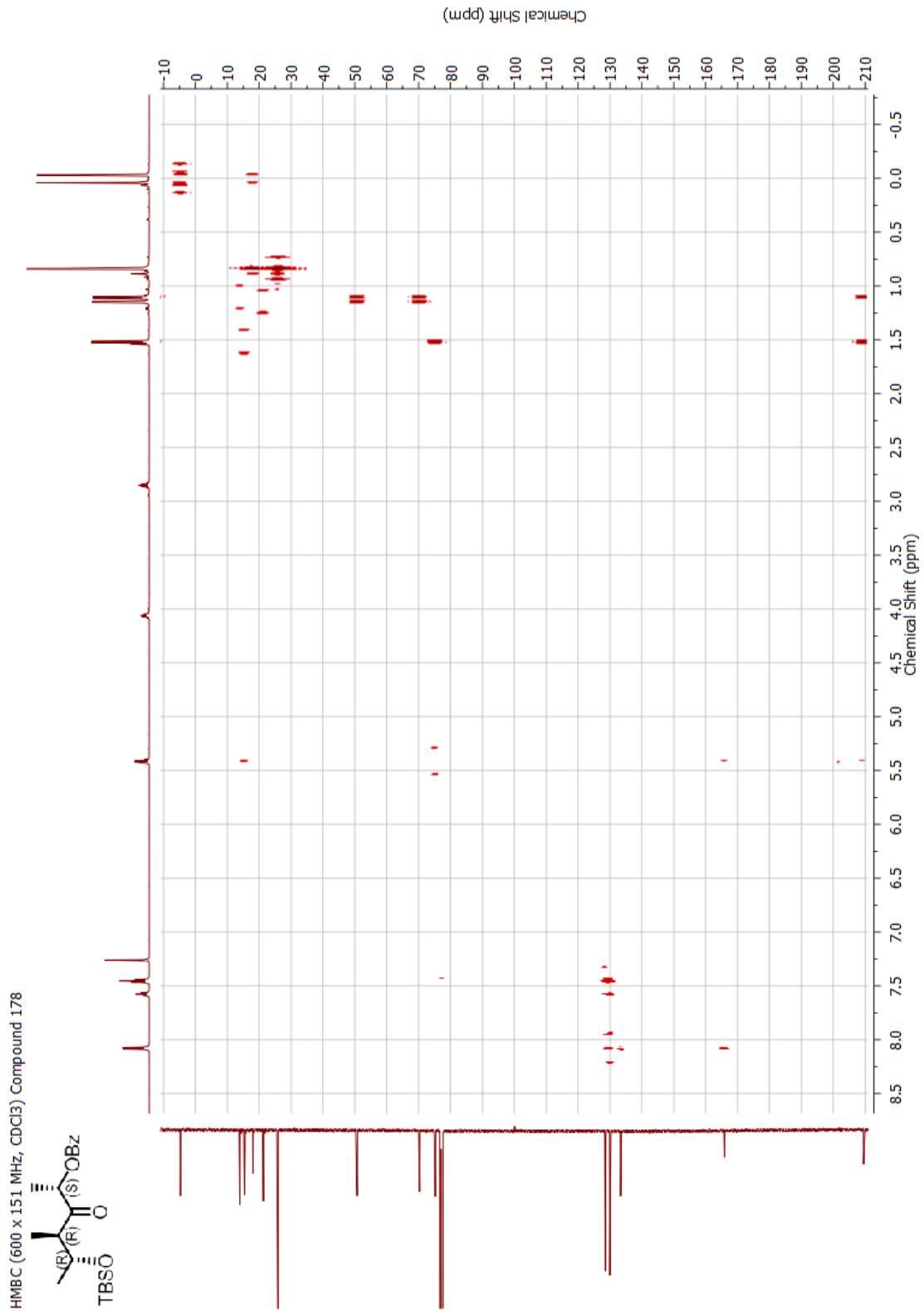


Appendix

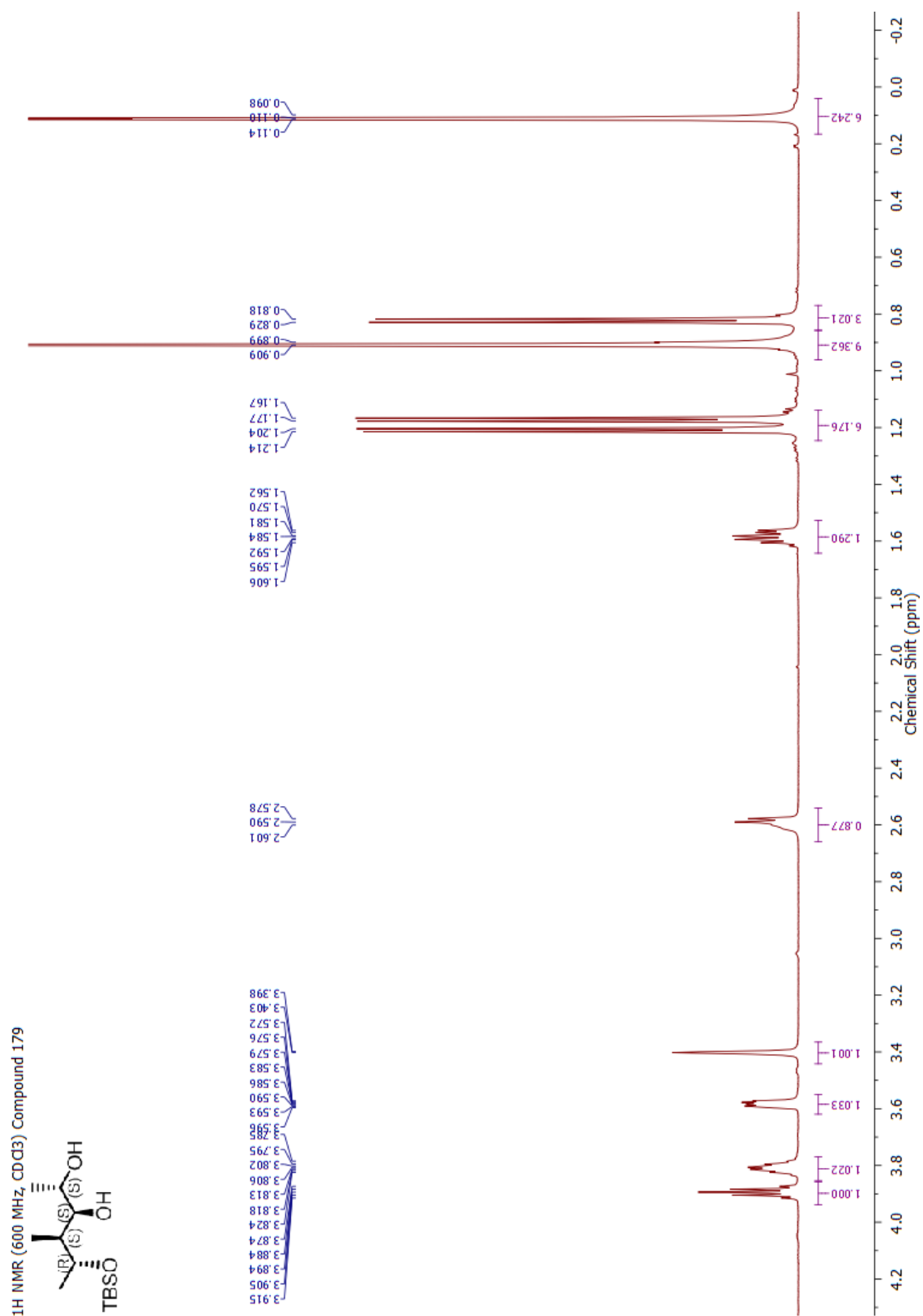
¹³C NMR (151 MHz, CDCl₃) Compound 178



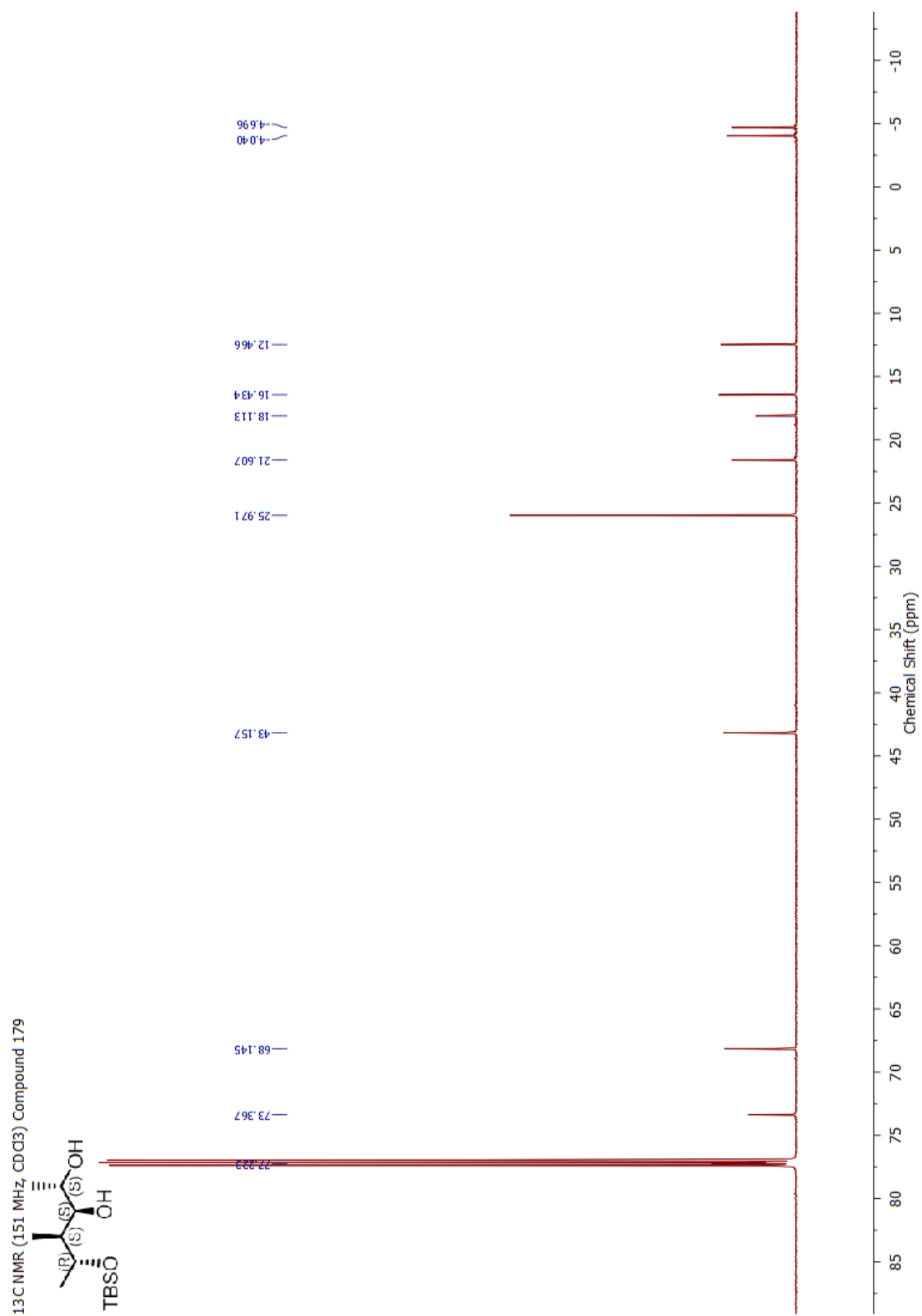
Appendix



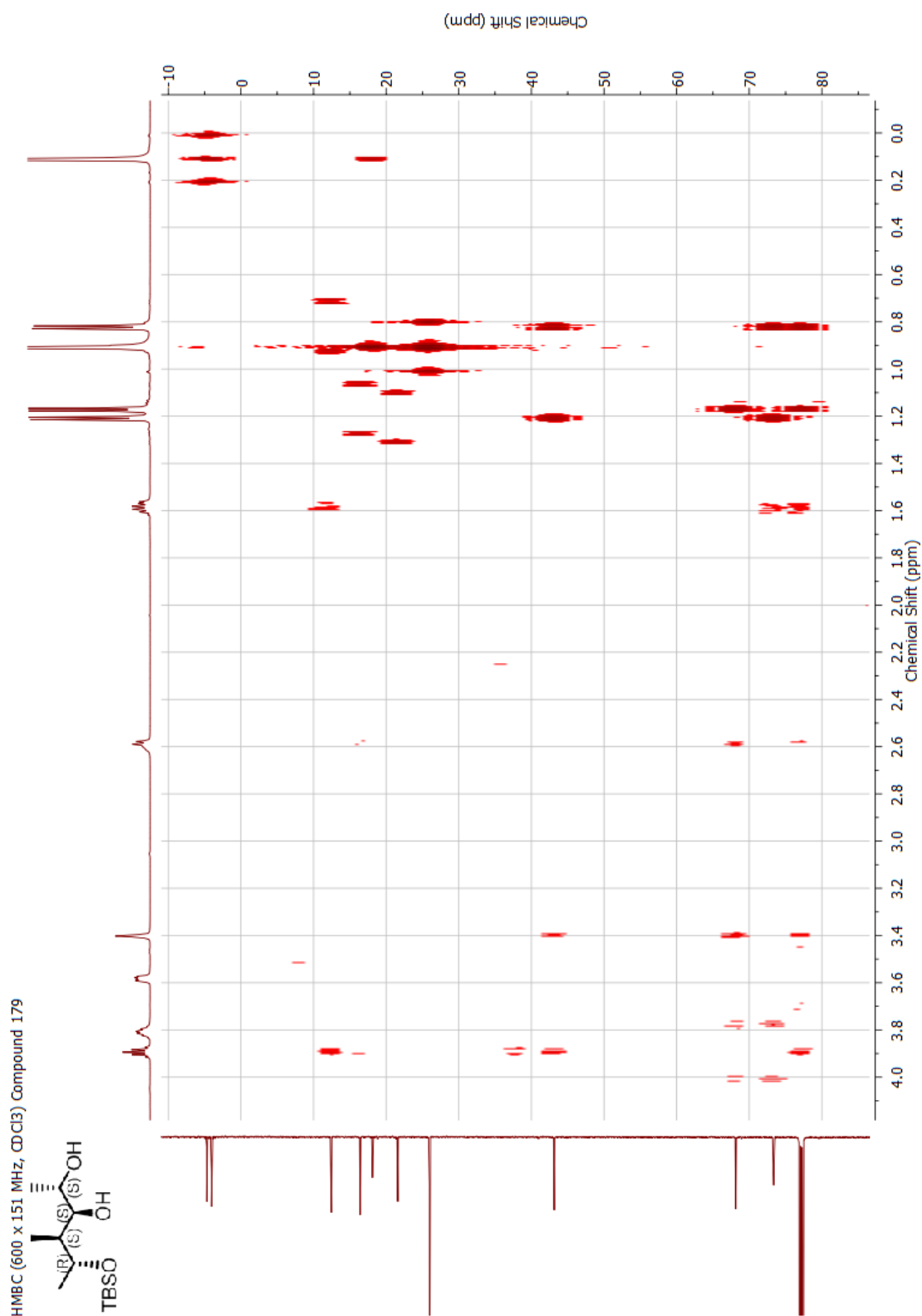
Appendix



Appendix

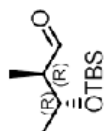


Appendix



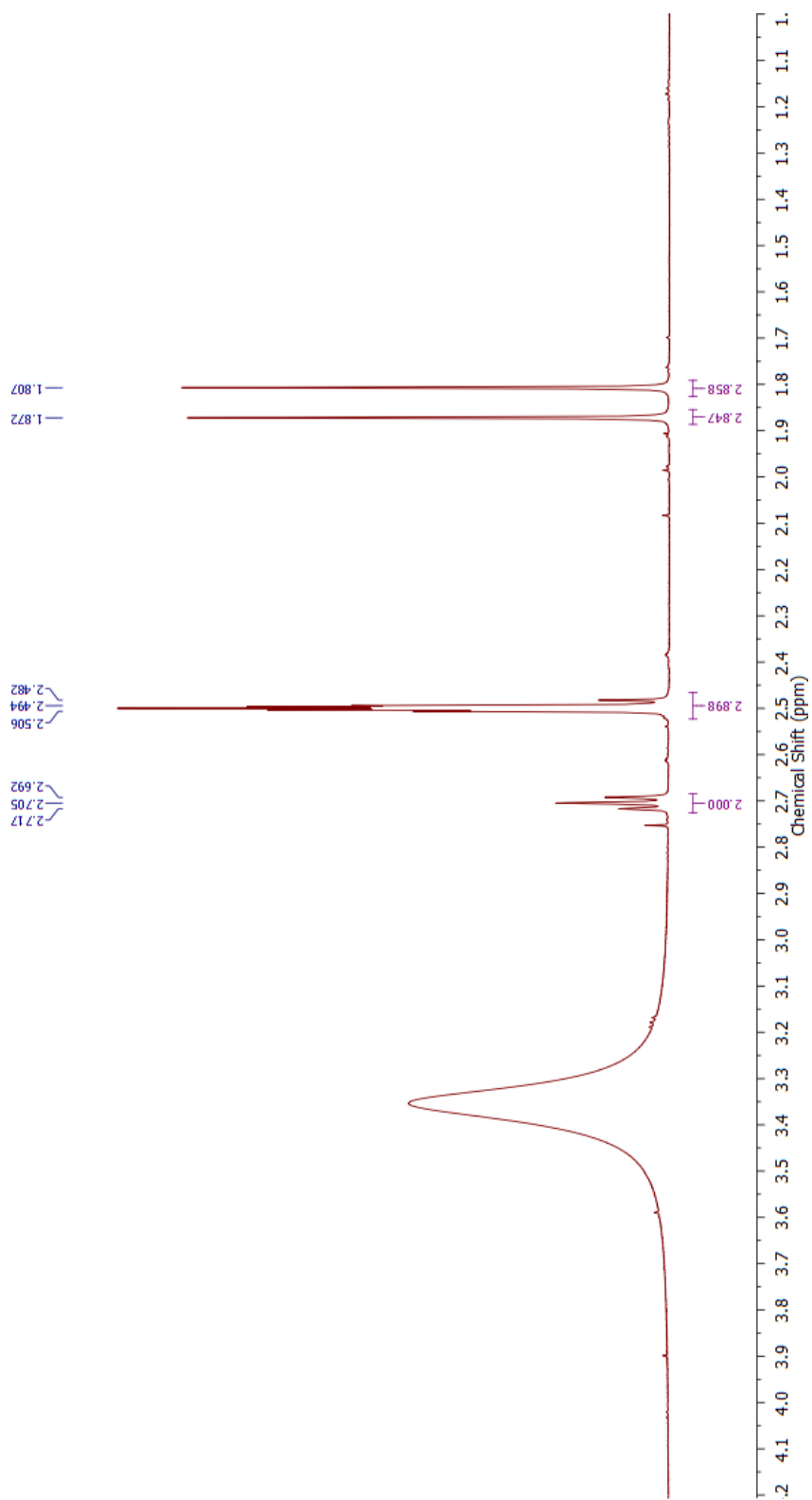
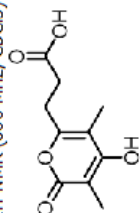
Appendix

¹H NMR (600 MHz, CDCl₃) Compound 180

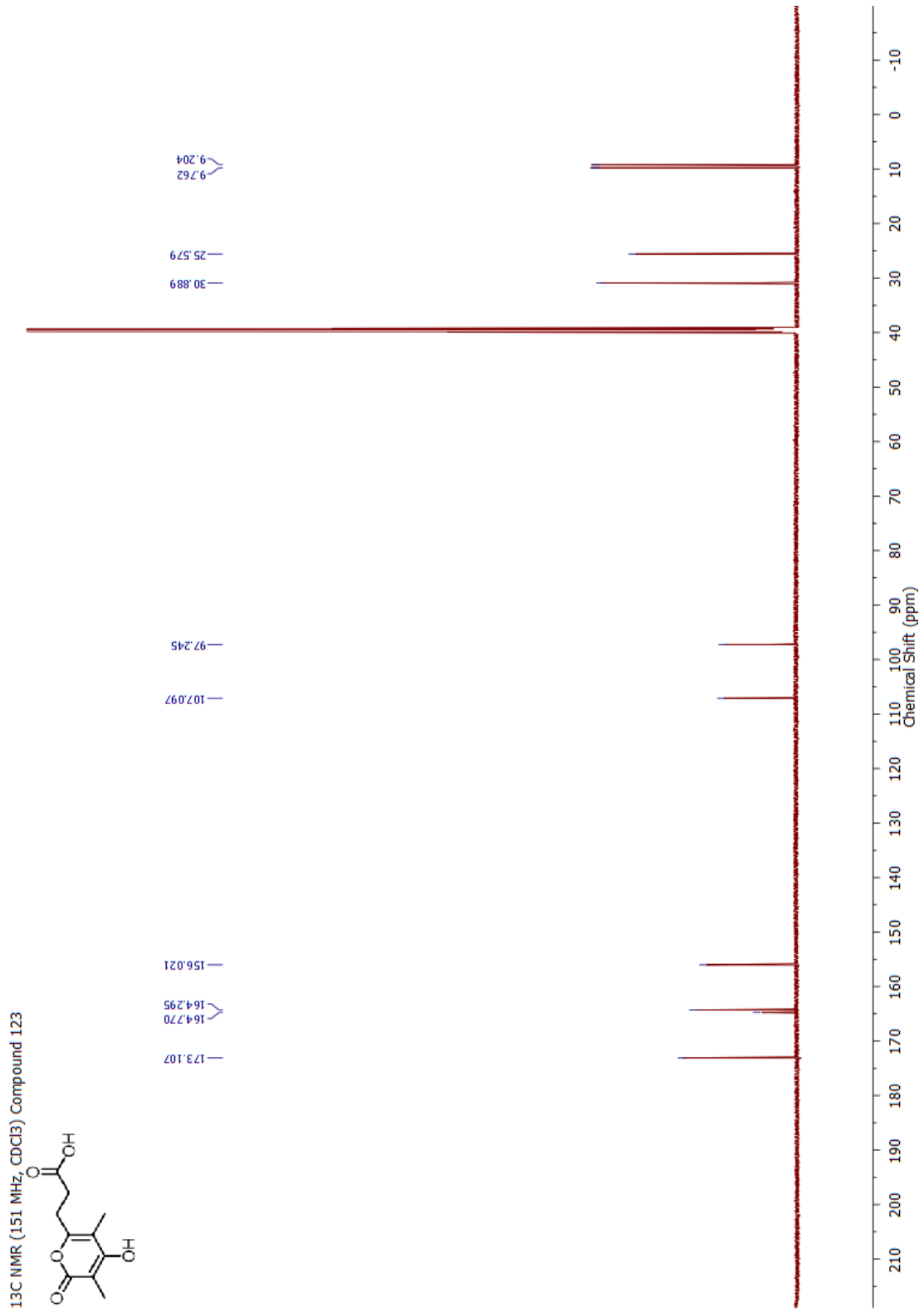


Appendix

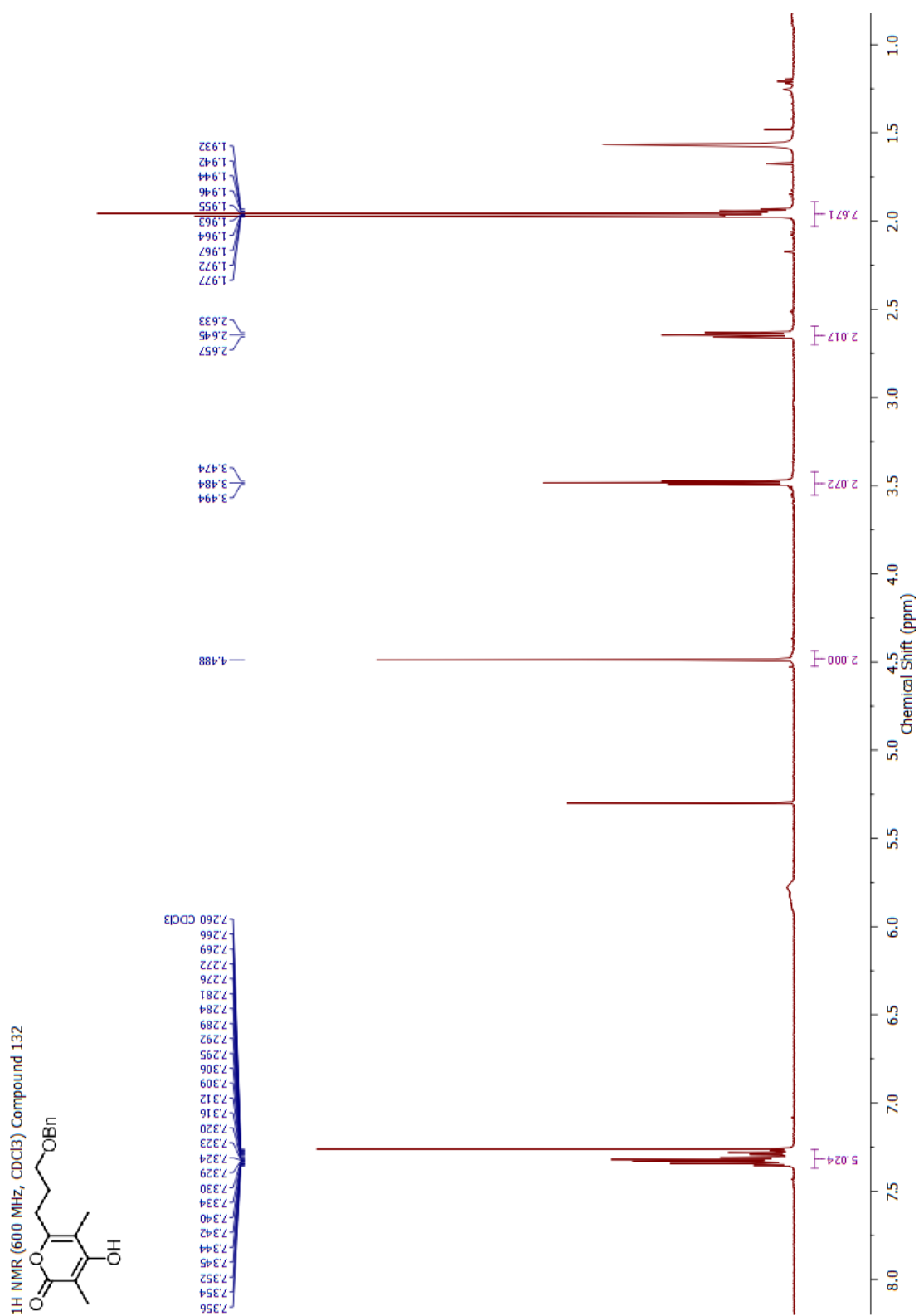
¹H NMR (600 MHz, CDCl₃) Compound 123



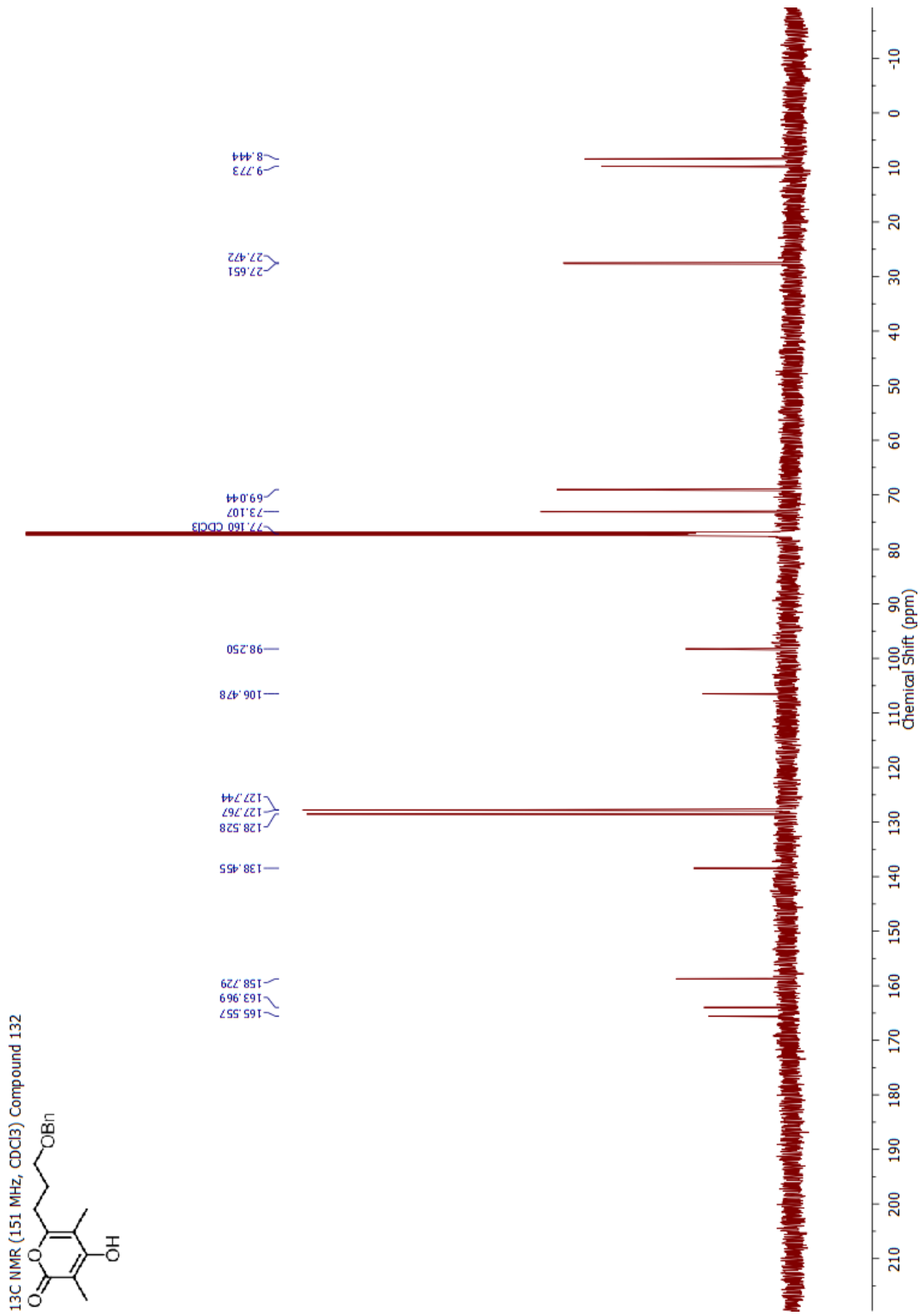
Appendix



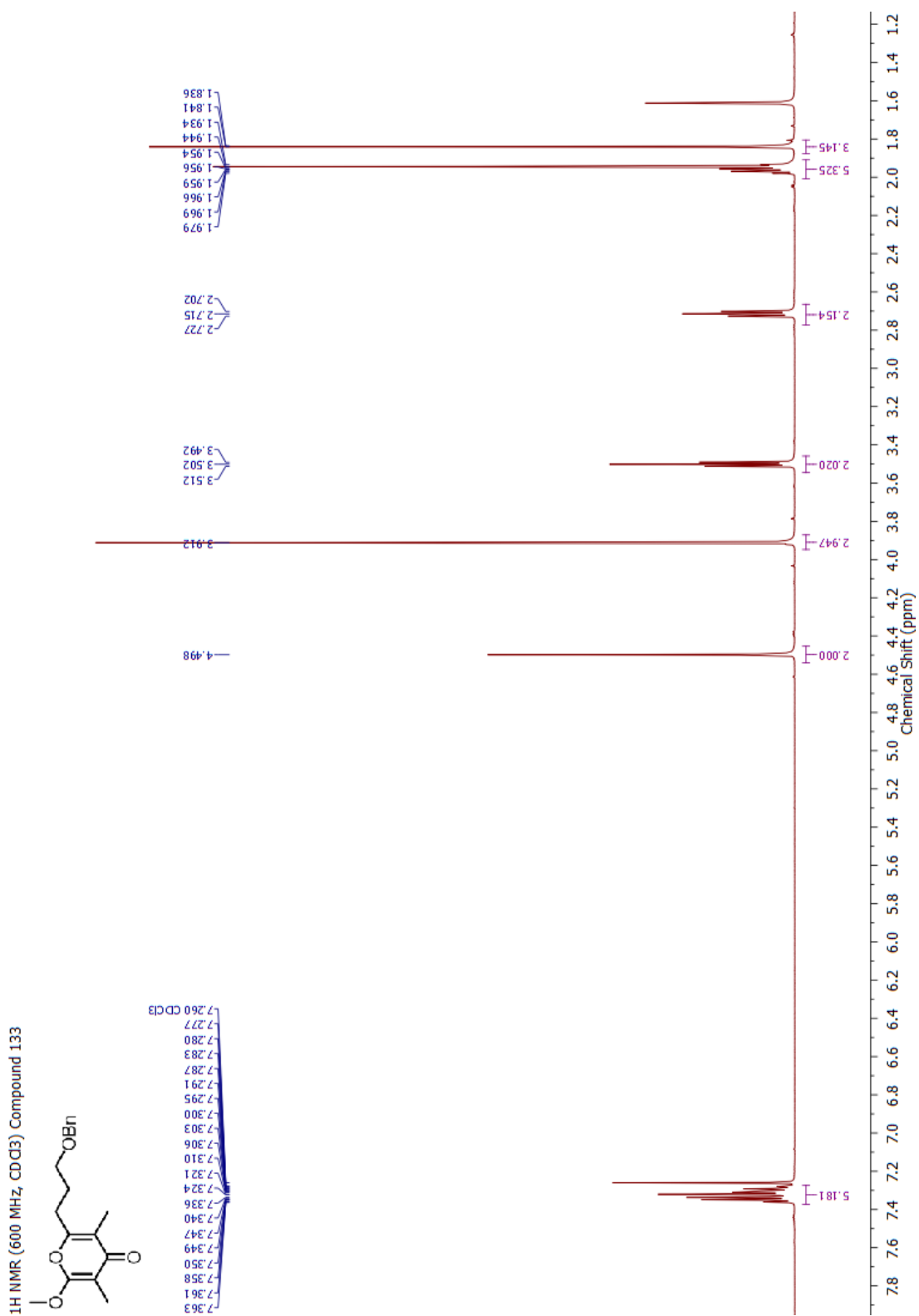
Appendix

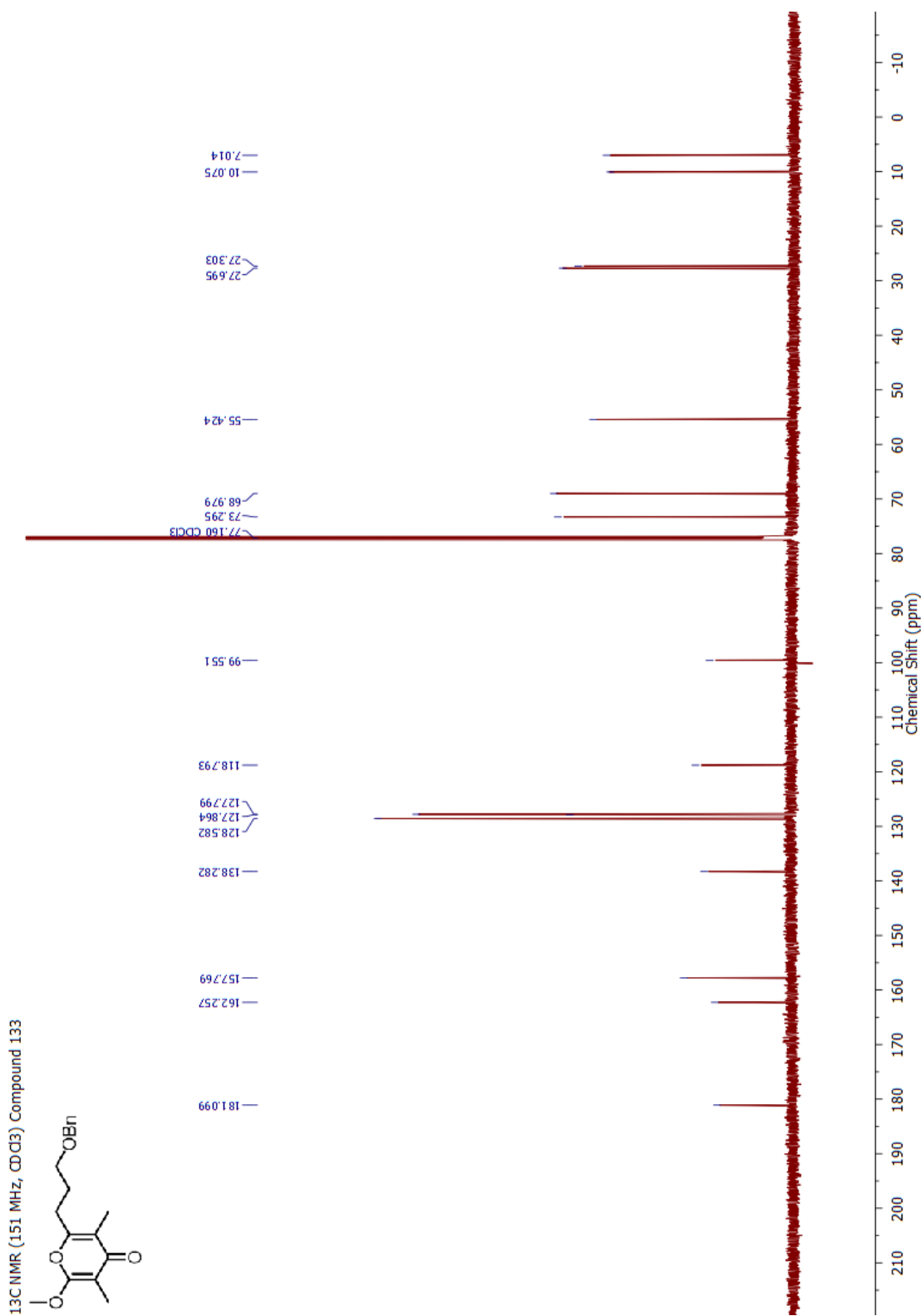


Appendix



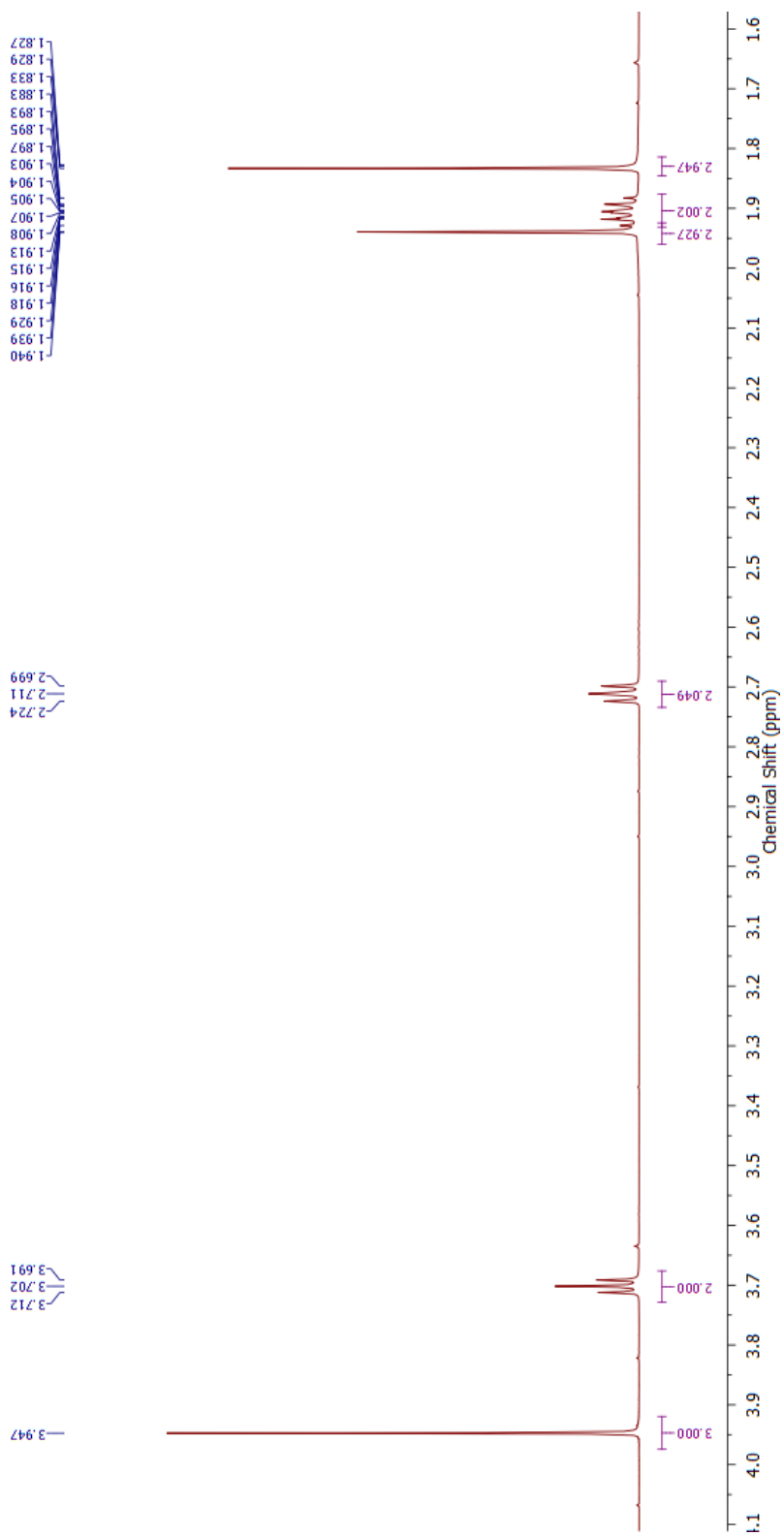
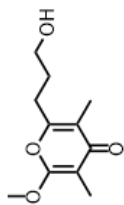
Appendix



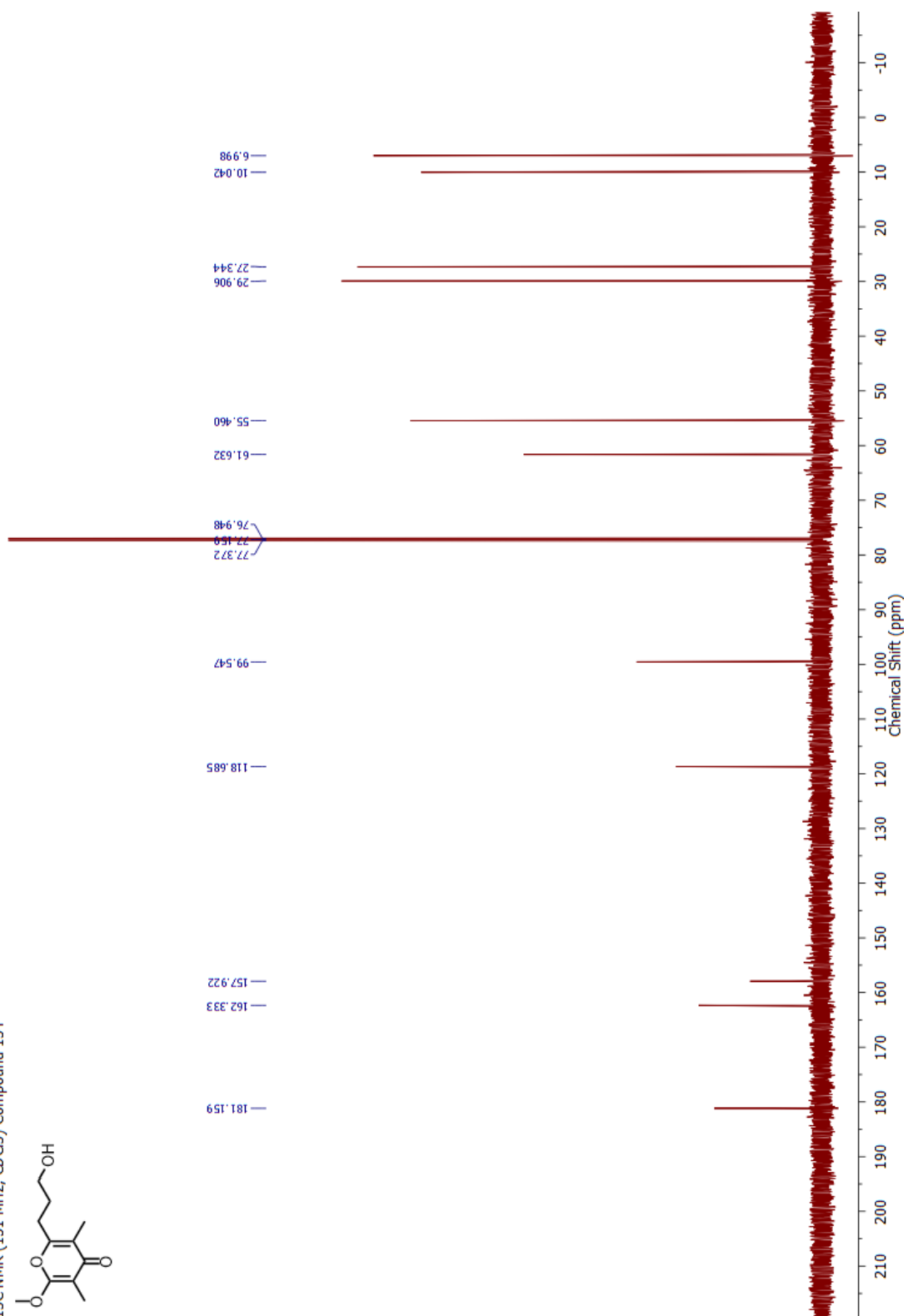
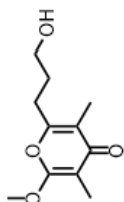


Appendix

¹H NMR (600 MHz, CDCl₃) Compound 134

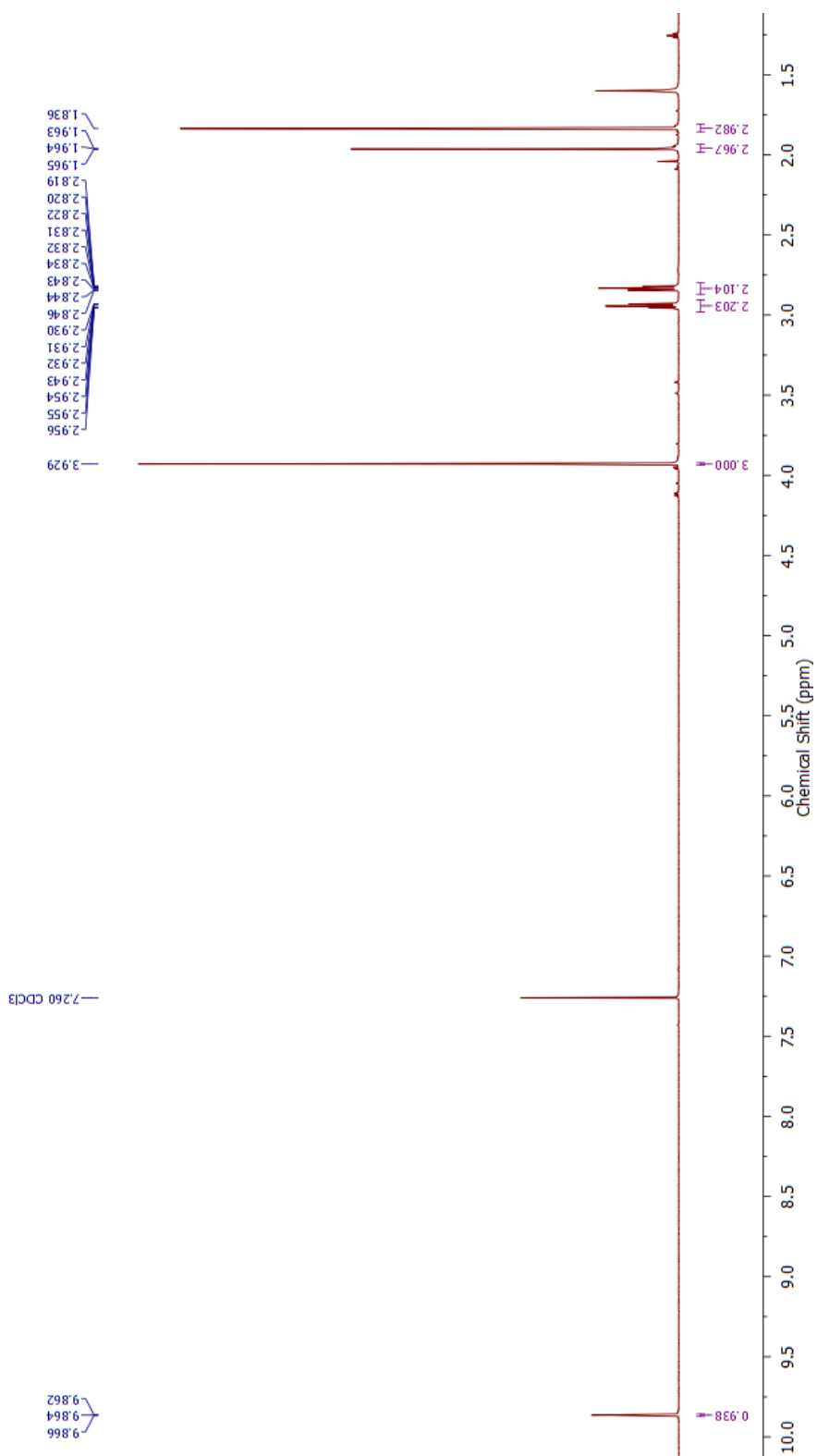
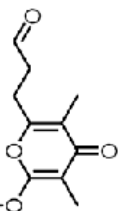


¹³C NMR (151 MHz, CDCl₃) Compound 134

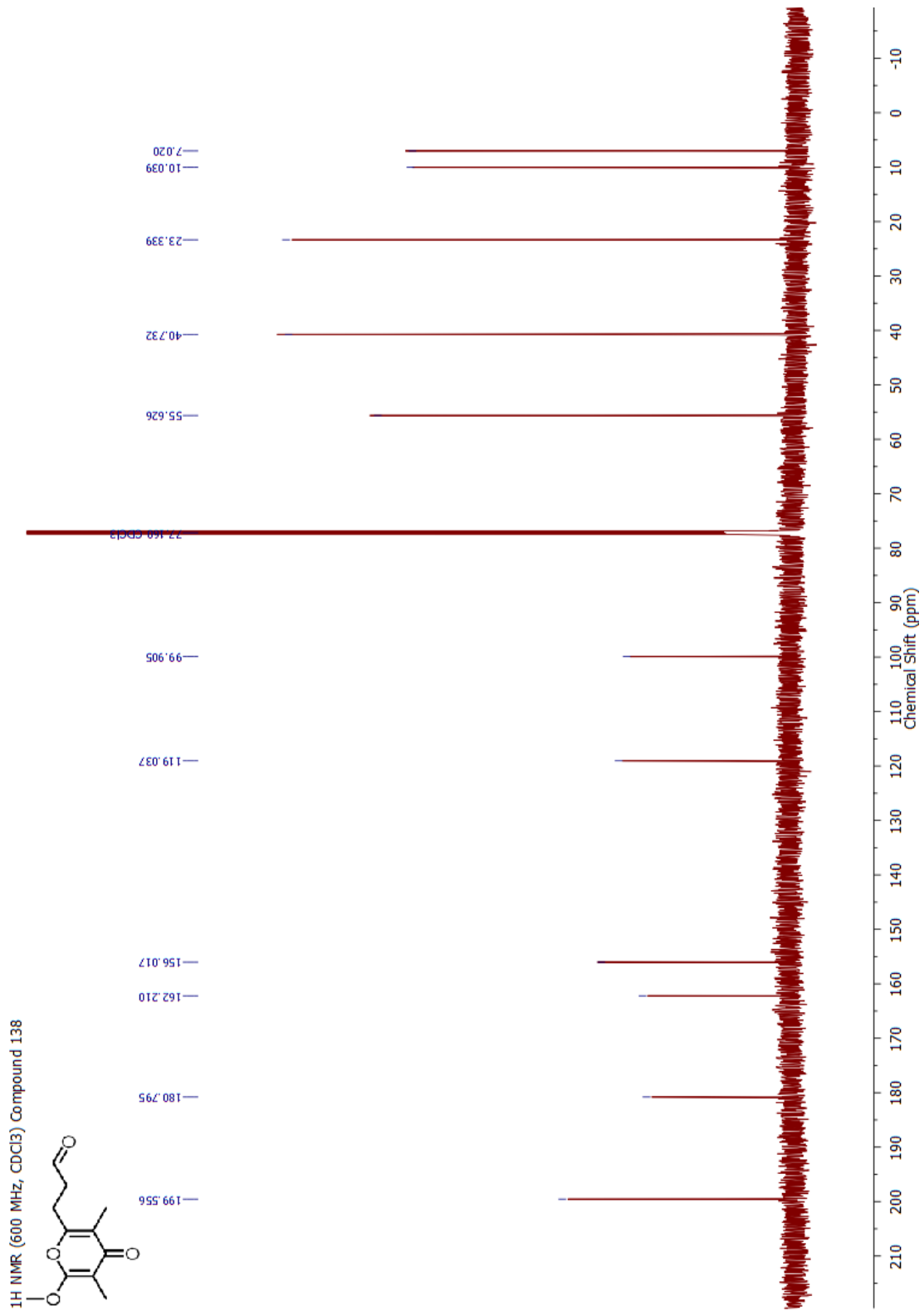


Appendix

¹H NMR (600 MHz, CDCl₃) Compound 138

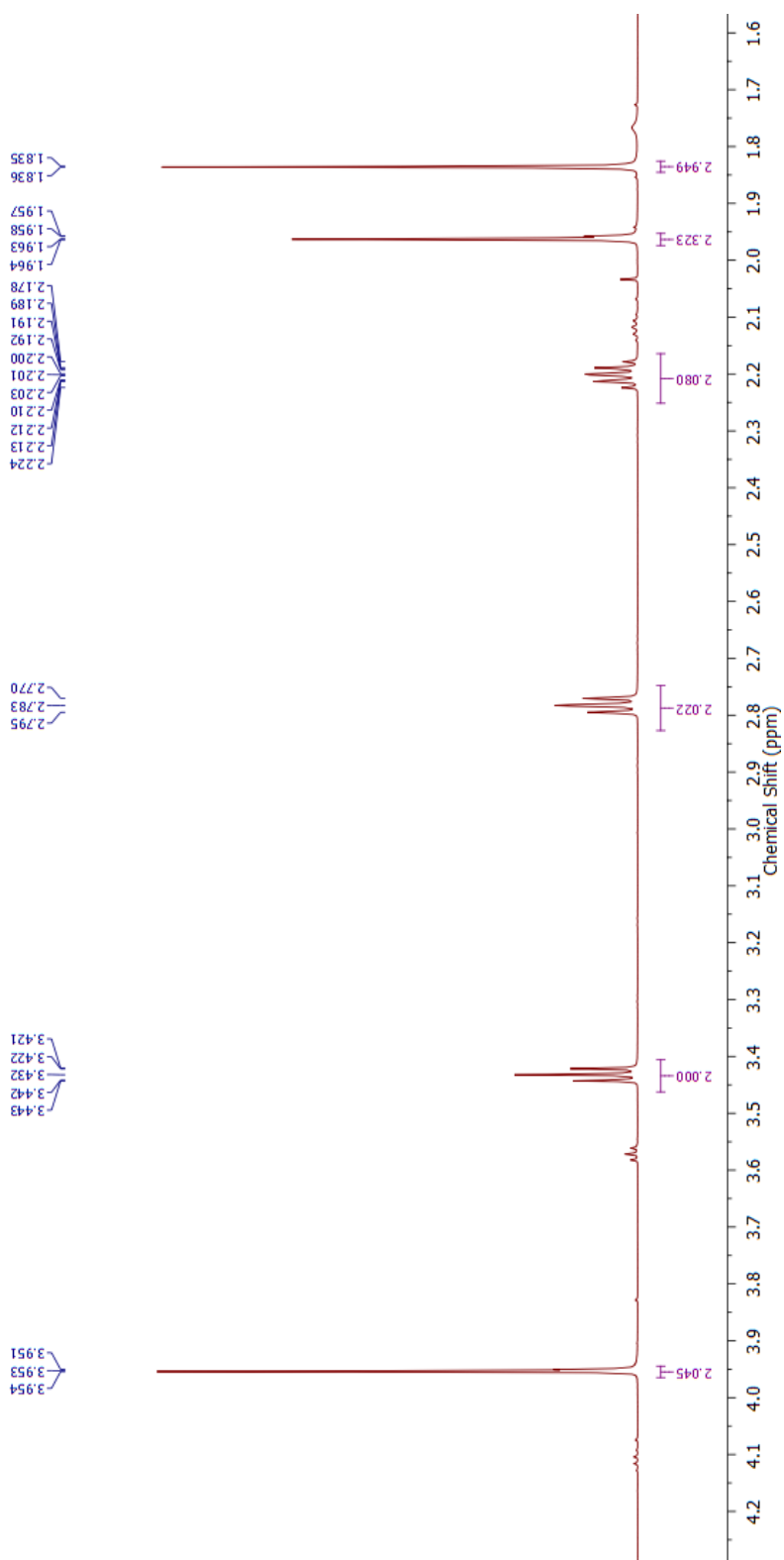
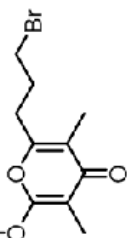


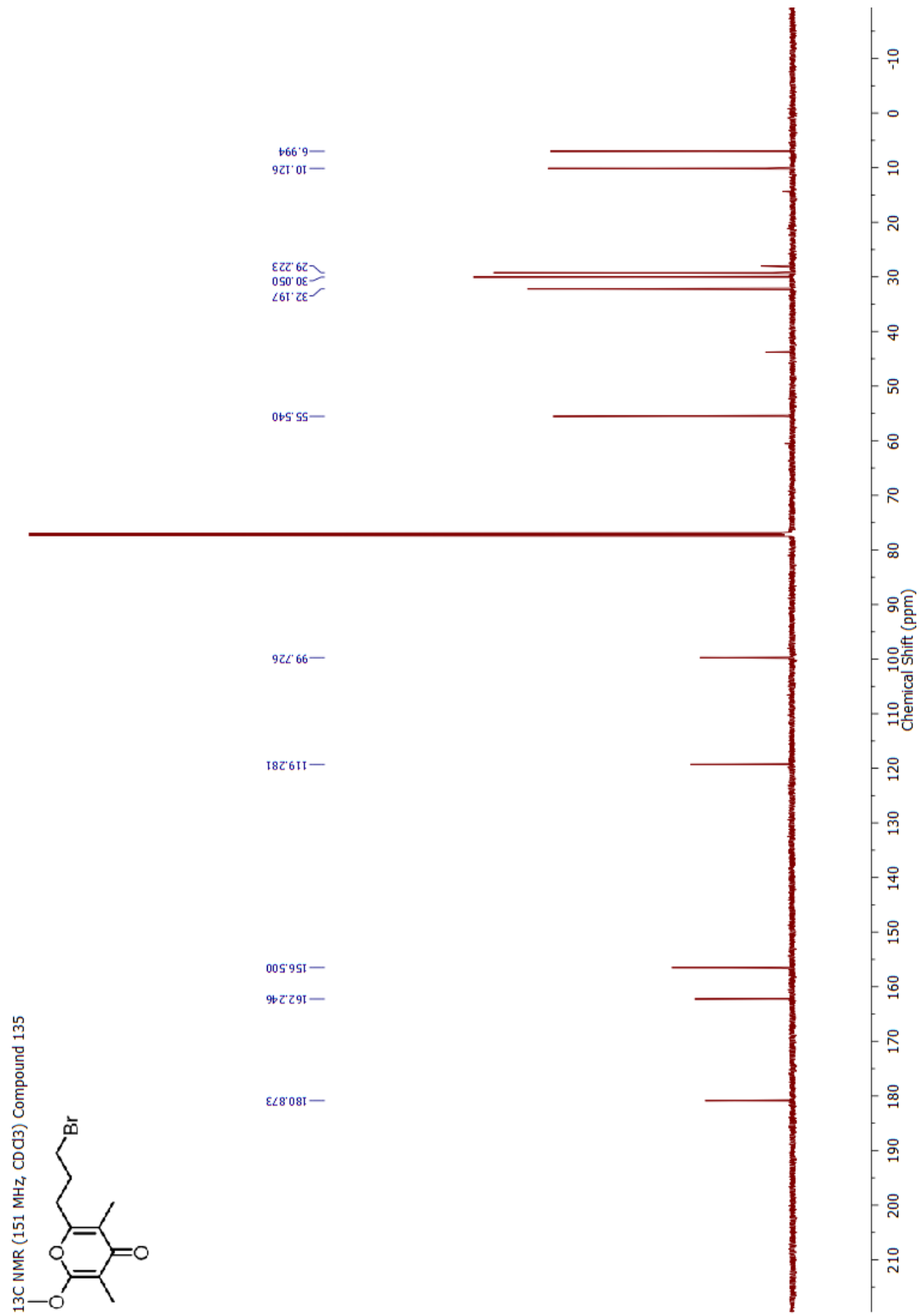
Appendix



Appendix

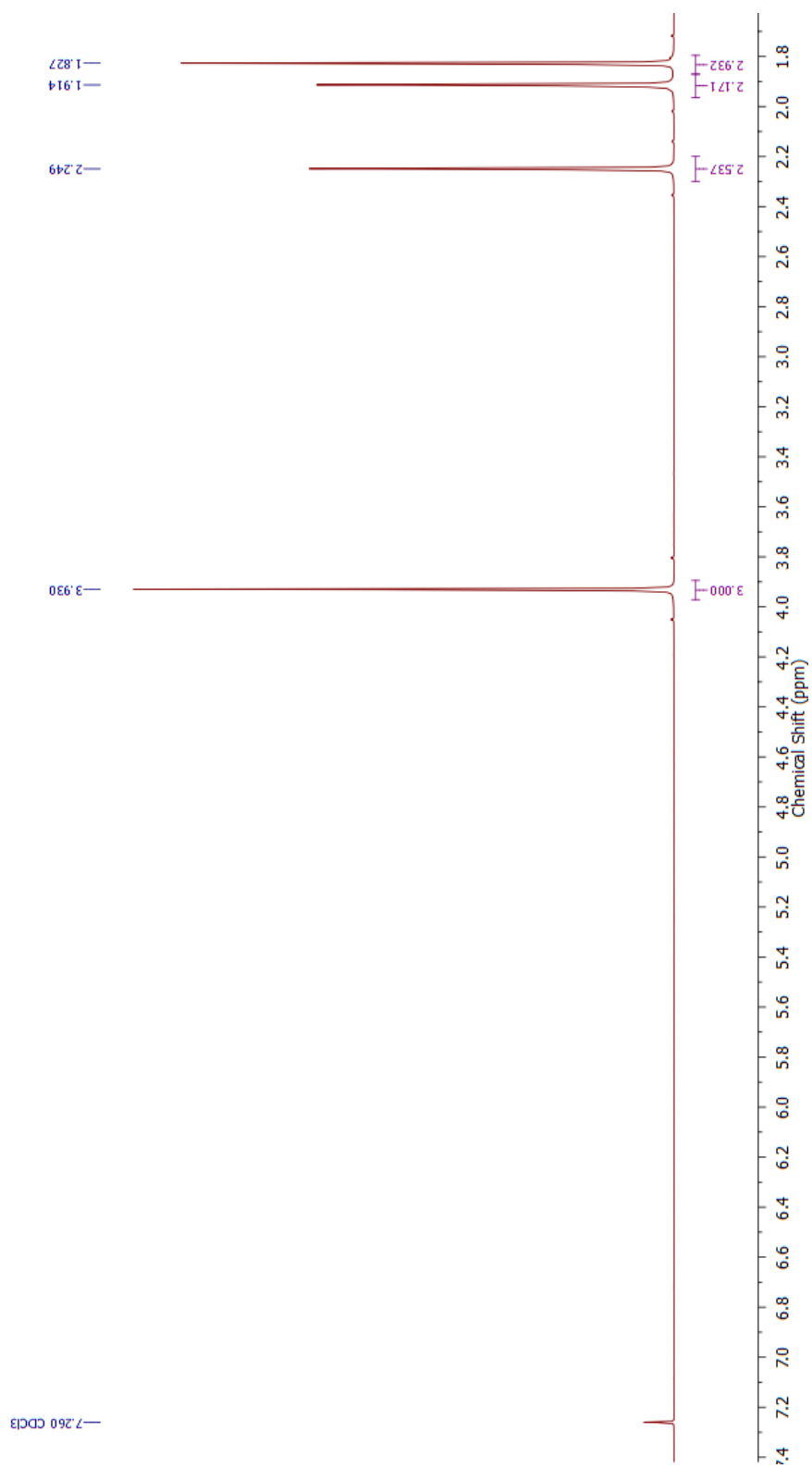
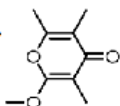
¹H NMR (600 MHz, CDCl₃) Compound 135



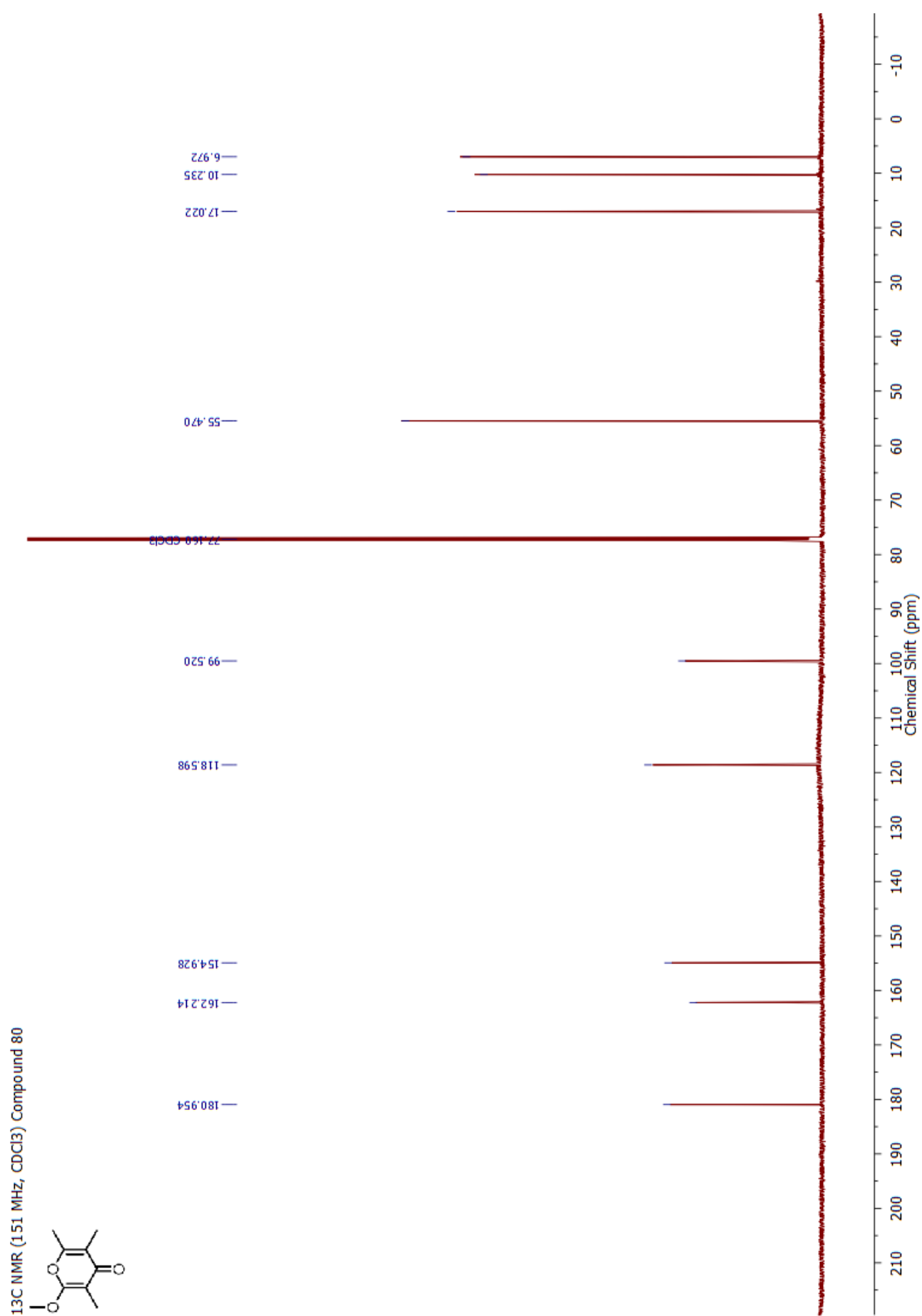


Appendix

¹H NMR (600 MHz, CDCl₃) Compound 80

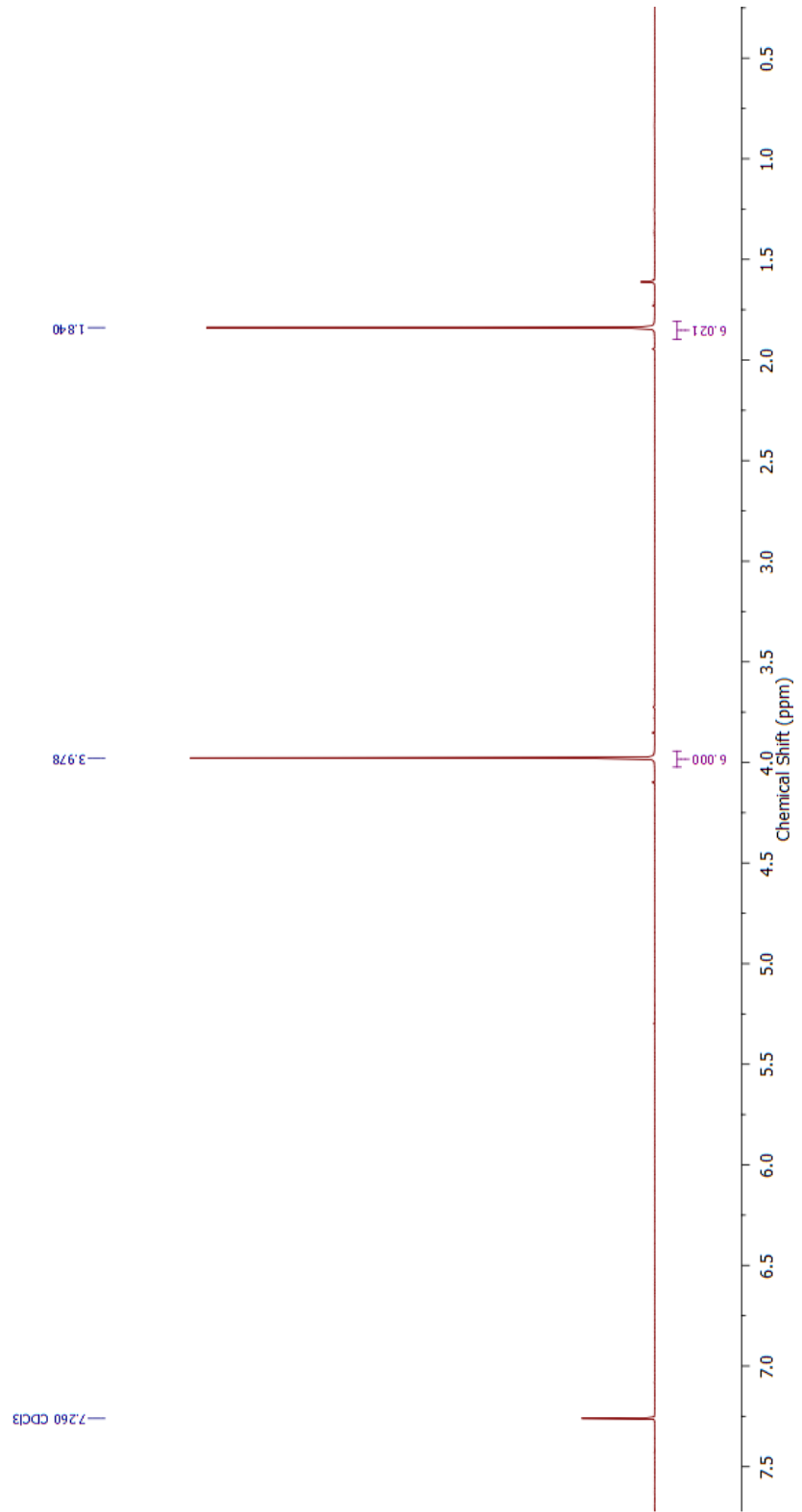
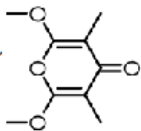


Appendix

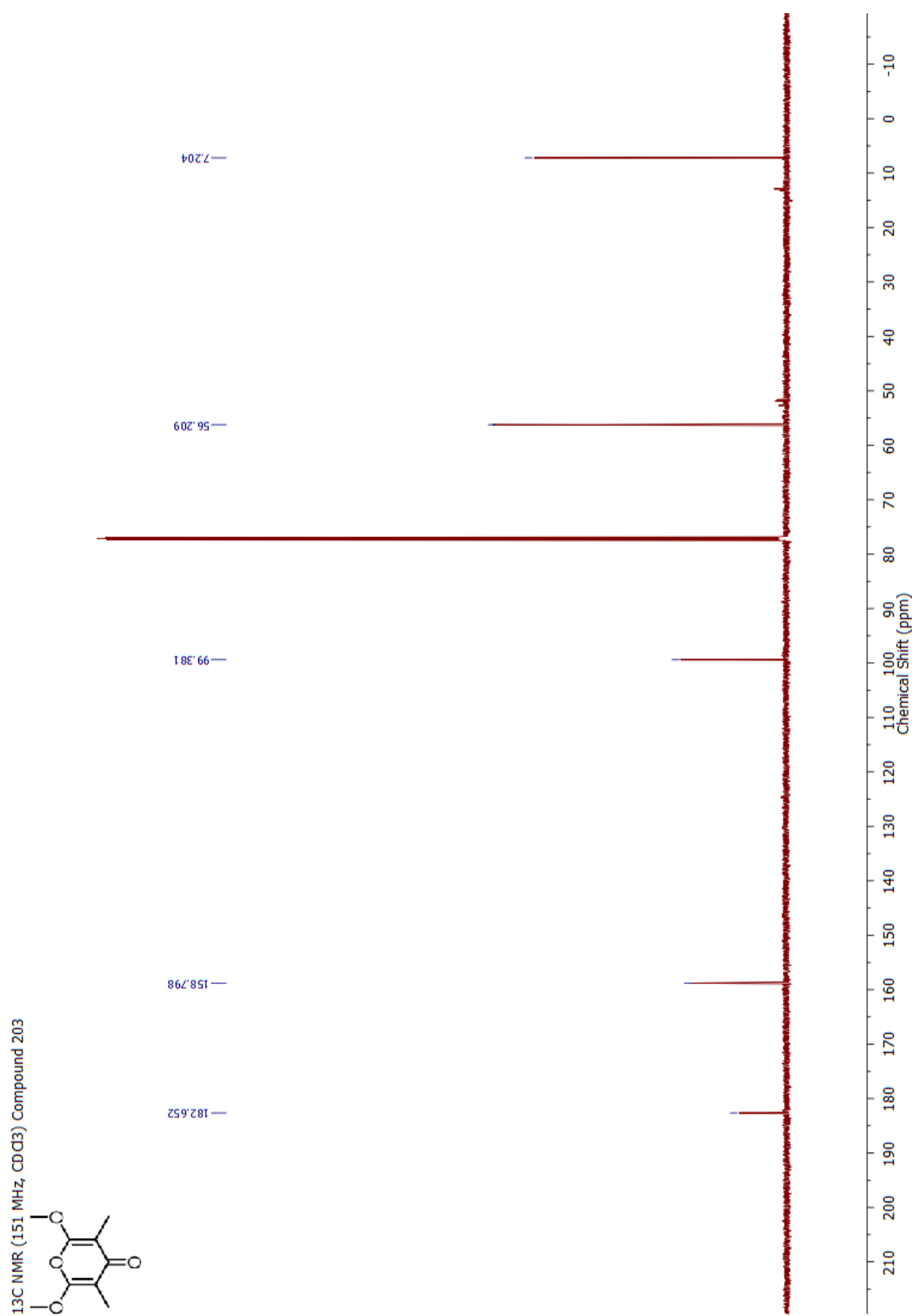


Appendix

¹H NMR (600 MHz, CDCl₃) Compound 203

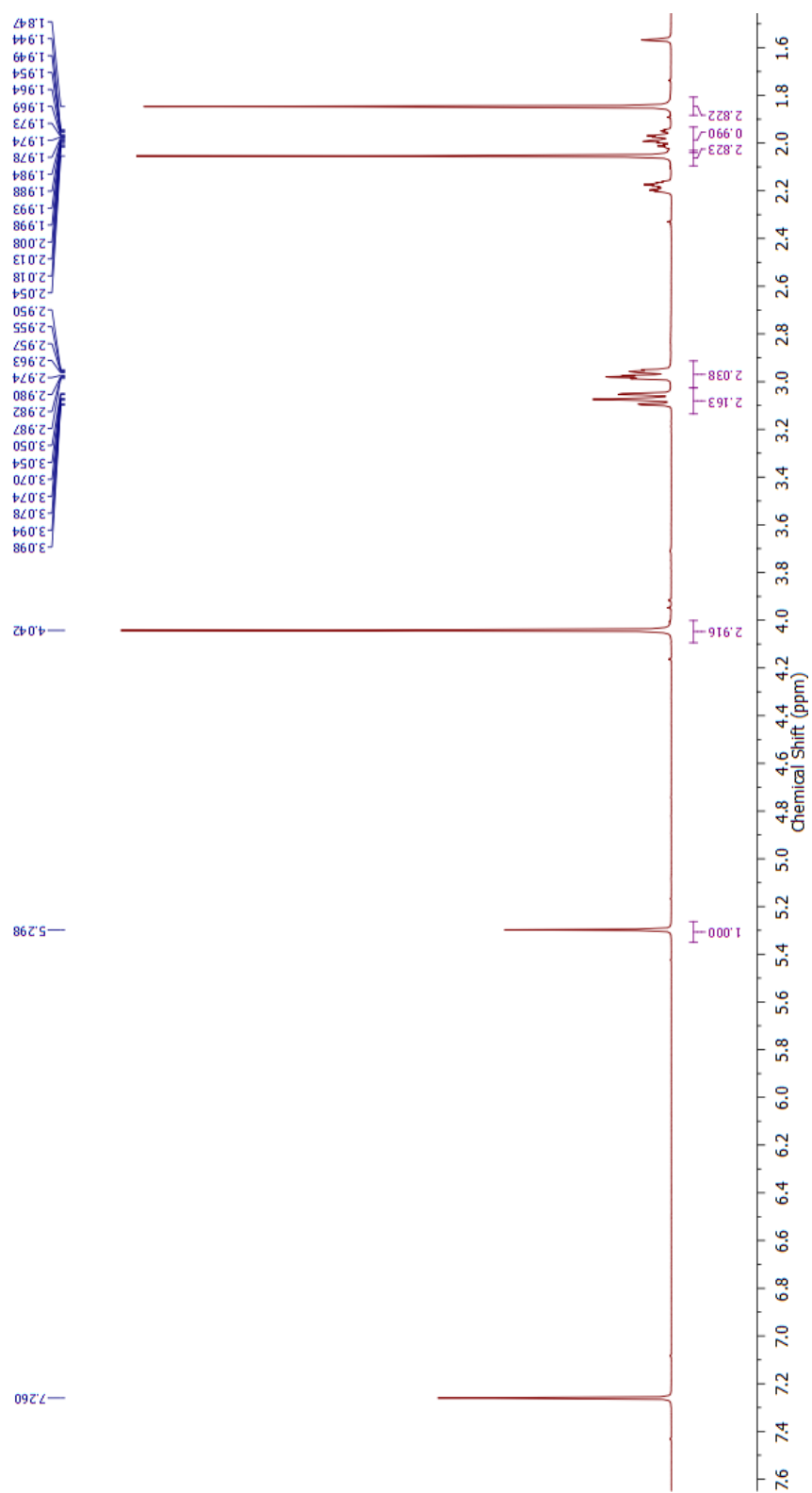
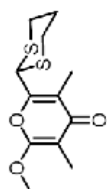


Appendix



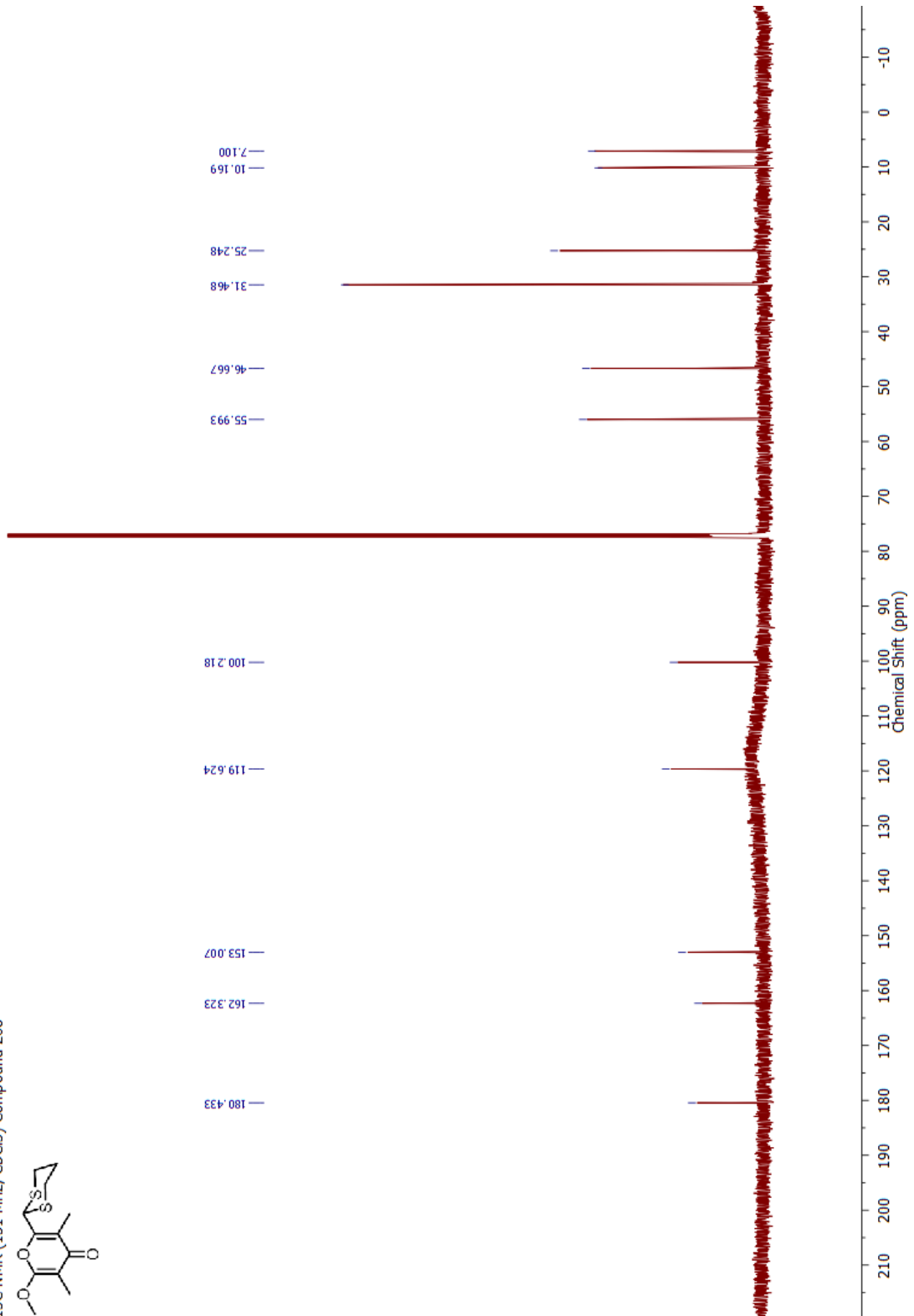
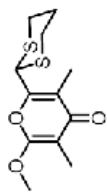
Appendix

¹H NMR (600 MHz, CDCl₃) Compound 208



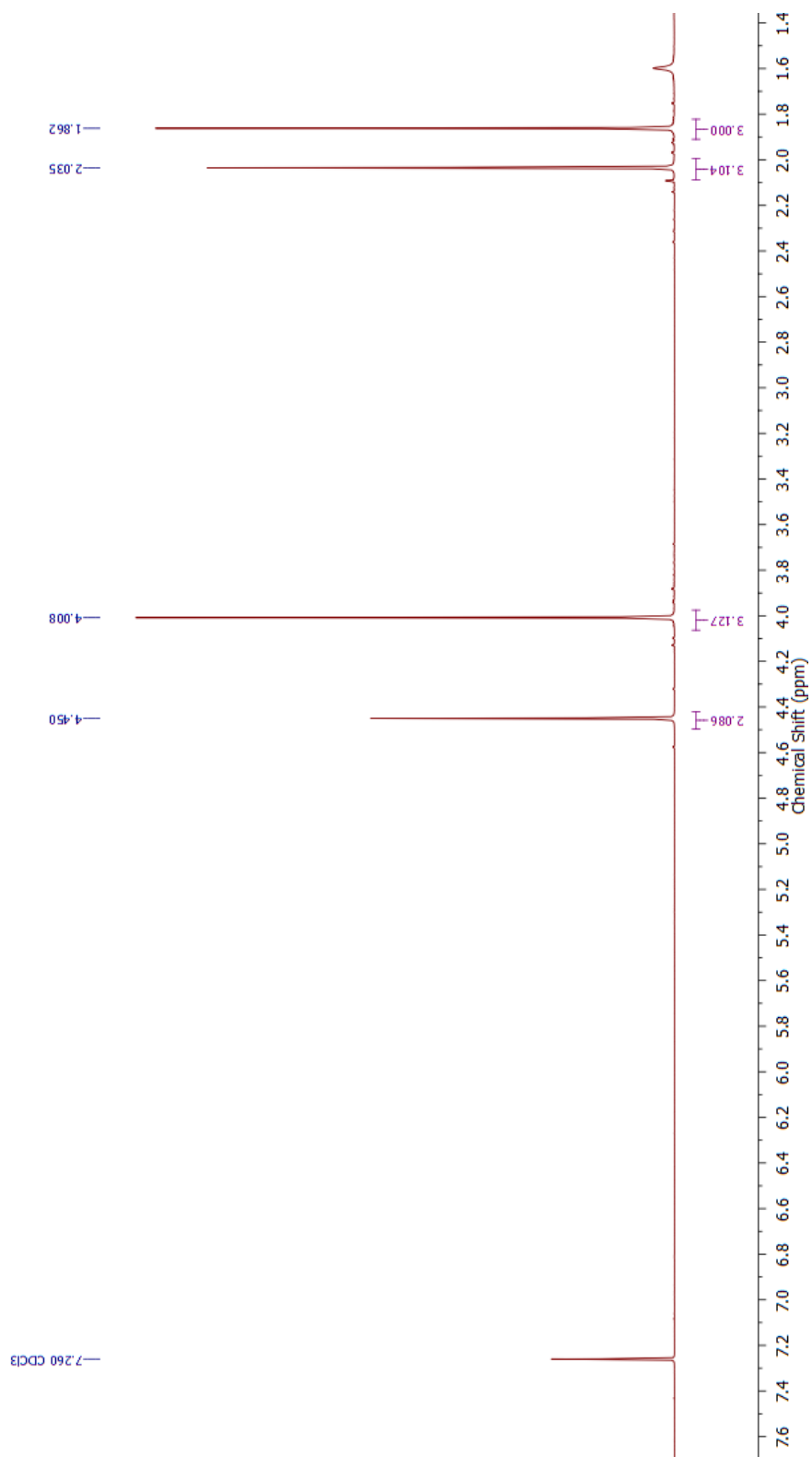
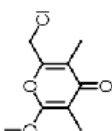
Appendix

¹³C NMR (151 MHz, CDCl₃) Compound 208

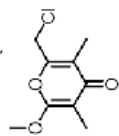


Appendix

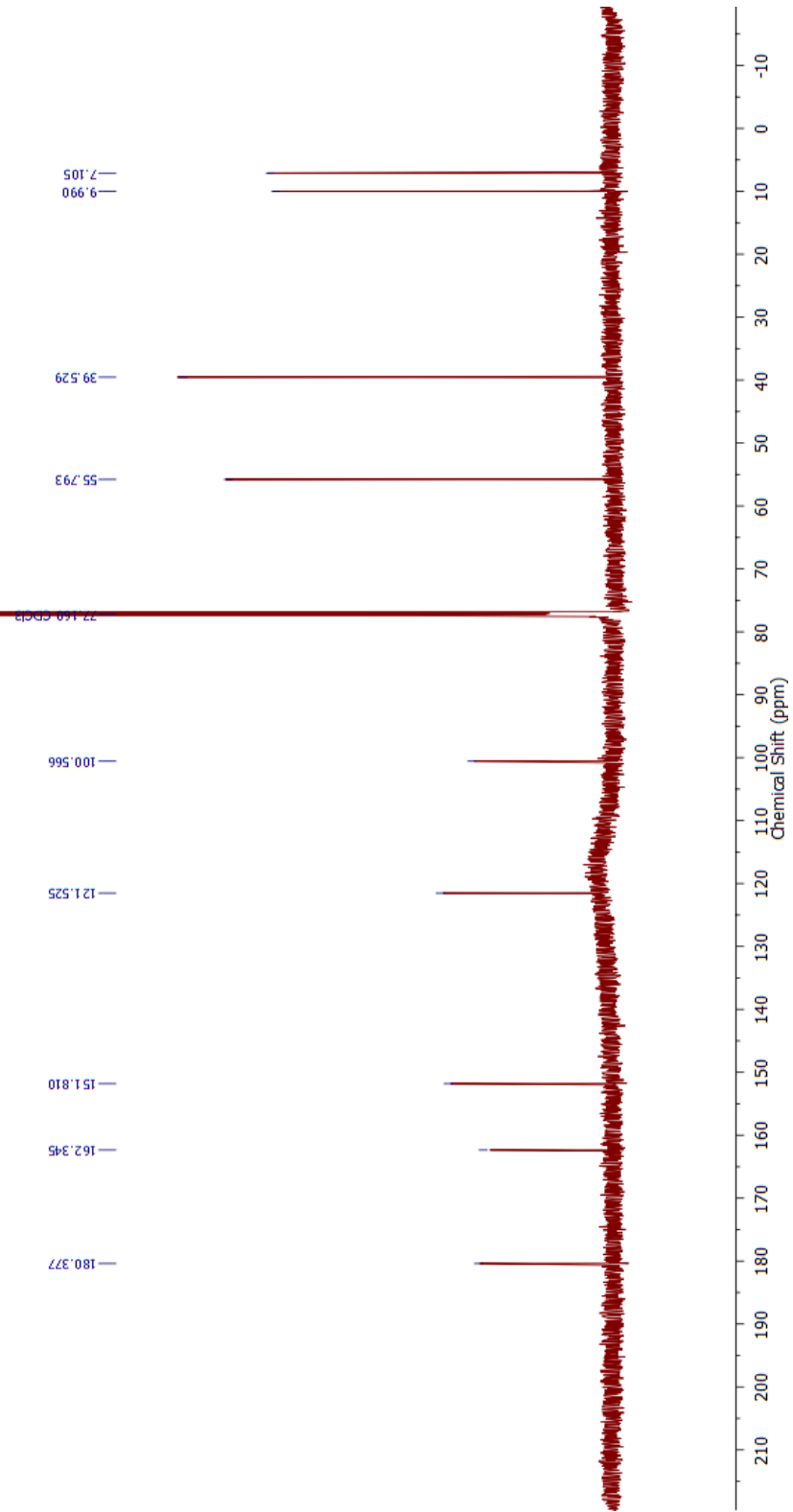
¹H NMR (600 MHz, CDCl₃) Compound 81



¹³C NMR (151 MHz, CDCl₃) Compound 81

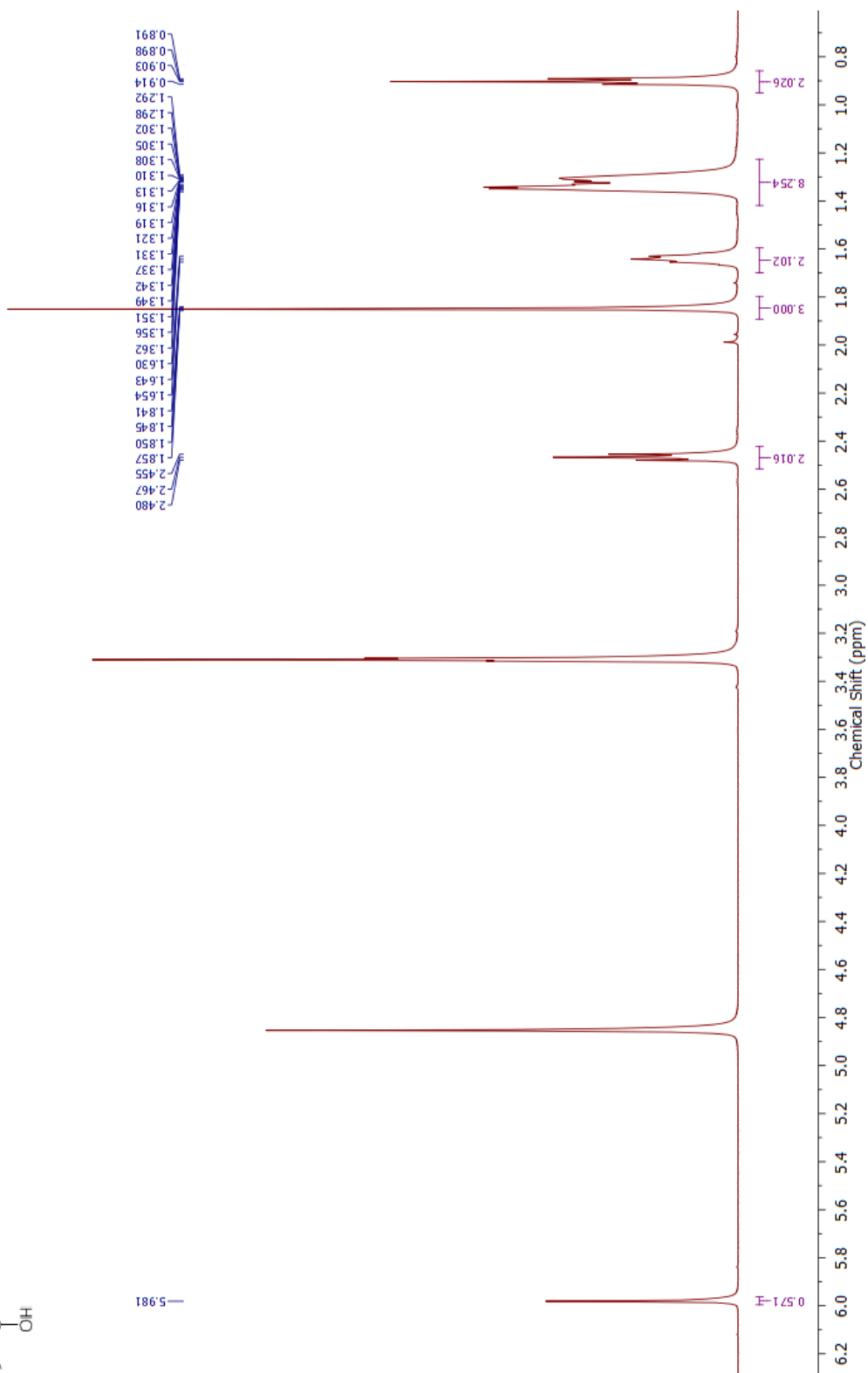
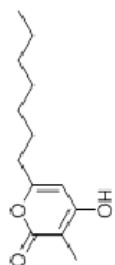


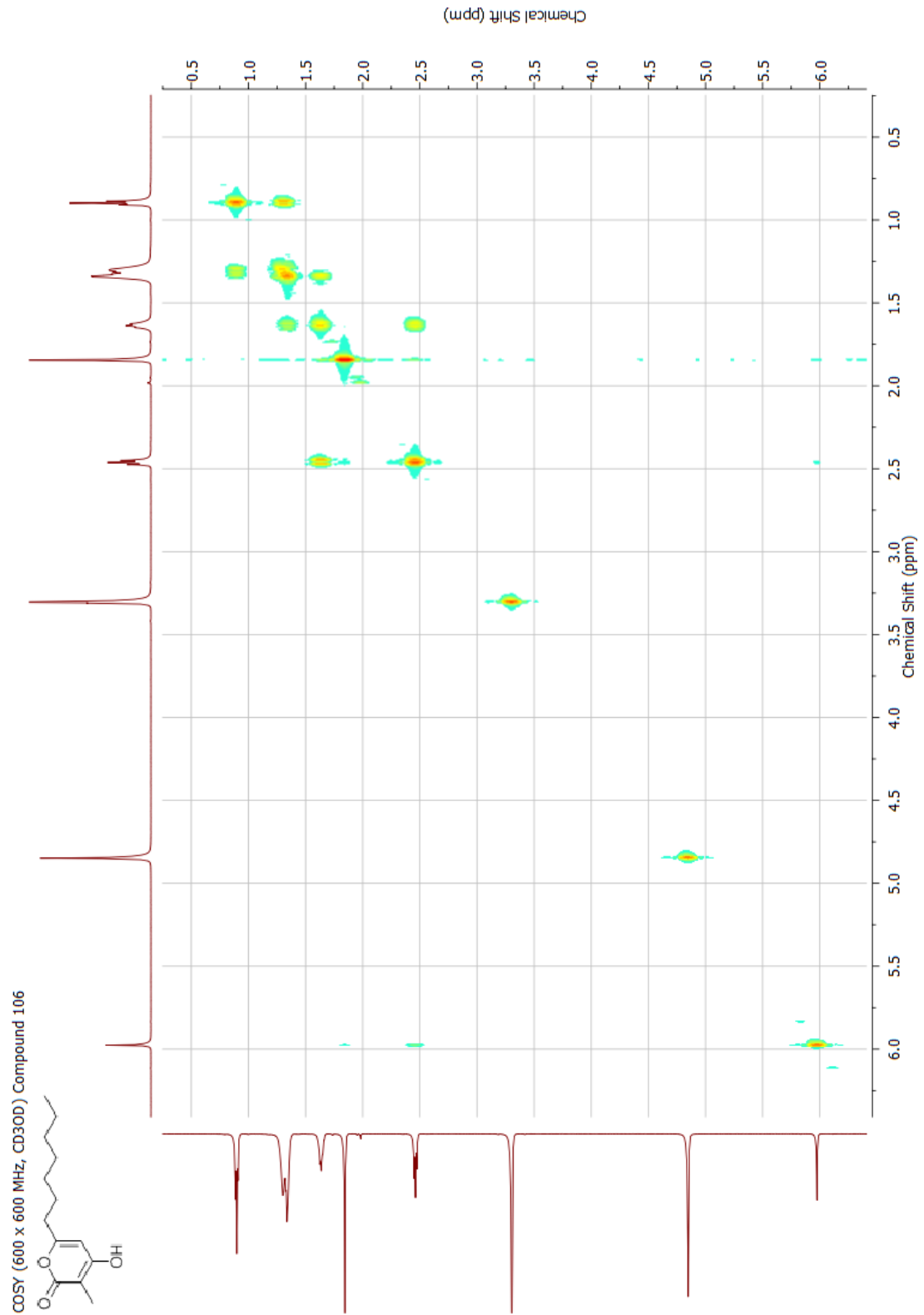
¹³C NMR (151 MHz, CDCl₃) δ 180.38, 162.35, 151.81, 121.53, 100.57, 77.16, 55.79, 39.53, 9.99, 7.11.



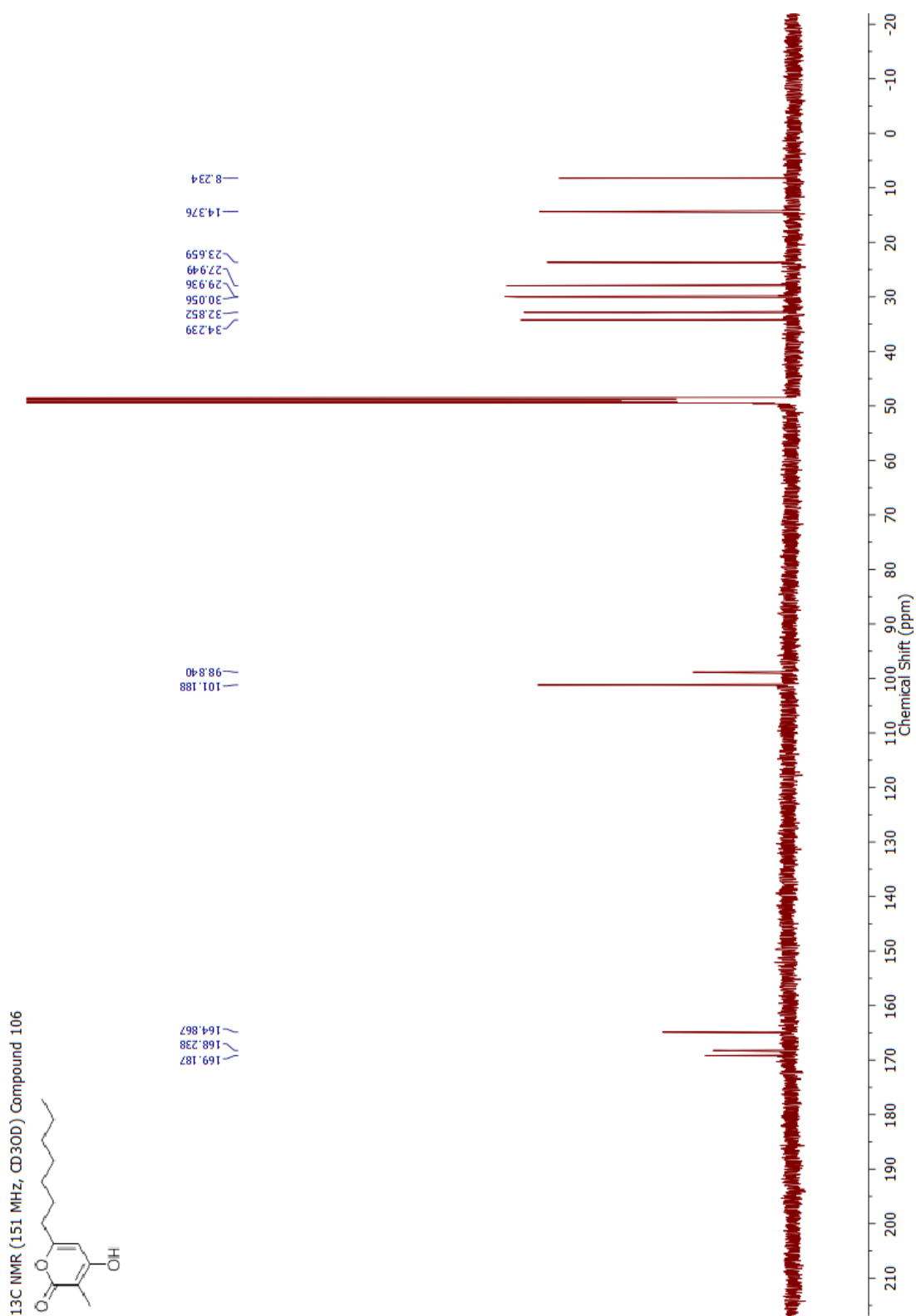
Appendix

¹H NMR (600 MHz, CD₃OD) Compound 106

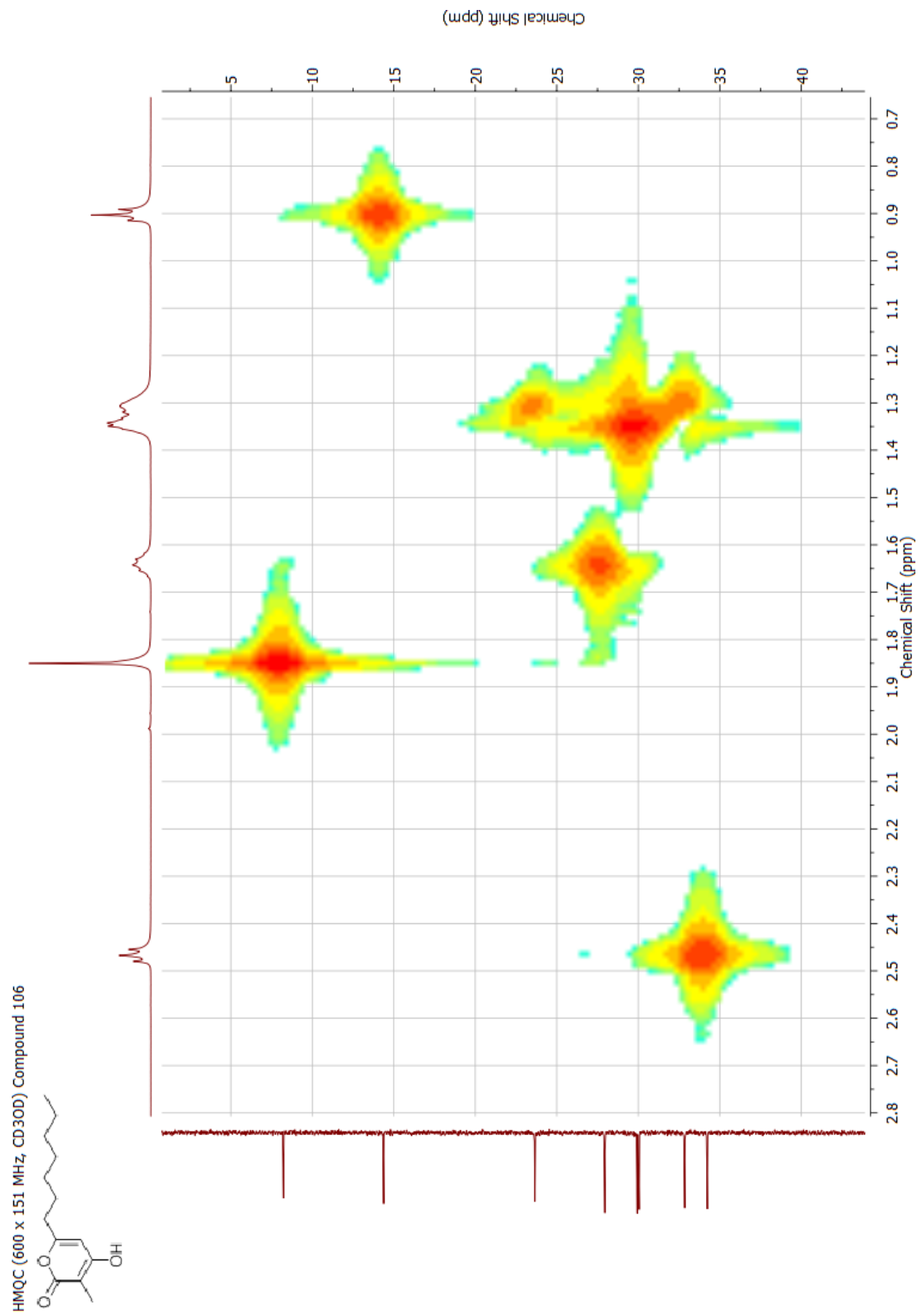




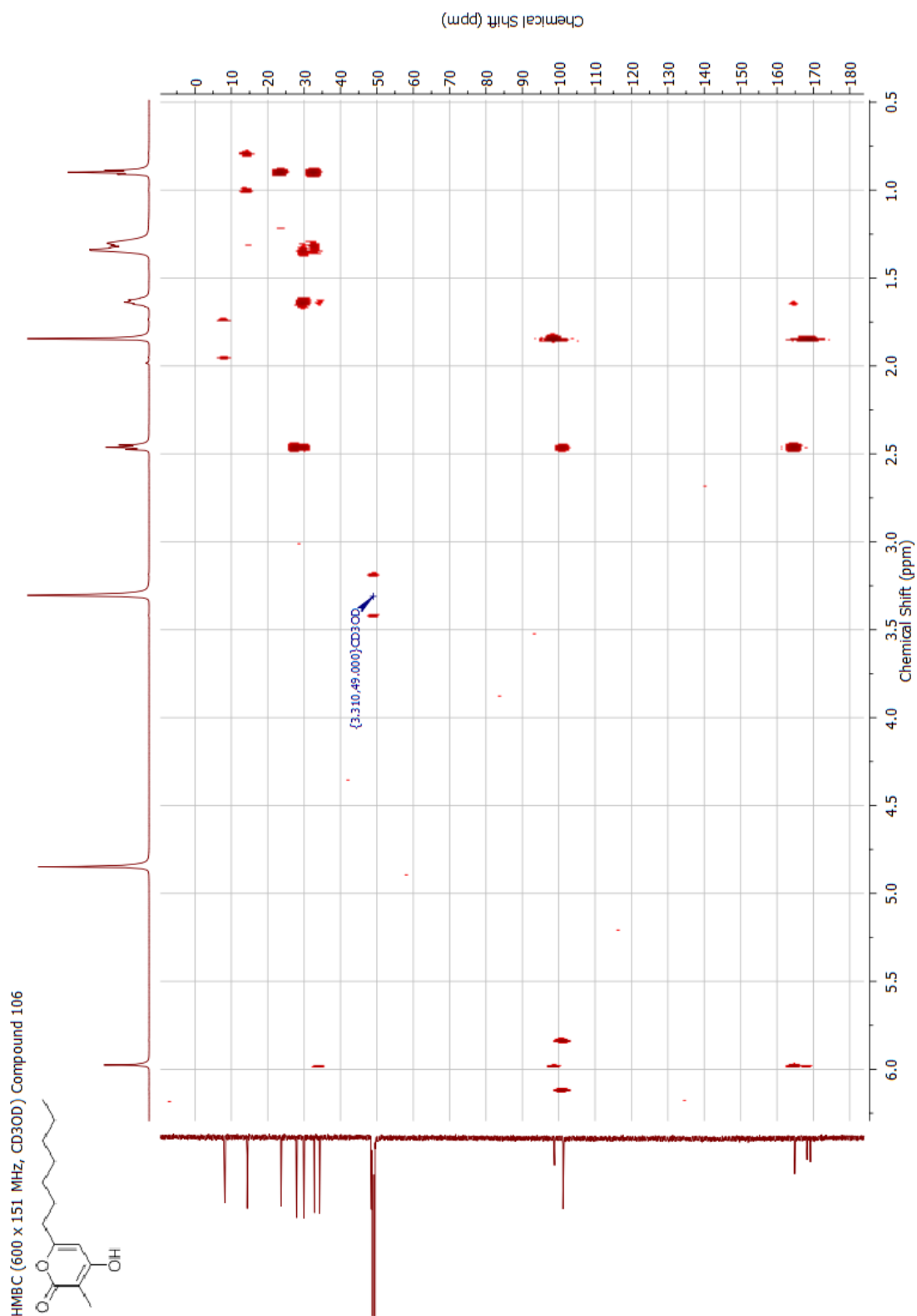
Appendix



Appendix

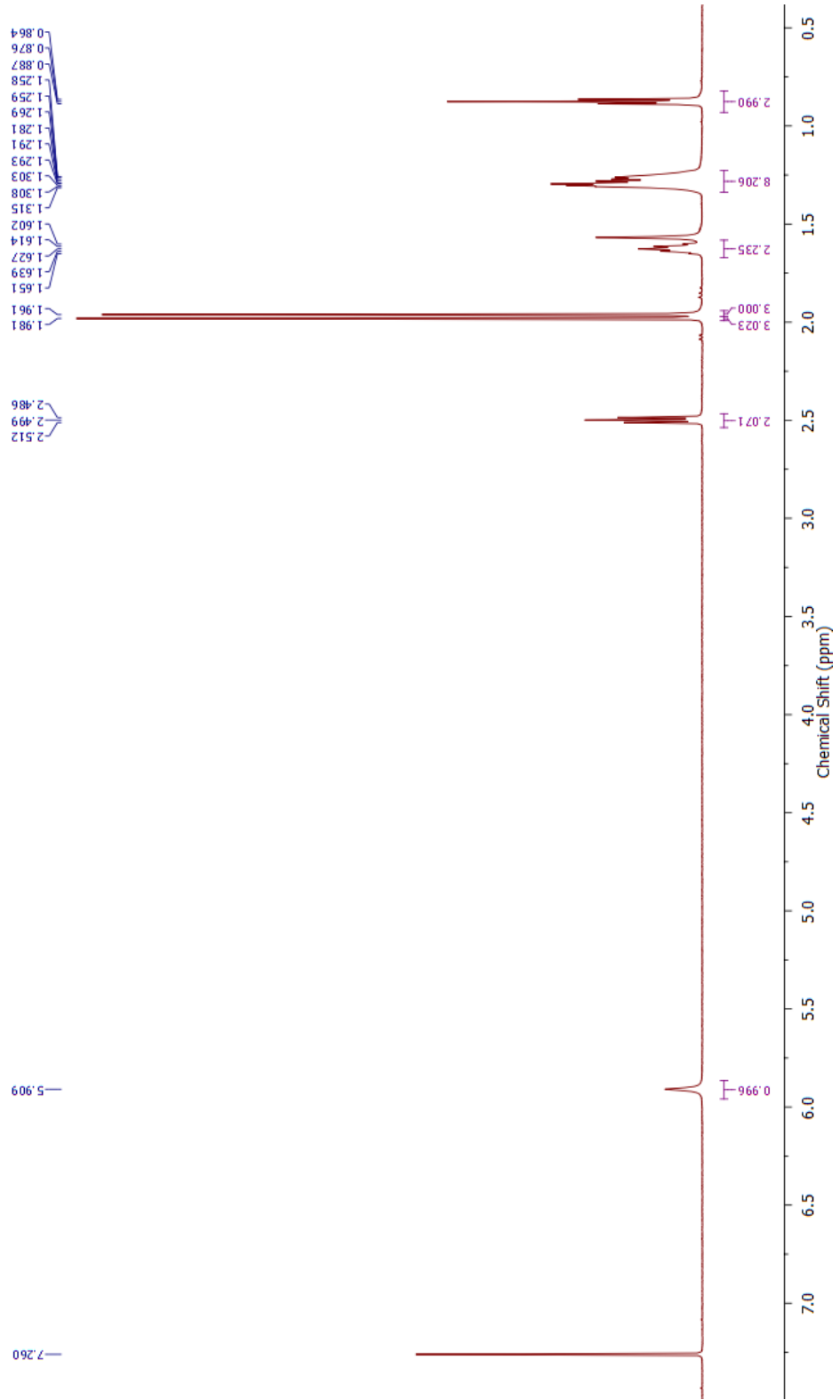
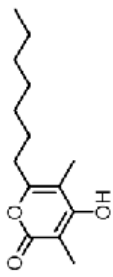


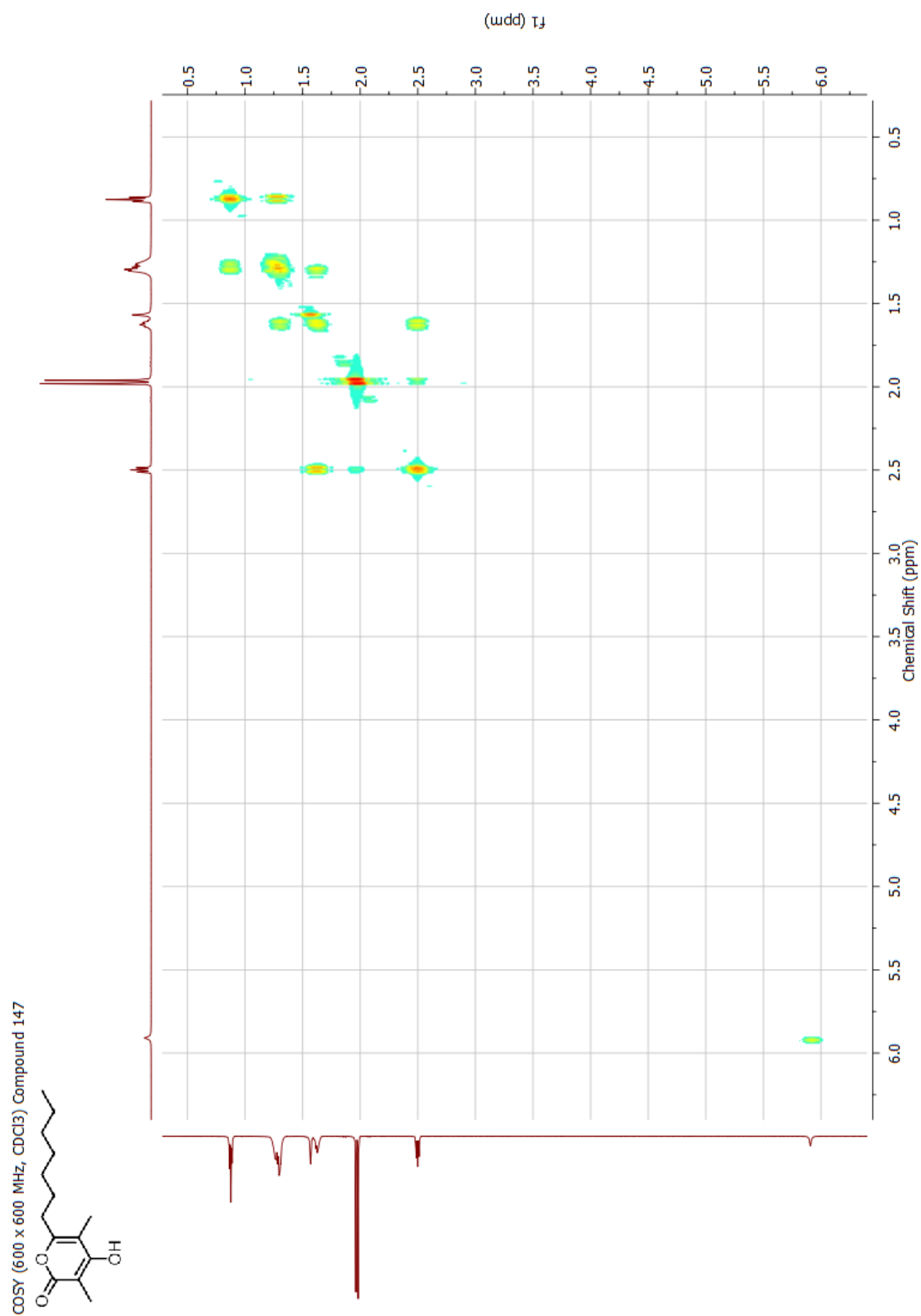
Appendix



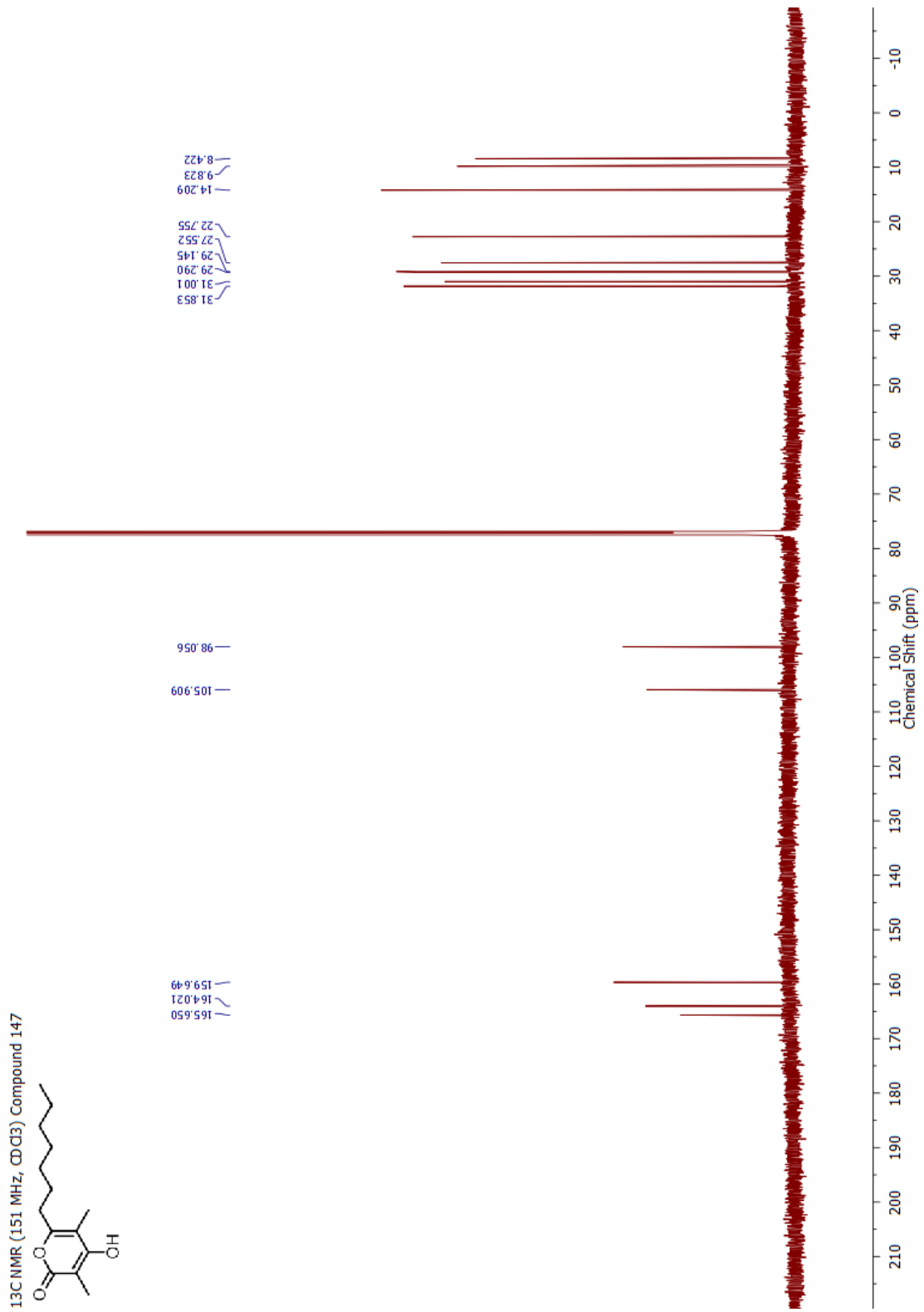
Appendix

¹H NMR (600 MHz, CDCl₃) Compound 147



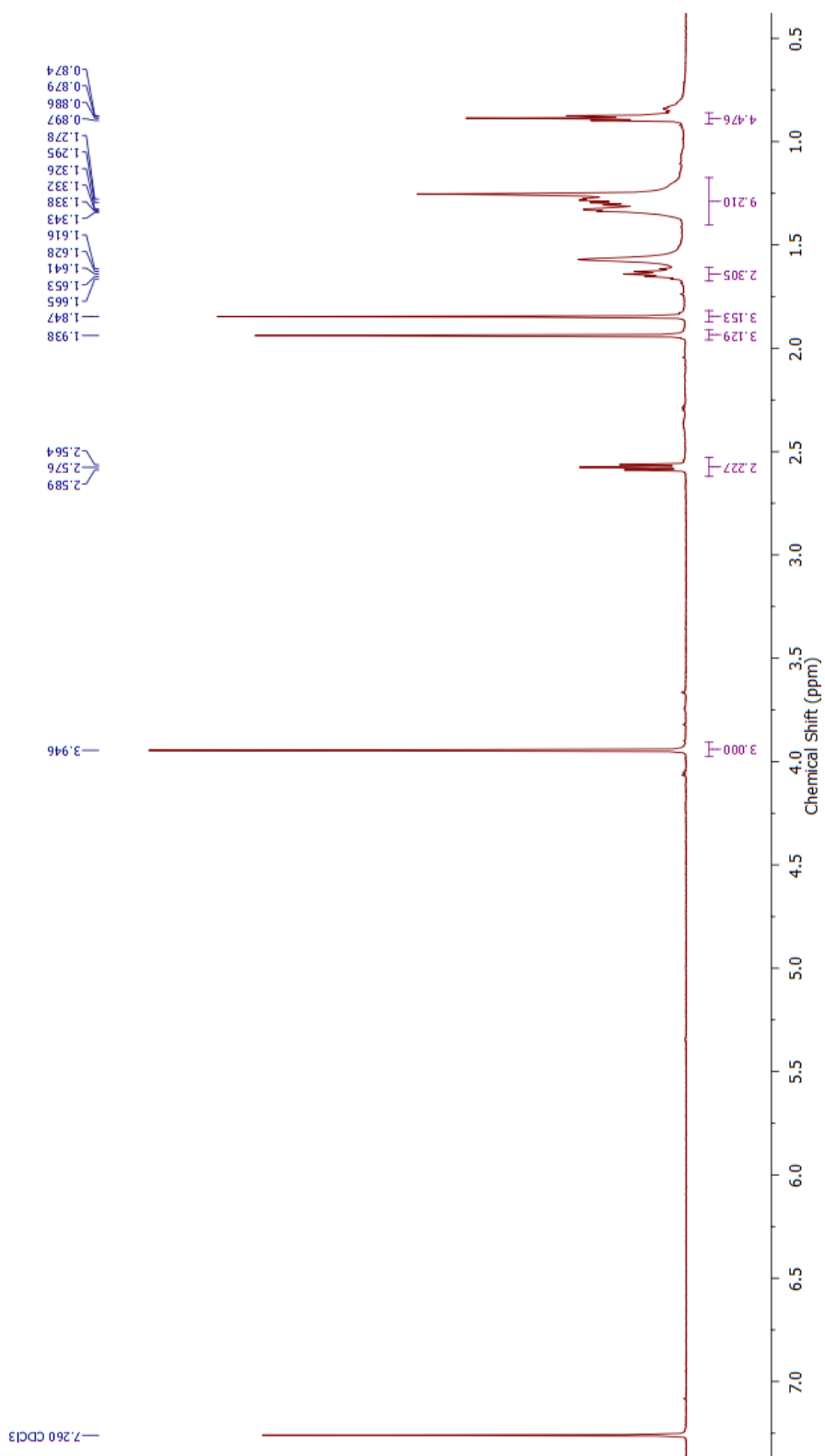


Appendix

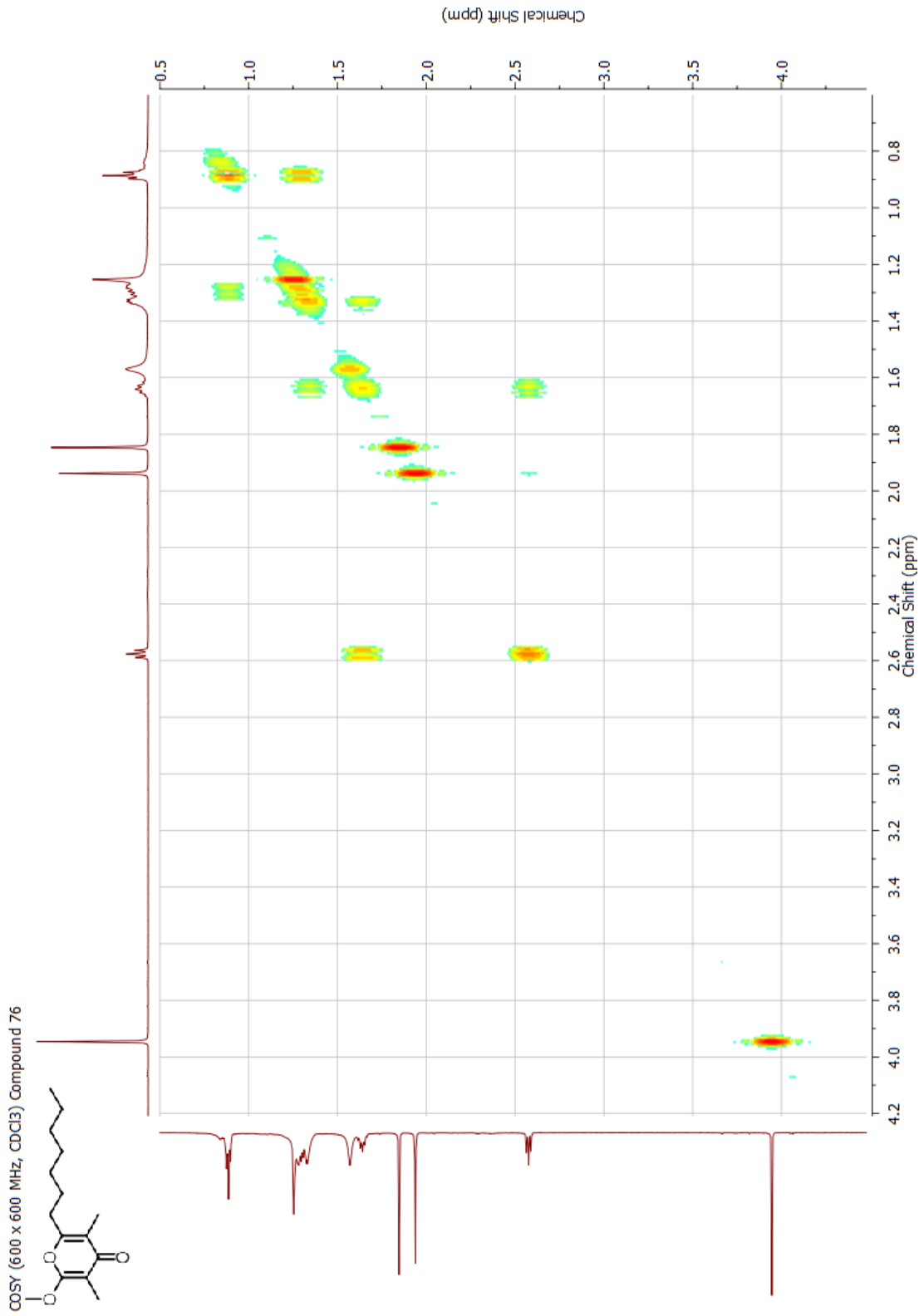


Appendix

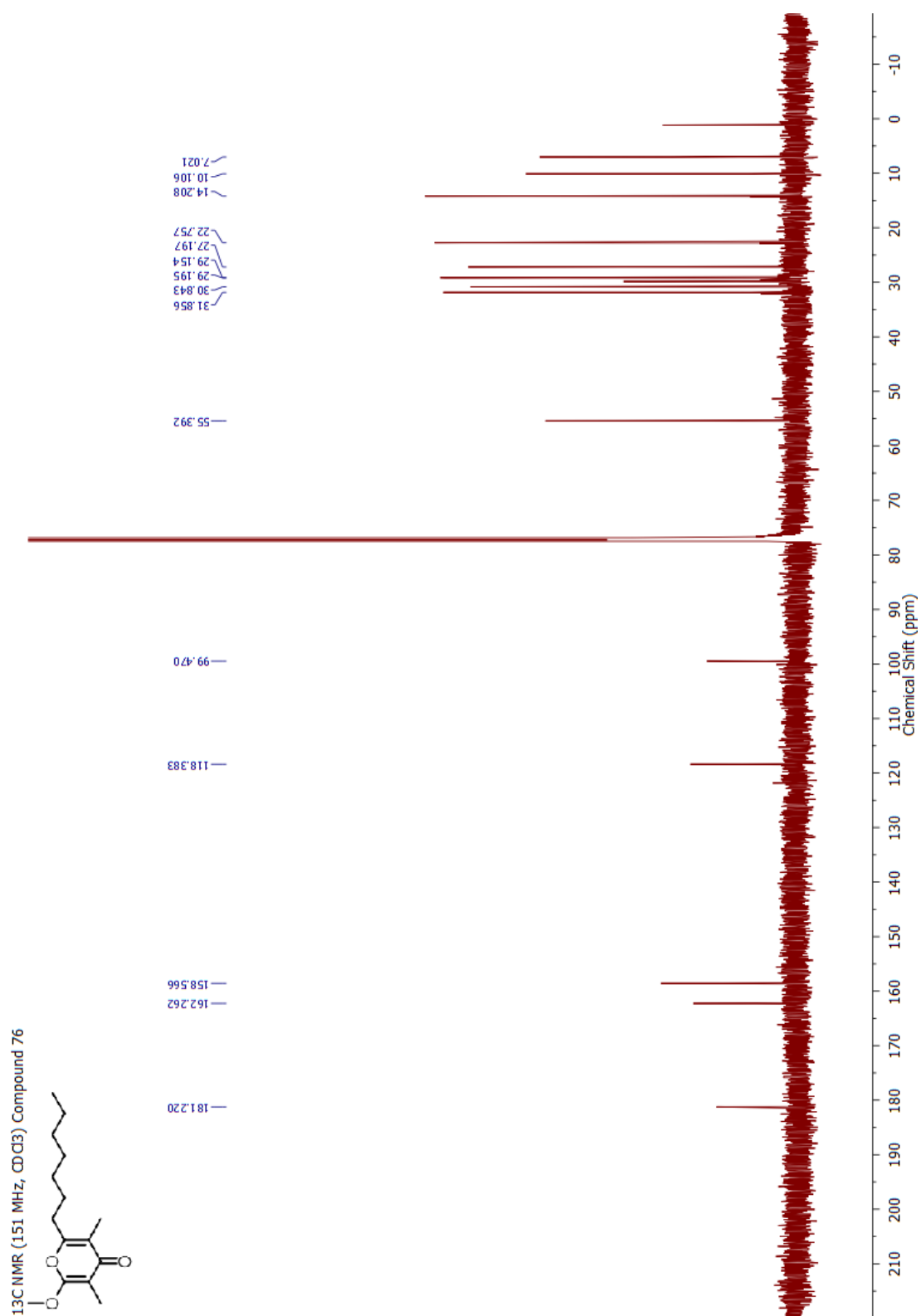
¹H NMR (600 MHz, CDCl₃) Compound 76



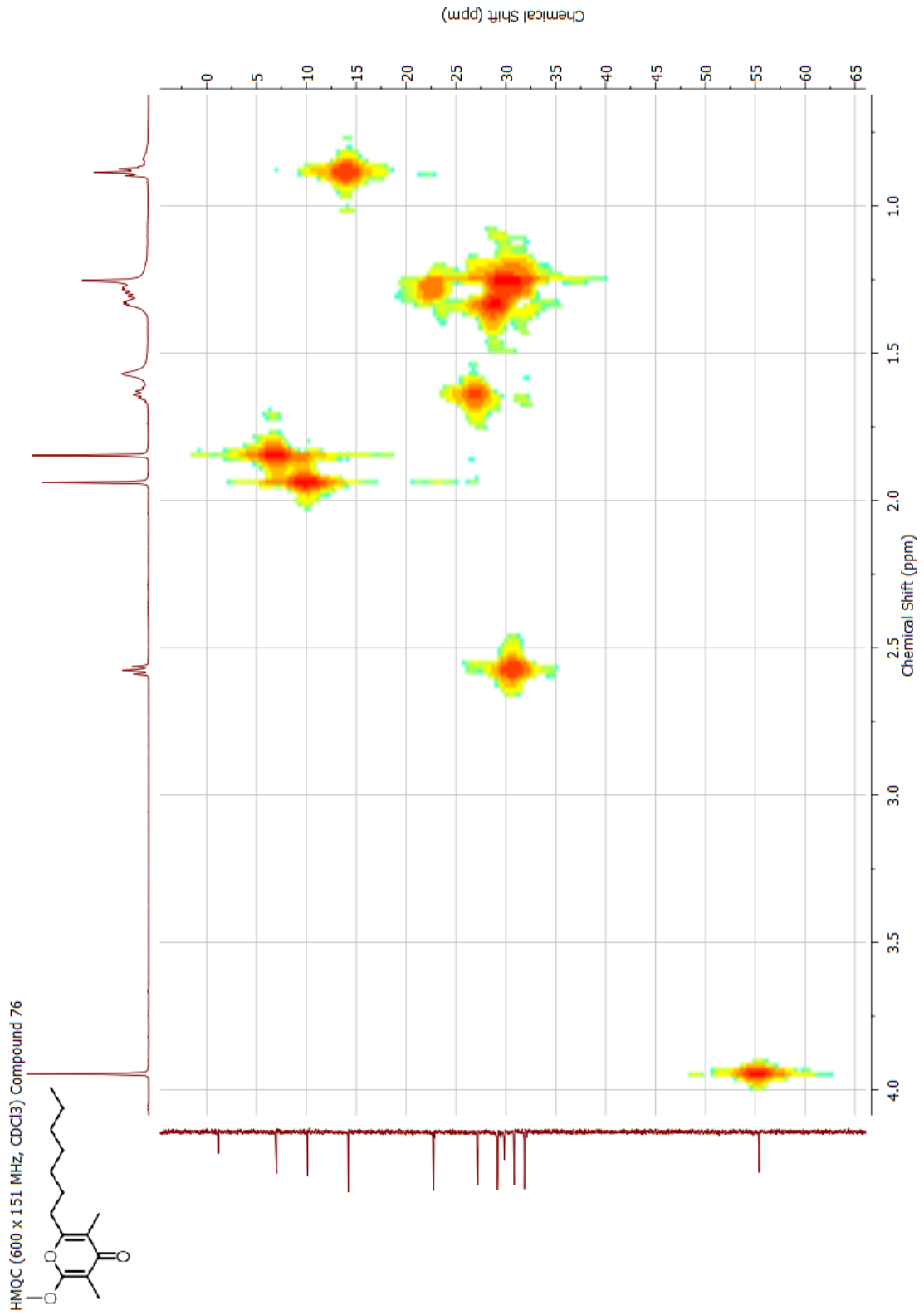
Appendix



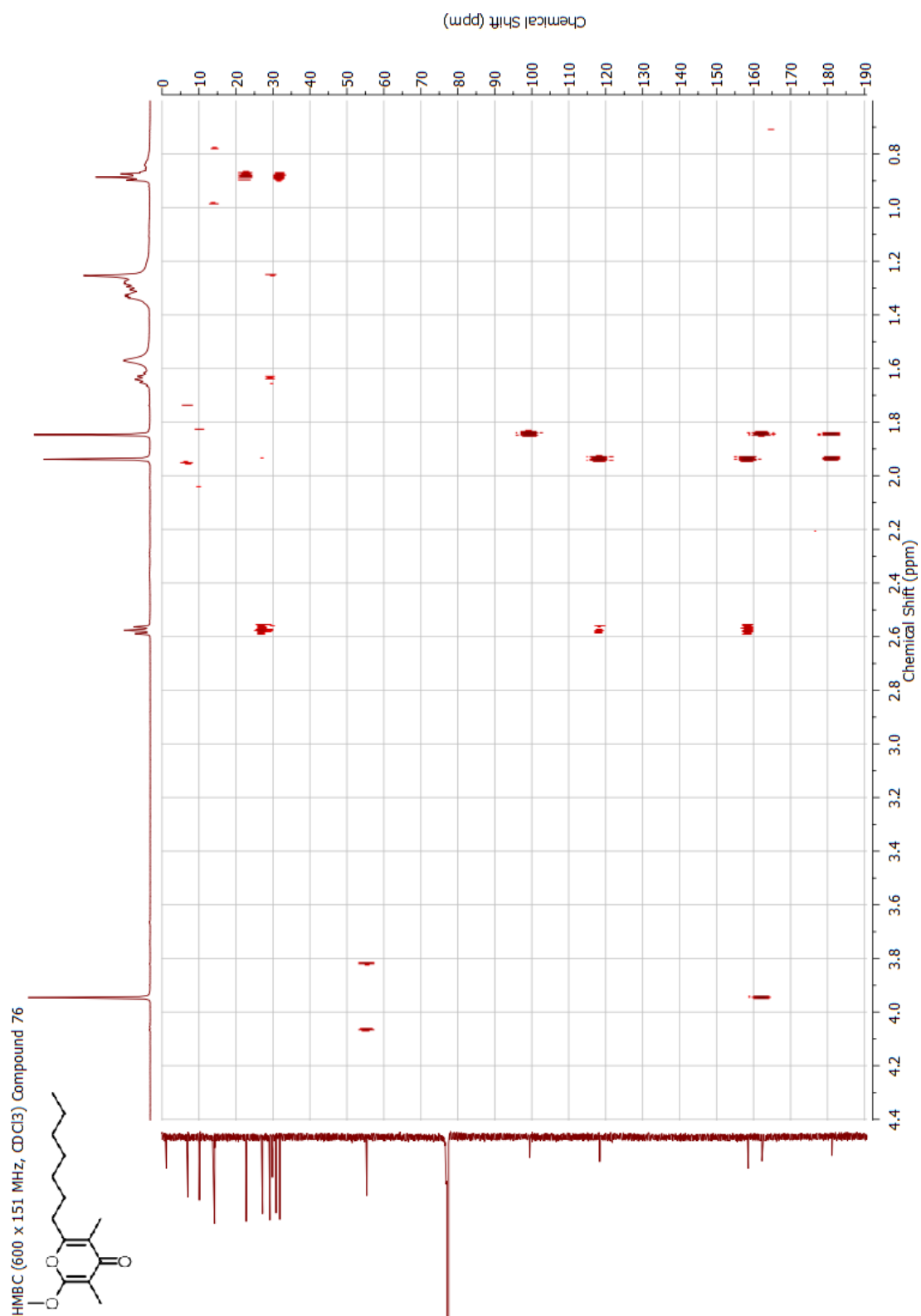
Appendix



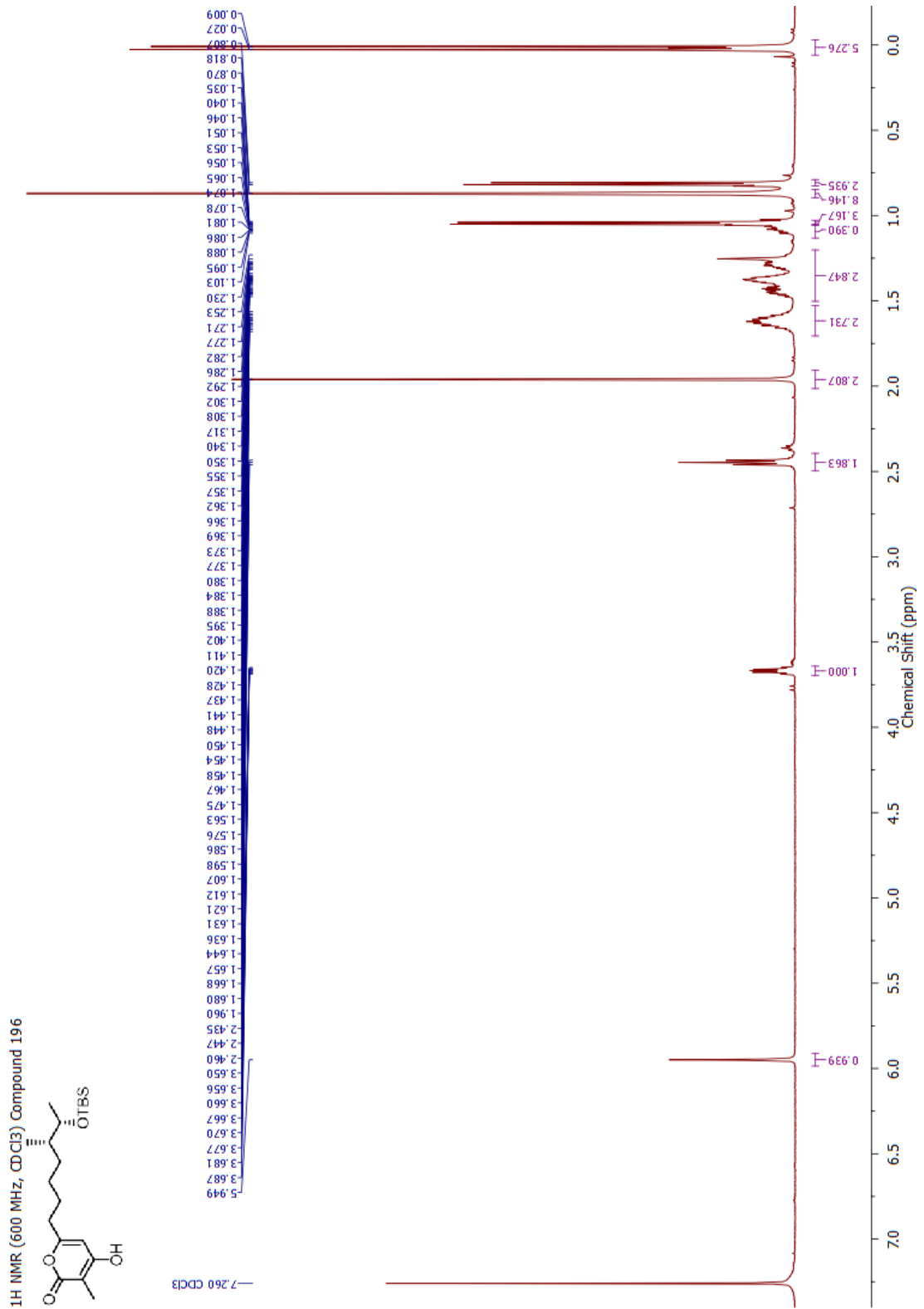
Appendix

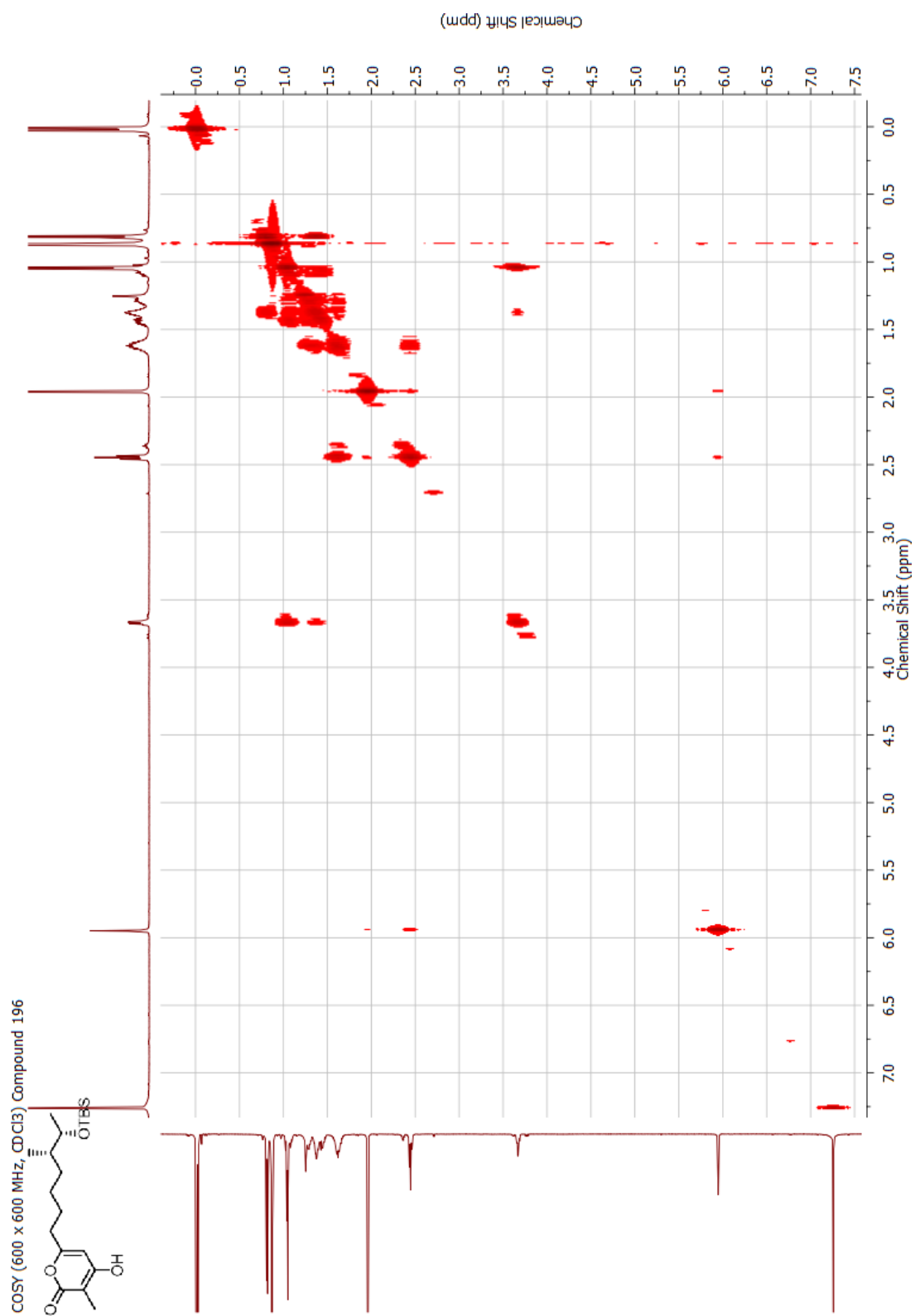


Appendix



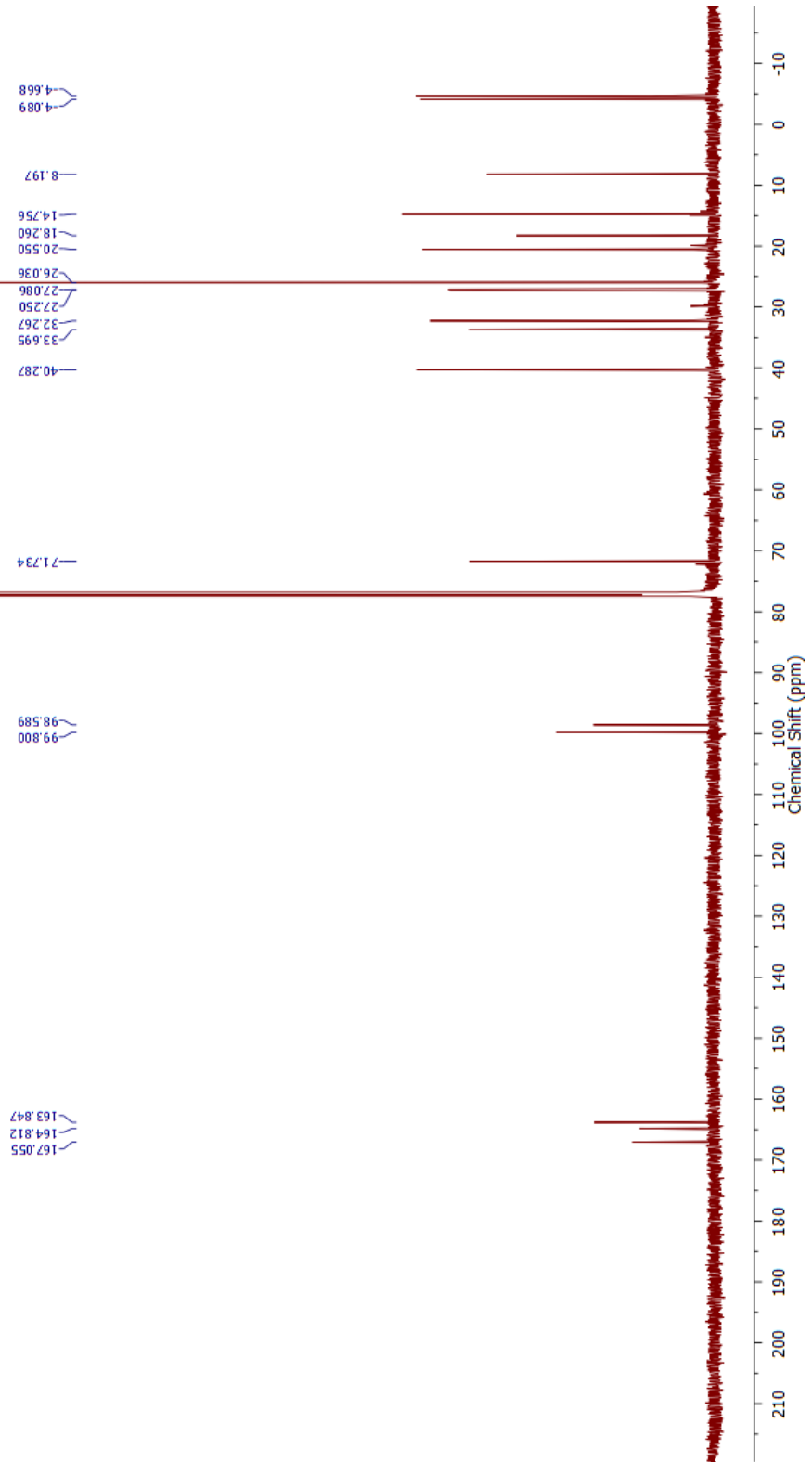
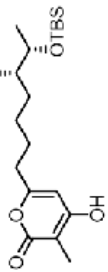
Appendix

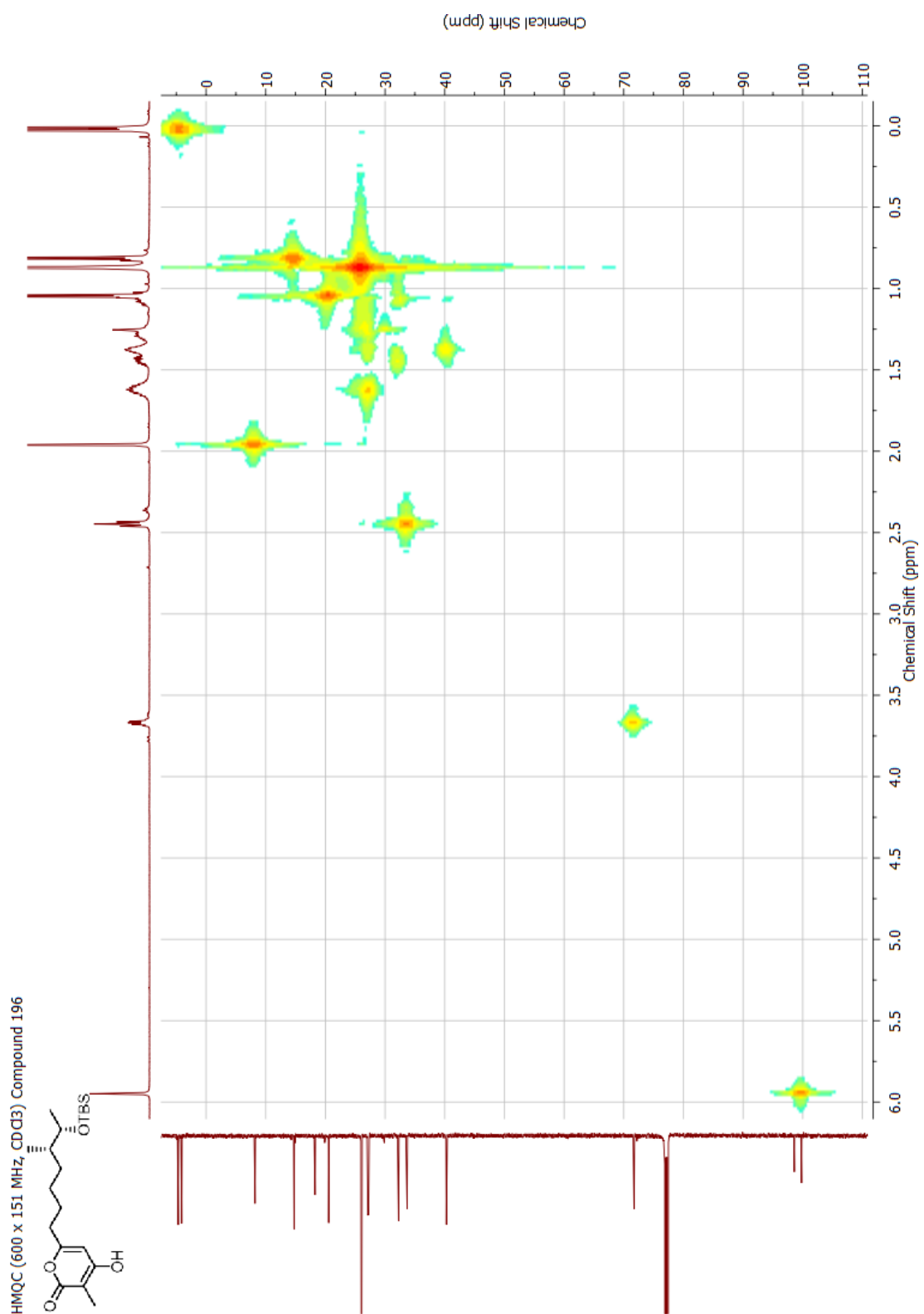




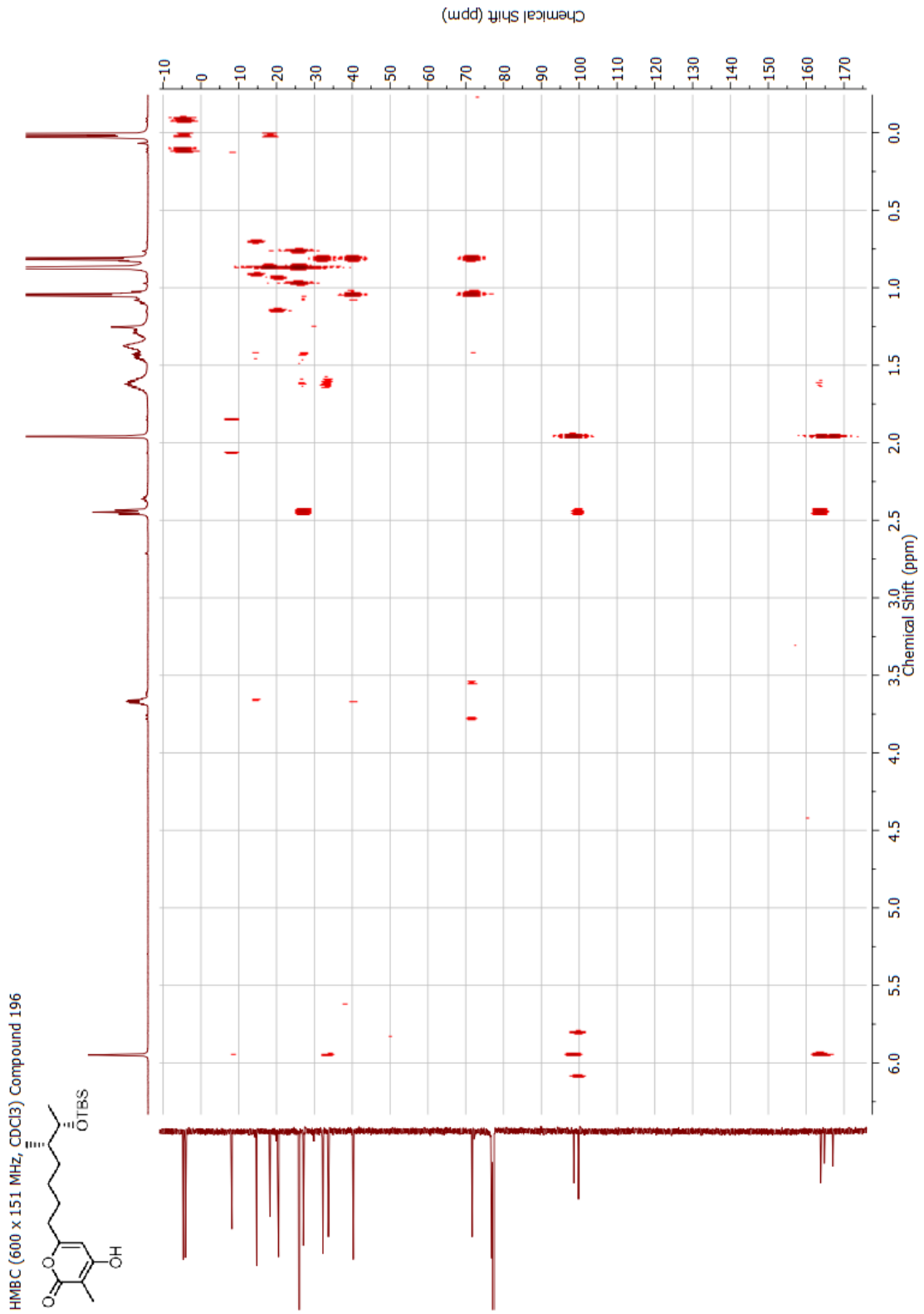
Appendix

¹³C NMR (151 MHz, CDCl₃) Compound 196



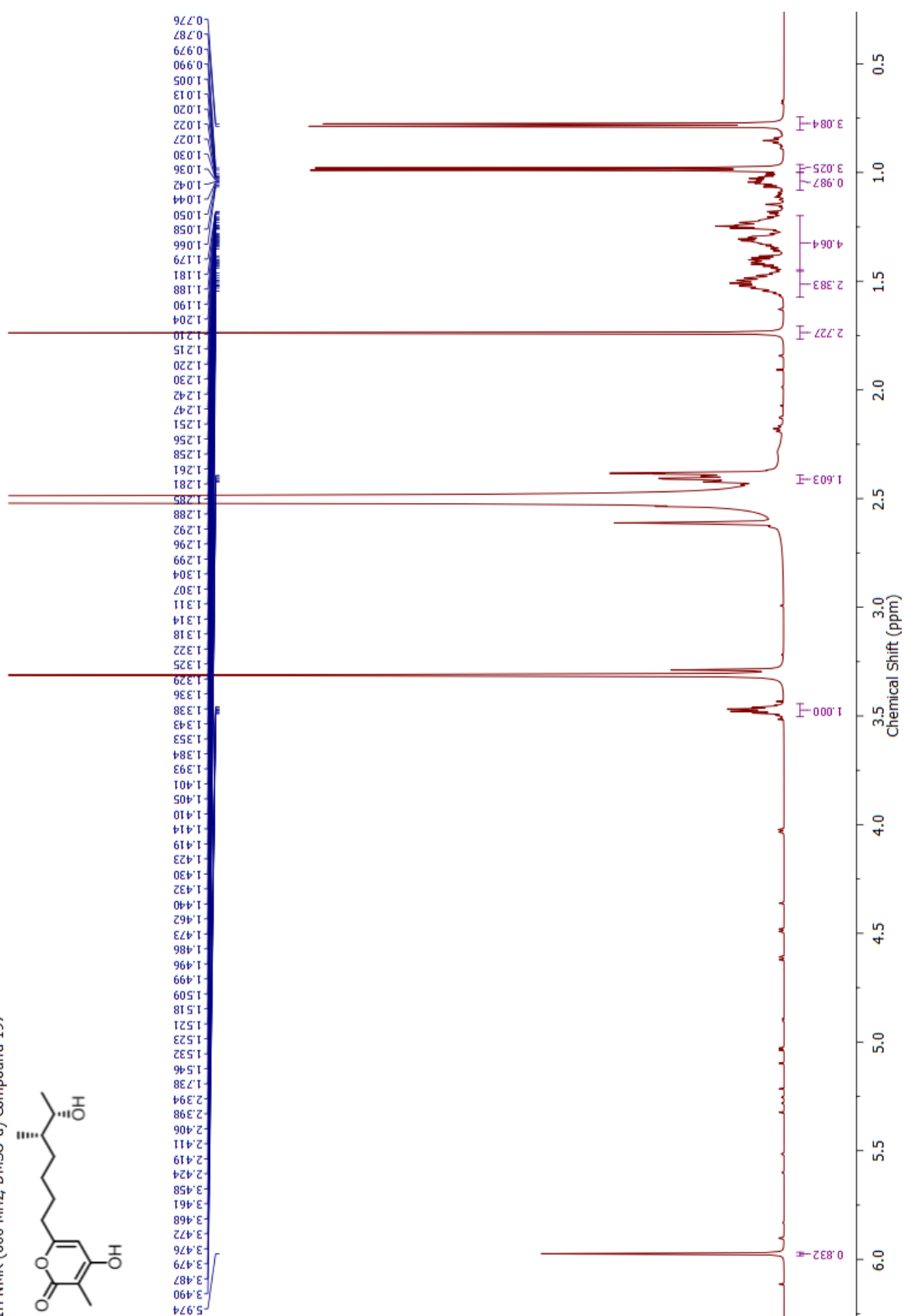
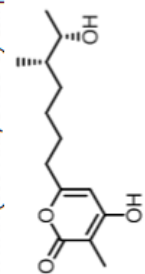


Appendix



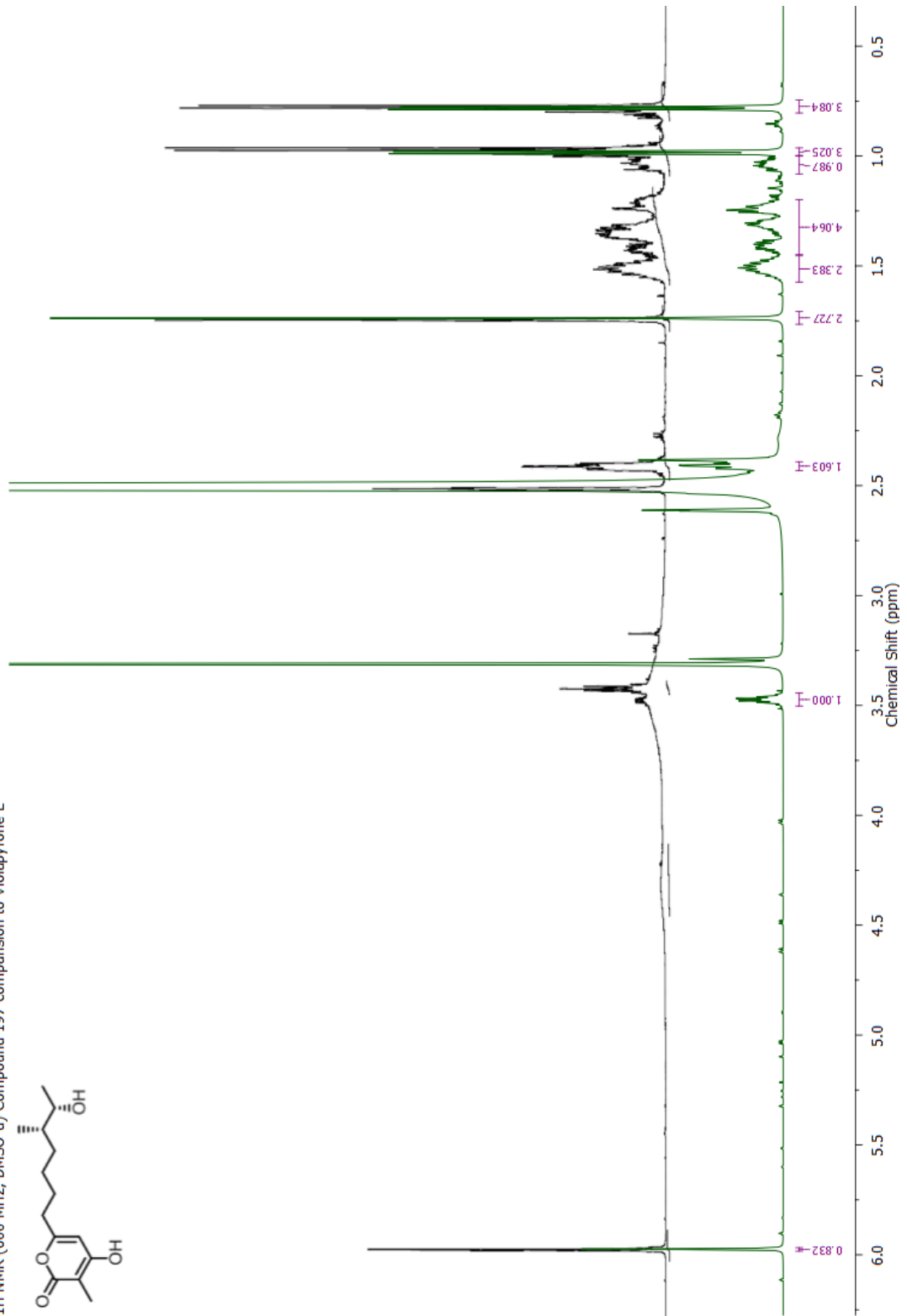
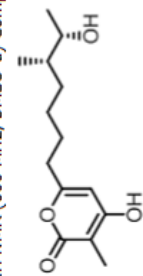
Appendix

¹H NMR (600 MHz, DMSO-d) Compound 197

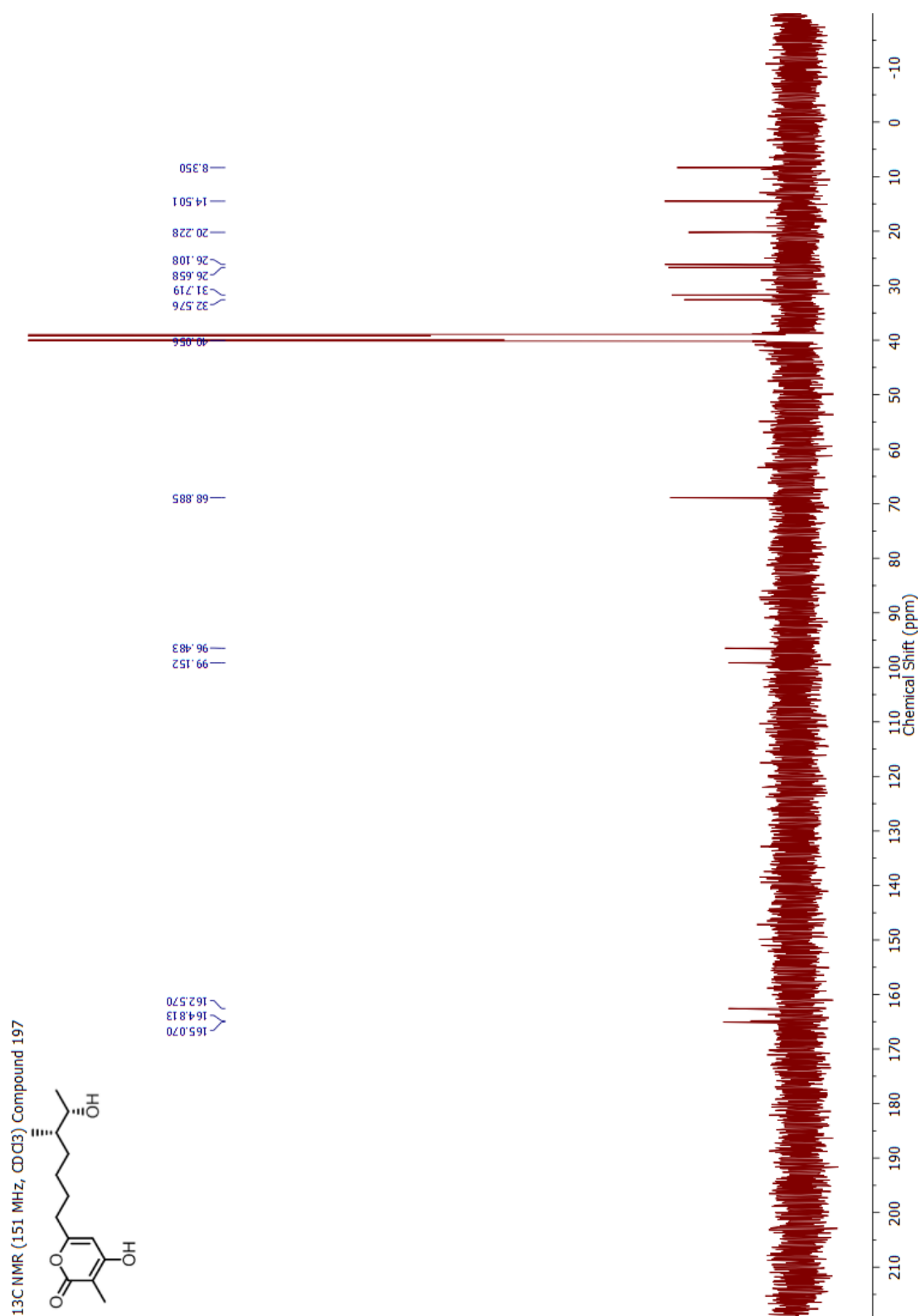


Appendix

¹H NMR (600 MHz, DMSO-d) Compound 197 comparison to Violapyrone E

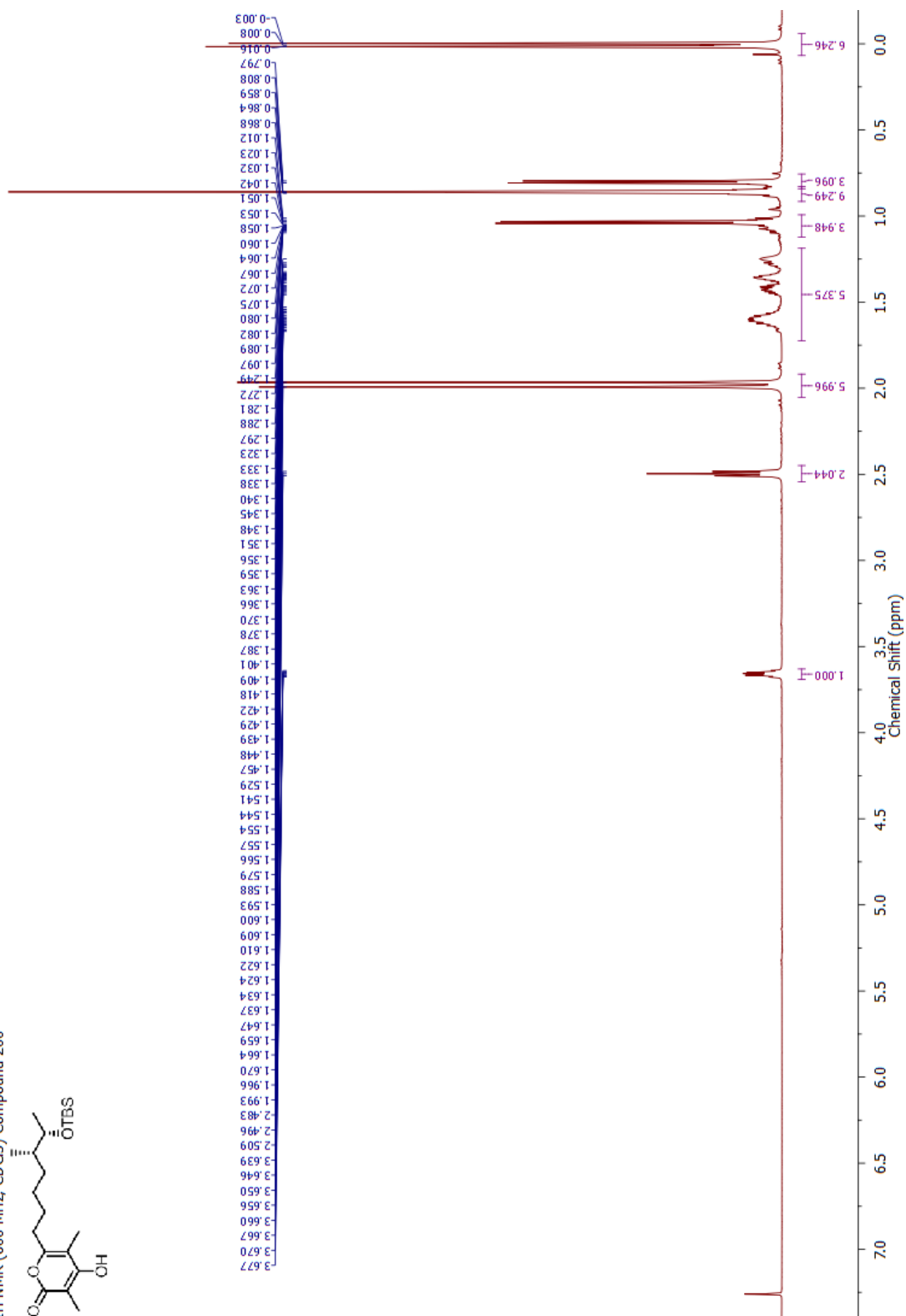
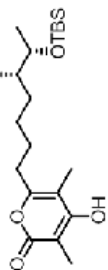


Appendix

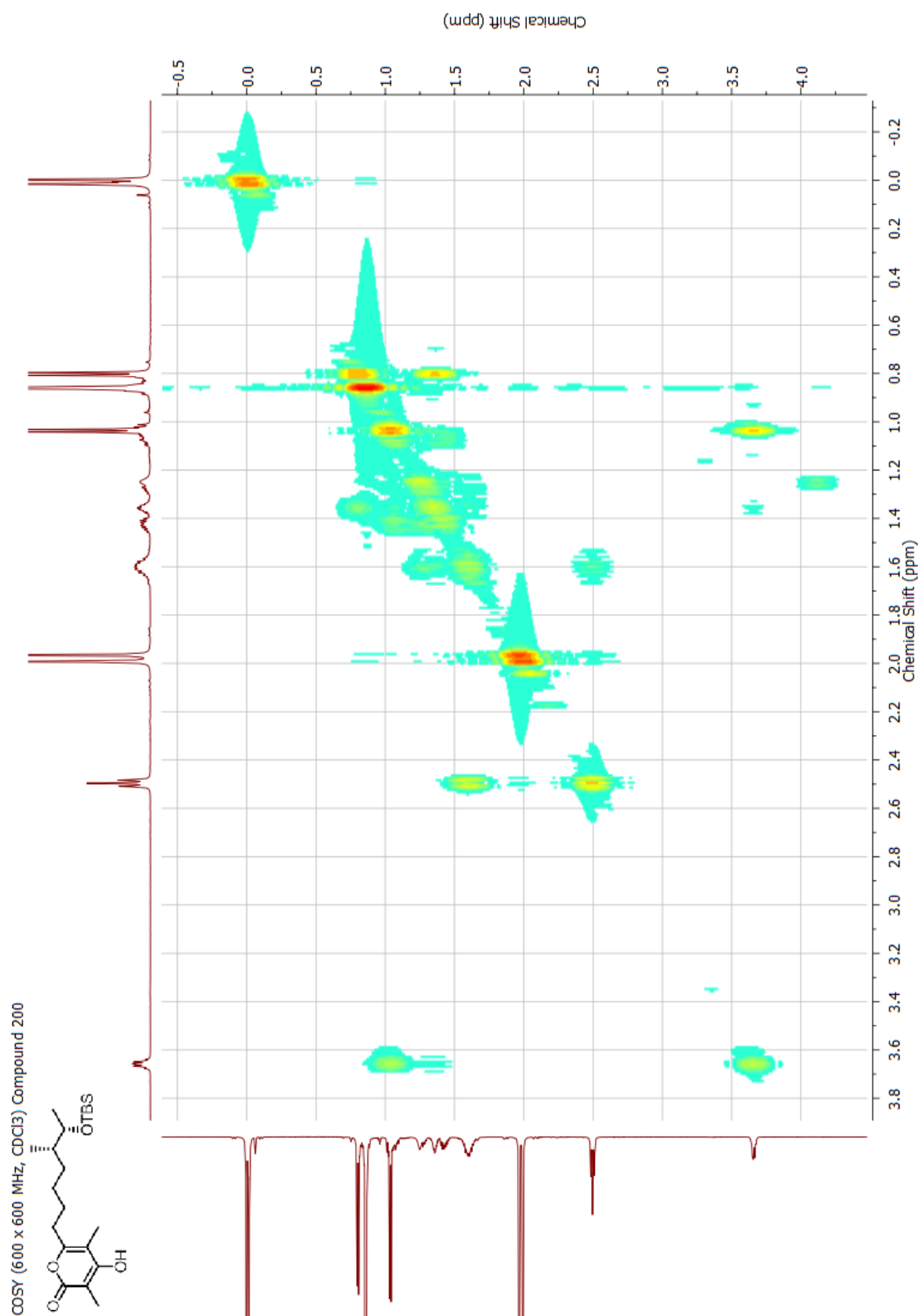


Appendix

¹H NMR (600 MHz, CDCl₃) Compound 200

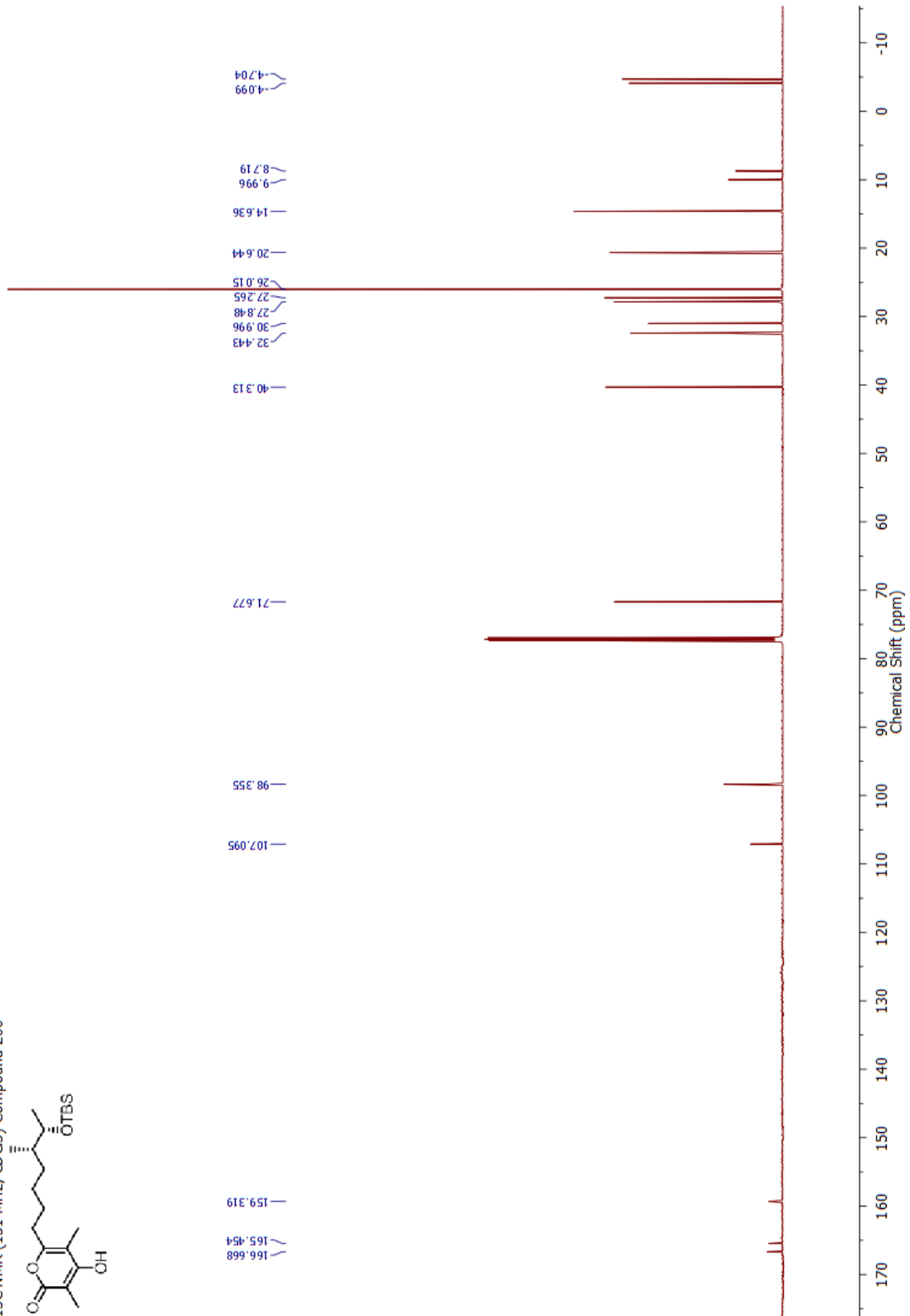


Appendix

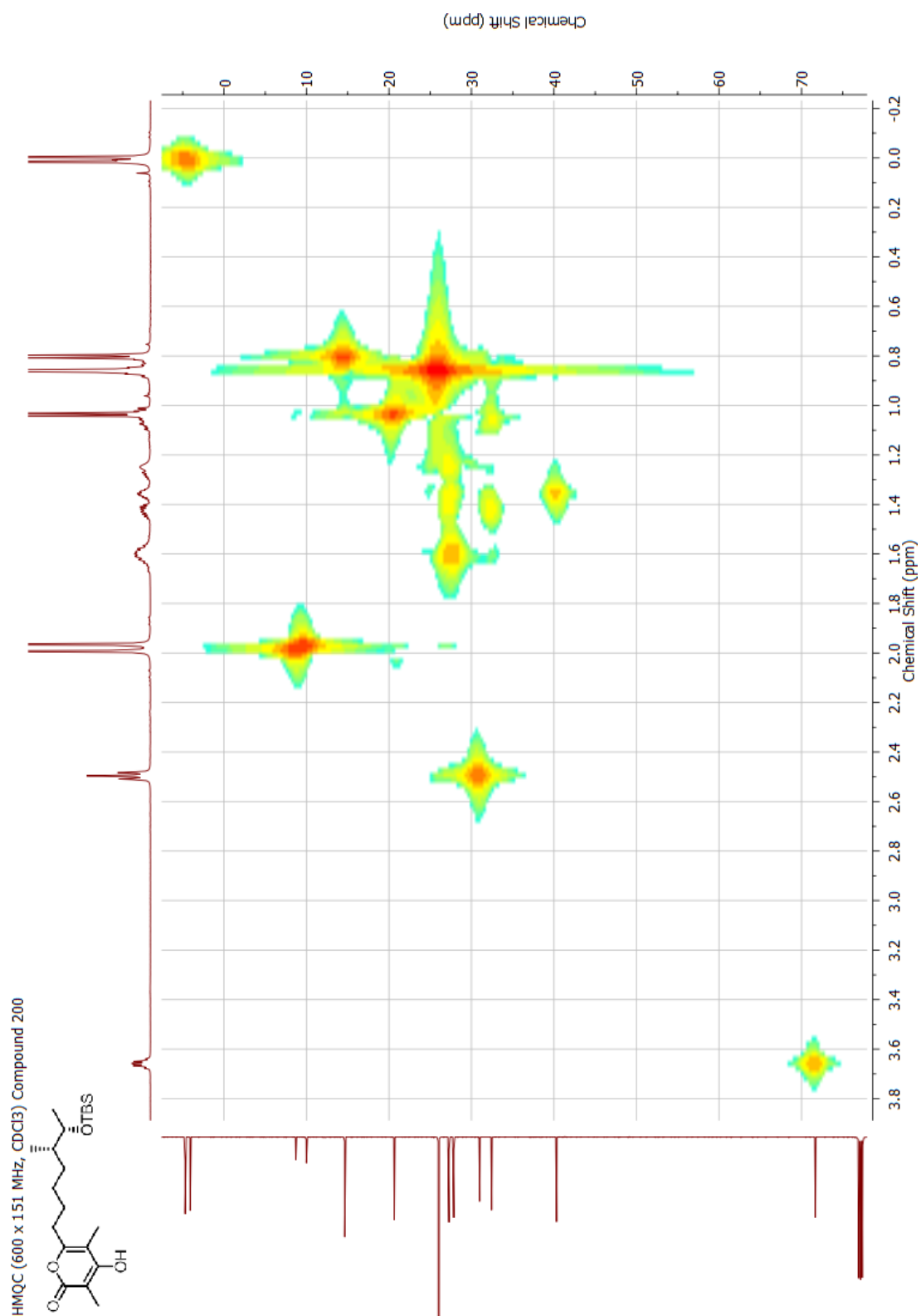


Appendix

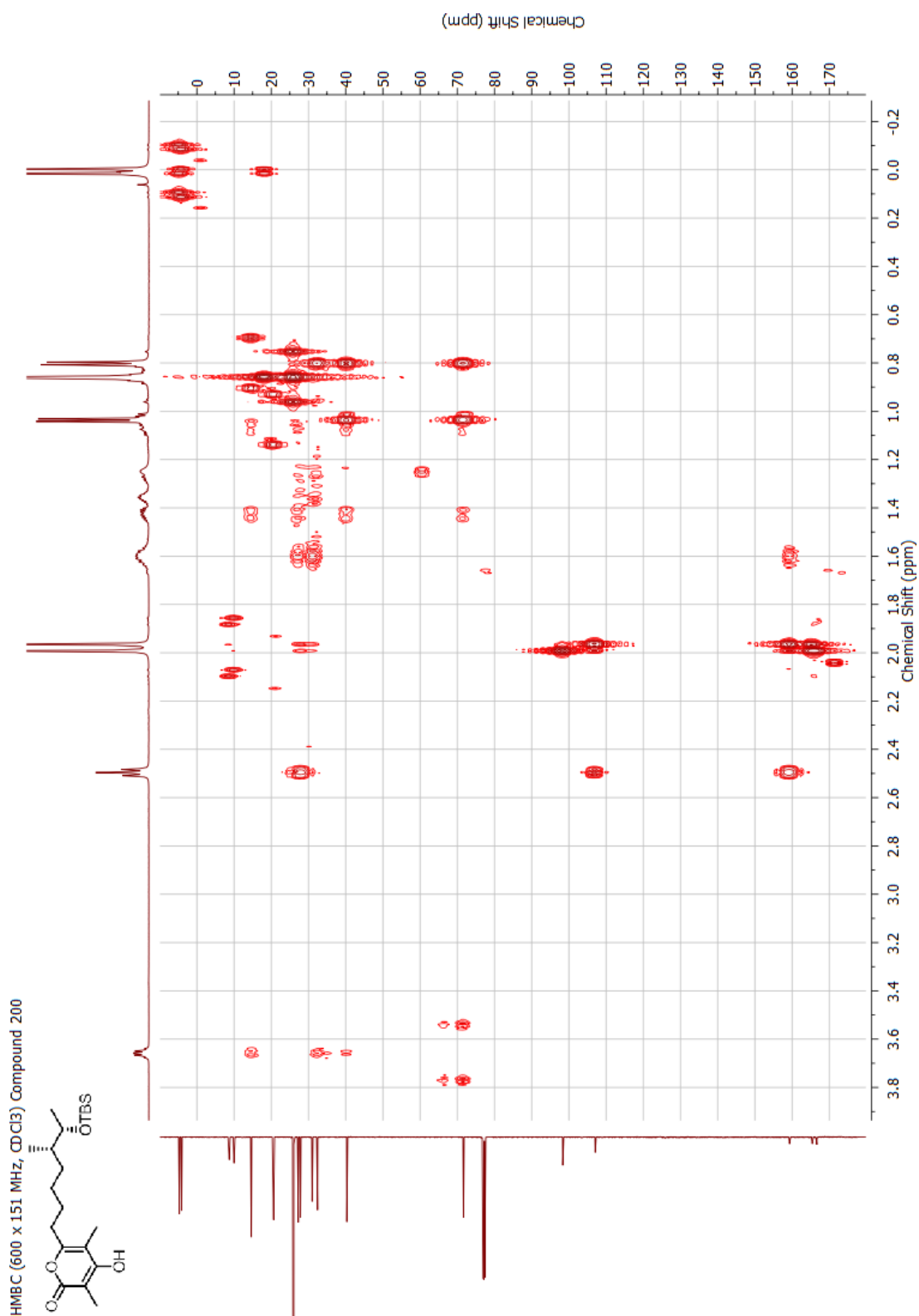
¹³C NMR (151 MHz, CDCl₃) Compound 200



Appendix

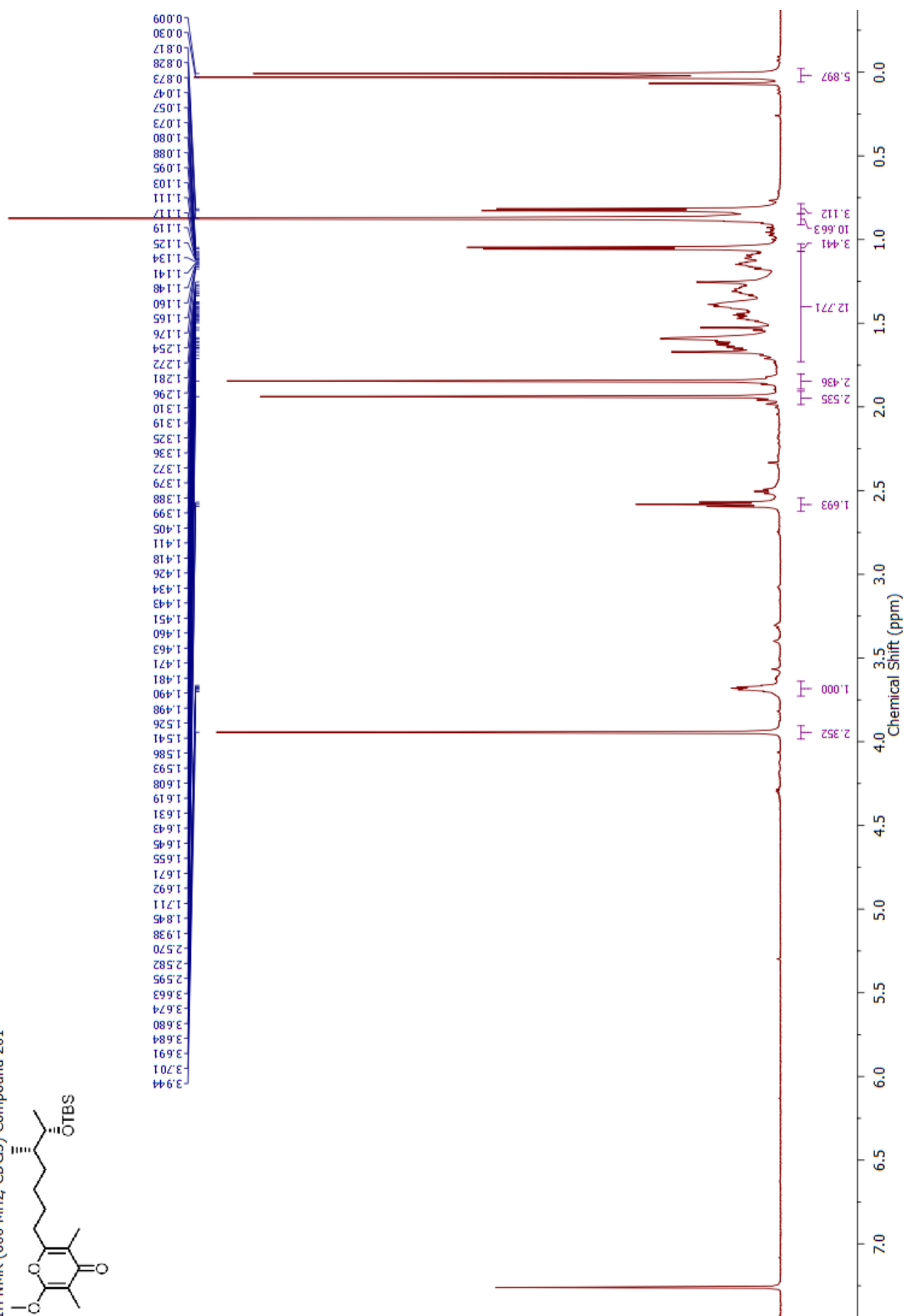
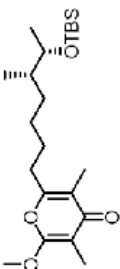


Appendix

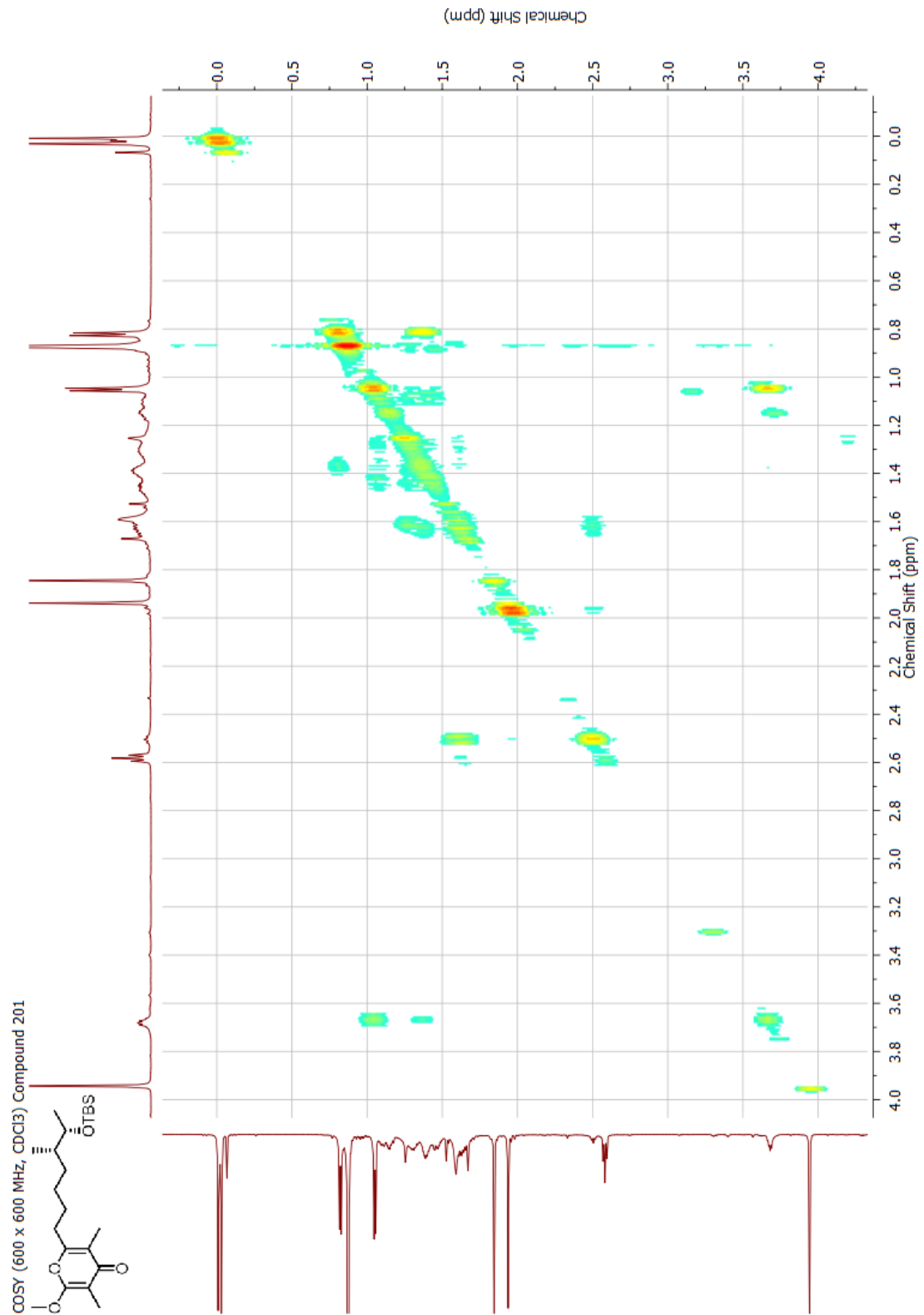


Appendix

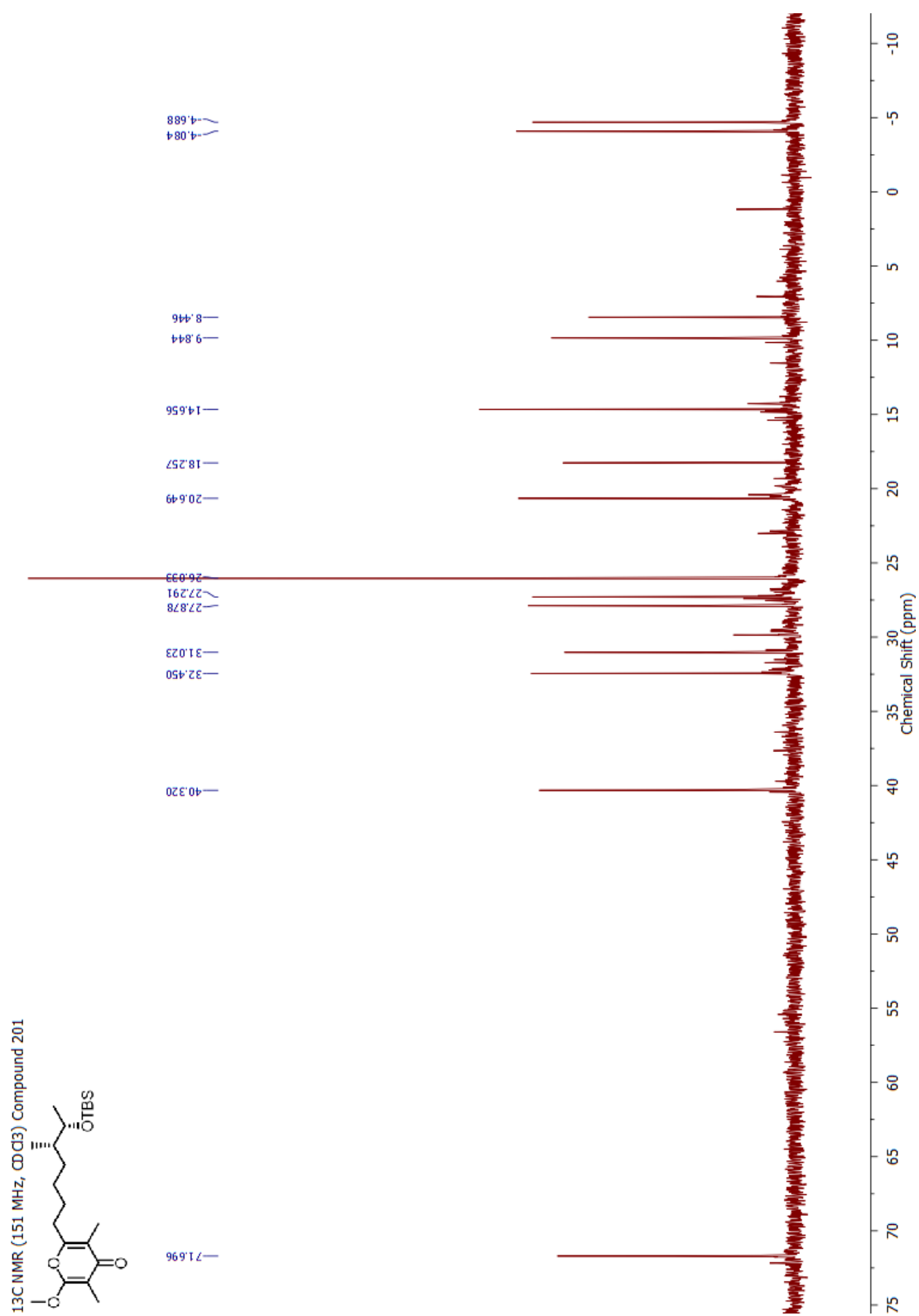
¹H NMR (600 MHz, CDCl₃) Compound 201

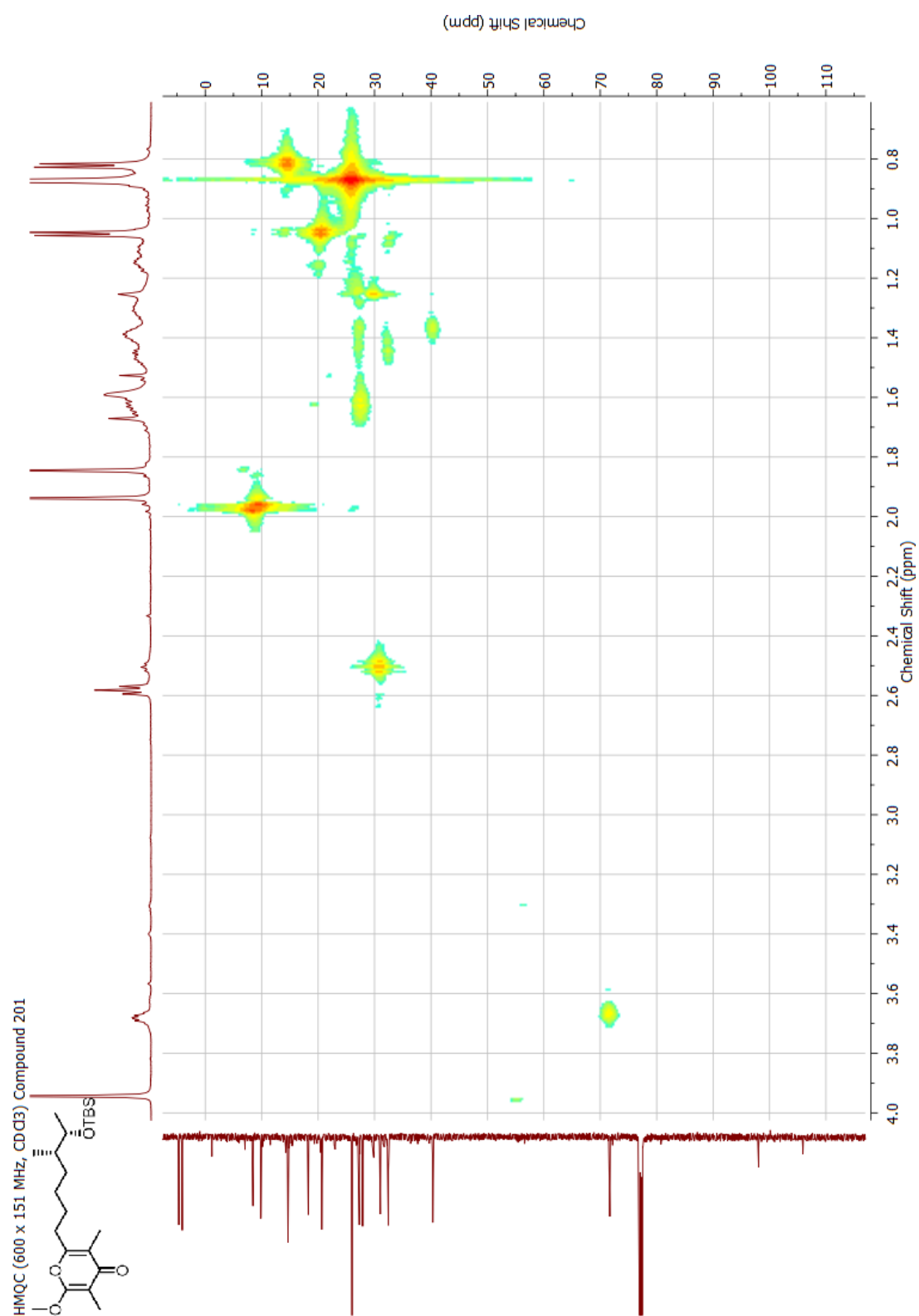


Appendix

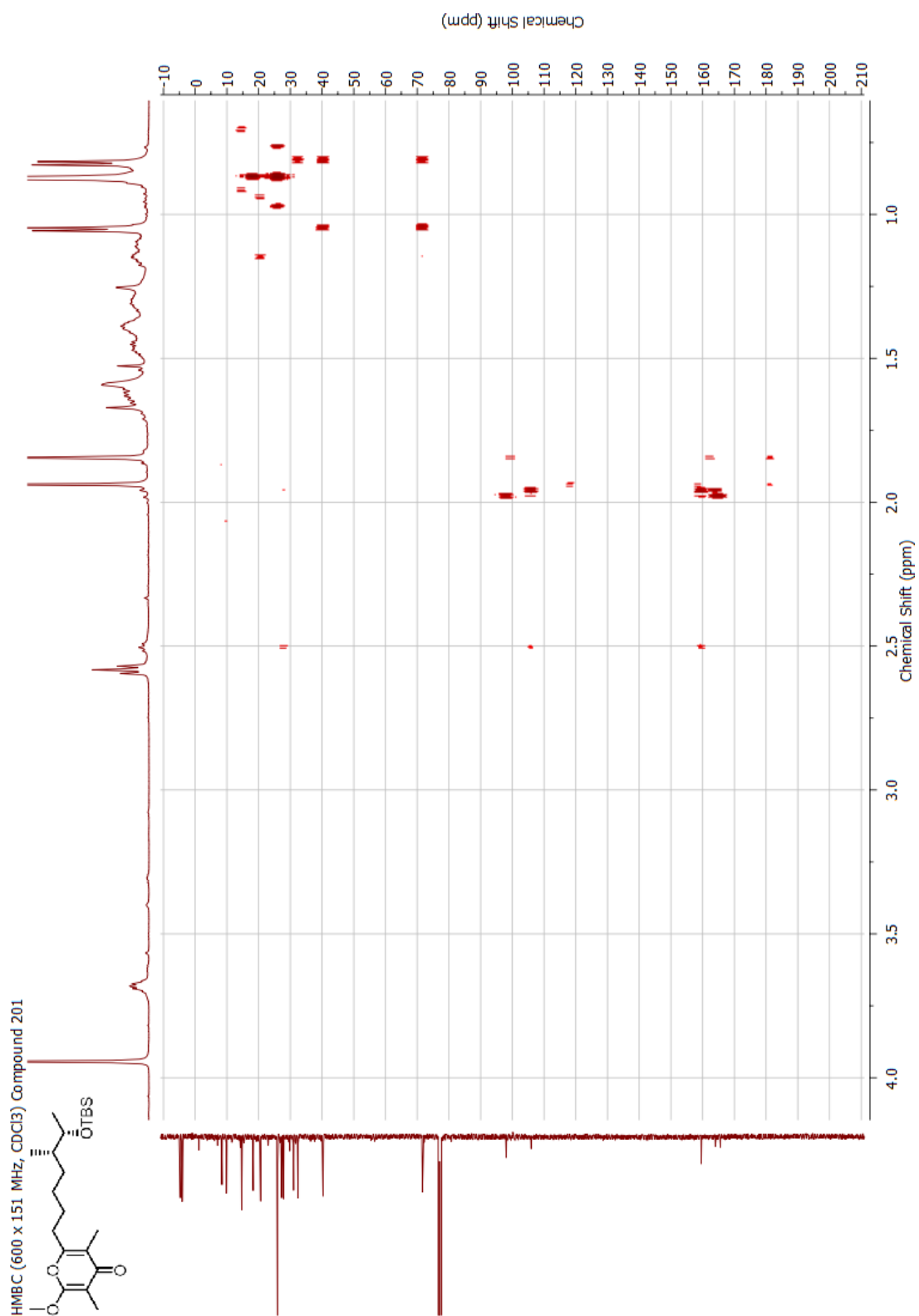


Appendix

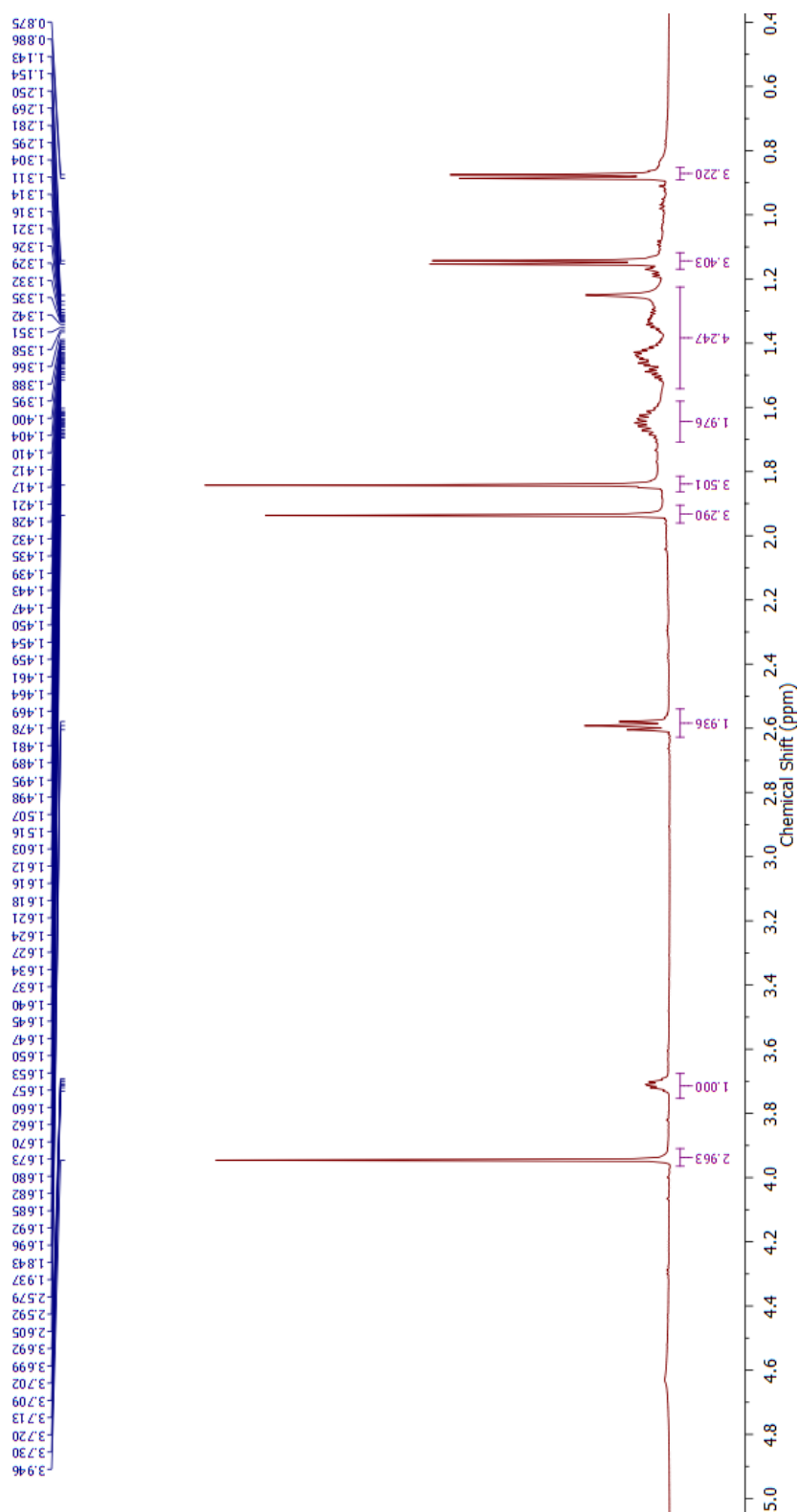
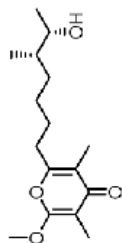




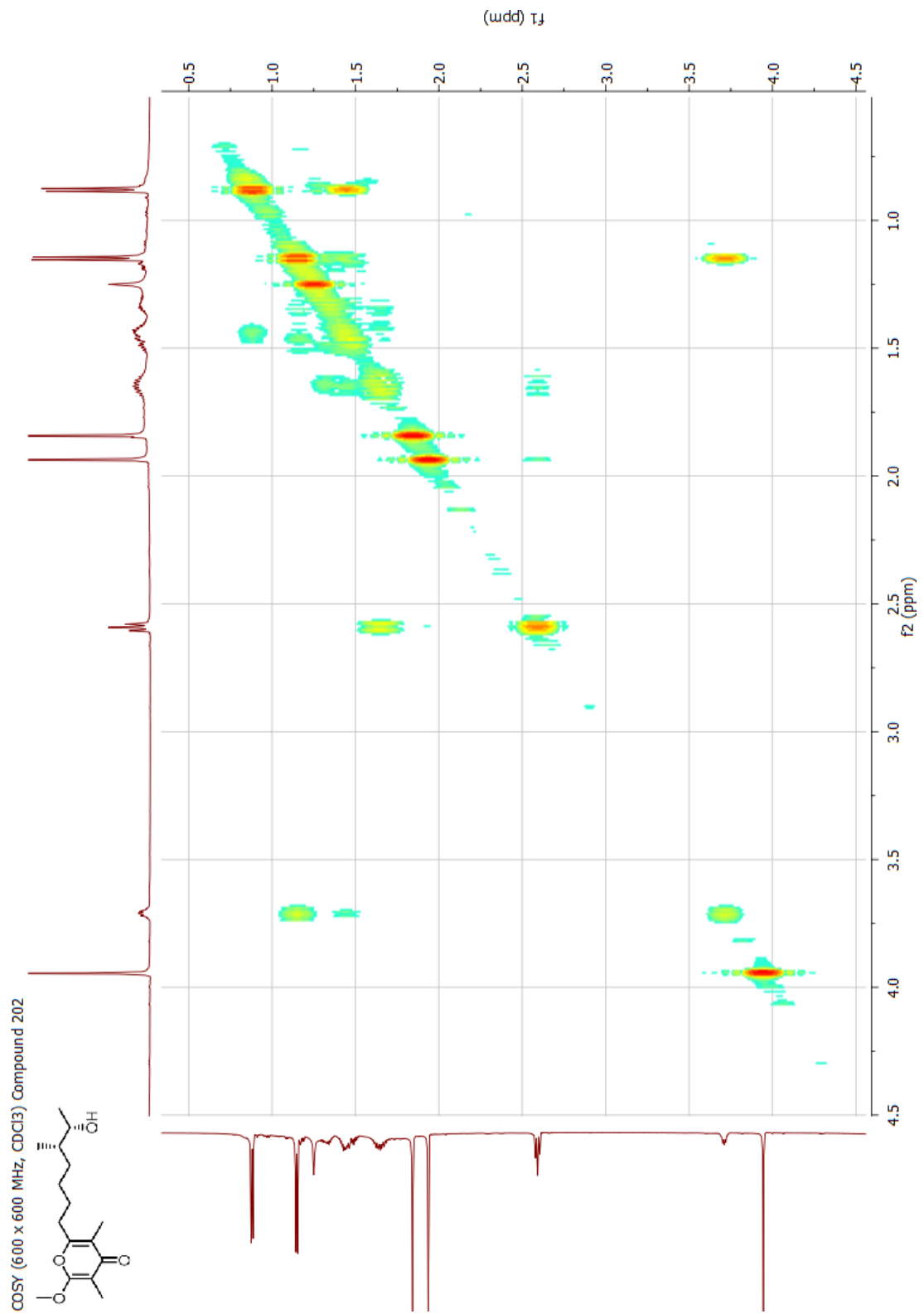
Appendix

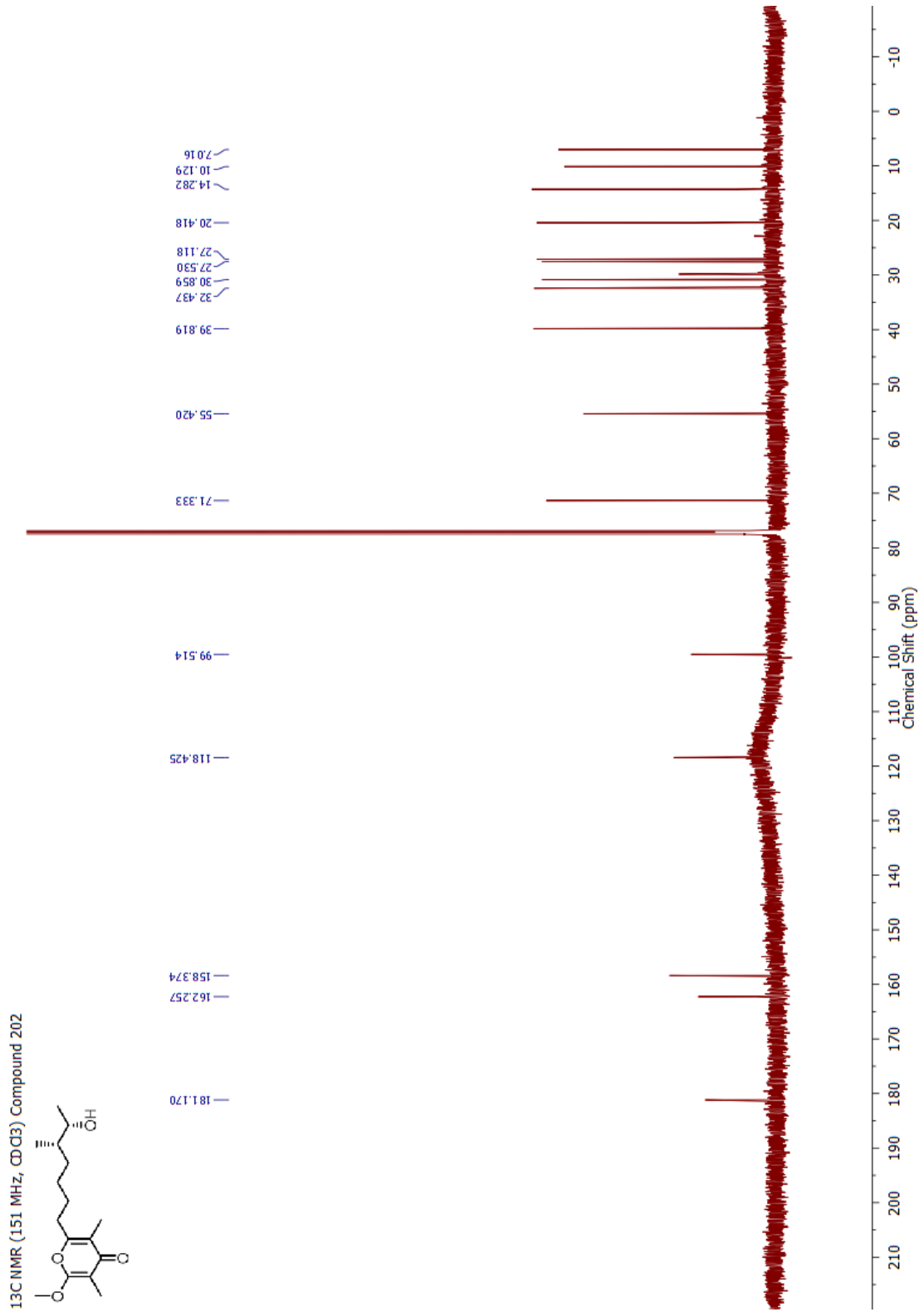


¹H NMR (600 MHz, CDCl₃) Compound 202

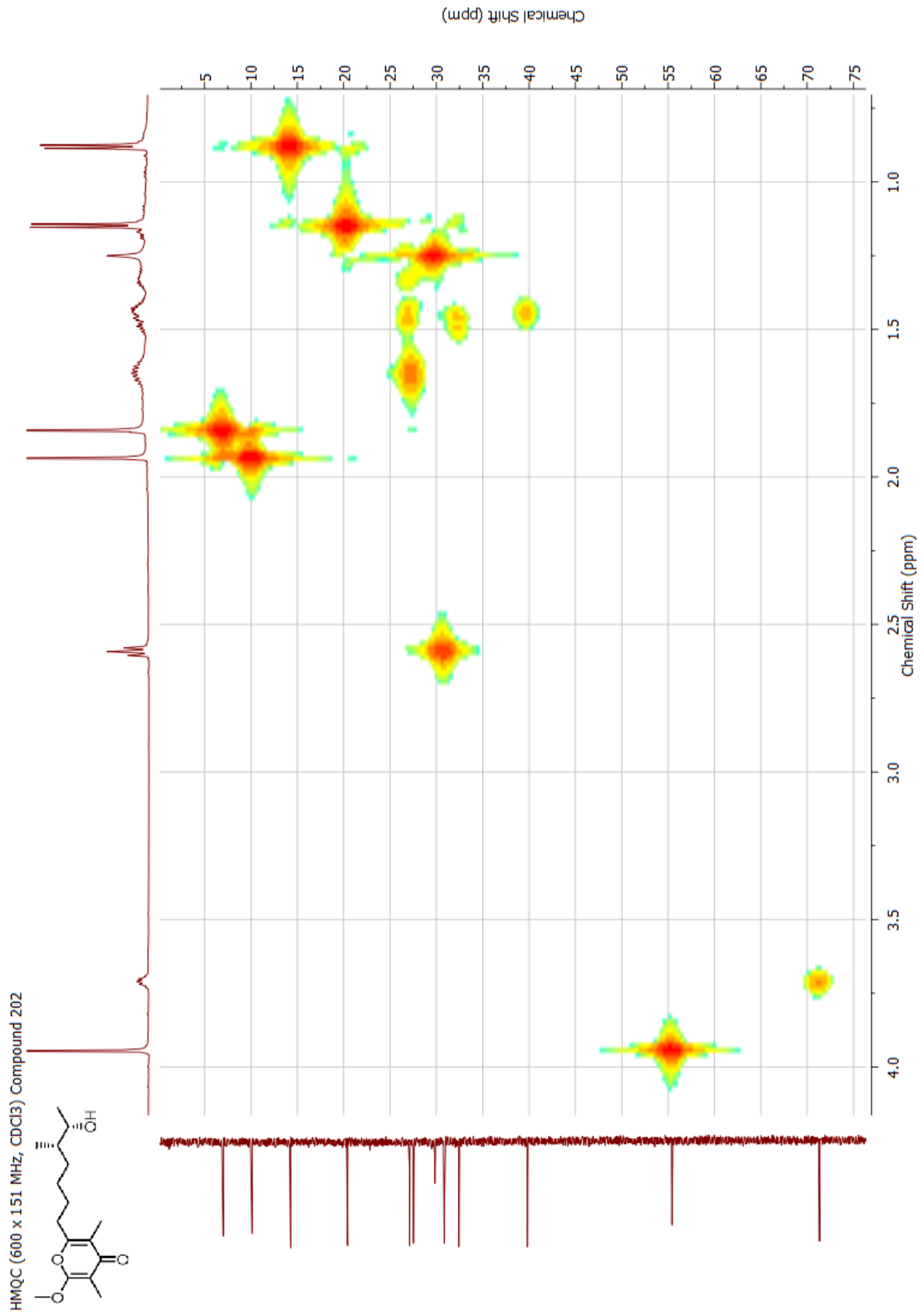


Appendix





Appendix



Appendix

